(12) INTERNATIONAL APPLICATION PUBLISHED UNDER THE PATENT COOPERATION TREATY (PCT)

(19) World Intellectual Property Organization
International Bureau

(43) International Publication Date
29 June 2023 (29.06.2023)

WIPO | PCT

(10) International Publication Number
WO 2023/118866 A1

(51) International Patent Classification:
C01B 32/15 (2017.01) *C01B 32/18* (2017.01)
C01B 32/05 (2017.01) *C01B 32/182* (2017.01)
C01B 32/152 (2017.01)

(21) International Application Number:
PCT/GB2022/053345

(22) International Filing Date:
21 December 2022 (21.12.2022)

(25) Filing Language: English

(26) Publication Language: English

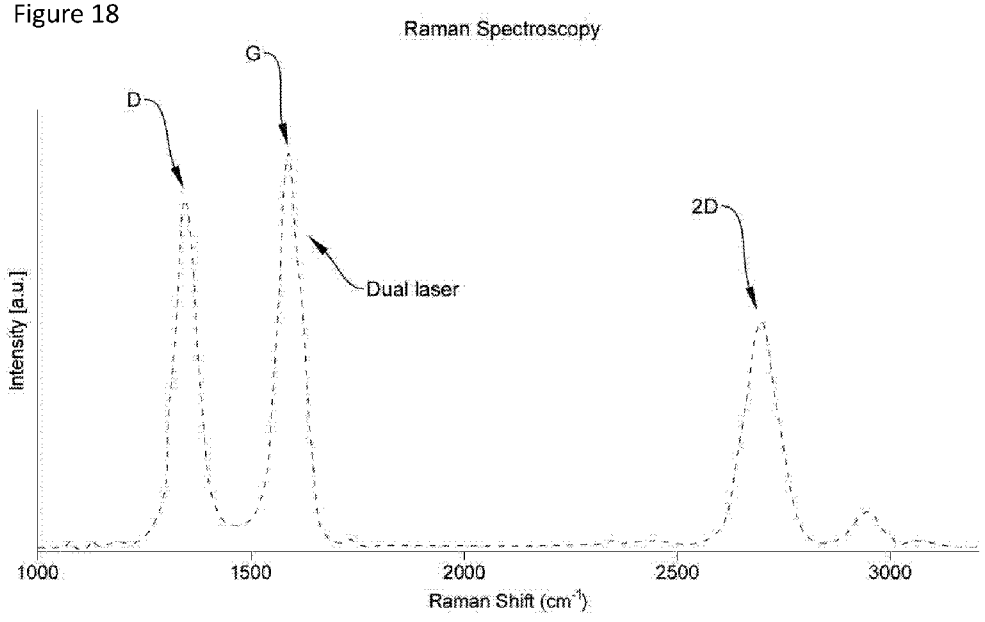
(30) Priority Data:

2118948.5	23 December 2021 (23.12.2021)	GB
2202353.5	22 February 2022 (22.02.2022)	GB
2202356.8	22 February 2022 (22.02.2022)	GB
2202357.6	22 February 2022 (22.02.2022)	GB
2202360.0	22 February 2022 (22.02.2022)	GB
2202362.6	22 February 2022 (22.02.2022)	GB
2202364.2	22 February 2022 (22.02.2022)	GB
2202366.7	22 February 2022 (22.02.2022)	GB
2202369.1	22 February 2022 (22.02.2022)	GB
2202372.5	22 February 2022 (22.02.2022)	GB
2202375.8	22 February 2022 (22.02.2022)	GB
2202376.6	22 February 2022 (22.02.2022)	GB
2202380.8	22 February 2022 (22.02.2022)	GB
2202382.4	22 February 2022 (22.02.2022)	GB
2202384.0	22 February 2022 (22.02.2022)	GB
2202387.3	22 February 2022 (22.02.2022)	GB
2202388.1	22 February 2022 (22.02.2022)	GB
2202389.9	22 February 2022 (22.02.2022)	GB

(71) Applicant: **INTEGRATED GRAPHENE HOLDING LIMITED** [GB/GB]; Euro House, Wellgreen Place, Stirling FK8 2DJ (GB).

(54) Title: LASER-INDUCED CARBON NANOSTRUCTURES

Figure 18



(57) Abstract: A method of manufacturing a carbon nanostructure, such as a carbon foam material, is disclosed. The method comprises the steps of: (a) using a first laser beam to irradiate an encapsulated or sub-surface region of a carbon pre-cursor material below a surface of the material, to create carbon foam in that sub-surface region, and a disorganised, amorphous non-graphene material above the carbon foam, and then (b) using a second laser beam to remove or ablate the disorganised, amorphous non-graphene material sitting above the carbon foam, to expose at least some of the carbon foam. The resultant carbon foam material shows a significant D peak; the 2D peak is significantly less than the G peak; and the peak D: peak G ratio is significantly above zero. In appearance and Raman signature, it appears similar to a carbon nano-onion material. It can be used in biosensors, supercapacitors and pseudo-capacitors.

WO 2023/118866 A1

[Continued on next page]

(72) **Inventors: CAFFIO, Marco**; c/o Integrated Graphene Holding Limited, Euro House, Wellgreen Place, Stirling FK8 2DJ (GB). **SEMPLE, Oliver**; c/o Integrated Graphene Holding Limited, Euro House, Wellgreen Place, Stirling FK8 2DJ (GB). **CAIRNS, Darren**; c/o Integrated Graphene Holding Limited, Euro House, Wellgreen Place, Stirling FK8 2DJ (GB).

(74) **Agent: ORIGIN LIMITED**; Twisden Works, Twisden Road, London NW5 1DN (GB).

(81) **Designated States** *(unless otherwise indicated, for every kind of national protection available)*: AE, AG, AL, AM, AO, AT, AU, AZ, BA, BB, BG, BH, BN, BR, BW, BY, BZ, CA, CH, CL, CN, CO, CR, CU, CV, CZ, DE, DJ, DK, DM, DO, DZ, EC, EE, EG, ES, FI, GB, GD, GE, GH, GM, GT, HN, HR, HU, ID, IL, IN, IQ, IR, IS, IT, JM, JO, JP, KE, KG, KH, KN, KP, KR, KW, KZ, LA, LC, LK, LR, LS, LU, LY, MA, MD, MG, MK, MN, MW, MX, MY, MZ, NA, NG, NI, NO, NZ, OM, PA, PE, PG, PH, PL, PT, QA, RO, RS, RU, RW, SA, SC, SD, SE, SG, SK, SL, ST, SV, SY, TH, TJ, TM, TN, TR, TT, TZ, UA, UG, US, UZ, VC, VN, WS, ZA, ZM, ZW.

(84) **Designated States** *(unless otherwise indicated, for every kind of regional protection available)*: ARIPO (BW, CV, GH, GM, KE, LR, LS, MW, MZ, NA, RW, SD, SL, ST, SZ, TZ, UG, ZM, ZW), Eurasian (AM, AZ, BY, KG, KZ, RU, TJ, TM), European (AL, AT, BE, BG, CH, CY, CZ, DE, DK, EE, ES, FI, FR, GB, GR, HR, HU, IE, IS, IT, LT, LU, LV, MC, ME, MK, MT, NL, NO, PL, PT, RO, RS, SE, SI, SK, SM, TR), OAPI (BF, BJ, CF, CG, CI, CM, GA, GN, GQ, GW, KM, ML, MR, NE, SN, TD, TG).

Published:

— *with international search report (Art. 21(3))*

— *in black and white; the international application as filed contained color or greyscale and is available for download from PATENTSCOPE*

LASER-INDUCED CARBON NANOSTRUCTURES

Field of the invention

This invention relates to the laser-induced production of carbon nanostructures, including turbostratic twisted multilayer carbon foam.

Background to the invention

Carbon nanostructures are both fascinating and the subject of intense research. Carbon nano-onions, also known as multi-layered fullerene, exemplify this. See 'Raman spectroscopy of polyhedral carbon nano-onions'. DOI: 10.1007/s00339-015-9315-9 and also 'Carbon nano-onions: unique carbon nano-structures with fascinating properties and their potential applications'. DOI:10.1016/j.ica.2017.07.021, the contents of which are incorporated by reference.

Another carbon nanostructure, graphene, has for many years been of great interest for applications including biosensors, electrochemical sensing systems, supercapacitors, electrodes, and fuel cells. Known methods of producing 3D graphene include the laser induced graphene production described in WO 2019/038558; when a suitable carbon pre-cursor material, such as polyimide film, is positioned on a supporting substrate, and irradiated with a CO_2 laser, then 3D graphene forms at the surface of the exposed polyimide film. Experience has shown that the thickness of the 3D graphene produced by this method is less than 50 μm; further, the 3D graphene itself can be brittle and adhere poorly to an underlying substrate and may flake off that substrate. It is hence unsuited to many applications.

A note on terminology used in the carbon nanostructure field: if we just take the term 'graphene', there are many different forms of 'graphene'; for example, the literature describes monolayer graphene, bilayer graphene, turbostratic graphene, graphene superlattices, graphene fiber, 3D graphene, graphene aerogel, crumpled graphene, and many other forms. This presents a definitional challenge because use of a specific term (e.g., '3D graphene') might imply a limitation to only that specific form of graphene. Further, The IUPAC (International Union for Pure and Applied Chemistry) recommends use of the name "graphite" for the three-

dimensional material, and "graphene" only when the reactions, structural relations or other properties of individual layers are discussed.

In this specification, we therefore use the term 'carbon foam' as a generalised term, and this term should be expansively construed to cover any carbon nanostructure, such as 3D carbon material foam, including turbostratic twisted multilayer 3D carbon material foam.

One instance of the term 'carbon foam' refers to a material that is manufactured using the methods described in this specification; this material has properties that are somewhat distinct from conventional graphene or conventional graphene foam. For example, graphene foam has several characteristics: it is hydrophobic, with low wettability. Raman analysis of a typical graphene foam reveals the following signatures: absence of a D peak; the 2D peak is higher than the G peak; the peak D: peak G ratio is close to zero. As we will describe in more detail below, the carbon foam generated in an implementation of this invention shares none of these characteristics; it is hydrophilic, with a contact angle below 20°; it lacks the tell-tale Raman signature of graphene: it shows a significant D peak; the 2D peak is significantly less than the G peak; the peak D: peak G ratio is significantly above zero. In appearance and Raman signature, it appears closer to carbon nano-onion material. The term 'carbon foam' hence also includes within its scope materials that are carbonaceous nanostructures, such as carbon nano-onion, carbon nano-horn, carbon nano-tubes, carbon nano-dots, nanodiamonds and fullerene, or combinations of any of these.

SUMMARY OF THE INVENTION

In this specification, we describe an approach in which the surface of a carbon pre-cursor is not converted to graphene at all; instead, a sub-surface or encapsulated region of the carbon pre-cursor is converted to a carbon foam by a focussed laser beam.

We generalise to the invention as defined in Claim 1, namely a method of manufacturing a carbon foam material comprising the steps of:

(a) using a first laser beam to irradiate an encapsulated or sub-surface region of a carbon pre-cursor material below a surface of the material, to create carbon foam in that sub-surface region, and a disorganised, amorphous non-graphene material above the carbon foam, and then

(b) using a second laser beam to remove or ablate the disorganised, amorphous non-graphene material sitting above the carbon foam, to expose at least some of the carbon foam.

The amorphous non-graphene material is 'above' the carbon foam in that it is closer to the laser generating the laser beam than the carbon foam is. One implementation of the invention is described as a 'Dual Laser' process, since two separate lasers are used in the production of the carbon foam material. The carbon foam material shows a significant D peak; the 2D peak is significantly less than the G peak; and the peak D: peak G ratio is significantly above zero. In appearance and Raman signature, it appears similar to a carbon nano-onion material. It can be used in biosensors, supercapacitors and pseudo-capacitors. In one implementation, the carbon foam is called 'Gii' carbon foam.

BRIEF DESCRIPTION OF THE FIGURES

The invention will be described with reference to implementations of the invention shown in the following Figures:

Figures 1 - 6 schematically show the Dual Laser process used to create carbon foam when a polyimide (PI) film, acting as the carbon pre-cursor, is positioned on a substrate.

Figure 7 is a scanning electron image showing the unique surface morphology of the carbon foam achieved using the Dual Laser method (x250).

Figure 8 is a scanning electron image showing the surface of conventional laser induced graphene.

Figure 9 - 14B schematically show the Dual Laser process used to create carbon foam when a PI film, acting as the carbon pre-cursor, is not positioned on a substrate.

Figure 15 are cyclic voltammography (CV) graphs for carbon foam electrodes produced using the Dual Laser method.

Figure 16A is a graph showing the peak separation ΔE_p as a function of scan rate for carbon foam electrodes produced using the Dual Laser method.

Figure 16B is a graph showing the peak separation ΔE_p as a function of scan rate for conventionally manufactured graphene electrodes.

Figure 17 is a comparison of electrochemical impedance spectroscopy results for carbon foam electrodes produced using the Dual Laser method and also conventionally manufactured graphene electrodes.

Figure 18A and **B** is a Raman analysis of a carbon foam sample made by the Dual Laser process.

Figure 18C is a Raman analysis of carbon nano-onion material.

Figure 19 are scanning electron images showing Dual Laser carbon foam and conventional graphene.

Figure 20 are schematic images of biosensors including Dual Laser carbon foam (this implementation of the carbon foam is called Gii-Sens).

Figure 21 - 23 are detailed processing flow charts for Dual Laser carbon foam (referred to as Gii-Sens, Gii-Sens+ and PPC Gii-Sens variants).

Figure 24 - 27 are schematic images of supercapacitor including Dual Laser carbon foam (this implementation of the carbon foam is called Gii-Cap).

Figure 28 - 29 are detailed processing flow charts for Dual Laser carbon foam (referred to as the Gii-Cap and Gii-Cap+ variants).

Figure 30 is a schematic cross section through an integrated lab-on-chip (LoC) device that includes a biosensor and supercapacitor made using Dual Laser carbon foam.

Figure 31 is an exploded view of a fully integrated LoC device.

Figure 32 shows the LoC device displaying quantitative results on its display.

Figure 33 is an exploded view of an environmental monitoring device that includes a Gii-Sens sensor.

Figure 34 is a view of the assembled environmental monitoring device

Figure 35 is a schematic cross section through a device that has a battery (e.g. a printed battery or a conventional battery) and also a Gii-Cap supercapacitor.

Figure 36 is a schematic view of a smart label; this has a battery (e.g. a printed battery or a conventional battery) and also a Gii-Cap supercapacitor.

Figure 37 a schematic cross section showing the basic layering of different materials in the Gii-Thru variant, which is a three-dimensional structure of the carbon foam.

Figure 38 - 42 are schematic views through various Gii-Thru Gii-Cap/Gii-Cap+ three-dimensional supercapacitor devices.

Figure 43A and 43B are detailed processing flow charts for Dual Laser carbon foam Gii-Thru Cap three-dimensional supercapacitor devices.

Figure 44A and 44B are schematic views of a Gii-Thru sensor used in a three-sample array microfluidic diagnostic device.

Figure 45A and 45B are schematic views of a Gii-Thru sensor used in an eight-sample array microfluidic diagnostic device**.**

Figure 46A shows a perspective view of a fully assembled multi sample array microfluidic diagnostic device.

Figure 46B is a top-down view of the multi sample array microfluidic diagnostic device.

Figures 47 and **48** are views of a microfluidic diagnostic device.

Figure 49 is a detailed manufacturing process flow for the High Sensitivity Low Cost Gii-Thru variant.

Figure 50 is a schematic of a high-speed reel to reel or reel to sheet manufacturing system for Gii carbon foam.

Figure 51 shows the detailed process flow for the Figure 50 system.

Figure 52 - 57A are scanning electron images showing Dual Laser carbon foam at various magnifications.

Figure 57B is a scanning electron image of a carbon nano-onion material made using a conventional process.

Figure 58 shows the Raman shifts for eight sheets of carbon foam made using the Dual Laser process.

Appendix 1 A Supercapacitor implementation with a hydrogel electrolyte

Figure 59 presents carbon foam cyclic voltammograms for positive voltages measured at 25 mV/s.

Figure 60 shows carbon foam cyclic voltammograms for negative voltages measured at 25 mV/s.

Figure 61 shows carbon foam galvanostatic charge discharge (GCD) curves measured at 0.5 mA/cm^2 for positive voltage windows.

Figure 62 shows carbon foam galvanostatic charge discharge (GCD) curves measured at 0.5 mA/cm^2 for negative voltage windows.

Figure 63 shows carbon foam galvanostatic charge discharge (GCD) data taken from five two-electrode devices.

Figure 64 shows carbon foam cyclic voltammograms recorded from five different two-electrode devices at high (left) and low (right) scan rates.

Figure 65 shows carbon foam cyclic voltammogram data for five additional systems, differing through the nature of the hydrogel electrolyte: (a) 3M $NaClO_4$ and PVA; (b) 1M $NaClO_4$ and PVA; (c) 2.5M $NaNO_3$ and PVA; (d) 3M $Mg(ClO_4)_2$ and PVA; and (e) 5M $NaClO_4$ and PVP.

Appendix 2 : Gii-Cap+ Hydrogel

Figure 66 are typical CV curves for Gii-Cap+ Hydrogel devices.

Figure 67 are typical GCD curves for Gii-Cap+ Hydrogel devices after conditioning.

Figure 68 shows post-conditioning Nyquist (left) and Bode (right) plots for Gii-Cap+ devices.

Appendix 3 GiiCap Iongel

Figure 69 - 74 are results for GiiCap Iongel devices.

Appendix 4 3-month Gii-Sens Assay Feasibility Proposal

Figure 75 - 78 are schematic views of assay procedures for a Gii-Sens 3D Carbon Foam assay system.

Figure 79 - 81 shows the surface chemistry for Gii-Sens 3D Carbon Foam.

Figure 82 - 83 shows a labeless assay exploration for Gii-Sens 3D Carbon Foam.

Appendix 6 Benchmark experimental conditions

Figure 84 - 86 are graphs comparing the performance of Gii-Sens carbon foam with graphene electrode materials.

Figure 87 - 89 are graphs comparing the performance of Gii-Sens carbon foam with carbon-based electrode materials.

Figure 90 - 92 are graphs comparing the performance of Gii-Sens carbon foam with Screen Printed Gold.

Appendix 7: Optimisation of the surface immobilization of anti human procalcitonin (cAb)

Figure 93 shows the direct assay procedure for optimisation of the surface immobilization of anti human procalcitonin (cAb).

Figure 94 is a surface immobilization reaction schematic.

Figure 95 shows Rct & ΔEp signal response for NHS functionalization of Gii-Sens electrodes.

Figure 96 shows cAb immobilisation on GiiSens electrodes.

Figure 97 shows signal response from 2000 pg/ml in direct assay format using 100 µg/ml cAb surface coating.

Note that Gii, Gii-Sens, Gii-Sens+, Gii-Cap, Gii-Cap+, Gii-Thru and PPC Gii are trademarks of the patent proprietor. 'Gii' refers generally to the carbon foam made using the Dual Laser process. 'Gii-Sens' refers to the Gii carbon foam used in a sensor, such as a biosensor. 'Gii-Cap' refers to the Gii carbon foam used in a supercapacitor. The + suffix refers to the Gii carbon foam when modified with a metal oxide layer or film. 'Gii-Thru' refers to the Gii carbon foam when arranged into a specific three dimensional structure. 'PPC' refers to a specific

manufacturing process, 'post printing conversion', where the Gii carbon foam is created after various screen printing steps have been completed.

Index to Figures

Dual laser process

11 IR laser
12 IR laser beam
13 interior of PI film
14 PI film
15 substrate
16 sub-surface carbon foam region
17 disorganised, amorphous, non-graphene material below the sub-surface carbon foam region
18 expanded region of disorganised, amorphous, non-graphene material above the sub-surface carbon foam region
20 CO2 laser
21 unique surface morphology of the exposed carbon foam region

Biosensor

201 polyimide substrate
202 carbon foam working electrode
203 carbon foam counter electrode
204 carbon foam reference electrode
205 screen printed silver connection tracks
206 dielectric layer
207 area where silver connection tracks overlap the electrodes

Gii-Cap Supercapacitor

241 array of carbon foam electrodes
242 screen printed silver connectors

243 dielectric layer
244 polyimide base layer
245 copper connection tabs
246 electrolyte layer
247 aluminium-laminate heat-seal pouch
250 rounded edges of a carbon foam digit

Combined Sensor and Supercapacitor

301 upper polyimide layer
302 Gii-Sens biosensor
303 lower polyimide layer
304 supercapacitor
305 plastic piece
306 microchannels
307 connector tracks
308 flexible electronics

310 inductive power loop
312 Gii-Cap supercapacitor
313 Gii-Sens biosensor
314 device layer with microelectronics
315 top panel
316 display
317 circular analyte well

Environmental monitor

330 Gii-Sens carbon foam sensor
331 Control electronics
332 PV solar cell
333 Gii-Cap carbon foam supercapacitor
334 Peelable back

Combined Supercapacitor and Battery

351 first polyimide layer
352 supercapacitor
353 second polyimide layer
354 battery
355 BMS (battery management system)
356 flexible electronics
357 electrical connections

Smart Label

360 flexible battery
361 supercapacitor
362 electronics module
363 exposed label surface
364 adhesive release liner 364

Gii-Thru Cap

371 PI film
372 screen printed conductive ink or paste layer
373 screen printed collector
374 dielectric isolator
375 encapsulated carbon foam layer
376 disorganised, amorphous non-graphene layer under the carbon foam layer
377 unique surface morphology layer

390 hydrogel electrolyte layer
391 carbon foam layer with unique surface morphology
392 PI film
393 screen printed carbon paste layer
394 screen printed silver connector layer

395 copper tab for the silver connector layer
396 dispensed dielectric isolation layer
397 second carbon foam layer with unique surface morphology
398 PI film
399 hydrogel electrolyte layer

400 dielectric isolation layer
401 screen printed silver collector layer
402 copper tab
403 screen printed carbon paste layer
404 carbon foam layer
405 PI film

Gii-Thru Sens

Three spot array microfluidic diagnostic device

440 analyte sample wells
441 laminated well spacer layer
442 polyimide film
443 screen printed conductive carbon layer
444A reference electrode connection
444B working electrode connection
444C counter electrode connection
447 screen printed dielectric layer
448A reference electrode
448B working electrode
448C counter electrode
449 reference electrode screen printed carbon layer

Eight spot array microfluidic diagnostic device

451 laminated well spacer

452 array of eight analyte wells
453 wells for a counter electrode
454 wells for a reference electrode
455 polyimide layer
456 polyimide layer
457 eight working electrodes
458 counter electrodes
459 reference electrodes
460 screen printed carbon connection interface layer
461 screen printed silver connection tracks
462 screen printed dielectric layer

470 top layer microfluidic foil
471 middle layer microfluidic foil
472 printed or moulded microfluidic fluid channel
473 bottom layer microfluidic foil with adhesive
474 Gii-Thru sensor
475 connectors

481 clear resin barb connectors
482 top foil
483 clear resin moulded microfluidic card
484 microfluidic channels
485 well unit
486 Gii-Thru sensor

DETAILED DESCRIPTION

We will start with a simplified, schematic walk-through of implementations of the invention. We give two walk-throughs; the first (**Figures 1 – 6**) will describe at a high level the carbon foam production process when the carbon pre-cursor (e.g. polyimide (PI) film, such as Kapton® film in this case) is mounted on a substrate; the second walk-through (**Figures 9 – 14**) covers the carbon foam production process when the polyimide film is not mounted on a substrate. In each case, we use a Dual Laser process; we will explain what the term means below.

In the first stage, (see **Figure 1**), laser 11 with wavelength A irradiates with laser beam 12 the interior 13 of polyimide film 14, positioned on a substrate 15 suitable for the end application. This laser can be a pulsed IR laser that delivers IR radiation with a 1064 nm wavelength.

As shown in **Figure 2**, the laser 11 with wavelength A is tuned so that a sub-surface region 16, is converted to carbon foam. The focus of laser A moves progressively through the interior 13 of the polyimide film 14 to create the entire carbon foam region 16. The carbon foam region 16 can be approximately 50μm or greater in depth or height – far taller than is possible with other methods. Note that there is no carbon foam created on the exposed surface (i.e. the surface that the laser beam is incident on) of the polyimide film 14 at any time. The region above the carbon foam 16 (i.e. closer to the laser than the carbon foam region 16) is not converted to carbon foam. The region 17 below the carbon foam region 16 (i.e. the lower surface of the PI film) is also not converted to carbon foam but is instead converted to a disorganised, amorphous non-graphene material that adheres to the underlying substrate 15.

Figure 3 shows that laser 11 with wavelength A causes a physical expansion at the region 18 above (i.e. closer to the laser than the carbon foam region 16) the internal carbon foam zone 16 due to trapped gasses. This region 18 is not 3D graphene, nor is it a polymer; it is a disorganised, amorphous material.

In a second stage, a laser 20 with wavelength B is now tuned on the disorganised, amorphous material region 18 above the carbon foam region 16, as shown in **Figure 4.** This can be a CO_2 laser with a 10.6 μm wavelength.

This laser 20 with wavelength B, as shown in **Figure 5,** ablates some or all of the region 18 above the carbon foam region16, exposing at least some of the underlying carbon foam region 16.

The laser 20 with wavelength B also gives the underlying carbon foam region a unique surface morphology 21, as shown in **Figure 6**.

We refer to the process described in **Figures 1 - 6** as a 'Dual Laser process'.

Figure 7 is a scanning electron image showing the unique surface morphology achieved using the Dual Laser method (x250). In this case, the carbon source was irradiated first with IR radiation of a wavelength of 1064 nm from a pulsed IR laser, with the radiation focussed into the carbon source and at progressive depths within the carbon source, and then the carbon source was irradiated with a laser beam at wavelength of 10.6 μm from a CO_2 laser. The approximate thickness of the carbon foam layer in this image is 220 μm.

The contrast with the surface morphology achieved using a conventional LIG method (x250), shown in **Figure 8,** is clear: there are clear raster lines, and the folding is less convoluted. The thickness of this layer of carbon foam is less than 50μm.

From the **Figure** 7 images, we may infer that the material created using the Dual Laser process does not have a surface morphology similar to conventional graphene foam; whilst it appears to be a turbostratic twisted multilayer 3D carbon-based material with a foam like structure, it is not necessarily what one would normally describe as 'graphene', in the conventional sense. Further details are in **Feature R** below.

In the preceding walk-through (**Figures 1 – 6**), we looked at the Dual Laser process when the carbon pre-cursor material (the polyimide film) is mounted on a substrate. In the following **Figures 9 -14**, we will look at the Dual Laser process when the polyimide film is not mounted on a substrate. The manufacturing processes we describe in detail later for the two implementations called Gii-Cap (a supercapacitor) and Gii-Sens (a sensor) use a standard 220mm x 180mm sheet of polyimide film that is not mounted on a substrate; this size can be accommodated in a standard laser scanning device, of the sort typically used for laser engraving, laser cutting and laser plotting that traces out a path defined by a standard CAD

program. The manufacturing processes also uses a standard flatbed screen printing device, and a standard conveyor dryer, again readily compatible with different sizes of thin PI film. Other sizes of polyimide sheet can be accommodated.

As described previously, laser 11 with wavelength A (e.g. IR laser) irradiates the interior 13 of PI film 14; the film 14 is now not mounted on a substrate, as shown in **Figure 9**. It can be a sheet that is supported at its edges, or rests temporarily upon a surface, or forms part of a reel of PI film when a continuous manufacturing (e.g. reel to reel or reel to sheet) system is used (see **Feature P** below).

The laser 11 with wavelength A is tuned so that a sub-surface region 16 is converted to carbon foam, as shown in **Figure 10**. The focus moves progressively through the film 14 to create the entire carbon foam region 16. The carbon foam region 16 can be approximately 50μm or greater in height – far deeper or taller than is possible with other methods.

There is no 3D graphene created on the exposed surface of the polymer film at any time. The region above the carbon foam is not converted to 3D graphene.

As shown in **Figure 11**, there is a physical expansion of the region 18 above the internal carbon foam zone 16 due to trapped gasses. This region is not 3D graphene, nor a polymer; it is a disorganised, amorphous material.

A laser 20 with wavelength B (e.g. CO_2) is now tuned on the region 18 above the carbon foam, as shown in **Figure 12**. The laser 20 with wavelength B ablates the region 18 above the carbon foam region 16, exposing at least some of the underlying carbon foam 16, as shown in **Figure 13**.

Just as when the polyimide film 14 is mounted on a substrate, the laser 20 with wavelength B also gives the underlying carbon foam 16 a unique surface morphology 21, as shown in **Figure 14.**

Some implementation specifics for this Dual Laser approach to carbon foam production now follow: in one example, a Nd:YAG solid state laser is the wavelength A laser and is positioned so that the IR laser radiation beam (wavelength of 1064 nm) produced by the solid-state laser

impacts the polyimide layer perpendicular to the layer. Optics focus the IR laser radiation laser beam to a volume of minimum beam convergence within the polyimide layer.

In an encapsulated or sub-surface region or locus around the minimum beam convergence the interaction of the laser light and the polyimide results in carbonization of the carbon source. This carbonization results in the production of carbon foam, such as a twisted or turbostratic multilayer carbon foam, in the encapsulated or sub-surface region and results in the production of a layer of a disorganised, amorphous non-graphene substance at the surface of the polyimide film.

While maintaining the laser beam focused at a particular depth within the polyimide layer, the laser is scanned laterally over the polyimide layer. In this way a path, wholly within the polyimide carbon source, is tracked and is converted to carbon foam. The polyimide is hence carbonized to a carbon foam in a pattern which corresponds to the path tracked by the scanned, focused IR laser beam.

In one set-up, the Nd:YAG IR laser was pulsed at a frequency of 80 kHz and the laser beam was scanned across the surface at a speed of 9.4 cm/s. Other embodiments utilised different parameters. For example, a pulse frequency of 50 kHz and a scan speed of 35.5 cm/s were also utilised to successfully produce carbon foam. The laser power is within a typical working range of 8 - 20 watts, with 12W optimum; the laser focal distance is within a typical working range of 50mm - 400mm.

Once a predetermined area within the polyimide layer has been irradiated in the above manner by the focused IR laser beam, the depth of the encapsulated or sub-surface region or locus in the polyimide is changed and the IR laser beam is again scanned over an area, in this case over the same predetermined area. A standard computer-controlled laser scanning system can be used that controls the X-Y position of a laser over the polyimide film. It may be necessary to pass the focussed IR laser radiation over the same area more than once to produce carbon foam. In this implementation, the focussed IR laser also irradiates adjacent, but not substantially overlapping, areas. This process of irradiating the carbon source with the focussed IR laser radiation at different focus depths is repeated until the desired depth of the polyimide layer has been exposed to the IR laser radiation and carbon foam has been formed in the encapsulated or

sub-surface region. The surface layer is however a disorganised, amorphous, non-graphene substance.

In the second step, the polyimide layer is exposed to radiation from a CO_2 laser to perform the ablation step, to expose at least some of the underlying carbon foam and to give the exposed carbon foam a particular surface morphology. The radiation from the CO_2 laser is scanned across the surface of the treated carbon source at a speed of 19 cm/s to match the pattern or area which had been irradiated with the IR laser. Other embodiments utilised different parameters. For example, a pulse frequency of 50 kHz and a scan speed of 35.5 cm/s were also utilised to successfully reveal the underlying carbon foam. The laser power is within a typical working range of 8 - 20 watts, with 12W optimum; the laser focal distance is within a typical working range of 50mm - 400mm.

As noted above, the CO_2 laser ablates the surface layer disorganised, amorphous, non-graphene substance, exposing the underlying carbon foam and altering the surface morphology of that carbon foam to generate an exposed, carbon foam with a greater number of defects compared to standard laser induced graphene; this gives the carbon foam exceptionally useful properties that are superior to standard laser induced graphene, as noted earlier.

Varying the laser parameters for either or both of the lasers (e.g. IR and the CO2 lasers), such as power, focus, wavelength, scanning speed, varies the carbon foam material properties, enabling carbon foam to be produced with properties that are optimised for different applications.

One useful property of the exposed carbon foam made by the Dual Laser process is a high degree of wettability: the contact angle can be less than 20°, making this carbon foam hydrophilic, in contrast with conventional graphene foam, which has a contact angle between 70° and 150°, making it hydrophobic. The hydrophilic property of the carbon foam produced by the Dual Laser process is highly relevant for two key applications, biosensors (an implementation is called Gii-Sens) and supercapacitors (an implementation is called Gii-Cap). For biosensors, high wettability leads to the liquid being tested (e.g. the liquid analyte) spreading rapidly and uniformly over the entire working electrode, leading to greater sensitivity, consistency and speed. For supercapacitors, high wettability means the electrolyte wets the supercapacitor electrodes better, leading to higher performance. Conventional

graphene foam can be processed to make it more wettable, but no such additional processing step is needed with this carbon foam implementation.

Another useful property of the exposed carbon foam made by the Dual Laser process is a high degree of antifouling: this could lead to enhanced sensitivity and extended life for biosensors. The carbon foam could be useful in applications where the build-up of contaminants or residues can harm the performance or lifetime of an element (e.g. filters, heating elements in electronic cigarettes; electrodes); the exposed carbon foam made by the Dual Laser process element can be used for the element, leading to an enhanced performance or lifetime.

The performance of carbon foam electrodes produced using this Dual Laser method has been explored by cyclic voltammography (CV), shown in **Figure 15**. Cyclic voltametric plots of the well characterised ferricyanide/ferrocyanide redox reaction were carried out with electrodes prepared using the method described above and with electrodes prepared using the known, conventional method of CO_2 laser irradiation. **Figure 15** shows the resulting CV plots taken at scan rates of 10 mV/s, 25 mV/s, 50 mV/s, 75 mV/s, 100 mV/s and 150 mV/s. Each plot shows data recorded with carbon foam electrodes produced using the present Dual Laser method (light line) and with 3D graphene electrodes produced using the known method of irradiation with CO_2 laser light (dark line). The peak in the negative current direction at around 0.22 V corresponds to the reduction of ferricyanide to ferrocyanide; and the peak in the positive current direction at around 0.28 V corresponds to the oxidation of ferrocyanide to ferricyanide.

Away from the prominent redox peaks, it is qualitatively apparent from these graphs that the CV plots recorded using carbon foam electrodes produced using the Dual Laser method disclosed in this specification have an appearance which is more rectangular than for plots recorded using 3D graphene electrodes produced by the known method. This is most apparent at the top of the voltage range (around 0.6 V) and for higher scan rates (see for example 100 mV/s). This increased rectangular appearance is indicative of an increased capacitive behaviour for electrodes prepared using the present Dual Laser method, reflecting the very high surface area of the twisted or turbostratic multilayer carbon foam produced by this method.

It is also apparent from the CV plots that the voltage separating the oxidation and the reduction peaks is consistently less for measurements performed using carbon foam electrodes produced by the Dual Laser method, compared to those measurements performed using 3D graphene

electrodes produced by a conventional, known method. The peak separation ΔE_p as a function of scan rate for CV measurements taken using a carbon foam electrode produced according to the presently disclosed method is plotted in **Figure 16(a),** and for CV measurements taken using a 3D graphene electrode produced according to a known method in **Figure 16(b).**

This data shows the narrowing of ΔE_p when the electrodes are prepared according to the Dual Laser method. The theoretical peak separation parameter for a reversible system such as the ferricyanide/ferrocyanide reversible redox reaction is 57 mV, but in practice this is sensitive to the effect that the electrode structure has on the electrochemistry. It is apparent that the voltage separation of the oxidation and reduction peaks in the cyclic voltametric plots is close to the theoretical value. This evidences the quality of the electrodes produced by both the known method and the Dual Laser method. Furthermore, the reduced separation demonstrated by the results recorded with carbon foam electrodes produced by the Dual Laser method shows that the porosity of the electrode produced in this way is improved over those produced by the conventional method.

Figure 17 shows a comparison of electrochemical impedance spectroscopy results of a system comprising carbon foam electrodes produced using the Dual Laser method (squares) and of a system comprising 3D graphene electrodes produced using a known method (circles). The Bode plot shows the variation in the phase angle as a function of frequency. The frequency responses of the two systems are clearly different. Specifically, measurements recorded using carbon foam electrodes produced using the Dual Laser method lack the peak in the phase angle signal observed at around 1 kHz for measurements recorded using 3D graphene electrodes produced using the conventional method. The response from the electrodes prepared using the Dual Laser method is indicative of a fast electron transfer response. The difference is a further clear demonstration that carbon foam produced by the Dual Laser method is distinct and distinguishable from 3D graphene produced by the conventional method.

Further details are apparent from **Figure 18A**. The Raman spectrum of carbon foam made by the Dual Laser process is shown in **Figure 18A** has three principal peaks. In particular, the D peak at around 1344 cm^{-1} is characteristic of the presence of lattice defects and the G peak at around 1577 cm^{-1} is characteristic of sp^2 carbon hybridisation, with the presence of distorted six-fold carbon rings. The 2D peak at around 2685 cm^{-1} is characteristic of second order transitions in the 3D graphene and the absence of a doublet structure here indicates a lack of

planar AB stacking which would be found in multilayer 2D graphene or graphite. Fitting the 2D peak with a single Lorentzian peak (having a full width at half maximum of 67 cm^{-1}) centred at 2685 cm^{-1} indicates that there are only one, or a few, carbon-foam-like layers present in the 3D carbon formed with the two methods. Analysis of the D/G peak ratio (0.85) for the Dual Laser process, indicates a higher defect density compared to a conventional laser-induced graphene process (0.67) that uses a single laser step, as shown in **Table 1** below.

Process	D/G	2D/G	D/D'
Dual Laser	**0.85 ± 0.1**	**0.95 ± 0.12**	**3.7 ± 1.3**
Conventional single laser	**0.67 ± 0.13**	**0.75 ± 0.05**	**2.6 ± 0.22**

Table 1

As we noted earlier, Raman analysis of a typical graphene foam reveals the following signatures: absence of a D peak; the 2D peak is higher than the G peak; the peak D: peak G ratio is close to zero. The carbon foam generated in an implementation of the invention shares none of these characteristics; it is highly hydrophilic, with a contact angle below 20°; it lacks the tell-tale Raman signature of graphene: **Figure 18A** shows, for the material made by the Dual Laser process: presence of a D peak; the 2D peak is lower than the G peak; the peak D: peak G ratio is above zero. **Figure 18B** is another Raman analysis of a carbon foam made by the Dual Laser process, again showing the presence of a D peak; the 2D peak is lower than the G peak; the peak D: peak G ratio is above zero. **Figure 18C** is a Raman analysis of carbon nano-onion material, see 'Raman spectroscopy of polyhedral carbon nano-onions'. DOI: 10.1007/s00339-015-9315-9, and the similarities with the Raman for the carbon foam made by the Dual Laser process is apparent. One reasonable interpretation is that the carbon foam made by the Dual Laser process is or includes carbon nano-onion material. See also **Figure 57A** and **Figure 57B** below.

Both the Dual Laser carbon foam and a conventional graphene made by a single laser process show a microporous structure, as shown in the **Figure 19** SEM images. Low magnification images show distinct differences in the surface morphology. The single laser surface shows a smoother, striated surface with rough edges and the carbon foam made by the Dual Laser process shows a rough surface. **Feature R** below revisits this area.

KEY FEATURES

In this section, we outline key **Features A - R** of an implementation of this invention. These features define the production of carbon foam in the Dual Laser manufacturing process described earlier; this process has many advantages over conventional CVD: we can compare the production of 1cm^2 of approximately 50µm thick carbon foam onto a plastic substrate (or indeed many other types of substrates) in **Table 2:**

Process	**Number of Steps**	**Time**	**Temp**	**Pressure**	**Cost**
CVD	6	300 mins	800 C	Vacuum	$50
Dual Laser Process	1	2 mins	20 C	Ambient	sub $1

Table 2

Features A - R define various aspects of a carbon foam manufacturing process that is highly scalable, high yield, highly reproducible and that can be easily adapted to many different applications that all use the same process. For example, the Dual Laser carbon foam is especially well suited to biosensors and electrochemical capacitors (e.g. supercapacitor and pseudo-capacitor applications).

For biosensor applications, the Dual Laser carbon foam has the following advantages over conventional graphene foam: higher electron transfer rates; greater detection sensitivity; larger electrochemically active area; greater reproducibility; lower cost; higher wettability; higher anti-fouling. One implementation of the biosensor is called Gii-Cap and we will describe this in more detail below.

For supercapacitors and other electronics applications, the carbon foam has the following advantages over conventional graphene foam: larger surface area; more porous structure; higher quality; lower sheet resistance; higher wettability; higher anti-fouling. One

implementation of the supercapacitor is called Gii-Cap and we will also describe this in more detail below.

The **Features A - R** are organised into the following four groups:

Group 1: Sub-surface carbon foam

Group 2: Dual laser processing

Group 3: Products

Group 4: Miscellaneous

We can expand on this organisation as follows:

Group 1: Sub-surface carbon foam

Feature A: Carbon foam created in a sub-surface region of a carbon pre-cursor material

Feature B: Carbon foam created in an encapsulated region of a carbon pre-cursor material

Feature C: Carbon foam created in a region of a carbon pre-cursor material, where the region has no substantial gas escape pathways

Feature D: Amorphous, non-graphene material adhering to the substrate

Group 2: Dual laser processing

Feature E: Carbon foam created by laser ablating a sub-surface carbon foam region

Feature F: Non-graphene carbon foam created by laser ablating a sub-surface carbon foam region

Feature G: Dual lasers operating at different frequency bands

Feature H: Electrical contacts positioned in carbon foam created by laser ablating a sub-surface carbon foam region

Feature I: Printing electrical contacts on the polyimide film and then creating the exposed carbon foam

Feature J: Tall tracks made in the carbon foam

Feature K: Applying the first and second lasers in different manufacturing facilities

Group 3: Products

Feature L1: Biosensors

Feature L2: Scalable, low-cost manufacture of a carbon foam biosensor using screen printing technology

Feature L3: Adding functionalised groups to the biosensor at a different manufacturing facility

Feature L4: Adding functionalised groups to the biosensor as part of the biosensor production process

Feature L5: Biosensor manufacture using PPC: Post Printing Conversion

Feature M1: Energy storage device

Feature M2: Screen printing layers of the carbon foam Supercapacitor

Feature M3: Carbon foam supercapacitor: the Common Collector

Feature M4: Carbon foam supercapacitor: the PPC manufacturing process

Feature M5: Carbon foam pseudo-capacitor: a metal oxide variant

Feature M6: Carbon foam supercapacitor: using an ionic-gel in low humidity environment

Feature N1: Electrical conductors

Feature N2: Combined Sensor and Supercapacitor

Feature N3: Combined Supercapacitor and Battery

Feature N4: The Smart Label

Feature N5: Combined Supercapacitor and Antenna

Feature N6: Combined Energy Scavenger + Supercapacitor.

Feature O1: 3D carbon foam structures: Gii-Thru for Gii-Cap

Feature O2: 3D carbon foam structures: Gii-Thru Stackable Gii-Cap/Gii-Cap+

Feature O3: 3D carbon foam structures: Gii-Thru for Gii-Sens: HISLOC

Feature O4 3D carbon foam structures: Gii-Thru for Gii-Sens: HISLOC manufacturing process

Group 4: Miscellaneous

Feature P: Scalable manufacturing of carbon foam: Gii 3

Feature Q: Various other carbon foam applications

Feature R: Non-graphene carbon foam

Turning now to **Group 1**:

Group 1: Sub-surface carbon foam

Feature A: Carbon foam created in a sub-surface region of a carbon pre-cursor material

We have described above, in the prior art section, how earlier approaches to laser induced graphene convert a surface layer of a carbon pre-cursor to 3D graphene. The resultant 3D graphene can however be somewhat brittle, may flake off from the underlying substrate and be generally unsuited to many real-world applications; further, the 3D graphene is typically relatively thin, with a depth of less than 50 μm.

In this specification, we describe an alternative approach in which the surface of the carbon pre-cursor is not converted to graphene at all; instead, it is only a sub-surface region of the carbon pre-cursor 14 that is converted to a carbon foam 16 by a focussed laser beam 12; in one implementation, a focussed IR beam 12 generates a temperature higher than 500°C at the sub-surface or encapsulated region inside a polyimide film 14 over a very short time, between 1 ns and 10 μs (i.e. at a rate of between around 5 x 10^7 °C/s and 2 x 10^{12} °C/s); this brief, intense heating is sufficient to form carbon foam 16 in this sub-surface or encapsulated region. There are no substantial gas escape paths from this sub-surface or encapsulated region 16; constraining the gaseous products to within the sub-surface or encapsulated region beneficially affects the structure of the carbon foam 16 formed in that sub-surface region. Formation of carbon foam 16 solely in a sub-surface region was an unexpected discovery; it was unexpected for several reasons, including a very low absorbance (absorbance of radiation per cm (base 10) of sub 50 or as low as sub 10 of the 1064 nm IR radiation by the polyimide carbon pre-cursor material.

The surface (e.g., the interface between the carbon pre-cursor material perpendicular and facing towards the laser and the gaseous environment surrounding the carbon pre-cursor material) expands under laser irradiation and is converted from the carbon pre-cursor material to a

disorganised, amorphous, non-graphene substance 18. This disorganised, amorphous, non-graphene substance 18 forms a layer that is typically at least 1% of the total thickness of the carbon pre-cursor material; for a 500 μm thick polyimide film, then typically the top 1μm - 10μm is converted to the disorganised, amorphous, non-graphene substance 18; below this upper surface layer, in the body of the carbon pre-cursor material, we have the region that is converted to a carbon foam 16.

The thickness of this carbon foam 16 is controlled by moving the focus of the laser beam progressively through the carbon pre-cursor material; unusually thick carbon foams structures can be made using this process: 50μm - 200 μm (approx.) thick carbon foam tracks have been achieved.

If the laser illuminates a carbon film pre-cursor material, such as a polyimide film that is suspended in space as shown in **Figures 9 - 14B** (i.e., is not mounted on a substrate), then, after irradiation, as we progressively move through the material, we have at the upper surface, i.e., facing the laser, a disorganised, amorphous, non-graphene substance 18; we then have the carbon foam region 16. The laser beam 12 does not generally approach the lower surface of the carbon pre-cursor material, so that the carbon foam region 16 sits over carbon pre-cursor material that has not been converted to a carbon foam. If the laser approaches the lower surface of the carbon pre-cursor material, then the carbon pre-cursor close to and at the lower surface is converted to a disorganised, amorphous, non-graphene substance.

Similarly, if the laser illuminates a carbon pre-cursor film, such as a polyimide (PI) film that is mounted on a substrate, as shown in **Figures 1 - 6**, then we have the same sequence of materials; in addition, the laser will usually approach the lower surface of the carbon pre-cursor material that lies against the substrate: the carbon pre-cursor close to and at the lower surface is then converted to a disorganised, amorphous, non-graphene substance 17. This disorganised, amorphous, non-graphene substance 17 adheres to the substrate 15; since the carbon foam region 16 is bonded to this disorganised, amorphous, non-graphene substance 17, the result is that the carbon foam region 16 is itself not bonded directly to the substrate 15, but is nevertheless securely attached via the intermediary disorganised, amorphous, non-graphene substance 17 to the substrate 15.

This approach enables carbon foam structures that are significantly thicker than is possible with earlier approaches that limited graphene foam formation to a surface region. Further, this approach enables carbon foam structures that adhere more robustly, although not directly, to an underlying substrate. Note that with this approach, carbon foam is not produced at any surface of the carbon pre-cursor material. Instead, carbon foam is produced solely in a sub-surface region inside the carbon pre-cursor material.

We can generalise to:

A method of manufacturing carbon foam material comprising the step of irradiating a sub-surface region of a carbon pre-cursor material, parameters of the laser beam being selected to create a carbon foam in that sub-surface region.

Feature B: **Carbon foam created in an encapsulated region of a carbon pre-cursor material**

In **Feature A** above, we defined the region in which the carbon foam is generated by laser irradiation as a 'sub-surface' region. Another way of describing the region is to qualify it as 'encapsulated'; this captures the 3-dimensional relationship of the carbon foam to its surroundings; the carbon foam 16 is 'encapsulated' by the original carbon precursor material and by the disorganised, amorphous, non-graphene substance 18 generated by laser irradiation at the upper surface of the carbon pre-cursor material 14.

We can generalise to:

A method of manufacturing carbon foam material comprising the step of irradiating an encapsulated region of a carbon pre-cursor material, parameters of the laser beam being selected to create a carbon foam in that encapsulated region.

Feature C: **Carbon foam created in a region of a carbon pre-cursor material, where the region has no substantial gas escape pathways**

We have seen above that a sub-surface or encapsulated region of the carbon pre-cursor is converted to a carbon foam and there are no substantial gas escape paths from this sub-surface or encapsulated region; constraining the gaseous products to within the sub-surface or encapsulated region affects the structure of the carbon foam 16 formed in that region.

We can generalise to:

A method of manufacturing carbon foam material comprising the step of irradiating an encapsulated, sub-surface region of a carbon pre-cursor material, parameters of the laser beam being selected to create a carbon foam in that region and in which no substantial gas escape pathways to a surface of the pre-cursor material are created by the laser beam.

Feature D: Amorphous, non-graphene material adhering to the substrate

We have seen earlier that if the laser 11 illuminates a carbon film 14 that is mounted on a substrate 15, then the laser carbonises the surface of the carbon film adjacent to the substrate 15 to form a disorganised, amorphous, non-graphene substance 17 adjacent to the substrate 15; this disorganised, amorphous, non-graphene substance 17 adheres to the substrate 15; since the internal, or sub-surface or encapsulated carbon foam region 16 is itself bonded to this disorganised, amorphous, non-graphene substance 17, the result is that the carbon foam region 16 is itself not directly attached to the substrate 15, but is nevertheless securely positioned on the substrate 15, via the intermediary disorganised, amorphous, non-graphene substance 17. The carbon foam region 16 is more securely bonded, compared to conventional laser induced graphene, and is less likely to flake off, even where the substrate is flexible, enabling for example biosensor applications where the substrate is often a thin and flexible structure.

We can generalise to:

A method of manufacturing carbon foam material comprising the step of irradiating an internal region of a carbon pre-cursor material, positioned on a substrate, parameters of the laser beam being selected to create a carbon foam in that region and to create a disorganised, amorphous, non-graphene material between the carbon foam region and the substrate; in which that

disorganised, amorphous, non-graphene material is adhering or otherwise attaching directly to the substrate.

Group 2: Dual laser processing

Feature E: Carbon foam created by laser ablating a sub-surface carbon foam region

Previous **Features A - D** have covered the creation of a carbon foam in a sub-surface or encapsulated region of the carbon pre-cursor material. Because the carbon foam is not formed on an exposed surface, and many applications require the carbon foam to be exposed (e.g., to be functionalised for biomedical sensing applications or for a supercapacitor), we can perform an additional step to expose at least some of the sub-surface or encapsulated carbon foam.

We have seen earlier that the laser irradiation using IR laser 11 forms a disorganised, amorphous, non-graphene material 18 over the sub-surface or encapsulated carbon foam 16: We now use a laser, typically a long IR CO_2 laser 20, to ablate or otherwise treat this disorganised, amorphous, non-graphene material 18 and hence expose the underlying carbon foam 16. This second laser 20 is typically de-focused, unlike the initial laser.

As noted earlier, we use a standard 220mm x 180mm polyimide sheet (but other sizes of polyimide sheet can be accommodated); this size that can be accommodated in a standard laser scanning device, of the sort typically used for laser engraving, laser cutting and laser plotting that traces out a path defined by a standard CAD program, and also a standard flatbed screen printing device, and a standard conveyor dryer. Other sizes of polyimide sheet can be accommodated.

We have found that this secondary laser irradiation step alters the morphology and other characteristics of the underlying carbon foam in surprising and favourable ways, to generate a twisted or turbostratic multilayer carbon foam not previously observed. Varying the CO2 laser 20 parameters can alter the carbon foam material properties, enabling carbon foam to be produced with properties that are optimised for different applications.

This newly exposed carbon foam includes one or more of the following properties:

- a readily controlled thickness or depth
- greater flexibility compared to the highly brittle graphene made using conventional laser processes.
- strong adhesion to any underlying flexible substrate
- high porosity
- high electrical conductivity
- increased capacitance or charge storage
- rapid absorption of organic solvents and water-based solutions
- higher hydrophilicity
- high EMI shielding
- enhanced electrode quality
- high wettability
- anti-fouling

Note that it is possible to alter one or more of these properties, as well as the size and extent of defects, and the size (including the relative size) of the Raman D and 2D peaks, by varying the laser parameters of either or both of the laser used in the Dual Laser process. In this way, it is possible to produce a carbon foam with properties tuned or especially suitable for different applications. It was surprising that the operation of the second ablation laser could enable the creation of a useable, exposed carbon foam region, especially one with properties that could be adjusted by varying the parameters of the first and/or second lasers.

We can generalise to:

A method of manufacturing carbon foam material comprising the steps of (a) a laser beam irradiating an encapsulated or sub-surface region of a carbon pre-cursor material, to create a carbon foam in that encapsulated or sub-surface region and a disorganised, amorphous non-graphene substance above the carbon foam, and then (b) laser ablation or treatment to remove the disorganised, amorphous non-graphene substance and to expose at least some of the carbon foam.

Feature F: Carbon foam created by laser ablating a sub-surface carbon foam region

In the preceding **Feature E**, we described the formation of carbon foam 16 in an encapsulated or sub-surface region of the carbon pre-cursor by irradiating that region with a laser 11 (e.g. an IR laser); that irradiation causes the overlying (in the direction of the laser) carbon pre-cursor material 14 to expand into a disorganised, amorphous, non-graphene substance 18; we then expose or reveal that carbon foam 16 by ablating the overlying disorganised, amorphous, non-graphene substance 18 with a second laser 20, e.g. a CO2 laser. This second irradiation step not only ablates the overlying disorganised, amorphous non-graphene substance 18 and hence exposes the underlying carbon foam 16, but also gives this underlying carbon foam an unexpected and unusual surface morphology 21 with very desirable characteristics; this resultant carbon foam may be a twisted or turbostratic, multilayer carbon foam.

However, because this foam may have characteristics (such as extensive defects, appearance, wettability and a Raman spectrum (See **Feature R** below) which are not associated with a graphene foam, in this **Feature F**, we explicitly describe this foam as a 'non-graphene carbon foam'. The term 'non-graphene carbon foam' hence (unlike the term 'carbon foam') explicitly excludes graphene foams, including twisted or turbostratic multilayer graphene foams, but extends to cover any other 3D carbon material foam.

We can generalise to:

A method of manufacturing non-graphene carbon foam comprising the steps of
(a) a laser beam irradiating an encapsulated or sub-surface region of a carbon pre-cursor material to create a carbon foam in that encapsulated or sub-surface region in the carbon pre-cursor material, and a disorganised, amorphous non-graphene substance above the carbon foam and then
(b) laser ablation or treatment to remove the disorganised, amorphous non-graphene substance and expose at least some of the underlying carbon foam and transform at least some of that underlying carbon foam into a non-graphene carbon foam.

Feature G: Dual lasers at different bands

We have seen in the preceding **Features E** and **F** that we may use two separate laser irradiation steps. These are usually carried out using two separate lasers: the first step, that creates the sub-

surface or encapsulated carbon foam, is typically done with a focused IR laser 11; and the second step involves laser irradiation at a longer wavelength with a de-focused CO2 laser 20, but other wavelengths (e.g., UV and visible) may also be used.

The second laser 20 ablates the material 18 sitting between the carbon foam 16 and the surface (e.g., a disorganised, amorphous non-graphene material) and exposes the underlying carbon foam 16. The exposed carbon foam 16 may also be altered (e.g., in its surface morphology 21) by the second laser, i.e. the term 'exposes' should be construed broadly to include not just revealing at least some of the pre-existing carbon foam, but also transforming or altering at least some of the pre-existing carbon foam into a 3D carbon material foam with characteristics that differ from those of the pre-existing graphene foam.

We can generalise to:

A method of manufacturing a carbon foam material comprising the steps of
(a) using a laser beam operating at a first band to irradiate an encapsulated or sub-surface region of a carbon pre-cursor material below a surface of the material, to create carbon foam in that encapsulated or sub-surface region, and then
(b) using a laser beam operating at a second band to remove or ablate material sitting above the carbon foam, to expose at least some of the carbon foam.

Feature H: Electrical contacts positioned in carbon foam created by laser ablating a sub-surface carbon foam region

We have seen earlier how we create a carbon foam, which may be a twisted or turbostratic, multilayer carbon foam: because this material has exceptional electrical properties (e.g., conductivity; capacitance), we can attach or locate one or more electrical contacts (including also electrical items such as flexible electronics, microprocessors, antennas, IoT devices, electrical interfaces) into the carbon foam. For printed tracks (e.g. screen printed silver tracks), these are screen printed onto the polyimide film (or other suitable substrate) and over and into the pre-existing 3D carbon material foam, so that the tracks make good electrical contact with the foam, and any structures formed on the foam, such as a functionalisation layer (for example,

see **Feature L** below where we describe how the carbon foam is functionalised to form a biosensor with an analyte-specific receptor layer).

We can generalise to:

A method of manufacturing carbon foam material comprising the steps of:

(a) using a laser beam operating at a first band to irradiate an encapsulated or sub-surface region of a carbon pre-cursor material below a surface of the material, to create carbon foam in that encapsulated or sub-surface region, and then

(b) using a laser beam operating at a second band to remove or ablate material sitting above the carbon foam, to expose at least some of the carbon foam; and

(c) attaching, printing or locating one or more electrical contacts into the carbon foam.

Feature I: Printing electrical contacts on the polyimide film and then creating the exposed carbon foam

In **Feature H**, we have seen that once the Dual Laser process is completed, then electrical contacts or circuits are added to contact the pre-existing carbon foam – e.g. simple silver electrical contacts can be screen printed on to the carbon foam. In this **Feature I**, we describe starting the process by first screen printing the electrical contacts on to the polyimide film, and then finishing the process by creating the exposed carbon foam using the second, laser ablation step of the Dual Laser process. This has some advantages, because the screen printing process can disturb or disrupt the carbon foam. This is a process we call 'PPC', an acronym for Post Printing Conversion, in which the screen printing steps are done before the Dual Laser process to create the carbon foam. In **Feature L5**, below we describe a biosensor manufactured using the PPC process.

So for screen printed tracks (e.g. screen printed silver tracks), these are screen printed onto the polyimide film (or other suitable substrate) in such a way that the carbon foam is subsequently formed around one end of the printed tracks, providing a contact area with a large surface and hence very good electrical connectivity. As with the alternative process described in **Feature H** above, the printed tracks also make good electrical contact with any structures formed on the foam, such as a functionalisation layer (for example, see **Feature L** below where we

describe how the carbon foam is functionalised to form a biosensor with an analyte-specific receptor layer).

An alternative sequence involves using the first laser beam to create the sub-surface carbon foam, then screen printing the electrical contacts, and then using the second laser beam to create the carbon foam in a way that makes good electrical contact with the electrical contacts.

We can generalise to:

A method of manufacturing carbon foam material comprising the steps of:

(a) screen printing electrical contacts onto or into a carbon pre-cursor material;

(b) using a laser beam operating at a first band to irradiate an encapsulated or sub-surface region of a carbon pre-cursor material below a surface of the material, to create carbon foam in that encapsulated or sub-surface region, and where steps (a) and (b) can be performed in the sequence (a) then (b) or (b) then (a); and

(c) using a laser beam operating at a second band to remove or ablate material sitting above the carbon foam, to expose at least some of the carbon foam to which the electrical contacts are connected.

Feature J: Tall tracks made in the carbon foam

We have seen earlier that the thickness of the sub-surface or encapsulated carbon foam region can far exceed the thickness of conventional graphene foams that are restricted to a surface layer: the laser focus of the first laser beam can be progressively moved down through the carbon pre-cursor material to create a deep or thick layer of sub-surface or encapsulated carbon foam. We then deploy the second laser irradiation step, ablating the material sitting between the carbon foam and the surface of the carbon pre-cursor material, resulting in an exposed region of carbon foam. The thickness or depth of this now-exposed carbon foam region can be at least 50μm; carbon foam of 300 μm thickness has been produced. Increased thickness is beneficial because it can result in better electrical conductivity, greater capacitance, and greater mechanical integrity.

We can generalise to:

A method of manufacturing carbon foam material comprising the steps:

(a) using a laser beam operating at a first band to irradiate an encapsulated or sub-surface region of a carbon pre-cursor material below a surface of the material, to create carbon foam in that encapsulated or sub-surface region, and then

(b) using a laser beam operating at a second band to remove or ablate material sitting above the carbon foam, to expose at least some of the carbon foam;

and where the carbon foam is at least 50μm in thickness or depth.

Feature K: Applying the first and second lasers in different manufacturing facilities

The specific properties or structure of the carbon foam that results from the second laser may be considered to be sensitive information because they define features of the final product; it may well be desirable for the first laser beam process to be carried out by a supplier of the carbon foam at that supplier's manufacturing facility, who then supplies that carbon foam to a customer, who in turn carries out the final stage, using the second laser beam, at their own manufacturing facility As we noted earlier, by varying the parameters of the first and also the second laser, it is possible to alter the carbon foam material properties, enabling carbon foam to be produced with properties that are optimised for different applications. Typical parameters that can be altered or tuned in this way include: intensity, wavelength, pulse frequency, pulse duration, pulse profile, scanning speed, focal distance, heat generated at the sub-surface or encapsulated region.

By splitting the manufacturing process in this way, the supplier is insulated from knowledge of the specific manufacturing processes used by a customer as part of the second laser, ablation process (e.g. how they vary the parameters of the second laser beam to give the exposed carbon foam the properties they require); the customer can keep the details of how they produce finished products confidential.

So the manufacturing process is a three-stage process involving the steps: (a) the first laser beam irradiating a sub-surface region of a carbon pre-cursor material at a manufacturing site to produce unfinished carbon foam product; (b) the unfinished carbon foam product being

transferred to a customer-controlled manufacturing site; and (c) the laser ablation or treatment taking place at the customer-controlled manufacturing site.

In addition, this approach enables large scale manufacturing (e.g. see **Feature P**) of the carbon foam produced by just the first laser process, reducing the cost of this material, which can be used across a number of different applications and customers. The more specialised products generated using the second laser beam may well be manufactured at much lower quantities than the carbon foam produced by just the first laser process. So this approach enables more efficient and lower cost manufacturing of the base material, i.e. the carbon foam produced by just the first laser process.

We can generalise to:

A method of manufacturing a device comprising the steps:

(a) using a laser beam operating at a first band to irradiate an encapsulated or sub-surface region of a carbon pre-cursor material below a surface of the material, to create carbon foam in that encapsulated or sub-surface region, and then

(b) using a laser beam operating at a second band to remove or ablate material sitting above the carbon foam, to expose at least some of the carbon foam;

in which step (a) is performed at one manufacturing facility and step (b) is performed at a different facility.

For **Features A - K**, the following optional features are especially relevant. Note that any one or more of the following optional features may each be combined with any one or more other, compatible optional features and with any one or more of **Features A – K:**

We will cover the following areas:

- the manufacturing processes
- the first laser beam parameters and control scheme
- attributes of the sub-surface or encapsulated region

- the carbon pre-cursor material
- the substrate supporting the carbon pre-cursor material
- the carbonisation at the surface that the laser beam is incident on
- the ablation laser beam or second laser beam
- the carbon foam

Note that any one or more of the following optional features may each be combined with any one or more other, compatible optional features and with any one or more of the other 'Features' listed in this specification (e.g., **Features A – R**).

The laser-based manufacturing process described above has many advantages over a conventional CVD process; we can list these as the following optional features:

- is a room temperature process.
- is an ambient pressure process.
- can be performed on a plastic substrate (compatible with any manufacturing process, not just silicon chip fabrication).
- can be done without a catalyst.
- takes approximately 2 minutes or less to manufacture 1cm^2 of approximately 50μm thick carbon foam onto a plastic substrate.
- enables a 3D carbon foam to be created on a flexible substrate
- requires no graphene or graphene oxide precursor.
- creates carbon foam material solely in the encapsulated or sub-surface region of the carbon pre-cursor material and not at any surface of the carbon pre-cursor material.
- uses a combination of industry standard, low cost and scalable (i) screen printing technology and (ii) computer-controlled laser scanning technology.
- can be adapted for high-speed, high volume reel-to-reel or reel-to-sheet production.

The first laser beam parameters and control scheme are important to the production of carbon foam; we define the relevant optional features here:

- parameters of the laser beam that irradiates the sub-surface or encapsulated region include one or more of: intensity, wavelength, pulse frequency, pulse duration, pulse

profile, scanning speed, focal distance, heat generated at the sub-surface or encapsulated region.

- varying the laser parameters alters the carbon foam material properties, enabling carbon foam to be produced with properties that are optimised for different applications.
- varying the laser parameters alters one or more of the following carbon foam material properties or parameters: size of defects, distribution of defects, extent of defects, type of defects, of the Raman D and 2D peaks, relative size of the Raman D and 2D peaks, thickness or depth, flexibility, adhesion, porosity, electrical conductivity, capacitance, absorption of organic solvents and water-based solutions, hydrophilicity, EMI shielding, electrode quality, wettability, contact angle, anti-fouling.
- laser beam generates a temperature higher than 500°C in the sub-surface or encapsulated region to form carbon foam.
- laser beam generates a temperature of over approximately 500°C in the sub-surface or encapsulated region to form carbon foam.
- laser pulse duration is between approximately 1 ns and 10 μs, giving a heating rate of between around 5 x 10^7 °C/s and 2 x 10^{12} °C/s.
- laser power is within a typical working range of 8 - 20 watts, with 12W optimum.
- laser focal distance is within a typical working range of 50mm - 400mm.
- laser pulse frequency is between approximately 50 kHz and 500 kHz.
- laser pulse frequency is between approximately 1 kHz and 2 MHz.
- laser wavelength is between approximately 0.7 μm – 2.5 μm.
- laser is scanned at between approximately 9cm/s and 40cm/s.
- parameters of the laser beam include focus parameters.
- parameters of the laser beam include diffraction parameters.
- parameters of the laser beam include interference pattern parameters.
- focus of the laser beam moves through the depth of the carbon pre-cursor material to generate carbon foam in the sub-surface or encapsulated region of the carbon pre-cursor that the focus passes through.
- focus of the laser beam moves at least approximately 50 μm through the depth of the carbon pre-cursor material to generate carbon foam in the sub-surface or encapsulated region of the carbon pre-cursor of at least 50 μm thickness .

- focus of the laser beam moves at least approximately 100 μm through the depth of the carbon pre-cursor material to generate carbon foam in the sub-surface or encapsulated region of the carbon pre-cursor of at least 100 μm thickness.
- laser beam scans (e.g., raster scans) or moves laterally across the carbon pre-cursor material to form a desired pattern.
- laser beam scans or moves laterally across the carbon pre-cursor material to form a desired pattern that includes non-overlapping regions or lines.
- laser beam is repeatedly scanned (e.g., raster scanned) or moved laterally across the carbon pre-cursor material with a focus or intensity maximum arranged to multiple different depths within the carbon pre-cursor material until carbon foam of the required pattern and depth has been created.
- laser beam is scanned at a scan rate of between 1.7 mm/s and 3550 m/s, or more typically between 35 mm/s and 350 mm/s and the scanning may be such that the number of pulses per inch (PPI) is between 100 and 10000 (relevant to the production of individual approximately polyimide sheets of size 220mm x 180mm).
- laser beam has a wavelength with substantially no absorbance by the carbon pre-cursor material.
- laser beam has a wavelength with very low absorbance by the carbon pre-cursor material, where the radiation absorbance per cm (base 10) is below 50, or below 20 or below 10.
- laser beam is an IR laser.
- laser beam is an IR laser with wavelength of between approximately 0.7 μm – 2.5 μm.
- laser beam is an IR laser with wavelength of between approximately 0.75 μm – 1.40 μm.

The attributes of the sub-surface or encapsulated region in which carbon foam is created can be defined by the following optional features:

- unlike conventional graphene foams, the sub-surface or encapsulated region can be over approximately 50 μm in thickness.
- a desired depth of the sub-surface or encapsulated region in the carbon pre-cursor material is achieved by moving the focus of the first laser beam through that depth.

- the sub-surface or encapsulated region can be at different depths below the surface of the carbon pre-cursor material facing the incident laser; the exact depth at which the sub-surface or encapsulated region is a function of various factors, such as laser intensity, the choice of carbon pre-cursor material used etc. For example, the sub-surface or encapsulated region can be at least approximately 10 μm, 20 μm, 30 μm, 40 μm, 50 μm or more below the surface of the carbon pre-cursor material.
- the sub-surface or encapsulated region can have a thickness of between approximately 10 μm and 200 μm.
- the sub-surface or encapsulated region is at a distance below the surface of the carbon pre-cursor material that is a function of various factors, such as laser intensity, other laser parameters, the choice of carbon pre-cursor material used etc. For example, the top of the sub-surface or encapsulated region can be below the surface by at least 1%, 10%, 20%, 30%, 40% of the total thickness of the carbon pre-cursor material.
- the sub-surface or encapsulated region is a volume of space centred at the mid-point of the minimum cross-section of the first laser beam and the volume is within 500 or 100 microns, or 1 micron of this mid-point.

The carbon pre-cursor material can be defined by the following optional features:

- the carbon pre-cursor material is made substantially of thermo-setting material.
- the carbon pre-cursor material is made substantially of non-thermo-plastic material.
- the carbon pre-cursor material is a thermo-setting film.
- the thermo-setting film is a polyimide film.
- carbon pre-cursor is a polyimide film.
- carbon pre-cursor is a polyimide polyimide film, the wavelength of the first laser is within the range of 0.7 μm to 2.5 μm.
- carbon pre-cursor is at least 50% carbon by mass, or at least 75% carbon by mass, or at least 90% carbon by mass.
- carbon pre-cursor is a film or sheet.
- the carbon pre-cursor material is flexible.
- the carbon pre-cursor material is a printed layer, such as a screen-printed layer.
- the carbon pre-cursor material has a thickness greater than 5 μm, or between 5 μm and 120 μm, or greater than 120 μm.

- the carbon pre-cursor material is substantially planar or flat and is oriented perpendicular to the first laser beam.
- the carbon pre-cursor material is homogeneous.
- the carbon pre-cursor material is heterogenous and comprises several different materials.
- carbon pre-cursor is supported on a substrate that is not made of a carbon pre-cursor.
- the absorption coefficient of the carbon pre-cursor material at the first laser beam wavelength is low.
- the absorption coefficient of the carbon pre-cursor material for the first laser beam is below 50 cm^{-1}, or below 20 cm^{-1}, or below 10 cm^{-1}
- the absorption coefficient of the carbon pre-cursor material for the second or ablation laser beam (see Group 3 Features below) is below 300 cm^{-1}
- the absorption coefficient of the carbon pre-cursor material for the second or ablation laser beam is 300±50 cm^{-1}
- the carbon pre-cursor material has a thermal conductivity of less than 1.0 W/mK (using a method according to ASTM D5470).
- the carbon pre-cursor material has a thermal conductivity of less than 0.5 W/mK (using a method according to ASTM D5470).
- carbon pre-cursor material is mounted on a substrate that is substantially optically transparent at the wavelength or wavelengths of the first and/or second laser beams.
- the carbon pre-cursor material carbon source comprises or is formed from one or more polymers.
- the carbon pre-cursor material comprises one or more of the following materials: polyimides (for example, poly(4,4'-oxydiphenylene-pyromellitimide), otherwise known as polyimide), polyetherimides (PEI), poly(methyl methacrylate) (PMMA) (e.g. spray-coated PMMA), polyurethanes (PU), polyesters, vinyl polymers, carbonized polymers, photoresist polymers, alkyds, urea-formaldehyde.
- the carbon pre-cursor comprises one or more of the following materials: poly(amic acids) (for example an aryl-containing poly (amic acid)) (for example poly(pyromellitic dianhydride-*co*-4,4'-oxydianiline), amic acid - otherwise known as polyamic acid); dianhydrides (for example aryl dianhydrides) (for example pyromellitic dianhydride); derivatives of said poly(amic acids); derivatives of said dianhydrides (e.g., derivates of pyromellitic dianhydride).

- the carbon pre-cursor comprises one or more of the following materials: aromatic materials (e.g., aromatic polymers); heteroaromatic materials (e.g., heteroaromatic polymers); polymers containing aromatic moieties; cyclic materials (e.g., polymers containing cyclic moieties); heterocyclic materials (e.g., polymers containing heterocyclic moieties); heteroaromatic materials (e.g., polymers containing heteroaromatic moieties).
- the carbon pre-cursor comprises material: containing one or more of aromatic bonds, or heteroaromatic bonds or hetero bonds (e.g., imide bonds).

A substrate can be thought of as a material that presents a surface on which the carbon pre-cursor is positioned; the specific materials, thickness and properties of the substrate are determined by the application: for example, for some sensors, the substrate could be a thin flexible plastic membrane; for other applications, the substrate could be a rigid polyimide board on which electronic circuitry can be mounted. The IR laser can irradiate the carbon source directly; alternatively, radiation from the IR laser may first pass through a substrate before reaching the carbon source, in which case there are two alternative scenarios: first, the substrate is substantially transparent to the IR radiation and the mechanism of carbon foam formation is as described above. But in a second scenario, the substrate is substantially non-transparent to the IR radiation: then, rapid thermal transfer from the substrate into the carbon pre-cursor material first produces a disorganised, amorphous non-graphene layer at the interface layer with the substrate, and carbon foam is then formed in a sub-surface or encapsulated region inside the carbon pre-cursor material.

The substrate on which the carbon pre-cursor material may be positioned and supported can be defined by the following optional features:

- the substrate is a plastic body, film, or foil.
- the substrate is flexible.
- the substrate is a polyimide circuit board.
- the substrate has very low absorbance of the first laser beam.
- the substrate is substantially optically transparent at the wavelength or wavelengths of the first laser beam.

- the substrate has a high absorbance of the first laser beam, absorbing greater than 60% of the first laser beam
- the substrate has a high absorbance of the first laser beam, absorbing greater than 60% of the first laser beam and has a thermal conductivity of at least 10 W/mK.
- the surface of the carbon pre-cursor material is converted to a disorganised, amorphous, non-graphene substance by the laser beam and that disorganised, amorphous, non-graphene substance adheres or bonds to the substrate and hence indirectly attaches the 3D carbon material foam to the substrate.
- the substrate is formed from one or more of the following: silicon (Si), silicon dioxide (SiO2), gallium nitride (GaN), gallium arsenide (GaAs), zinc oxide (ZnO).
- the substrate is silicon wafer.
- the substrate is a silicon dioxide wafer.
- the substrate is a wafer comprising both silicon and silicon dioxide.
- the substrate is a carbon source.
- the substrate is not a carbon source, e.g. is a metal, dielectric material, a screen-printed dielectric material.
- the carbon pre-cursor is positioned 'above' the substrate (e.g. the carbon pre-cursor is positioned closer to the laser sources than the substrate).
- the carbon pre-cursor is positioned 'below' the substrate (e.g. the carbon pre-cursor is positioned further from the laser sources than the substrate).

The carbonisation at the surface that the laser beam is incident on can be defined by the following optional features:

- the surface of the carbon pre-cursor material is converted to a disorganised, amorphous, non-graphene substance by the first laser beam.
- the disorganised, amorphous, non-graphene substance occupies a thickness below the surface of the adjacent carbon pre-cursor material that is approximately 1%, or less than approximately 1%, or less than approximately 5%, or less than approximately 10%, of the total thickness of the carbon pre-cursor material.
- the disorganised, amorphous, non-graphene substance extends to a distance below the surface of the carbon pre-cursor material that is at least 10 μm.

- the disorganised, amorphous, non-graphene substance extends from the outer surface into the body of the carbon pre-cursor material to a depth of 10 μm or less, or to a depth of 20 μm or less, or to a depth of 30 μm or less, or to a depth of 40 μm or less, or to a depth of 50 μm or less, or to a depth of 100 μm or less.

The ablation laser beam or second laser beam can be defined by the following optional features:

- parameters of the laser beam include one or more of: intensity, wavelength, pulse duration, pulse profile, scanning speed, heat generated at the sub-surface or encapsulated region.
- varying the laser parameters alters the carbon foam material properties, enabling carbon foam to be produced with properties that are optimised for different applications.
- varying the laser parameters alters one or more of the following carbon foam material properties or parameters: type of carbon nanostructures present (e.g. carbon nano-onion etc), size of defects, distribution of defects, extent of defects, type of defects, of the Raman D and 2D peaks, relative size of the Raman D and 2D peaks, thickness or depth, flexibility, adhesion, porosity, electrical conductivity, capacitance, absorption of organic solvents and water-based solutions, hydrophilicity, EMI shielding, electrode quality, wettability, contact angle, anti-fouling.
- laser beam that ablates the amorphous, non-graphene substance that is formed above the encapsulated or sub-surface region in the carbon pre-cursor (the 'second laser beam') is a CO2 laser.
- the second laser beam alters the carbon foam as part of the process of exposing it.
- the second laser beam alters the morphology of the carbon foam as part of the process of exposing it.
- The second laser beam is automatically controlled to be scanned (e.g., raster scanned) across the same regions, and/or overlapping regions and/or non-overlapping regions.
- wavelength of the laser beam that ablates the amorphous, non-graphene substance is between 8 μm -15 μm.
- the second laser beam is a long IR laser, or a UV laser or a visible light laser.
- the second laser beam has a pulse frequency of between 50 kHz and 500 kHz and a scan speed of between 9cm/s and 40cm/s.

- the absorption coefficient of the carbon pre-cursor material is above 100 cm^{-1} for the second laser beam, or above 200 cm^{-1} for the second laser beam.
- the absorption coefficient of the carbon pre-cursor material is 300±50 cm^{-1} for the second laser beam.
- laser power is within a typical working range of 8 - 20 watts, with 12W optimum.
- laser focal distance is within a typical working range of 50mm - 400mm.
- the second laser beam is scanned in a pattern that includes non-overlapping regions or lines.
- the second laser beam is scanned in a pattern that matches the scan pattern of the first laser beam.
- the second laser beam is de-focussed.
- the manufacturing process is a three-stage process involving the steps: (a) the first laser beam irradiating a sub-surface region of a carbon pre-cursor material at a manufacturing site to produce unfinished carbon foam product; (b) the unfinished carbon foam product being transferred to a customer-controlled manufacturing site; and (c) the laser ablation or treatment taking place at the customer-controlled manufacturing site.

The carbon foam can be defined by the following optional features:

- the carbon foam is at least 50 μm in thickness.
- the carbon foam is between 50 μm to 300 μm in thickness.
- the carbon foam is or includes a twisted or turbostratic multilayer foam.
- the carbon foam is or includes a carbon foam with a spatial distribution of defects leading to high electrochemical reactivity.
- the carbon foam is or includes a carbon foam with vacancy position basal plane defects leading to high electrochemical reactivity.
- the carbon foam has a Carbon: Oxygen ratio of between 25: 1 and 50:1.
- the carbon foam has a fast electron transfer constant.
- the carbon foam has one or more of the following properties
    - a readily controlled thickness or depth
    - greater flexibility compared to the highly brittle graphene made using conventional laser processes.
    - strong adhesion to an underlying flexible substrate

- high porosity
- high electrical conductivity
- increased capacitance or charge storage
- rapid absorption of organic solvents and water-based solutions
- higher hydrophilicity
- high EMI shielding
- enhanced electrode quality
- a contact angle of approximately 20° or less

- the properties of the carbon foam are selected by choosing specific laser parameters to generate carbon foam material with one or more of the following desired properties or parameters: size of defects, distribution of defects, extent of defects, type of defects, of the Raman D and 2D peaks, relative size of the Raman D and 2D peaks, thickness or depth, flexibility, adhesion, porosity, electrical conductivity, capacitance, absorption of organic solvents and water-based solutions, hydrophilicity, EMI shielding, electrode quality, wettability, contact angle, anti-fouling.

Group 3: Products

Feature L1: Biosensor

The carbon foam made by the Dual Laser method described above, has broad applications across many different types of sensors. For simplicity, we will use the phrase 'carbon foam' in this **Feature L** to refer to any carbon foam or 3D carbon material foam made by the methods described in this specification. **Appendix 1** includes more details on this area, describing in more detail a biosensor that includes carbon foam that has been functionalised by adding a receptor that is specific to a target or analyte, and a linker that enables the receptor to attach indirectly to the carbon foam; (some receptors cannot be attached directly to the carbon foam because of poor stability when in contact with surfaces; instead a linker has to be used as an intermediary between the carbon foam and the receptor. During manufacture, the linker is first added to the carbon foam, and then the receptor is added to the linker.)

For biosensor applications, the functionalised carbon foam has the following advantages over conventional graphene foam: higher electron transfer rates; greater detection sensitivity; larger

electrochemically active area; greater reproducibility; lower cost; enhanced wettability, with a contact angle of approximately 20° or less.

At a high level, functionalised carbon foam is useful in a sensor because of its ability to generate a detectable change in state; its high sensitivity is a function of its large surface area. It can be used to detect specific chemicals, specific gases, mechanical stress, and temperature, as well as other variables. We will look briefly at each category.

First, chemical sensors: chemical detection systems rely on detecting the electrical response of the carbon foam when in the presence of the target chemical; many different detection principles can be used, such as changes in capacitance, electrical resistance, voltammetry, redox potentials, and charge transfer resistance.

For example, when a specific analyte or target binds to the carbon foam, that binding can be detected because it modifies the surface of the carbon foam. Biomolecules are added to the carbon foam, such as specific antibodies or aptamers (aptamers are short, single-stranded DNA or RNA molecules that can selectively bind to a specific target, including proteins, peptides, carbohydrates, small molecules, toxins, and live cells). When the target is present and binds to the aptamer, then the morphology of the aptamer is altered (e.g., reducing the surface area) and the capacitance of the combined carbon foam and aptamer system measurably reduces.

Highly sensitive and highly selective sensors can be built using this principle; since there is a quantitative reduction in a measurable variable (e.g. capacitance), it is possible to build a LOC (laboratory on chip) that includes not just the carbon foam and aptamer biosensor, but also a power source on the LOC, such as a supercapacitor or other energy store using the carbon foam as its electrodes, and circuitry to measure the variable, compute a biosensor output and to display on a screen of the LOC that output (e.g. presence or absence of the target; concentration of the target); **Feature O3** (Gii-Thru for Gii-Sens: HISLOC) describes this further.

Carbon foam sensors can also measure the redox potential of the target; for example, a current peak could be detected where the oxidation of the target chemical is catalysed by specific catalysts added to the carbon foam; quantitative measurement of the target concentration is possible since the current is typically a function of concentration of the target chemical.

Other techniques that have been applied to conventional graphene sensors, such as thermal conductivity measurement to detect specific chemicals, electrical resistance measurement to infer temperature, physical morphing, or transformation in the presence of specific chemicals, piezoresistive deformation to detect motion, can all be applied to carbon foam sensors made by the Dual Laser method described above.

An important application that makes use of the very large electrochemically active area and fast electron transfer rates of the carbon foam produced by the Dual Laser method is an electroanalytical sensing electrode (an implementation is called 'Gii-Sens') that is optimised for biosensing.

It can, for example, be used in point of care diagnostic devices; the sensing electrode has very high sensitivity, reliability, purity, wettability and conductivity.

Figure 20A is a perspective view of a biosensor called Gii-Sens. The assembly is made up of a polyimide substrate 201; a working electrode 202 made of Gii carbon foam; a counter electrode 203, made of Gii carbon foam; a reference electrode 204, made of a screen printed silver-silver chloride; three screen printed silver connection tracks 205; and a screen printed dielectric layer 206.

Figures 20B - 20D show the four main manufacturing stages. **Figure 20B** shows Step 1, in which the Dual Laser process creates the Gii carbon foam working electrode 202 (area is 18.94 mm^2) and the counter electrode 203 (area is 20.84 mm^2) using the polyimide substrate 201 as the pre-cursor.

Figure 20C shows Step 2, in which the silver-silver chloride reference electrode 204 (area is 8.99 mm^2) is screen printed onto the polyimide substrate 201.

Figure 20D shows Step 3, in which silver connection tracks 205 are screen printed onto the polyimide substrate 201; these overlap carbon foam electrodes at electrical contact region 207. The silver track area is 1x 18.85mm^2 and for three, it is 3x 56.55mm^2. The area of overlap with an underlying carbon foam electrode is 1x 2.21mm^2 and for three, it is 3x 6.63mm^2.

Figure 20E shows Step 4, in which dielectric layer 206 is screen printed over the carbon foam electrodes 202, 203, 204 and the silver connection tracks 205. The active areas for the electrodes are as follows: working electrode 202: 12.64mm^2; counter electrode 203: 14.18mm^2; reference electrode 204: 2.59mm^2. The exposed area of the silver connection tracks 205 are 1x 7.15mm^2 and 2x 21.45mm^2.

Figure 20F shows a single polyimide sheet on which an array of 100 carbon foam working electrodes and counter electrodes have been created using the Step 1 Dual Laser process described above. The sheet is a standard type of polyimide sheet, 220mm x 180mm, to enable handling with standard screen printing and laser scanning equipment; it can be A5 size or any other suitable size.

Figure 20G and **20H** shows the final form of the sheet, after Step 4 has been completed. The 100 individual units can be cut and assembled into 100 finished Gii-Sens biosensors.

One specific use case for Gii-Sens sensing electrodes is in a reversible polymer displacement sensor mechanism for electrochemical glucose monitoring. Graphene sensors for this use case have been proposed: see 'Polymer indicator displacement assay: electrochemical glucose monitoring based on boronic acid receptors and graphene foam competitively binding with poly-nordihydroguaiaretic acid' Wikeley et al. DOI: 10.1039/d1an01991k. This paper describes a pyrene-derivatised boronic acid chemo-receptor for glucose is adsorbed onto a graphene foam electrode. Spontaneous oxidative polymerisation of nordihydroguaiaretic acid (NHG) onto the graphene foam electrode leads to a redox active film (poly-NHG) covalently attached to the boronic acid receptors. Oxidation of poly-NHG frees the boronic acid receptors to interact with glucose from the solution phase, which is detected due to competitive binding when reduced poly-NHG re-binds to the boronic acid functional groups. The sensor shows the anticipated boronic acid selectivity of fructose glucose. The ratio of charges under the voltammetric peaks for poly-NHG unbound and bound is employed for glucose sensing with an approximately linear analytical range from 1 to 50 mM glucose in aqueous pH 7 buffer.

The Gii-Sens sensing electrode implementation has many advantages over current sensing electrodes, such as graphene sensors:

- lowers limits of detection using amplification-free, enzyme-free, label-free electrochemical biosensing

- enhanced reproducibility
- optimises useful dynamic range
- minimises background noise
- reduces protocol times and operations
- scalable for low-cost manufacturing
- high sensitivity and selectivity
- gives quantitative digital result
- can be printed into specific patterns, e.g., interdigitated patterns, enabling miniaturised, integrated devices
- can translate existing biorecognition and test formats (e.g., ELISA, PCR, RT-PCR) to electrochemical microfluidics POC without compromising performance quality
- impedance based measurements can be made with very high sensitivity, reliability, and very low background signal interference.
- replaces costly large scale laboratory testing and low sensitivity lateral flow testing
- can be implemented in microfluidic assays (single or multi-target) and Lab-on-a-chip (LOC) devices
- can be used in any sensor application where the user aims to immobilise (bio)molecules of interest (e.g., carboxyl/n-hydroxysuccinimide moieties can be added to the sensor surface to provide a platform for subsequent immobilisation conjugation chemistry reactions)
- can be used across a wide range of diagnostics: POC (point of care) human and animal health, food safety, in-situ environmental health and safety, agricultural health and safety -all with enhanced sensitivity, selectivity, and reproducibility for biosensing because of its pure and high specific surface area.
- enhanced wettability (e.g. contact angle below approximately 20°)
- enhanced anti-fouling properties

We can generalise to:

A method of manufacturing a biosensor including a sensing electrode comprising carbon foam made, at least in part, by the method defined in any of Features A – K above.

L2: Scalable, low-cost manufacture of a carbon foam biosensor using screen printing technology

We have seen above how screen printing is used extensively in the manufacturing process: this is a well-known, scalable, predictable and low-cost technology. The detailed manufacturing process for the Gii-Sens carbon foam biosensor is shown in **Figure 21**.

We can generalise to the following:

A method of manufacturing a biosensor including sensor electrodes, such as a working electrode, a counter electrode, each comprising carbon foam made, at least in part, by the method defined in any of Features A – K above, and the method includes screen printing electrical connection tracks over each electrode and at least partly covering the electrodes and connection tracks with a screen printed dielectric.

Optional features include the following:

- the method defined above in which in a Step 1, the Dual Laser process creates a carbon foam working electrode and a counter electrode using a PI substrate as the pre-cursor.
- the method defined above in which in a Step 2, a reference electrode, such as a silver-silver chloride electrode, is screen printed onto the PI substrate.
- the method defined above in which in a Step 3, connection tracks, such as silver tracks, are screen printed onto the PI substrate to overlap the carbon foam electrodes. NB the order of Step 2 and 3 can be reversed.
- the method defined above in which in a Step 4, a dielectric layer is screen printed over at least some of the carbon foam electrodes and the silver connection tracks.

Other aspects are:

A biosensor including sensor electrodes, such as a working electrode, and a counter electrode, each comprising carbon foam made, at least in part, by the method defined in any of Features A – **K** above, and each electrically connected to screen printed tracks and also at least partly covered by a screen printed dielectric.

A point of care diagnostics device including a biosensor as defined above.

L3: Adding functionalised groups to the biosensor at a different manufacturing facility

For Gii-Sens biosensors, the biosensor is manufactured in one facility, but the customer adds the functionalised groups to which biomolecules can attach in a different facility, typically their own facility, hence speeding up the development and testing of these functionalised groups and also protecting their trade secrets and know-how in these functionalised groups and the final design of the biosensor.

We can generalise to:

A method of manufacturing, in one manufacturing facility, a biosensor including sensor electrodes, such as a working electrode, a counter electrode, each comprising carbon foam made, at least in part, by the method defined in any of Features A – K above, and the method includes the further step of adding, at a different manufacturing facility, functionalised groups to the working electrode.

L4: Adding functionalised groups to the biosensor as part of the biosensor production process

For Gii-Sens+ biosensors, the manufacturing process includes adding functionalised groups. **Figure 22** shows the detailed manufacturing process for Gii-Sens+.

We can generalise to:

A method of manufacturing in one manufacturing facility a biosensor including sensor electrodes, such as a working electrode, a counter electrode, each comprising carbon foam made, at least in part, by the method defined in any of Features A – K above, and the method includes the further step of adding, at that manufacturing facility, functionalised groups to the working electrode.

L5: Biosensor manufacture using PPC: Post Printing Conversion

A PPC variant of the Gii-Sens manufacturing process is shown in **Figure 23**. PPC is an acronym for Post Printing Conversion, in which the screen printing steps are done before the Dual Laser process to create the carbon foam. The specific steps are as follows:

1. Screen print carbon layer on to a substrate (e.g. polyimide,)
2. Screen print Ag/AgCl reference electrode
3. Screen print Ag electrical connection tracks
4. Screen print dielectric
4. Create carbon foam in the substrate using the Dual Laser process

All screen printing steps (1 -3) could be done using a reel to reel or reel-to-sheet process, and then the carbon foam is created using the Dual Laser process and the material then kept flat and stacked.

Also, only the first laser process (sub-surface foam creation) could be done in the factory, which then ships the sheets to a customer and the customer does the second stage of the Dual Laser process (laser ablation); the customer can add functionalised groups at their own manufacturing facility, different from the facility where the first laser process step (or both laser process steps) in the Dual Laser process is carried out. Alternatively, functionalisation can take place at the facility where the Dual Laser process is carried out.

Screen printing before creating the carbon foam has advantages: because we are not drying the carbon foam, it is not as hydrophobic. The carbon layer acts as a bridge between the carbon foam formed in the polyimide (e.g. carbon foam and the non-graphene disorganised amorphous foam) and the silver connections.

We can generalise to:

A method of manufacturing a biosensor including sensor electrodes, such as a working electrode, and a counter electrode, each comprising carbon foam made, at least in part, by the

method defined in any of Features A – K above, and the method includes the steps of (a) screen printing a carbon layer on the substrate; (b) screen printing electrical connection tracks and a reference electrode; (c) screen printing a dielectric layer over the carbon and the electrical connection tracks and the reference electrode; and then (d) creating carbon foam sensor electrodes using a process defined in any of Features A – K above.

Feature M1: Energy storage device: the Supercapacitor

Because the carbon foam manufactured using any of the **Features A – K** has a very large electrochemically active area and fast electron transfer rates, it is an ideal material for capacitor or supercapacitor or pseudo-capacitor electrodes.

An important application is a supercapacitor (an implementation is called 'Gii-Cap') or other energy storage device (e.g., Li-ion batteries). For supercapacitors and other electronics applications, the carbon foam has the following advantages over conventional graphene foam: larger surface area; more porous structure; higher quality; lower sheet resistance; higher wettability.

The carbon foam can be treated with a metal oxide or other pseudo-capacitive material, a variant we call Gii-Cap+, (e.g. to create a metal oxide layer or film) for pseudo-capacitance, and that metal oxide film has an exceptionally large surface area and a fast surface Faradic mechanism.

Note that when we use the term Gii-Cap, we include the Gii-Cap+ variant, unless the context makes it explicitly clear that we are specifically excluding the Gii-Cap+ variant. Note also that we use the term 'supercapacitor' to include both (i) an electric double-layer (EDLC) capacitor, where charge is stored electrostatically with no interaction between the electrode and electrolyte ions, and also (ii) a pseudo-capacitor, where there is electron charge transfer between the electrode and the electrolyte and any energy storage device which uses a combination of electric double-layer capacitance and pseudo-capacitance. Note finally that the term 'supercapacitor' should be expansively construed to cover any electrochemical capacitor, including EDLC supercapacitors, pseudo-capacitors, and hybrids of these. The Gii-Cap+

variant is predominantly a pseudo-capacitor, but we nevertheless refer to it as a 'supercapacitor'.

The carbon foam electrodes in the Gii-Cap supercapacitor enhance both the electrostatic double-layer capacitance and the electrochemical pseudocapacitance, compared with conventional supercapacitors. **Appendix 2** provides more detail on the supercapacitor, and describes an implementation where a hydrogel electrolyte (e.g. a high molarity salt) envelops interdigitated carbon foam electrodes in an active area to produce an enhanced operational voltage window.

The EDLC supercapacitor Gii-Cap and pseudo-capacitor Gii-Cap+ implementations have many advantages over conventional rechargeable batteries:

- fast charging
- high power
- recyclable
- non-explosive
- flexible form and shape
- can use a solid gel electrolyte or a polymeric electrolyte (e.g. an ionic gel or a hydrogel) that is solid at room temperature, having a high transition temperature far in excess of normal use temperatures (e.g. 90° C); this greatly minimises the risk of electrolyte leakage.

It can be used across a very broad range of devices and power storage requirements, such as Lab-on-a-chip (LOC), IoT devices, e-mobility, UAV, EV applications.

We can generalise to:

An energy storage device, such as a supercapacitor, in which the energy storage electrodes comprise carbon foam material made, at least in part, by the method defined in any of Features A – K above.

Feature M2: Screen printing layers of the carbon foam Supercapacitor

Figure 24 is an exploded perspective view of the Gii-Cap supercapacitor. It is made up of an array of carbon foam electrodes 241, connected to a pair of screen printed silver connectors 242, made using the Dual Laser process described above. A dielectric layer 243 is screen printed over the carbon foam electrodes 241 and the screen printed silver connectors 242. Carbon foam electrodes 241 are formed on a polyimide base layer 244. A pair of copper connection tabs 245 connect to the pair of screen printed silver connectors 242. An electrolyte layer 246 covers the carbon foam electrodes 241 (e.g. an ion gel electrolyte such as a polymeric hydrogel electrolyte that is a gel or semi-solid at room temperature to minimise leakage risks, and reversibly liquifies at over 90C, and so can be applied as a liquid during manufacture). The assembly is sealed within an aluminium-laminate heat-seal pouch 247.

Figure 25 is an exploded perspective view of the supercapacitor assembly: it is made up of an interdigitated array of carbon foam electrodes 241 that form the supercapacitor; screen printed silver connector tracks 242 provide electrical current to the carbon foam electrodes 241 and are covered by electrically insulating dielectric layer 243. A polyimide sheet 244 forms the base of the assembly.

Figures 26A - H shows the manufacturing sequence. **Figure 26A** shows step 1, the creation of the interdigitated carbon foam electrodes using the Dual Laser process. The enlarged area in **Figure 26B** shows the interdigitated carbon foam electrodes in more detail; the Group A electrodes form one set of electrodes, and the Group B electrodes form the other set of electrodes; capacitive coupling between the two groups of electrodes stores energy. The approximate thickness of the carbon foam electrodes is 20 - 30 μm.

Figure 26C shows step 2, screen printing the silver collectors. One silver connector A' provides current to the Group A electrodes, and silver connector B' provides current to the Group B electrodes. The approximate thickness of a silver layer is 20 - 40 μm and several layers may be applied.

We use a 'common collector' layout: a typical interdigitated supercapacitor has two long silver collectors, with graphene digits extending from one side of each of the long silver collectors. The long silver collectors present a significant resistance because of their length and use a significant amount of silver. Also, printing the curved parts of the collectors is difficult. In the

'common collector' approach shown in **Figure 26D**, we have carbon foam digits C extending from both sides of a shared collector 242: this maximises space utilisation of the digits and hence capacitance, reduces the amount of collector material needed and eliminates difficult curved collector parts.

The region 250 of the carbon foam digits that connect to a common collector have rounded edges; these reduce the chance of stress fractures forming and increases the reliability of the electrical connection.

Figure 26F shows Step 3, screen printing the dielectric layer 243 over the silver collectors to electrically insulate them; the approximate thickness is 10 - 30 µm.

Figure 26G shows Step 4, adding copper connection tabs 245 (made from conductive metallic tape) to connect to the silver collectors 242. **Figure 26H** shows Step 5, depositing electrolyte layer 246 over the interdigitated carbon foam digits. The electrolyte could be a hydrogel and salt combination (see **Appendix** 2). **Figure 26I** shows Step 6, packaging the entire assembly into aluminium-laminate heat-seal pouch 247, leaving just copper connection tabs 245 exposed. Note also that Step 4, adding the copper connection tabs 245, could be done before Step 2 (screen printing the silver collector) as well as after Step 5, depositing electrolyte layer 246 over the interdigitated carbon foam digits.

Figure 27 shows how a single polyimide sheet will accommodate 6 of these Gii-Cap assemblies of 220mm x 180mm size; other sizes (e.g. A4, A5, A6 or different from A-series standard sizes) are also possible.

The detailed Gii-Cap manufacturing process is shown in **Figure 28**.

The specifications for one production run of Gii-Cap supercapacitors is shown in **Table 3** below, using a hydrogel electrolyte.

Description	EDL supercapacitor
Format	A7 V4
Voltage Window	2.5V

Capacitance	4.06 ±0.10mF (measured at 65mA)
Equivalent series resistance	0.77 ± 0.04 Ohm
Time Constant	0.016 ± 0.001s
Energy	0.0033 ± 0.0001mWh (measured at 65mA)
Power	355.77 ± 9.11mW (measured at 390mA)
Peak Power	2.03W
N	6

Table 3

We can generalise to:

An energy storage device, such as a supercapacitor in which energy storage electrodes comprise carbon foam material made, at least in part, by the method defined in any of Features A – K above;

and in which screen printed electrical connection tracks are formed over at least a part of each electrode and a screen printed dielectric layer at least partly covers the electrodes and connection tracks.

Feature M3: Carbon foam supercapacitor: the Common Collector

We have seen above how a 'common collector' is used.

We can generalise to:

An energy storage device, such as a supercapacitor, in which energy storage electrodes comprise carbon foam material made, at least in part, by the method defined in any of Features A – K above and are arranged in an interdigitated pattern;

and in which screen printed electrical connection tracks are formed over at least a part of each electrode, and in which a single electrical connection track connects to underlying digits that extend perpendicularly from both sides of the electrical connection track.

Feature M4: Carbon foam supercapacitor: the PPC manufacturing process

The PPC (Post Printing Conversion) is shown in **Figure 29**. The steps are:

1. Silver collectors screen printed on to a substrate (e.g. polyimide).
2. Screen print carbon over silver collectors and then dry.
3. Screen print dielectric over carbon layer and then dry.
4. Create carbon foam in the carbon layer using the Dual Laser process; the carbon foam is attached to the underlying polyimide substrate via a non-graphene intermediary layer.
5. Dispense electrolyte.
6. Add copper/aluminium etc tabs to contact the silver collectors (could also be step 1).
7. Add lid/pouch.

All screen printing steps (1 -3) could be done using a reel to reel process, and then the carbon foam is created using the Dual Laser process and the material then kept flat and stacked. Also, only the first laser process (sub-surface carbon material foam creation) could be done in the factory, which then ships the sheets to a customer and the customer does the second stage of the Dual Laser process (laser ablation) and steps 5 - 7.

Screen printing before creating the carbon foam has advantages: if the carbon foam is made first, it can have sharp edges; a silver screen printed layer applied over these sharp edges can crack at these sharp edges. But by screen printing before creating the carbon foam, we do not have this problem. Also, because we are not drying the carbon foam, it is not hydrophobic.

We can generalise to:

A method of manufacturing an energy storage device, such as a supercapacitor or pseudo-capacitor;

and the method includes the step of (a) screen printing electrical connectors on to a substrate; (b) screen printing a carbon layer over the electrical collectors; (c) screen printing a dielectric over at least some of the carbon layer; then (d) creating carbon foam energy storage electrodes at least in part by the method defined in any of Features A – K above.

Feature M5: Carbon foam pseudo-capacitor: a metal oxide variant

A metal oxide electrochemical deposition process (e.g. MnO_x for +ve; Fe_xO_x for -ve) is used to create the Gii-Cap+ variant; this much higher capacitance compared to the standard Gii-Cap device (see **Table 4**).

Description	Pseudocapacitor
Format	A7 V4
Voltage Window	2V
Capacitance	856 ± 120mF (measured at 65mA)
Equivalent series resistance	0.81 ± 0.03 Ohm
Time Constant	4.0 ± 0.8s
Energy	0.48 ± 0.07mWh (measured at 65mA)
Power	277.91 ± 13.94mW (measured at 390mA)
Peak Power	1.23W
N	12

Table 4

This metal oxide electrochemical deposition process can be applied to the Gii-Cap Supercap manufacturing process and also the PPC process and hence all Gii-Cap products can also be Gii-Cap+ products. A detailed process flow chart is at **Figure 29**.

We can generalise to:

A method of manufacturing an energy storage device, such as a supercapacitor or pseudo-capacitor, in which energy storage electrodes comprise carbon foam material made, at least in part, by the method defined in any of Features A – K above;

and the method includes the step of applying an electrochemical deposition process of a pseudo-capacitive material, such as a metal oxide, to the energy storage electrodes.

Feature M6: Carbon foam supercapacitor: using an ionic-gel in low humidity environment

We use an ionic gel (ionic liquid with fumed silica SiO_2) that gives 3V - 6V voltage. It is solid below 90°C and so will not leak during shipment and normal use and hence is especially useful in smart labels and IoT devices; above 90°C it liquifies and hence can be printed where the electrochemical printing process is done at over 90°C. Ion-gel is usually made with ionic liquid (e.g. *1-ethyl-3-methylimidazolium tetrafluoroborate* (EMIMBF4) plus a gel-forming agent (e.g. fumed silica SiO2).

Normally, manufacturing is done in an inert (e.g. Argon) atmosphere because the presence of O_2 and H_2O can lead to reduced voltages and stability.

The optimal sweet spot of O_2 and H_2O levels where we get the optimal balance between increased capacitance and decreased voltage as described in more detail in Appendix 3 ("GiiCap Iongel).

We can generalise to:

A method of manufacturing an energy storage device, such as a supercapacitor, in which energy storage electrodes comprise carbon foam material made, at least in part, by the method defined in any of Features A – K above;

and the method includes the step of applying an ionic gel in a low humidity but non-inert environment, in which the levels of O_2 and H_2O in the environment and measured and controlled to optimise the capacitance of the energy storage device.

In the preceding sections covering **Features M1 - M6**, we have looked at some general features of the Gii-Cap carbon foam supercapacitor. In the following sections, covering **Features N - S**, we look at some more specific products that implement Gii-Cap.

Feature N1: Electrical conductor

For devices like the biosensor described above, it is possible and desirable to fabricate the electrical conductors that provide the measurement signal connection from carbon foam material made by the Dual Laser method: because these electrical conductors are very low resistance, the sensitivity is maximised. Electrodes (e.g. the biosensor working electrodes that are functionalised, as well as the reference electrode that is described above as being screen-printed; the capacitor plate electrodes) are examples of electrical conductors covered by this **Feature N1**. Also, electrodes whose primary function is to merely carry signals and current are also covered by this **Feature N1** - e.g. to replace conventional silver connection tracks, such as the screen printed Ag electrical connection tracks we describe above that are in biosensors.

We can generalise to:

A method of manufacturing an electrical conductor, in which the electrical conductor comprises carbon foam made, at least in part, by the method defined in any of Features A – K above.

An electrical conductor including carbon foam made, at least in part, by the method defined in any of Features A – K above.

Feature N2: Combined Sensor and Supercapacitor

Features L1 - L4 above describes the biosensor that uses the carbon foam made by the Dual Laser method in its sensor electrode; **Features M1 - M6** describe a supercapacitor and a pseudo-capacitor that uses the carbon foam made by the Dual Laser method in its electrodes.

Highly sensitive and highly selective biosensors can be built that combine both this biosensor and this supercapacitor into a single, integrated device that also includes electronic circuitry to measure the variable being detected or measured, compute a biosensor output, and send that output to a POC diagnostics device or display that output on a display screen of the device (e.g., presence or absence of the target; concentration of the target).

Figure 30 is a schematic cross section through this integrated LOC device: there are two separate polyimide film layers, an upper layer 301 including a functionalised carbon foam

biosensor (Gii-Sens) 302 as described in **Feature L** and the lower one 303 including a supercapacitor 304 (Gii-Cap) as described in **Feature M**. Although back-to-back polyimide layers are shown, they could be side-by-side; there could be a single polyimide film that integrates the biosensor 302, and the supercapacitor 304 together onto a single item.

A plastic piece 305 with microchannels 306 provides the microfluidics system that distributes the test fluid over the biosensor 302; sub-surface carbon foam electrodes or conventional connector tracks 307 as described in **Feature O** lead from the biosensor to the flexible electronics 308 (e.g. a microcontroller that measures the change in electro-chemical properties of the biosensor in the presence of the target analyte; a display panel to show diagnostics results; a power management system that controls the power from the supercapacitor 304 to the electronics 308). The supercapacitor 304 (Gii-Cap) is charged with power (e.g. through a wireless inductive process (not shown) controlled by the microcontroller) and powers up the biosensor measurement process and an integrated display on which quantitative measurements are shown. Alternatively, a rechargeable secondary battery (not shown) or a non-rechargeable primary battery (not shown) could charge the supercapacitor 304, and the supercapacitor 304 then powers the biosensor measurement process. Another variant is for a rechargeable secondary battery (not shown) or a non-rechargeable primary battery (not shown) to charge the supercapacitor 304, and also power the biosensor measurement process. The supercapacitor 304 is then reserved for powering up a high-power process, such as a wireless data transmission, so that the LOC becomes a self-contained LOC device that can both perform a diagnostic process and also wirelessly transmit results data, without the need for a user to approach the LOC, as would be required if the LOC used conventional NFC (near-field communications). The electrical connector tracks from the supercapacitor 304 to the flexible electronics 308 are not shown.

An exploded view of a fully integrated LoC device is show in **Figure 31**. Moving up from the lowest layer, we have (i) an inductive power loop 310; (ii) the Gii-Cap supercapacitor 312 wirelessly powered by the inductive loop 310; (iii) the Gii-Sens biosensor 313; (iv) a layer 314 with the electronics for the biosensor that are powered by the supercapacitor 312 and microfluidics channels; (v) a top panel 315 that includes a display 316, again powered by the supercapacitor, and also the circular well 317 into which the sample is delivered.

Figure 32 shows the LOC displaying quantitative results on its display.

Figure 33 shows an exploded view of an environmental monitoring device that includes a Gii-Sens sensor 330 configured to detect environmental parameters, such as CO2 level, volatile organic compounds and other atmospheric pollutants. Gii-Sens is not limited to being a biosensor but can detect any molecules that the carbon foam sensor electrodes can be functionalised to detect. The environmental monitoring device includes a Gii-Sens sensor 330 and related control and wireless transmission (e.g. LoRaWAN) electronics 331, and a PV solar cell 332 and a Gii-Cap supercapacitor 333. A secondary or primary battery (which could be a printed battery) is included in electronics 331, and, working together with PV solar cell 332, powers those electronics and charges the Gii-Cap supercapacitor 333. The Gii-Sens sensor can also be configured to measure temperature, humidity and pressure. The device has a back 334 that can be peeled away to reveal a sticky surface, so that the device can be stuck on a wall etc. The PV solar cell, in conjunction with the secondary or primary battery on electronics 331, provides power to charge the Gii-Cap supercapacitor 333 and the supercapacitor 333 in turn provides the peak bursts of power needed for data transmissions. The device can be permanently installed and remain in situ for many years, requiring no battery changes at all, unlike current environmental monitoring devices. It can detect atmospheric pollutants with a signal to noise ratio that is better than conventional devices. The assembled device is shown in **Figure 34**.

Many other types of devices can be implemented with a combined carbon foam sensor and carbon foam supercapacitor; for example:

- any biosensor that would benefit from being able to transmit data e.g. wirelessly, where the data transmission is powered by the supercapacitor, for example, wearable health monitoring devices, such as continuous glucose monitors, other wearable monitors sensing levels of electrolytes, potassium, sodium, lactose.
- any sensor device (i.e. not necessarily a biosensor) that would benefit from being able to transmit data e.g. wirelessly, where the data transmission is powered by the supercapacitor.
- any IoT device that would benefit from being able to transmit data e.g. wirelessly, where the data transmission is powered by the supercapacitor.
- the device may include electronics that are powered by the supercapacitor.

- the device may include a battery to charge the energy storage device and/or power device electronics.
- the device may include a PV cell to charge the energy storage device and/or a secondary battery in the device and/or power device electronics.

We can generalise to:

A method of manufacturing a device that includes both a sensor, and an energy storage device, such as a supercapacitor, in which both the sensor and the energy storage device comprise a carbon foam material made, at least in part, by the method defined in any of Feature A – K above.

A sensor device, such as a biosensor, including (a) a sensing electrode comprising carbon foam material made, at least in part, by the method defined in any of Features A – K above and (b) an energy storage device, such as a supercapacitor, in which the energy storage device comprises carbon foam material made, at least in part, by the method defined in any of Features A – K above.

A point of care diagnostics device including (a) a sensing electrode comprising carbon foam material made, at least in part, by the method defined in any of Features A – K above and (b) an energy storage device, such as a supercapacitor, in which the energy storage device comprise carbon foam material made, at least in part, by the method defined in any of Features A – K above.

Feature N3: Combined Supercapacitor and Battery

In this example, we combine two different power sources into a single device to form a consolidated or hybrid power source: the device has a battery (e.g. a printed battery or a conventional battery) and a supercapacitor that uses the carbon foam made by the Dual Laser method in its electrodes; they work together in a complimentary manner. The battery can be a use-once, non-rechargeable battery (a 'primary' battery) or it can be a rechargeable battery (a 'secondary' battery).

The power sources have complimentary roles: the battery can provide a slow, long-term charge to the supercapacitor or power for electronics that consume relatively low levels of power; the supercapacitor can provide a fast, high-power discharge and power functions that need much higher levels of power (e.g. a wireless data connection function and a data payload transmission function). Note that the supercapacitor can be an EDL supercapacitor or a pseudo-capacitor, or any other form of energy storage device. The device could be used where you need occasional high power (e.g., to power a transmitter to connect to a data network and send a data payload), but the device needs to be self-contained and to last many months or years in the field: the device could be a high value asset tracking label, which only occasionally needs to broadcast its information, but needs to do so at higher power than a conventional printed battery can supply.

A schematic is shown in **Figure 35.** There are two separate polyimide film layers, one layer 351 including a supercapacitor (Gii-Cap) 352 as described in **Feature M** and one layer 353 including a battery 354, such as a printed battery; this may include electrodes made using the Dual Laser process fabricated carbon foam or a conventional process. It is possible also to fabricate the printed battery 354 and the supercapacitor 352 on the same piece of polyimide, although yield may suffer since any defect in either the printed flexible battery or the supercapacitor will lead to a rejected device.

Sub-surface carbon foam electrodes as described above (or conventional printed electrodes) lead from the supercapacitor (Gii-Cap)352 and also the printed battery 354 to a BMS (battery management system) 355; the BMS 355 provides power to flexible electronics 356; sub-surface carbon foam electrodes or conventional connector tracks 357 connect different parts of the flexible electronics 356. The BMS 355 controls the flow of power from the battery 354 to the electronics 356; the battery 354 may trickle charge the supercapacitor 352. (The supercapacitor may also be a primary power source, designed to be charged once at the factory and not subsequently re-charged.)

The battery 354 could be a printed battery, and can be a re-chargeable secondary printed battery or a single-use non-rechargeable primary battery; the battery 354 can trickle charge the supercapacitor 352 and provide power for the sensors or other device electronics 356; the supercapacitor 352 then provides power (e.g. transient peak power) for a circuit with short demands for relatively high bursts of power, such as a data transmitter. As noted above, the

printed battery, supercapacitor, electronics can all be part of a single, integrated device - e.g. all on a single substrate, or on separate but attached substrates.

Although back-to-back polyimide layers are shown, they could be side-by-side; also, there could be a single polyimide film that integrates the battery 354, and the supercapacitor 352 together onto a single item.

The battery 354, supercapacitor 352, electronics 356 could all be formed on the substrate or substrates as part of a continuous or batch manufacturing process (e.g. you do not take a previously manufactured battery and combine it with the supercapacitor). This enables interconnects to be constructed as an integral part of the manufacturing process, leading to lower cost, faster manufacturing and greater performance (e.g. where the interconnects are shorter).

The device can be used for a smart label (see below), or IoT environmental monitoring device (e.g. temperature or humidity sensor), train seat occupancy sensor, medical monitoring device (e.g. continuous blood glucose monitor). More generally, the device may include electronics that are powered by the battery; the device may include electronics that are powered by the supercapacitor; the device may include a data transmitter that is powered by the supercapacitor; the battery may be a printed battery; the battery may be a primary battery or a secondary battery.

We can generalise to:

A method of manufacturing an integrated device including a battery and a supercapacitor, the battery providing long term power and the supercapacitor providing short term power at a higher level than the battery, in which the supercapacitor comprises a carbon foam material made, at least in part, by the method defined in any of Features A – K above.

An integrated device including a battery and a supercapacitor, the battery providing long term power and the supercapacitor providing short term power at a higher level than the battery, in which the supercapacitor comprises carbon foam material made, at least in part, by the method defined in any of Features A – K above.

Feature N4: The Smart Label

One important application is the smart label, shown in **Figure 36**, with the bottom surface shown on the left side and the exposed label surface 363 with human readable text shown on the right; the label includes an adhesive release liner 364 so that the bottom surface can be attached to a package, component etc. The label includes a thin, flexible, battery 360 that is printed onto a polyimide film and then the Gii-cap supercapacitor 361 is formed on the same polyimide layer, (or a different polyimide layer that is joined to the printed battery polyimide film). The thin, flexible, battery may be a non-rechargeable, primary battery or a rechargeable secondary battery. The supercapacitor powers the data transmitter; the printed battery powers the smart label electronics, including sensor, and the power management electronics. The smart label includes human readable, printed information 363 on one surface; the reverse side

The smart label includes an electronics module 362 with power management, sensors (e.g. solid-state vibration, temperature, pressure, GPS etc sensors) and data transmit electronics such as an LTE transmitter, or, for ultra-low cost, a LoRaWan transmitter. The supercapacitor 361 provides enough peak power to send useful data packages once a data connection has been established, so there is no need to simply include this data in an 'advertising' signal; instead, the smart label can establish a data connection with a data receiver and then send the data payload once the connection has been established; it can hence be reasonably assured that its data has been received. More generally, the device may include electronics that are powered by the battery; the device may include electronics that are powered by the supercapacitor; the device may include a data transmitter that is powered by the supercapacitor; the battery may be a printed battery; the battery may be a primary battery or a secondary battery.

For scalable manufacturing (e.g. producing millions of smart labels at low cost), reel to sheet manufacturing of the smart label is desirable (See **Feature P: Gii 3** below).

We can generalise to:

A smart label including a battery and a supercapacitor, the battery providing long term power and the supercapacitor providing short term power at a higher level than the battery, in which the supercapacitor comprises carbon foam material made, at least in part, by the method defined in any of Features A – K above;

and the smart label includes electronics, such as sensor electronics, powered by the battery and a data transmitter powered by the supercapacitor.

Feature N5: Combined Supercapacitor and Antenna

The supercapacitor from the preceding example in **Feature M** could power an antenna, but not be integrated with a battery: for example, it could be powered from solar cells or extracting power from local WiFi or from a wireless charger (e.g., Qi standard).

We can generalise to:

A method of manufacturing an integrated device including an antenna and a supercapacitor, in which the supercapacitor powers the antenna and comprises carbon foam material made, at least in part, by the method defined in any of Features A – K above.

An integrated device including an antenna and a supercapacitor, in which the supercapacitor powers the antenna and comprises carbon foam material made, at least in part, by the method defined in any of Features A – K above.

Feature N6: Combined Energy Scavenger + Supercap

One useful feature is to combine an energy scavenger with the carbon foam supercapacitor into a device. The energy scavenger could be a solid state energy harvester, such as a solar cell, or vibration energy harvester (e.g. piezoelectric fibre based), or thermoelectric generator (e.g. Seebeck generator). The supercapacitor can provide power (e.g. transient power) for a circuit with short demands for relatively high bursts of power, such as a data transmitter and antenna. The device may also include a primary battery (e.g. a non-rechargeable printed battery) or a secondary, rechargeable battery.

The energy scavenger can be on the same substrate as the supercapacitor or on separate but joined substrates; the supercapacitor can be on the same side of the substrate as the energy scavenger or on the opposite side.

Where a battery is included in the device (e.g. a printed rechargeable secondary battery), the energy harvester charges the battery, and the battery provides power to low power sub-systems (e.g. a sensor) and also charges the supercapacitor; the supercapacitor provides the transient high power for data transmission. Alternatively, the energy harvester can directly charge the supercapacitor.

This approach can be used for a smart label, or IoT environmental monitoring device (e.g. temperature or humidity sensor), train seat occupancy sensor, wearables, medical monitoring device (e.g. continuous blood glucose monitor). This approach is especially useful where there is a need to continuously (or with high regularity) power a device - for example, where continuous monitoring of environmental or personal health conditions is required.

The device can include a LoRaWan or other ultra-low power transmitter. The supercapacitor can provide enough peak power to send useful data packages once a data connection has been established, so there is no need to simply include this data in an advertising signal; instead, the smart label can establish a data connection with a data receiver and hence be assured that its data has been received.

More generally, the energy scavenger may be a solid state energy harvester, such as a solar cell, or vibration energy harvester (e.g. piezoelectric fibre based), or thermoelectric generator (e.g. Seebeck generator); the device may include one or more sensors powered by the energy scavenge; the energy scavenger may charge the supercapacitor; the device may include a primary or secondary battery; the device may be a smart label, or IoT environmental monitoring device (e.g. temperature or humidity sensor), train seat occupancy sensor, wearable, or medical monitoring device

We can generalise to:

A data logging device including an energy scavenger system and a supercapacitor, in which the supercapacitor powers an antenna and comprises carbon foam material made, at least in part, by the method defined in any of Features A – K above.

Feature O1: 3D carbon foam structures: Gii-Thru for Gii-Cap

In earlier sections, the carbon foam in the Gii-Cap supercapacitor is formed into a single, planar layer of interdigitated digits. In this section, we describe a three-dimensional structure of the carbon foam which enable the carbon foam supercapacitor electrodes to be formed as a 3D structure of parallel plates - the energy storage is potentially larger than a mono-layer of interdigitated graphene foam digits.

Figure 37 shows the basic layering of different materials in the core structure. Multiple screen printing steps are performed on a sheet of PI polyimide film 371. First, a conductor, such as a carbon ink or carbon paste layer 372, is screen printed on to the lower surface of the polyimide film 371. Then, a collector 373, e.g. a screen printed silver collector, is screen printed over the carbon layer 372. And then, a dielectric layer 374 is screen printed over the collector.

Figure 38 shows a carbon foam layer formed in the polyimide film 371 using the Dual Laser process described above: more specifically, an IR laser forms an encapsulated carbon foam layer 375 in the PI film 371; below this carbon foam layer is a disorganised, amorphous non-graphene layer 376 that forms at the lower surface of the PI film 371. A C02 ablation laser exposes the previously encapsulated carbon foam layer 370, giving the exposed surface layer 377 a unique morphology.

This structure provides an electrically conductive pathway from the collector layer 373, through the conductive ink or paste layer 372, through the disorganised, amorphous non-graphene layer 376 and then to the carbon foam layer 375. In this way, the electric potential of a large area of carbon foam 375 can be raised, enabling it to function as a capacitive plate; the structure forms part of a half-cell.

Typical thicknesses are as follows: polyimide film 371: 127µm; carbon ink layer: 20 µm; silver collector layer 373:30 µm; dielectric layer: 40 µm; carbon foam layer 375 and disorganised, amorphous non-graphene layer 376: 127 µm; unique surface morphology layer 377: 25 µm.

Note that the Gii-Cap+ (the variant that uses a metal oxide electrochemical deposition process (e.g. MnO_x for +ve; Fe_xO_x for -ve - see Feature M2 above) and that delivers much higher capacitance compared to the standard Gii-Cap device can be used in Gii-Thru.

We can generalise to

An energy storage device, such as a supercapacitor, including:
(i) a carbon pre-cursor film;
(ii) a screen printed conductive paste or ink layer, on the surface of the carbon pre-cursor film;
(iii) a screen printed collector layer over the screen printed conductive paste or ink layer;
(iv) a screen printed dielectric layer over the collector layer;
(v) energy storage electrodes that comprise carbon foam material made from the carbon pre-cursor film at least in part by the method defined in any of Features A – K above, and in which an electrically conductive path is formed from the carbon foam material to the collector layer, via the conductive paste or ink layer.

Feature O2: 3D carbon foam structures: Gii-Thru Stackable Gii-Cap/Gii-Cap+

It is possible to stack a number of the structures described in **Figure 38** on top of one another; since the surface area of the carbon foam layer can be large (significantly larger than the surface area of the digits in the planar interdigitated supercapacitor described earlier) this enables high performance supercapacitors to be produced.

A half-cell is shown in **Figure 39.** It includes (moving progressively down through the structure) a hydrogel electrolyte layer 390, carbon foam layer with unique surface morphology 391 in a PI film 392; screen printed carbon paste layer 393; screen printed silver connector layer 394 with external copper tab 395 connection point; screen printed dielectric isolation layer 396; a second carbon foam layer with unique surface morphology 397 in a PI film 398, and at the base of the stack a hydrogel electrolyte layer 399. It may help to relate this structure to the **Figure 38** schematic: in **Figure 40A**, we group together at A the four main layers shown in **Figure 38**, i.e. moving down through the stack, the carbon foam layer, then the carbon ink layer, then the silver collector layer, and then the dielectric layer. **Figure 40B** is a cross-section through the **Figure 40A** structure, showing the group A features. **Figure 40B** is the same cross-section, but this time labelling all of the **Figure 39** elements.

A full cell is shown in **Figure 41A** and **41B**. In **Figure 41A** we only label the features that are also present in Figure 39 (using the same numbering). So it includes a hydrogel electrolyte layer 390, carbon foam layer with unique surface morphology 391 in a PI film 392; screen printed carbon paste layer 393; screen printed silver connector layer 394 with external copper tab 395 connection point; and a screen printed dielectric isolation layer 396.

In **Figure 41B**, we now add in the additional layers; moving progressively down through the structure, we have a screen printed dielectric isolation layer 400, then screen printed silver collector layer 401 with copper tab 402, then screen printed carbon paste layer 403, and then carbon foam layer with unique surface morphology 404 in a PI film 405.

In **Figure 41C**, we group together at A the four main layers shown in **Figure 38**; the four top layers are in the inverse order, and we group these together at B. Group A and Group B are separated by a hydrogel (e.g. polymeric hydrogel) electrolyte layer 399, dispensed using a conventional electrolyte dispensing system.

Figure 41D is a cross section through this structure, showing Group A and Group B layers, separated by the hydrogel (e.g. polymeric hydrogel) electrolyte layer 399. **Figure 41E** is the same cross-section, but this time with the individual layers numbered as per the schematic of **Figure 38.**

Figure 41F is a perspective view of the assembled supercapacitor.

Figure 42 shows a 4 stack of full cell supercapacitors; the carbon foam layers are shown at A, and the polymeric hydrogel electrolyte is shown at B. Additional cells can be added to the stack to give the require performance.

Figure 43A shows the detailed manufacturing flow for the Gii-Thru supercapacitor and **Figure 43B** shows the detailed manufacturing flow for the Gii-Thru Multi-stack supercapacitor

We can generalise to:

An energy storage device, such as a supercapacitor, including a sub-assembly comprising:
(i) a carbon pre-cursor film;

(ii) a screen printed conductive paste or ink layer, on the surface of the carbon pre-cursor film;
(iii) a screen printed collector layer over the screen printed conductive paste or ink layer;
(iv) a screen printed dielectric layer over the collector layer;
(v) energy storage electrodes that comprise carbon foam material made, at least in part, from the carbon pre-cursor film by the method defined in any of Features A – K above, and in which an electrically conductive path is formed from the carbon foam material to the collector layer, via the conductive paste or ink layer;

and in which multiple sub-assemblies are formed into a stack and in which adjacent energy storage electrodes are separated by an ionic gel electrolyte.

Feature O3: 3D carbon foam structures: Gii-Thru for Gii-Sens: HISLOC

The Gii-Thru structure described in **Figure 38** can be used not just for a supercapacitor, but also for a Gii-Sens sensor, such as a biosensor.

For microfluidics, the Gii-Thru HISLOC (High Sensitivity Low Cost) platform approach enables the liquids and the carbon foam sensors to be on the upper face of the biosensor device and for the electrical connections that connect to the carbon foam sensors to be on the lower face of the biosensor device. Microfluidics conventionally use functionalised gold electrodes where the electrical connectors that connect to the functionalised gold electrodes are all co-planar; the Gii-Thru biosensor has cost, yield and performance advantages over these functionalised gold electrodes. And moving the electrical connections to the bottom or base of the biosensor enables greater miniaturisation and compatibility with POC (point-of-care) systems.

Figure 44A is a cross-sectional schematic view through a Gii-Thru sensor used in a three sample array microfluidic diagnostic device. At the top level are three sample wells 440; the fluid to be analysed flows into each of these wells 440. The wells 440 are formed as small, apertures in a laminated well spacer layer 441, that sits over a polyimide film layer 442.

In the polyimide film layer 442 are formed three functionalised carbon foam regions that form the reference electrode 448A, working electrode 448B, and counter electrode 448C; the upper surface of each electrode 448A - 448C is exposed to the analyte fluid present in the well 440.

The base of the reference electrode 448A may include an Ag-AgCl layer (or screen printed carbon layer) 449; at the base of the working electrode 448B is a screen printed conductive carbon layer 443; at the base of the counter electrode 448C is another screen printed conductive carbon layer 443. In this way, reference electrode 448A is in electrical contact with reference electrode connection 444A; the working electrode 448B is in electrical contact with working electrode connection 444B; and the counter electrode 448C is in electrical contact with counter electrode connection 444C.

A screen printed dielectric layer 447 forms the base of the structure.

So what is interesting about this structure is that the electrode connections 444A - C are not co-planar with the functionalised carbon foam electrodes 448A - C, as they would be with conventional screen printed sensors. Instead, they are in a plane below the functionalised carbon foam electrodes 448A - C, on the opposite side to the wells 440. This structure enables greater miniaturisation and compatibility with POC (point-of-care) systems.

Figure 44B shows an isometric exploded view of the **Figure 44A** microfluidic diagnostic device. The three sample wells 440 sit in laminated well spacer layer 441, which sits over the polyimide film layer 442. The reference electrode 448A, working electrode 448B and counter electrode 448C are shown; the end of reference electrode 448A is covered by Ag-AgCl layer or screen printed carbon layer 449; the working electrode 448B and counter electrode 448C are covered by screen printed conductive carbon layer 443. As noted above, reference electrode 448A is in electrical contact with reference electrode connection 444A; the working electrode 448B is in electrical contact with working electrode connection 444B; and the counter electrode 448C is in electrical contact with counter electrode connection 444C.

Note that the three functionalised carbon foam regions 448A - C are shown as planar squares lying at different planes; this is however just an artefact of the CAD used to create the figure and the carbon foam regions 448A - C are better represented in **Figure 44A**. Screen printed dielectric layer 447 forms the base of the structure.

Figure 44A and **44B** above show a three-spot array microfluidic diagnostic device. In **Figure 45A** and **Figure 45B**, we show an eight-spot array microfluidic diagnostic device. In isometric **Figure 45A**, a laminated well spacer 451 includes an array of eight analyte wells 452 for the

working electrodes, plus wells 453 for a counter electrode and wells 454 for a reference electrode; laminated well spacer 451 sits over the polyimide layer 455. Gii carbon foam in polyimide layer 456 forms the eight working electrodes 457 and the counter electrode 458 and are made using the Dual Laser process. Note also that the carbon foam electrodes 457, 458 are shown as planar squares lying at three different planes; this is however just an artefact of the CAD and the carbon foam form a continuous region in polyimide layer 455.

A reference electrode 459 is covered with a thin screen printed Ag-AgCl layer. A thin screen printed carbon connection interface layer 460 sits under the working electrodes 457 and the counter electrodes 458; screen printed silver connection tracks 461 form an electrical connection to all electrodes 457, 458 and 459. A screen printed dielectric layer 462 then forms the case of the device. **Figure 45B** is a pair of top down views of the **Figure 45A** device; the lower view shows the underlying connection track paths.

Figure 46A shows a perspective view of a fully assembled multi sample array microfluidic diagnostic device; **Figure 46B** is a top down view.

We can generalise to

A microfluidic diagnostic device including sample wells positioned on an upper face of the device, reference, working and counter electrodes, made from a carbon pre-cursor film at least in part by the method defined in any of Features A – K above, are in a layer below the sample wells, and reference, working and counter electrode connections are in layer below the reference, working and counter electrodes .

Figure 47A shows an exploded view of a microfluidic diagnostic device comprised of multiple laminate layers; it includes a three-spot array (3SA) microfluidic biosensor that implements Gii-Thru, as shown in **Figure 44A**. The top layer 470 of the device is a microfluidic foil; the middle layer 471 is a microfluidic foil with adhesive, and includes a printed or moulded microfluidic fluid channel 472, and the bottom layer 473 is a microfluidic foil with adhesive. The Gii-Thru sensor 474 is a three-spot array (3SA) biosensor and includes connectors 475. **Figure 47B** is a top down view showing the internal structure. The Gii-Thru sensor 473 can be replaced with a different biosensor (e.g. an 8SA) for greater flexibility.

Figure 48B shows an exploded view of a microfluidic diagnostic device comprised of a printed or moulded microfluidic card and it includes a three-spot array (3SA) microfluidic biosensor that implements Gii-Thru, as shown in **Figure 44A**. This device includes clear resin barb connectors 481, a top foil 482, a clear resin moulded microfluidic card 483 with microfluidic channels 484, a well unit 485 made of microfluidic foil with adhesive and the Gii-Thru sensor 486. Again, the Gii-Thru sensor 486 can be replaced with a different biosensor (e.g. an 8SA) for greater flexibility and the moulded microfluidic card 483 can be replaced with different designs of microfluidic features to allow for different assay platforms. **Figure 45B** is a top down and side view.

Feature O4: 3D carbon foam structures: Gii-Thru for Gii-Sens: HISLOC manufacturing process

The HISLOC manufacturing process can be summarised as follows:

1. Screen print carbon layer on the underside of the polyimide film.
2. Screen print silver connections.
3. Screen print silver/silver chloride reference electrodes (steps 3 and 4 can be re-ordered as 4 then 3).
4. Screen print dielectric.
5. Create Gii carbon foam sensor electrodes in the polyimide film using the Dual Laser process.

Detailed manufacturing process flows are shown in **Figure 49**

We can generalise to:

A lab-on-chip device, including a sub-assembly comprising:
(i) a carbon pre-cursor film;
(ii) a screen printed conductive paste or ink layer, on the surface of the carbon pre-cursor film;
(iii) a screen printed conductive layer over the screen printed conductive paste or ink layer;
(iv) a screen printed reference electrode;
(v)) a screen printed dielectric layer over the collector layer;

(vi) sensor electrodes that comprise carbon foam material made from the carbon pre-cursor film at least in part by the method defined in any of Features A – K above, and in which an electrically conductive path is formed from the carbon foam material to the conductive layer, via the conductive paste or ink layer.

Group 4

Feature P: Scalable manufacturing: G-ii 3

Gii-3 is a scalable manufacturing plant with reel-to-reel or reel-to-sheet production of all of the Gii-based materials described above. A key commercially advantage is that Gii 3 manufacturing does not need bespoke equipment - it uses off the shelf computer controlled lasers for the Dual Laser carbon foam manufacturing and conventional screen printing and drying technology: these are well known, well understood manufacturing processing steps and equipment, leading to repeatability and reliability.

Figure 50 is a schematic of the overall manufacturing process and **Figure 51** shows the detailed process flow.

We can generalise to:

A method of manufacturing a device including one or more electrodes, each comprising carbon foam material;

in which the method includes passing a continuous reel of a carbon pre-cursor film through a sequence of operations required to manufacture the carbon foam material made, at least in part, by the method defined in any of Features A – K above.

Feature Q: Various other Gii Applications

The Gii carbon foam described in this specification can be used in a wide variety of applications, including many applications for which conventional graphene foam has been considered to be suitable.

We can generalise to:

A device including a carbon foam material made, at least in part, by the method defined in any of **Feature A – K** above, where the device is one of the following types of devices:

- Hall effect sensor: the carbon foam shows a response to magnetic fields.
- Tactile sensor for e.g. robotics; prototype sensors using Gii carbon foam with polydimethylsiloxane (PDMS) embedded into and over the structure, as an active layer in piezoresistive based pressure sensors for use in robotic touch sensing applications have been shown: a few layers of carbon foam is able to present sensitivity to pressures with sensitivity of 0.0418 mV/kPa over a range of 0 to > 50kPa. See DOI:10.4028/p-oy94hj. and DOI: 1109/CDE52135.2021.9455738. The contents of these are incorporated by reference to the fullest extent permissible.
- Infectious diseases sensor.
- Biosensor where the Gii carbon foam is subject to π–π non-covalent functionalization with pyrene carboxylic acid (PCA) for interleukin 10 impedimetric detection. See DOI:10.1016/j.bios.2022.114954, the contents which is incorporated by reference to the fullest extent permissible.
- Constant monitoring chemical sensor.
- Glucose monitoring sensor: A reversible polymer displacement sensor mechanism for electrochemical glucose monitoring has been shown; a pyrene-derivatised boronic acid chemo-receptor for glucose is adsorbed onto a carbon foam electrode, competitively binding with poly-nordihydroguaiaretic acid. See DOI:10.1039/D1AN01991K, the contents which is incorporated by reference to the fullest extent permissible.
- Lactic acid sensor: Synthetic organic receptor molecules are employed based on boronic acids attached to carbon foam to provide functionality and selectivity in competitive analyte binding, using surface redox polymer indicator displacement. See DOI:10.1016/j.snb2022.133089, the contents which is incorporated by reference to the fullest extent permissible.
- Gas detection sensor, such as hydrogen peroxide and oxygen detection using Gii carbon foam immersed in a phosphate buffer solution of pH 7nanoparticulate polymer of

intrinsic microporosity (PIM-1). See DOI:10.1016/j.elecom.2022.107394, the contents which is incorporated by reference to the fullest extent permissible.

- Optical detector.
- Self-charging hybrid energy generation device.
- Green gas conversion into useful chemical.
- Fuel cell, e.g. hydrogen fuel cell.
- Filters, including gas permeable filter.
- Heating device.

Feature R: Non-graphene carbon material foam

Conventional graphene foam appears, under a scanning electron microscope, to have large, open ring-like structures, typically 500 μm in size. The carbon foam generated using the Dual Laser process looks very different; **Figures 52 - 57A** are SEM images of this Gii carbon foam.

Figure 57B is a SEM of a carbon nano-onion, see 'Raman spectroscopy of polyhedral carbon nano-onions'. DOI: 10.1007/s00339-015-9315-9 and also 'Carbon nano-onions: unique carbon nano-structures with fascinating properties and their potential applications'. DOI:10.1016/j.ica.2017.07.021. The similarities to the Gii carbon foam are apparent.

As noted earlier, graphene foam has a number of characteristics: it is hydrophobic, with low wettability. Raman analysis of a typical graphene foam reveals the following signatures: absence of a D peak; the 2D peak is higher than the G peak; the peak D: peak G ratio is close to zero. Yet the carbon foam generated using the Dual Laser process shares none of these characteristics; it is hydrophilic, with a contact angle below 20°; it lacks the tell-tale Raman spectrum signature of graphene: it shows a significant D peak; the 2D peak is significantly less than the G peak; the peak D: peak G ratio is significantly above zero. **Figure 58** shows the Raman shifts for eight sheets of carbon foam made using the Dual Laser process, showing the consistency of the Raman signature. It also shows a significant D peak; the 2D peak is less than the G peak; the peak D: peak G ratio is above zero. As we noted earlier, this Raman spectrum has much in common with carbon nano-onions. see also **Figure 18C**, also from 'Raman spectroscopy of polyhedral carbon nano-onions'. DOI: 10.1007/s00339-015-9315-9.

The specific Dual Laser parameters used to create this low electrical resistance carbon nano-onion variant of Gii carbon foam are in **Table 5** below:

	First Laser	Second laser
Laser machine	S300	S300
Laser wavelength (nm)	Flexx - IR 1064nm	CO2 10600nm
Power (Watts)	11	36
Speed (mm/s)	810.11	188.15
PPI (pulses per inch)	n/a	1000
Frequency (Hz)	80000	n/a
DPI (Dot/inch)	1000	1000
Offset (mm)	0	15
Passes	1	1

Table 5

We can generalise to the following:

A carbon foam material made, at least in part, by the method defined in any of Features A – K above and that is hydrophilic, with a contact angle below 20°.

A carbon foam material made, at least in part, by the method defined in any of Features A – K above and with a Raman spectrum exhibiting a significant D peak; the 2D peak is less than the G peak; the peak D: peak G ratio is above zero.

A carbon nano-onion material made, at least in part, by the method defined in any of Features A – K above.

Note that any of the devices described earlier, e.g. sensors, pressure sensors, biosensors, Hall Effect sensors, supercapacitors, hydrogen fuel cells, filters, may be characterised by their use of these materials and so we can generalise to the following:

A device including a carbon foam material made, at least in part, by the method defined in any of Features A – K above and that is hydrophilic, with a contact angle below 20°.

A device including a carbon foam material made, at least in part, by the method defined in any of Features A – K above and with a Raman spectrum exhibiting a significant D peak; the 2D peak is less than the G peak; the peak D: peak G ratio is above zero.

A device including a carbon nano-onion material, made, at least in part, by the method defined in any of Features A – K above.

Appendix 1 A Supercapacitor implementation with a hydrogel electrolyte

Appendix 2 Gii-Cap+ Hydrogel

Appendix 3 GiiCap Iongel

Appendix 4 3-month Gii-Sens® Assay Feasibility Proposal

Appendix 5 Sensor implementations where a receptor is bonded to a 3D carbon foam material through a linker

Appendix 6 Benchmark experimental conditions:

Appendix 7 Optimisation of the surface immobilization of anti-human procalcitonin (cAb)

Note that **Appendices 1 - 7** describe specific implementations of Gii carbon foam.

Appendix 8 Consolidated list of Features and Optional Features

Appendix 1 A Supercapacitor implementation with a hydrogel electrolyte

Background

A supercapacitor is a device which stores electrical charge. In terms of its make-up and function, a supercapacitor lies between an electrolytic capacitor and a rechargeable battery.

The properties of a supercapacitor make it superior over a rechargeable battery in applications where short charging times are required and also in applications where numerous charge/discharge cycles are used. Shortcomings of a supercapacitor over a battery include a lesser capacity to store energy over a long period of time.

Operational limitations of a supercapacitor are imposed by the material properties of the components. In particular, the maximum voltage at which a supercapacitor can operate, i.e. to which it can be charged, is dependent on the stability of the electrolyte and/or the electrodes. The maximum voltage of a capacitor is an important parameter, particularly so as the amount of energy stored by a capacitor is proportional to the square of the voltage. A supercapacitor with an organic electrolyte generally supports a higher voltage than one with an aqueous electrolyte. By utilising an organic electrolyte, the supercapacitor designer may produce a device with a working range of 2.5 to 2.7 V. In contrast, aqueous electrolytes, although often preferable for reasons of reduced cost and reduced toxicity, generally produce a device with a lower working voltage range. Known symmetric aqueous supercapacitors are generally unable to support voltages higher than 1.3 – 1.5 V. If electrodes of different materials are used, this voltage limit may reach 1.8 – 2.0 V. The limitation for an aqueous based supercapacitor is due to the electrolysis of water which in principle occurs when it is exposed to a potential difference of 1.23 V. In practice however in order to overcome the effect of overpotential a larger potential difference is required before electrolysis occurs.

Electrodes based on carbon have been associated with supercapacitors since the early days of their development. Initially carbon was of interest as an electrode material because it provided the possibility to manufacture electrodes with large surface areas. It was only later in the development of supercapacitor devices that the importance of the so-called double layer at the electrode surfaces was realised. This complex and often ill-understood phenomenon, which is linked to the use of carbon as an electrode material, is at the heart of the high capacitance values associated with supercapacitors. Supercapacitor devices which comprise carbon-based

electrodes are considered to involve a double layer at the electrode surface, and the energy is stored electrostatically. Such supercapacitors are referred to as electrostatic double-layer capacitors, or EDLCs.

Other categories of supercapacitor exist. Electrochemical pseudocapacitors utilise metal oxide electrodes or conducting polymer electrodes. In contrast to the electrostatic charge storage mechanism of EDLCs, the charge storage in a pseudocapacitor is largely electrochemical. A third type of supercapacitor is the hybrid capacitor. A hybrid capacitor has asymmetric electrodes. One electrode is typically of carbon and has an electrostatic charge storage character; the other electrode is typically a lithium containing or a lithium doped material, which exhibits mainly electrochemical charge storage character.

Conventionally a supercapacitor can be thought of and is modelled as a series connection of two capacitors, one associated with each electrode. Each capacitor is positioned at the interface between electrode and the electrolyte, and is formed from the supercapacitor electrode, a dielectric layer formed from solvent molecules present in the electrolyte (called the inner Helmholtz plane), and a layer of charge carriers supplied by the electrolyte as counter-charges to charge on the electrode (called the outer Helmholtz plane). This triple structure of electrode, inner Helmholtz plane and outer Helmholtz plane forming a capacitive system at each electrode is referred to as the double layer, or electrical double layer.

Summary of this Appendix 1 Feature

A first aspect of the feature provides a symmetric supercapacitor device comprising: two electrodes, wherein each electrode comprises carbon foam as described in this specification (see for example **Features A – K** in **Appendix 8**); and an ion gel or hydrogel electrolyte enveloping the electrodes in an active area.

We have found that a symmetric supercapacitor device according to the above combination of features produces an enhanced operational voltage window. Referring to the device as symmetric means that the electrodes comprise, and may be composed of, the same material.

The operational voltage window, or window of operation, of a supercapacitor is a key parameter of such a device and is determined by the breakdown voltage of the electrolyte. For

an aqueous electrolyte-based supercapacitor, the breakdown of water is generally responsible for limiting the operational voltage window.

Although the reasons for the unexpectedly large operational window observed with the presently disclosed device are not understood in detail, and without any constraint to theory, it is apparent that the exceptional properties are a consequence of the combination of carbon foam electrodes and the electrolyte, and in particular a consequence of the interface between these elements.

The large operational window of the present device equates in electrochemical terms to an unexpectedly large overpotential at the electrode. The overpotential is the potential difference beyond the thermodynamic redox potential for a particular reduction/oxidation reaction which is required for that reaction to occur. Overpotential is generally an ill-understood phenomenon, partly because there are many factors which contribute to it. For example, the overpotential is dependent on the electrode material, on the electrode morphology, and on the nature of the electrolyte. In the present feature, the large surface area presented to the electrolyte by the carbon foam electrodes is thought likely to play a role in the device performance. How ions diffuse to the electrode surface from the bulk of the electrolyte and the associated depletion of charge carriers at the electrode surface is known to have an effect on overpotential. This may play a role in the present device. Diffusion rates of charge carriers in the electrolyte may be affected by the presence of hydrated ions which are larger in size than un-hydrated ions. There may also be effects on the overpotential arising from the interaction between the charge carriers and the morphology of the carbon foam electrodes. The presence of the ion gel or hydrogel polymer is thought also to have an effect, possibly steric and related to the carbon foam morphology, on the diffusion of charge carriers to the electrode surface.

A hydrogel is a gel in which the liquid constituent is water, and which may be formed from a network of polymer chains. A supercapacitor in which the dielectric is formed by a hydrogel electrolyte would be expected to have the performance characteristics associated with an aqueous electrolyte-based supercapacitor. Against this expectation however, the present inventors have found that the performance of a supercapacitor according to the first aspect, i.e. a symmetric device, wherein the electrodes are of the same material, these electrodes comprising carbon foam and being enveloped in a hydrogel electrolyte, outstrips that expected of an aqueous based device. The operational voltage window of the device is unexpectedly

enhanced over an aqueous electrolyte-based device. The window of operation is more akin to an organic solvent-based supercapacitor.

Polyvinyl alcohol (PVA), polyvinylpyrrolidone (PVP), sodium polyacrylate, acrylate polymers and copolymers with an abundance of hydrophilic groups are examples of polymers which may be utilised in hydrogels. Fluorinated hydrogels may be used. The combination of a hydrogel and ionic charge carriers helps to achieve the surprisingly large window of operation achieved by the present system.

The electrodes of the device presently disclosed are situated on the substrate and the electrolyte is present on top of the electrodes in a manner which seals at least part of the electrode structure, thus forming an active area. The active area of the supercapacitor is an area of the supercapacitor comprising electrolyte and electrodes in which charge is stored.

The electrodes of the device may have an interdigitated geometry, i.e. they may be interdigitated. An interdigitated electrode geometry helps to maximize the capacitance of the supercapacitor. An interdigitated electrode geometry additionally enables a device without a separator. Supercapacitors normally include a separator between oppositely facing electrodes to prevent short circuiting between the electrodes. The absence of a separator eases construction of a supercapacitor device. A separator may also have negative effects on device performance, for example by inhibiting charge flow leading to lowered charge/discharge rates. The absence of a separator avoids these negative performance effects.

An interdigitated electrode geometry is well suited to a symmetric device. It is clearly more complicated to construct an interdigitated electrode geometry structure if the materials of the opposing electrodes are different than if the electrodes are of the same material. If the electrodes are of the same material, then the electrodes can be manufactured, possibly in situ, in one method step. If different electrode materials are used, then a plurality of manufacture steps are required, greatly complicating the process of manufacture.

The absence of a separator additionally removes any negative effects that a separator may have on device performance, for example inhibition of charge flow leading to lowered charge/discharge rates.

The hydrogel electrolyte may comprise a concentration of charge carriers which is sufficiently high to produce said enhanced operational voltage window.

It may be that the enhanced operational voltage window is dependent on the concentration of charge carriers.

The charge carriers may have a redox potential supporting the enhanced operational voltage window.

The charge carriers may be provided by an aqueous solution of an acid, by an aqueous solution of an alkali, or by an aqueous solution of a salt. Acids which may be used include sulphuric acid. Alkalis which may be used include potassium hydroxide.

The hydrogel electrolyte may comprise a mixture of a hydrogel and a salt. The electrolyte may be composed of a hydrogel, whose hydrogeling polymer may be for example PVA or PVP. The salt may be, for example, $NaClO_4$ or $NaNO_3$ or $Mg(ClO_4)_2$. The molarity of the salt may be for example 0.5M or greater, for example 1M or greater, for example 2M or greater, for example 2.5M or greater, for example 3M or greater, for example approximately 5M. The molarity of the salt may be for example between 1M and 10M, or it may be for example between 2.5M and 7.5M.

Salts which may be used include phosphonium salts, perchlorate salts, nitrate salts and arsenate salts. Examples of salts include sodium sulphate, sodium disulphate, sodium persulphate, sodium perchlorate, lithium perchlorate, magnesium perchlorate, sodium nitrate, lithium hexafluoride arsenate. Aqueous solutions of these salts may be used in the electrolyte to provide ionic carriers.

The charge carriers may be ions. The charge carriers may be hydrated ions.

A hydrated ion is an ion in an aqueous environment. Polar water molecules arrange themselves around the ion forming a hydration sphere centred on the ion. The details of the mechanism behind the surprisingly wide enhanced operational voltage window observed with the present feature are ill understood and the inventors do not wish to be constrained by theory. Nevertheless, the surprising advantageous properties of the present device are the result of a

synergy between the electrode and the dielectric materials. The enhanced performance is an expression of a lack of water splitting under voltage conditions where the person skilled in the art would expect electrolysis to occur. It is expected that the interface between the electrode and the electrolyte lies at the origin of its performance. It is possible that there is a synergetic interaction between the size of the charge carriers, possibly hydrated, and the size of pores present in the electrodes. A hydrogel comprises a network of polymer chains and this chain network of the hydrogel may also have a physical (steric) effect which limits the exposure of water molecules to potential difference which can cause their splitting.

The increased size of hydrated ions is thought to combine with the porous structure of the carbon foam electrode to hinder diffusion close to the electrode surface, with the consequence that the overpotential is increased.

The electrodes of the symmetric supercapacitor device may comprise porous carbon foam. Optionally the electrodes may comprise no additional binder material.

Porous carbon foam electrodes are believed to combine with the charge carriers in the electrolyte to increase the overpotential and thereby enhance the operational window of the supercapacitor.

Carbon foam consists of one or more 2D carbon sheets (each sheet being a layer of sp2 bonded carbon) folded back on one another to form a three-dimensional structure rather than a planar sheet. Carbon foam lacks the regular AB stacking of planar carbon sheets found in graphite or multilayer 2D carbon. A carbon foam material is typically porous. Carbon foam has a high surface area. The porosity of the carbon foam and as a result the surface area of the foam can be controlled by varying parameters of the growth method. This has the advantage that the porosity of the electrodes of the device can be controlled during a manufacturing process of the electrodes.

The carbon foam electrodes may be on a substrate. The carbon foam electrodes may be on a polyimide substrate. The polyimide substrate may be polyimide. The substrate may form a substrate of the supercapacitor device. The substrate may be sufficiently thin so as to be flexible, resulting in a supercapacitor device which is flexible. It may be that the substrate

comprises (e.g. is formed from) one or more of the following materials: polyimides (for example, poly(4,4'-oxydiphenylene-pyromellitimide), otherwise known as polyimide), polyetherimides (PEI), poly(methyl methacrylate) (PMMA) (e.g. spray-coated PMMA), polyurethanes (PU), polyesters, vinyl polymers, carbonized polymers, photoresist polymers, alkyds, urea-formaldehyde.

These substrate materials can be utilised as a source of carbon which is transformed to carbon foam using the Dual Laser process described above. Production of carbon foam in this way can be achieved by irradiating a polyimide substrate (for example) with radiation, for example laser radiation. This produces carbon foam which is chemically fixed indirectly to the substrate via an intermediary layer of an amorphous non-graphene substance which is directly attached to the substrate (see earlier in this specification), resulting in a robust structure. The electrodes are thus produced in situ by using part of the substrate as a carbon source, i.e. as a reagent for producing carbon foam. The structure can at the same time as being robust be flexible. A flexible device is advantageous in many respects. A device which is flexible can be advantageously packaged, for example by rolling it up. A device which is flexible can also be attached to surfaces of curved structures, for example.

The substrate may be substantially planar. The substrate may be a film, for example a thin film. The substrate may have a thickness of greater than 5 μm. The substrate may have a thickness of less than 120 μm. The substrate may have a thickness of between 5 μm and 120 μm. The thickness of the substrate may be substantially uniform across the surface of the substrate. The substrate may be flexible. The substrate may be pliable.

The substrate may be a polyimide tape (e.g. a polyimide tape) having a first surface and a second surface.

The electrodes may be mass balanced to optimise the operational voltage window.

A supercapacitor can be considered as two capacitors connected together in series. To maximise the capacity of the supercapacitor, the capacity of the two constituent capacitors should be equal. This can be engineered by adjusting the surface area of the individual electrodes, thus compensating for other factors contributing to the capacity, such as the nature of the solvated ions. This process of adjusting the individual electrodes is called mass

balancing. Mass balancing of the electrodes has the advantage that the capacity of the superconductor device can be maximised, and the lifetime of the supercapacitor can be extended.

In a second aspect, there is a method of manufacturing a symmetric supercapacitor device according to the first aspect, whereby:

the electrodes are formed on a substrate;

an electrolyte precursor comprising charge carriers and a hydrogel is applied to the electrodes;

the electrolyte is formed from the precursor, causing the electrodes to be embedded in the electrolyte in an active area.

Electrodes of carbon foam may be made by converting part of the substrate (if said substrate is or comprises a carbon source) to carbon foam, or by using chemical or physical deposition methods, such as physical vapour deposition (PVD), chemical vapour deposition (CVD), molecular beam epitaxy (MBE), sputtering, laser induced growth, pulsed laser deposition, cathodic arc deposition, spin coating, dip coating or sol-gel methods. In this way, the electrodes are produced on the substrate in situ.

The electrolyte precursor may be prepared by preparing an aqueous solution of charge carriers and by mixing this aqueous solution with a hydrogel. The electrodes may be formed using laser radiation.

When preparing the electrolyte precursor the undesirability of precipitation or crystallisation of the salt in the electrolyte should be kept in mind. Precipitation of salt, or any solid, from the electrolyte may lead to cracking of the device, or to other defects of the device, or defects in the performance of the device. This places an upper limit on the concentration of the salt solution. It may be advantageous to avoid using a supersaturated solution of salt. The precise upper concentration limit may depend on the particulars of the chemicals present. For sodium perchlorate, the inventors have found that a concentration of 5M produces an electrolyte which avoids precipitation or crystallisation of the salt and also, in combination with the other features, gives a supercapacitor device with an operational window beyond that which would be expected from a consideration of the individual components. The electrolyte may comprise a salt solution with a concentration of greater than 4M. The electrolyte may comprise a salt

solution with a concentration of greater than 3M, or greater than 2M, or greater than 1M, or greater than 0.5M.

At higher concentrations, salt was observed to readily precipitate from the electrolyte gel, and too quickly for a viable device. This precipitation may be caused by evaporation of water. Water loss through hydrolysis may be another cause. In any case, the inventors found that although an electrolyte gel could be formed using concentrations of sodium perchlorate up to 16.5 M, the problem of precipitation was observed at all concentrations upwards of 10 M.

When manufacturing the hydrogel electrolyte, a high molar solution of salt may be used.

Smaller concentrations of salt solution are generally advantageous for cost reasons.

The carbon foam layer may be between 10 μm and 100 μm thick. This facilitates a flexibility in the device. The device may be rolled up to become more compact.

A gap of between 100 μm and 1000 μm may separate the electrodes from each other. The capacity of the device has a dependency on the gap between the electrodes and consequently regulation of this gap affects the amount of charge which can be stored.

The operational window of the present device may be greater than 1.5 V, or it may be greater than 2 V, or it may be greater than 2.5 V.

Optional and preferred features of any one aspect of the system may be features of any other aspect of the system.

Appendix 1 Description of the Drawings

We reference the following Figures in which:

Figure 59 presents carbon foam cyclic voltammograms for positive voltages measured at 25 mV/s.

Figure 60 presents carbon foam cyclic voltammograms for negative voltages measured at 25 mV/s.

Figure 61 presents carbon foam galvanostatic charge discharge (GCD) curves measured at 0.5 mA/cm^2 for positive voltage windows.

Figure 62 presents carbon foam galvanostatic charge discharge (GCD) curves measured at 0.5 mA/cm^2 for negative voltage windows.

Figure 63 presents carbon foam galvanostatic charge discharge (GCD) data taken from five two-electrode devices.

Figure 64 presents carbon foam cyclic voltammograms recorded from five different two-electrode devices at high (left) and low (right) scan rates.

Figure 65 presents carbon foam cyclic voltammogram data for five additional systems, differing through the nature of the hydrogel electrolyte: (a) 3M $NaClO_4$ and PVA; (b) 1M $NaClO_4$ and PVA; (c) 2.5M $NaNO_3$ and PVA; (d) 3M $Mg(ClO_4)_2$ and PVA; and (e) 5M $NaClO_4$ and PVP.

Appendix 1 Detailed Description

Two-electrode supercapacitor

A typical carbon foam supercapacitor device according to this feature has interdigitated carbon foam electrodes, as shown in Figure 26. To re-cap, a polyimide substrate supports the supercapacitor electrodes which are composed in this example of carbon foam and which are arranged in an interdigitated comb geometry, and which form an interdigitated electrode structure. A silver current collector runs down each side of the device serving to electrically unify each opposing electrode. The non-substrate sides of the interdigitated electrode structure is enveloped in a hydrogel. It is possible to add a polyimide lid to contain the hydrogel, or otherwise package the device in a suitable manner.

As explained earlier, the carbon foam electrodes may be formed on the polyimide substrate. By exposing a suitable substrate, being one which provides a source of carbon, in this example a polyimide substrate, to a laser beam, carbon foam is created over the substrate. Carbon foam produced in this way grows out of the substrate and is adhered indirectly to the substrate. The substrate and a carbon foam electrode formed in situ in this manner form one body.

The carbon foam electrodes were produced using an infrared CO2 laser under ambient conditions. The substrate was commercial polyimide film with a nominal thickness of 127 microns. One example has eleven parallel strips of carbon foam for each electrode. This number can clearly be varied. The carbon foam strips for the positive electrode are offset from the carbon foam strips for the second electrode, thus forming the interdigitated structure.

The electrode dimensions are as set out in **Table 6:**

Mass balance ratio	1.18
Positive half-cell 'electrode fingers'	
Length (cm)	0.4
Width (cm)	0.0472
Thickness (cm)	0.005
Number of fingers	11
Total Area exposed (cm^2)	0.20768
Negative half-cell 'electrode fingers'	
Length (cm)	0.4
Width (cm)	0.04
Thickness (cm)	0.005
Number of fingers	11
Total Area exposed (cm^2)	0.176
Distance between fingers (cm)	0.04
Total active electrode surface area (cm^2)	**0.38368**
Total active electrode volume (cm^3)	**0.0019184**

Table 6

Three-electrode device

In addition to the two-electrode supercapacitor device, a three-electrode test device additionally comprising a reference electrode has also been fabricated. The three-electrode device comprises a working electrode, a counter electrode and an Ag/AgCl reference electrode. Each

of the working electrode and the counter electrode is made from carbon foam, produced in this particular embodiment by the Dual Laser illumination of a polyimide substrate, as described earlier. This device is used to determine the voltage range within which the $NaClO_4$ hydrogel electrolyte is stable. The three-electrode device was left to stabilise for at least one hour following fabrication before any measurements were performed.

Preparation of the hydrogel electrolyte

Each of the two-electrode and the three-electrode devices disclosed is based on a 5M solution of sodium perchlorate and the electrolyte was prepared in the manner now described. A 5M solution of sodium perchlorate was prepared by dissolving sodium perchlorate (98% purity from Sigma-Aldrich) in deionised water (quantities used: 3.061g of NaClO4 was dissolved in 5ml deionised H2O). The sodium perchlorate solution was then stirred with a magnetic stirrer on a hot plate at 120°C while polyvinyl alcohol (PVA, 99% hydrolyzed, Sigma-Aldrich) was added. For every 10 mL of solution, 1.5 g of PVA was dissolved. The mixture of sodium perchlorate solution and PVA was removed from the hot plate and allowed to cool, whereupon it forms a white opaque gel-like solution. The gel solution is then heated to 120°C, until it liquefies and turns clear. It is then deposited onto the graphene electrodes. After deposition on the electrode surfaces, the liquified hydrogel electrolyte material solidifies in approximately 5 minutes at room temperature. The quantity of electrolyte which is deposited on the electrodes depends on the surface area to be covered. For the test device, 150 μL of electrolyte was deposited.

Experimental results from the three-electrode device

The performance which is obtainable from a supercapacitor is ultimately limited by the stability of the electrolyte.

To test the electrolyte stability in the present system, several experiments were run using the three-electrode device herein described. Differential pulse voltammetry (DPV) was initially used to select which voltage windows were investigated by cyclic voltammetry (CV) and galvanostatic charge discharge (GCD) measurements.

i Cyclic voltammetry

Cyclic voltammetric measurements were carried out to determine the stability of the electrolyte. In a standard three electrode measurement the potential between the working and reference electrodes was swept at a constant rate from an open circuit potential (OCP; nominal 0 V) to a predetermined upper limit, before being swept down again. The current response at the working electrode was monitored during this time.

Results of these measurements are shown in **Figure 59** and **Figure 60**. **Figure 59** shows results in which the voltage is scanned from OCP in a positive direction.

The upper set of results shows four voltammograms of maximum potential 1 V, 1.2 V, 1.3 V and 1.4 V. The lower set of results additionally includes a voltammogram of maximum potential 1.6 V. As the upper voltage limit increases beyond 1.2 V the shape of the cyclic voltammogram becomes less "square-like". The tail which becomes increasingly prominent as the end scan voltage becomes larger is indicative of electrolyte degradation, probably due to electrolysis of water. These voltammograms indicate that the electrolyte is stable up to +1.2V.

Figure 60 shows a similar set of results but taken for negative voltages. These data suggest that the electrolyte is stable to –1.4 V.

Taken together, the data in **Figures 59** and **60** give a working window for the device of 2.6 V. This is considerably higher than anything expected from using a water-based electrolyte.

ii Galvanostatic Charge Discharge (GCD) Data

Galvanostatic charge discharge (GCD) measurements were performed to determine coulombic efficiency from charge and discharge times. In these measurements a current is applied between the counter and working electrodes, and the voltage response of the working electrode (with reference to the reference electrode) is measured. GCD curves measured using a discharge current of 2×10^{-5} A (0.5 mA/cm^2) for selected voltage windows are shown in **Figure 61** for positive voltages. The curves plateau beyond 1.2 V which indicates electrolyte degradation. GCD curves for selected negative voltage windows are shown in **Figure 62**.

Significant plateauing is seen for voltage windows up to -1.6 V and -1.8 V, indicating electrolyte degradation. A voltage window of -1.4 V has a triangular shaped GCD curve and indicating stability.

Results from the cyclic voltammetry measurements and from the galvanostatic charge discharge measurements on the three-electrode system are summarised in the following tables.

The first table, Table 7, summarises average coulombic efficiency, areal discharge capacitance and discharge energy data for positive voltage windows.

EW	**Average Coulombic**	**stdev**	**Average Discharge**	**stdev**	**Discharge Energy from GCD**
[V]	**[%]**	**[%]**	**[mF/cm^2]**	**[mF/cm^2]]**	**[J]**
1	93.9	0.91	1.59	5.66E-02	3.12E-05
1.1	91.7	1.32	1.69	6.23E-02	4.02E-05
1.2	**87.8**	**1.30**	**1.82**	**7.53E-02**	**5.17E-05**
1.4	54.9	7.04	2.95	3.56E-01	1.14E-04
1.6	25.3	2.71	9.60	1.32E+00	4.05E-04

Table 7

The second table, Table 8, summarises average coulombic efficiency, areal discharge capacitance and discharge energy data for negative voltage windows.

EW [V]	**Average Coulombic efficiency**	**Stdev**	**Average Disch. Areal Cap.**	**stdev**	**Discharge Energy from GCD [J]**
-1	87.86	9.911	1.2970	0.311	2.65E-05
-1.2	87.98	7.354	1.5103	0.577	3.84E-05
-1.4	**87.04**	**5.636**	**1.8482**	**1.012**	**5.72E-05**
-1.6	82.21	5.419	3.1486	2.598	1.30E-04
-1.8	67.16	17.728	5.3844	4.637	2.88E-04

Table 8

In these summary tables, the coulombic efficiency is the ratio of the stored and delivered energy measured in the second GCD cycle; the areal capacitance in mF/cm^2 is calculated by the following formula:

$$Areal\ Capacitance\ \left[\frac{mF}{cm^2}\right] = \frac{2 * E_{(dis)charge}[J]}{A_{geometric}\ [cm^2] * (EW)^2\ [V^2]} * 1000$$

and the discharge energy is the integral over time of the charge and discharge portions of the GCD curve.

The GCD curves indicate that +1.2 V and -1.4 V are realistic positive and negative voltage limits.

These values of voltage limits and areal capacitances allow a mass balance to be calculated according to the following formula:

$$\frac{m^+}{m^-} = \frac{C^- \Delta E^-}{C^+ \Delta E^+}$$

where m^+ = mass of positive electrode, m^- = mass of negative electrode, C^+ = capacitance (F) of positive electrode, C^- = capacitance (F) of negative electrode, ΔE^+ = positive voltage window limit, ΔE^- = negative voltage window limit.

Experimental results from the two-electrode device – supercapacitor performance

Galvanostatic charge discharge (GCD) data were collected for the two-electrode supercapacitor device for a range of applied current densities from 0.25 mA/cm^2 to 30 mA/cm^2. **Figure 63** plots GCD results taken from five different devices (CH1 – CH5). A voltage window of 2.6 V is utilised to collect these data, with greater electrolyte stability being observed at higher current densities. Further performance data for the two-electrode supercapacitor are presented in **Figure 64**, showing cyclic voltammograms recorded from five different devices (devices #1 to #5) according to the present implementation at scan rates from 0.01 V/s to 5 V/s.

The cyclic voltammograms in the right hand column were recorded at low scan rates (0.01 V/s, 0.025 V/s, 0.05 V/s, 0.075 V/s, 0.1 V/s, 0.25 V/s and 0.5 V/s) and those in the left hand column at high scan rates (0.75 V/s, 1 V/s, 2 V/s, 3 V/s, 4 V/s and 5 V/s). The trend shown in these data is to higher electrolyte stability at higher scan rates. In each set of cyclic voltammograms shown in **Figure 64**, faster scan voltages result in larger differences in the current response between ramping the voltage up and ramping the voltage down.

In addition to the above disclosed devices, devices were constructed in a similar way but with the hydrogel electrolyte comprising (a) 3M $NaClO_4$ and PVA, (b) 1M $NaClO_4$ and PVA, (c) 2.5M $NaNO_3$ and PVA, (d) 3M $Mg(ClO_4)_2$ and PVA, and (e) 5M $NaClO_4$ and PVP.

Cyclic voltametric measurements on these additional devices are shown in Figure [.] 10. For each electrolyte a cyclic voltammogram was run between 0 V and 0.7 V; between 0 V and 0.8 V; between 0 V and 0.9 V; between 0 V and 1.0 V; between 0 V and 1.2 V; between 0 V and 1.3 V; and between 0 V and 1.4 V. Similarly, for each electrolyte a cyclic voltammogram was run between 0 V and -0.7 V; between 0 V and -0.8 V; between 0 V and -0.9 V; between 0 V and -1.0 V; between 0 V and -1.2 V; between 0 V and -1.3 V; and between 0 V and -1.4 V. These data are shown in **Figure 65**.

The data indicate that in each device the electrolyte is stable to the limits of -1.4 V and +1.1 V, and to +1.2 V for each of (d) 3M $Mg(ClO_4)_2$ and PVA, and (e) 5M $NaClO_4$ and PVP.

Further variations and modifications may be made within the scope of the disclosure.

Appendix 1 Concepts

1. A symmetric supercapacitor device comprising:
   two electrodes, wherein each electrode comprises carbon foam material; and
   a hydrogel electrolyte enveloping the electrodes in an active area.

2. The symmetric supercapacitor device according to concept 1, wherein said hydrogel electrolyte comprises a mixture of a hydrogel and a salt.

3. The symmetric supercapacitor device according to either concept 1 or concept 2, comprising ionic charge carriers.

4. The symmetric supercapacitor device of concept 3, wherein the ionic charge carriers are hydrated.

5. The symmetric supercapacitor device according to any one of the preceding concept, wherein said electrodes comprise carbon foam.

6. The symmetric supercapacitor device according to any one of the preceding concept, wherein said electrodes comprise carbon foam material.

7. The symmetric supercapacitor device according to any one of concepts 1, 5 and 6, wherein the carbon foam material is formed on a substrate.

8. The symmetric supercapacitor device according to concept 7, wherein the substrate is a polyimide substrate.

9. The symmetric supercapacitor device according to either concept 7 or concept 8, wherein the substrate forms a substrate of the device.

10. The symmetric supercapacitor device according to any of the preceding concept, wherein the symmetric supercapacitor device is flexible.

11. A method of manufacturing a symmetric supercapacitor device according to any of concept 1 to 10, whereby:

the electrodes are formed on a substrate;

an electrolyte precursor comprising charge carriers and a hydrogel is applied to the electrodes;

the electrolyte is formed from the precursor, causing the electrodes to be embedded in the electrolyte in an active area.

12. The method of manufacturing a symmetric supercapacitor device according to concept 11, whereby the electrolyte precursor is prepared by preparing an aqueous solution of charge carriers and by mixing this aqueous solution with a hydrogel.

13. The method of manufacturing a symmetric supercapacitor device according to either concept 11 or concept 12, whereby the electrodes are formed in situ.

14. The method of manufacturing a symmetric supercapacitor device according to any one of concepts 11 to claim 13, whereby the electrodes are formed by irradiating said substrate with laser radiation.

Appendix 2 : Gii-Cap+ Hydrogel

In this **Appendix 2** section, we demonstrate the effectiveness of Gii carbon foam as an ideal substrate onto which pseudocapacitive materials can be deposited, yielding greatly enhanced capacitance compared to Gii carbon foam as the sole electrode material. For context, these carbon foam -only devices show full cell specific capacitances in the 0.25 – 0.4 mF/cm2 region.

Sample Preparation

A7-sized Gii-Caps were electrodeposited in order to cast a layer of pseudocapacitive material onto them. Both v4 and v5 designs are suitable for electrodeposition, yielding similar performance. Results for v4 samples will be detailed in this document.

Sheets containing 6 Gii-Cap devices (2 rows, 3 columns) were first cut in half, yielding two 3-device half-sheets. The two half-sheets were mounted on an in-house made jig and placed inside the electrodeposition tank, MiniPlant 3. Samples were first deposited with MnOx, rinsed with deionised water and subsequently deposited with FexOy. After FexOy deposition, they were rinsed again and dried in air at 40^{o}C for at least 2 hours.

The specifics of the deposition are follows. Manganese oxide precursor solution contained a mixture of manganese acetate tetrahydrate (40 mM) and a surfactant (Tween20, 0.1 wt%). Depositions were carried out by constant-current pulses. ON time was 0.5 seconds, OFF time 2 seconds. ON current applied was 744 mA (19.14 mA/cm2, based on the nominal geometric area of the electrode). OFF current was 0 mA, i.e. open circuit. MnOx was deposited for a total of 390 cycles (3.7 C/cm2 per electrode). The FexOy precursor solution comprised of a 40 mM Fe-TEA complex (TEA is triethanolamine). It contained FeCl3, TEA, and NaOH. Deposition was also carried out by constant-current pulses. ON time was 1s, OFF time 2s. ON current applied was 233 mA (6 mA/cm2), with OFF current set to 0 mA. The deposition was performed for 1,000 cycles, resulting in 6 C/cm2 per electrode.

After depositions were complete and samples dried, they were singulated into individual devices. A quasi-reference electrode (RE) comprising screen printed Ag/AgCl ink (used for monitoring individual electrode potentials during testing) was fixed along one of the device's edges, outside the working area. Electrolyte was then applied to the devices' working area and

extended onto the RE. The electrolyte used was an aqueous hydrogel, containing NaClO4 as the salt and PVA (Polyvinyl alcohol) as the gelling agent. A stock batch of hydrogel contains 199.5 g NaClO4 monohydrate, 256.9 ml deionised water and 42.4 g PVA. The mixture is solid at room temperature, becoming liquid at temperatures close to water's boiling point. In order to dispense the hydrogel, it was heated to 94°C to liquify it. It was dispensed by pipetting the liquid electrolyte onto the active area and RE, typically 3 – 4 ml per device. Hydrogel on the samples was then allowed to cool, resolidifying after approximately 10 minutes. Following solidification, excessive electrolyte evaporation was prevented by applying a polyimide film onto the devices. Once the lid was applied, the devices were ready for testing

Electrochemical Testing Parameters

Samples were electrochemically tested using a Biologic VMP-3 potentiostat/galvanostat. They were subjected to an initial performance characterisation, followed by 500 charge-discharge cycles (conditioning protocol), and completed with a final characterisation. The nominal values reported are those obtained in the second characterisation step. The conditioning protocol was applied to bring the samples to a more stable and consistent performance.

During testing, voltage was controlled at the cell level (absolute difference between positive and negative electrodes), with 0 V as the minimum and 2 V as the maximum. The potential differences between each electrode and the common RE were also measured, enabling the calculation of individual electrode performance metrics.

The two characterisation steps are known as Ragone tests. They were identical and comprised of the following:

a) Cyclic voltammetry (CV). Three scan rates used: 50, 100 and 250 mV/s. Five cycles per scan rate were applied.
b) Galvanostatic Charge-Discharge (GCD). Seven current densities were tested: 1, 2.5, 5, 7.5, 10, 20 and 30 mA/cm2 (based on total device geometric area = 12.96 cm2). Five cycles were performed at each current density.
c) Electrochemical Impedance Spectroscopy (EIS). Voltage-controlled, using a 1V DC applied voltage and 10 mV AC signal. Measured in 1 MHz – 10 mHz region.

The conditioning step was achieved by performing 500 GCDs at 10 mA/cm2.

Nominal capacitance values were calculated from GCDs after conditioning at 5 mA/cm2. ESR (Equivalent Series Resistance) was calculated from the voltage drop at the beginning of the discharge half-cycle in GCD. Reported ESR values are also from the final GCD at 5 mA/cm2. ESR can also be calculated from the Nyquist Plot attained from EIS. Results obtained are nearly identical.

Results and Conclusions

A total of 48 devices accounted for in the averages. Samples from batches 3258 and 3259 were employed. Typical CV curves are shown in **Figure 66**. The full cell response (left panel) shows a quasi-rectangular shape, indicating that the storage mechanism is not purely capacitive. This is expected, as both MnOx and FexOy are redox-active materials. Most of the capacitance of the device is concentrated at cell voltages above 0.5 V, as seen by the small envelope of the full cell curve in the region 0 – 0.5 V. The explanation for this smaller capacitance at low cell voltages can be seen on the half-cell curves, shown on the right panel of **Figure 66.** From this graph, it can be seen that MnOx acts as the positive electrode, while FexOy is the negative electrode. MnOx is a near-ideal pseudocapacitive material, as demonstrated by the largely rectangular shape of its CV (grey trace).

Meanwhile, the FexOy electrode shows a more asymmetric response with respect to potential. Most of its capacitance is concentrated at potentials below 0 V vs Ag/AgCl. At potentials > 0 V vs Ag/AgCl, FexOy displays little capacitance, as seen by the small envelope of the blue trace at these potentials. This asymmetric FexOy response therefore explains the smaller capacitance at low voltages obtained in the full cell.

Figure 66 shows Post-conditioning CV curves from sample 3258-1#4, obtained at 100 mV/s. Left panel shows full cell CV, while right panel displays the half-cell curves obtained during the full cell measurement.

Capacitance calculations were performed using the GCD curves, as these provide more accurate values. A typical GCD curve after conditioning is shown in **Figure 67**, with both full and half-cell measurements displayed. The device shows a good capacitive response with a quasi-triangular curve. The full cell presents a linear discharge from the maximum voltage down to ~0.5 V, indicating near-ideal capacitive behaviour enabled by the pseudocapacitance of MnOx and FexOy. As seen in the CV curves, FexOy shows an asymmetric capacitance vs potential relationship, which explains the faster discharge at cell voltages below 0.5 V.

Figure 67 shows post-conditioning GCD curves from sample 3258-1#4, obtained at 5 mA/cm2. Full cell and corresponding half-cell responses shown in top line, middle line and the bottom line, respectively.

In addition to different pseudocapacitive behaviour with respect to potential, the MnOx and FexOy electrodes also show different levels of capacitance. Both electrodes occupy the same geometric area in the device, however the MnOx electrode experiences a much smaller electrochemical window within the device (see differences between maximum and minimum electrode potentials in **Figure 66** and **Figure 67**). The reason for the smaller MnOx window (0.65±0.06 V) is its larger specific capacitance compared to FexOy (1.35±0.06 V window). For the devices assessed in this study, The MnOx capacitance after conditioning reached 246.8±36.0 mF/cm2, while that of the FexOy electrodes was 171.4±38.4 mF/cm2. These Gii-Cap+ devices are therefore symmetric in terms of electrode dimensions but asymmetric in terms of electrode composition and potential split.

Since a full cell is effectively two capacitors (formed by the double layer between an electrode and electrolyte counterions) in series, the total cell capacitance will be lower than that of a single electrode. The average full cell capacitance after conditioning was 52.5±9.4 mF/cm2. At the same current density as used for reporting nominal capacitance (64.8 mA, 5 mA/cm2 at the cell level), the ESR calculated from the voltage drop at the beginning of discharge was 0.85±0.12 Ω.

EIS measurements further confirm the good capacitive response of these devices, as seen in **Figure 68**. From the Nyquist plot, it is possible to estimate ESR by locating the point at which the curve crosses the y-axis. In the case of the sample shown in **Figure 68**, the ESR calculated from EIS was 0.78 Ω, which matches well with the 0.73 Ω calculated from GCD for the same sample. The Bode plot provides information about behaviour of the devices at different frequencies. At high frequencies, e.g. 100 – 10000 Hz, the devices function essentially like resistors, with a 0^{o} phase angle. As the frequency drops, phase angle increases, indicating a larger capacitance contribution (an ideal capacitor has a -90^{o} phase angle). When the phase angle surpasses the 45^{o} mark, the device is considered majority capacitive in nature. Hence, the time at which the 45^{o} phase shift occurs can be considered the characteristic time constant of the device. For the samples in this study, the average time constant was 4.48±1.18 seconds.

This time constant can be understood as a cycle time threshold for effective capacitive response. At cycle times below the time constant, the device will not operate fully adequately.

Figure 68 shows post-conditioning Nyquist (left) and Bode (right) plots from sample 3258-1#4, obtained from potentiostatic EIS at 1V DC (full cell). Inset in left panel shows a magnified view of the high frequency response.

Considering that devices utilising Gii as their sole electrode material display specific capacitances of 0.25 – 0.4 mF/cm2, the addition of pseudocapacitve materials has enhanced the energy storage capacity of these Gii-Caps more than 100x. Moreover, the addition of these metal oxides does not significantly increase the ESR of these devices, maintaining their usefulness in high power applications. The electrodeposition process is controllable, enabling the fabrication of cells with less deposited material, and therefore less total capacitance, if desired. The resulting devices are asymmetric in nature, with MnOx as the primary positive electrode and FexOy as its negative counterpart.

Appendix 3 GiiCap Iongel

Goal: To demonstrate the specific capacitance, and electrochemically stable window (ESW) of an electrolyte formulation, comprising room temperature molten salts *1-ethyl-3-methylimidazolium tetrafluoroborate* ($EMIMBF_4$) and fumed silica, known as *Iongel* in conjunction with *GiiCap*® A7 devices at a 'low' humidity and an 'air-free' argon atmosphere environment.

Experimental Conditions:

All electrochemical tests were conducted under a '3-electrode' setup wherein a regular interdigitated A7 device was manufactured with a 'working' electrode and 'counter' electrode area ratio of 1:2, and a third quasi-reference electrode comprising screen printed AgCl ink for monitoring individual electrode potentials during testing.

Electrolyte, *Iongel*, was prepared and stored in an air-free environment.

Prior to application onto the A7 device for testing, the Iongel was heated to 90C and subsequently dispensed onto the A7 by 'doctor blading' a thin and consistent layer. The electrolyte was allowed to cool before the devices were ready for testing and connection. For air-free devices, testing was conducted in the same air-free environment wherein electrolyte was stored and dispensed, where the devices were connected to the electrochemical testing instrument: *Biologic VMP-3* potentiostat.

For the low humidity environment, devices were transferred to a humidity controlled chamber set to 20% relative humidity and sealed and connected to the instrument.

For each humidity, a range of maximum electrode potentials (Emax) in Volts (V) close to nominal literature values for the neat electrolyte[1] were tested. They were:

Positive: 2.0, 1.9, 1.8, 1.7, 1.6, 1.5

Negative: -2.0, -1.9, -1.8, -1.7, -1.6

For each humidity and electrode potential combination, N=8 samples were made from scratch.

Electrochemical testing parameters:

A standard protocol was used, where the testing window was 0.0 – Emax V Vs. OCV. OCV was

quantified as 0.25 V Vs. AgCl Qref.

Electrochemical tests were broken down into 3 stages: a) Ragone Characterisation; b) Long-Term (LT) cycling; c) Ragone Characterisation (post).

Ragone characterisation both before and after LT cycling comprised: OCV, 1 hour; Cyclic Voltammetry (CV) at 100, 1000 mV/s with 5 cycles each; Galvanostatic Charge-Discharge (GCD) at 5, 10 mA/cm^2 with 10 cycles each; Potentio-electrical impedance spectroscopy (PEIS) between 10 MHz – 0.01 Hz.

LT cycling comprised: CV at 750 mV/s for 5000 cycles.

Determination of electrochemical stability was by visual post-mortem analysis of electrode damage and electrolyte discolouration; and assessment of Coulombic efficiency change over the LT cycling period. Determination of device performance was determined from Specific Capacitance by GCD after the 5000 LT cycles.

Conclusion:

ESW was determined by plotting Coulombic Efficiency of the LT CV cycles versus number of cycles. When Coulombic efficiency remained consistent throughout the 5000 cycles, it would be determined that the cycling Emax was stable for the given environmental condition. From this analysis, it was found that at 20% relative humidity air, Iongel-A7 devices were stable at negative and positive electrode potentials of -1.6 and +1.6 V respectively. While in the air-free environment, negative and positive ESW were determined to be -1.8 and +1.7 V respectively

In terms of performance evaluation, it was found that at the positive window, 20% relative humidity and air-free devices had specific capacitances of 2.11 and 1.60 mF/cm^2 respectively. The negative window specific capacitances at 20% and air-free environments were 1.55 and 2.11 mF/cm^2

Figures 69, 70, and **71** are relevant results.

Figures 72, 73 and **74** are further relevant results.

Appendix 4 3-month Gii-Sens Assay Feasibility Proposal

Objective:

To use critical reagents to the Gii-Sens 3D Carbon Foam assay system to deliver a proof of feasibility project.

Phase 1: Surface immobilisation

Goal: Maximise the mAb (2) surface immobilisation. Evaluate the most convenient surface chemistry to immobilise the mAb onto the surface.

Deliverable: Data supporting the maximum surface coverage and procedure of choice.

Phase 3: Target analyte sensing range and LOD

Goal: Electrochemical immunoassay procedure and results. Establish the electrochemical immunoassay steps (incubation times, concentrations, volumes) and establish the parameters yielding most sensitive analytical assay.

Deliverable: Data supporting the electroanalytical immunoassay performance.

Experimental Section

Solution compositions

Surface Chemistry

10 mM Pyrene butyric acid in DMF

4 mM EDC / 10 mM SulfoNHS

PBS 0.1 M pH 7.2

Read out

1mM $K_3Fe(CN)_6$ + 1mM $K_4Fe(CN)_6$ in 0.02 M KCl

0,02 M PBS

Sensor Modification Procedure

10 µL PyrBuOOH onto sensor Surface incubated in wet chamber for 2 h before allowing for spontaneous solvent evaporation

15 µL EDC/NHS for 30 min

10 µL A1 or C1 mAb in PBS for 1 h

Electrochemical Techniques

Electrochemical impedance

Applied voltage = 0 V

Amplitude = 0.01VRMS

Frequency Range - 5000 - 0.1 Hz

Assay Procedures

Direct assay: Labeless: See **Figures 75** and **76.**

Direct assay: Labeless and Reagentless See **Figures** 77 and **78.**

Calibration Plots

- Replicates per point, n = 5 (minimum) different disposable sensors (single read out, sensors disposed)
- Each calibration plot contains data obtained in subsequent days and by different operators (inter and intra assay variability)

Phase 1: Surface Chemistry

The surface chemistry of choice was Pyr-COOH modified graphene and EDC/NHS conjugation of capture mAb (A1 and C1) following the **Figure 79** scheme showing surface immobilisation reaction schematics.

The concentration of surface immobilised mAb (A1 and C1) was screened using electrochemical impedance spectroscopy. (See experimental section). See **Figures 80 (**mAb

A1 immobilisation on Gii-Sens® surface. Inset normalised signal) and **Figure 81** (mAb C1 immobilisation on Gii-Sens® surface. Inset normalised signal).

Both A1 and C1 showed a logical surface coverage trend. Based on normalised curves A1 showed and marginally larger surface coverage. The optimum coverage range was screened to be between 15 to 250 µg/mL. That range on concentration was estimated enough to provide best performance of the sensor.

Phase 3: Assay and target analyte exploration

The more in-depth evaluation of the assay potential and the benefits of using Gii-Sens® as sensing electrochemical platform was conducted always in labeless assay format.
In parallel to that it was also explored a reagentless format, where the solutions used to both incubate and generate a read-out signal were just buffer, as described in the experimental section. The dynamic range of the assay was explored also at high concentrations also looking to identify the potential to extend that concentration range.

Due to the interesting results obtained during the investigations described above and general time limitations the sensitivity of the assay was explored down to 10 pg/mL and the aim was to explore the high concentration range up to 1000 ng/mL.

Labeless assay exploration

The labeless assay as described previously consisted in an assay that does not require a secondary antibody, but uses a particular electrochemical read out solution. During this investigation that electrochemical solution was also used as carrier solution, hence eliminating the need for washing steps or any other assay complications.

The first concentration range explored was from 10 ng/mL to 10 pg/mL, both for A1 and C1 modified sensors. See **Figure 82** which shows labeless dose response curve for A1 (top) and C1 (bottom) sensor vs. varying concentrations of N1 antigen. Surface coating > 60 µg/mL and assay incubation time of 6 minutes for all cases

Both A1 and C1 showed similar responses and achieved good preliminary dose response curve characteristics for the concentration range studied.

In order to further investigate how to enhance the performance of the assay the overall concentration range was divided and explored in different sensitivity ranges using the same data obtained.

Labeless and reagentless assay exploration

The labeless assay as described previously consists of an assay that does not require a secondary antibody. In the case of reagentless the presence of an electrochemical read out solution is also unnecessary as all the incubations and measurements are done in just buffer solution that also acts as carrier solution, further eliminating the need for extra washing steps.

The first concentration range explored was from 10 ng/mL to 10 pg/mL, both for A1 and C1 modified sensors. See **Figure 83** which shows labeless and reagentless dose response curve for A1 (top) and C1 (bottom) sensor vs. varying concentrations of N1 antigen. Surface coating > 60 µg/mL and assay incubation time of 6 minutes for all cases

Both A1 and C1 showed similar responses and achieved good preliminary dose response curve characteristics for the concentration range studied.

Appendix 5 Sensor implementations where a receptor is bonded to a 3D carbon foam material through a linker

Background

Sensors are analytical devices that detect changes or reactions and respond to some type of input from the environment. In recent years, the use of sensors has increased owing to their advantages such as high specificity and sensitivity, rapid and reliable results, easy handling, and point of care diagnostics. Due to these advantages, sensors have paved their way into a variety of technical areas such as chemical and medical diagnostics, environmental impact analysis, food industry, and marine sectors.

Different forms of graphene and its derivatives have been utilized in the production and development of sensors, especially biosensors. The electrochemical, physical and chemical properties of graphene make it a material of interest for these applications. However, conventional graphene (e.g., a 2D graphene) is difficult to handle during practical applications, due to its ultra-thin structure and flexibility, which causes it to easily curl, crease and corrugate. This significantly decreases the analytical performance of the sensors, especially with respect to their sensitivities. To date, numerous strategies and techniques have been carried out to make different types of graphene (e.g., different morphologies, different surface properties, different functionalized derivatives such as graphene quantum dots, graphene oxide, or reduced graphene oxide) and these cause difference in the sensing performance among the sensors.

E.A. Obaje, G.Cummins, H.Schulze, S.Mahmood, M.P.Y.Desmulliez and T.T. Bachmann, Journal of Interdisciplinary Nanomedicine, 2016; 0(0), doi: 10.1002/jin2.16 investigates the electrochemical performance of a newly fabricated sensor in relation to the function of its underlying composite materials and evaluates the choice of carbon and dielectric pastes by characterising properties like surface roughness, wetting and susceptibility of unspecific DNA binding.

L.H.Hess, A. Lyuleeva, B.M.Blaschke, M.Sachsenhauser, M. Seifert, and J.A.Garrido, ACS Appl. Materials & Interfaces, 2014, 6, 9705-9710 describes a platform for biosensing applications based on polymer-modified CVD-grown graphene transistors.

C. Fenzl, P. Nayak, T. Hirsch, O.S. Wolfbeis, H.N.Alshareef, and A.J. Baeumner, ACS Sensors, 2017,2, 616-620 describes a laser-scribed graphene (LSG) electrode as highly sensitive and reliable biosensor transducers in blood serum analysis.

S. Singal, A.K.Srivastava, S. Dhakate, A.M. Biradar and Rajesh, RSC Advances, 2015, 5, 74994-75003 describes electroactive graphene-multi-walled carbon nanotube hybrid supported impedimetric immunosensor for the detection of human cardiac troponin-I.

Despite all the prior art, there is a continued need to improve the sensing activities of those graphene-based sensors. Further, there remains a desire to improve sensitivities of said sensors without compromising at least one of the other aspects of those sensors such as their robustness, stability, durability, convenience of functionalization and/or ease of manufacturing.

Summary of this Appendix 5 Feature

In a first aspect, there is provided a sensor comprising: (i) a carbon foam electrode, (ii) a linker, and (iii) a receptor, wherein the receptor is bonded to the carbon foam electrode through the linker. The carbon foam electrode is made, at least in part, by the method defined in any of Features A – K above.

In a second aspect, there is provided a method of manufacturing a sensor according to the first aspect, comprising the steps in sequence of: (i) providing a carbon foam electrode as described in the first aspect; (ii) treating the carbon foam electrode with a linker; and (iii) treating the linker-modified carbon foam electrode obtained in step (ii) with a receptor.

In a third aspect, there is provided a method of sensing a target comprising the steps in sequence of: (i) providing a sensor according to the first aspect; (ii) contacting the sensor with a sample containing or suspected of containing the target; (iii) measuring a response of the sensor; and optionally (iv) correlating the response to the level of the target in the sample.

The carbon foam material typically has a folded structure, which affords the carbon foam a porous morphology with a high specific surface area. Without wishing to be bound by any theory, it is believed that the analytical performance of the sensors is affected by the morphology as well as the accessible surface area of the carbon foam. A 3D structure leads to

an increase in the available surface area, allowing linkers and receptors such as enzymes, proteins, nucleic acids, and antibodies to be efficiently bonded to the carbon foam, thus improving sensor performance with respect to sensitivities.

Additionally, it is also desirable to build the sensors with a very thick carbon foam layer. Preferably the layer thickness of the carbon foam is more than 50 μm. Since the carbon foam can be porous, this thick carbon foam layer is expected to provide even greater surface area, which is advantageous in enhancing analytical performance especially sensing properties as compared to other conventional graphene-based sensors.

The linker

In the context of the present feature, the carbon foam is modified by a linker as part of the process to form a required sensor. The carbon foam described above (e.g., the thick, porous carbon foam with folded structure) provides an improved base for modification since increased surface area is available for interaction with the linker, leading to improved sensitivities of the sensors.

The modified carbon foam is then treated by a receptor to obtain the sensor. Therefore, the linker functions as an intermediate between the carbon foam and the receptor. It may be that at least part of the linker is disposed (e.g., dispersed) within the carbon foam. It may be that the whole linker is disposed (e.g., dispersed) within the carbon foam.

The linker can be selected from nanoparticles, polymers, polymer brushes, ligands, organic compounds comprising one or more functional groups, molecules bonded to the carbon foam covalently or non-covalently, or mixtures thereof. Typically, the linker is selected from polymers (e.g. (meth)acrylate polymers), organic compounds comprising one or more functional groups, carbodiimides, diazonium compounds, or mixtures thereof.

Typically, organic compounds described above comprises one or more functional groups which are independently selected from oxygen, nitrogen, sulphur, halide, hydroxyl, carbonyl, carboxyl, amine, amino, amide, hydrophilic polymers, or mixtures thereof, optionally in combination with linear, branched or cyclic alkyl, alkylenyl, alkynyl, aryl residues, acryl, acyl, acyloxy, alkoxy, alkyleneoxy, or mixtures thereof. In the same embodiments, said optional

structures may be C1-C20 linear, branched or cyclic alkyl, alkylenyl, alkynyl, aryl residues, acryl, acyl, acyloxy, alkoxy, alkyleneoxy, or mixtures thereof. Still in the same embodiments, optionally, the organic compounds with the functional groups described above may further comprise one or more cyclic moieties that optionally comprise one or more heteroatoms, and at least one of the cyclic moieties is linked directly or indirectly to at least one of said functional groups, or the linker is a derivative that is an ester or salt of such an organic compound, or a compound that releases such an organic compound in reaction with the required 3D carbon foam. Representatively, the linker is selected from the organic compounds as described above in this paragraph.

Representatively, the linker is selected from 1-pyrenebutyric acid, N-hydroxysuccinimide (NHS), pyrene-1-carboxylic acid succinimidyl ester, 1-Aminopyrene, N-(1-pyrene) maleimide, or mixtures thereof.

The linker may be bonded to the carbon foam covalently or non-covalently. For example, diazonium compounds (e.g., diazonium salts) may be bonded to the carbon foam covalently. For non-covalent bonding, the linker may be bonded to the carbon foam by at least one of the followings: π–π interaction, ionic bonding, hydrogen bonding, hydrophobic or hydrophilic effect, electrostatic interaction, polymer wrapping, adsorption, grafting (e.g., photo grafting). For example, the linker comprising one or more cyclic moieties as described above (e.g., 1-pyrenebutyric acid, N-hydroxysuccinimide (NHS), pyrene-1-carboxylic acid succinimidyl ester, 1-Aminopyrene, N-(1-pyrene) maleimide, or mixtures thereof) may be bonded to the carbon foam by π–π interaction.

In the context of the present feature, a receptor is bonded to the carbon foam through the linker. The receptor is thus indirectly bonded. When at least part of the linker or preferably the whole linker is disposed (e.g., dispersed) within the carbon foam, it may be that at least part of or the whole receptor is also disposed (e.g., dispersed) within the carbon foam.

By ‘receptor’ herein is meant to encompass any molecule capable of responding to a target material (i.e., a target) presented in a sample to be analysed. The sample can be a biological, chemical, optical, physical or mechanical sample, typically a biological sample. Hence, the target is meant to encompass but not limited to biological materials, chemical substances or mixtures, optical objects, physical or mechanical items, and the like, typically biological

materials. The term 'responding' can include but are not limited to biological, and/or chemical, and/or optical, and/or physical, and/or mechanical interactions, typically biological and/or chemical interactions. These typical interactions can include but are not limited to bonding, or hybridising, or hydrophobic effects between the receptors and the targets.

Accordingly, the receptor can include but are not limited to one of the followings: an electrochemical receptor, a chemical receptor, a bioreceptor, an optical receptor, a physical or mechanical receptor. The receptor can be selected from but is not limited to crown ethers, ligands, catalysts, boric acids, carbohydrates, aptamers, proteins, enzymes, antibodies, antigens, microorganisms, nucleic acids, fatty acids, fatty acid esters, molecularly imprinted polymers, metal-organic frameworks, polypeptides or oligopeptides capable of forming a ligand binding, cells, cell organelles, or other cellular components, or mixtures thereof.

Typically, the receptor is a bioreceptor (i.e., the sensor is a biosensor). Typically, the receptor is selected from aptamers, proteins, enzymes, antibodies, antigens, microorganisms, nucleic acids, polypeptides or oligopeptides capable of forming a ligand binding, cells, cell organelles, or other cellular components, or mixtures thereof. More typically, the receptor is selected from proteins (e.g., immunoproteins, non-immunological proteins, immunoglobulin binding proteins, sugar binding proteins), nucleic acids, antibodies, enzymes (e.g., oxidoreductases enzymes (preferably glucose oxidase, alcohol oxidase or lactate oxidase enzymes), dehydrogenase enzymes), or mixtures thereof. Representatively, the receptor is selected from immunoglobulin A (IgA), glucose dehydrogenase, streptavidin, or mixtures thereof.

Typically, the target is a biomaterial. The biomaterial can include but are not limited to deoxyribonucleic acids (DNA), ribonucleic acids (RNA), peptides, proteins, protein complexes, nucleic acids, antibodies, antigens, lipids, fatty acids, fatty acid esters, vitamins, microorganisms, micelles, cells, cell organelles, or other cellular components, viruses, enzymes, or mixtures thereof. Typically, the biomaterial is selected from deoxyribonucleic acids (DNA), ribonucleic acids (RNA), peptides, proteins, nucleic acids, antibodies, antigens, enzymes, or mixtures thereof. More typically, the biomaterial is selected from proteins, nucleic acids, antibodies, enzymes or mixtures thereof. It is further understood that under the context of the present feature, both the bioreceptor and the biomaterial can be naturally occurred or synthetically produced.

The receptor can be attached to the linker. The receptor can be physically, biologically and/or chemically bonded to the linker. Typically, the receptor is chemically bonded to the linker. Herein, the chemical bond can include but are not limited to a covalent bond, a non-covalent bond (e.g., an ionic bond), a metallic bond, a hydrogen bond, a chelated bond, as well as those non-covalent interactions such as van der Waals force, π–π interaction, hydrophobic or hydrophilic effect and electrostatic interaction. Typically, the receptor (e.g., the bioreceptor) is covalently bonded to the linker. Typically, the receptor (e.g., the bioreceptor) is bonded (e.g., covalently) to one or more functional groups (e.g., functional groups of the organic compounds as described previously) comprised in the linker. For example, a bioreceptor can be covalently bonded to a carboxyl group, or an amino or amine, or an amide group of a linker (e.g., 1-pyrenebutyric acid, N-hydroxysuccinimide (NHS), pyrene-1-carboxylic acid succinimidyl ester, 1-Aminopyrene, N-(1-pyrene) maleimide).

The sensors

The sensors according to the present feature typically comprise a layer of carbon foam that can be produced by the Dual Laser treatment methods disclosed earlier. Typically, the carbon foam has a layer thickness of more than 50 μm, preferably more than 100μm, more preferably more than 200 μm and still more preferably more than 300 μm. Typically, at least part of the linker or the whole linker is disposed (e.g., dispersed) within the carbon foam. Optionally, at least part of the receptor or the whole receptor is also disposed (e.g., dispersed) within the carbon foam (i.e., when at least part of the linker or preferably the whole linker is disposed (e.g., dispersed) within the carbon foam). Typically, at least part of the linker and optionally at least part of the receptor is disposed (e.g., dispersed) at a depth below the surface of the carbon foam (e.g., the carbon foam layer) which is more than 1% of the total depth of said carbon foam, preferably more than 5% of the total depth, more preferably more than 10%, even more preferably more than 15%, still more preferably more than 20%. Typically, at least part of the linker and optionally at least part of the receptor is disposed (e.g., dispersed) at a depth below the surface of the carbon foam (e.g., the carbon foam layer) which is more than 1μm below the surface of said carbon foam, preferably more than 5 μm, more preferably more than 10 μm, even more preferably more than 15 μm, most preferably more than 20 μm. It may be that the whole linker and optionally the whole receptor is disposed (e.g., dispersed) at a depth below the surface of the carbon foam (e.g., the carbon foam layer) which is more than 1% of the total depth of said carbon foam. It may be that the carbon foam layer has a thickness of any of the

ranges as describe above (e.g., at least more than 50 μm). By 'dispersed' herein is meant that the linker (and optionally the receptor) molecules that are at least partly disposed within the carbon foam, are distributed therein to form a plurality of discrete domains other than a single cluster. It may be that said domains are distributed uniformly and/or continuously (e.g., distributed as a uniform and/or continuous layer) within said carbon foam. Without wishing to be bound by any theory, it is believed that the displacements of the linker (and optionally the receptor) lead to improved functionalisation of the carbon foam hence enhanced sensing activities (i.e., sensitivities) of the sensors.

Additionally, and optionally, neither the linker nor the receptor is disposed (e.g., dispersed) throughout the entire depth of the carbon foam (e.g., the carbon foam layer). In other words, the core of said carbon foam remains unmodified by either the linker or the receptor.

It may be that the linker is selected from 1-pyrenebutyric acid, N-hydroxysuccinimide (NHS), pyrene-1-carboxylic acid succinimidyl ester, 1-Aminopyrene, N-(1-pyrene) maleimide, or mixtures thereof and the receptor is selected from immunoglobulin A (IgA), glucose dehydrogenase, streptavidin, or mixtures thereof.

It may be that the sensor also includes a substrate. In the first method to obtain the carbon foam, if a carbon source is provided on or adjacent to a substrate, the final sensor may include said substrate as a component part. In the second method wherein use of a substrate is necessary, the final sensor may also include said substrate as a component part. Obtained by either method, the carbon foam may be optionally adhered to the substrate within the sensor. The substrate so included in the sensor may have the characteristics according to one of the features and/or one of the possible combinations of those features described previously for the substrate used in the production of the carbon foam. Alternatively, it is not necessary for the sensor to include a substrate. In other words, even if the carbon foam is produced adhered to a substrate, it may be removed therefrom as part of the preparation for the subsequent modification.

Typically, the sensor according to the present feature is a chemical, physical or mechanical, biological, or optical sensor, preferably a biosensor (i.e., when the receptor is a bioreceptor). Typically, the sensor (e.g., the biosensor) takes the form as an electrode or an electrode device. The sensor (e.g., the biosensor) may include a multi-electrode platform, for example, a three-electrode platform comprising a counter electrode (CE), a working electrode (WE) and a

reference electrode (E or RE)). The electrode (e.g., WE) may be made up of modified carbon foam (i.e., carbon foam modified by a receptor through a linker) of the present feature. The other electrodes (e.g., CE and/or RE) may also be carbon foam based, preferably carbon foam based, more preferably the same carbon foam based without any modifications. All electrodes may have the same or different dimensions.

The sensor (e.g., the biosensor) may be provided as a product wherein said sensor is contained within a packaging, and the product preferably comprises instructions for use. Typically, the packaging comprises a primary packaging within which the sensor is contained. It may be that the sensor is provided on an adaptor which is contained within a primary packaging. Suitable examples for a primary packaging are protective covers, pockets, folders, envelopes, boxes, containers, cartons, cases, and the like. Optionally, the packaging further comprises a secondary packaging. Such secondary packaging is typically a packaging that holds one sensor or a plurality of sensors together. Suitable examples for a secondary packaging are plastic cartons, cardboard cartons, blister packs, boxes (e.g., cardboard or plastic boxes), cases, containers, cardboard or plastic crates, trays, wrapped bundles with or without one or more air pockets, and the like. Still optionally, the packaging may comprise a tertiary packaging which may be selected from boxes, cases, cartons, containers, and the like. Suitably, at least one of the packaging described above can protect the sensor from light (e.g., direct sunlight), moisture, physical and/or chemical damages and contaminants. The instructions may give detailed information for the steps of using the sensors in accordance with the third aspect of the feature. The instructions may be supplied in the printed form of a label, a booklet, a brochure, or a leaflet. The instructions may also be printed on the packaging of the product.

Manufacturing of the sensors

In the second aspect, there is provided a method of manufacturing a sensor according to the first aspect, wherein the steps include: (i) providing carbon foam; (ii) treating the carbon foam with a linker; and (iii) treating the linker-modified carbon foam with a receptor.

It may be that the method comprises a step of manufacturing the carbon foam before providing and treating the carbon foam with a linker. The carbon foam is accordingly produced by one of the laser treatment methods disclosed herein, typically the first or the second method, more typically the first method. It may be that the carbon foam so produced is adhered to, attached

to, or provided on a substrate. Typically, said carbon foam may be removed from said substrate before the treatment of a linker in step (ii). In other words, the carbon foam in step (i) is provided without a substrate. Alternatively, said carbon foam does not need to be removed (e.g., said carbon foam remains adhered to said substrate). In other words, the carbon foam in step (i) is provided with a substrate.

It may be that the carbon foam is incubated with the linker. It may be that the incubation happens in a buffer preferably a buffer solution. Additionally or optionally, the modification by linker may require at least one of the following conditions: light (ultraviolet light, visible light, or infrared radiation), or heat. After the incubation, the linker-modified carbon foam may be cleaned.

It may be that the linker-modified carbon foam is incubated with the receptor. After the incubation, the sensor so obtained may be cleaned prior to use. After cleaning, the sensor may be passivated. The passivation is understood to block the remaining activated sites that are not functionalised by the receptor.

The receptor used to treat the linker-modified carbon foam in step (iii).

The sensor may be an electrode or an electrode device comprising a multi-electrode platform. The manufacturing steps described above may thus be applicable to manufacturing of an electrode. When the sensor is an electrode device comprising a multi-electrode platform, the above-described manufacturing steps are applicable to producing a working electrode (WE), and the method further comprises the following additional steps of producing a counter electrode (CE) and a reference electrode (E or RE).

Use of the sensors

In the third aspect, there is provided a method of using a sensor, comprising steps in sequence of : (i) providing a sensor according to the first aspect; (ii) contacting the sensor with a sample containing or suspected of containing a target, (iii) measuring a response of the sensor and (iv) optionally, the response is correlated to the level of the target in the sample.

The target can be a target disclosed herein, typically a biological material disclosed herein. The sample can be a sample disclosed herein, typically a biological sample disclosed herein.

Before use, the sensor (e.g., the biosensor) can be suitably stored at ambient conditions (e.g., room temperature around 20°C and 1 atmospheric pressure). Typically, the sensor is stored in dry conditions. After use, the sensor can be suitably disposed (i.e., the sensor is a disposable sensor).

It may be that the sensor is immersed into a sample. The sample may contain a phosphate buffered saline (PBS). The concentration of a target in a sample may be at least 1ppm. The equilibration time may be at least 0.5 minute, or at least 1 minute, or at least 10 minutes, or at least 30 minutes, typically not more than 2 hours, or not more than 1 hour, or not more than 40 minutes. It may be that after contacting the sample, the sensor is cleaned before a response is being measured. It may be that the sensor is cleaned by rinsing with a PBS. It may be that after cleansing, the sensor is dried (e.g., by a gas flow, or by natural dry).

It may be that a response is measured by differential pulse voltammograms, and/or impedance spectroscopy. It may be that a response measured is further correlated to the level of the target in the sample. It may be that the method comprises steps (i), (ii) and (iii) as described above, and additionally comprises steps in sequence of (iv) contacting the sensor with one or more samples containing known levels of the target (i.e. control samples); (v) measuring response of the sensor to those one or more control samples; (vi) comparing the response to the sample containing or suspected of containing the target with the response to the one or more control samples; and (vii) correlating the response to the sample containing or suspected of containing the target to the level of said target in said sample.

Appendix 5 concepts

1. A sensor comprising: (i) carbon foam (ii) a linker, and (iii) a receptor, wherein the receptor is bonded to the carbon foam through the linker.

2. A sensor according to concept 1, wherein the carbon foam is obtainable by a method of concentrating infrared radiation in at least one locus within a carbon source,

thereby producing the carbon foam within said at least one locus, and said infrared radiation is provided by a laser beam that is an infrared laser beam.

3. A sensor according to concept 2, wherein concentrating infrared radiation comprises diffracting the infrared radiation to form an interference pattern each of whose fringes is within a locus within the carbon source.

4. A sensor according to concept 2 or concept 3, wherein the at least one locus is moved laterally within the carbon source and/or the at least one locus is moved within the depth of the carbon source.

5. A sensor according to any one of concepts 2 to 4, wherein the infrared radiation irradiates the carbon source directly, or the infrared radiation passes through a substrate prior to irradiating the carbon source, wherein said carbon source is provided on or adjacent to a surface of said substrate.

6. A sensor according to any one of concepts 2 to 5, wherein the carbon source is additionally irradiated with an additional radiation, and this additional irradiation is performed prior to, or simultaneously to, or following the step of concentrating infrared radiation in at least one locus within the carbon source.

7. A sensor according to concept 6, wherein the additional radiation is rastered over the surface of the carbon source.

8. A sensor according to concept 6 or concept 7, wherein the additional radiation irradiates the carbon source directly, or passes through the substrate as described in concept 5 prior to irradiating the carbon source.

9. A sensor according to any one of the preceding concepts, wherein at least part of the linker is disposed, preferably dispersed, within the carbon foam; and optionally at least part of the receptor is disposed preferably dispersed within the carbon foam.

10. A sensor according to any one of the concepts 2 to 9, wherein the carbon foam has a layer thickness of more than 50μm, preferably more than 100μm, more preferably more than 200 μm and still more preferably more than 300 μm.

11. A sensor according to concept 1, wherein the carbon foam is obtainable by a method of providing a carbon source on or adjacent to a surface of a substrate and exposing at least a portion of the carbon source comprising carbon-containing material and/or at least a portion of the substrate to a laser beam, thereby converting at least a portion of the carbon source into the carbon foam.

12. A sensor according to concept 5, 8 or 11, wherein the substrate comprises one or more of the followings: silicone, silicon dioxide, gallium nitride, gallium arsenide, zinc oxide; or alternatively one or more polymers; or alternatively one or more metals selected from aluminium, copper, gold or other metals, or oxides, nitrides or arsenides of said metals.

13. A sensor according to any one of the preceding concepts, wherein the carbon foam comprises oxygen at an atomic percentage of less than 3%, preferably less than 1.5%, and/or nitrogen at an atomic percentage of less than 3%.

14. A sensor according to any one of the preceding concepts, wherein the linker is selected from nanoparticles, polymers, polymer brushes, ligands, organic compounds comprising one or more functional groups, molecules bonded to the carbon foam covalently or non-covalently, or mixtures thereof.

15. A sensor according to concept 14, wherein the linker is selected from polymers preferably (meth)acrylate polymers, organic compounds comprising one or more functional groups, carbodiimides, diazonium compounds, or mixtures thereof.

16. A sensor according to concept 15, wherein the one or more functional groups are independently selected from oxygen, nitrogen, sulphur, halide, hydroxyl, carbonyl, carboxyl, amine, amino, amide, hydrophilic polymers, or mixtures thereof, optionally in combination with linear, branched or cyclic alkyl, alkylenyl, alkynyl, aryl residues, acryl, acyl, acyloxy, alkoxy, alkyleneoxy, or mixtures thereof.

17. A sensor according to concept 16, wherein the organic compound further comprises one or more cyclic moieties that optionally comprise one or more heteroatoms, and at least one of the cyclic moieties is linked directly or indirectly to at least one of the functional groups, or the linker is a derivative that is an ester or salt of said organic compound, or a compound that releases said organic compound in reaction with the carbon foam .

18. A sensor according to concept 17, wherein the linker is selected from 1-pyrenebutyric acid, N-hydroxysuccinimide (NHS), pyrene-1-carboxylic acid succinimidyl ester, 1-Aminopyrene, N-(1-pyrene) maleimide, or mixtures thereof.

19. A sensor according to concept 17 or concept 18, wherein the linker is bonded to the carbon foam by π–π interaction.

20. A sensor according to any one of the preceding concepts, wherein the receptor is one of the followings: an electrochemical receptor, a chemical receptor, a bioreceptor, an optical receptor, a physical or mechanical receptor, preferably a bioreceptor.

21. A sensor according to claim 20, wherein the receptor is selected from crown ethers, catalysts, boric acids, concept, ligands, aptamers, proteins, enzymes, antibodies, antigens, microorganisms, nucleic acids, fatty acids, fatty acid esters, molecularly imprinted polymers, metal-organic frameworks, polypeptides or oligopeptides capable of forming a ligand binding, cells, cell organelles, or other cellular components, or mixtures thereof, preferably selected from proteins, nucleic acids, antibodies, enzymes, or mixtures thereof.

22. A sensor according to concept 21, wherein the receptor is selected from immunoglobulin A (IgA), glucose dehydrogenase, streptavidin, or mixtures thereof.

23. A sensor according to any one of the preceding concepts, wherein the receptor is physically, biologically and/or chemically bonded to the linker, preferably chemically bonded, more preferably covalently bonded.

24. A method of manufacturing a sensor according to any one of the preceding concept, comprising the steps in sequence of: (i) providing a carbon foam as described in any one of concept 1 to 13, 19; (ii) treating the carbon foam with a linker as described in any one of concept 1, 14 to 19, 23; and (iii) treating the linker-modified carbon foam obtained in step (ii) with a receptor as described in any one of concept 1, 20 to 23.

25. A method of sensing a target comprising the steps in sequence of: (i) providing a sensor according to any one of concept 1 to 23; (ii) contacting the sensor with a sample containing or suspected of containing the target; (iii) measuring a response of the sensor; and optionally (iv) correlating the response to the level of the target in the sample.

Note also that the sensor described in this **Appendix 5** may be the Gii-Sens carbon foam sensor described earlier in this specification.

Appendix 6 Benchmark experimental conditions

1 mM Potassium Ferri/Ferrocyanide in 0.1 M Strontium Nitrate and minimum number of five replicates randomly picked. Cyclic voltammetry at 25 and 200 mV/s scan rate performed as comparative technique. Various features were investigated and conclusions were drawn to evaluate the difference electrode materials performances.

Electrochemical Impedance Spectroscopy was performed at equilibrium potential with 5 mV amplitude and from 0.1 to 100 kHz frequencies

Sensor built-in or external silver/silver chloride reference electrode was used.

Gii Sens carbon foam vs. conventional Graphene electrode materials

Gii Sens carbon foam sensors were evaluated and compared against other commercially available graphene-based sensors. See **Figure 84**.

The obtained reduction and oxidation peak current recorded shows a 25 % greater efficiency in terms of current density per geometrical area. This is clear reflection of the larger available electrochemically available area provided by Gii Sens 3D carbon foam. See **Figure 85**.

From cyclic voltammetry the evaluation of the reduction – oxidation peak separation can be interpreted as a measure of the electron redox responsiveness of the surface to voltage scan and its ability to effectively perform rapid redox reactions. The research shows that the reduction – oxidation peak separation remains below 70 mV and shows no increased separation from 25 to 200 mV/s.

Other graphene electrode surface showed larger voltage separation from reduction to oxidation, indicative of less efficient redox faradaic reaction and a clear detrimental effect associated with faster scan rates. See **Figure 86.**

The value of charge transfer resistance at the different surfaces shows a dramatic improvement at Gii Sens sensor surface. This illustrates the massive potential of Gii Sens for implementing impedance based measurements with reliability and little background signal interference.

Gii Sens vs. other Carbon-based materials

Carbon based electrode materials are very common in electroanalytical applications . Carbon paste electrodes are a common material for screen printed sensors. They are most widespread electrode surface in real point-of-care applications due to their fabrication flexibility and affordability. On the other end of carbon-based materials they are glassy carbon surfaces, with expected better performance but a limited availability for flexible manufacturing and affordability. See **Figure 87.**

The performance of Gii Sens carbon foam shows a match with that of pure glassy carbon material in terms of available electrochemically active area whilst increasing by 50 % the area available at equivalent size carbon paste electrodes. See **Figure 88.**

The reduction – oxidation peak separation obtained from cyclic voltammetry shows first the poor performance of carbon paste materials and its high dependence to slow scan rates to deliver relatively acceptable redox reactions at its surface. The response of Gii Sens even outperforms that of pure glassy carbon at any scan rate, showing its great potential to combine the flexibility in manufacturing terms and excellent performance. See **Figure 89.**

The measure of surface charge transfer resistance comes to emphasize that Gii Sens holds a tremendous potential as impedance based sensing surface above glassy carbon and opening a field still unreachable for carbon paste electrode materials.

Gii Sens vs. Screen Printed Gold

Screen printed gold sensors are hosts of two of the most important properties to make a sensor material feasible for real electrochemistry sensing applications: Flexible fabrication procedures and excellent electrochemical response. Two commercially available examples of screen printed gold were evaluated. See **Figure 90**. Gii Sens carbon foam proves to also host those properties whilst adding affordability.

The recorded reduction and oxidation peak current recorded shows at least a 20 % increase in available electrochemically active area per geometrical area unit. See **Figure 91**.

As expected screen printed gold shows the most responsive electrode surface material of the evaluated lot, however Gii-Sens matches and even improves that performance specially at fast scan rates. See **Figure 92.**

Charge transfer resistance at the electrode surface comparing screen printed gold and Gii Sens also highlights the great potential of the Gii carbon foam material; in all cases it shows lower resistivity associated values.

The comparison of Gii Sens with screen printed gold aims to show the winning comparison in terms of ease of manufacturing and outstanding performance, whereas the affordability and scalability are definitively beneficial inherent features of Gii Sens sensors.

Conclusions

The performance of Gii Sens sensors outplays any other carbon-based or even graphene sensor available in the market. Even screen printed gold surfaces are outperformed, which eliminates any shadow of doubt over the total convenience of using Gii Sens surface as the ultimate electrochemical platform for sensing. Gii Sens shows for the first time the perfect choice for manufacturing and scalable material for electroanalytical applications while maintaining a top performance, ensuring maximum sensitivity and flexibility for implementing into large throughput and point-of-care applications

Appendix 7 Optimisation of the surface immobilization of anti human procalcitonin (cAb)

Objective:

Optimisation of the surface immobilization of anti human procalcitonin (cAb)

Summary of Results

- Surface NHS production method selected. Matching existing standard manufacturing process
- Optimal cAb surface coverage achieved using 100 µg/ml cAb.
- For standard bare Gii-Sens® sensors the usual %CV is 7%. For all sensors across the experiments shown in this report the %CV for the 100 µg/ml cAb coating is 10%.
- Successful detection of 2000 pg/ml Ag in direct assay format using 100 µg/ml cAb coating. Signal output has a %CV of 10%.

Experimental Section

Solution compositions

Surface Chemistry

NHS modification

Pyrene NHS

Capture Antibody (cAb):

Product Name: Anti – h PCT 4004 SPTN – 5

Antigen (Ag):

Product Name : Recombinant PCT antigen

Echem Read out solution

1mM K3Fe(CN)6 + 1mM K4Fe(CN)6 in 20 mM KCl

cAb Immobilization Solution

Anti – h PCT in 1 x PBS (pH 7.2)

Antigen (Ag) Detection Solution

1mM K3Fe(CN)6 + 1mM K4Fe(CN)6 in 20 mM KCl + Ag

Electrochemical Techniques

Electrochemical impedance

Applied voltage: OCP

Amplitude: 0.01 V_{RMS}

Frequency Range: 100000 - 0.1 Hz

Cyclic Voltammetry

Scan Rate: 25mV/s

Start potential: -0.3 V

Upper potential: 0.6 V

V Lower potential: -0.3 V

Assay Procedures

NHS immobilisation

- Prepare 10 mM Pyr NHS in DMF
- Drop-cast 10 µL of onto the working electrode of each sensor.
- Place sensors inside an airtight box and leave incubating for 12 to 18 h

- Confirm the PyrNHS / DMF has fully evaporated from the surface

cAb Immobilization Procedure

- Place NHS GiiSens+ sensor onto a flat surface.
- Drop-cast 10 μL of cAb onto the working electrode of each sensor.
- Place sensors inside a sealed container with a water bath for 2 hours.
- Remove sensors and gently rinse the solution off with a DI water before gently drying with N_2 gas stream.

Assay Procedure: Direct assay 1 - see **Figure 93**

1) cAb readout - Electrochemical read out solution applied to sensor surface before EIS measurement taken.

2) Solution removal – Electrochemical read out solution removed from sensor surface.

3) t'1 readout – Antigen spiked electrochemical read out solution applied to sensor surface before EIS measurment taken. Approximately 1 min between solution addition & measurement.

4) t'2 readout – EIS measurment taken. Approximately 6 min between solution additon & measurement.

5) t'3 readout – EIS measurment taken. Approximately 11 min between solution addiditon & measurement.

See Annex for Electrochemical readout procedures

1. Characterisation Plots

- Replicates per point, n = 5 (minimum) different disposable sensors (single read out, sensors disposed)

Phase 1: Surface Chemistry

The surface chemistry of choice was NHS modified carbon foam followed by conjugation of the cAb via amide bond formation following the scheme below. See **Figure 94:** Surface immobilization reaction schematic.

The NHS production on the carbon foam surface was monitored using electrochemical impedance spectroscopy & cyclic voltammetry. See **Figure 95:** Rct & ΔEp signal response for NHS functionalization of GiiSens ® electrodes.

The increase in Rct & ΔEp relative to the bare electrode confirms NHS functionalization of the carbon foam electrode.

A range of cAb concentrations between 50 – 800 µg/ml were screened using electrochemical impedance spectroscopy. See **Figure 96**: cAb immobilisation on GiiSens ® electrodes.

A logical increase of Rct with cAb concentration is observed for immobilizations on NHS modified sensors. The optimum coverage was estimated 100 µg/ml cAb on NHS electrodes, that concentration was estimated to provide best performance of the sensor without wasting material for little gain. At this concentration an excellent level of reproducibility is observed (%CV 3%).

Phase 2: Electrochemical Signal

The electrochemical signal generated was evaluated for a direct assay, this means no utilization of a secondary antibody to assist the antigen detection.

An antigen concentration of 2000 pg/ml was selected for investigation of the direct assay. The surface antibody coating was fixed at 100 µg/ml as per the results in Phase 1 of this report. Ag – Ab incubation

time was selected as a preliminary assay parameter for investigation. See **Figure 97**: Signal response from 2000 pg/ml in direct assay format using 100 µg/ml cAb surface coating.

The 100 µg/ml cAb again shows a good level of reproducibility (%CV 8%). The distinction between the Avg. Rct of the cAb is clear, giving a distinct quantifiable signal output (ΔRct). The ΔRct signal output also shows an acceptable level of reproducibility with the %CV ≥ 10% at each readout time. The stability of the output signal between 1 , 6 & 11 m shows no additional Ab – Ag interaction takes place after the first measurement. The 5-minute time gap between measurements is due to the length of time the EIS measurement takes. The assay incubation time is optimal as low as 1 minute for a 2000 pg/ml Ag sample.

cAb Concentration (µg/ml)	**Analysis Solution**	**Electrochemical Analysis Parameters**	
50, 100 , 200, 400 & 800	**20mM KCl + 1mM potassium ferricyanide + 1mM potassium ferrocyanide**	<u>Cyclic Voltammetry</u> Scan Rate: 25mV/s Potential Window: -0.3 – 0.6 V	<u>EIS</u> Applied voltage: OCP Amplitude: 0.01 V_{RMS} Frequency Range: 100000 - 0.1 Hz

Table 9: Key experimental & electrochemical parameters for cAb immobilizations

Ag concentration (pg/ml)	**cAb Concentration (µg/ml)**	**Analysis Solution**	**Electrochemical Analysis Parameters**

2000	**100**	**20mM KCl + 1mM potassium ferricyanide + 1mM potassium ferrocyanide**	EIS Applied voltage: OCP Amplitude: 0.01 V_{RMS} Frequency Range: 100000 - 0.1 Hz

Table 10: Key experimental & electrochemical parameters for Ag detection

Appendix 8

Consolidated list of Features and Optional Features

This **Appendix 8** is a consolidated list of Features and Optional Features. Note that any one or more of the following **Features A – R** may each be combined with any one or more other, compatible **Features A – R** and with any one or more of the Optional Features.

Group 1: Sub-surface carbon foam

Feature A: Carbon foam created in a sub-surface region of a carbon pre-cursor material

Feature B: Carbon foam created in an encapsulated region of a carbon pre-cursor material

Feature C: Carbon foam created in a region of a carbon pre-cursor material, where the region has no substantial gas escape pathways

Feature D: Amorphous, non-graphene material adhering to the substrate

Group 2: Dual laser processing

Feature E: Carbon foam created by laser ablating a sub-surface carbon foam region

Feature F: Non-graphene carbon foam created by laser ablating a sub-surface carbon foam region

Feature G: Dual lasers

Feature H: Electrical contacts positioned in carbon foam created by laser ablating a sub-surface carbon foam region

Feature I: Printing electrical contacts on the polyimide film and then creating the exposed carbon foam

Feature J: Tall tracks made in the carbon foam

Feature K: Applying the first and second lasers in different manufacturing facilities

Group 3: Products

Feature L1: Biosensors

Feature L2: Scalable, low-cost manufacture of a carbon foam biosensor using screen printing technology

Feature L3: Adding functionalised groups to the biosensor at a different manufacturing facility

Feature L4: Adding functionalised groups to the biosensor as part of the biosensor production process

Feature L5: Biosensor manufacture using PPC: Post Printing Conversion

Feature M1: Energy storage device: the supercapacitor

Feature M2: Specifics of the carbon foam supercapacitor

Feature M3: Carbon foam supercapacitor: the Common Collector

Feature M4: Carbon foam supercapacitor: the PPC manufacturing process

Feature M5: Carbon foam pseudo-capacitor: a metal oxide variant

Feature M6: Carbon foam supercapacitor: using an ionic-gel in low humidity environment

Feature N1: Electrical conductors

Feature N2: Combined Sensor and Supercapacitor

Feature N3: Combined Supercapacitor and Battery

Feature N4: The Smart Label

Feature N5: Combined Supercapacitor and Antenna

Feature N6: Combined Energy Scavenger + Supercapacitor.

Feature O1: 3D carbon foam structures: Gii-Thru for Gii-Cap

Feature O2: 3D carbon foam structures: Gii-Thru Stackable Gii-Cap/Gii-Cap+

Feature O3: 3D carbon foam structures: Gii-Thru for Gii-Sens: HISLOC

Feature O4 3D carbon foam structures: Gii-Thru for Gii-Sens: HISLOC manufacturing process

Group 4: Miscellaneous

Feature P: Scalable manufacturing of carbon foam: Gii 3

Feature Q: Various other carbon foam applications

Feature R: Non-graphene carbon foam

Feature A: **Carbon foam created in a sub-surface region of a carbon pre-cursor material**

A method of manufacturing carbon foam material comprising the step of irradiating a sub-surface region of a carbon pre-cursor material, parameters of the laser beam being selected to create a carbon foam, in that sub-surface region.

A laser induced carbon foam material made by a laser beam configured to irradiate a sub-surface region of a carbon pre-cursor material, parameters of the laser beam being selected to create a carbon foam in that sub-surface region.

A device including a laser induced carbon foam material manufactured by irradiating a sub-surface region of a carbon pre-cursor material, parameters of the laser beam being selected to create a carbon foam in that sub-surface region.

Feature B: **Carbon foam created in an encapsulated region of a carbon pre-cursor material**

A method of manufacturing carbon foam material comprising the step of irradiating an encapsulated region of a carbon pre-cursor material, parameters of the laser beam being selected to create a carbon foam in that encapsulated region.

A laser induced carbon foam material made by a laser beam configured to irradiate an encapsulated region of a carbon pre-cursor material, parameters of the laser beam being selected to create a carbon foam in that encapsulated region.

A device including a laser induced carbon foam material manufactured by irradiating an encapsulated region of a carbon pre-cursor material, parameters of the laser beam being selected to create a carbon foam in that encapsulated region.

Feature C: **Carbon foam created in a region of a carbon pre-cursor material, where the region has no substantial gas escape pathways**

A method of manufacturing carbon foam material comprising the step of irradiating an encapsulated, sub-surface region of a carbon pre-cursor material, parameters of the laser beam being selected to create a carbon foam in that region and in which no substantial gas escape pathways to a surface of the pre-cursor material are created by the laser beam.

A laser induced carbon foam material by a laser beam configured to irradiate an encapsulated, sub-surface region of a carbon pre-cursor material, parameters of the laser beam being selected to create a carbon foam in that region and in which no substantial gas escape pathways to a surface of the pre-cursor material are created by the laser beam.

A device including a laser induced carbon foam material manufactured by irradiating an encapsulated, sub-surface region of a carbon pre-cursor material, parameters of the laser beam being selected to create a carbon foam, in that region and in which no substantial gas escape pathways to a surface of the pre-cursor material are created by the laser beam.

Feature D: Amorphous, non-graphene material adhering to the substrate

A method of manufacturing carbon foam material comprising the step of irradiating an internal region of a carbon pre-cursor material, positioned on a substrate, parameters of the laser beam being selected to create a carbon foam in that region and to create a disorganised, amorphous, non-graphene material between the carbon foam region and the substrate; in which that disorganised, amorphous, non-graphene material is adhering or otherwise attaching directly to the substrate.

A laser induced carbon foam material made by a laser beam configured to irradiate an internal region of a carbon pre-cursor material, positioned on a substrate, parameters of the laser beam being selected to create a carbon foam in that region and to create a disorganised, amorphous, non-graphene material between the graphene region and the substrate, that disorganised, amorphous, non-graphene material adhering or otherwise attaching directly to the substrate.

A device including a laser induced carbon foam material manufactured by irradiating an internal region of a carbon pre-cursor material, positioned on a substrate, parameters of the laser beam being selected to create a carbon foam in that region and to create a disorganised,

amorphous, non-graphene material between the graphene region and the substrate, that disorganised, amorphous, non-graphene material adhering or otherwise attaching directly to the substrate.

Feature E: Carbon foam created by laser ablating a sub-surface carbon foam region

A method of manufacturing graphene material comprising the steps of (a) a laser beam irradiating an encapsulated or sub-surface region of a carbon pre-cursor material, to create a carbon foam in that encapsulated or sub-surface region and a disorganised, amorphous non-graphene substance above the carbon foam, and then (b) laser ablation or treatment to remove at least some of the disorganised, amorphous non-graphene substance and to expose at least some of the carbon foam.

A laser induced, carbon foam made by (a) a laser beam irradiating an encapsulated or sub-surface region of a carbon pre-cursor material, to create a carbon foam in that encapsulated or sub-surface region and a disorganised, amorphous non-graphene substance above the carbon foam, and then (b) laser ablation or treatment to remove the disorganised, amorphous non-graphene substance and to expose at least some of the carbon foam.

A device including a laser induced carbon foam material manufactured by (a) a laser beam irradiating an encapsulated or sub-surface region of a carbon pre-cursor material, to create a carbon foam in that encapsulated or sub-surface region and a disorganised, amorphous non-graphene substance above the carbon foam, and then (b) laser ablation or treatment to remove the disorganised, amorphous non-graphene substance and to expose at least some of the carbon foam.

Feature F: Non-graphene carbon foam created by laser ablating a sub-surface carbon foam region

A method of manufacturing non-graphene carbon foam comprising the steps of

(a) a laser beam irradiating an encapsulated or sub-surface region of a carbon pre-cursor material to create a carbon foam in that encapsulated or sub-surface region in the carbon pre-

cursor material, and a disorganised, amorphous non-graphene substance above the carbon foam, and then

(b) laser ablation or treatment to remove the disorganised, amorphous non-graphene substance and expose at least some of the underlying carbon foam and transform at least some of that underlying carbon foam into a non-graphene carbon foam.

A laser induced carbon foam made by:

(a) a laser beam irradiating an encapsulated or sub-surface region of a carbon pre-cursor material to create a carbon foam in that encapsulated or sub-surface region in the carbon pre-cursor material, and a disorganised, amorphous non-graphene substance above the carbon foam, and then

(b) laser ablation or treatment to remove the disorganised, amorphous non-graphene substance and expose at least some of the underlying carbon foam and transform at least some of that underlying carbon foam into a non-graphene carbon foam.

A device including a laser induced carbon foam made by:

(a) a laser beam irradiating an encapsulated or sub-surface region of a carbon pre-cursor material to create a carbon foam in that encapsulated or sub-surface region in the carbon pre-cursor material, and a disorganised, amorphous non-graphene substance above the carbon foam, and then

(b) laser ablation or treatment to remove the disorganised, amorphous non-graphene substance and expose at least some of the underlying carbon foam and transform at least some of that underlying carbon foam into a non-graphene carbon foam.

Feature G: Dual lasers operating at different frequency bands

A method of manufacturing a carbon foam material comprising the steps of

(a) using a laser beam operating at a first band to irradiate an encapsulated or sub-surface region of a carbon pre-cursor material below a surface of the material, to create carbon foam in that encapsulated or sub-surface region, and then

(b) using a laser beam operating at a second band to remove or ablate material sitting above the carbon foam, to expose at least some of the carbon foam.

A laser induced carbon foam made by:

(a) using a laser beam operating at a first band to irradiate an encapsulated or sub-surface region of a carbon pre-cursor material below a surface of the material, to create carbon foam in that encapsulated or sub-surface region, and then

(b) using a laser beam operating at a second band to remove or ablate material sitting above the carbon foam, to expose at least some of the carbon foam.

A device including a laser induced carbon foam material manufactured by

(a) using a laser beam operating at a first band to irradiate an encapsulated or sub-surface region of a carbon pre-cursor material below a surface of the material, to create carbon foam in that encapsulated or sub-surface region, and then

(b) using a laser beam operating at a second band to remove or ablate material sitting above the carbon foam, to expose at least some of the carbon foam.

Feature H: Electrical contacts positioned in carbon foam created by laser ablating a sub-surface carbon foam region

A method of manufacturing carbon foam material comprising the steps of:

(a) using a laser beam operating at a first band to irradiate an encapsulated or sub-surface region of a carbon pre-cursor material below a surface of the material, to create carbon foam in that encapsulated or sub-surface region, and then

(b) using a laser beam operating at a second band to remove or ablate material sitting above the carbon foam, to expose at least some of the carbon foam; and

(c) attaching, printing or locating one or more electrical contacts into the carbon foam.

A laser induced carbon foam made by:

(a) using a laser beam operating at a first band to irradiate an encapsulated or sub-surface region of a carbon pre-cursor material below a surface of the material, to create carbon foam in that encapsulated or sub-surface region, and then

(b) using a laser beam operating at a second band to remove or ablate material sitting above the carbon foam, to expose at least some of the carbon foam;

(c) attaching, printing or locating one or more electrical contacts into the carbon foam.

A device including a laser induced carbon foam material manufactured by:

(a) using a laser beam operating at a first band to irradiate an encapsulated or sub-surface region of a carbon pre-cursor material below a surface of the material, to create carbon foam in that encapsulated or sub-surface region, and then

(b) using a laser beam operating at a second band to remove or ablate material sitting above the carbon foam, to expose at least some of the carbon foam; and

(c) attaching, printing or locating one or more electrical contacts into the carbon foam.

Feature I: Printing electrical contacts on the polyimide film and then creating the exposed carbon foam

A method of manufacturing carbon foam material comprising the steps of:

(a) screen printing electrical contacts onto or into a carbon pre-cursor material;

(b) using a laser beam operating at a first band to irradiate an encapsulated or sub-surface region of a carbon pre-cursor material below a surface of the material, to create carbon foam in that encapsulated or sub-surface region, and where steps (a) and (b) can be performed in the sequence (a) then (b) or (b) then (a); and

(c) using a laser beam operating at a second band to remove or ablate material sitting above the carbon foam, to expose at least some of the carbon foam to which the electrical contacts are connected.

A laser induced carbon foam material made by:

(a) screen printing electrical contacts onto or into a carbon pre-cursor material;

(b) using a laser beam operating at a first band to irradiate an encapsulated or sub-surface region of a carbon pre-cursor material below a surface of the material, to create carbon foam in that encapsulated or sub-surface region, and where steps (a) and (b) can be performed in the sequence (a) then (b) or (b) then (a); and

(c) using a laser beam operating at a second band to remove or ablate material sitting above the carbon foam, to expose at least some of the carbon foam to which the electrical contacts are connected.

A device including a laser induced carbon foam material manufactured by:

(a) screen printing electrical contacts onto or into a carbon pre-cursor material;

(b) using a laser beam operating at a first band to irradiate an encapsulated or sub-surface region of a carbon pre-cursor material below a surface of the material, to create carbon foam in that encapsulated or sub-surface region, and where steps (a) and (b) can be performed in the sequence (a) then (b) or (b) then (a); and

(c) using a laser beam operating at a second band to remove or ablate material sitting above the carbon foam, to expose at least some of the carbon foam to which the electrical contacts are connected.

Feature J: Tall tracks made in the carbon foam

A method of manufacturing carbon foam material comprising the steps:

(a) using a laser beam operating at a first band to irradiate an encapsulated or sub-surface region of a carbon pre-cursor material below a surface of the material, to create carbon foam in that encapsulated or sub-surface region, and then

(b) using a laser beam operating at a second band to remove or ablate material sitting above the carbon foam, to expose at least some of the carbon foam;

and where the carbon foam is at least 50μm in thickness or depth.

A laser induced carbon foam material made by:

(a) using a laser beam operating at a first band to irradiate an encapsulated or sub-surface region of a carbon pre-cursor material below a surface of the material, to create carbon foam in that encapsulated or sub-surface region, and then

(b) using a laser beam operating at a second band to remove or ablate material sitting above the carbon foam, to expose at least some of the carbon foam;

and where the carbon foam is at least 50μm in thickness or depth.

A device including a laser induced carbon foam material manufactured by:

(a) using a laser beam operating at a first band to irradiate an encapsulated or sub-surface region of a carbon pre-cursor material below a surface of the material, to create carbon foam in that encapsulated or sub-surface region, and then

(b) using a laser beam operating at a second band to remove or ablate material sitting above the carbon foam, to expose at least some of the carbon foam;

and where the carbon foam is at least 50μm in thickness or depth.

Feature K: Applying the first and second lasers in different manufacturing facilities

A method of manufacturing a device comprising the steps:

(a) using a laser beam operating at a first band to irradiate an encapsulated or sub-surface region of a carbon pre-cursor material below a surface of the material, to create carbon foam in that encapsulated or sub-surface region, and then

(b) using a laser beam operating at a second band to remove or ablate material sitting above the carbon foam, to expose at least some of the carbon foam;

in which step (a) is performed at one manufacturing facility and step (b) is performed at a different facility.

A laser induced carbon foam material made by:

(a) using a laser beam operating at a first band to irradiate an encapsulated or sub-surface region of a carbon pre-cursor material below a surface of the material, to create carbon foam in that encapsulated or sub-surface region, and then

(b) using a laser beam operating at a second band to remove or ablate material sitting above the carbon foam, to expose at least some of the carbon foam;

in which step (a) is performed at one manufacturing facility and step (b) is performed at a different facility.

A device including a laser induced carbon foam material manufactured by:

(a) using a laser beam operating at a first band to irradiate an encapsulated or sub-surface region of a carbon pre-cursor material below a surface of the material, to create carbon foam in that encapsulated or sub-surface region, and then

(b) using a laser beam operating at a second band to remove or ablate material sitting above the carbon foam, to at least some of the expose carbon foam;

in which step (a) is performed at one manufacturing facility and step (b) is performed at a different facility.

Feature L1: Biosensor

A method of manufacturing a biosensor including a sensing electrode comprising carbon foam made, at least in part, by the method defined in any of Features A – K above.

A biosensor including a sensing electrode comprising carbon foam made, at least in part, by the method defined in any of Features A – **K** above.

A point of care diagnostics device including a biosensor with a sensing electrode comprising carbon foam made, at least in part, by the method defined in any of Features A – K above.

Feature L2: Scalable, low-cost manufacture of a carbon foam biosensor using screen printing technology

A method of manufacturing a biosensor including sensor electrodes, such as a working electrode, and a counter electrode, each electrode comprising carbon foam made, at least in part, by the method defined in any of Features A – K above, and the method includes screen printing electrical connection tracks over each electrode and at least partly covering the electrodes and connection tracks with a screen printed dielectric.

A biosensor including sensor electrodes, such as a working electrode, and a counter electrode, each electrode comprising carbon foam made, at least in part, by the method defined in any of Features A – K above, and where the biosensor includes (i) electrical connection tracks that have been screen printed over each electrode and (ii) a screen printed dielectric that at least partly covers the electrodes and connection tracks.

Feature L3: Adding functionalised groups to the biosensor at a different manufacturing facility

A method of manufacturing, in one manufacturing facility, a biosensor including sensor electrodes, such as a working electrode, a counter electrode, each comprising carbon foam made, at least in part, by the method defined in any of Features A – K above, and the method includes the further step of adding, at a different manufacturing facility, functionalised groups to at least the working electrode.

A biosensor including sensor electrodes, such as a working electrode, and a counter electrode, each electrode comprising carbon foam made, at least in part, by the method defined in any of Features A – K above at one manufacturing facility, and where the biosensor includes

functionalised groups that have been added to at least the working electrode at a different manufacturing facility.

Feature L4: Adding functionalised groups to the biosensor as part of the biosensor production process

A method of manufacturing in one manufacturing facility a biosensor including sensor electrodes, such as a working electrode, a counter electrode, each comprising carbon foam made, at least in part, by the method defined in any of Features A – K above, and the method includes the further step of adding, at that manufacturing facility, functionalised groups to the working electrode.

A biosensor including sensor electrodes, such as a working electrode, and a counter electrode, each electrode comprising carbon foam made, at least in part, by the method defined in any of Features A – K above at one manufacturing facility, and where the biosensor includes functionalised groups that have been added to at least the working electrode at that same manufacturing facility.

Feature L5: Biosensor manufacture using PPC: Post Printing Conversion

A method of manufacturing a biosensor including sensor electrodes, such as a working electrode, and a counter electrode, each comprising carbon made, at least in part, by the method defined in any of Features A – K above, and the method includes the steps of (a) screen printing a carbon layer on a carbon pre-cursor substrate; (b) screen printing electrical connection tracks and a reference electrode; (c) screen printing a dielectric layer over the carbon layer and the electrical connection tracks and the reference electrode; and then (d) creating carbon foam sensor electrodes using a process defined in any of Features A – K above.

A biosensor including sensor electrodes, such as a working electrode, and a counter electrode, where the biosensor includes (a) a carbon layer screen printed on a carbon pre-cursor substrate; (b) screen printed electrical connection tracks and a screen printed reference electrode; (c) a dielectric layer screen printed over the carbon layer and the electrical connection tracks and the

reference electrode; and then (d) carbon foam sensor electrodes made using a process defined in any of Features A – K above.

Feature M1: Energy storage device

A method of manufacturing an energy storage device, such as a supercapacitor or pseudo-capacitor, in which energy storage electrodes comprise carbon foam material made, at least in part, by the method defined in any of Features A – K above.

An energy storage device, such as a supercapacitor or pseudo-capacitor, in which the energy storage electrodes comprise carbon foam material made, at least in part, by the method defined in any of Features A – K above.

Feature M2: Screen printing layers of the carbon foam Supercapacitor

A method of manufacturing an energy storage device, such as a supercapacitor or pseudo-capacitor in which energy storage electrodes comprise carbon foam material made, at least in part, by the method defined in any of Features A – K above;

and the method includes the step of screen printing electrical connection tracks over at least a part of each electrode and at least partly covering the electrodes and connection tracks with a screen printed dielectric layer.

An energy storage device, such as a supercapacitor or pseudo-capacitor, in which energy storage electrodes comprise carbon foam material made, at least in part, by the method defined in any of Features A – K above;

including screen printed electrical connection tracks formed over at least a part of each electrode and a screen printed dielectric layer that at least partly covers the electrodes and connection tracks.

Feature M3: Carbon foam supercapacitor: the Common Collector

A method of manufacturing an energy storage device, such as a supercapacitor or pseudo-capacitor, in which energy storage electrodes comprise carbon foam material made, at least in part, by the method defined in any of Features A – K above and are arranged in an interdigitated pattern;

and the method includes the step of screen printing electrical connection tracks over at least a part of each electrode, in which a single electrical connection track connects to underlying digits that extend perpendicularly from both sides of the electrical connection track.

An energy storage device, such as a supercapacitor or pseudo-capacitor, in which energy storage electrodes comprise carbon foam material made, at least in part, by the method defined in any of Features A – K above and are arranged in an interdigitated pattern;

and in which screen printed electrical connection tracks are formed over at least a part of each electrode, and in which a single electrical connection track connects to underlying digits that extend perpendicularly from both sides of the electrical connection track.

Feature M4: Carbon foam supercapacitor: the PPC manufacturing process

A method of manufacturing an energy storage device, such as a supercapacitor or pseudo-capacitor;

and the method includes the step of (a) screen printing electrical connectors on to a substrate; (b) screen printing a carbon layer over the electrical collectors; (c) screen printing a dielectric over at least some of the carbon layer; then (d) creating carbon foam energy storage electrodes at least in part by the method defined in any of Features A – K above.

An energy storage device, such as a supercapacitor or pseudo-capacitor;

including (a) screen printed electrical connectors on a substrate; (b) screen printing a carbon layer over the electrical collectors; (c) screen printing a dielectric over at least some of the carbon layer; then (d) creating carbon foam energy storage electrodes at least in part by the method defined in any of Features A – K above.

Feature M5: Carbon foam super-capacitor: a metal oxide variant

A method of manufacturing an energy storage device, such as a supercapacitor or pseudo-capacitor, in which energy storage electrodes comprise carbon foam material made, at least in part, by the method defined in any of Features A – K above;

and the method includes the step of applying an electrochemical deposition process of a pseudo-capacitive material, such as a metal oxide, to the energy storage electrodes.

An energy storage device, such as a supercapacitor or pseudo-capacitor;

including (a) energy storage electrodes comprised of carbon foam material made, at least in part, by the method defined in any of Features A – K above; and (b) a pseudo-capacitive material, such as a metal oxide, applied to the energy storage electrodes.

Feature M6: Carbon foam supercapacitor: using an ionic-gel in low humidity environment

A method of manufacturing an energy storage device, such as a supercapacitor or pseudo-capacitor, in which energy storage electrodes comprise carbon foam material made, at least in part, by the method defined in any of Features A – K above;

and the method includes the step of applying an ionic gel electrolyte in a low humidity but non-inert environment, in which the levels of O_2 and H_2O in the environment and measured and controlled to optimise the capacitance of the energy storage device.

An energy storage device, such as a supercapacitor or pseudo-capacitor;

including (a) energy storage electrodes comprised of carbon foam material made, at least in part, by the method defined in any of Features A – K above; and (b) an ionic gel electrolyte that has been applied in a low humidity but non-inert environment, in which the levels of O_2 and H_2O in the environment and measured and controlled to optimise the capacitance of the energy storage device.

Feature N1: Electrical conductor

A method of manufacturing an electrical conductor, in which the electrical conductor comprises carbon foam made, at least in part, by the method defined in any of Features A – K above.

An electrical conductor including carbon foam made, at least in part, by the method defined in any of Features A – K above.

Feature N2: Combined Sensor and Supercapacitor

A method of manufacturing a device that includes both a sensor, and an energy storage device, such as a supercapacitor, in which both the sensor and the energy storage device comprise a carbon foam material made, at least in part, by the method defined in any of Features A – K above.

A sensor device, such as a biosensor, including (a) a sensing electrode comprising carbon foam material made, at least in part, by the method defined in any of Features A – K above and (b) an energy storage device, such as a supercapacitor, in which the energy storage device comprises carbon foam material made, at least in part, by the method defined in any of Features A – K above.

A point of care diagnostics device including (a) a sensing electrode comprising carbon foam material made, at least in part, by the method defined in any of Features A – K above and (b) an energy storage device, such as a supercapacitor, in which the energy storage device comprise carbon foam material made, at least in part, by the method defined in any of Features A – K above.

Feature N3: Combined Supercapacitor and Battery

A method of manufacturing an integrated device including a battery and a supercapacitor, the battery providing long term power and the supercapacitor providing short term power at a higher level than the battery, in which the supercapacitor comprises a carbon foam material made, at least in part, by the method defined in any of Features A – K above.

An integrated device including a battery and a supercapacitor, the battery providing long term power and the supercapacitor providing short term power at a higher level than the battery, in which the supercapacitor comprises carbon foam material made, at least in part, by the method defined in any of Features A – K above.

Feature N4: The Smart Label

A method of manufacturing a smart label comprising the steps of combining or integrating a battery and a supercapacitor, the battery providing long term power and the supercapacitor providing short term power at a higher level than the battery, in which the supercapacitor comprises carbon foam material made, at least in part, by the method defined in any of Features A – K above;

and the smart label includes electronics, such as sensor electronics, powered by the battery and a data transmitter powered by the supercapacitor.

A smart label including a battery and a supercapacitor, the battery providing long term power and the supercapacitor providing short term power at a higher level than the battery, in which the supercapacitor comprises carbon foam material made, at least in part, by the method defined in any of Features A – K above;

and the smart label includes electronics, such as sensor electronics, powered by the battery and a data transmitter powered by the supercapacitor.

Feature N5: Combined Supercapacitor and Antenna

A method of manufacturing an integrated device including an antenna and a supercapacitor, in which the supercapacitor powers the antenna and comprises carbon foam material made, at least in part, by the method defined in any of Features A – K above.

An integrated device including an antenna and a supercapacitor, in which the supercapacitor powers the antenna and comprises carbon foam material made, at least in part, by the method defined in any of Features A – K above.

Feature N6: Combined Energy Scavenger + Supercapacitor.

A method of manufacturing an integrated device comprising the steps of combining or integrating an energy scavenger system and a supercapacitor, in which the supercapacitor powers an antenna and comprises carbon foam material made, at least in part, by the method defined in any of Features A – K above.

A data logging device including an energy scavenger system and a supercapacitor, in which the supercapacitor powers an antenna and comprises carbon foam material made, at least in part, by the method defined in any of Features A – K above.

Feature O1: 3D carbon foam structures: Gii-Thru for Gii-Cap

A method of manufacturing an energy storage device comprising the steps of
(i) providing a carbon pre-cursor film;
(ii) screen printing a conductive paste or ink layer, on the surface of the carbon pre-cursor film;
(iii) screen printing a collector layer over the screen printed conductive paste or ink layer;
(iv) screen printing a dielectric layer over the collector layer;
(v) making energy storage electrodes that comprise carbon foam material from the carbon pre-cursor film at least in part by the method defined in any of Features A – K above
and in which an electrically conductive path is formed from the carbon foam material to the collector layer, via the conductive paste or ink layer.

An energy storage device, such as a supercapacitor, including:
(i) a carbon pre-cursor film;
(ii) a screen printed conductive paste or ink layer, on the surface of the carbon pre-cursor film;
(iii) a screen printed collector layer over the screen printed conductive paste or ink layer;
(iv) a screen printed dielectric layer over the collector layer;
(v) energy storage electrodes that comprise carbon foam material made from the carbon pre-cursor film at least in part by the method defined in any of Features A – K above, and in which an electrically conductive path is formed from the carbon foam material to the collector layer, via the conductive paste or ink layer.

Feature O2: 3D carbon foam structures: Gii-Thru Stackable Gii-Cap/Gii-Cap+

A method of manufacturing an energy storage device comprising the steps of
(i) providing a carbon pre-cursor film;
(ii) screen printing a conductive paste or ink layer, on the surface of the carbon pre-cursor film;
(iii) screen printing a collector layer over the screen printed conductive paste or ink layer;
(iv) screen printing a dielectric layer over the collector layer;
(v) making energy storage electrodes that comprise carbon foam material from the carbon pre-cursor film at least in part by the method defined in any of Features A – K above
and in which an electrically conductive path is formed from the carbon foam material to the collector layer, via the conductive paste or ink layer;
and in which multiple sub-assemblies are formed into a stack and in which adjacent energy storage electrodes are separated by an ionic gel electrolyte.

An energy storage device, such as a supercapacitor, including a sub-assembly comprising:
(i) a carbon pre-cursor film;
(ii) a screen printed conductive paste or ink layer, on the surface of the carbon pre-cursor film;
(iii) a screen printed collector layer over the screen printed conductive paste or ink layer;
(iv) a screen printed dielectric layer over the collector layer;
(v) energy storage electrodes that comprise carbon foam material made from the carbon pre-cursor film at least in part by the method defined in any of Features A – K above, and in which an electrically conductive path is formed from the carbon foam material to the collector layer, via the conductive paste or ink layer;
and in which multiple sub-assemblies are formed into a stack and in which adjacent energy storage electrodes are separated by an ionic gel electrolyte.

Feature O3: 3D carbon foam structures: Gii-Thru for Gii-Sens: HISLOC

A microfluidic diagnostic device including sample wells positioned on an upper face of the device, reference, working and counter electrodes, made from a carbon pre-cursor film at least in part by the method defined in any of Features A – K above, are in a layer below the sample wells, and reference, working and counter electrode connections are in layer below the reference, working and counter electrodes .

Feature O4 3D carbon foam structures: Gii-Thru for Gii-Sens: HISLOC manufacturing process

A method of manufacturing a lab-on-chip device comprising the steps of
(i) providing a carbon pre-cursor film;
(ii) screen printing a conductive paste or ink layer on the surface of the carbon pre-cursor film;
(iii) screen printing a conductive layer over the screen printed conductive paste or ink layer;
(iv) screen printing a reference electrode;
(v) screen printing a dielectric layer over the collector layer;
(vi) making sensor electrodes that comprise carbon foam material from the carbon pre-cursor film at least in part by the method defined in any of Features A – K above;
and in which an electrically conductive path is formed from the carbon foam material to the conductive layer, via the conductive paste or ink layer.

A lab-on-chip device, including a sub-assembly comprising:
(i) a carbon pre-cursor film;
(ii) a screen printed conductive paste or ink layer, on the surface of the carbon pre-cursor film;
(iii) a screen printed conductive layer over the screen printed conductive paste or ink layer;
(iv) a screen printed reference electrode;
(v) a screen printed dielectric layer over the collector layer;
(vi) sensor electrodes that comprise carbon foam material made from the carbon pre-cursor film at least in part by the method defined in any of Features A – K above, and in which an electrically conductive path is formed from the carbon foam material to the conductive layer, via the conductive paste or ink layer.

Feature P: Scalable manufacturing of carbon foam: Gii 3

A method of manufacturing a device including one or more electrodes, each comprising carbon foam material;

in which the method includes passing a continuous reel of a carbon pre-cursor film through a sequence of operations required to manufacture the carbon foam material made, at least in part, by the method defined in any of Features A – K above.

Feature Q: Various other carbon foam applications

A device including a carbon foam material made, at least in part, by the method defined in any of Features A – K above, where the device is one of the following types of devices:

- Hall effect sensor: the carbon foam shows a response to magnetic fields.
- Tactile sensor for e.g. robotics; prototype sensors using Gii carbon foam with polydimethylsiloxane (PDMS) embedded into and over the structure, as an active layer in a piezoresistive based pressure sensors for use in robotic touch sensing applications.
- Infectious diseases sensor.
- Biosensor where the Gii carbon foam is subject to π–π non-covalent functionalization with pyrene carboxylic acid (PCA) for interleukin 10 impedimetric detection.
- Constant monitoring chemical sensor.
- Glucose monitoring sensor: A reversible polymer displacement sensor mechanism for electrochemical glucose monitoring; a pyrene-derivatised boronic acid chemo-receptor for glucose is adsorbed onto a carbon foam electrode, competitively binding with poly-nordihydroguaiaretic acid.
- Lactic acid sensor: Synthetic organic receptor molecules are employed based on boronic acids attached to carbon foam to provide functionality and selectivity in competitive analyte binding, using surface redox polymer indicator displacement.
- Gas detection sensor, such as hydrogen peroxide and oxygen detection using Gii carbon foam immersed in a phosphate buffer solution of pH 7nanoparticulate polymer of intrinsic microporosity (PIM-1).
- Optical detector.
- Self-charging hybrid energy generation device.
- Green gas conversion into useful chemical.
- Fuel cell, e.g. hydrogen fuel cell.
- Filters, including gas permeable filter.

- Heating device.

Feature R: Non-graphene carbon material foam

A carbon foam material made, at least in part, by the method defined in any of Features A – K above and that is hydrophilic, with a contact angle below 20°.

A carbon foam material made, at least in part, by the method defined in any of Features A – K above and with a Raman spectrum exhibiting a significant D peak; the 2D peak is less than the G peak; the peak D: peak G ratio is above zero.

A carbon nano-onion material made, at least in part, by the method defined in any of Features A – K above.

A device including a carbon foam material made, at least in part, by the method defined in any of Features A – K above and that is hydrophilic, with a contact angle below 20°.

A device including a carbon foam material made, at least in part, by the method defined in any of Features A – K above with a Raman spectrum exhibiting a significant D peak; the 2D peak is less than the G peak; the peak D: peak G ratio is above zero.

A device including a carbon nano-onion material, made, at least in part, by the method defined in any of Features A – K above.

Optional features

Note that any one or more of the following optional features may each be combined with any one or more other, compatible optional features and with any one or more of the main Features **A - R**.

The manufacturing processes

- the manufacturing process is a room temperature process.
- the manufacturing process is an ambient pressure process.
- can be done on a plastic substrate (compatible with any manufacturing process, not just silicon chip fabrication).
- can be done without a catalyst.
- the manufacturing process takes approximately 2 minutes or less to manufacture 1cm^2 of approximately 50μm thick carbon foam onto a plastic substrate.
- the manufacturing process enables a 3D carbon foam to be created on a flexible substrate.
- the manufacturing process requires no graphene or graphene oxide precursor.
- the manufacturing process creates carbon foam material solely in the encapsulated, sub-surface region of the carbon pre-cursor material and not at any surface of the carbon pre-cursor material.
- the manufacturing process uses a combination of industry standard, low cost and scalable (i) screen printing technology and (ii) computer-controlled laser scanning technology.
- the manufacturing process uses, or can be adapted for, high-speed, high volume reel-to-reel or reel-to-sheet production.

The first laser beam parameters and control scheme

- the first laser beam and the second laser beam are generated by different laser systems.
- the first laser beam and the second laser beam are generated by the same laser systems.
- parameters of the laser beam that irradiates the sub-surface or encapsulated region include one or more of: intensity, wavelength, pulse frequency, pulse duration, pulse profile, scanning speed, focal distance, heat generated at the sub-surface or encapsulated region.
- varying the laser parameters alters the carbon foam material properties, enabling carbon foam to be produced with properties that are optimised for different applications.
- varying the laser parameters alters one or more of the following carbon foam material properties or parameters: type of carbon nanostructures present (e.g. carbon nano-onion etc),

size of defects, distribution of defects, extent of defects, type of defects, of the Raman D and 2D peaks, relative size of the Raman D and 2D peaks, thickness or depth, flexibility, adhesion, porosity, electrical conductivity, capacitance, absorption of organic solvents and water-based solutions, hydrophilicity, EMI shielding, electrode quality, wettability, contact angle, anti-fouling.

- laser beam generates a temperature of higher than 500°C at the sub-surface or encapsulated region to form carbon foam.
- laser beam generates a temperature of over 500°C at the sub-surface or encapsulated region to form carbon foam.
- laser pulse duration is between 1 ns and 10 μs, giving a heating rate of between around 5 x 10^7 °C/s and 2 x 10^{12} °C/s.
- laser power is within a typical working range of 8 - 20 watts, with 12W optimum.
- laser focal distance is within a typical working range of 50mm - 400mm.
- laser pulse frequency is between 50 kHz and 500 kHz.
- laser pulse frequency is between 1 kHz and 2 MHz.
- laser wavelength is between 0.7 μm – 2.5 μm.
- laser is scanned at between 9cm/s and 40cm/s (or ± 50% of these ranges).
- parameters of the laser beam include focus parameters.
- parameters of the laser beam include diffraction parameters.
- parameters of the laser beam include interference pattern parameters.
- focus of the laser beam moves through the depth of the carbon pre-cursor material to generate carbon foam in the sub-surface or encapsulated region of the carbon pre-cursor
- focus of the laser beam moves at least approximately 50 μm through the depth of the carbon pre-cursor material to generate carbon foam in the sub-surface or encapsulated region of the carbon pre-cursor.
- focus of the laser beam moves at least 100 μm through the depth of the carbon pre-cursor material to generate carbon foam in the sub-surface or encapsulated region of the carbon pre-cursor.
- laser beam scans (e.g., raster scans) or moves laterally across the carbon pre-cursor material to form a desired pattern.
- laser beam scans or moves laterally across the carbon pre-cursor material to form a desired pattern that includes non-overlapping regions or lines.

- laser beam is repeatedly scanned (e.g., raster scanned) or moved laterally across the carbon pre-cursor material with a focus or intensity maximum arranged to multiple different depths withing the carbon pre-cursor material until carbon foam of the required pattern and depth has been created.
- laser beam is scanned at a scan rate of between 1.7 mm/s and 3550 m/s, or more typically between 35 mm/s and 350 mm/s and the scanning may be such that the number of pulses per inch (PPI) is between 100 and 10000 (relevant to the production of individual approximately polyimide sheets of size 220mm x 180mm).
- laser beam has a wavelength with substantially no, or very low, absorbance by the carbon pre-cursor material.
- laser beam has a wavelength with very low, absorbance by the carbon pre-cursor material

  where the radiation absorbance per cm (base 10) is below 50, or below 20 or below 10.
- laser beam is an IR laser.
- laser beam is an IR laser with wavelength of between 0.7 μm – 2.5 μm.
- laser beam is an IR laser with wavelength of between 0.75 μm – 1.40 μm.

Attributes of the sub-surface or encapsulated region

- a desired depth of the sub-surface or encapsulated region in the carbon pre-cursor material is achieved by moving the focus of the first laser beam through that depth.
- sub-surface or encapsulated region is at least 10 μm below the surface of the carbon pre-cursor material.
- sub-surface or encapsulated region is at least 20 μm below the surface of the carbon pre-cursor material.
- sub-surface or encapsulated region is at least 30 μm below the surface of the carbon pre-cursor material.
- sub-surface or encapsulated region is at least 40 μm below the surface of the carbon pre-cursor material.
- sub-surface or encapsulated region is at least 50 μm below the surface of the carbon pre-cursor material.
- unlike conventional graphene foams, the sub-surface or encapsulated region can be over approximately 50 μm in thickness.

- sub-surface or encapsulated region has a thickness of between 10 μm and 200 μm.
- the sub-surface or encapsulated region can be at different depths below the surface of the carbon pre-cursor material facing the incident laser; the exact depth at which the sub-surface or encapsulated region is a function of various factors, such as laser intensity or other laser parameters, the choice of carbon pre-cursor material used etc. For example, the sub-surface or encapsulated region can be at least approximately 10 μm, 20 μm, 30 μm, 40 μm, 50 μm or more below the surface of the carbon pre-cursor material.
- sub-surface or encapsulated region is at a distance below the surface of the carbon pre-cursor material that is at least 1% of the total thickness of the carbon pre-cursor material, or at least 10% of the total thickness of the carbon pre-cursor material, or at least 20% of the total thickness of the carbon pre-cursor material, or at least 30% of the total thickness of the carbon pre-cursor material, or at least 40% of the total thickness of the carbon pre-cursor material.
- sub-surface or encapsulated region is volume of space centred at the centre of the minimum cross-section of the first laser beam and the volume is within 500 microns of this centre, or 100 microns of this centre, or 1 micron of this centre.

The carbon pre-cursor material

- the carbon pre-cursor material is made substantially of thermo-setting material.
- the carbon pre-cursor material is made substantially of non-thermo-plastic material.
- the carbon pre-cursor material is a thermo-setting film.
- the thermo-setting film is a polyimide film.
- carbon pre-cursor is a polyimide film.
- carbon pre-cursor is a polyimide film, the wavelength of the first laser is within the range of 0.7 μm to 2.5 μm.
- carbon pre-cursor is at least 50% carbon by mass, or at least 75% carbon by mass, or at least 90% carbon by mass.
- carbon pre-cursor is a film or sheet.
- the carbon pre-cursor material is flexible.
- the carbon pre-cursor material is a printed layer, such as a screen-printed layer.

- the carbon pre-cursor material has a thickness greater than 5 μm, or between 5 μm and 120 μm, or greater than 120 μm.
- the carbon pre-cursor material is substantially planar or flat and is oriented perpendicular to the first laser beam.
- the carbon pre-cursor material is homogeneous.
- the carbon pre-cursor material is heterogenous, and comprises several different materials.
- carbon pre-cursor is supported on a substrate that is not made of a carbon pre-cursor.
- the absorption coefficient of the carbon pre-cursor material at the first laser beam wavelength is low.
- the absorption coefficient of the carbon pre-cursor material for the first laser beam is below 50 cm^{-1}, or below 20 cm^{-1}, or below 10 cm^{-1}
- the absorption coefficient of the carbon pre-cursor material for the second or ablation laser beam is below 300 cm^{-1}
- the absorption coefficient of the carbon pre-cursor material for the second or ablation laser beam is 300±50 cm^{-1}
- the carbon pre-cursor material has a thermal conductivity of less than 1.0 W/mK (using a method according to ASTM D5470).
- the carbon pre-cursor material has a thermal conductivity of less than 0.5 W/mK (using a method according to ASTM D5470).
- carbon pre-cursor material is mounted on a substrate that is substantially optically transparent at the wavelength or wavelengths of the laser beam.
- the carbon pre-cursor material carbon source comprises or is formed from one or more polymers.
- the carbon pre-cursor material comprises one or more of the following materials: polyimides (for example, poly(4,4'-oxydiphenylene-pyromellitimide), otherwise known as polyimide), polyetherimides (PEI), poly(methyl methacrylate) (PMMA) (e.g., spray-coated PMMA), polyurethanes (PU), polyesters, vinyl polymers, carbonized polymers, photoresist polymers, alkyds, urea-formaldehyde.
- the carbon pre-cursor comprises one or more of the following materials: poly(amic acids) (for example an aryl-containing poly (amic acid)) (for example poly(pyromellitic dianhydride-*co*-4,4'-oxydianiline), amic acid - otherwise known as polyamic acid); dianhydrides (for example aryl dianhydrides) (for example pyromellitic dianhydride);

derivatives of said poly(amic acids); derivatives of said dianhydrides (e.g., derivates of pyromellitic dianhydride).

- the carbon pre-cursor comprises one or more of the following materials: aromatic materials (e.g., aromatic polymers); heteroaromatic materials (e.g., heteroaromatic polymers); polymers containing aromatic moieties; cyclic materials (e.g., polymers containing cyclic moieties); heterocyclic materials (e.g., polymers containing heterocyclic moieties); heteroaromatic materials (e.g., polymers containing heteroaromatic moieties).
- the carbon pre-cursor comprises material: containing one or more of aromatic bonds, or heteroaromatic bonds or hetero bonds (e.g., imide bonds).

The substrate supporting the carbon pre-cursor material

- the substrate is a plastic body, film, or foil.
- the substrate is flexible.
- the substrate is a polyimide circuit board.
- the substrate has very low absorbance of the first laser beam.
- the substrate is substantially optically transparent at the wavelength or wavelengths of the first laser beam.
- the substrate has a high absorbance of the first laser beam, absorbing greater than 60% of the first laser beam.
- the substrate has a high absorbance of the first laser beam, absorbing greater than 60% of the first laser beam and has a thermal conductivity of at least 10 W/mK.
- the surface of the carbon pre-cursor material is converted to a disorganised, amorphous, non-graphene substance by the laser beam and that disorganised, amorphous, non-graphene substance adheres or bonds to the substrate and hence indirectly attaches the 3D carbon material foam to the substrate.
- the substrate is formed from one or more of the following: silicon (Si), silicon dioxide (SiO2), gallium nitride (GaN), gallium arsenide (GaAs), zinc oxide (ZnO).
- the substrate is silicon wafer.
- the substrate is a silicon dioxide wafer.
- the substrate is a wafer comprising both silicon and silicon dioxide.
- the substrate is a carbon source.

- the substrate is not a carbon source, e.g. is a metal, dielectric material, a screen-printed dielectric material.
- the carbon pre-cursor is positioned 'above' the substrate (e.g. the carbon pre-cursor is positioned closer to the laser sources than the substrate).
- the carbon pre-cursor is positioned 'below' the substrate (e.g. the carbon pre-cursor is positioned further from the laser sources than the substrate).

The carbonisation at the surface that the laser beam is incident on

- the surface of the carbon pre-cursor material is converted to a disorganised, amorphous, non-graphene substance by the laser beam.
- disorganised, amorphous, non-graphene substance occupies a thickness from the surface of the adjacent carbon pre-cursor material that is approximately 1%, or less than approximately 1%, or less than approximately 5%, or less than approximately 10%, of the total thickness of the carbon pre-cursor material.
- disorganised, amorphous, non-graphene substance extends a distance from its surface into the body of the carbon pre-cursor material that is at least 10 μm.
- the disorganised, amorphous, non-graphene substance extends from its outer surface into the body of the carbon pre-cursor material to a depth of 10 μm or less, or to a depth of 20 μm or less, or to a depth of 30 μm or less, or to a depth of 40 μm or less, or to a depth of 50 μm or less, or to a depth of 100 μm or less.

The carbonisation at the physical interface with a substrate supporting the carbon pre-cursor material

- the carbon pre-cursor material is converted to a disorganised, amorphous, non-graphene substance by the laser beam at the physical interface with the substrate to a depth defined by parameters of the laser beam.
- the disorganised, amorphous, non-graphene substance is at one region adhering or otherwise attaching to the carbon foam and is at another region adhering or otherwise attaching to the substrate, hence giving stability to the carbon foam.
- the disorganised, amorphous, non-graphene substance occupies a thickness, measured from the interface of the carbon pre-cursor material with the substrate, that is

approximately 1%, or less than approximately 1%, or less than approximately 5%, or less than approximately 10%, of the total thickness of the carbon pre-cursor material.

- the disorganised, amorphous, non-graphene substance occupies a thickness from the interface of the carbon pre-cursor material with the substrate that is at least 10 μm.
- the disorganised, amorphous, non-graphene substance extends from the interface of the carbon pre-cursor material with the substrate to a depth of 10 μm or less, or to a depth of 20 μm or less, or to a depth of 30 μm or less, or to a depth of 40 μm or less, or to a depth of 50 μm or less, or to a depth of 100 μm or less.

The ablation laser beam or second laser beam

- parameters of the laser beam include one or more of: intensity, wavelength, pulse frequency, pulse duration, pulse profile, scanning speed, focal distance, heat generated at the sub-surface or encapsulated region.
- varying the laser parameters alters the carbon foam material properties, enabling carbon foam to be produced with properties that are optimised for different applications.
- varying the laser parameters alters one or more of the following carbon foam material properties or parameters: type of carbon nanostructures present (e.g. carbon nano-onion etc), size of defects, distribution of defects, extent of defects, type of defects, of the Raman D and 2D peaks, relative size of the Raman D and 2D peaks, thickness or depth, flexibility, adhesion, porosity, electrical conductivity, capacitance, absorption of organic solvents and water-based solutions, hydrophilicity, EMI shielding, electrode quality, wettability, contact angle, anti-fouling.
- laser beam that ablates the amorphous, non-graphene substance that is formed above the encapsulated or sub-surface region in the carbon pre-cursor (the 'second laser beam') is a CO2 laser.
- the second laser beam alters the carbon foam as part of the process of exposing it.
- the second laser beam alters the morphology of the carbon foam as part of the process of exposing it.
- the second laser beam is automatically controlled to be scanned across the same regions, and/or overlapping regions and/or non-overlapping regions.
- wavelength of the laser beam that ablates the amorphous, non-graphene substance is between 8 μm -15 μm.

- the second laser beam is a long IR laser, or a UV laser or a visible light laser.
- the second laser beam has a pulse frequency of between 50 kHz and 500 kHz and a scan speed of between 9cm/s and 40cm/s.
- the absorption coefficient of the carbon pre-cursor material is above 100 cm^{-1} for the second laser beam, or above 200 cm^{-1} for the second laser beam.
- the absorption coefficient of the carbon pre-cursor material is 300±50 cm^{-1} for the second laser beam.
- laser power is within a typical working range of 8 - 20 watts, with 12W optimum.
- laser focal distance is within a typical working range of 50mm - 400mm.
- the second laser beam is scanned in a pattern (e.g., a raster) that includes non-overlapping regions or lines.
- the second laser beam is scanned in a pattern that matches the scan pattern of the first laser beam.
- the second laser beam is de-focussed.
- the second laser beam is the same as the laser beam that irradiates the encapsulated or sub-surface region of a carbon pre-cursor material, to create a carbon foam in that encapsulated or sub-surface region.
- the manufacturing process is a three-stage process involving the steps: (a) the first laser beam irradiating a sub-surface region of a carbon pre-cursor material at a manufacturing site to produce unfinished carbon foam product; (b) the unfinished carbon foam product being transferred to a customer-controlled manufacturing site; and (c) the laser ablation or treatment taking place at the customer-controlled manufacturing site.

The carbon foam

- the carbon foam is a multilayer twisted or turbostratic carbon foam.
- the carbon foam is a non-graphene carbon foam.
- the carbon foam includes carbonaceous nanostructures, such as carbon nano-onion, carbon nano-horn, carbon nano-tubes, carbon nano-dots, nanodiamonds and fullerene, or combinations of any of these.
- the carbon foam is at least approximately 50 μm in thickness.
- the carbon foam is between approximately 50 μm to 300 μm in thickness.
- the carbon foam is or includes a twisted or turbostratic multilayer foam.

- the carbon foam is or includes a carbon foam with a spatial distribution of defects leading to high electrochemical reactivity.
- the carbon foam is or includes a carbon foam with vacancy position basal plane defects leading to high electrochemical reactivity.
- the carbon foam has a Carbon: Oxygen ratio of between 25: 1 and 50:1.
- the carbon foam has a fast electron transfer constant.
- the carbon foam has one or more of the following properties compared to conventional graphene foam made using conventional laser processes: a more readily controlled thickness or depth; greater flexibility compared to the highly brittle graphene made using conventional laser processes; stronger adhesion to an underlying flexible substrate; higher porosity; higher electrical conductivity; increased capacitance or charge storage; faster absorption of organic solvents and water-based solutions; higher hydrophilicity; a contact angle of below approximately 20°; enhanced anti-fouling properties; higher EMI shielding; enhanced electrode quality.

Biosensor use case

- the carbon foam is functionalised as a biosensor.
- the carbon foam is functionalised as a biosensor by adding a receptor that is specific to a target or analyte.
- the carbon foam is functionalised as a biosensor with a reversible polymer displacement sensor mechanism for electrochemical glucose monitoring.
- the reversible polymer displacement sensor includes a pyrene-derivatised boronic acid chemo-receptor for glucose that is adsorbed onto an electrode comprising the carbon foam.
- the carbon foam is functionalised as a biosensor by adding a receptor that is specific to a target or analyte, and a linker that enables the receptor to attach to the carbon foam.
- the linker is selected from nanoparticles, polymers, polymer brushes, ligands, organic compounds comprising one or more functional groups, molecules bonded to the carbon foam covalently or non-covalently, or mixtures thereof.
- the linker is selected from polymers preferably (meth)acrylate polymers, organic compounds comprising one or more functional groups, carbodiimides, diazonium compounds, or mixtures thereof.

- the one or more functional groups are independently selected from oxygen, nitrogen, sulphur, halide, hydroxyl, carbonyl, carboxyl, amine, amino, amide, hydrophilic polymers, or mixtures thereof, optionally in combination with linear, branched or cyclic alkyl, alkylenyl, alkynyl, aryl residues, acryl, acyl, acyloxy, alkoxy, alkyleneoxy, or mixtures thereof.
- the organic compound further comprises one or more cyclic moieties that optionally comprise one or more heteroatoms, and at least one of the cyclic moieties is linked directly or indirectly to at least one of the functional groups, or the linker is a derivative that is an ester or salt of said organic compound, or a compound that releases said organic compound in reaction with the carbon foam.
- the linker is selected from 1-pyrenebutyric acid, N-hydroxysuccinimide (NHS), pyrene-1-carboxylic acid succinimidyl ester, 1-Aminopyrene, N-(1-pyrene) maleimide, or mixtures thereof.
- the linker is bonded to the carbon foam by π–π interaction.
- the receptor is one of the followings: an electrochemical receptor, a chemical receptor, a bioreceptor, an optical receptor, a physical or mechanical receptor, preferably a bioreceptor.
- the receptor is selected from crown ethers, catalysts, boric acids, concept, ligands, aptamers, proteins, enzymes, antibodies, antigens, microorganisms, nucleic acids, fatty acids, fatty acid esters, molecularly imprinted polymers, metal-organic frameworks, polypeptides or oligopeptides capable of forming a ligand binding, cells, cell organelles, or other cellular components, or mixtures thereof, preferably selected from proteins, nucleic acids, antibodies, enzymes, or mixtures thereof.
- the receptor is selected from immunoglobulin A (IgA), glucose dehydrogenase, streptavidin, or mixtures thereof.
- the receptor is physically, biologically and/or chemically bonded to the linker, preferably chemically bonded, more preferably covalently bonded.

Supercapacitor use case

- the carbon foam forms an electrode in an energy storage device, such as an electrochemical capacitor, a supercapacitor, pseudo-capacitor or capacitor.
- the carbon foam is treated with a metal oxide film to provide pseudo-capacitance.

- the carbon foam forms at least one electrode in an energy storage device, such as an electrochemical capacitor, a supercapacitor, pseudo-capacitor or capacitor, and a hydrogel electrolyte envelops the or each electrode in an active area to produce an enhanced operational voltage window.
- the carbon foam forms an electrode in a battery.
- the carbon foam forms an electrical conductor.

CLAIMS

1. A method of manufacturing a carbon foam material comprising the steps of:

(a) using a first laser beam to irradiate an encapsulated or sub-surface region of a carbon pre-cursor material below a surface of the material, to create carbon foam in that sub-surface region, and a disorganised, amorphous non-graphene material above the carbon foam, and then

(b) using a second laser beam to remove or ablate the disorganised, amorphous non-graphene material sitting above the carbon foam, to expose at least some of the carbon foam.

The first laser beam parameters and control scheme

2. The method of Claim 1 in which the first laser beam operates at a first band and the second laser beam operates at a second band.

3. The method of any preceding Claim in which the first laser beam and the second laser beam are generated by different laser systems.

4. The method of any preceding Claim in which the first laser beam and the second laser beam are generated by the same laser system.

5. The method of any preceding Claim in which the parameters of the first laser beam that irradiates the sub-surface or encapsulated region include one or more of: intensity, wavelength, pulse frequency, pulse duration, pulse profile, scanning speed, focal distance, heat generated at the sub-surface or encapsulated region.

6. The method of any preceding Claim in which the varying the laser parameters of the first laser beam alters the carbon foam material properties, enabling carbon foam to be produced with properties that are optimised for different applications.

7. The method of any preceding Claim in which varying the laser parameters of the first laser beam alters one or more of the following carbon foam material properties or parameters: type of carbon nanostructures present, size of defects, distribution of defects, extent of defects, type of defects, of the Raman D and 2D peaks, relative size of the Raman D and 2D peaks,

thickness or depth, flexibility, adhesion, porosity, electrical conductivity, capacitance, absorption of organic solvents and water-based solutions, hydrophilicity, EMI shielding, electrode quality, wettability, contact angle, anti-fouling.

8. The method of any preceding Claim in which no substantial gas escape pathways to a surface of the pre-cursor material are created by the first laser beam.

9. The method of any preceding Claim in which the first laser beam generates a temperature of higher than 500°C at the sub-surface or encapsulated region to form carbon foam.

10. The method of any preceding Claim in which the first laser beam pulse duration is between 1 ns and 10 μs, giving a heating rate of between around 5×10^7 °C/s and 2×10^{12} °C/s.

11. The method of any preceding Claim in which the first laser beam power is within a typical working range of 8 - 20 watts, with 12W optimum.

12. The method of any preceding Claim in which the first laser beam focal distance is within a typical working range of 50mm - 400mm.

13. The method of any preceding Claim in which the first laser beam pulse frequency is between 50 kHz and 500 kHz.

14. The method of any preceding Claim in which the first laser beam pulse frequency is between 1 kHz and 2 MHz.

15. The method of any preceding Claim in which the first laser beam wavelength is between 0.7 μm – 2.5 μm.

16. The method of any preceding Claim in which the first laser is scanned at between 9cm/s and 40cm/s or ± 50% of these ranges.

17. The method of any preceding Claim in which the parameters of the first laser beam include focus parameters.

18. The method of any preceding Claim in which the parameters of the first laser beam include diffraction parameters.

19. The method of any preceding Claim in which the parameters of the first laser beam include interference pattern parameters.

20. The method of any preceding Claim in which the focus of the first laser beam moves through the depth of the carbon pre-cursor material to generate carbon foam in the sub-surface or encapsulated region of the carbon pre-cursor.

21. The method of any preceding Claim in which the focus of the first laser beam moves at least approximately 50 μm through the depth of the carbon pre-cursor material to generate carbon foam in the sub-surface or encapsulated region of the carbon pre-cursor.

22. The method of any preceding Claim in which the focus of the first laser beam moves at least 100 μm through the depth of the carbon pre-cursor material to generate carbon foam in the sub-surface or encapsulated region of the carbon pre-cursor.

23. The method of any preceding Claim in which the first laser beam scans, for example, raster scans, or moves laterally across the carbon pre-cursor material to form a desired pattern.

24. The method of any preceding Claim in which the first laser beam scans or moves laterally across the carbon pre-cursor material to form a desired pattern that includes non-overlapping regions or lines.

25. The method of any preceding Claim in which the first laser beam is repeatedly scanned (e.g., raster scanned) or moved laterally across the carbon pre-cursor material with a focus or intensity maximum arranged to multiple different depths withing the carbon pre-cursor material until carbon foam of the required pattern and depth has been created.

26. The method of any preceding Claim in which the first laser beam is scanned at a scan rate of between 1.7 mm/s and 3550 m/s, or more typically between 35 mm/s and 350 mm/s and the scanning may be such that the number of pulses per inch (PPI) is between 100 and 10000

(relevant to the production of individual approximately polyimide sheets of size 220mm x 180mm).

27. The method of any preceding Claim in which the first laser beam has a wavelength with substantially no, or very low, absorbance by the carbon pre-cursor material.

28. The method of any preceding Claim in which the first laser beam has a wavelength with very low, absorbance by the carbon pre-cursor material.

29. The method of any preceding Claim in which the carbon pre-cursor material radiation absorbance per cm (base 10) is below 50, or below 20 or below 10.

30. The method of any preceding Claim in which the first laser beam is an IR laser.

31. The method of any preceding Claim in which the first laser beam is an IR laser with wavelength of between 0.7 μm – 2.5 μm.

32. The method of any preceding Claim in which the first laser beam is an IR laser with wavelength of between 0.75 μm – 1.40 μm.

Attributes of the sub-surface or encapsulated region

33. The method of any preceding Claim in which a desired depth of the sub-surface or encapsulated region in the carbon pre-cursor material is achieved by moving the focus of the first laser beam through that depth.

34. The method of any preceding Claim in which the sub-surface or encapsulated region is at least 10 μm below the surface of the carbon pre-cursor material.

35. The method of any preceding Claim in which the sub-surface or encapsulated region is at least 20 μm below the surface of the carbon pre-cursor material.

36. The method of any preceding Claim in which the sub-surface or encapsulated region is at least 30 μm below the surface of the carbon pre-cursor material.

37. The method of any preceding Claim in which the sub-surface or encapsulated region is at least 40 μm below the surface of the carbon pre-cursor material.

38. The method of any preceding Claim in which the sub-surface or encapsulated region is at least 50 μm below the surface of the carbon pre-cursor material.

39. The method of any preceding Claim in which unlike conventional graphene foams, the sub-surface or encapsulated region can be over approximately 50 μm in thickness.

40. The method of any preceding Claim in which the sub-surface or encapsulated region has a thickness of between 10 μm and 200 μm.

41. The method of any preceding Claim in which the sub-surface or encapsulated region can be at different depths below the surface of the carbon pre-cursor material facing the incident laser; and the exact depth at which the sub-surface or encapsulated region is a function of various factors, such as laser intensity or other laser parameters, and the choice of carbon pre-cursor material used.

42. The method of any preceding Claim in which the sub-surface or encapsulated region is at a distance below the surface of the carbon pre-cursor material that is at least 1% of the total thickness of the carbon pre-cursor material, or at least 10% of the total thickness of the carbon pre-cursor material, or at least 20% of the total thickness of the carbon pre-cursor material, or at least 30% of the total thickness of the carbon pre-cursor material, or at least 40% of the total thickness of the carbon pre-cursor material.

43. The method of any preceding Claim in which the sub-surface or encapsulated region is a volume of space centred at the centre of the minimum cross-section of the first laser beam and the volume is within 500 microns of this centre, or 100 microns of this centre, or 1 micron of this centre.

The carbon pre-cursor material

44. The method of any preceding Claim in which the carbon pre-cursor material is made substantially of thermo-setting material.

45. The method of any preceding Claim in which the carbon pre-cursor material is made substantially of non-thermo-plastic material.

46. The method of any preceding Claim in which the carbon pre-cursor material is a thermo-setting film.

47. The method of any preceding Claim in which the thermo-setting film is a polyimide film.

48. The method of any preceding Claim in which the carbon pre-cursor is a polyimide film.

49. The method of any preceding Claim in which the carbon pre-cursor is a polyimide film, and the wavelength of the first laser is within the range of 0.7 μm to 2.5 μm.

50. The method of any preceding Claim in which the carbon pre-cursor is at least 50% carbon by mass, or at least 75% carbon by mass, or at least 90% carbon by mass.

51. The method of any preceding Claim in which the carbon pre-cursor is a film or sheet.

52. The method of any preceding Claim in which the carbon pre-cursor material is flexible.

53. The method of any preceding Claim in which the carbon pre-cursor material is a printed layer, such as a screen-printed layer.

54. The method of any preceding Claim in which the carbon pre-cursor material has a thickness greater than 5 μm, or between 5 μm and 120 μm, or greater than 120 μm.

55. The method of any preceding Claim in which the carbon pre-cursor material is substantially planar or flat and is oriented perpendicular to the first laser beam.

56. The method of any preceding Claim in which the carbon pre-cursor material is homogeneous.

57. The method of any preceding Claim in which the carbon pre-cursor material is heterogenous, and comprises several different materials.

58. The method of any preceding Claim in which the carbon pre-cursor is supported on a substrate that is not made of a carbon pre-cursor.

59. The method of any preceding Claim in which the absorption coefficient of the carbon pre-cursor material at the first laser beam wavelength is low.

60. The method of any preceding Claim in which the absorption coefficient of the carbon pre-cursor material for the first laser beam is below 50 cm^{-1}, or below 20 cm^{-1}, or below 10 cm^{-1}.

61. The method of any preceding Claim in which the absorption coefficient of the carbon pre-cursor material for the second or ablation laser beam is below 300 cm^{-1}.

62. The method of any preceding Claim in which the absorption coefficient of the carbon pre-cursor material for the second or ablation laser beam is 300±50 cm^{-1}.

63. The method of any preceding Claim in which the carbon pre-cursor material has a thermal conductivity of less than 1.0 W/mK (using a method according to ASTM D5470).

64. The method of any preceding Claim in which the carbon pre-cursor material has a thermal conductivity of less than 0.5 W/mK (using a method according to ASTM D5470).

65. The method of any preceding Claim in which the carbon pre-cursor material is mounted on a substrate that is substantially optically transparent at the wavelength or wavelengths of the laser beam.

66. The method of any preceding Claim in which the carbon pre-cursor material carbon source comprises or is formed from one or more polymers.

67. The method of any preceding Claim in which the carbon pre-cursor material comprises one or more of the following materials: polyimides (for example, poly(4,4'-oxydiphenylene-pyromellitimide), otherwise known as polyimide), polyetherimides (PEI), poly(methyl methacrylate) (PMMA) (e.g., spray-coated PMMA), polyurethanes (PU), polyesters, vinyl polymers, carbonized polymers, photoresist polymers, alkyds, urea-formaldehyde.

68. The method of any preceding Claim in which the carbon pre-cursor comprises one or more of the following materials: poly(amic acids) (for example an aryl-containing poly (amic acid)) (for example poly(pyromellitic dianhydride-*co*-4,4'-oxydianiline), amic acid - otherwise known as polyamic acid); dianhydrides (for example aryl dianhydrides) (for example pyromellitic dianhydride); derivatives of said poly(amic acids); derivatives of said dianhydrides (e.g., derivates of pyromellitic dianhydride).

69. The method of any preceding Claim in which the carbon pre-cursor comprises one or more of the following materials: aromatic materials (e.g., aromatic polymers); heteroaromatic materials (e.g., heteroaromatic polymers); polymers containing aromatic moieties; cyclic materials (e.g., polymers containing cyclic moieties); heterocyclic materials (e.g., polymers containing heterocyclic moieties); heteroaromatic materials (e.g., polymers containing heteroaromatic moieties).

70. The method of any preceding Claim in which the carbon pre-cursor comprises material: containing one or more of aromatic bonds, or heteroaromatic bonds or hetero bonds (e.g., imide bonds).

The substrate supporting the carbon pre-cursor material

71. The method of any preceding Claim in which the carbon pre-cursor is positioned on or adjacent to a substrate.

72. The method of any preceding Claim in which the carbon pre-cursor is positioned 'above' the substrate (e.g. the carbon pre-cursor is positioned closer to the laser sources than the substrate).

73. The method of any preceding Claim in which the carbon pre-cursor is positioned 'below' the substrate (e.g. the carbon pre-cursor is positioned further from the laser sources than the substrate).

74. The method of any preceding Claim in which the substrate is a plastic body, film, or foil.

75. The method of any preceding Claim in which the substrate is flexible.

76. The method of any preceding Claim in which the substrate is a polyimide circuit board.

77. The method of any preceding Claim in which the substrate has very low absorbance of the first laser beam.

78. The method of any preceding Claim in which the substrate is substantially optically transparent at the wavelength or wavelengths of the first laser beam.

79. The method of any preceding Claim in which the substrate has a high absorbance of the first laser beam, absorbing greater than 60% of the first laser beam.

80. The method of any preceding Claim in which the substrate has a high absorbance of the first laser beam, absorbing greater than 60% of the first laser beam and has a thermal conductivity of at least 10 W/mK.

81. The method of any preceding Claim in which the surface of the carbon pre-cursor material is converted to a disorganised, amorphous, non-graphene substance by the laser beam and that disorganised, amorphous, non-graphene substance adheres or bonds to the substrate and hence indirectly attaches the 3D carbon material foam to the substrate.

82. The method of any preceding Claim in which the substrate is formed from one or more of the following: silicon (Si), silicon dioxide (SiO2), gallium nitride (GaN), gallium arsenide (GaAs), zinc oxide (ZnO).

83. The method of any preceding Claim in which the substrate is silicon wafer.

84. The method of any preceding Claim in which the substrate is a silicon dioxide wafer.

85. The method of any preceding Claim in which the substrate is a wafer comprising both silicon and silicon dioxide.

86. The method of any preceding Claim in which the substrate is a carbon source.

87. The method of any preceding Claim in which the substrate is not a carbon source, e.g. a metal, dielectric material, a screen-printed dielectric material.

The carbonisation at the surface that the laser beam is incident on

88. The method of any preceding Claim in which the surface of the carbon pre-cursor material is converted to a disorganised, amorphous, non-graphene substance by the first laser beam.

89. The method of any preceding Claim in which the disorganised, amorphous, non-graphene substance occupies a thickness from the surface of the carbon pre-cursor material that is approximately 1%, or less than approximately 1%, or less than approximately 5%, or less than approximately 10%, of the total thickness of the carbon pre-cursor material.

90. The method of any preceding Claim in which the disorganised, amorphous, non-graphene substance occupies a thickness from the surface of the carbon pre-cursor material that is at least 10 μm.

91. The method of any preceding Claim in which the disorganised, amorphous, non-graphene substance extends from its outer surface into the body of the carbon pre-cursor material to a depth of 10 μm or less, or to a depth of 20 μm or less, or to a depth of 30 μm or less, or to a depth of 40 μm or less, or to a depth of 50 μm or less, or to a depth of 100 μm or less.

The carbonisation at the physical interface with a substrate supporting the carbon pre-cursor material

92. The method of any preceding Claim in which the carbon pre-cursor is positioned on or adjacent to a substrate.

93. The method of any preceding Claim in which the carbon pre-cursor material is converted to a disorganised, amorphous, non-graphene substance by the laser beam at the physical interface with the substrate to a depth defined by parameters of the laser beam.

94. The method of any preceding Claim in which the disorganised, amorphous, non-graphene substance is at one region adhering or otherwise attaching to the carbon foam and is at another region adhering or otherwise attaching to the substrate, hence giving stability to the carbon foam.

95. The method of any preceding Claim in which the disorganised, amorphous, non-graphene substance occupies a thickness, measured from the interface of the carbon pre-cursor material with the substrate, that is approximately 1%, or less than approximately 1%, or less than approximately 5%, or less than approximately 10%, of the total thickness of the carbon pre-cursor material.

96. The method of any preceding Claim in which the disorganised, amorphous, non-graphene substance occupies a thickness from the interface of the carbon pre-cursor material with the substrate that is at least 10 μm.

97. The method of any preceding Claim in which the disorganised, amorphous, non-graphene substance extends from the interface of the carbon pre-cursor material with the substrate to a depth of 10 μm or less, or to a depth of 20 μm or less, or to a depth of 30 μm or less, or to a depth of 40 μm or less, or to a depth of 50 μm or less, or to a depth of 100 μm or less.

The ablation laser beam or second laser beam

98. The method of any preceding Claim in which parameters of the second laser beam include one or more of: intensity, wavelength, pulse frequency, pulse duration, pulse profile, scanning speed, focal distance, heat generated at the sub-surface or encapsulated region.

99. The method of any preceding Claim in which varying the second laser parameters alters the carbon foam material properties, enabling carbon foam to be produced with properties that are optimised for different applications.

100. The method of any preceding Claim in which varying the laser parameters of the second laser beam alters one or more of the following carbon foam material properties or parameters: type of carbon nanostructures present, size of defects, distribution of defects, extent of defects, type of defects, of the Raman D and 2D peaks, relative size of the Raman D and 2D peaks, thickness or depth, flexibility, adhesion, porosity, electrical conductivity, capacitance, absorption of organic solvents and water-based solutions, hydrophilicity, EMI shielding, electrode quality, wettability, contact angle, anti-fouling.

101. The method of any preceding Claim in which the second laser beam is a CO2 laser.

102. The method of any preceding Claim in which the second laser beam alters the carbon foam as part of the process of exposing it.

103. The method of any preceding Claim in which the second laser beam alters the morphology of the carbon foam as part of the process of exposing it.

104. The method of any preceding Claim in which the second laser beam is automatically controlled to be scanned across the same regions, and/or overlapping regions and/or non-overlapping regions.

105. The method of any preceding Claim in which the wavelength of the second laser beam that ablates the amorphous, non-graphene substance is between 8 μm -15 μm.

106. The method of any preceding Claim in which the second laser beam is a long IR laser, or a UV laser or a visible light laser.

107. The method of any preceding Claim in which the second laser beam has a pulse frequency of between 50 kHz and 500 kHz and a scan speed of between 9cm/s and 40cm/s.

108. The method of any preceding Claim in which the absorption coefficient of the carbon pre-cursor material is above 100 cm^{-1} for the second laser beam, or above 200 cm^{-1} for the second laser beam.

109. The method of any preceding Claim in which the absorption coefficient of the carbon pre-cursor material is 300±50 cm^{-1} for the second laser beam.

110. The method of any preceding Claim in which the laser power is within a typical working range of 8 - 20 watts, with 12W optimum.

111. The method of any preceding Claim in which the second laser focal distance is within a typical working range of 50mm - 400mm.

112. The method of any preceding Claim in which the second laser beam is scanned in a pattern (e.g., a raster) that includes non-overlapping regions or lines.

113. The method of any preceding Claim in which the second laser beam is scanned in a pattern that matches the scan pattern of the first laser beam.

114. The method of any preceding Claim in which the second laser beam is de-focussed.

115. The method of any preceding Claim in which the second laser beam is the same as the laser beam that irradiates the encapsulated or sub-surface region of a carbon pre-cursor material, to create a carbon foam in that encapsulated or sub-surface region.

116. The method of any preceding Claim in which the manufacturing process is a three-stage process involving the steps: (a) the first laser beam irradiating a sub-surface region of a carbon pre-cursor material at a manufacturing site to produce unfinished carbon foam product; (b) the unfinished carbon foam product being transferred to a customer-controlled manufacturing site; and (c) the laser ablation or treatment taking place at the customer-controlled manufacturing site.

The carbon foam

117. The method of any preceding Claim in which the carbon foam is or includes a multilayer twisted or turbostratic carbon foam.

118. The method of any preceding Claim in which the carbon foam is or includes a non-graphene carbon foam.

119. The method of any preceding Claim in which the carbon foam includes carbonaceous nanostructures, such as carbon nano-onion, carbon nano-horn, carbon nano-tubes, carbon nano-dots, nanodiamonds and fullerene, or combinations of any of these.

120. The method of any preceding Claim in which the carbon foam is at least approximately 50 μm in thickness.

121. The method of any preceding Claim in which the carbon foam is between approximately 50 μm to 300 μm in thickness.

122. The method of any preceding Claim in which the carbon foam is or includes a carbon foam with a spatial distribution of defects leading to high electrochemical reactivity.

123. The method of any preceding Claim in which the carbon foam is or includes a carbon foam with vacancy position basal plane defects leading to high electrochemical reactivity.

124. The method of any preceding Claim in which the carbon foam has a Carbon: Oxygen ratio of between 25: 1 and 50:1.

125. The method of any preceding Claim in which the carbon foam has a fast electron transfer constant.

126. The method of any preceding Claim in which the carbon foam has one or more of the following properties compared to conventional graphene foam made using conventional laser processes: a more readily controlled thickness or depth; greater flexibility compared to the highly brittle graphene made using conventional laser processes; stronger adhesion to an underlying flexible substrate; higher porosity; higher electrical conductivity; increased capacitance or charge storage; faster absorption of organic solvents and water-based solutions;

higher hydrophilicity; a contact angle of below approximately 20°; enhanced anti-fouling properties; higher EMI shielding; enhanced electrode quality.

Biosensor use case

127. The method of any preceding Claim in which the carbon foam is functionalised as a biosensor.

128. The method of any preceding Claim in which the carbon foam is functionalised as a biosensor by adding a receptor that is specific to a target or analyte.

129. The method of any preceding Claim in which the carbon foam is functionalised as a biosensor with a reversible polymer displacement sensor mechanism for electrochemical glucose monitoring.

130. The method of any preceding Claim in which the reversible polymer displacement sensor includes a pyrene-derivatised boronic acid chemo-receptor for glucose that is adsorbed onto an electrode comprising the carbon foam.

131. The method of any preceding Claim in which the carbon foam is functionalised as a biosensor by adding a receptor that is specific to a target or analyte, and a linker that enables the receptor to attach to the carbon foam.

132. The method of any preceding Claim in which the linker is selected from nanoparticles, polymers, polymer brushes, ligands, organic compounds comprising one or more functional groups, molecules bonded to the carbon foam covalently or non-covalently, or mixtures thereof.

133. The method of any preceding Claim in which the linker is selected from polymers preferably (meth)acrylate polymers, organic compounds comprising one or more functional groups, carbodiimides, diazonium compounds, or mixtures thereof.

134. The method of any preceding Claim in which the one or more functional groups are independently selected from oxygen, nitrogen, sulphur, halide, hydroxyl, carbonyl, carboxyl,

amine, amino, amide, hydrophilic polymers, or mixtures thereof, optionally in combination with linear, branched or cyclic alkyl, alkylenyl, alkynyl, aryl residues, acryl, acyl, acyloxy, alkoxy, alkyleneoxy, or mixtures thereof.

135. The method of any preceding Claim in which the organic compound further comprises one or more cyclic moieties that optionally comprise one or more heteroatoms, and at least one of the cyclic moieties is linked directly or indirectly to at least one of the functional groups, or the linker is a derivative that is an ester or salt of said organic compound, or a compound that releases said organic compound in reaction with the carbon foam.

136. The method of any preceding Claim in which the linker is selected from 1-pyrenebutyric acid, N-hydroxysuccinimide (NHS), pyrene-1-carboxylic acid succinimidyl ester, 1-Aminopyrene, N-(1-pyrene) maleimide, or mixtures thereof.

137. The method of any preceding Claim in which the linker is bonded to the carbon foam by π–π interaction.

138. The method of any preceding Claim in which the receptor is one of the followings: an electrochemical receptor, a chemical receptor, a bioreceptor, an optical receptor, a physical or mechanical receptor, preferably a bioreceptor.

139. The method of any preceding Claim in which the receptor is selected from crown ethers, catalysts, boric acids, concept, ligands, aptamers, proteins, enzymes, antibodies, antigens, microorganisms, nucleic acids, fatty acids, fatty acid esters, molecularly imprinted polymers, metal-organic frameworks, polypeptides or oligopeptides capable of forming a ligand binding, cells, cell organelles, or other cellular components, or mixtures thereof, preferably selected from proteins, nucleic acids, antibodies, enzymes, or mixtures thereof.

140. The method of any preceding Claim in which the receptor is selected from immunoglobulin A (IgA), glucose dehydrogenase, streptavidin, or mixtures thereof.

141. The method of any preceding Claim in which the receptor is physically, biologically and/or chemically bonded to the linker, preferably chemically bonded, more preferably covalently bonded.

Supercapacitor use case

142. The method of any preceding Claim in which the carbon foam forms an electrode in an energy storage device, such as an electrochemical capacitor, supercapacitor, pseudo-capacitor or capacitor.

143. The method of any preceding Claim in which the carbon foam is treated with a metal oxide film or other pseudo-capacitive material to provide pseudo-capacitance.

144. The method of any preceding Claim in which the carbon foam forms at least one electrode in an energy storage device, such as an electrochemical capacitor, supercapacitor, pseudo-capacitor or capacitor, and a hydrogel electrolyte envelops the or each electrode in an active area to produce an enhanced operational voltage window.

145. The method of any preceding Claim in which the carbon foam forms an electrode in a battery.

146. The method of any preceding Claim in which the carbon foam forms an electrical conductor.

The manufacturing processes detail

147. The method of any preceding Claim including the step of screen printing electrical contacts onto or into the carbon pre-cursor material before using the first laser beam.

148. The method of any preceding Claim including the step of screen printing electrical contacts onto or into the carbon pre-cursor material after using the first and the second laser beam.

149. The method of any preceding Claim in which the manufacturing method is a room temperature process.

150. The method of any preceding Claim in which the manufacturing method is an ambient pressure process.

151. The method of any preceding Claim in which the manufacturing method can be done on a plastic substrate.

152. The method of any preceding Claim in which the manufacturing method enables a 3D carbon foam to be created on a flexible substrate.

153. The method of any preceding Claim in which the manufacturing method creates carbon foam material solely in the encapsulated, sub-surface region of the carbon pre-cursor material and not at any surface of the carbon pre-cursor material.

154. The method of any preceding Claim in which the manufacturing method uses a combination of industry standard, low cost and scalable (i) screen printing technology and (ii) computer-controlled laser scanning technology.

155. The method of any preceding Claim in which the manufacturing method uses high-speed, high volume reel-to-reel or reel-to-sheet production.

156. The method of any preceding Claim in which step (a) of Claim 1 is performed at one manufacturing facility and step (b) of Claim 1 is performed at a different facility.

157. The method of any preceding Claim comprising the steps of (a) screen printing electrical contacts onto or into a carbon pre-cursor material; (b) using a laser beam operating at a first band to irradiate an encapsulated or sub-surface region of a carbon pre-cursor material below a surface of the material, to create carbon foam in that encapsulated or sub-surface region, and where steps (a) and (b) can be performed in the sequence (a) then (b) or (b) then (a); and then (c) using a laser beam operating at a second band to remove or ablate material sitting between the carbon foam and the surface of the carbon pre-cursor material, to expose at least some of the carbon foam to which the electrical contacts are connected.

Applications

158. The method of any preceding Claim when used for manufacturing a biosensor including a sensing electrode comprising carbon foam made, at least in part, by the method defined in any preceding manufacturing method claim.

159. The method of any preceding Claim when used for manufacturing a biosensor including sensor electrodes, such as a working electrode, a counter electrode, each comprising carbon foam made, at least in part, by the method defined in any preceding manufacturing method claim, and the method includes screen printing electrical connection tracks over each electrode and at least partly covering the electrodes and connection tracks with a screen printed dielectric.

160. The method of any preceding Claim when used for manufacturing, in one manufacturing facility, a biosensor including sensor electrodes, such as a working electrode, a counter electrode, each comprising carbon foam made, at least in part, by the method defined in any preceding manufacturing method claim, and the method includes the further step of adding, at a different manufacturing facility, functionalised groups to the working electrode.

161. The method of any preceding Claim when used for manufacturing in one manufacturing facility a biosensor including sensor electrodes, such as a working electrode, a counter electrode, each comprising carbon foam made, at least in part, by the method defined in any preceding manufacturing method claim, and the method includes the further step of adding, at that manufacturing facility, functionalised groups to the working electrode.

162. The method of any preceding Claim when used for manufacturing a biosensor including sensor electrodes, such as a working electrode, and a counter electrode, each comprising carbon made, at least in part, by the method defined in in any preceding manufacturing method claim, and the method includes the steps of (a) screen printing a carbon layer on the substrate; (b) screen printing electrical connection tracks and a reference electrode; (c) screen printing a dielectric layer over the carbon and the electrical connection tracks and the reference electrode; and then (d) creating carbon foam sensor electrodes using a process defined in any preceding manufacturing method claim.

163. The method of any preceding Claim when used for manufacturing an energy storage device, such as a supercapacitor or pseudo-capacitor, in which energy storage electrodes

comprise carbon foam material made, at least in part, by the method defined in any preceding manufacturing method claim.

164. The method of any preceding Claim when used for manufacturing an energy storage device, such as a supercapacitor or pseudo-capacitor in which energy storage electrodes comprise carbon foam material made, at least in part, by the method defined in any preceding manufacturing method claim;

and the method includes the step of screen printing electrical connection tracks over at least a part of each electrode and at least partly covering the electrodes and connection tracks with a screen printed dielectric layer.

165. The method of any preceding Claim when used for manufacturing an energy storage device, such as a supercapacitor or pseudo-capacitor, in which energy storage electrodes comprise carbon foam material made, at least in part, by the method defined in any preceding manufacturing method claim and are arranged in an interdigitated pattern;

and the method includes the step of screen printing electrical connection tracks over at least a part of each electrode, in which a single electrical connection track connects to underlying digits that extend perpendicularly from both sides of the electrical connection track.

166. The method of any preceding Claim when used for manufacturing an energy storage device, such as a supercapacitor or pseudo-capacitor;

and the method includes the step of (a) screen printing electrical connectors on to a substrate; (b) screen printing a carbon layer over the electrical collectors; (c) screen printing a dielectric over at least some of the carbon layer; then (d) creating carbon foam energy storage electrodes at least in part by the method defined in any preceding manufacturing method claim.

167. The method of any preceding Claim when used for manufacturing an energy storage device, such as a supercapacitor or pseudo-capacitor, in which energy storage electrodes comprise carbon foam material made, at least in part, by the method defined in any preceding manufacturing method claim;

and the method includes the step of applying an electrochemical deposition process of a pseudo-capacitive material, such as a metal oxide, to the energy storage electrodes.

168. The method of any preceding Claim when used for manufacturing an energy storage device, such as a supercapacitor or pseudo-capacitor, in which energy storage electrodes comprise carbon foam material made, at least in part, by the method defined in any preceding manufacturing method claim;

and the method includes the step of applying an ionic gel in a low humidity but non-inert environment, in which the levels of O_2 and H_2O in the environment and measured and controlled to optimise the capacitance of the energy storage device.

169. The method of any preceding Claim when used for manufacturing an electrical conductor, in which the electrical conductor comprises carbon foam made, at least in part, by the method defined in any preceding manufacturing method claim.

170. The method of any preceding Claim when used for manufacturing a device that includes both a sensor, and an energy storage device, such as a supercapacitor, in which both the sensor and the energy storage device comprise a carbon foam material made, at least in part, by the method defined in any preceding manufacturing method claim.

171. The method of any preceding Claim when used for manufacturing an integrated device including a battery and a supercapacitor, the battery providing long term power and the supercapacitor providing short term power at a higher level than the battery, in which the supercapacitor comprises a carbon foam material made, at least in part, by the method defined in any preceding manufacturing method claim.

172. The method of any preceding Claim when used for manufacturing an integrated device including an antenna and a supercapacitor, in which the supercapacitor powers the antenna and comprises carbon foam material made, at least in part, by the method defined in any preceding manufacturing method claim.

173. The method of any preceding Claim when used for manufacturing a device including one or more electrodes, each comprising carbon foam material;

in which the method includes passing a continuous reel of a carbon pre-cursor film through a sequence of operations required to manufacture the carbon foam material made, at least in part, by the method defined in any preceding manufacturing method claim.

Devices

174. A device including carbon foam material made, at least in part, by the method defined in any preceding manufacturing method claim.

175. The device of any preceding device claim, being a data logging device including an energy scavenger system and a supercapacitor, in which the supercapacitor powers an antenna and comprises carbon foam material made, at least in part, by the method defined in any preceding manufacturing method claim.

176. The device of any preceding device claim, being an energy storage device, such as a supercapacitor, including:
(i) a carbon pre-cursor film;
(ii) a screen printed conductive paste or ink layer, on the surface of the carbon pre-cursor film;
(iii) a screen printed collector layer over the screen printed conductive paste or ink layer;
(iv) a screen printed dielectric layer over the collector layer; and
(v) energy storage electrodes that comprise carbon foam material made, at least in part, from the carbon pre-cursor film by the method defined in any preceding manufacturing method claim, and in which an electrically conductive path is formed from the carbon foam material to the collector layer, via the conductive paste or ink layer.

177. The device of any preceding device claim, being a smart label including a battery and a supercapacitor, the battery providing long term power and the supercapacitor providing short term power at a higher level than the battery, in which the supercapacitor comprises carbon foam material made, at least in part, by the method defined in any preceding manufacturing method claim;

and the smart label includes electronics, such as sensor electronics, powered by the battery and a data transmitter powered by the supercapacitor.

178. The device of any preceding device claim, being a smart label including a battery and a supercapacitor, the battery providing long term power and the supercapacitor providing short term power at a higher level than the battery, in which the supercapacitor comprises carbon foam material made, at least in part, by the method defined in any preceding manufacturing method claim;

and the smart label includes electronics, such as sensor electronics, powered by the battery and a data transmitter powered by the supercapacitor, where the supercapacitor provides sufficient power to the data transmitter to enable the data transmitter to establish a data connection with a basestation or hub and to transmit a data payload once that data connection has been established.

179. The device of any preceding device claim, being an energy storage device, such as a supercapacitor, including a sub-assembly comprising:

(i) a carbon pre-cursor film;

(ii) a screen printed conductive paste or ink layer, on the surface of the carbon pre-cursor film;

(iii) a screen printed collector layer over the screen printed conductive paste or ink layer;

(iv) a screen printed dielectric layer over the collector layer;

(v) energy storage electrodes that comprise carbon foam material made, at least in part, from the carbon pre-cursor film by the method defined in any preceding manufacturing method claim, and in which an electrically conductive path is formed from the carbon foam material to the collector layer, via the conductive paste or ink layer;

and in which multiple sub-assemblies are formed into a stack and in which adjacent energy storage electrodes are separated by an ionic gel electrolyte.

180. The device of any preceding device claim, being a microfluidic diagnostic device including sample wells positioned on an upper face of the device, reference, working and counter electrodes, made, at least in part, from a carbon pre-cursor film by the method defined in any preceding manufacturing method claim, are in a layer below the sample wells, and reference, working and counter electrode connections are in layer below the reference, working and counter electrodes

181. The device of any preceding device claim, being a lab-on-chip device, including a sub-assembly comprising:

(i) a carbon pre-cursor film;

(ii) a screen printed conductive paste or ink layer, on the surface of the carbon pre-cursor film;

(iii) a screen printed conductive layer over the screen printed conductive paste or ink layer;

(iv) a screen printed reference electrode;

(v)) a screen printed dielectric layer over the collector layer;

(vi) sensor electrodes that comprise carbon foam material made, at least in part, from the carbon pre-cursor film by the method defined in any preceding manufacturing method claim, and in which an electrically conductive path is formed from the carbon foam material to the conductive layer, via the conductive paste or ink layer.

182. The device of any preceding device claim, being a device including a laser induced carbon foam material manufactured by

(a) using a laser beam operating at a first band to irradiate an encapsulated or sub-surface region of a carbon pre-cursor material below a surface of the material, to create carbon foam in that sub-surface region, and then

(b) using a laser beam operating at a second band to remove or ablate material sitting between the carbon foam and the surface of the carbon pre-cursor material, to expose at least some of the carbon foam.

183. The device of any preceding device claim, being a device including a laser induced carbon foam material manufactured by

(a) using a laser beam operating at a first band to irradiate an encapsulated or sub-surface region of a carbon pre-cursor material below a surface of the material, to create carbon foam in that sub-surface region, and then

(b) using a laser beam operating at a second band to remove or ablate material sitting between the carbon foam and the surface of the carbon pre-cursor material, to expose at least some of the carbon foam; in which the device is or includes one of the following: a Hall effect sensor; a tactile sensor for e.g. robotics; an infectious diseases sensor; a biosensor; a constant monitoring chemical sensor; a glucose monitoring sensor; a lactic acid sensor: a gas detection sensor, a self-charging hybrid energy generation device; a green gas conversion device; a fuel cell, e.g. hydrogen fuel cell; a filter, including a gas permeable filter; a heating device.

Carbon foam

184. A laser induced carbon foam made by:

(a) using a laser beam operating at a first band to irradiate an encapsulated or sub-surface region of a carbon pre-cursor material below a surface of the material, to create carbon foam in that sub-surface region, and then

(b) using a laser beam operating at a second band to remove or ablate material sitting between the carbon foam and the surface of the carbon pre-cursor material, to expose at least some of the carbon foam.

185. A laser induced carbon foam made using the method defined in any preceding manufacturing method claim.

186. A laser induced carbon foam made using the method defined in any preceding manufacturing method claim, the carbon foam including one or more carbonaceous nanostructures, such as carbon nano-onion, carbon nano-horn, carbon nano-tubes, carbon nano-dots, nanodiamonds and fullerene, or combinations of any of these.

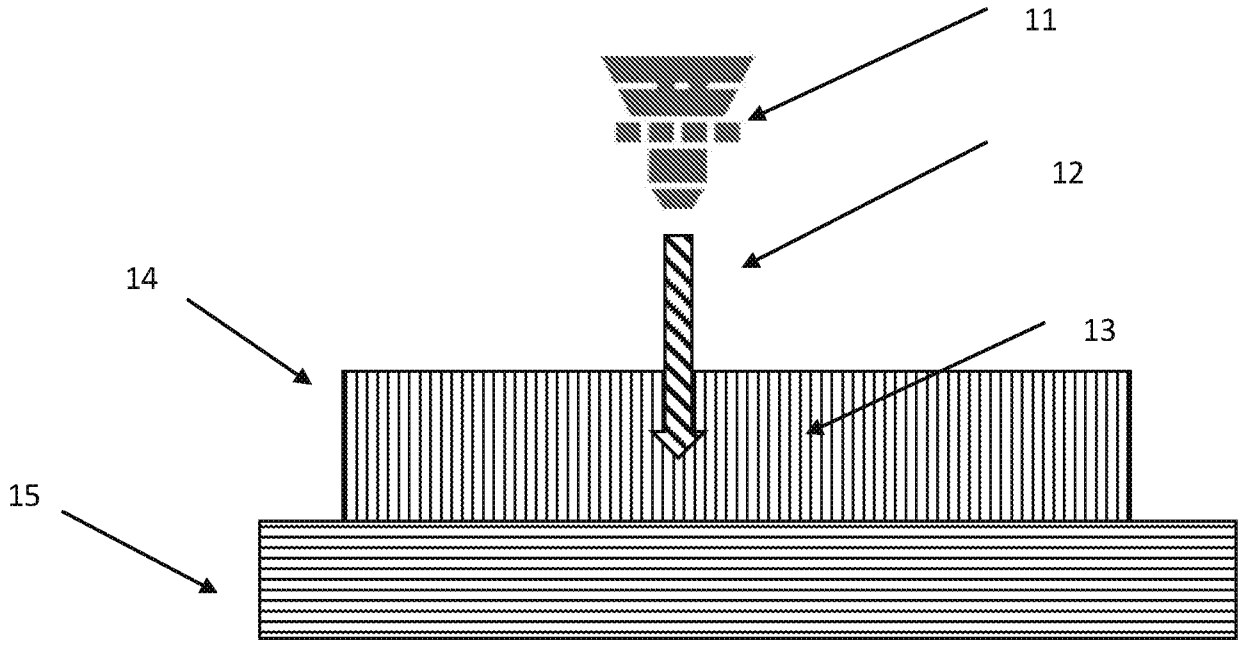


Figure 1

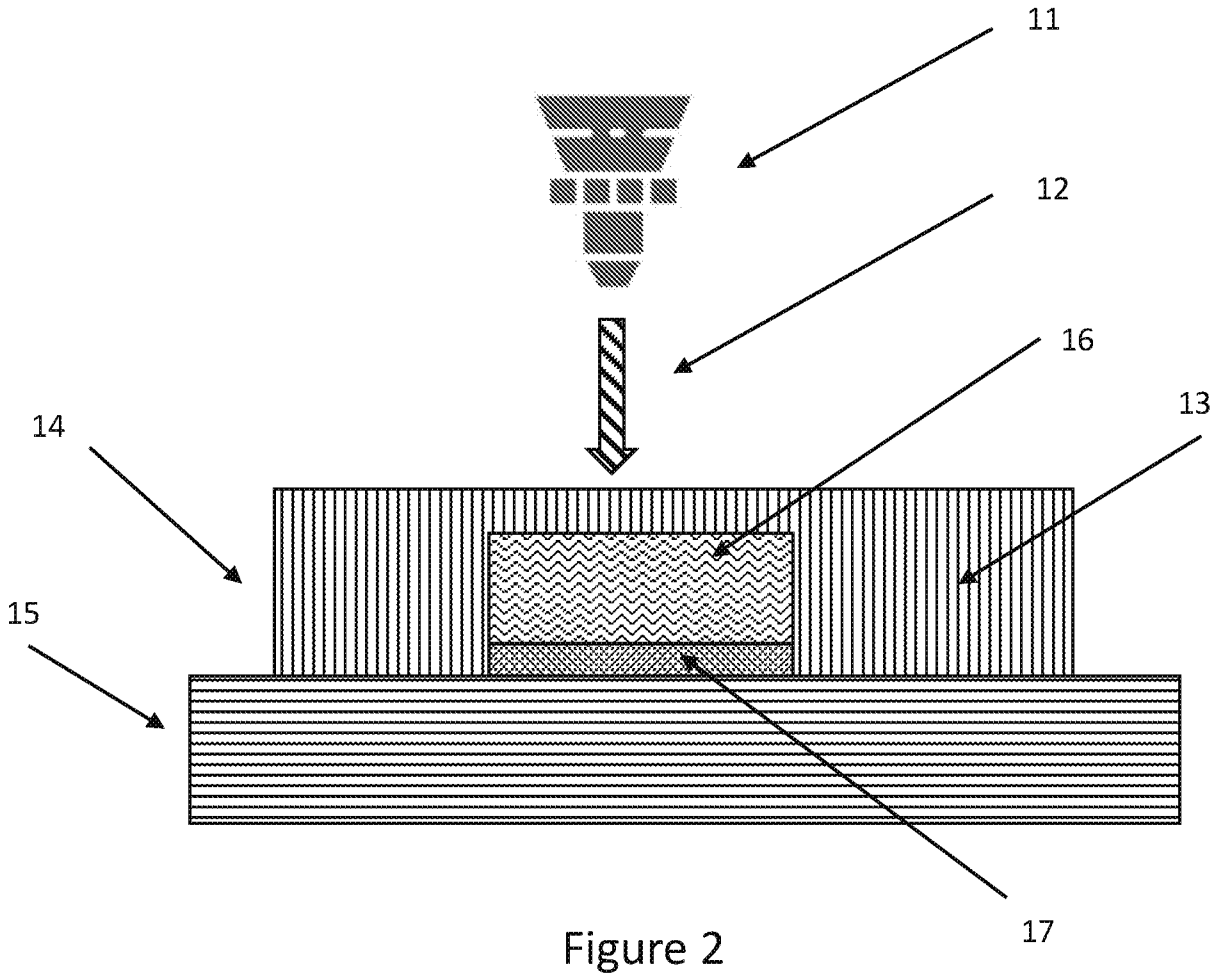


Figure 2

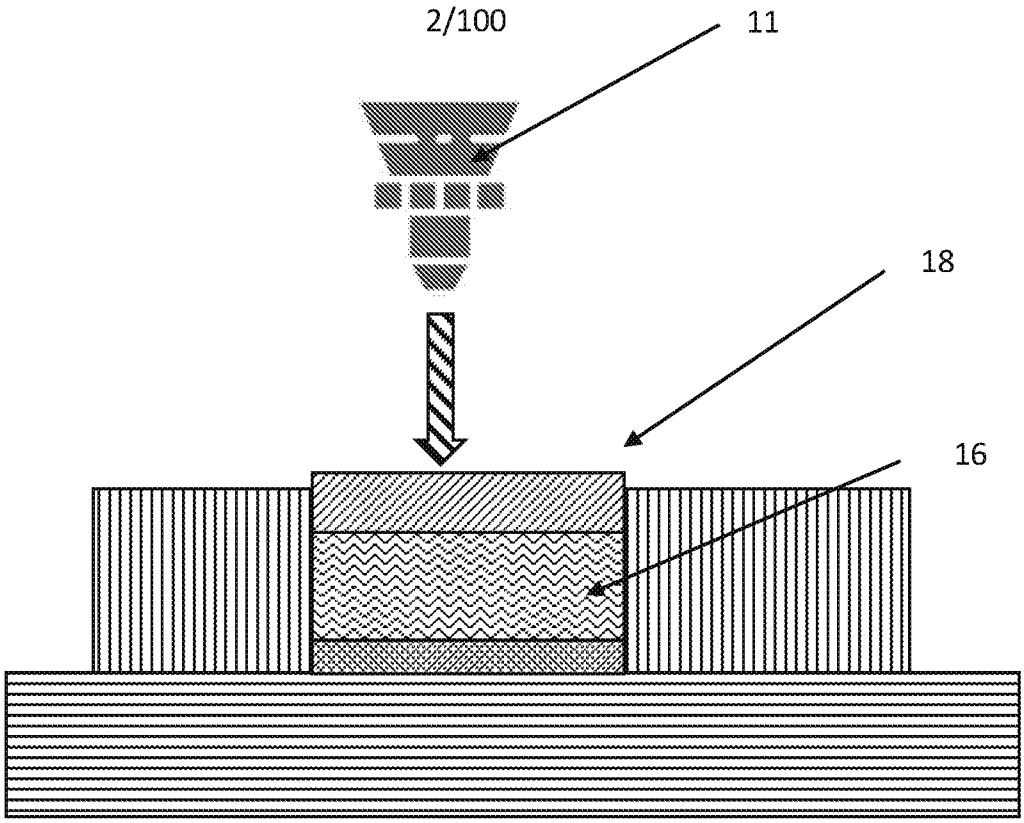


Figure 3

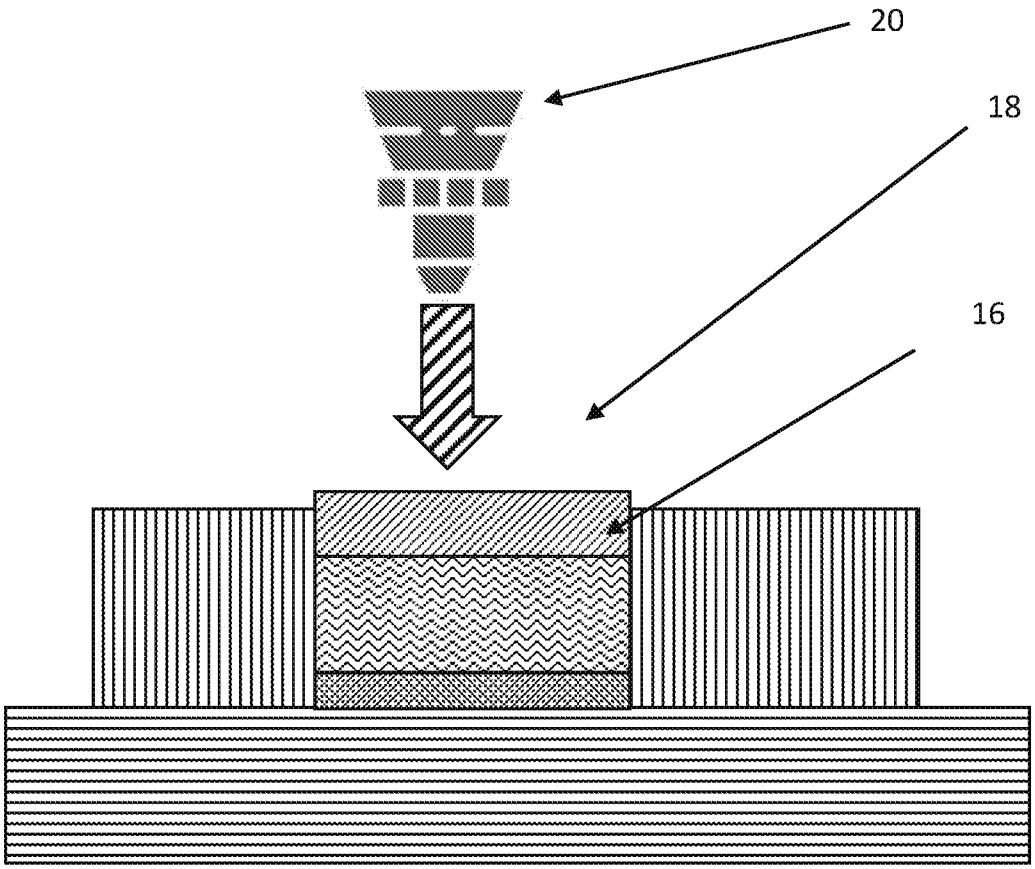


Figure 4

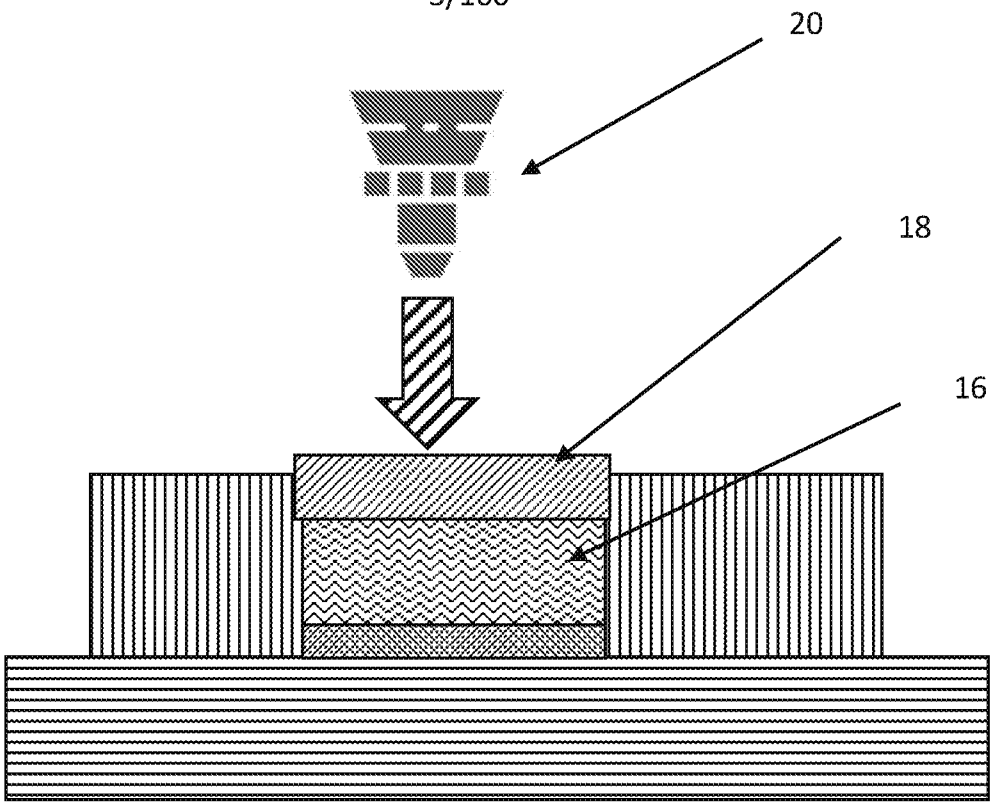


Figure 5

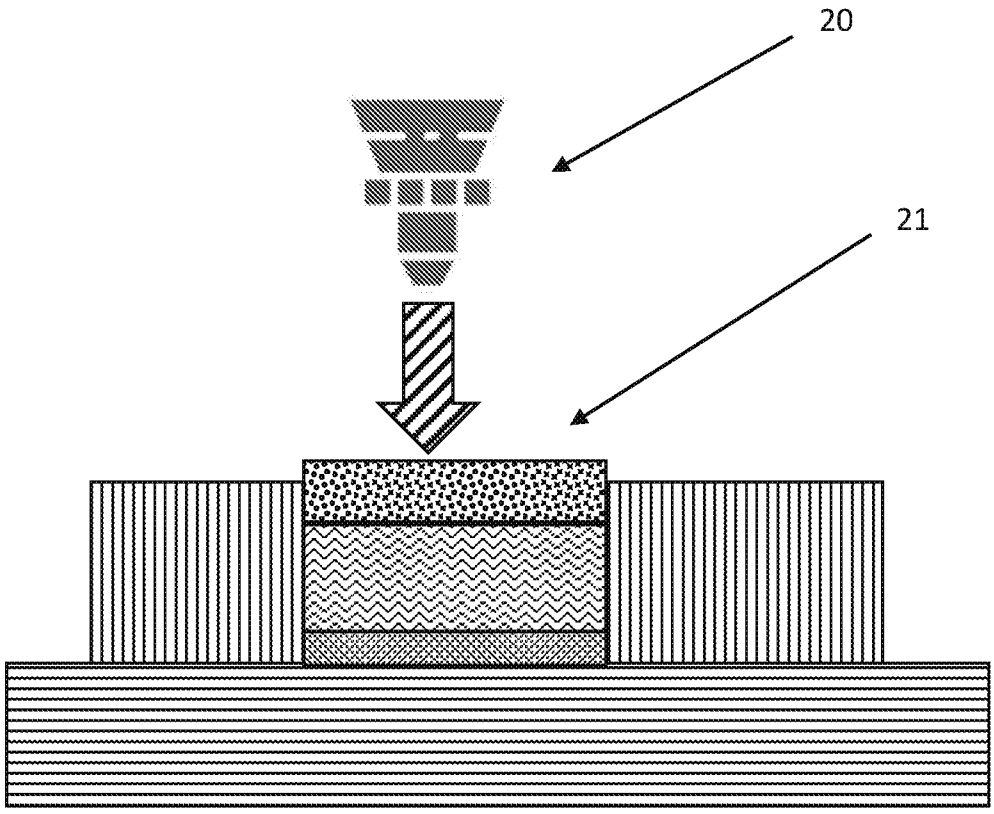


Figure 6

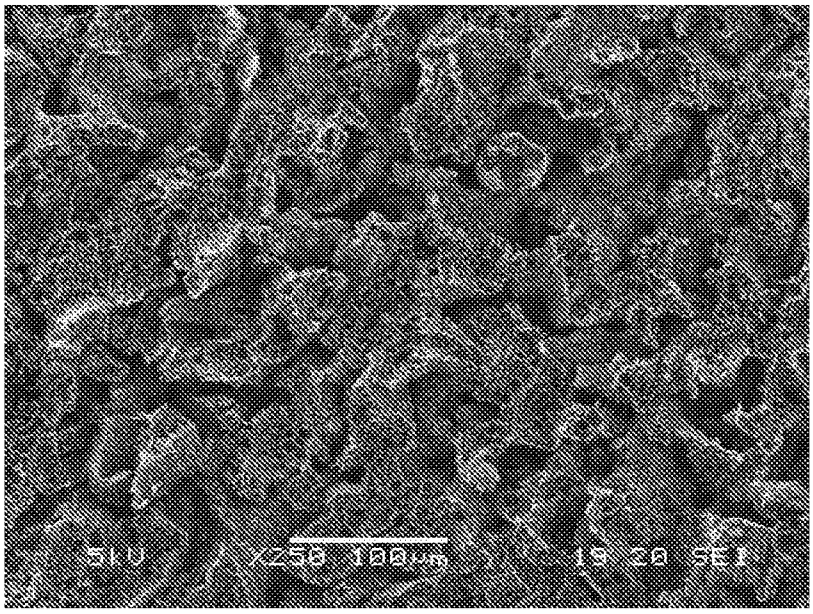


Figure 7

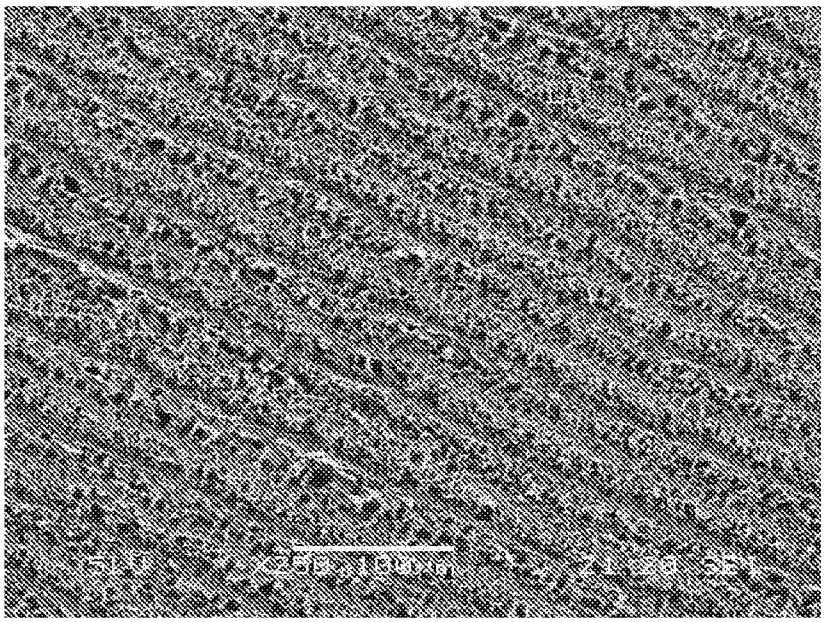


Figure 8

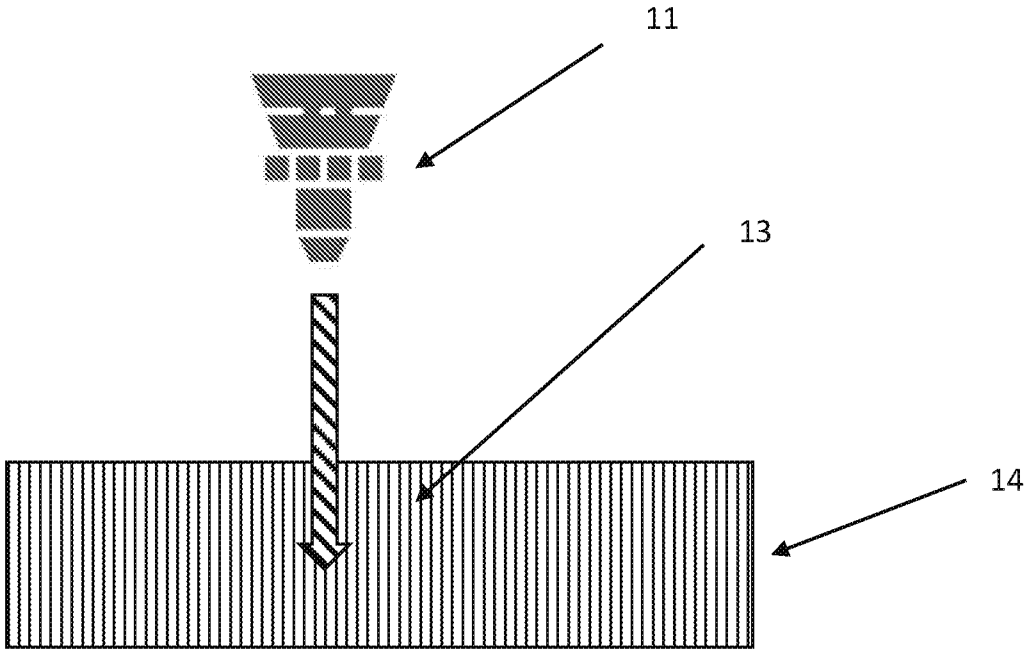


Figure 9

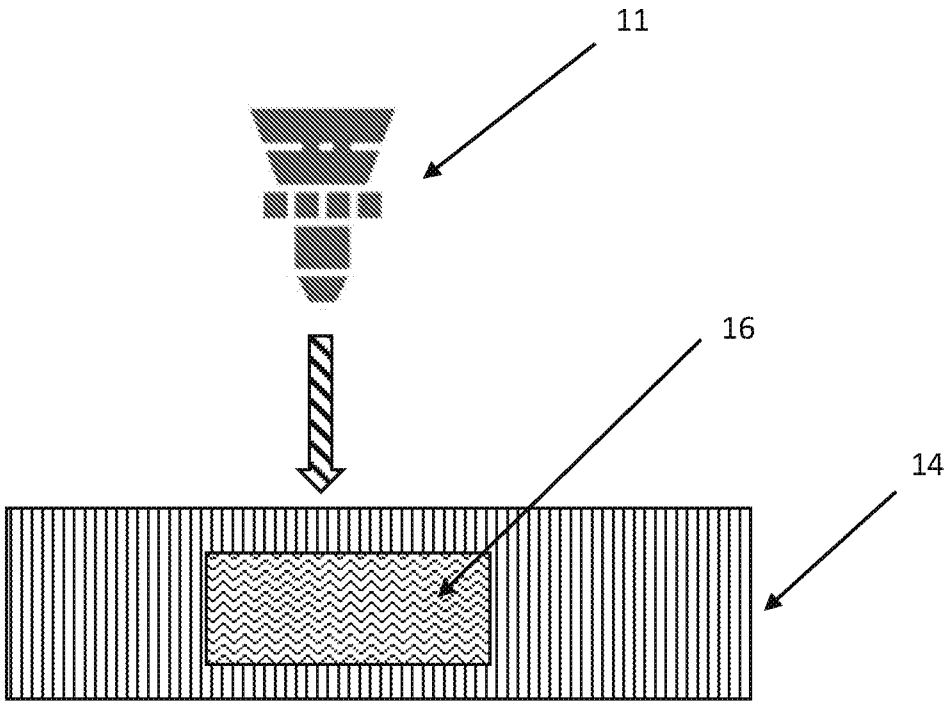


Figure 10

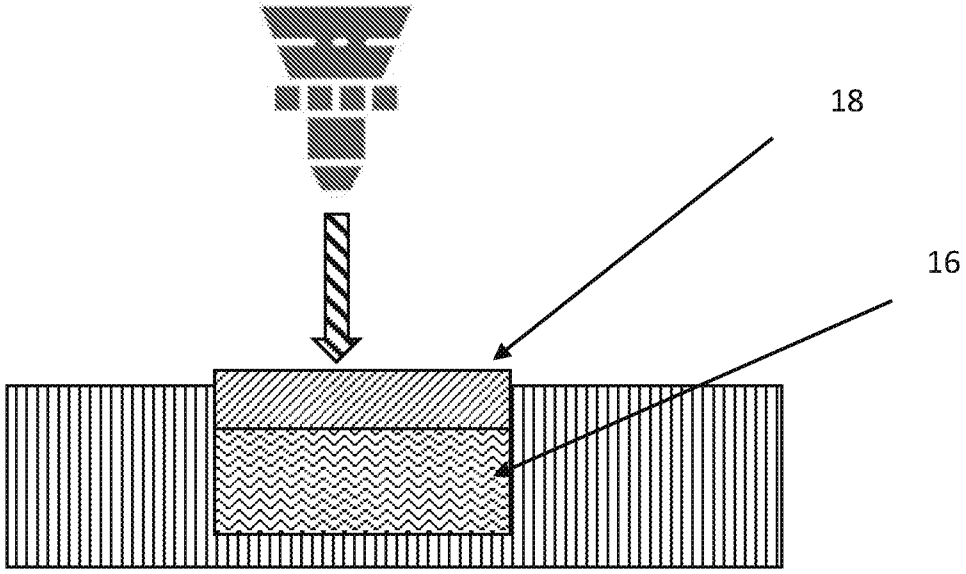


Figure 11

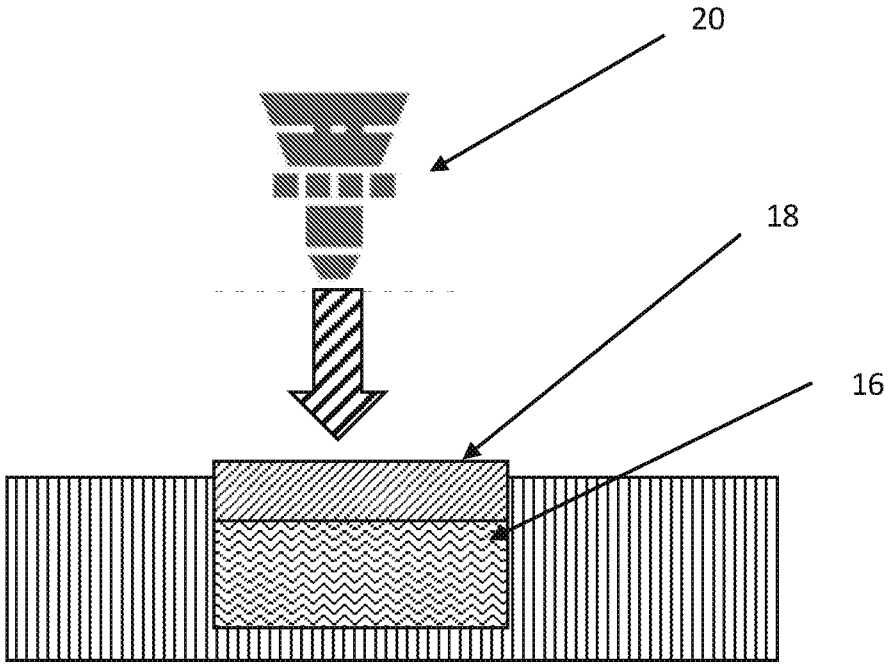


Figure 12

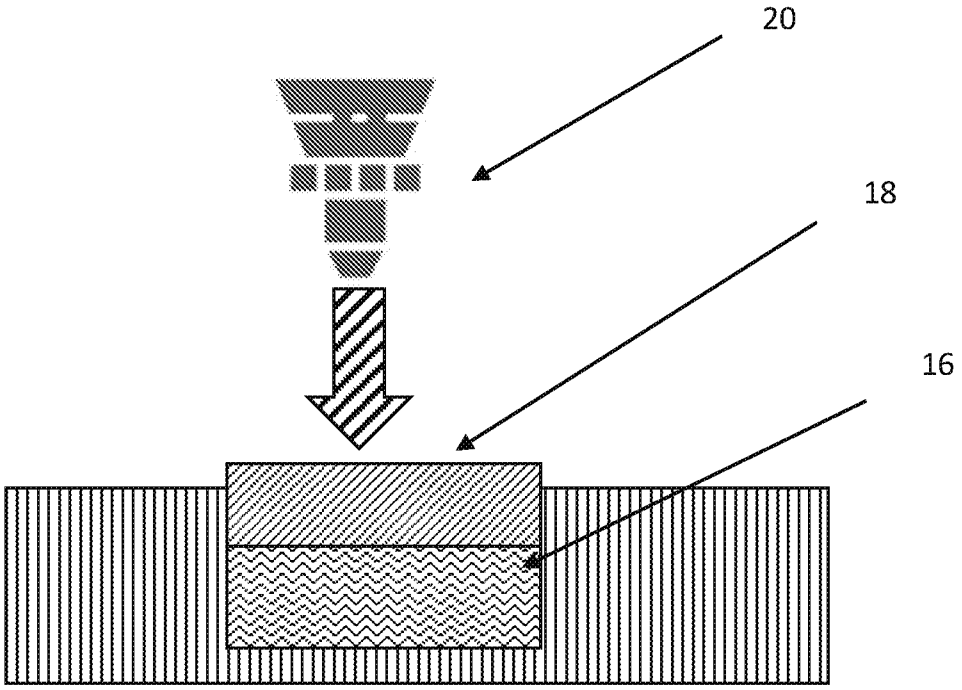


Figure 13

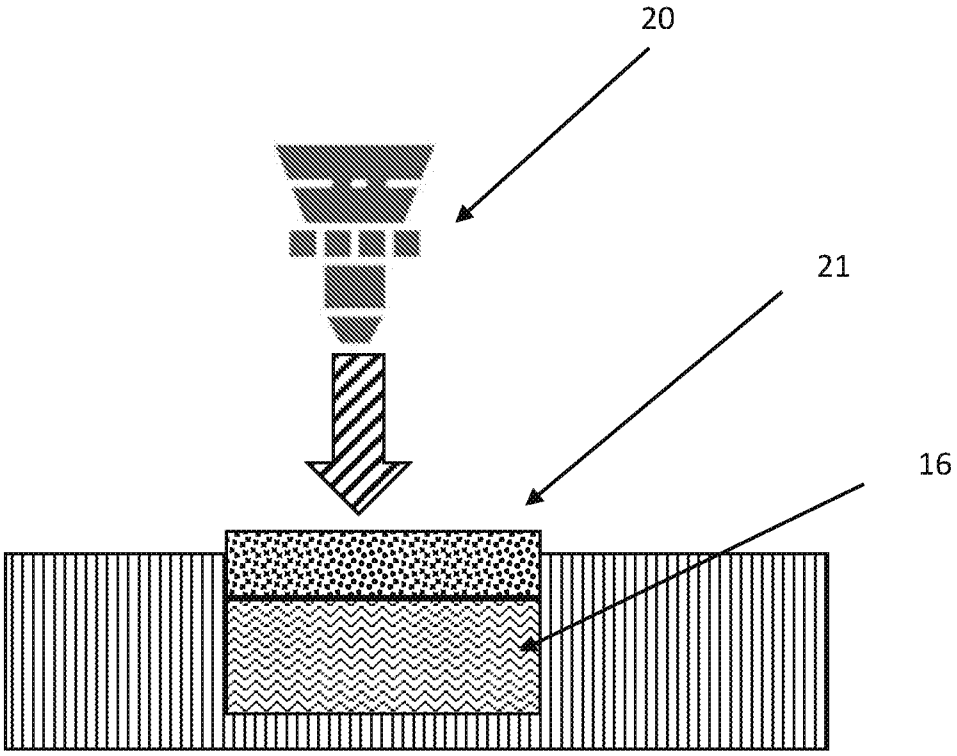


Figure 14A

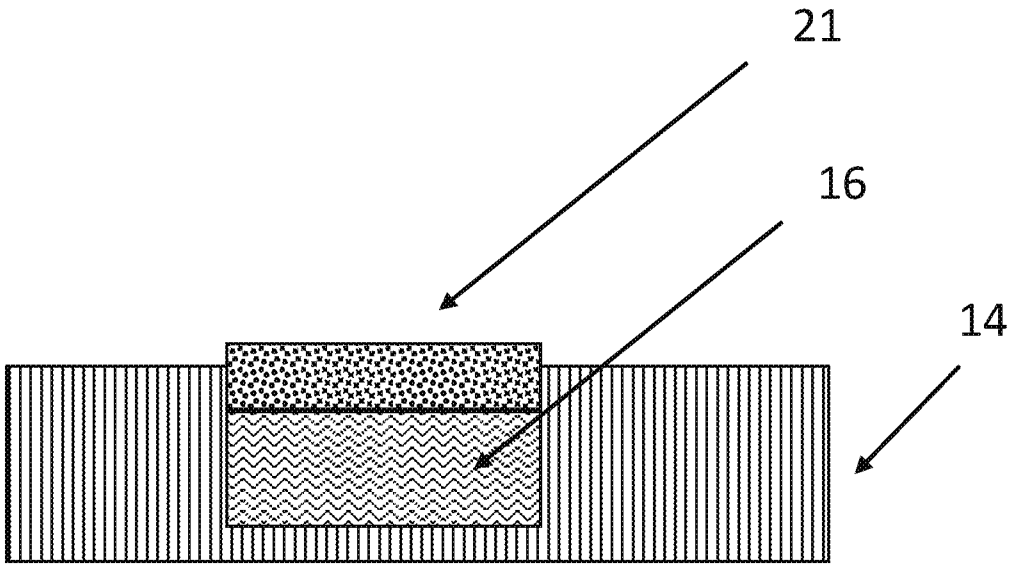


Figure 14B

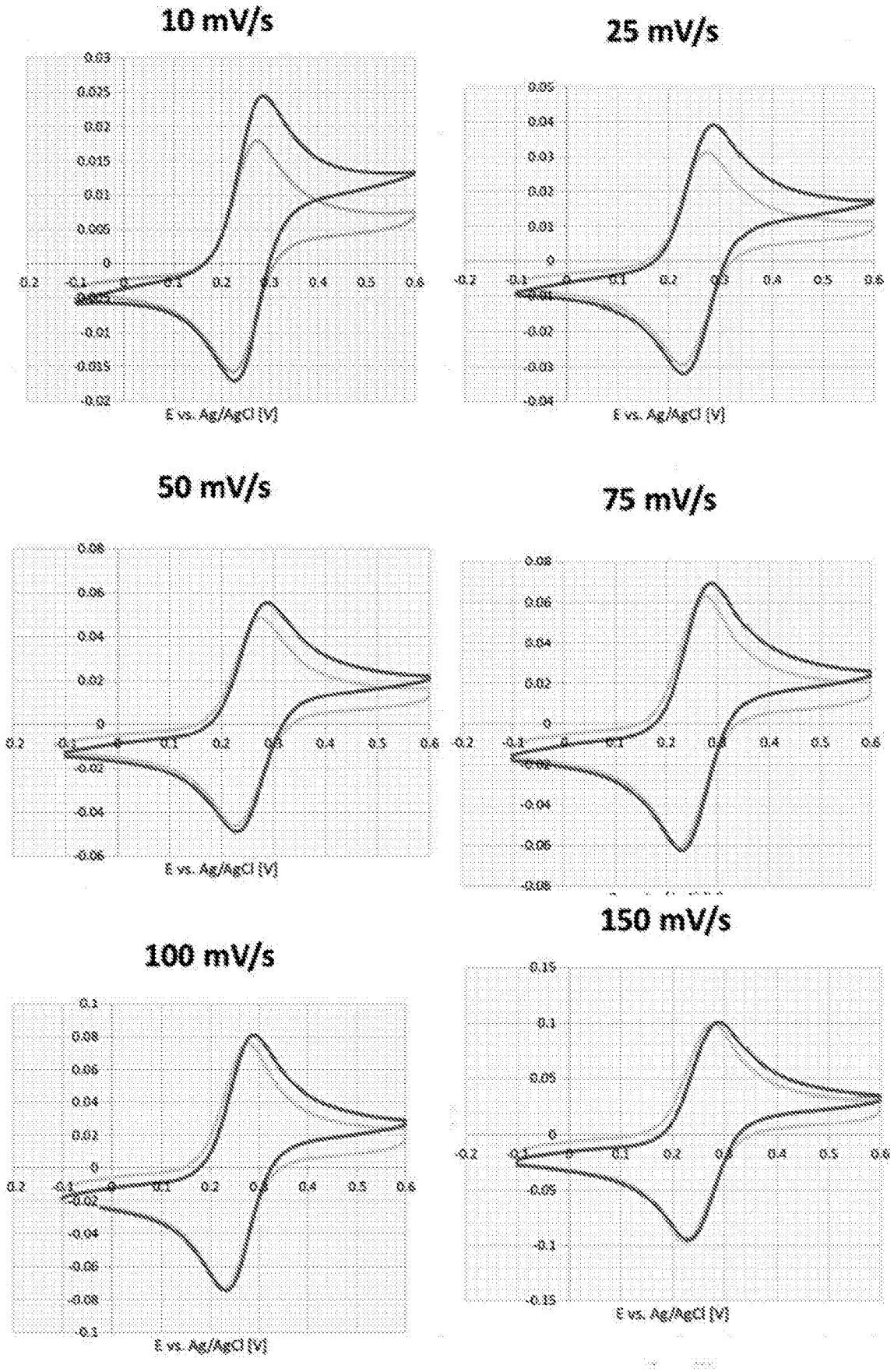
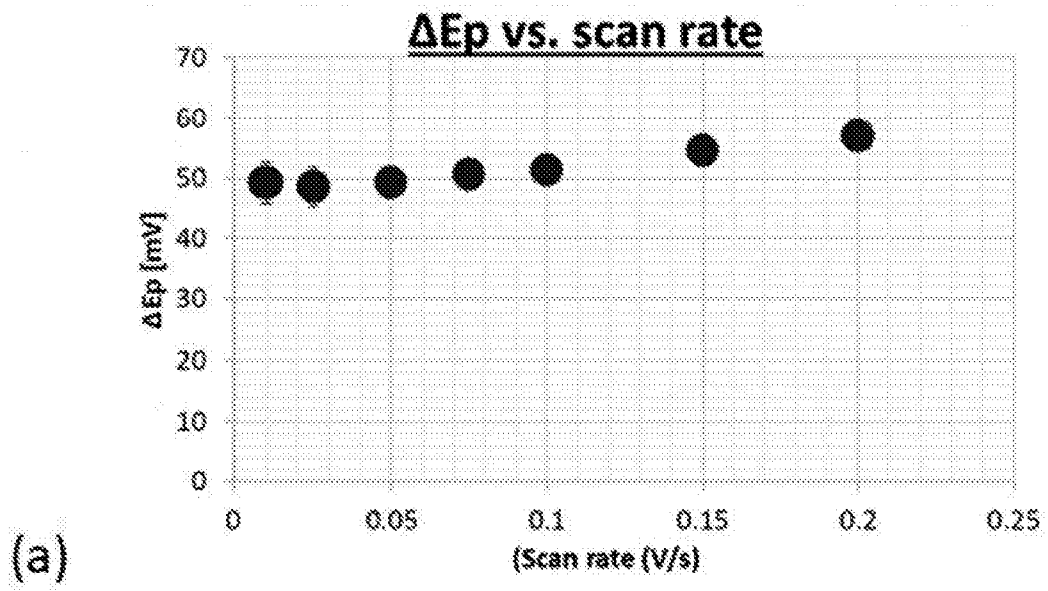
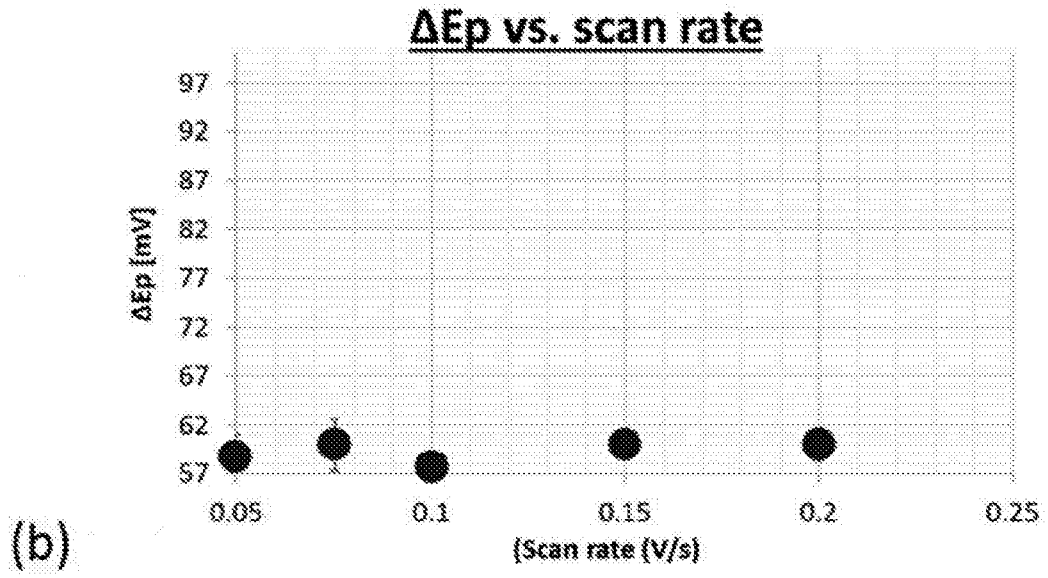

10 mV/s
E vs. Ag/AgCl [V]
25 mV/s
E vs. Ag/AgCl [V]
50 mV/s
E vs. Ag/AgCl [V]
75 mV/s
150 mV/s
E vs. Ag/AgCl [V]
100 mV/s
E vs. Ag/AgCl [V]

Figure 15


ΔEp vs. scan rate
70
60
50
40
30
20
10
0
ΔEp [mV]
0
0.05
0.1
0.15
0.2
0.25
(Scan rate (V/s)

(a)


ΔEp vs. scan rate
97
92
87
82
77
72
67
62
57
ΔEp [mV]
0.05
0.1
0.15
0.2
0.25
(Scan rate (V/s)

(b)

Figure 16

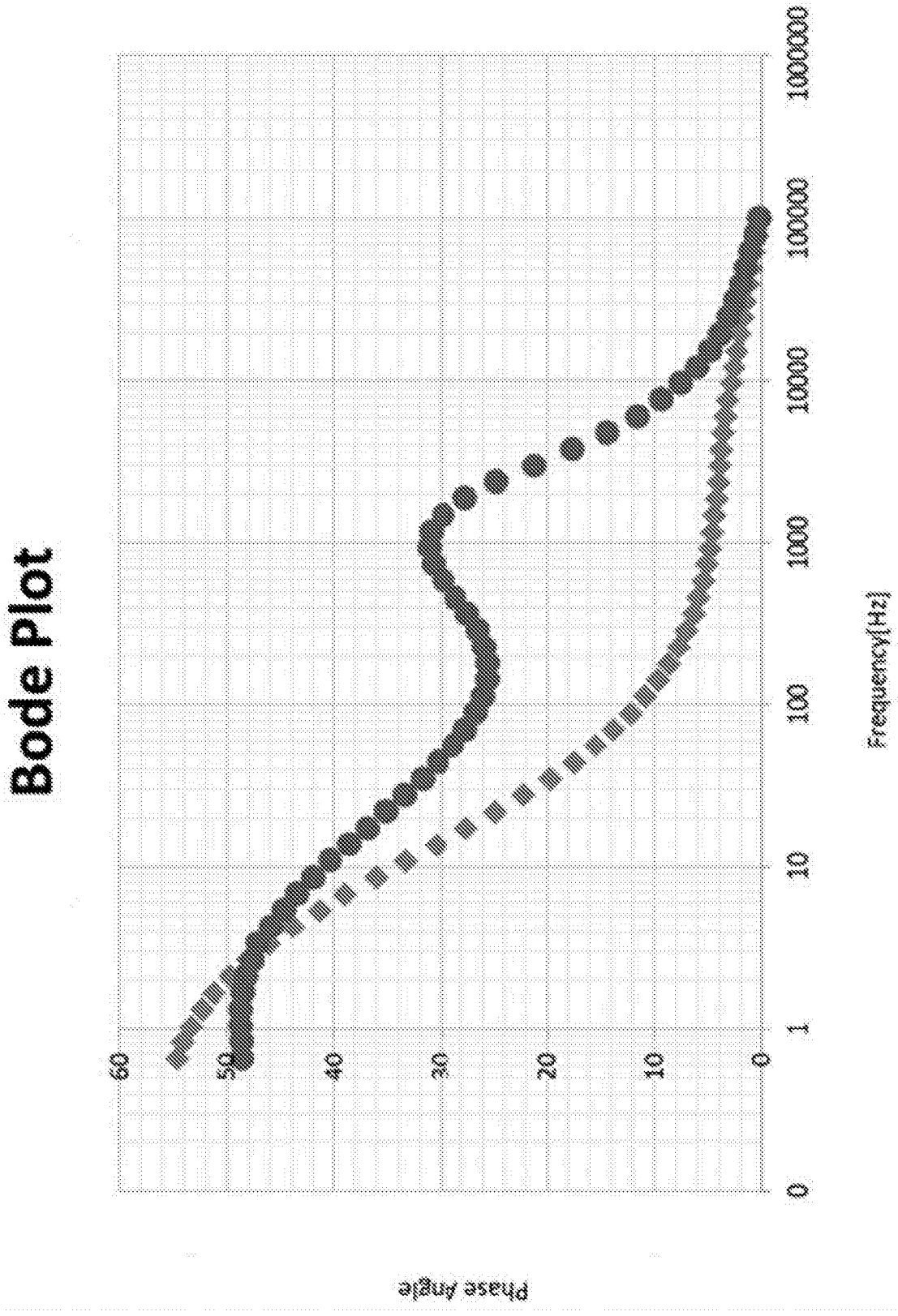

Bode Plot
Phase Angle
60
50
40
30
20
10
0
0
1
10
100
1000
10000
100000
1000000
Frequency[Hz]

Figure 17

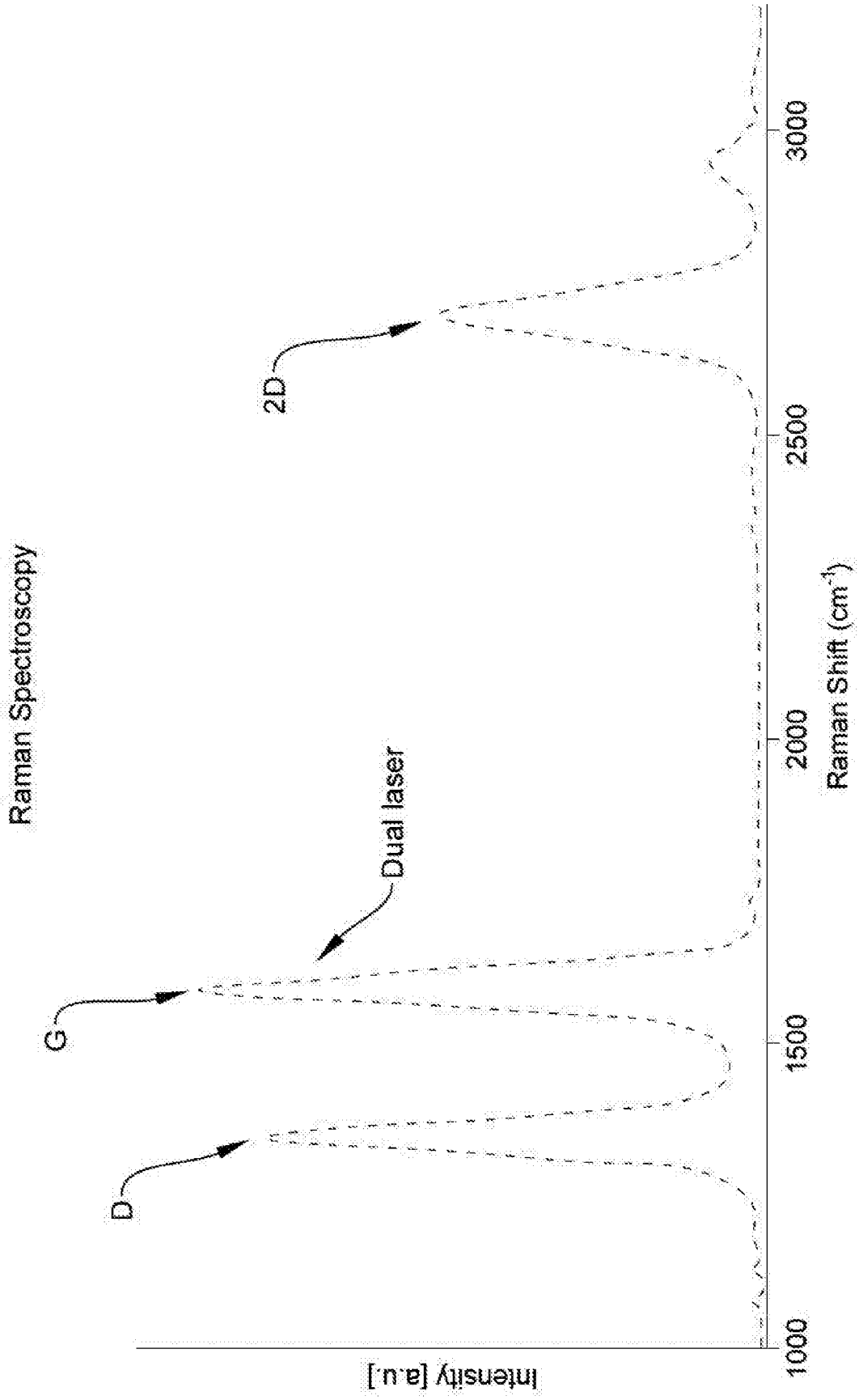

Raman Spectroscopy
Dual laser
D
G
2D
Intensity [a.u.]
1000
1500
2000
2500
3000
Raman Shift (cm-1)

Figure 18

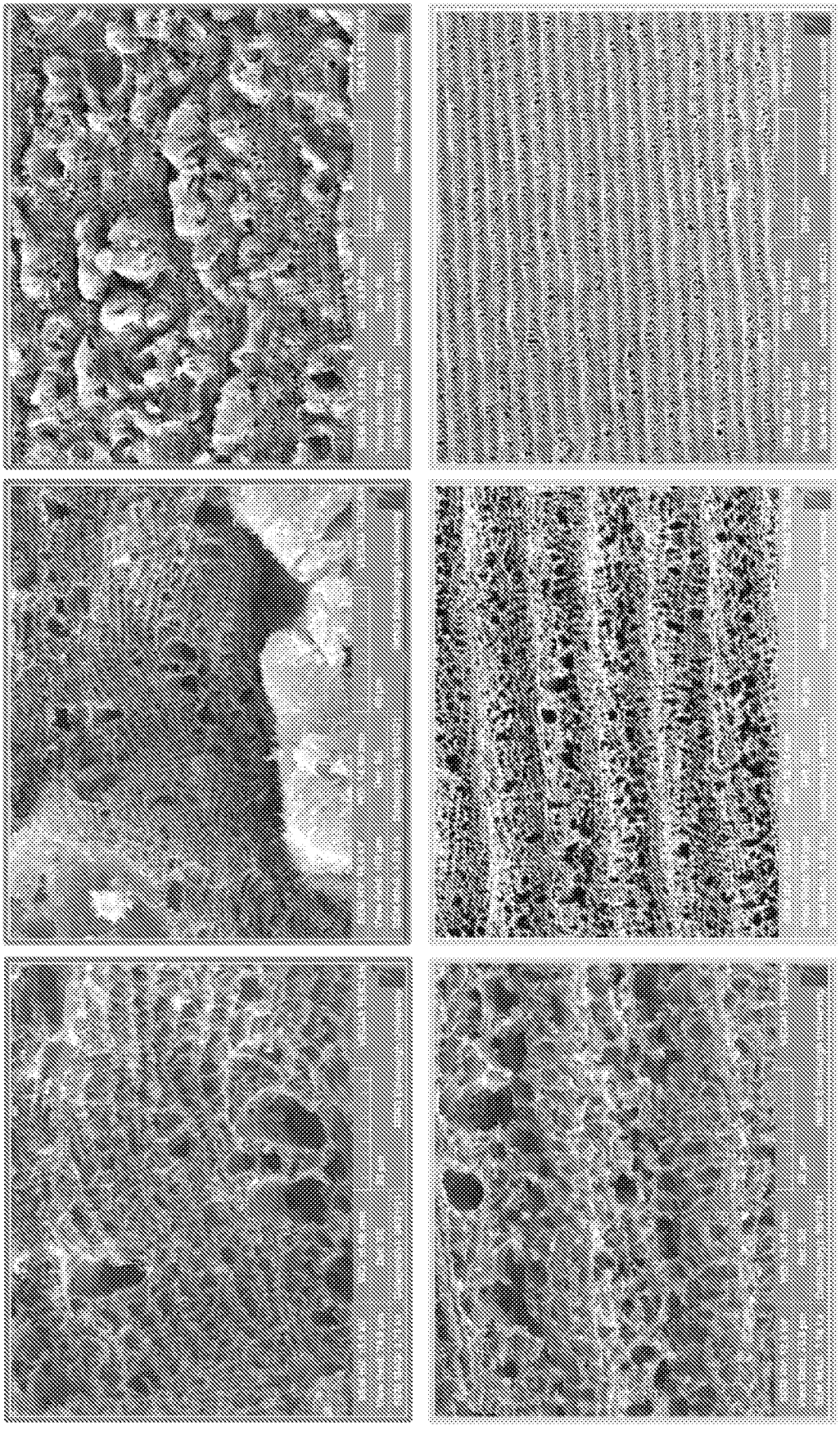


Figure 19

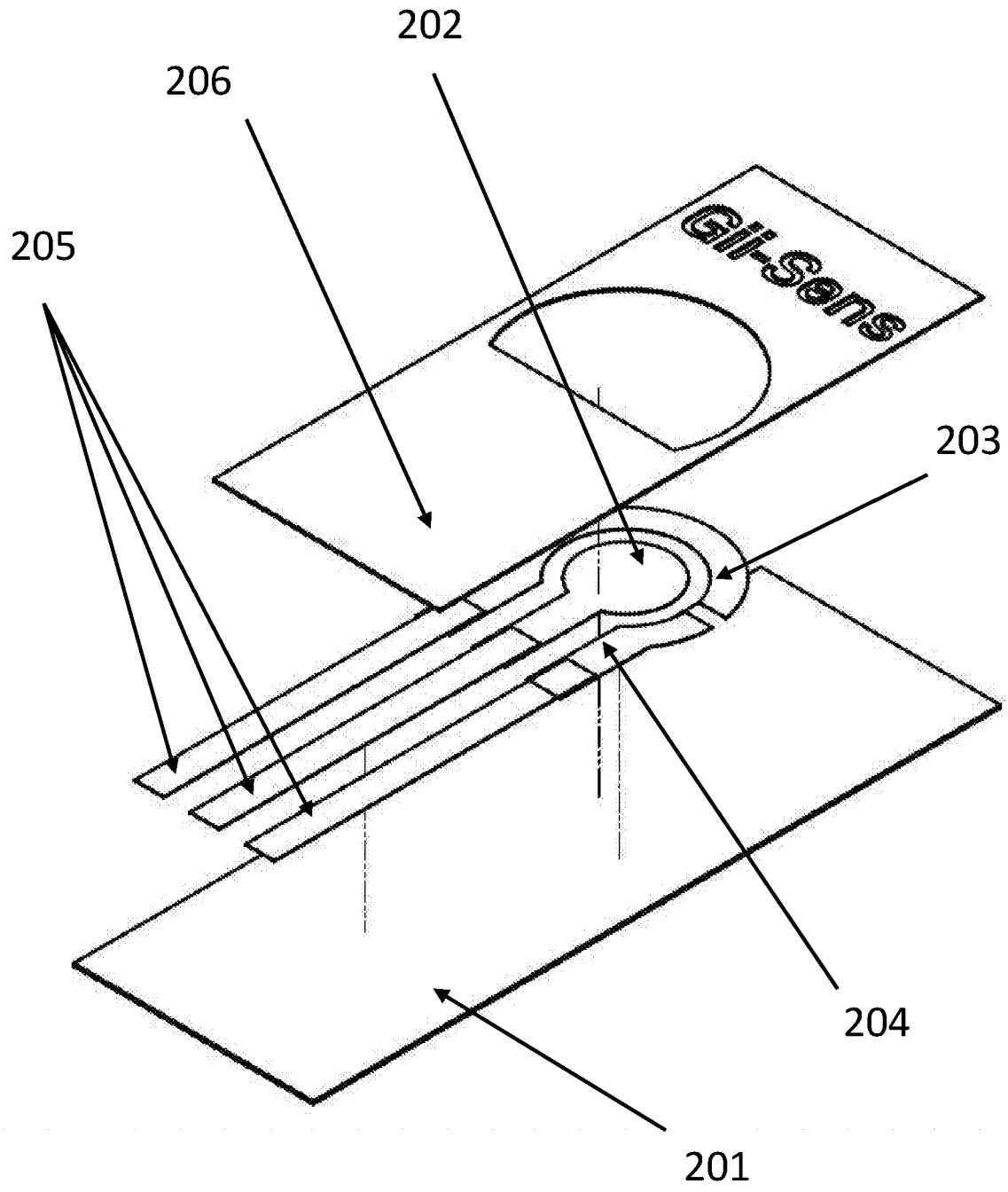


Figure 20A

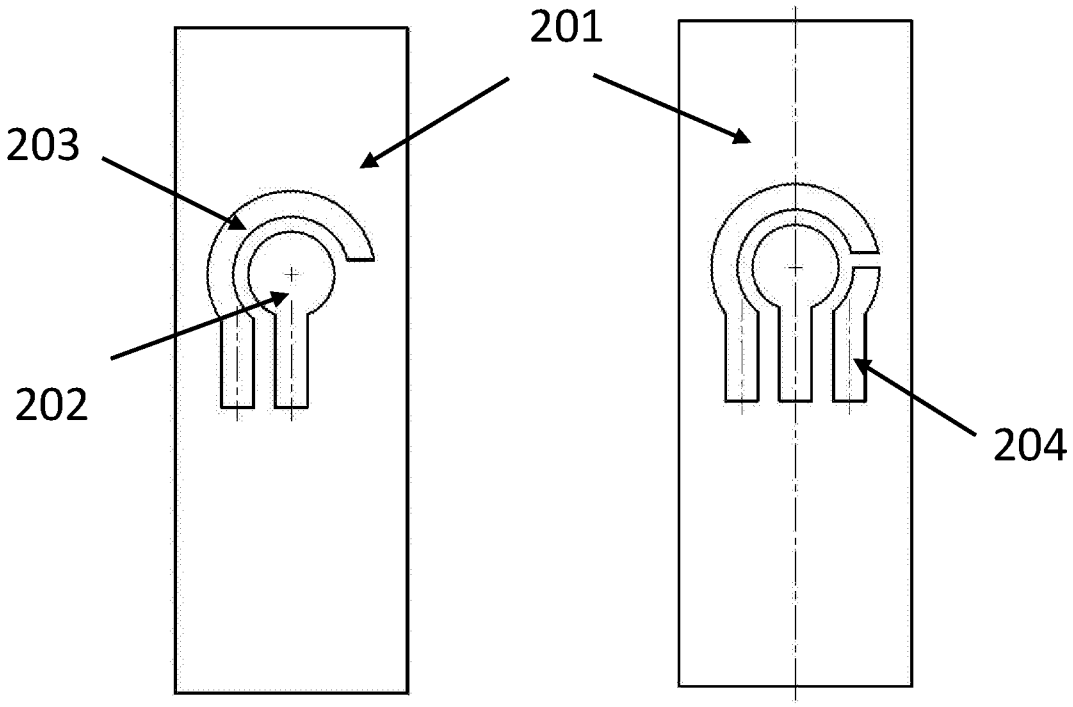


Figure 20B

Figure 20C

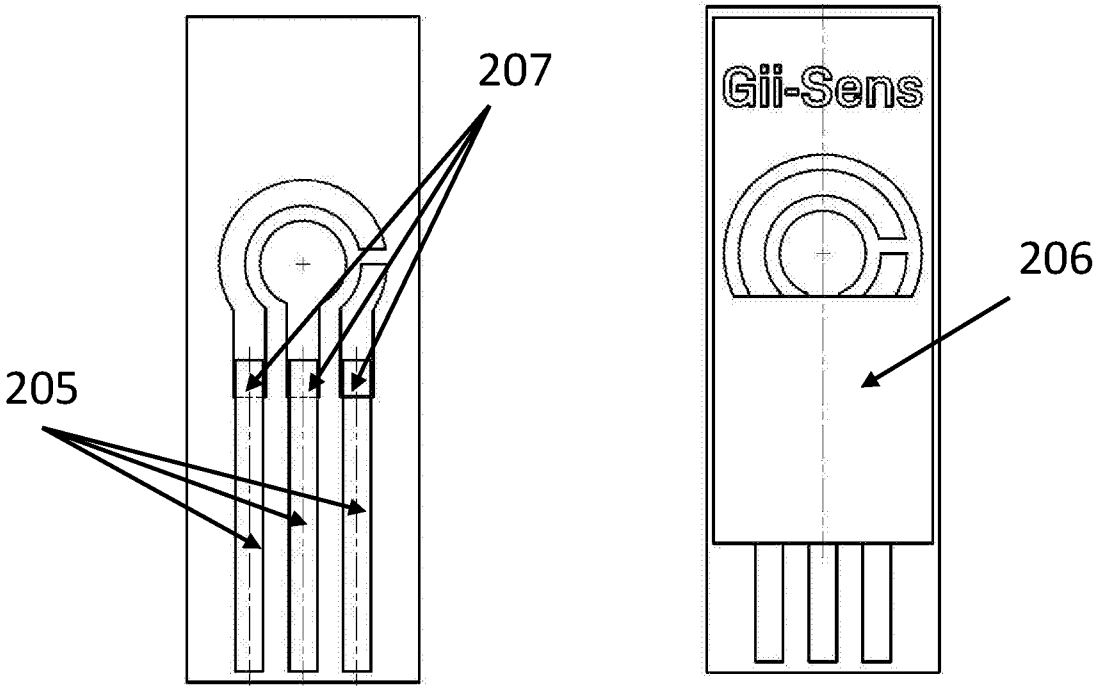


Figure 20D

Figure 20E

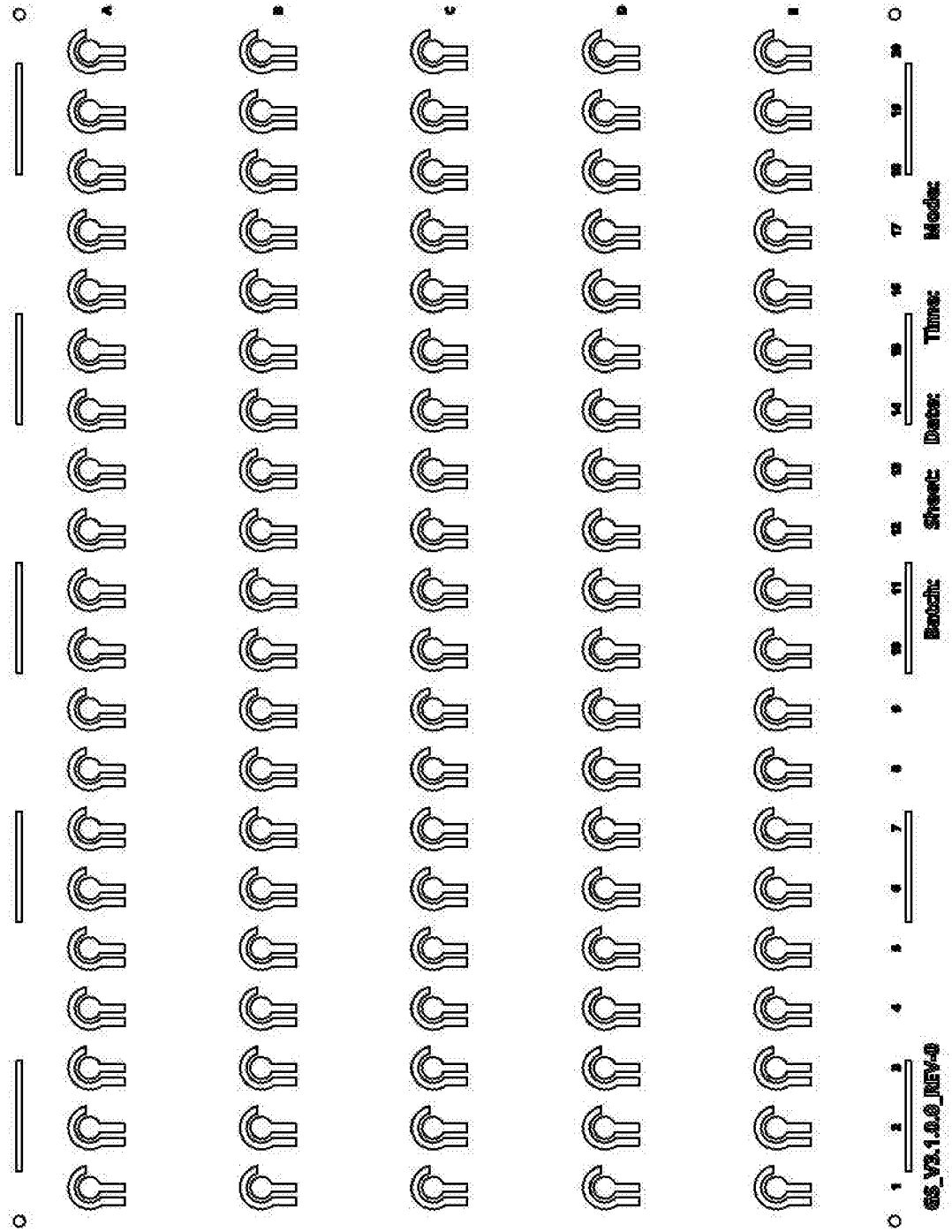


Figure 20F

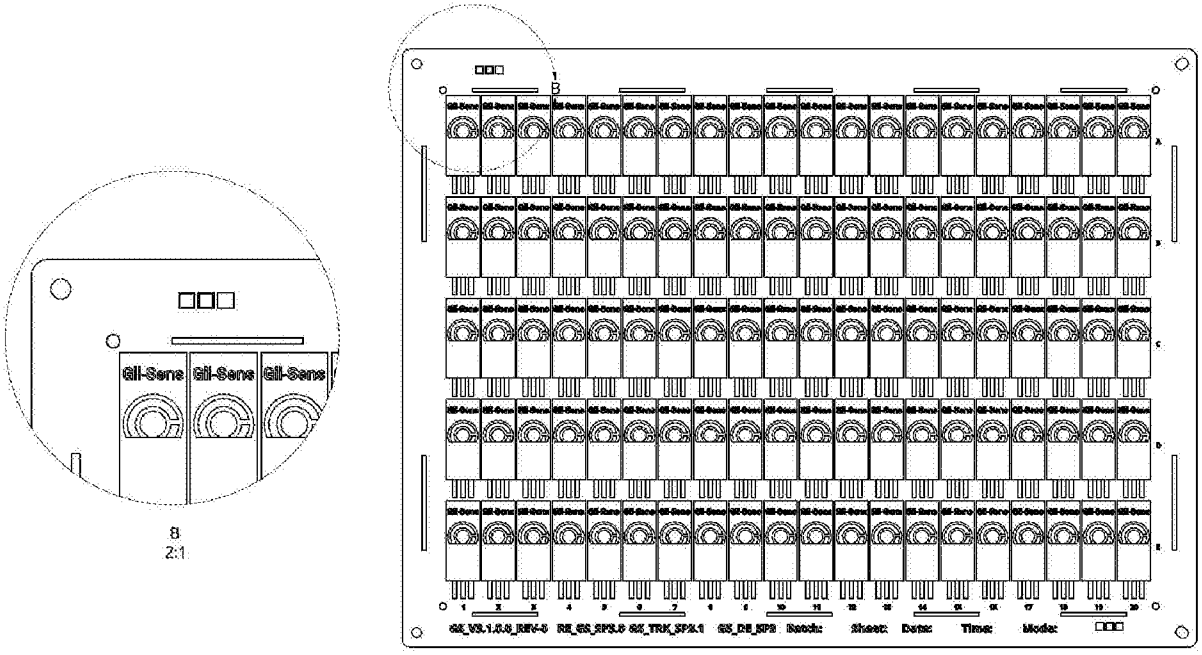


Figure 20G

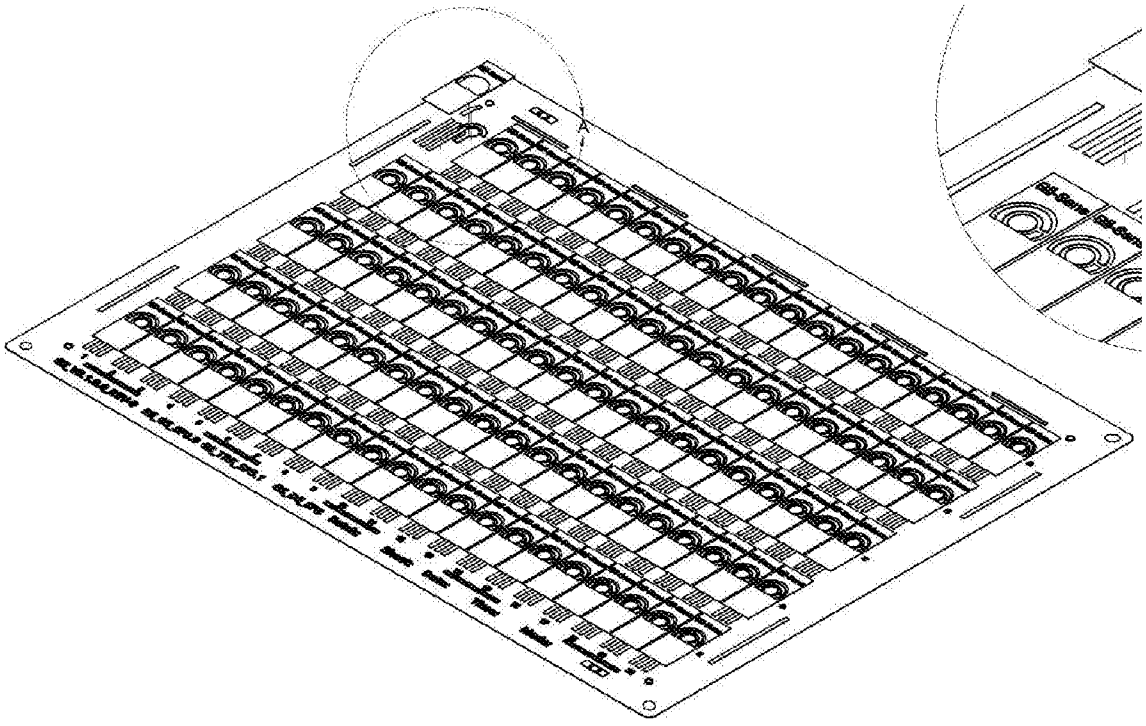


Figure 20H

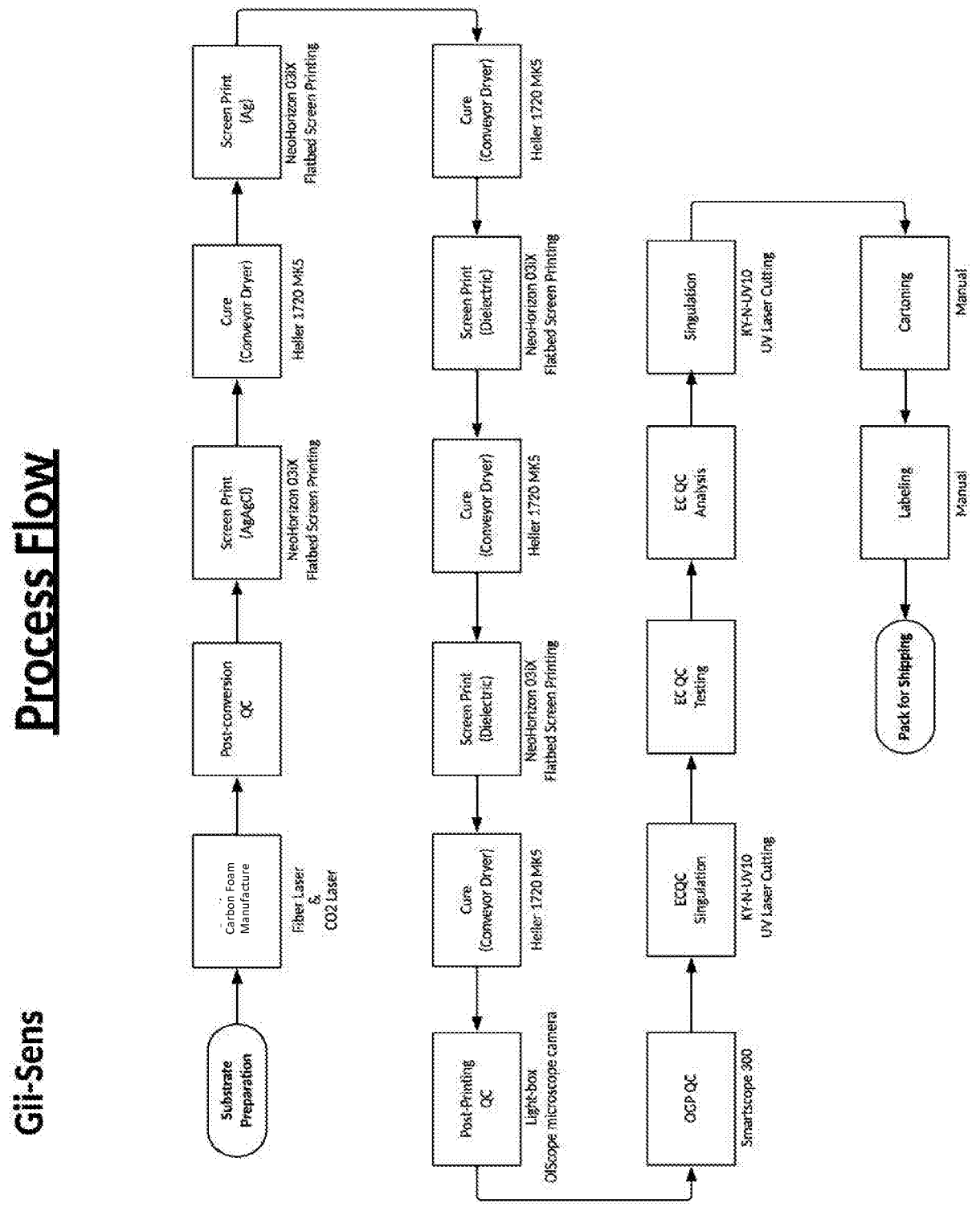

Gii-Sens
Process Flow
Substrate Preparation
Carbon Foam Manufacture
Fiber Laser & CO2 Laser
Post-conversion QC
Screen Print (Ag/AgCl)
NeoHorizon 03iX Flatbed Screen Printing
Cure (Conveyor Dryer)
Heller 1720 MK5
Screen Print (Ag)
NeoHorizon 03iX Flatbed Screen Printing
Cure (Conveyor Dryer)
Heller 1720 MK5
Screen Print (Dielectric)
NeoHorizon 03iX Flatbed Screen Printing
Cure (Conveyor Dryer)
Heller 1720 MK5
Screen Print (Dielectric)
NeoHorizon 03iX Flatbed Screen Printing
Cure (Conveyor Dryer)
Heller 1720 MK5
Post-Printing QC
Light-box OlScope microscope camera
OCP QC
Smartscope 380
ECQC Singulation
KY-N-UV10 UV Laser Cutting
EC QC Testing
EC QC Analysis
Singulation
KY-N-UV10 UV Laser Cutting
Cartoning
Manual
Labeling
Manual
Pack for Shipping

Figure 21

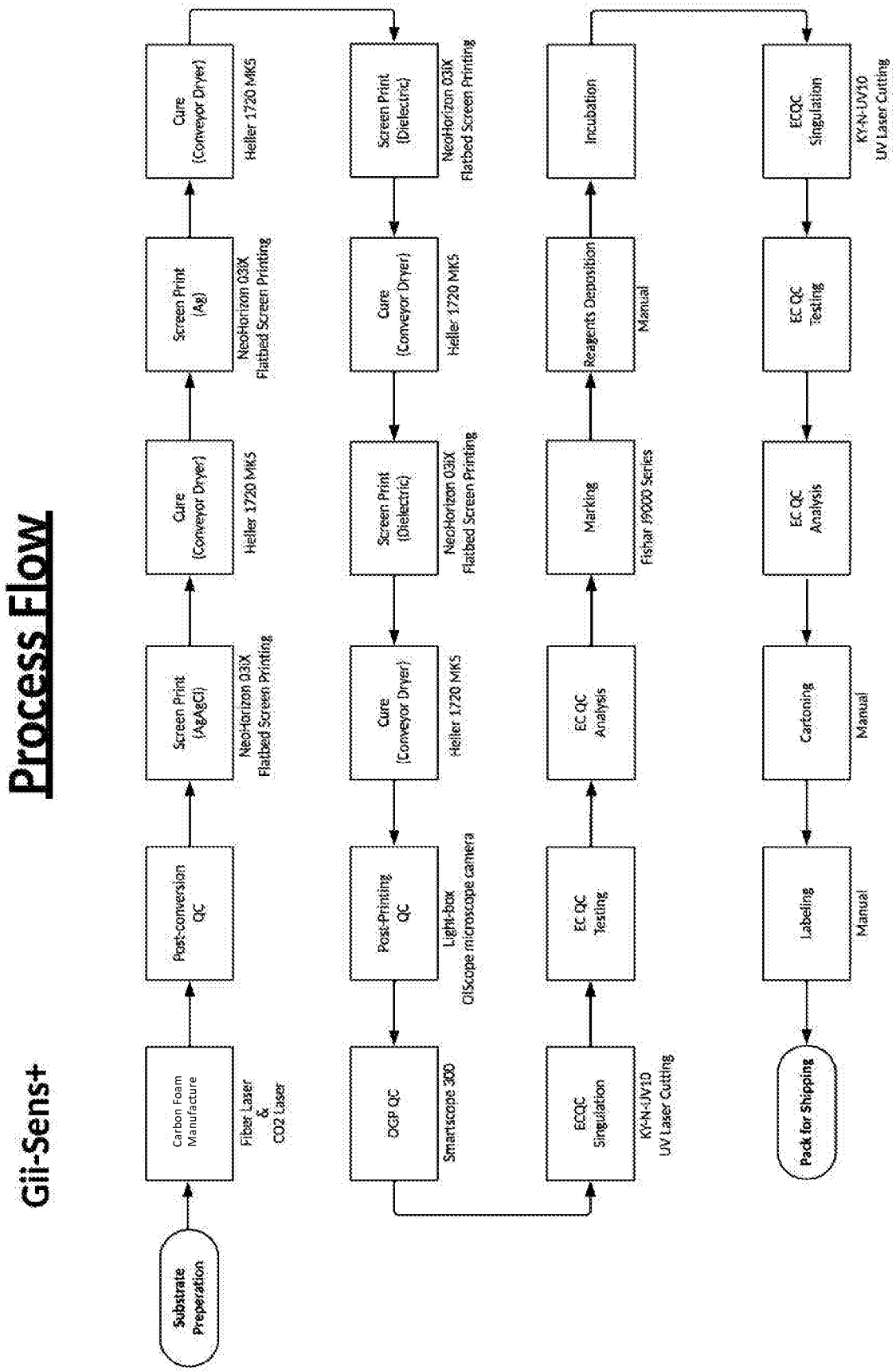

Gii-Sens+
Process Flow
Substrate Preperation
Carbon Foam Manufacture
Fiber Laser & CO2 Laser
Post-conversion QC
Screen Print (Ag/AgCl)
NeoHorizon 03iX Flatbed Screen Printing
Cure (Conveyor Dryer)
Heller 1720 MK5
Screen Print (Ag)
NeoHorizon 03iX Flatbed Screen Printing
Cure (Conveyor Dryer)
Heller 1720 MK5
DGP QC
Smartscope 300
Post-Printing QC
Light-box OiScope microscope camera
Cure (Conveyor Dryer)
Heller 1720 MK5
Screen Print (Dielectric)
NeoHorizon 03iX Flatbed Screen Printing
Cure (Conveyor Dryer)
Heller 1720 MK5
Screen Print (Dielectric)
NeoHorizon 03iX Flatbed Screen Printing
ECQC Singulation
KY-N-UV10 UV Laser Cutting
EC QC Testing
EC QC Analysis
Marking
Fishar I9000 Series
Reagents Deposition
Manual
Incubation
ECQC Singulation
KY-N-UV10 UV Laser Cutting
EC QC Testing
EC QC Analysis
Cartoning
Manual
Labeling
Manual
Pack for Shipping

Figure 22

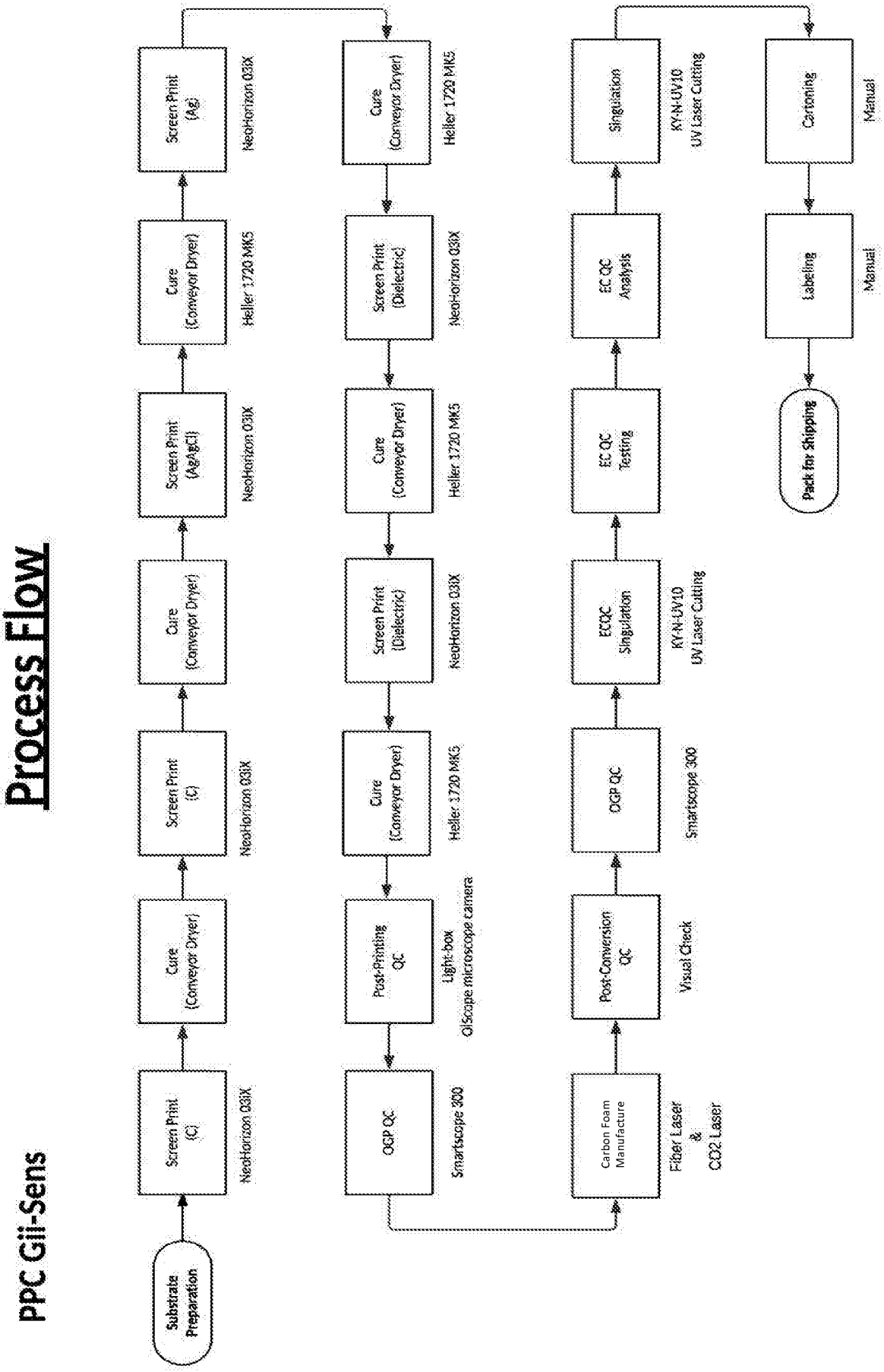

PPC Gii-Sens
Process Flow
Substrate Preparation
Screen Print (C)
NeoHorizon 03iX
Cure (Conveyor Dryer)
Screen Print (C)
NeoHorizon 03iX
Cure (Conveyor Dryer)
Screen Print (Ag/AgCl)
NeoHorizon 03iX
Cure (Conveyor Dryer)
Heller 1720 MK5
Screen Print (Ag)
NeoHorizon 03iX
OGP QC
Smartscope 300
Post-Printing QC
Light-box
OScope microscope camera
Cure (Conveyor Dryer)
Heller 1720 MK5
Screen Print (Dielectric)
NeoHorizon 03iX
Cure (Conveyor Dryer)
Heller 1720 MK5
Screen Print (Dielectric)
NeoHorizon 03iX
Cure (Conveyor Dryer)
Heller 1720 MK5
Carbon Foam Manufacture
Fiber Laser & CO2 Laser
Post-Conversion QC
Visual Check
OGP QC
Smartscope 300
EC QC Singulation
KY-N-UV10 UV Laser Cutting
EC QC Testing
EC QC Analysis
Singulation
KY-N-UV10 UV Laser Cutting
Pack for Shipping
Labeling
Manual
Cartoning
Manual

Figure 23

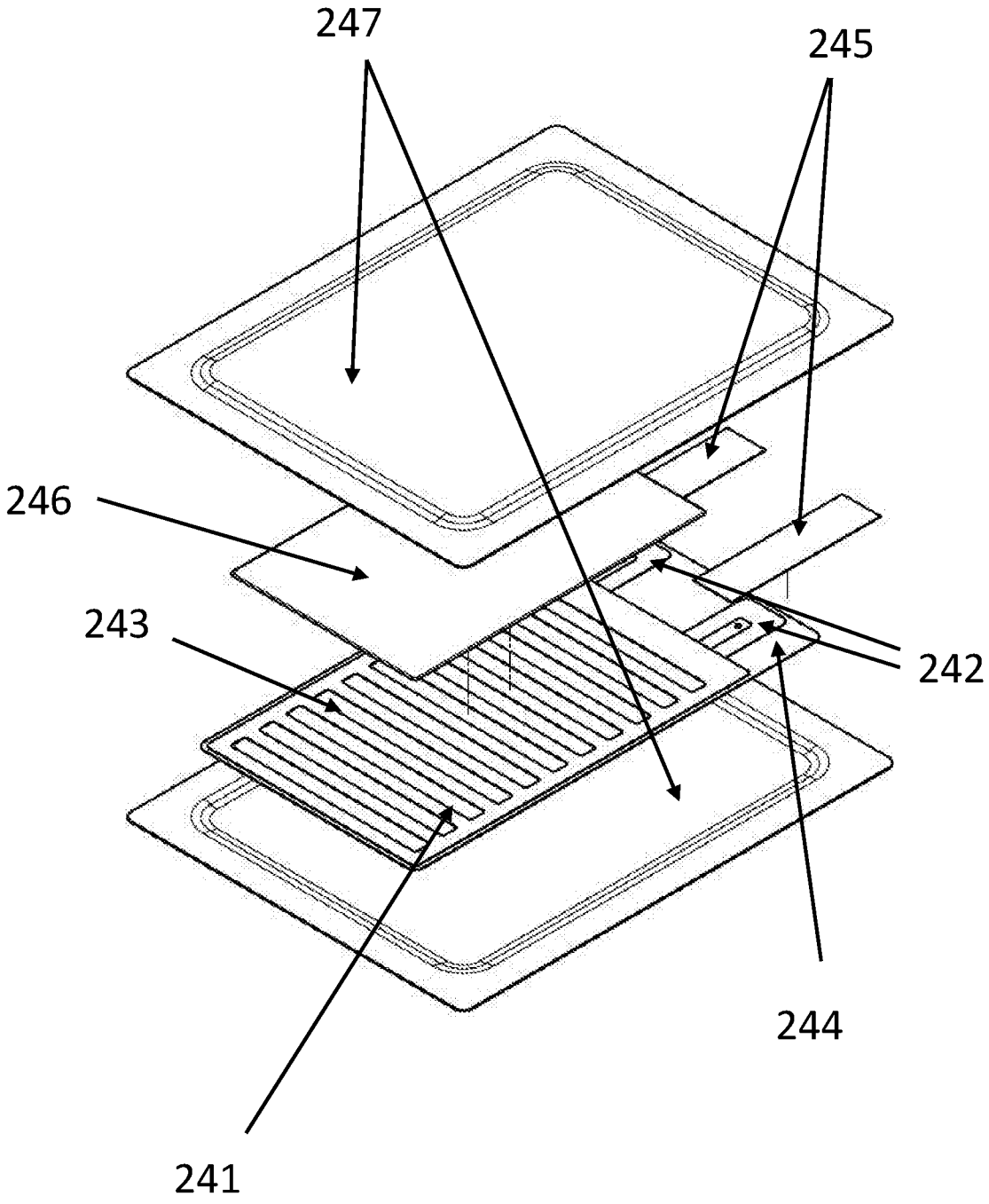


Figure 24

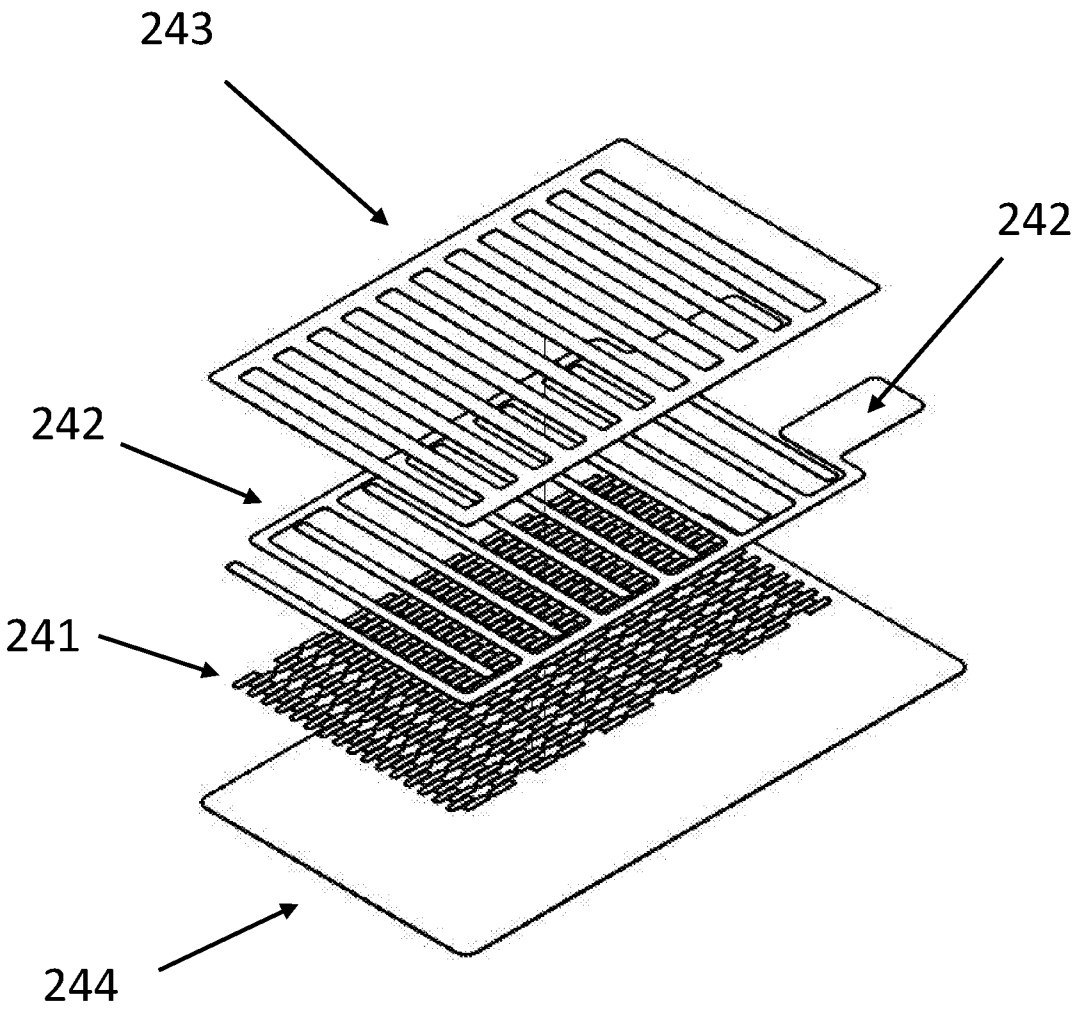


Figure 25

Step 1

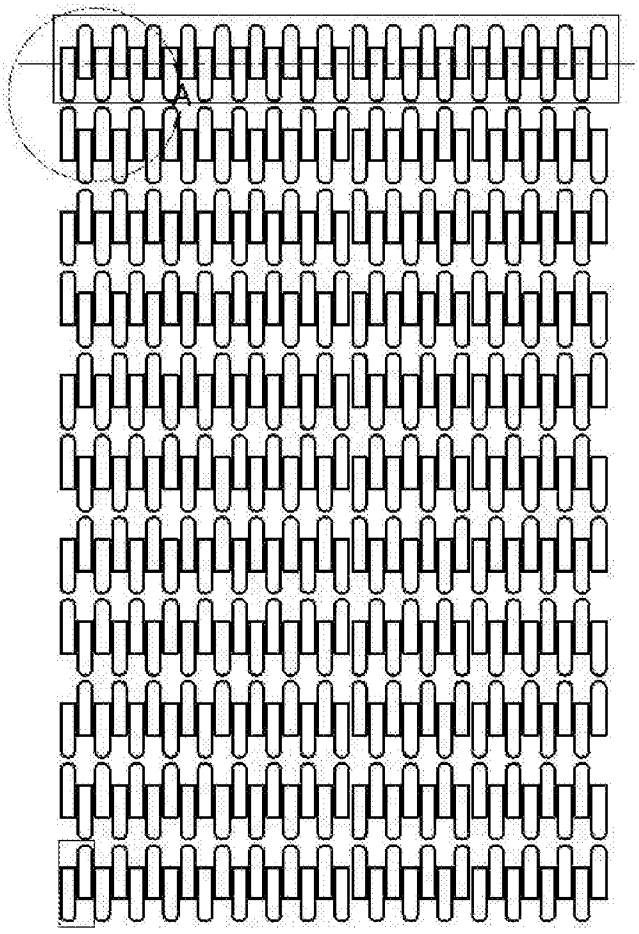


Figure 26A

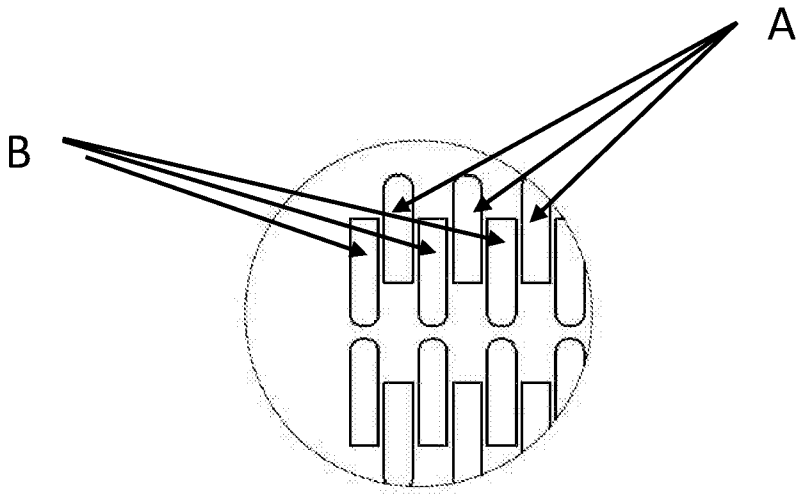


Figure 26B

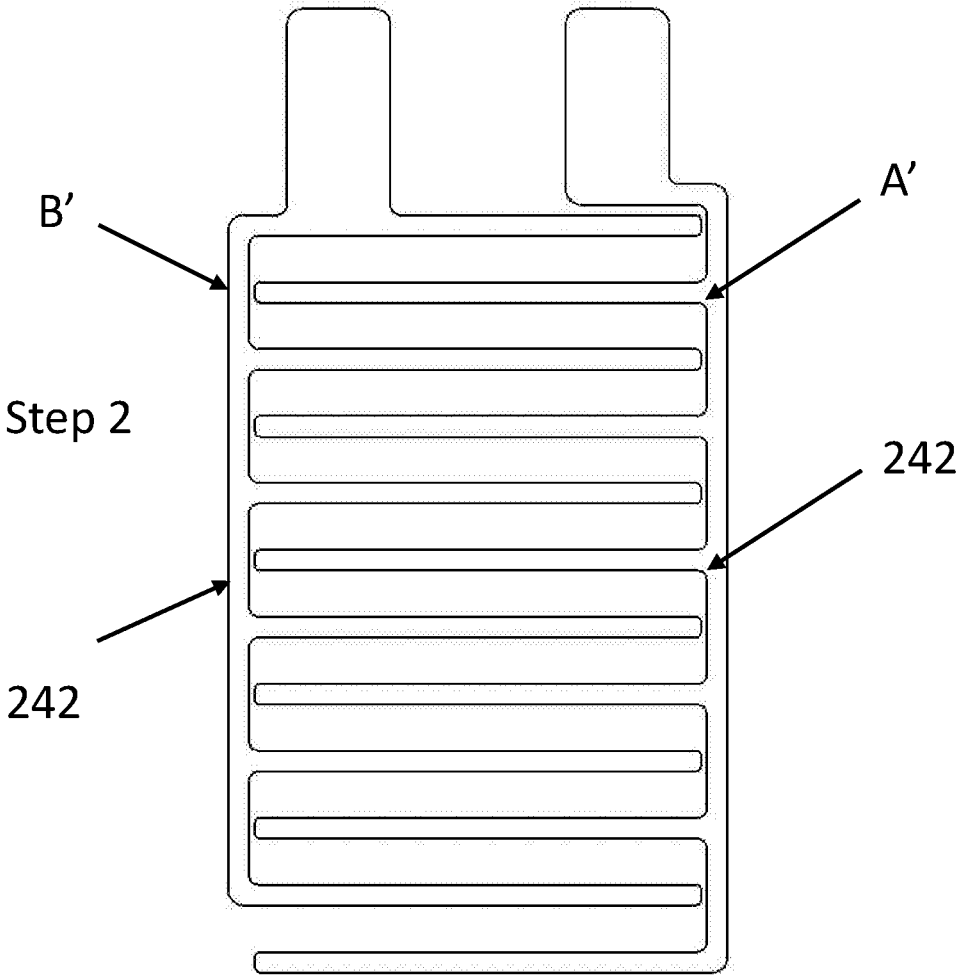


Figure 26C

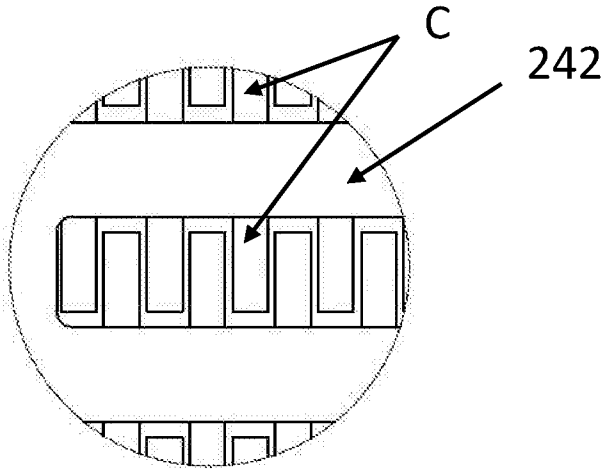


Figure 26D

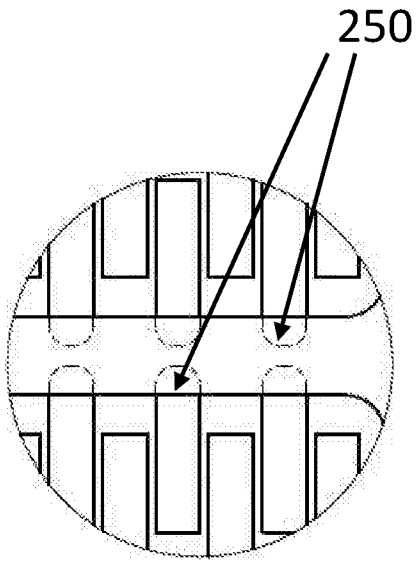


Figure 26E

Step 3

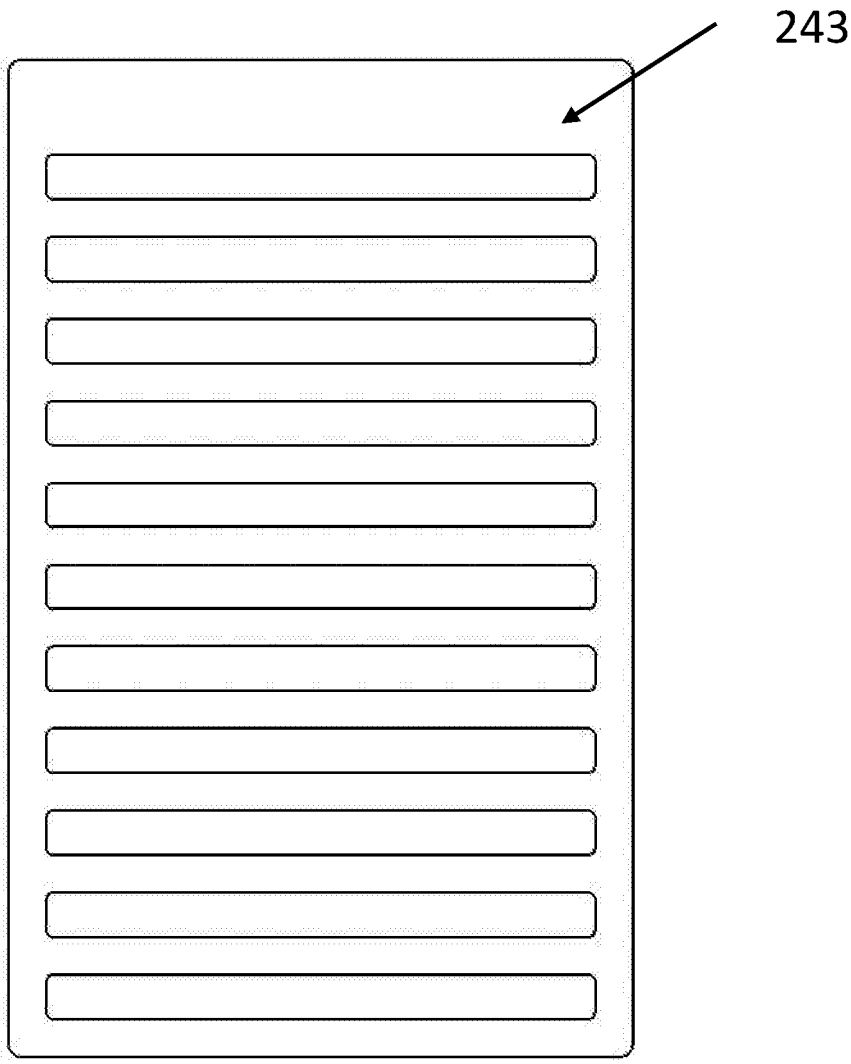


Figure 26F

Step 4

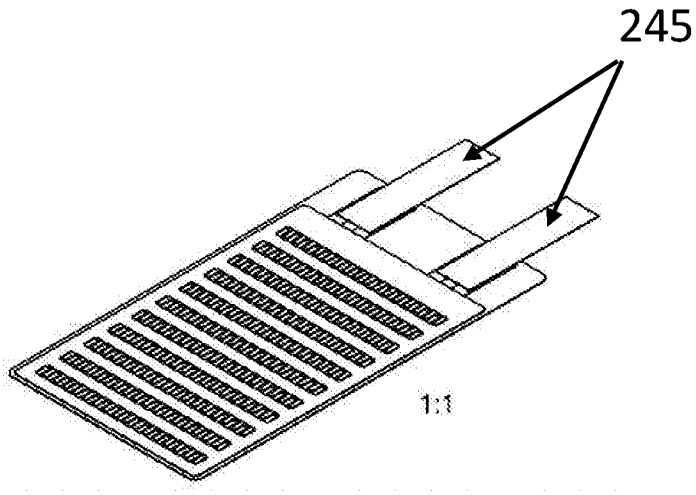


Figure 26G

Step 5

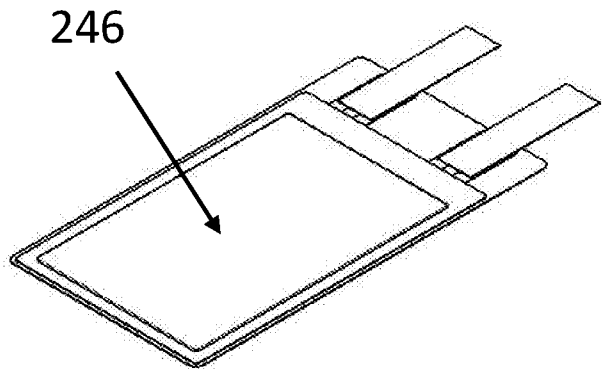


Figure 26H

Step 6

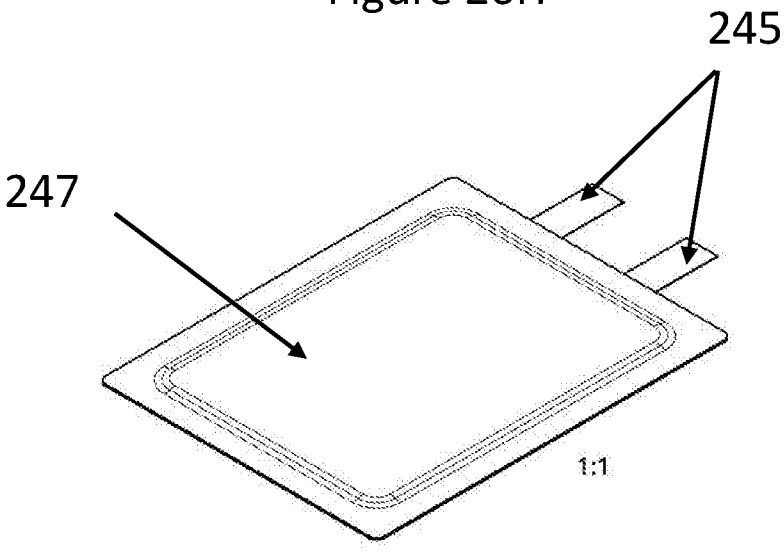


Figure 26I

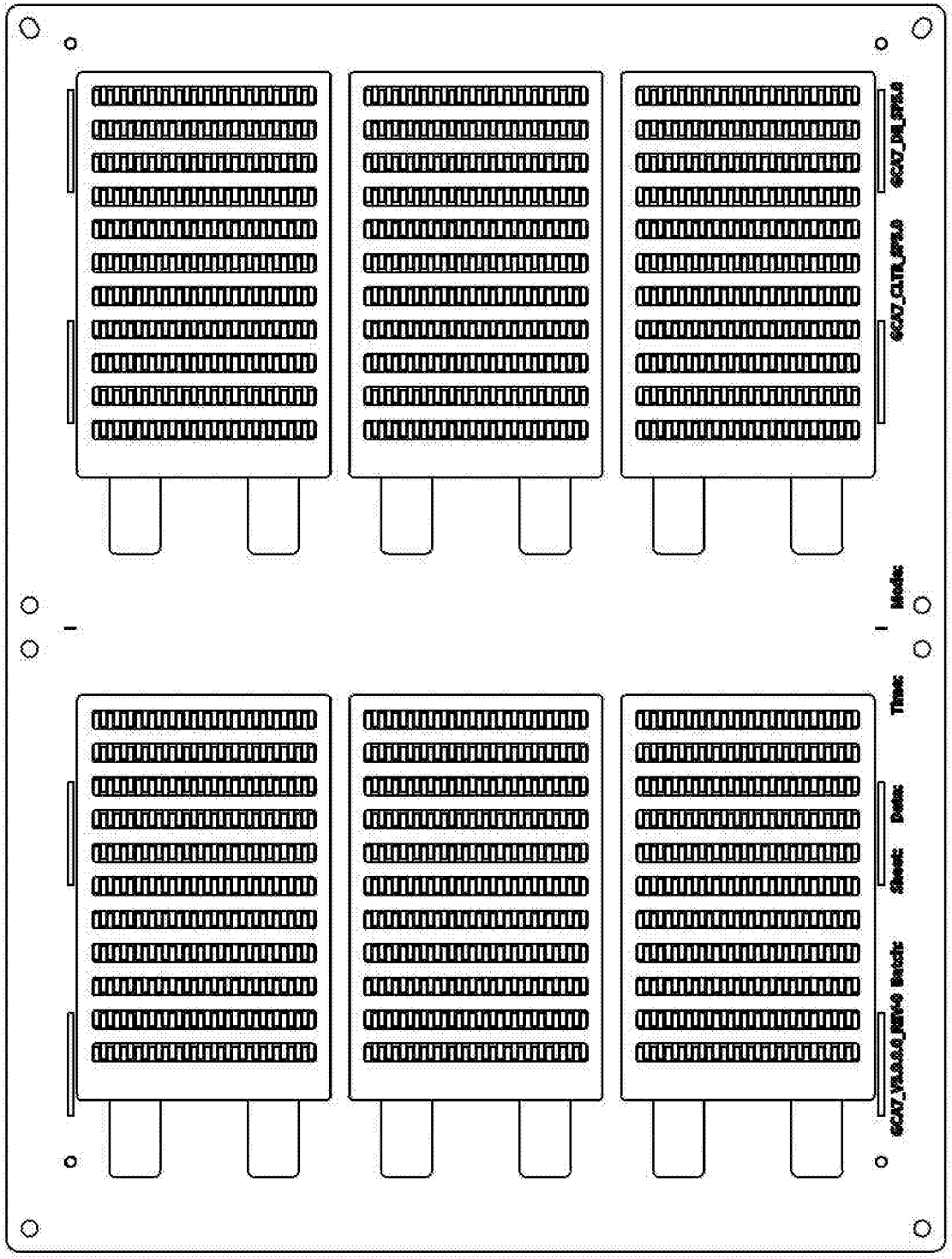


Figure 27

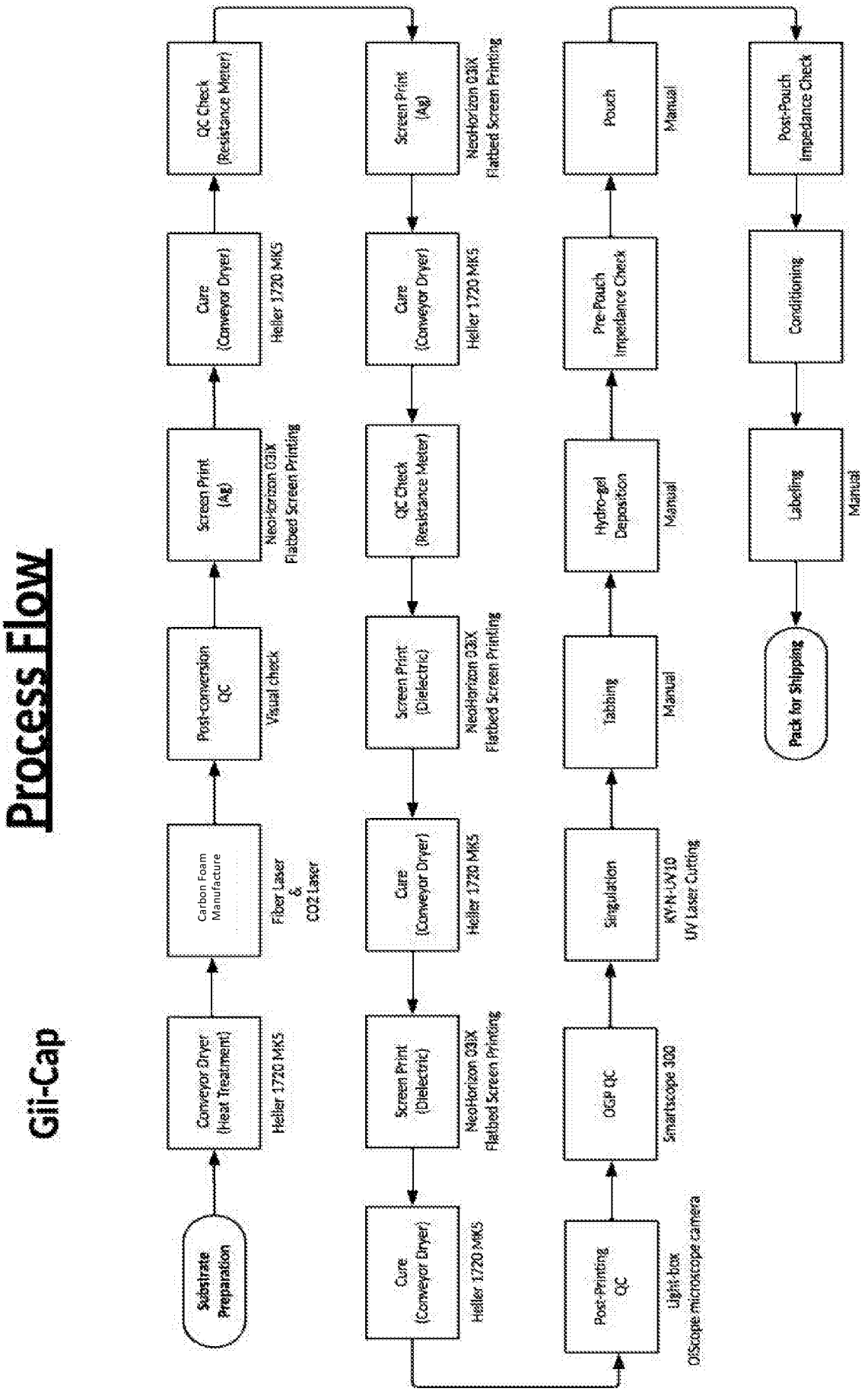

Process Flow
Gii-Cap
Substrate Preparation
Conveyor Dryer (Heat Treatment)
Heller 1720 MK5
Carbon Foam Manufacture
Fiber Laser & CO2 Laser
Post-conversion QC
Visual check
Screen Print (Ag)
NeoHorizon 03iX Flatbed Screen Printing
Cure (Conveyor Dryer)
Heller 1720 MK5
QC Check (Resistance Meter)
Screen Print (Dielectric)
NeoHorizon 03iX Flatbed Screen Printing
Cure (Conveyor Dryer)
Heller 1720 MK5
Screen Print (Dielectric)
NeoHorizon 03iX Flatbed Screen Printing
Cure (Conveyor Dryer)
Heller 1720 MK5
Screen Print (Ag)
NeoHorizon 03iX Flatbed Screen Printing
QC Check (Resistance Meter)
Post-Printing QC
Light-box OScope microscope camera
OGP QC
Smartscope 300
Singulation
KYN-UV10 UV Laser Cutting
Tabbing
Manual
Hydro-gel Deposition
Manual
Pre-Pouch Impedance Check
Pouch
Manual
Post-Pouch Impedance Check
Conditioning
Labeling
Manual
Pack for Shipping

Figure 28

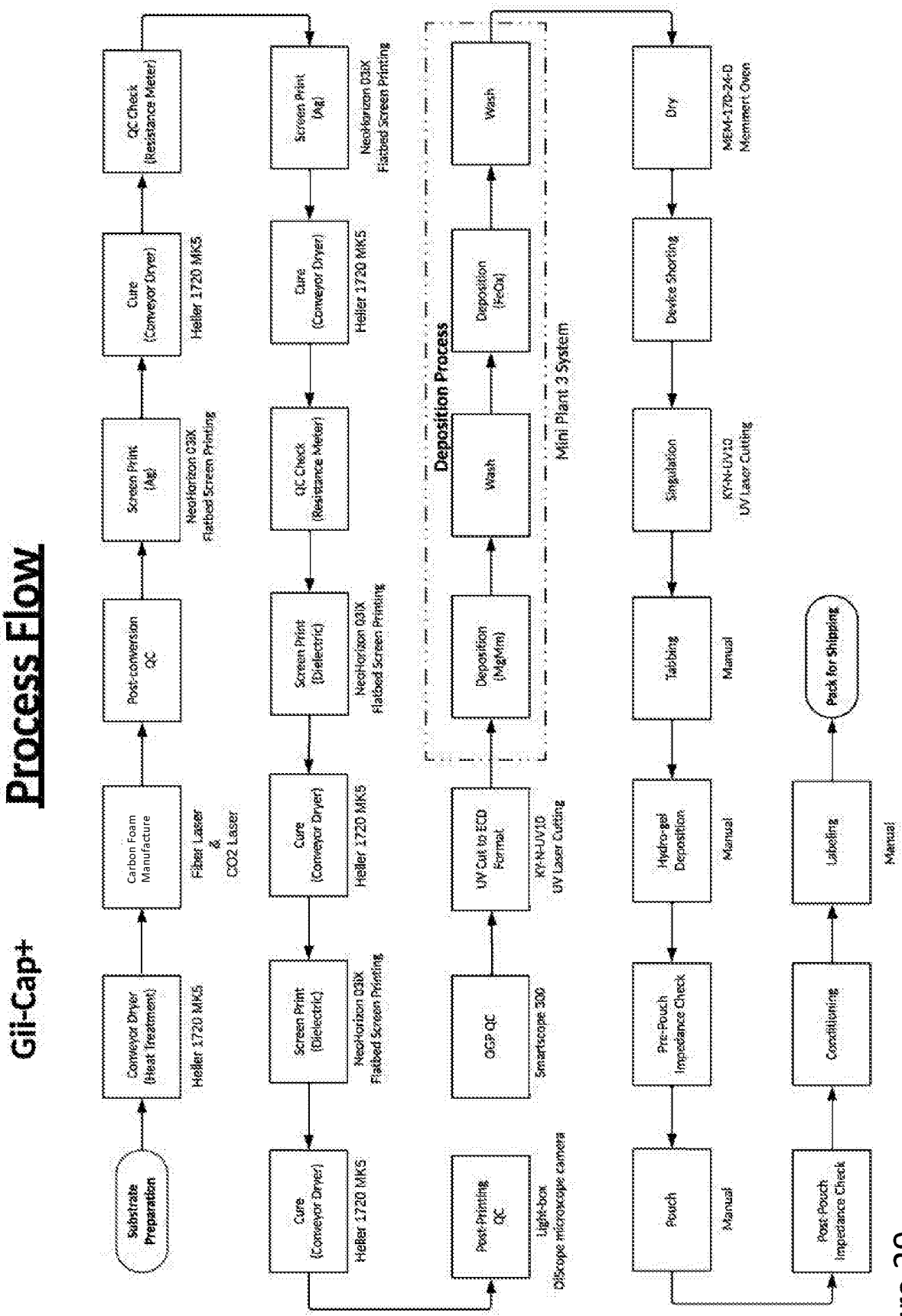

Gii-Cap+
Process Flow
Substrate Preparation
Conveyor Dryer (Heat Treatment)
Heller 1720 MK5
Carbon Foam Manufacture
Fiber Laser & CO2 Laser
Post-conversion QC
Screen Print (Ag)
NeoHorizon 03X Flatbed Screen Printing
Cure (Conveyor Dryer)
Heller 1720 MK5
QC Check (Resistance Meter)
Screen Print (Dielectric)
NeoHorizon 03X Flatbed Screen Printing
Cure (Conveyor Dryer)
Heller 1720 MK5
Post-Printing QC
Light-box
Olscope microscope camera
Screen Print (Ag)
NeoHorizon 03X Flatbed Screen Printing
Cure (Conveyor Dryer)
Heller 1720 MK5
QC Check (Resistance Meter)
Screen Print (Dielectric)
NeoHorizon 03X Flatbed Screen Printing
Cure (Conveyor Dryer)
Heller 1720 MK5
QSP QC
Smartscope 300
UV Cut to ECD Format
KY-N-UV10
UV Laser Cutting
Deposition Process
Deposition (MgMm)
Wash
Deposition (ReOx)
Wash
Mini Plant 3 System
Dry
MEM-170-24-D
Memmert Oven
Device Shorting
Singulation
KY-N-UV10
UV Laser Cutting
Tabbing
Manual
Hydro-gel Deposition
Manual
Pre-Pouch Impedance Check
Pouch
Manual
Post-Pouch Impedance Check
Conditioning
Labeling
Manual
Pack for Shipping

Figure 29

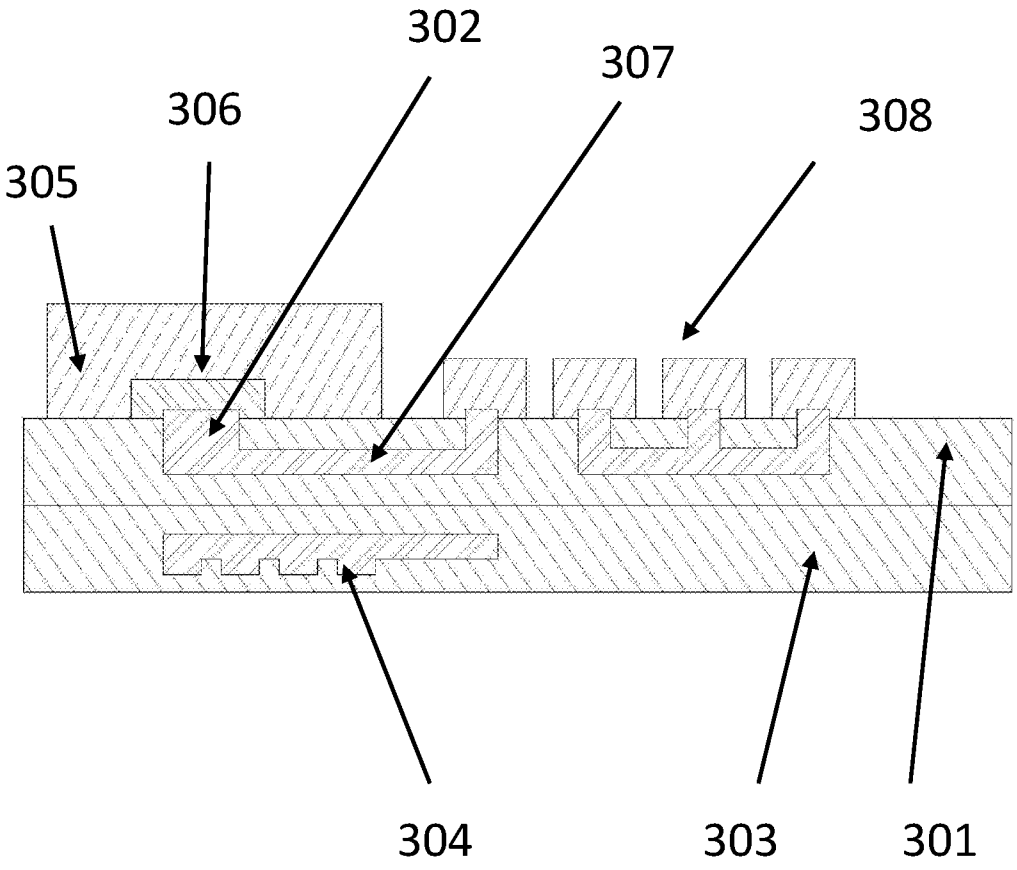


Figure 30

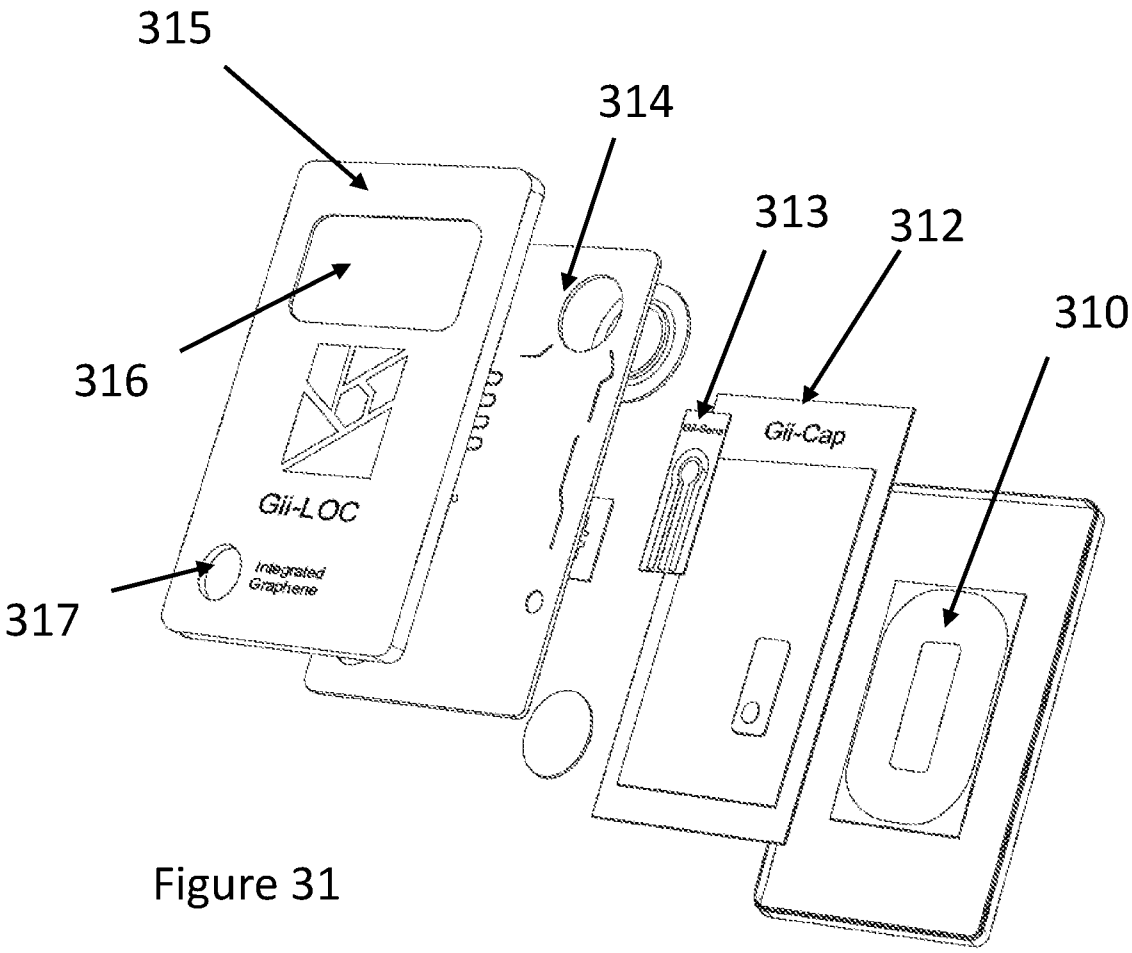


Figure 31

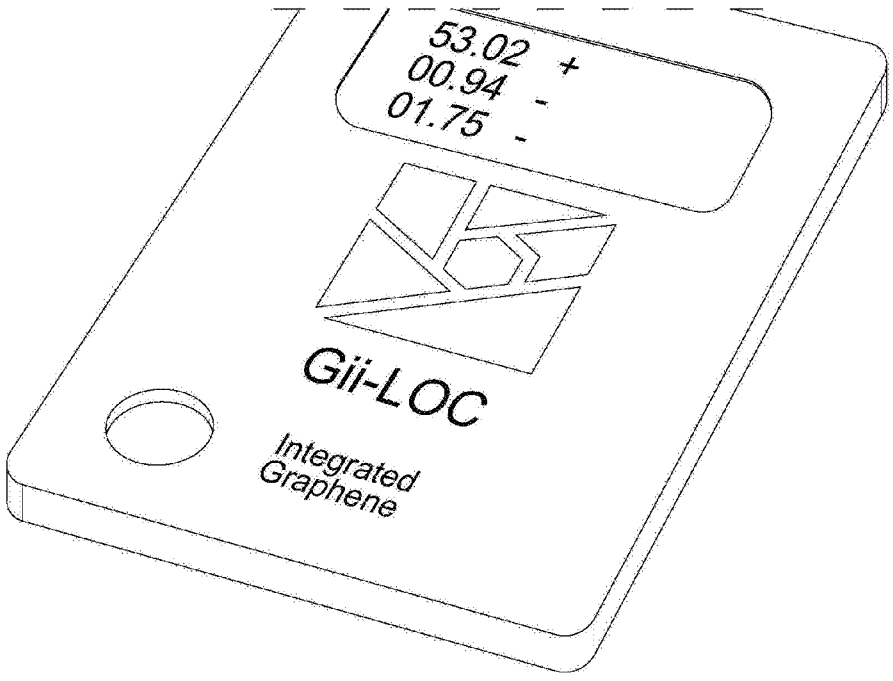


Figure 32

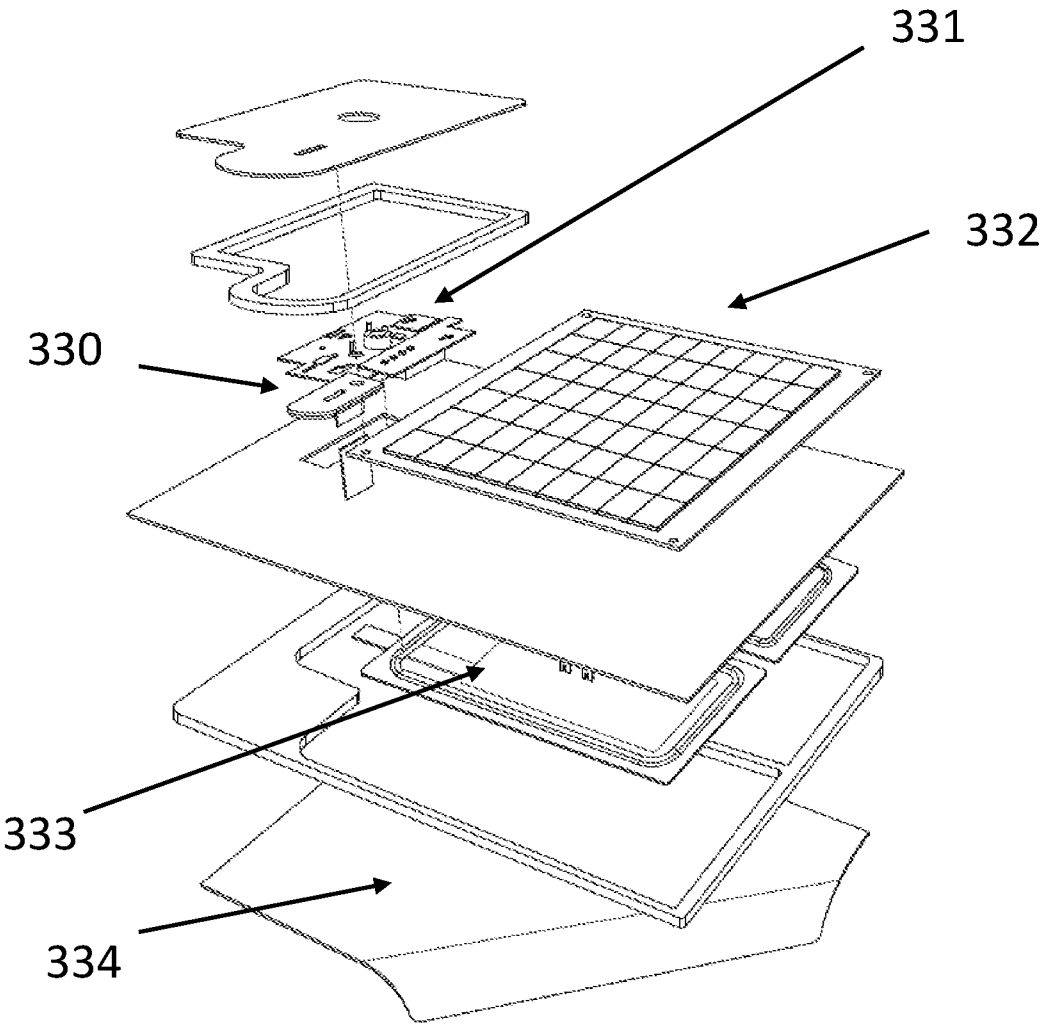


Figure 33

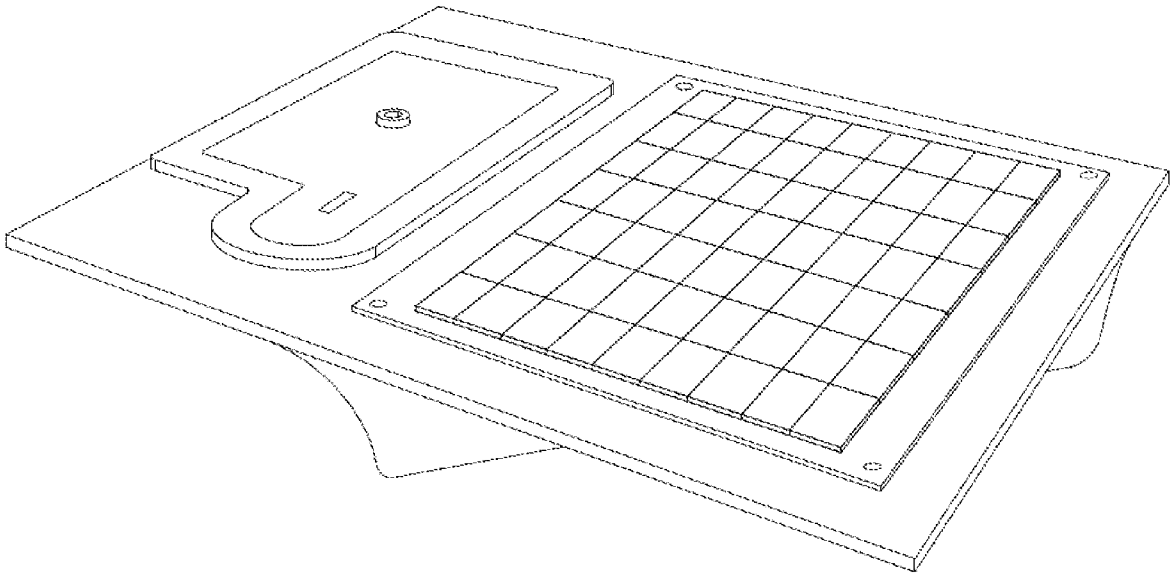


Figure 34

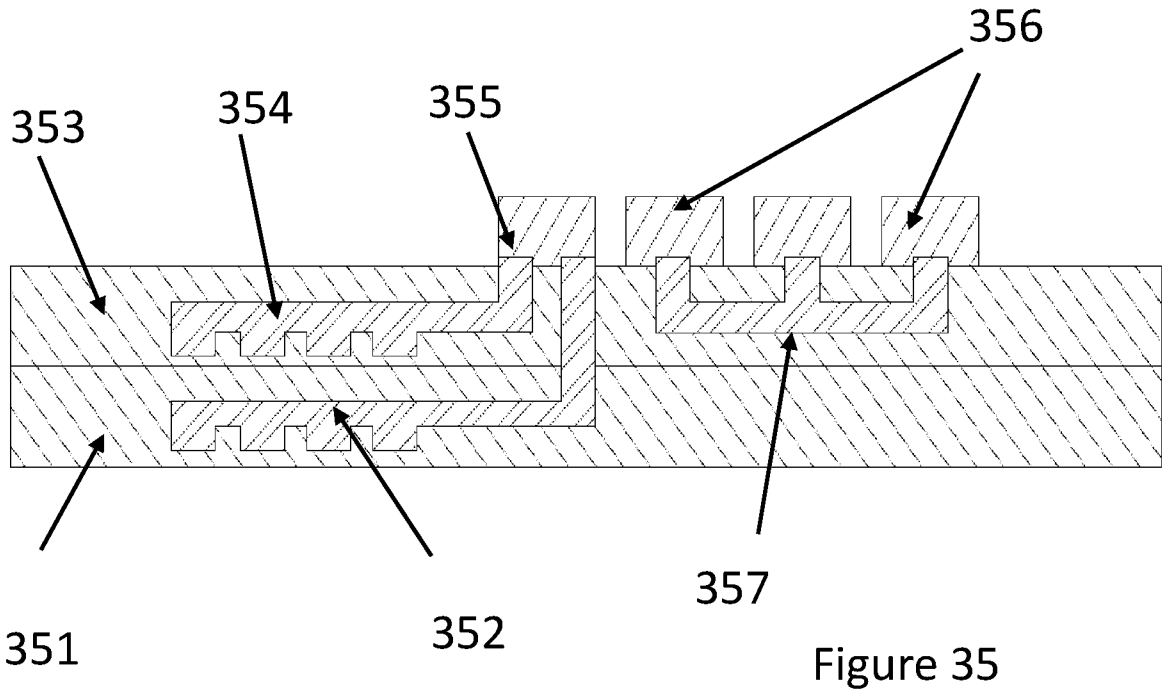


Figure 35

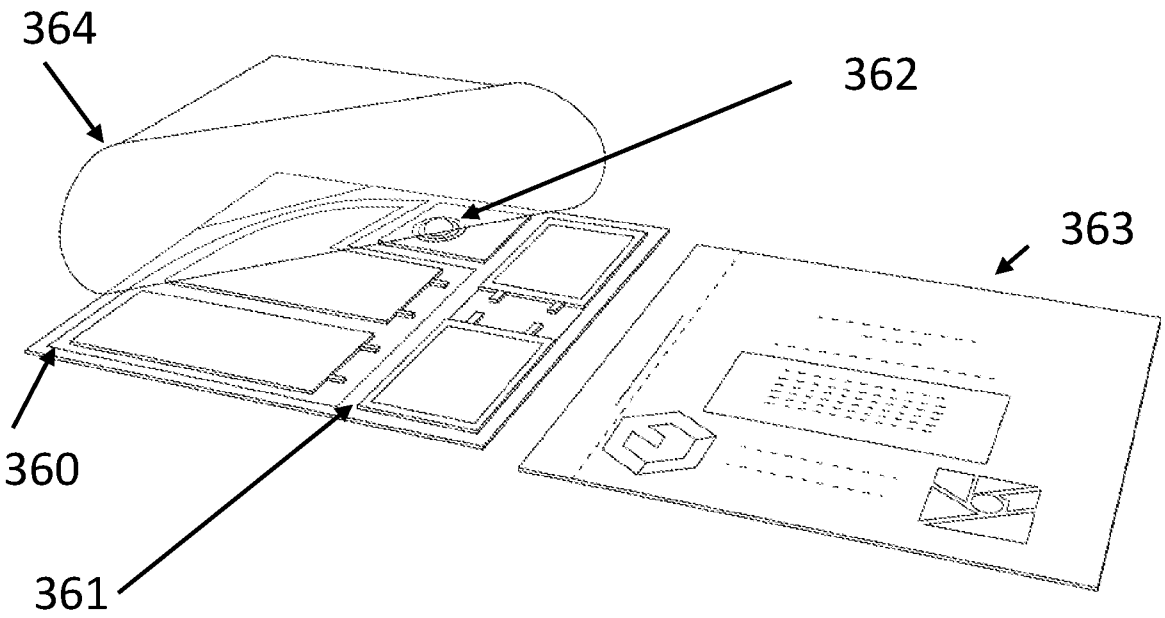


Figure 36

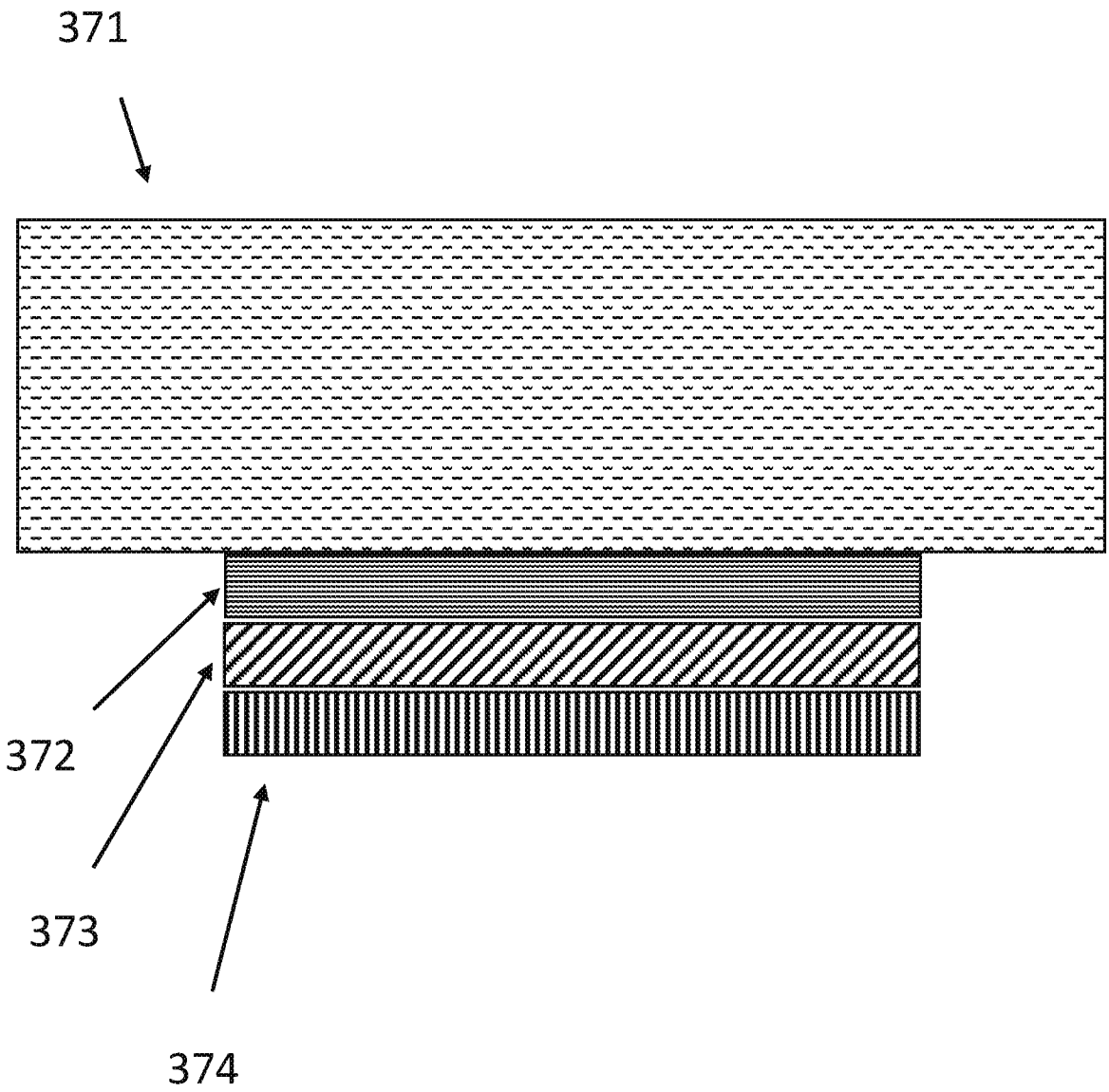


Figure 37

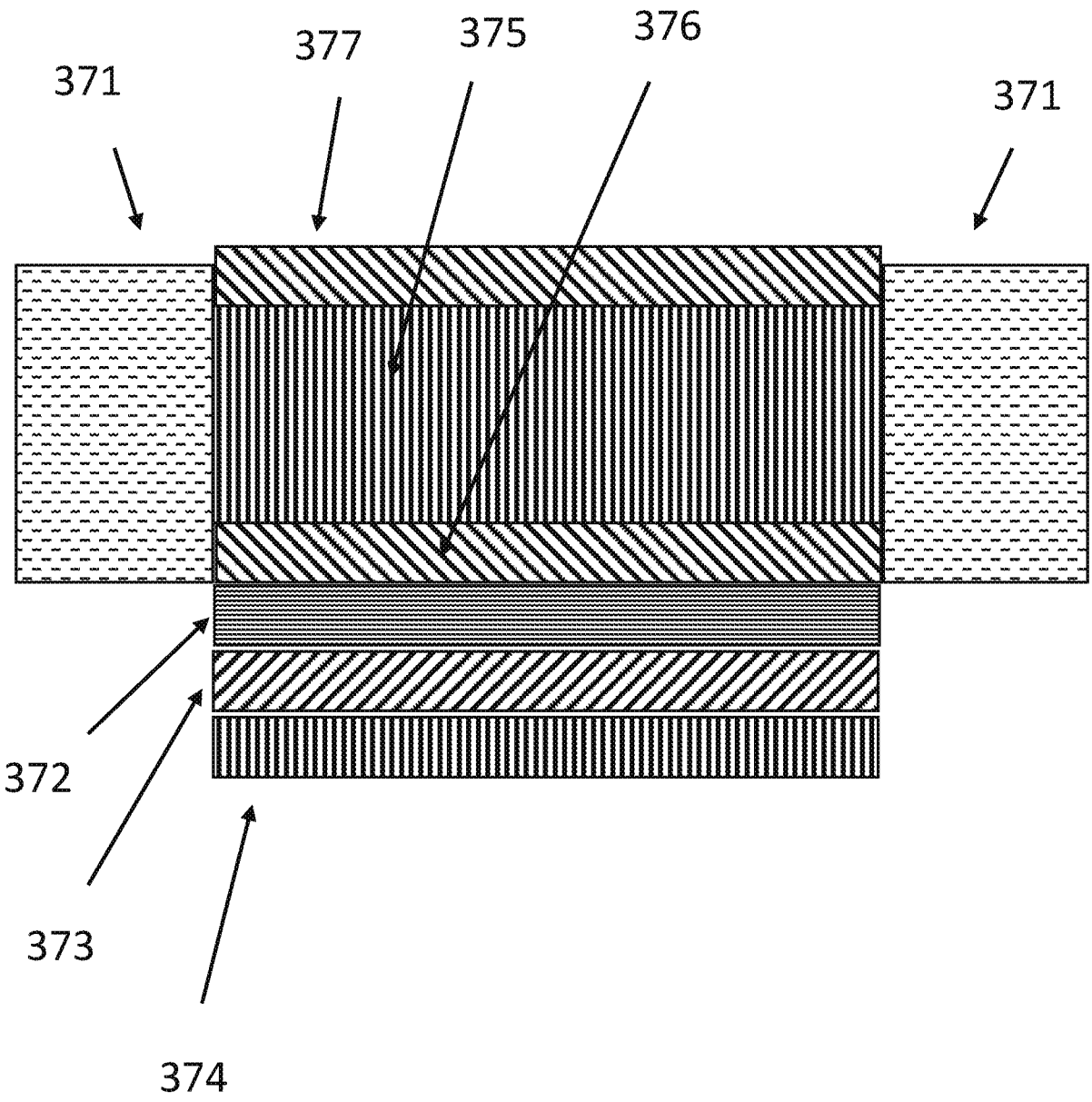


Figure 38

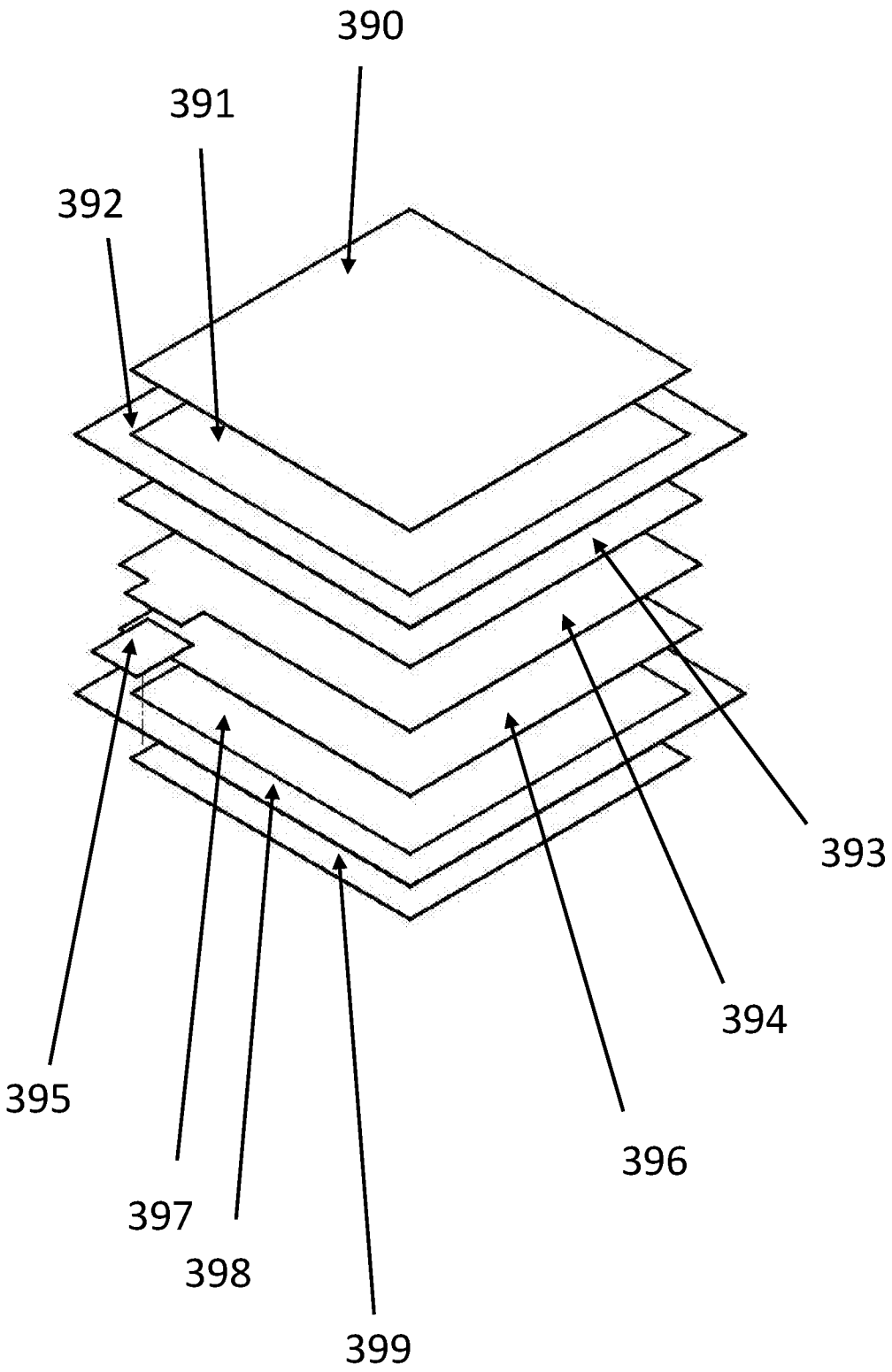
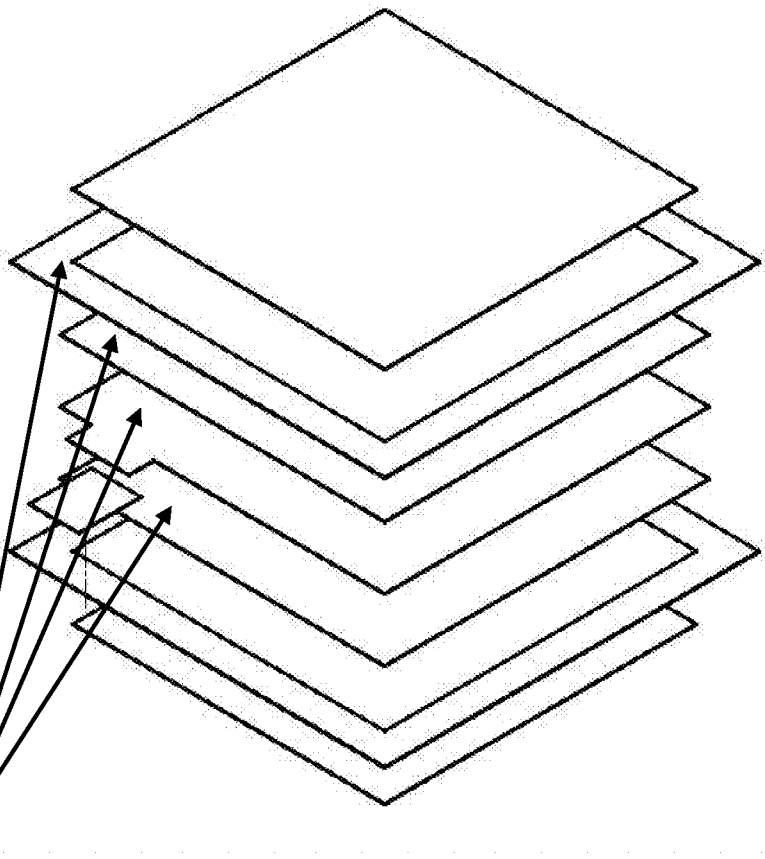


Figure 39



A

Figure 40A

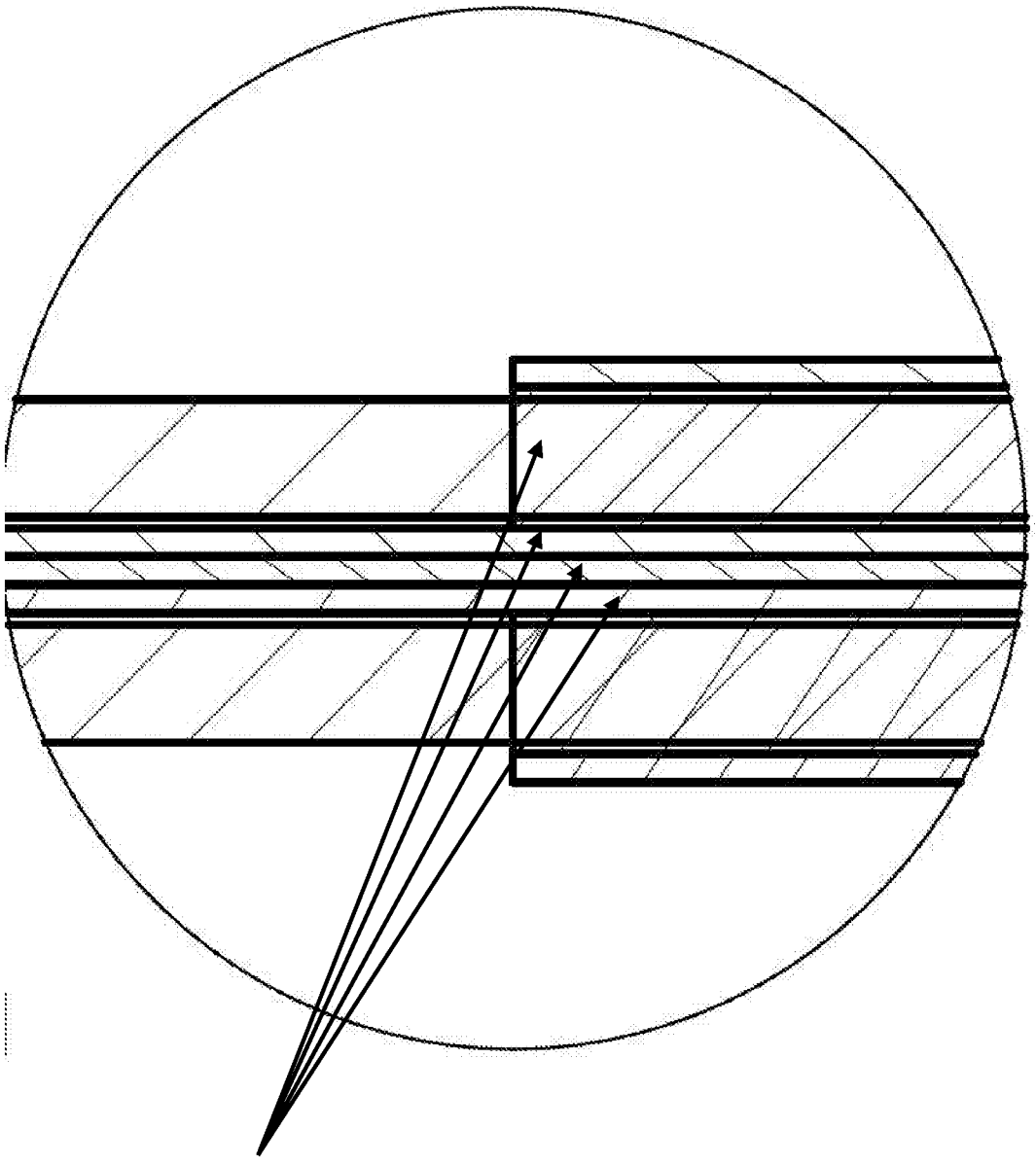


Figure 40B

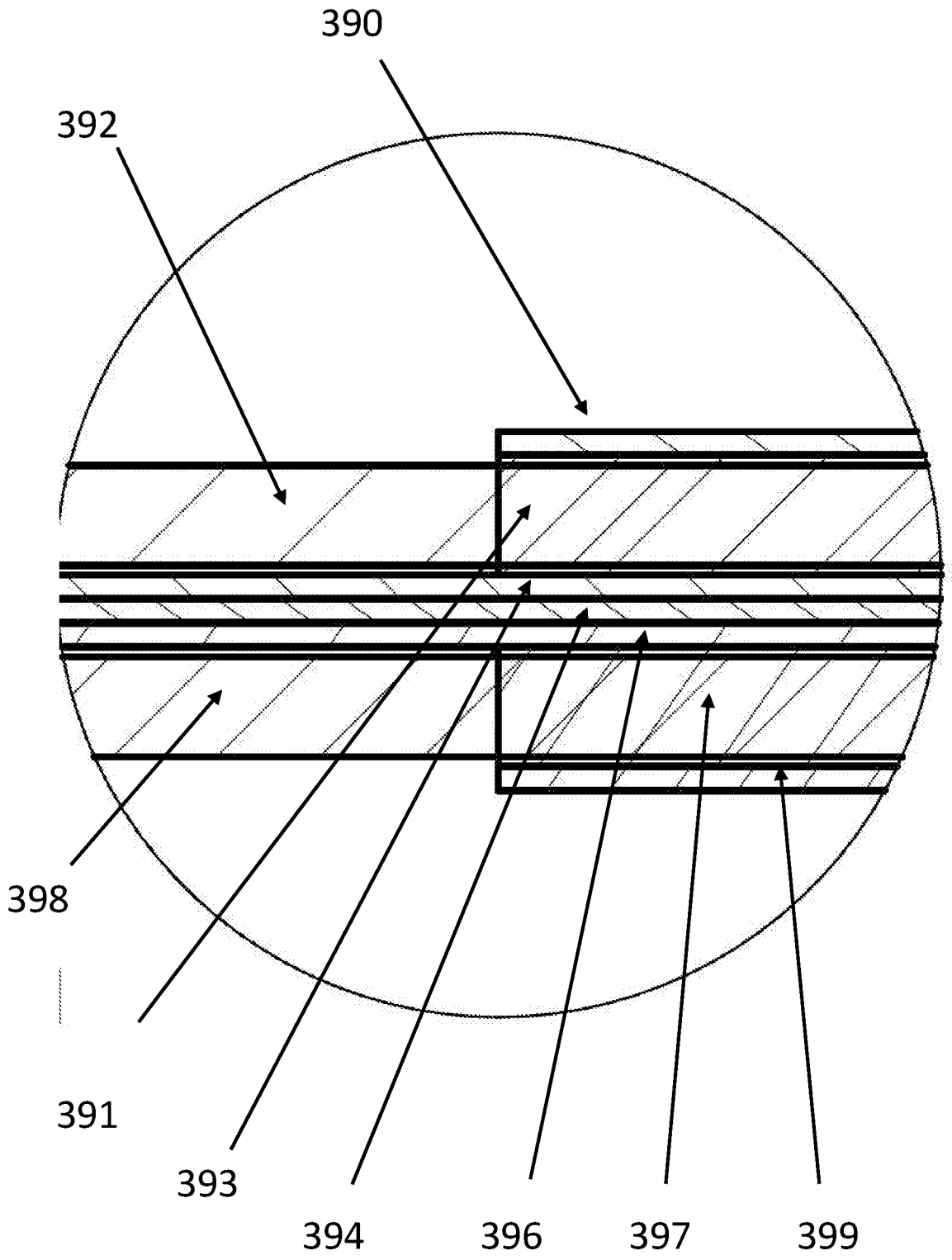


Figure 40C

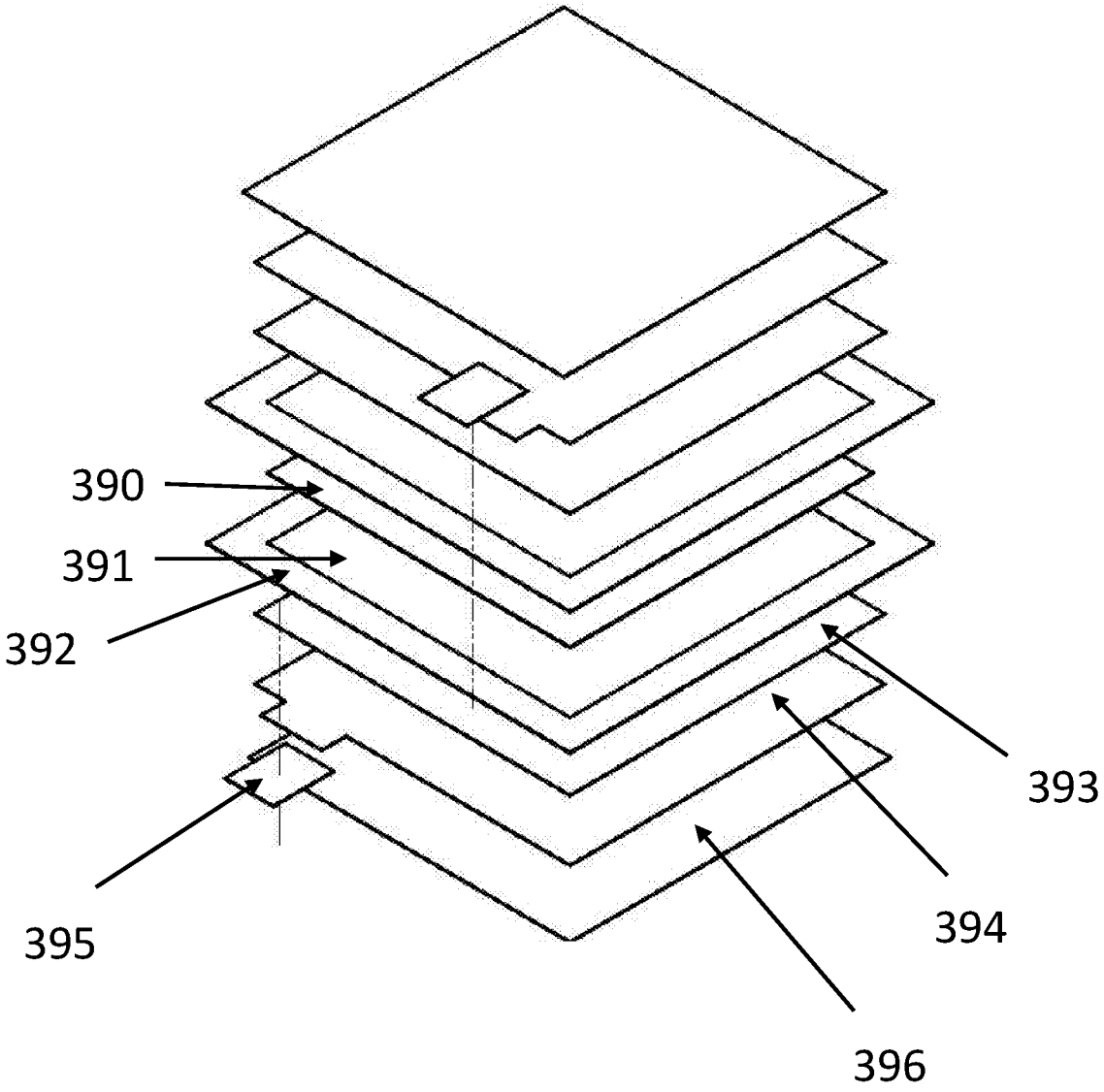


Figure 41A

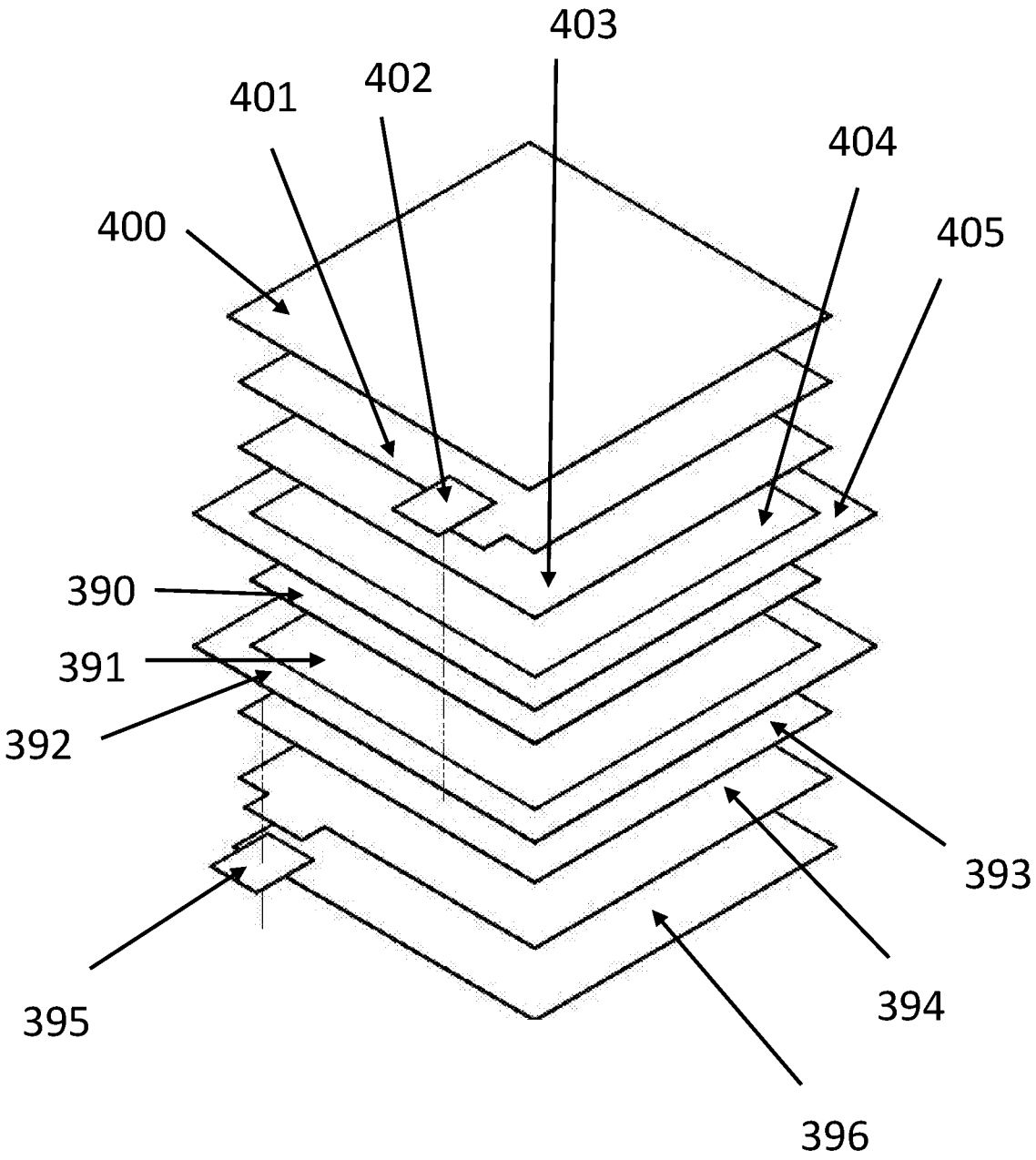


Figure 41B

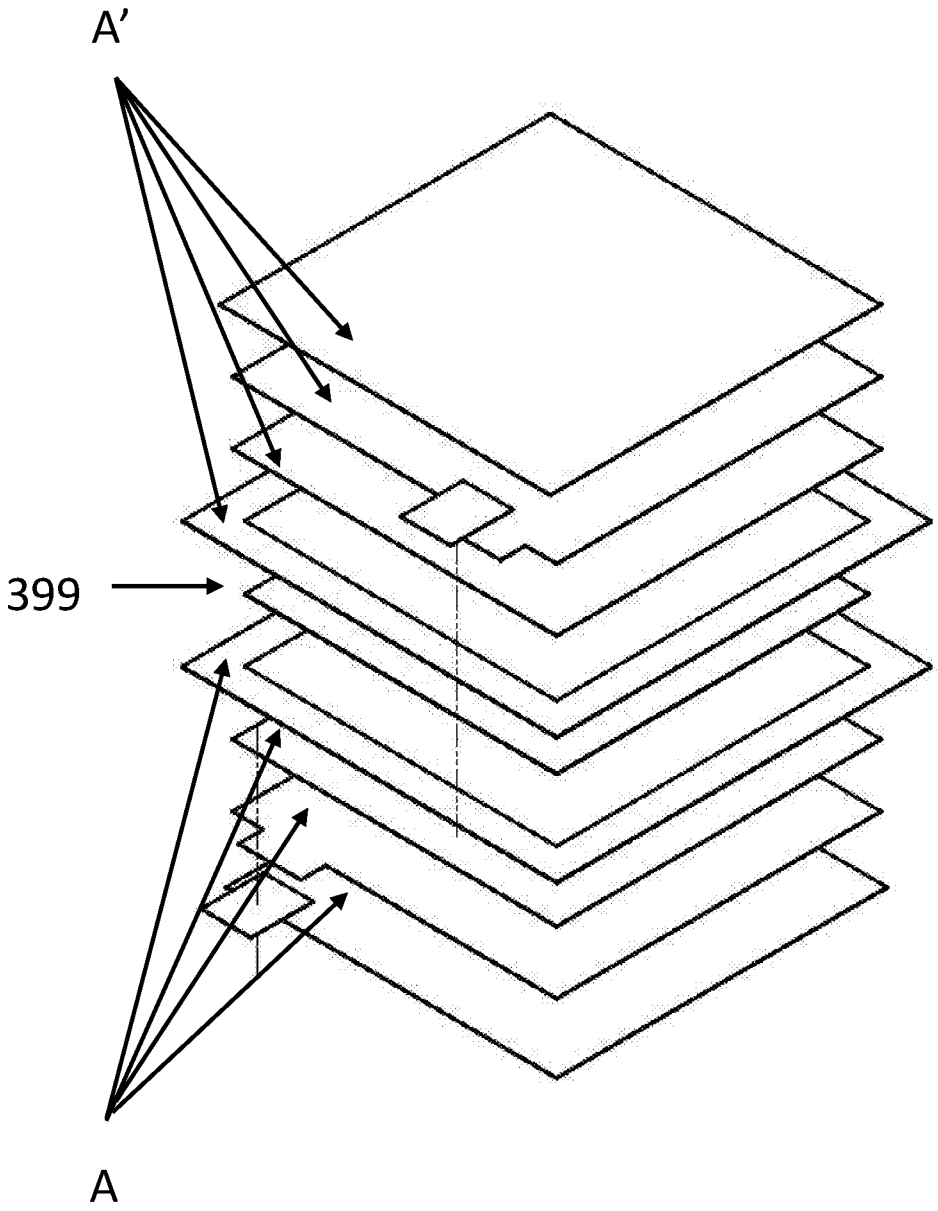


Figure 41C

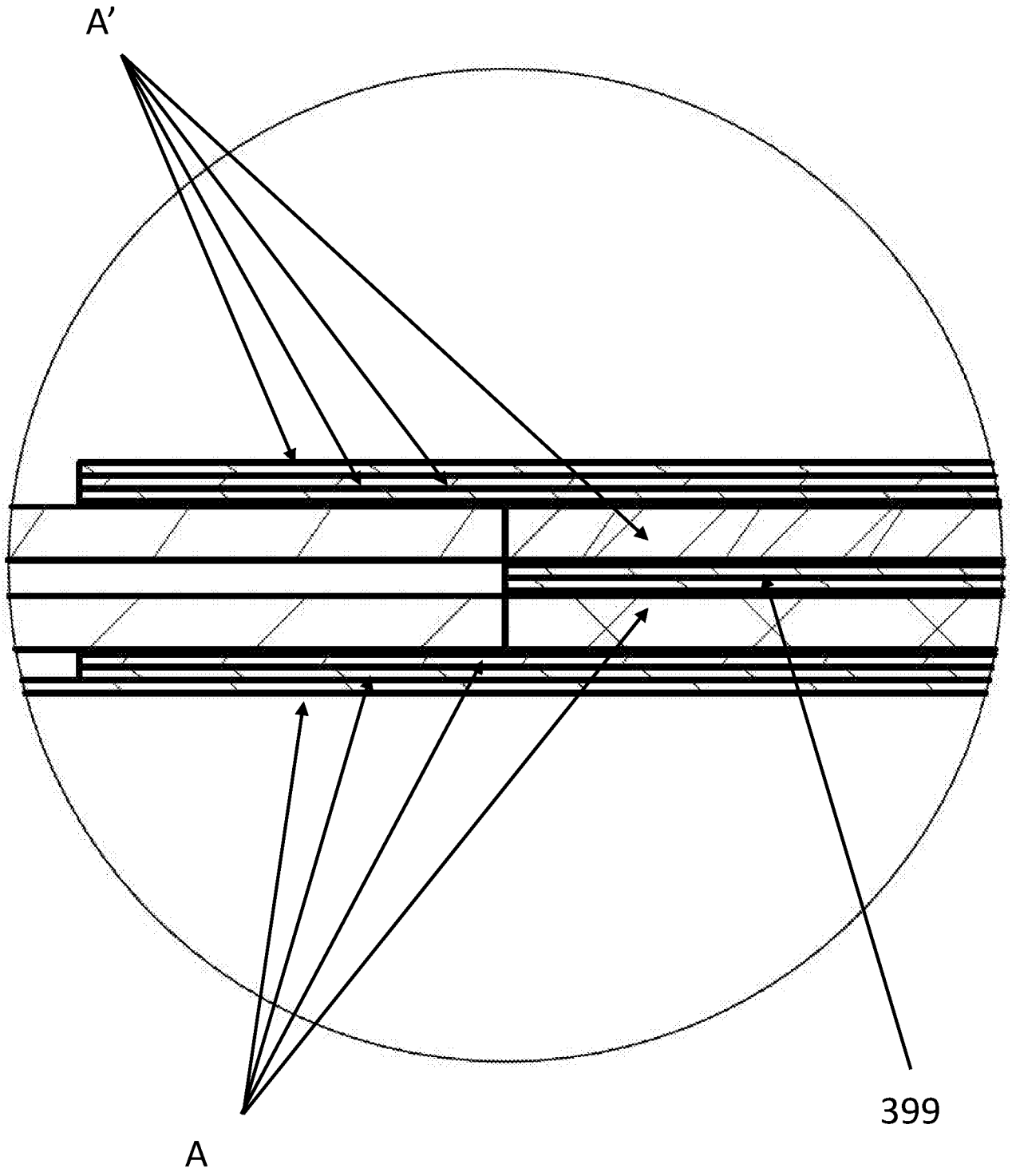


Figure 41D

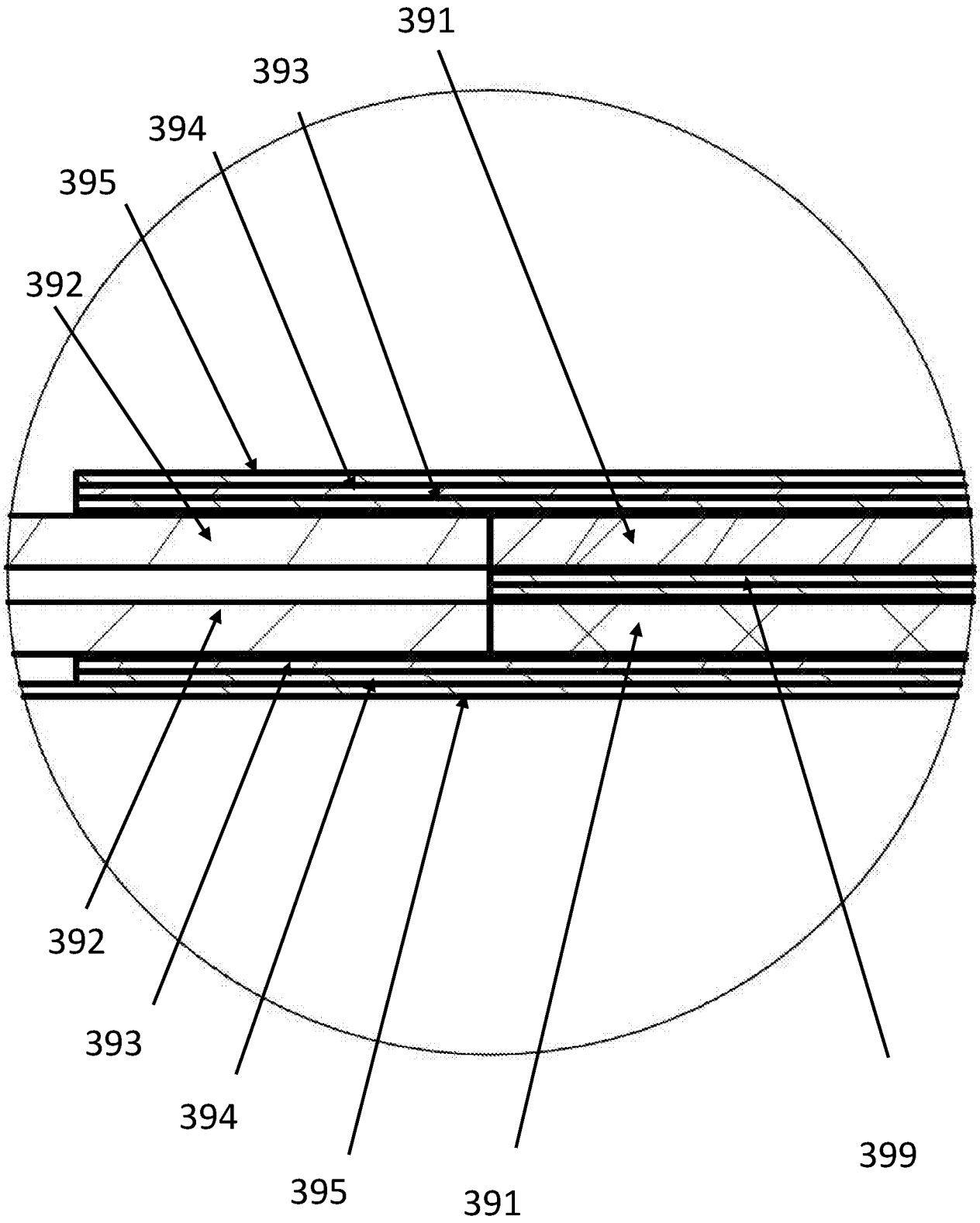


Figure 41E

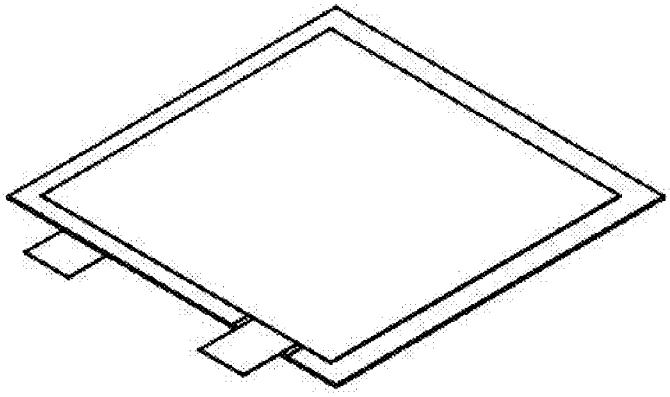


Figure 41F

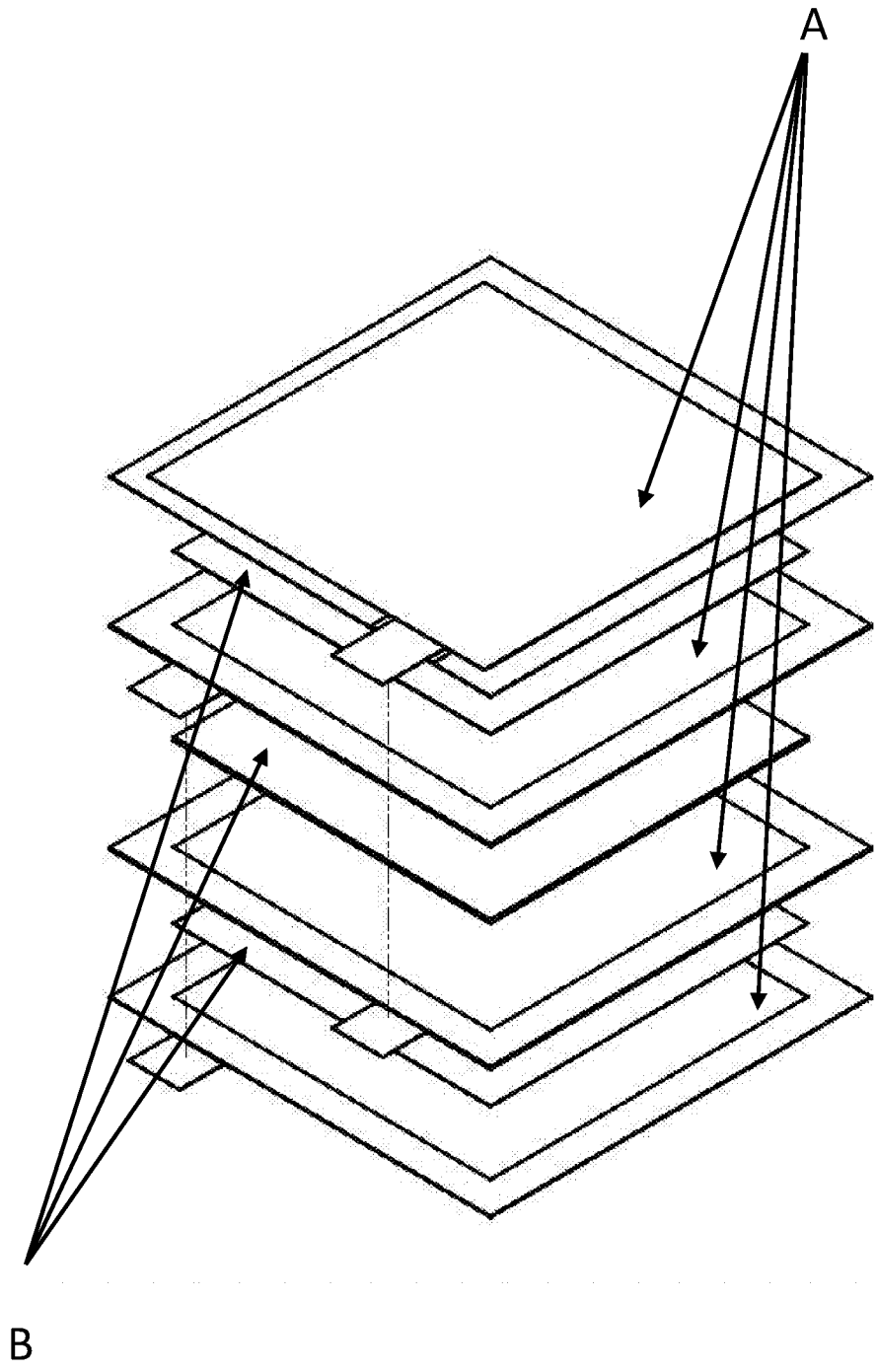


Figure 42

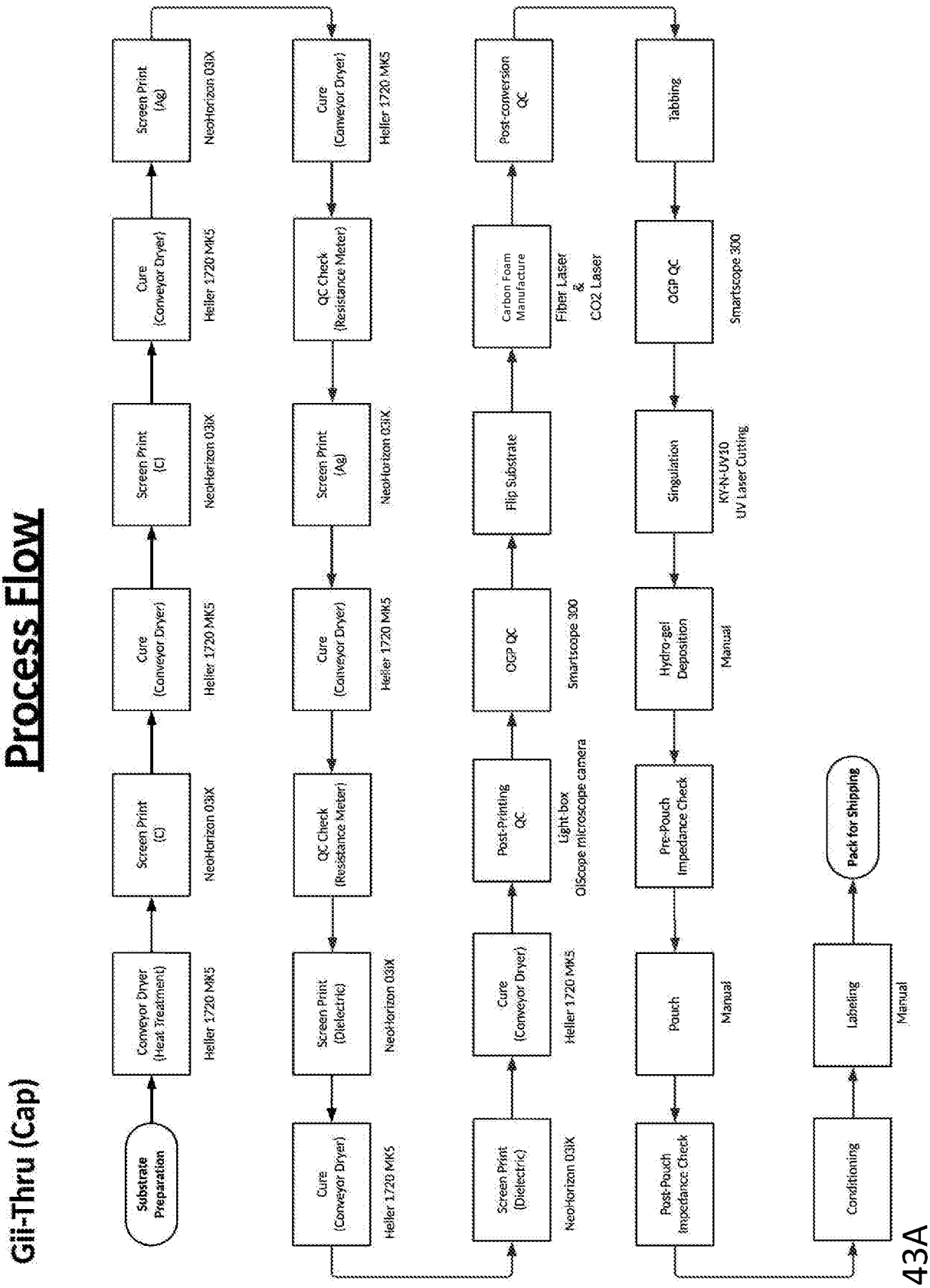

Process Flow
Gii-Thru (Cap)
Substrate Preparation
Conveyor Dryer (Heat Treatment)
Heller 1720 MK5
Screen Print (C)
NeoHorizon 03iX
Cure (Conveyor Dryer)
Heller 1720 MK5
Screen Print (C)
NeoHorizon 03iX
Cure (Conveyor Dryer)
Heller 1720 MK5
Screen Print (Ag)
NeoHorizon 03iX
Cure (Conveyor Dryer)
Heller 1720 MK5
QC Check (Resistance Meter)
Screen Print (Ag)
NeoHorizon 03iX
Cure (Conveyor Dryer)
Heller 1720 MK5
QC Check (Resistance Meter)
Screen Print (Dielectric)
NeoHorizon 03iX
Cure (Conveyor Dryer)
Heller 1720 MK5
Post-Printing QC
Light-box OiScope microscope camera
OGP QC
Smartscope 300
Flip Substrate
Carbon Foam Manufacture
Fiber Laser & CO2 Laser
Post-conversion QC
Screen Print (Dielectric)
NeoHorizon 03iX
Pre-Pouch Impedance Check
Hydro-gel Deposition
Manual
Singulation
KY-N-UV10 UV Laser Cutting
OGP QC
Smartscope 300
Tabbing
Post-Pouch Impedance Check
Pouch
Manual
Conditioning
Labeling
Manual
Pack for Shipping

Figure 43A

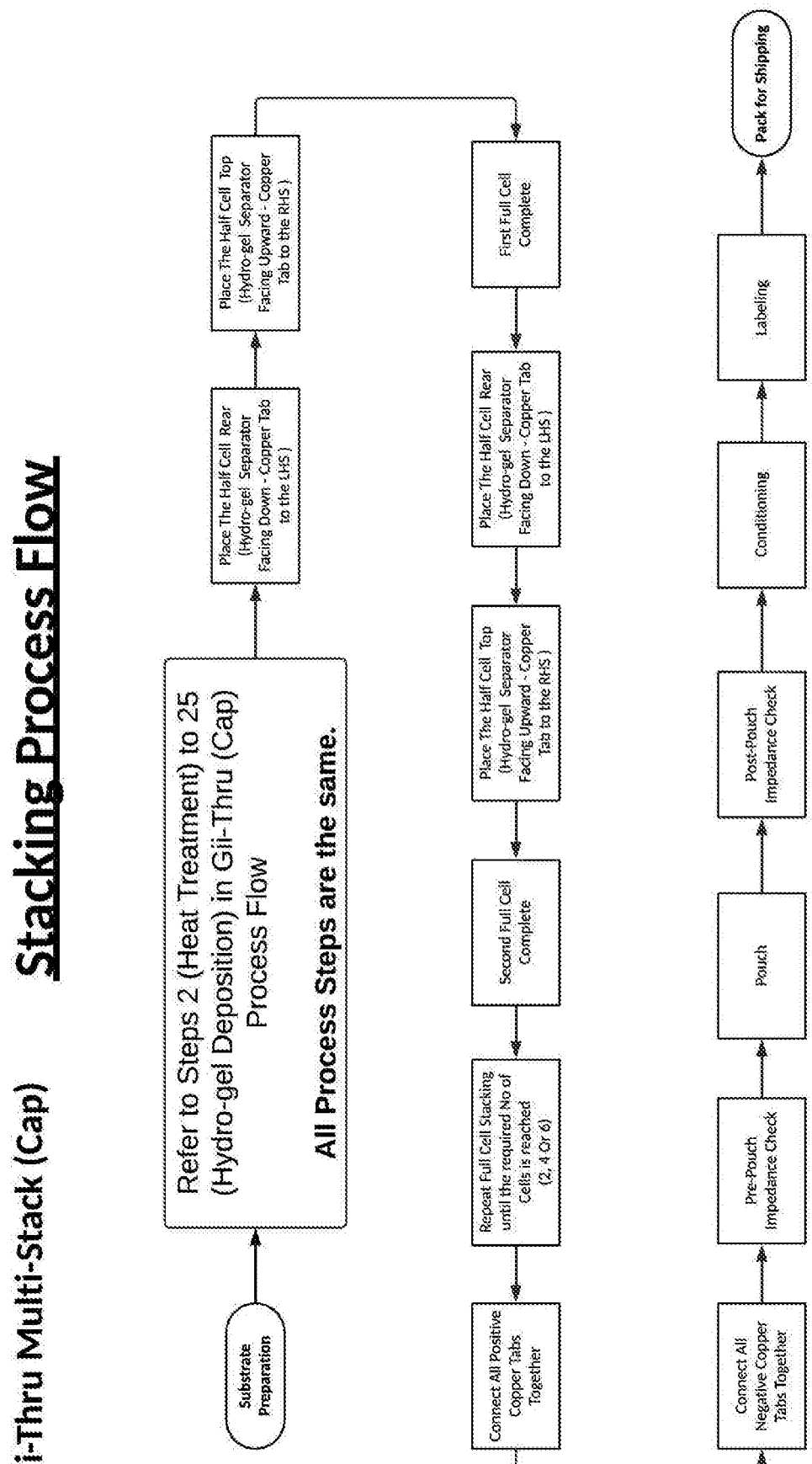

Gii-Thru Multi-Stack (Cap)
Stacking Process Flow
Substrate Preparation
Refer to Steps 2 (Heat Treatment) to 25 (Hydro-gel Deposition) in Gii-Thru (Cap) Process Flow
All Process Steps are the same.
Place The Half Cell Rear (Hydro-gel Separator Facing Down - Copper Tab to the LHS)
Place The Half Cell Top (Hydro-gel Separator Facing Upward - Copper Tab to the RHS)
First Full Cell Complete
Place The Half Cell Rear (Hydro-gel Separator Facing Down - Copper Tab to the LHS)
Place The Half Cell Top (Hydro-gel Separator Facing Upward - Copper Tab to the RHS)
Second Full Cell Complete
Repeat Full Cell Stacking until the required No of Cells is reached (2, 4 Or 6)
Connect All Positive Copper Tabs Together
Connect All Negative Copper Tabs Together
Pre-Pouch Impedance Check
Pouch
Post-Pouch Impedance Check
Conditioning
Labeling
Pack for Shipping

Figure 43B

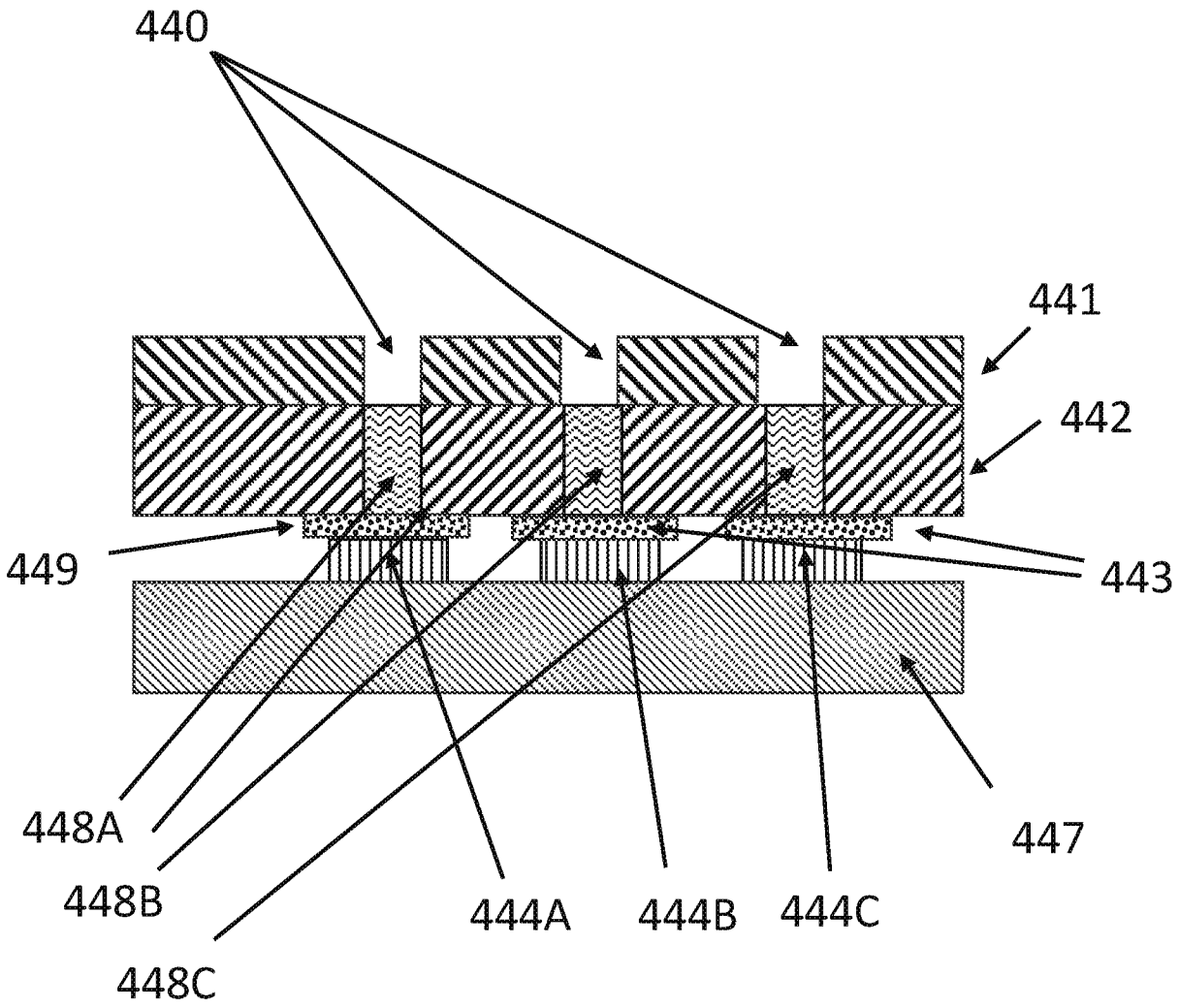


Figure 44A

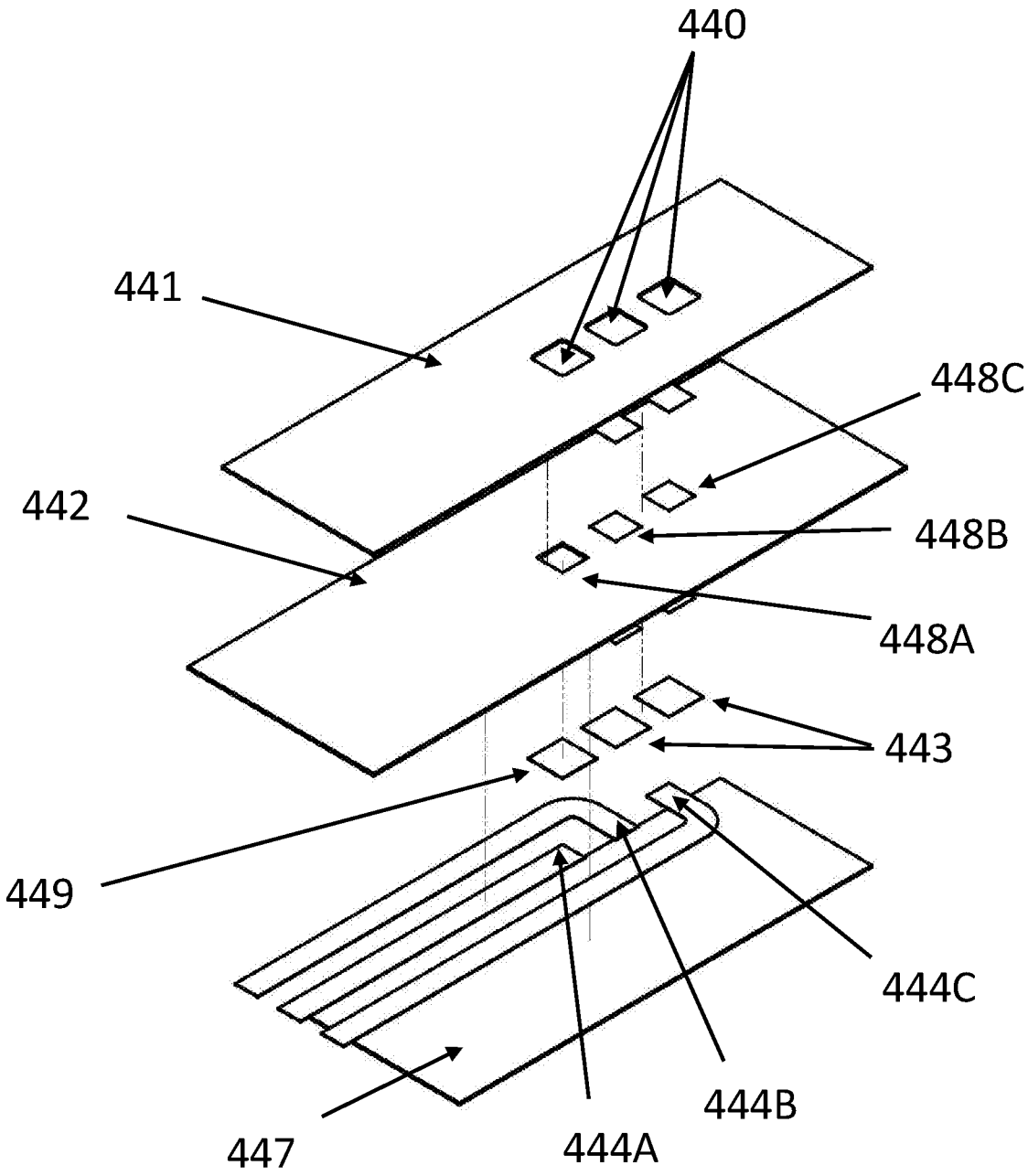


Figure 44B

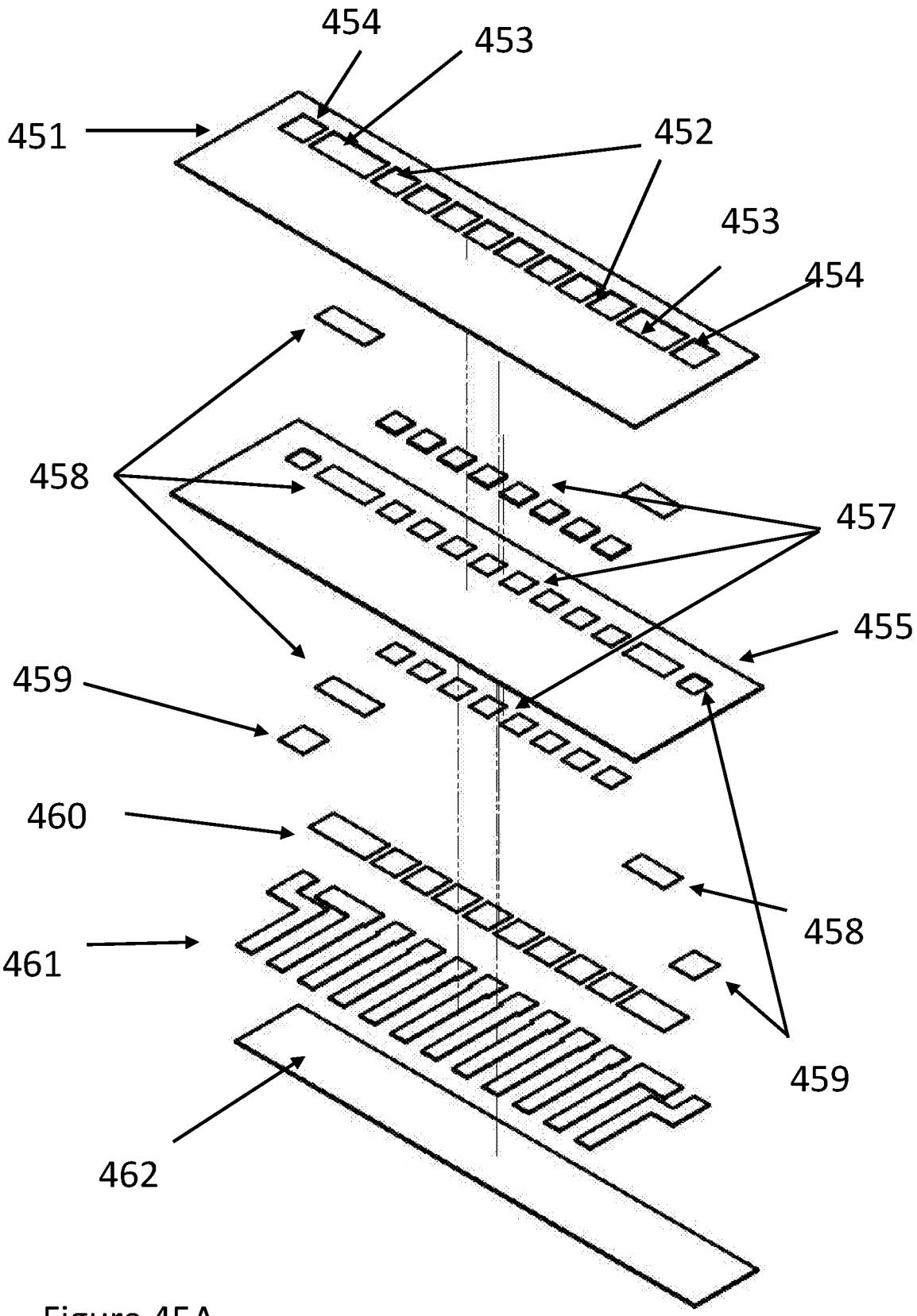


Figure 45A

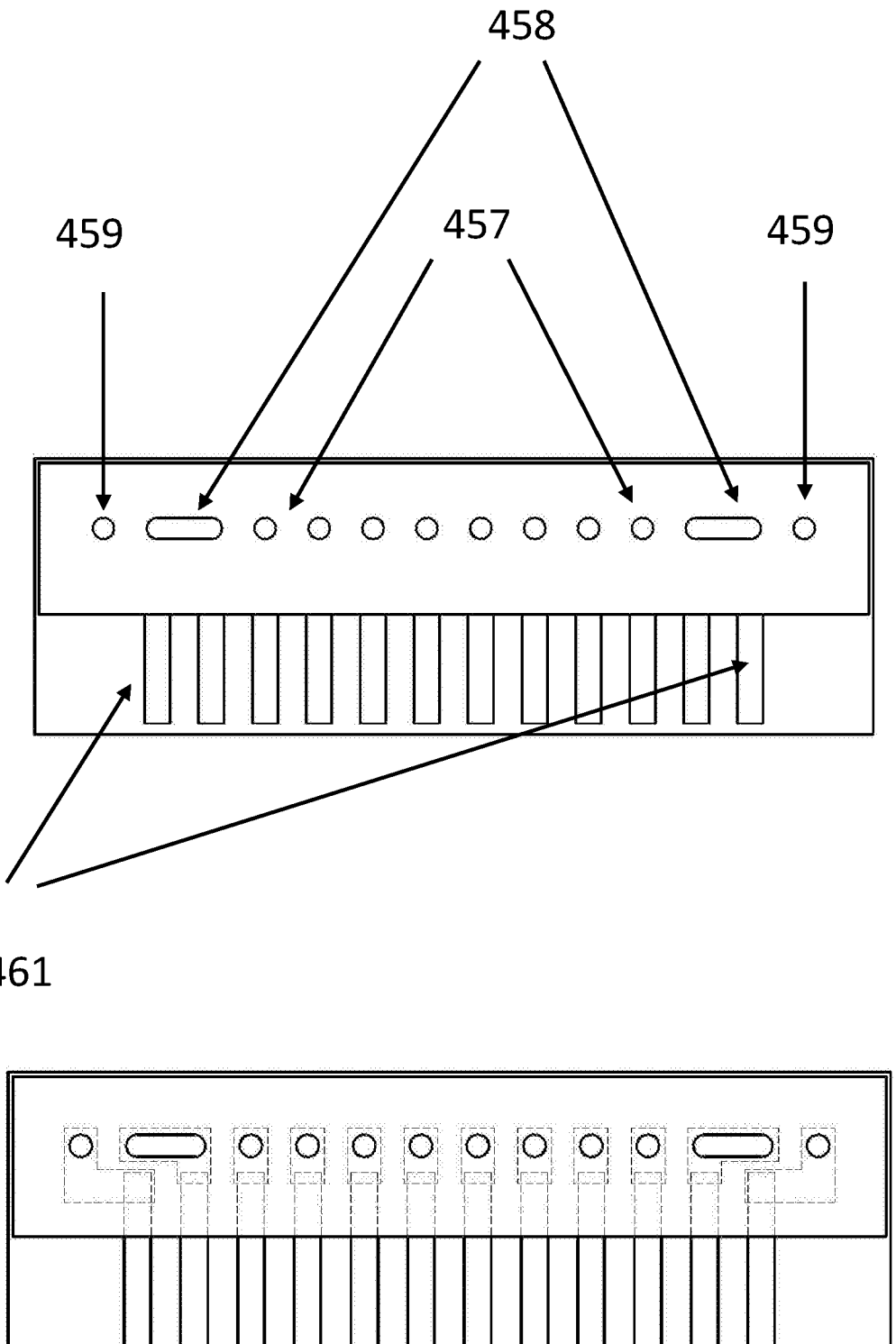


Figure 45B

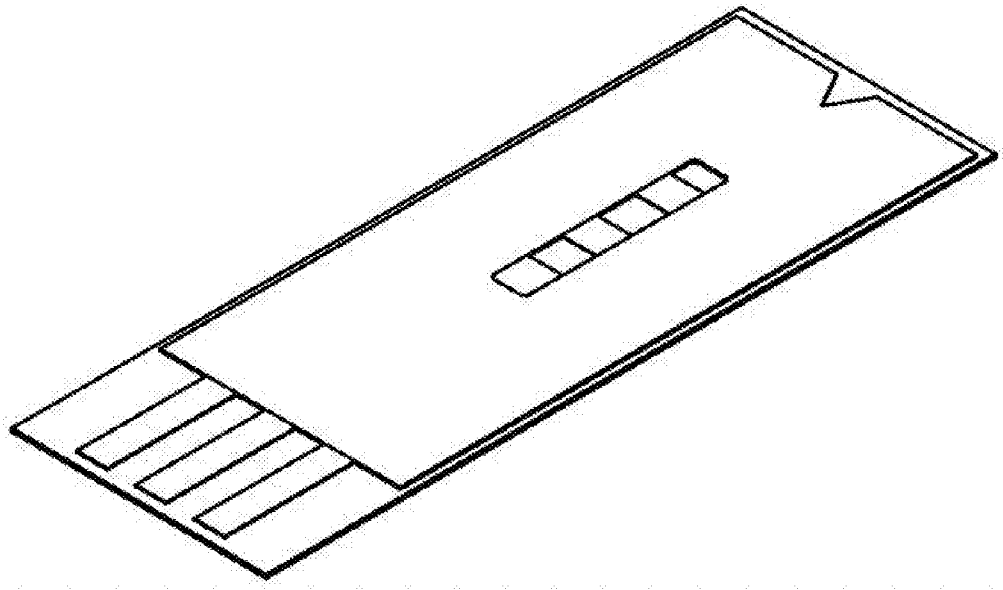


Figure 46A

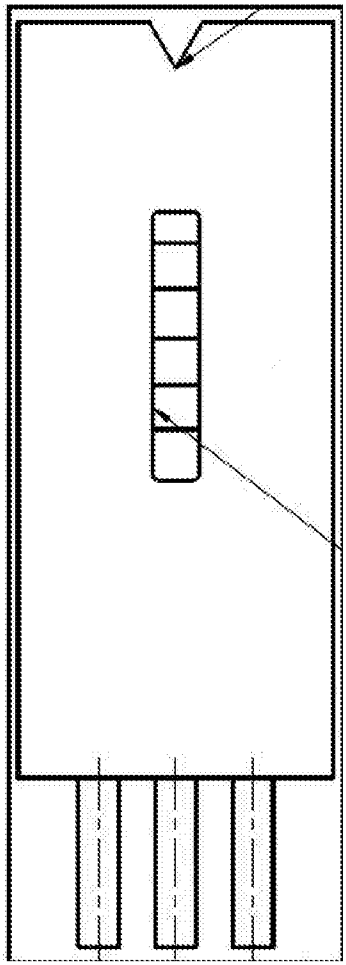


Figure 46B

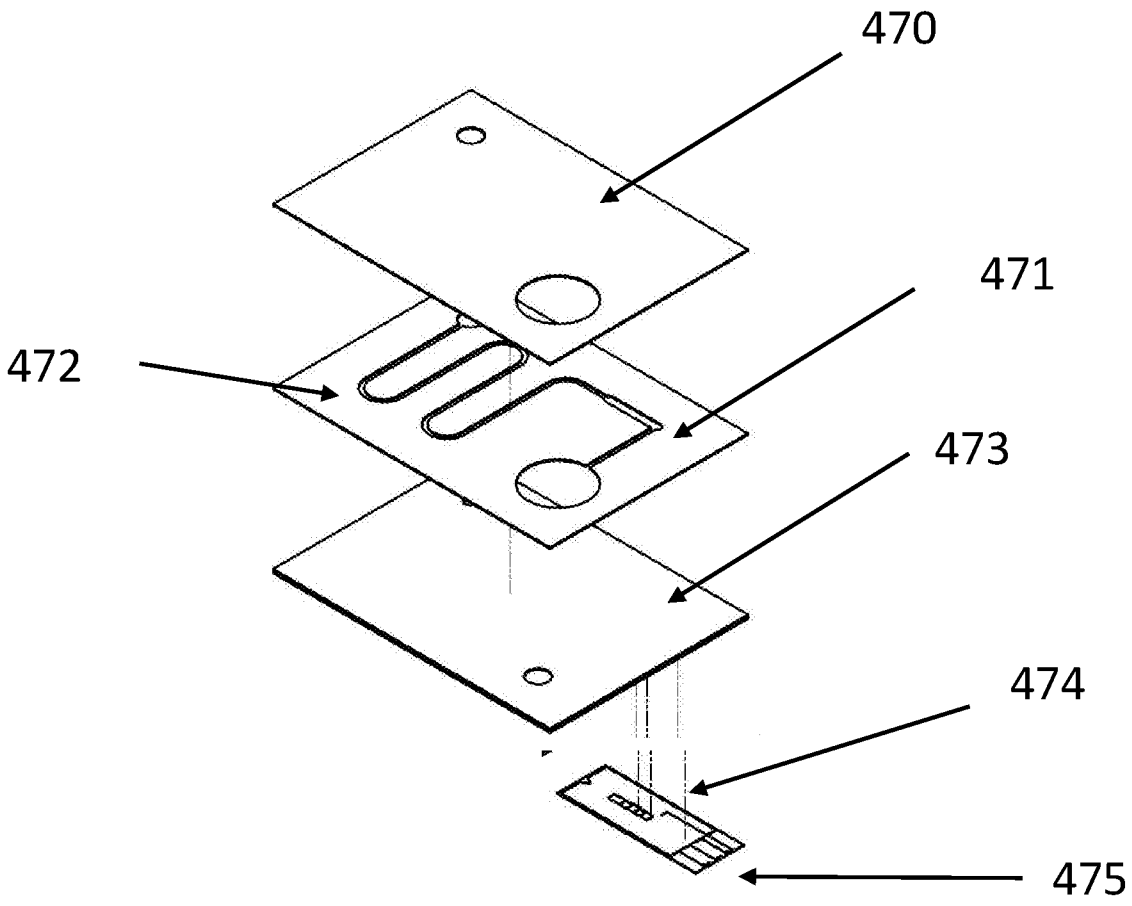


Figure 47A

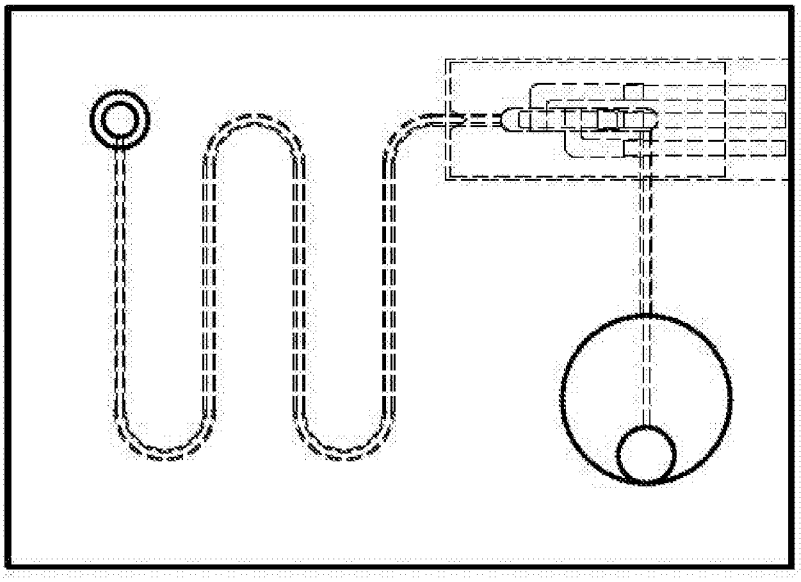


Figure 47B

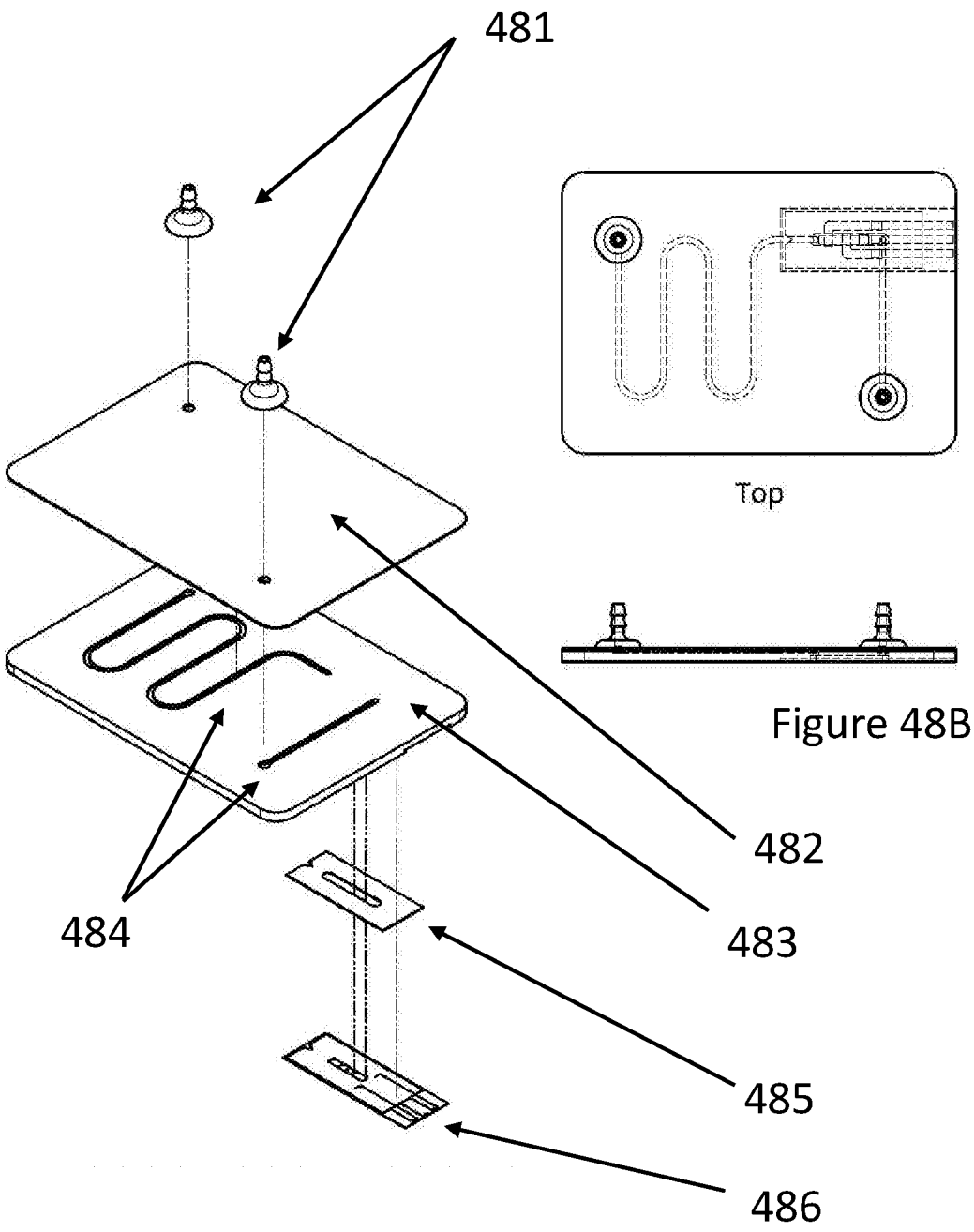


Figure 48A

Figure 48B

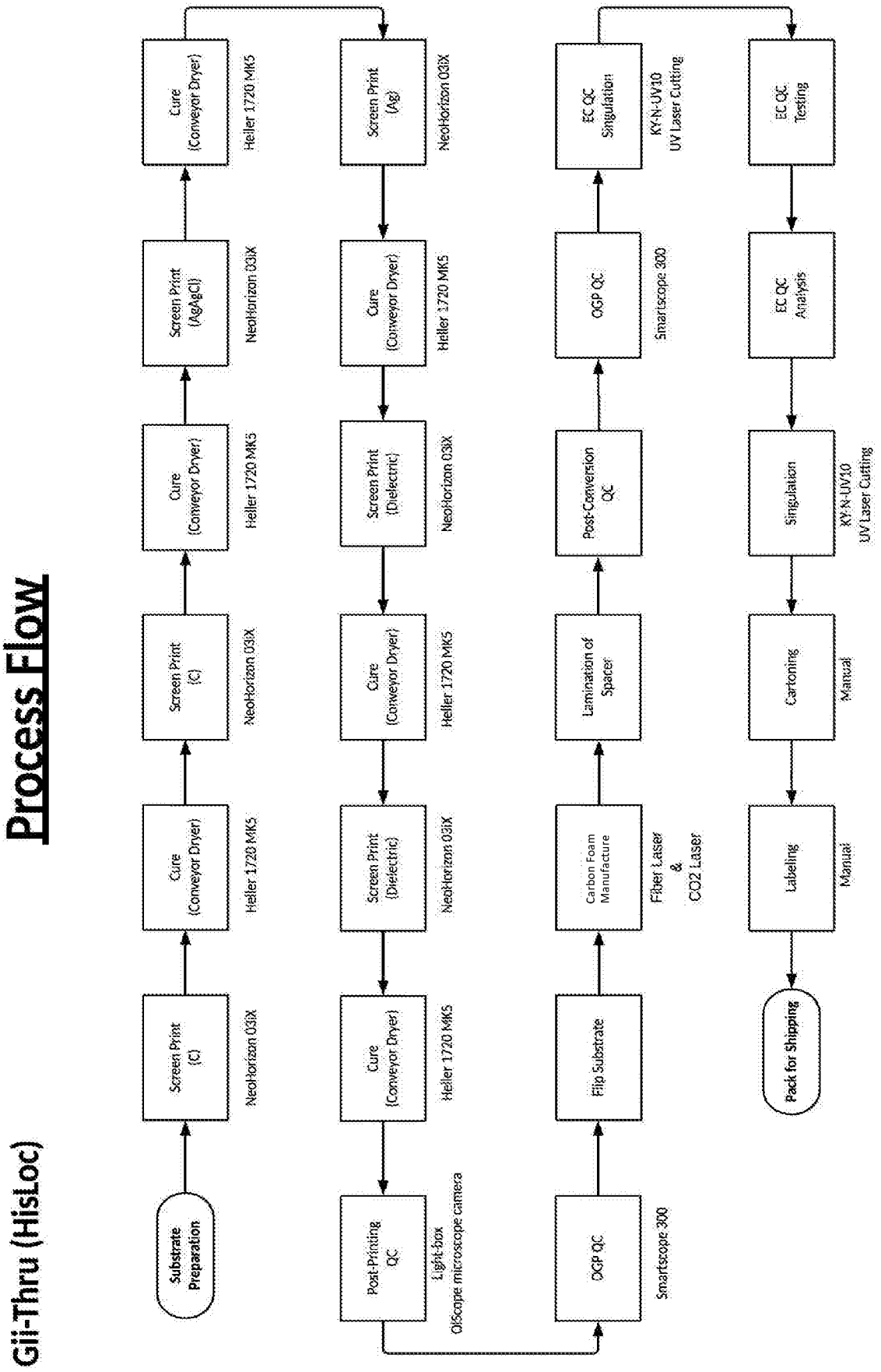

Gii-Thru (HisLoc)
Process Flow
Substrate Preparation
Screen Print (C)
NeoHorizon 03iX
Cure (Conveyor Dryer)
Heller 1720 MK5
Screen Print (C)
NeoHorizon 03iX
Cure (Conveyor Dryer)
Heller 1720 MK5
Screen Print (Ag/AgCl)
NeoHorizon 03iX
Cure (Conveyor Dryer)
Heller 1720 MK5
Post-Printing QC
Light-box
Olscope microscope camera
Cure (Conveyor Dryer)
Heller 1720 MK5
Screen Print (Dielectric)
NeoHorizon 03iX
Cure (Conveyor Dryer)
Heller 1720 MK5
Screen Print (Dielectric)
NeoHorizon 03iX
Cure (Conveyor Dryer)
Heller 1720 MK5
Screen Print (Ag)
NeoHorizon 03iX
Cure (Conveyor Dryer)
Heller 1720 MK5
OGP QC
Smartscope 300
Flip Substrate
Carbon Foam Manufacture
Fiber Laser & CO2 Laser
Lamination of Spacer
Post-Conversion QC
OGP QC
Smartscope 300
EC QC Singulation
KY-N-UV10 UV Laser Cutting
Pack for Shipping
Labeling
Manual
Cartoning
Manual
Singulation
KY-N-UV10 UV Laser Cutting
EC QC Analysis
EC QC Testing

Figure 49

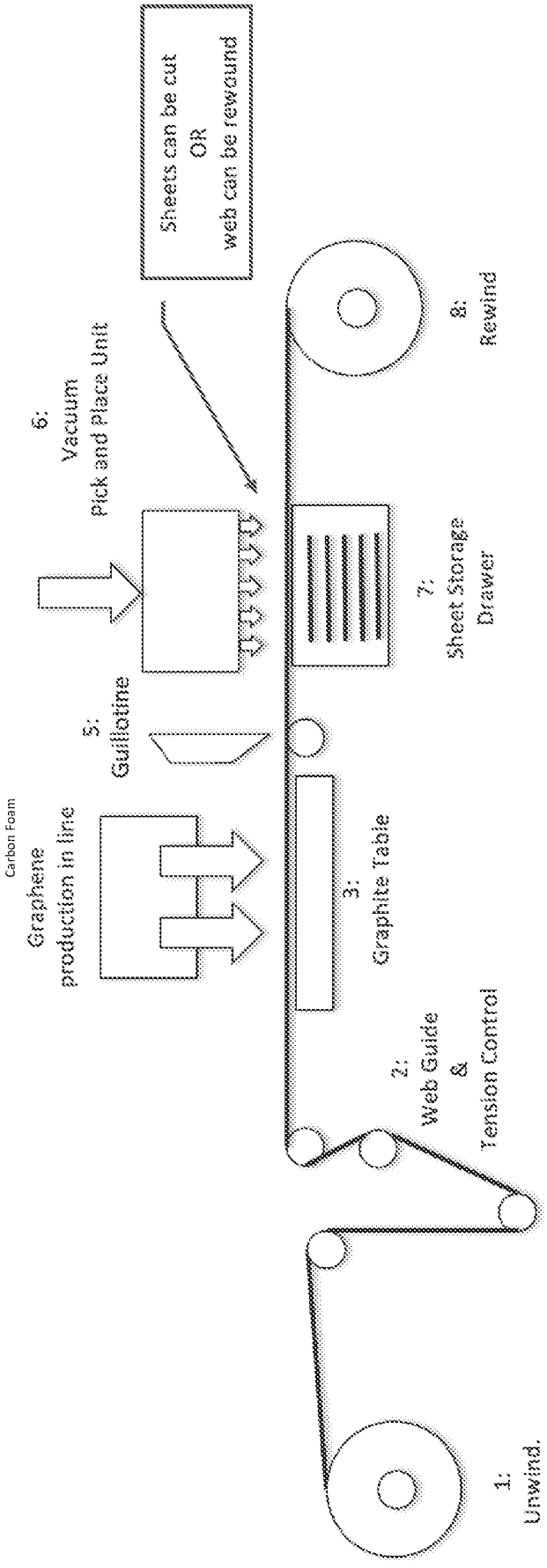

Sheets can be cut
OR
web can be rewound
6:
Vacuum
Pick and Place Unit
5:
Guillotine
Carbon Foam
Graphene
production in line
3:
Graphite Table
2:
Web Guide
&
Tension Control
1:
Unwind
Web
7:
Sheet Storage
Drawer
8:
Rewind

Figure 50

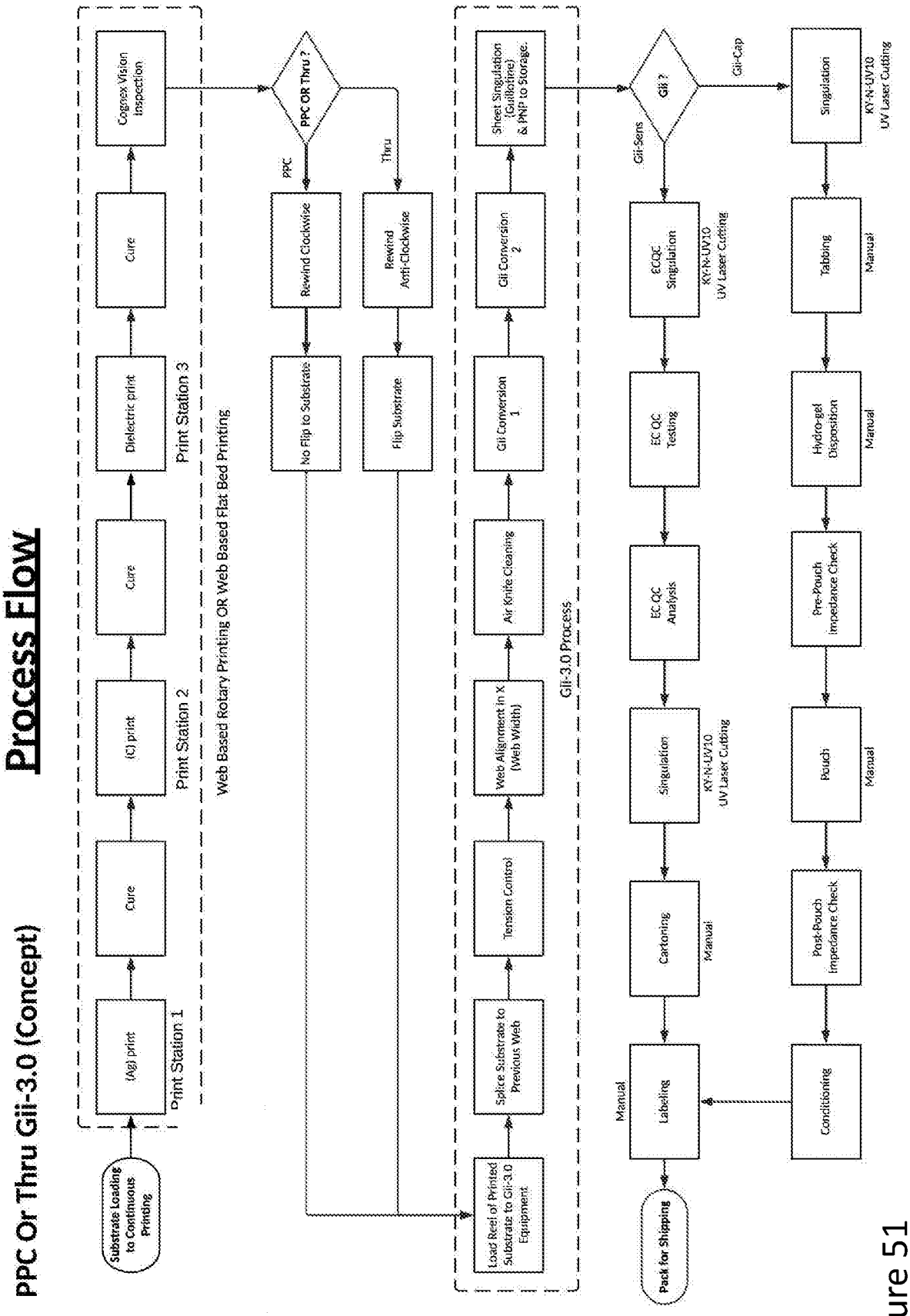
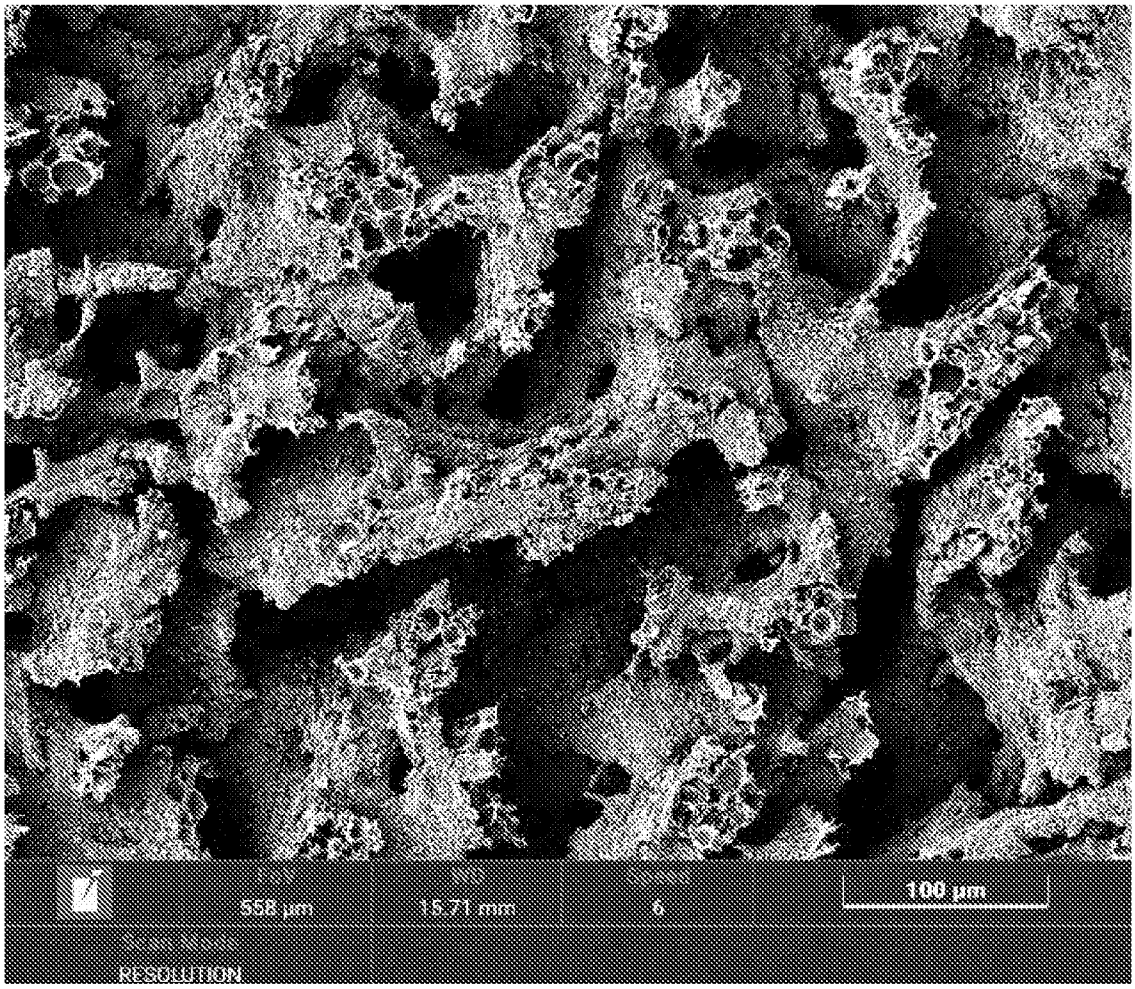
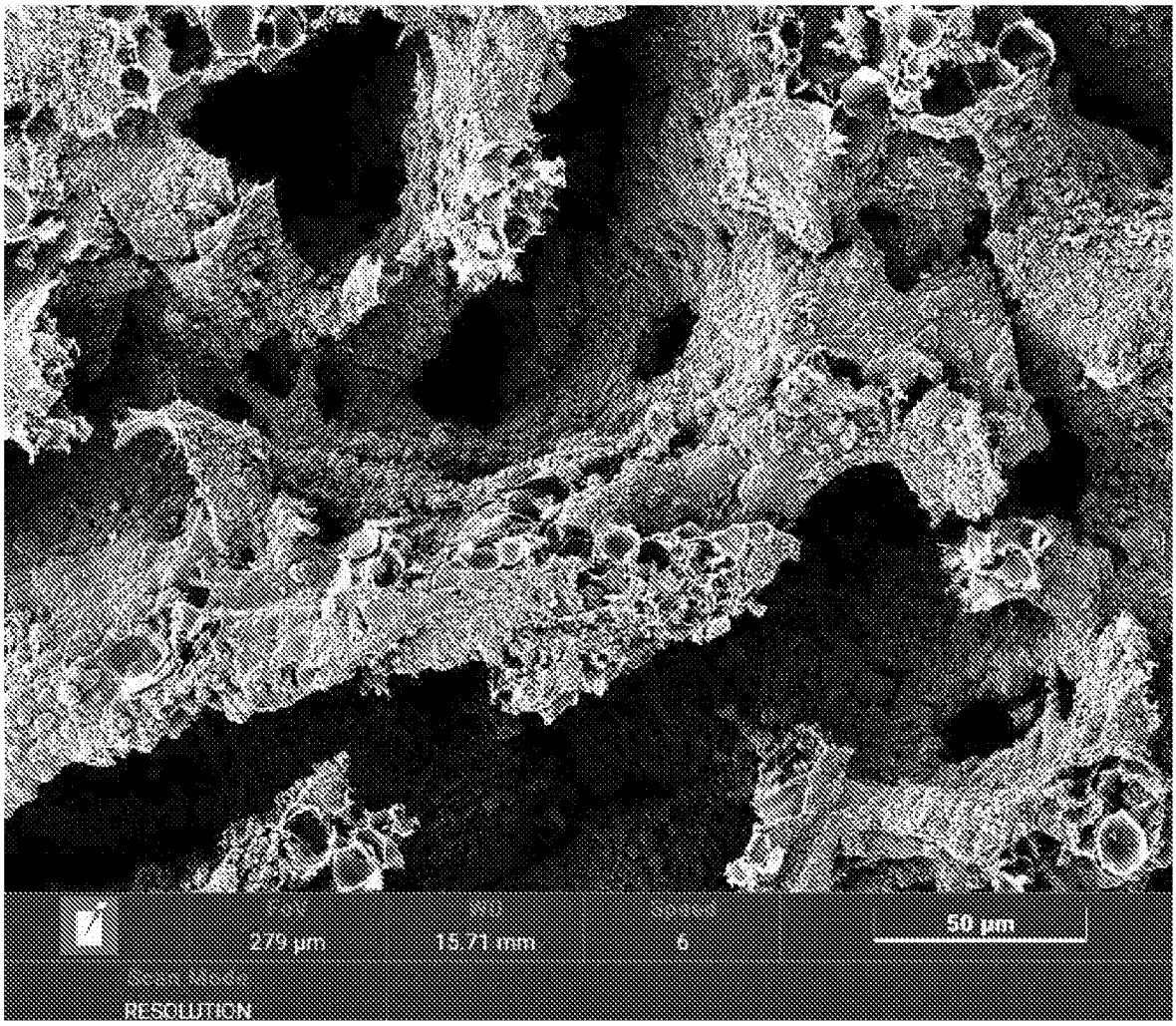

PPC Or Thru Gii-3.0 (Concept)
Process Flow
Substrate Loading to Continuous Printing
(Ag) print
Cure
(C) print
Cure
Dielectric print
Cure
Cognex Vision Inspection
Print Station 1
Print Station 2
Print Station 3
Web Based Rotary Printing OR Web Based Flat Bed Printing
PPC OR Thru ?
PPC
Thru
Rewind Clockwise
Rewind Anti-Clockwise
No Flip to Substrate
Flip Substrate
Load Reel of Printed Substrate to Gii-3.0 Equipment
Splice Substrate to Previous Web
Tension Control
Web Alignment in X (Web Width)
Air Knife Cleaning
Gii Conversion 1
Gii Conversion 2
Sheet Singulation (Guillotine) & PNP to Storage.
Gii-3.0 Process
Gii ?
Gii-Sens
Gii-Cap
ECQC Singulation
KY-N-UV10 UV Laser Cutting
EC QC Testing
EC QC Analysis
Singulation
KY-N-UV10 UV Laser Cutting
Cartoning
Manual
Labeling
Manual
Pack for Shipping
Conditioning
Post-Pouch Impedance Check
Pouch
Manual
Pre-Pouch Impedance Check
Hydro-gel Disposition
Manual
Tabbing
Manual
Singulation
KY-N-UV10 UV Laser Cutting

Figure 51



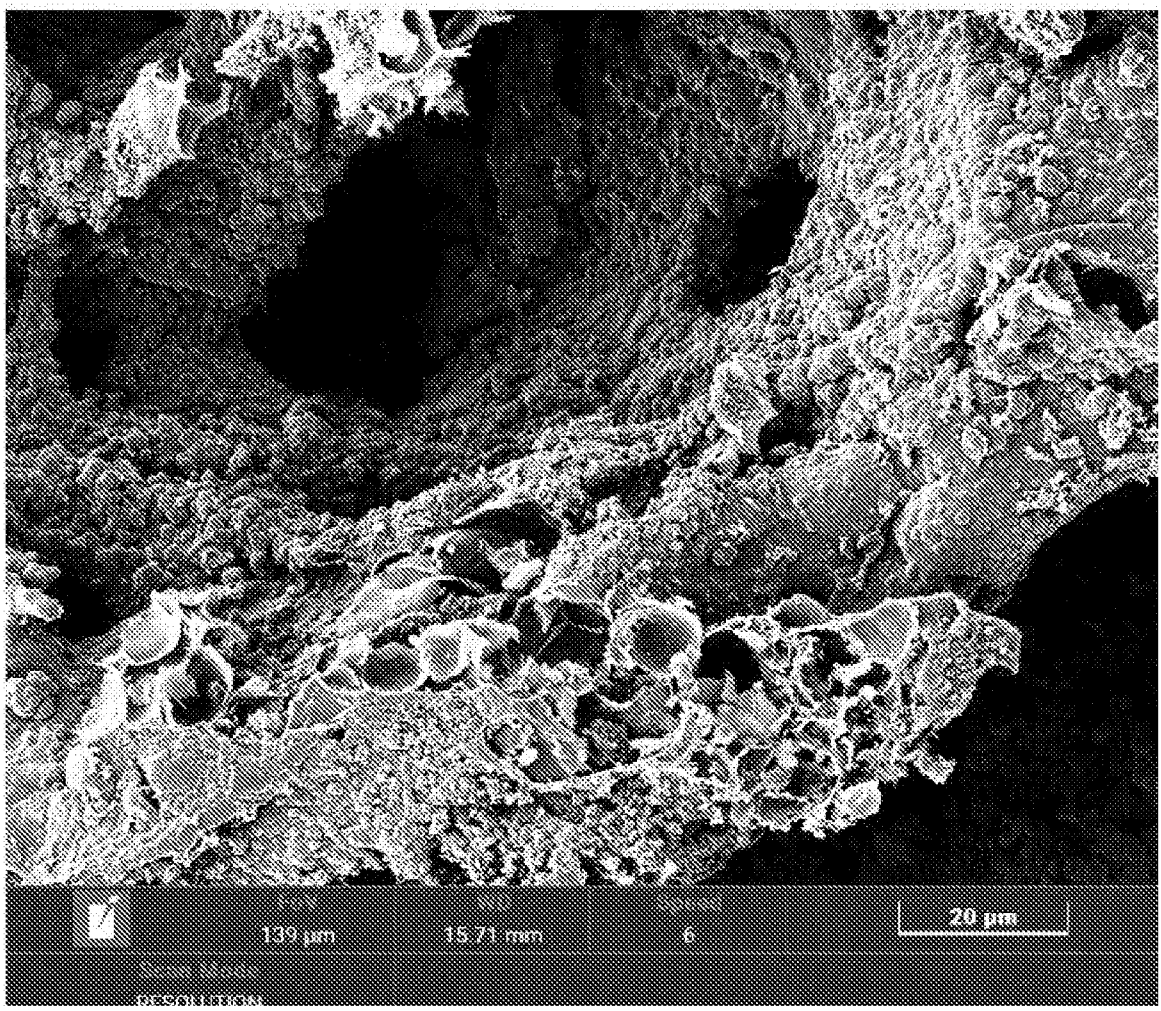
100 µm

Figure 52



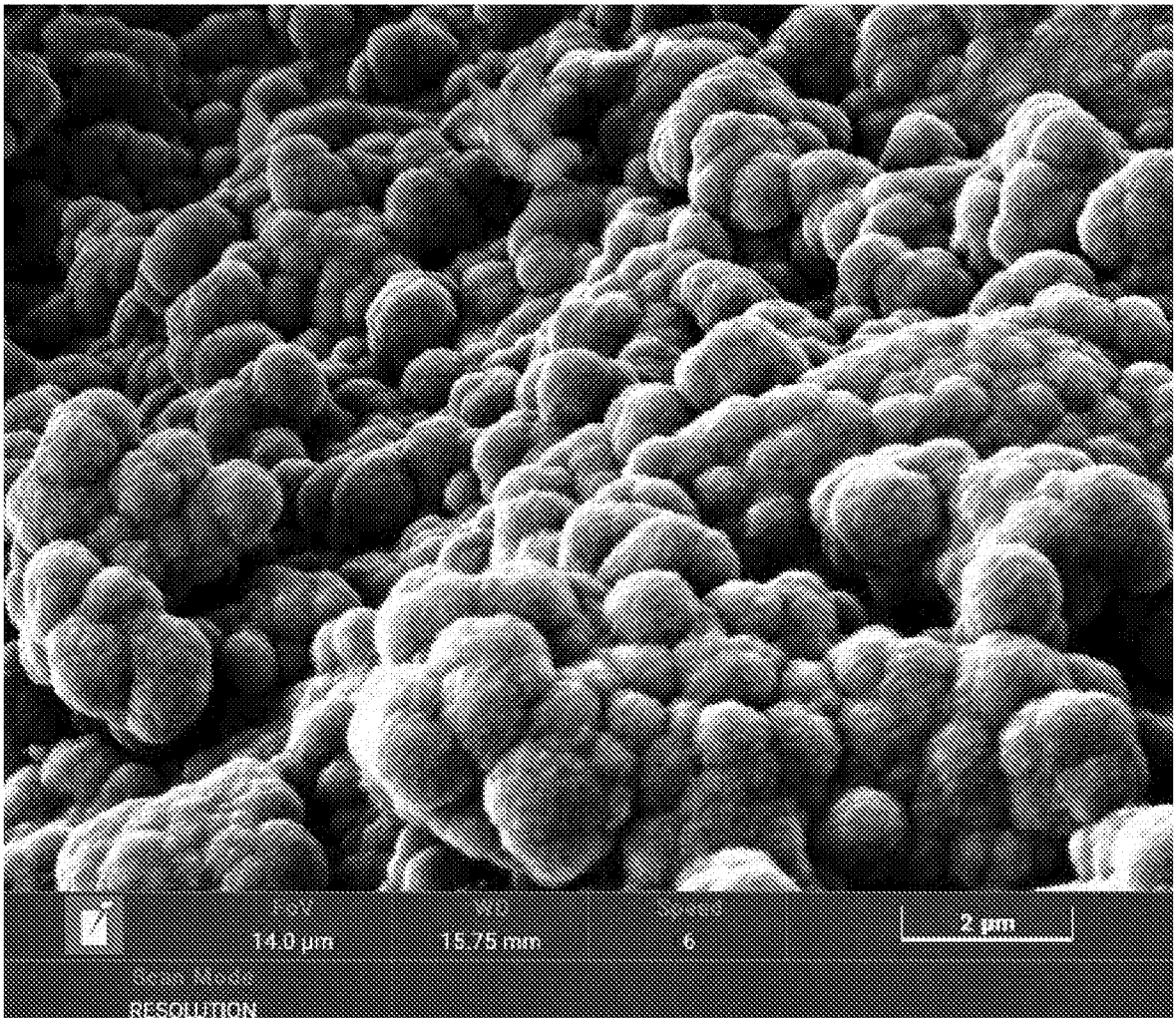
50 µm

Figure 53



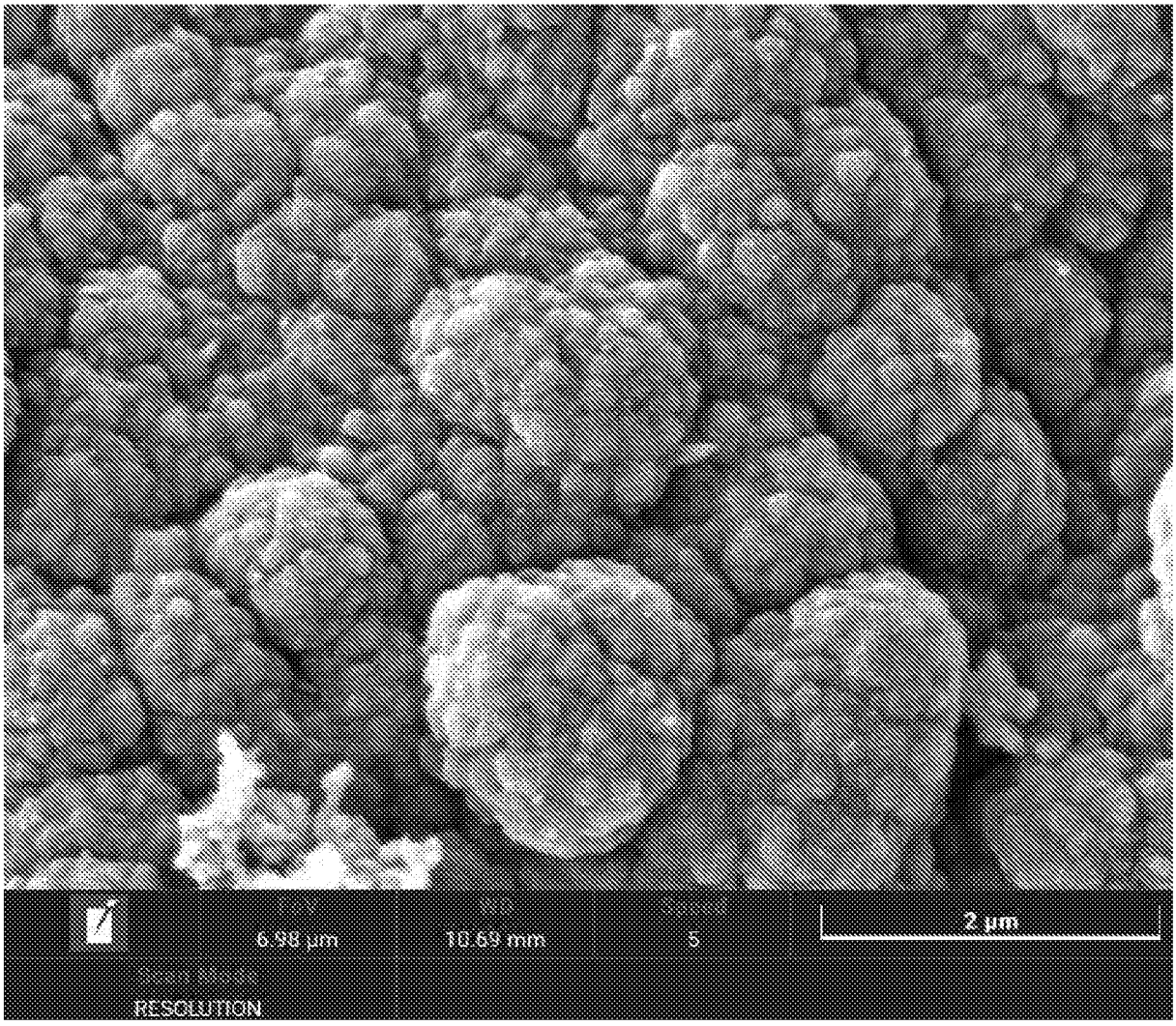
20 µm

Figure 54



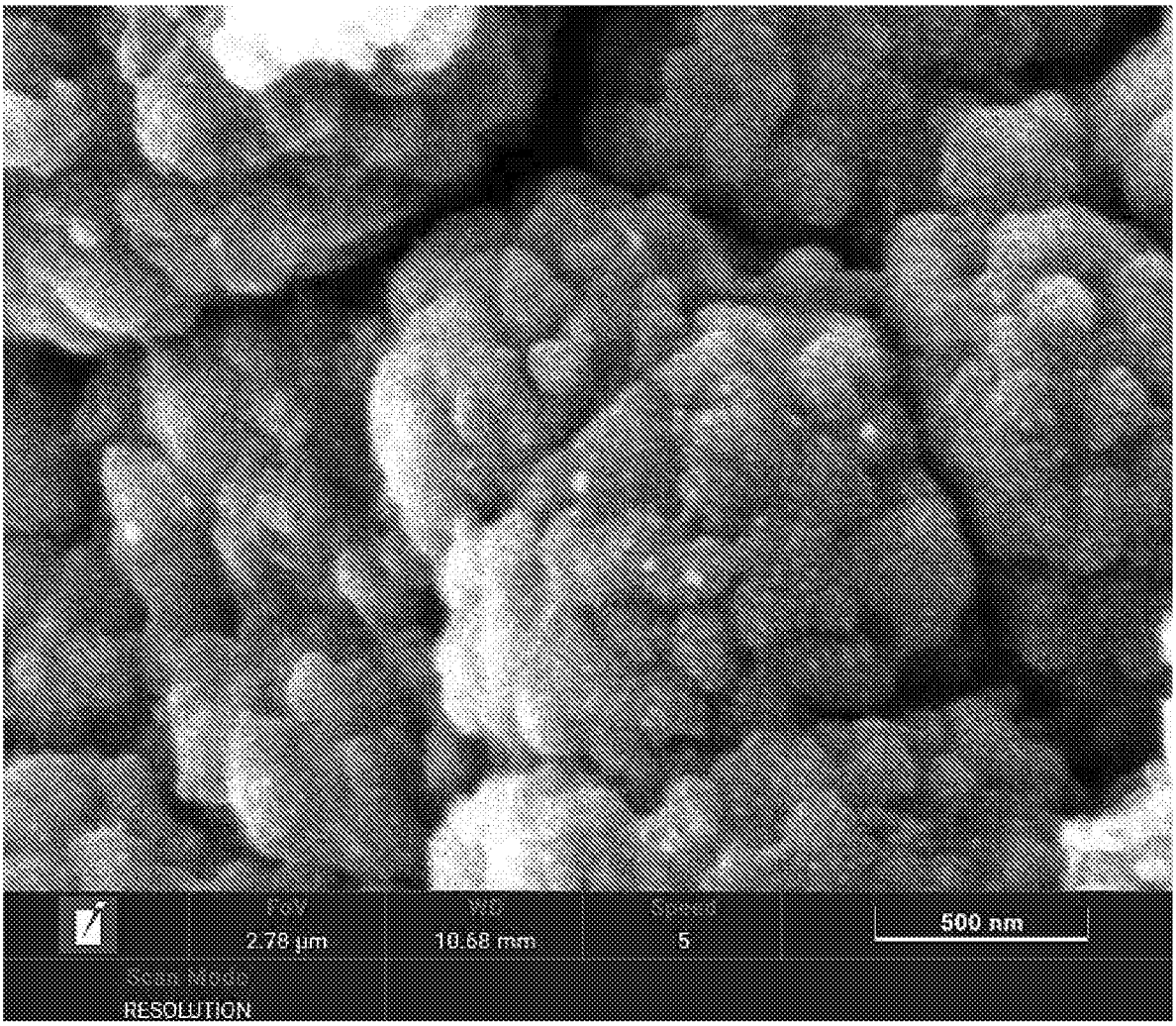
2 µm

Figure 55



2 µm

Figure 56



500nm

Figure 57

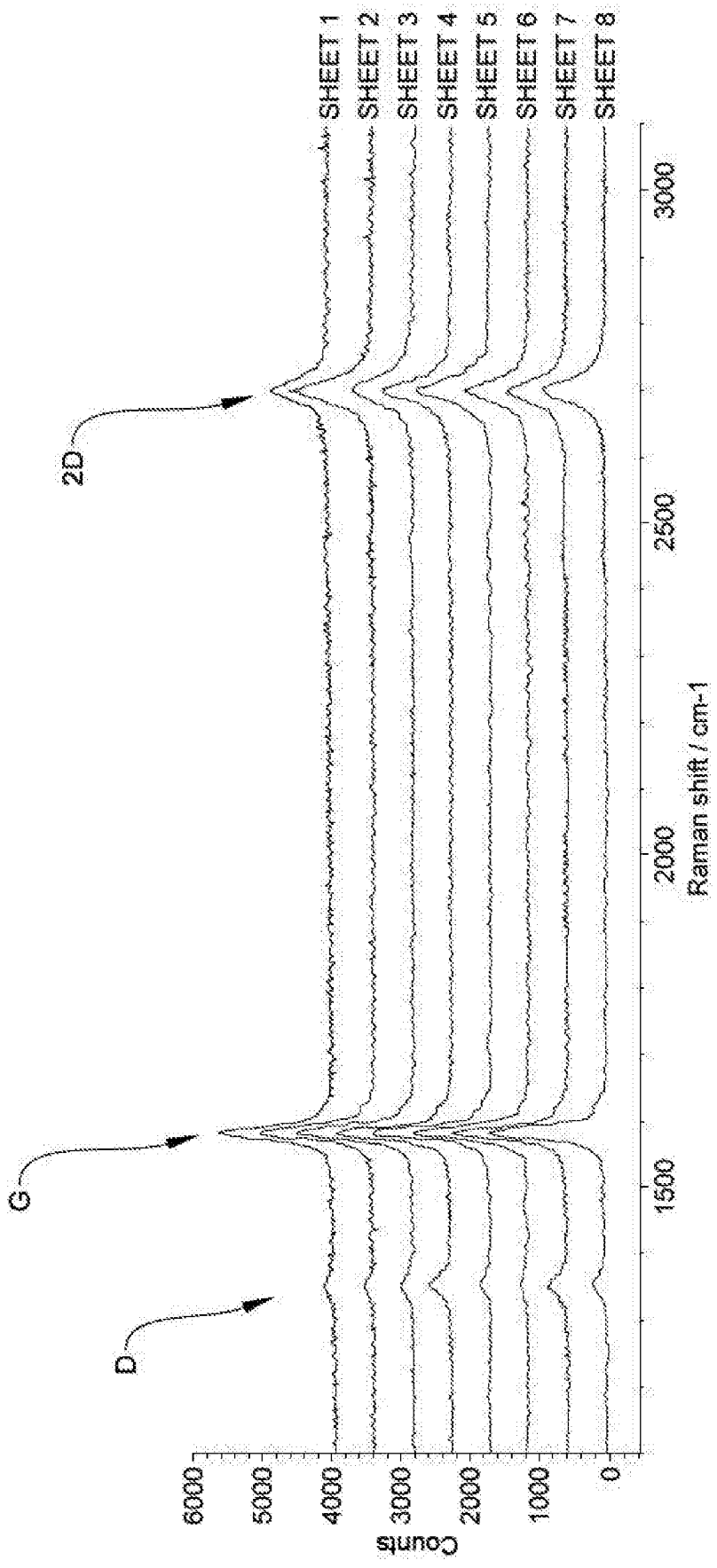

SHEET 1
SHEET 2
SHEET 3
SHEET 4
SHEET 5
SHEET 6
SHEET 7
SHEET 8
2D
G
D
Counts
6000
5000
4000
3000
2000
1000
0
1500
2000
2500
3000
Raman shift / cm-1

Figure 58

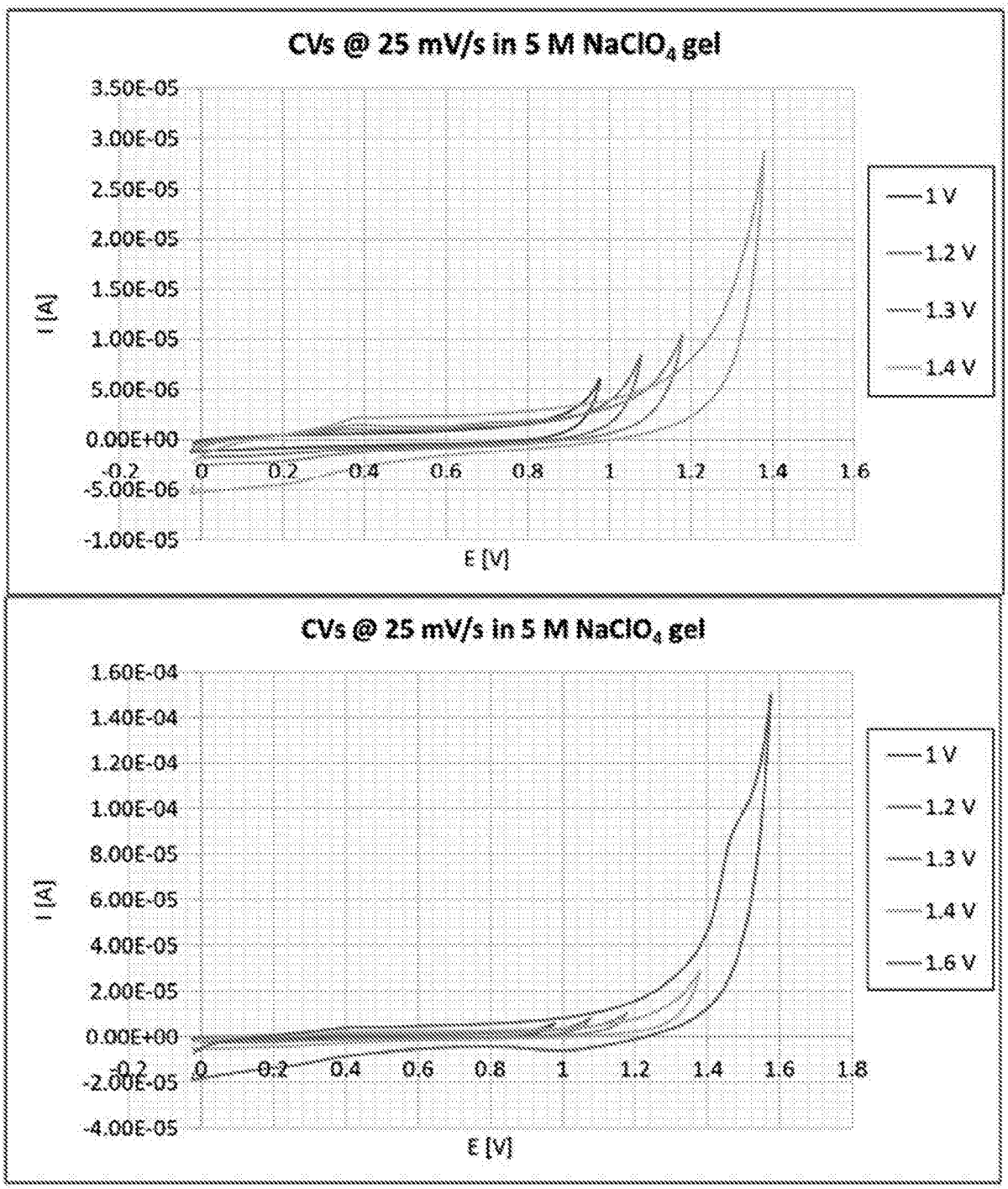

CVs @ 25 mV/s in 5 M NaClO4 gel
I [A]
E [V]
3.50E-05
3.00E-05
2.50E-05
2.00E-05
1.50E-05
1.00E-05
5.00E-06
0.00E+00
-5.00E-06
-1.00E-05
-0.2
0
0.2
0.4
0.6
0.8
1
1.2
1.4
1.6
1 V
1.2 V
1.3 V
1.4 V
CVs @ 25 mV/s in 5 M NaClO4 gel
I [A]
E [V]
1.60E-04
1.40E-04
1.20E-04
1.00E-04
8.00E-05
6.00E-05
4.00E-05
2.00E-05
0.00E+00
-2.00E-05
-4.00E-05
-0.2
0
0.2
0.4
0.6
0.8
1
1.2
1.4
1.6
1.8
1 V
1.2 V
1.3 V
1.4 V
1.6 V

Figure 59

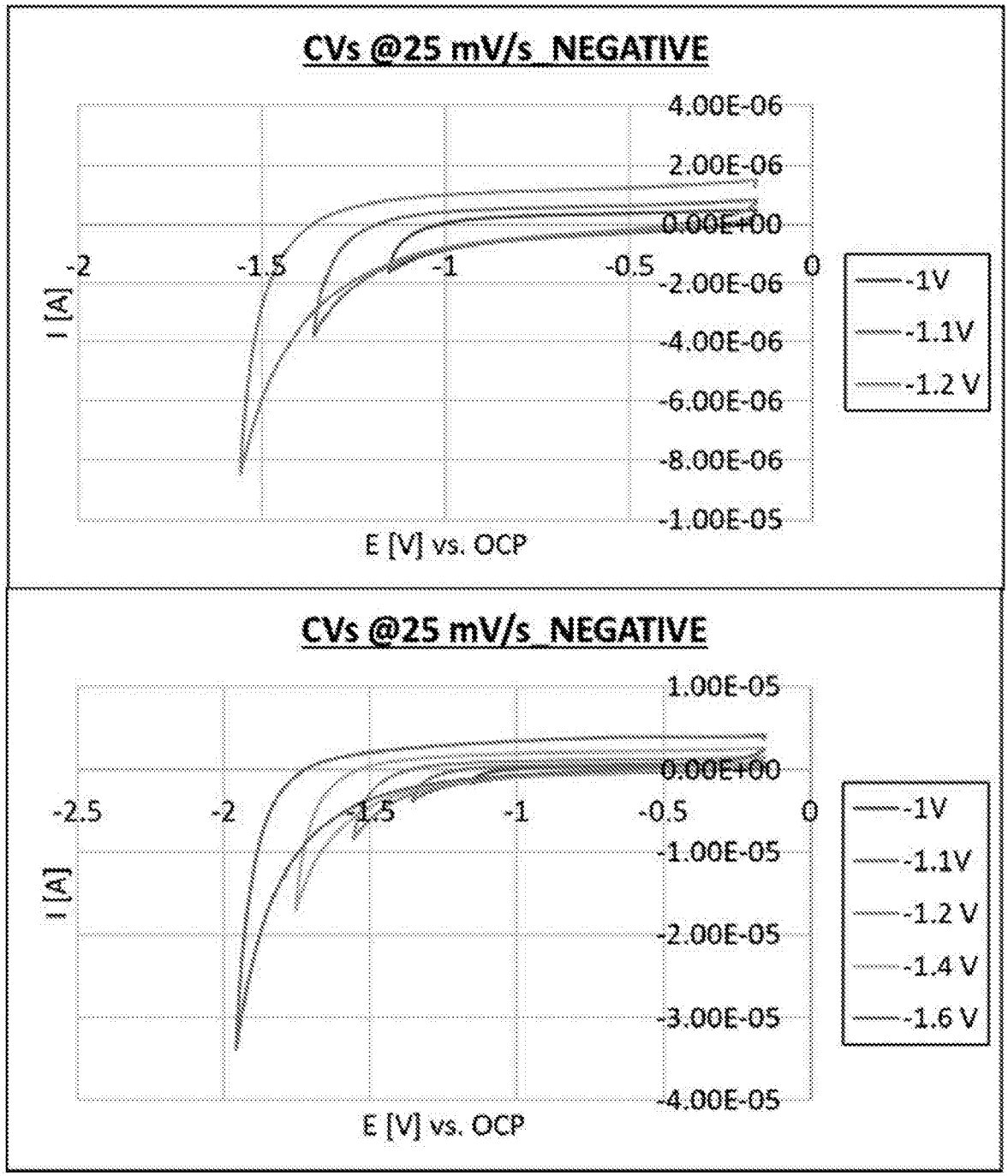

CVs @25 mV/s_NEGATIVE
4.00E-06
2.00E-06
0.00E+00
-2.00E-06
-4.00E-06
-6.00E-06
-8.00E-06
-1.00E-05
-2
-1.5
-1
-0.5
0
I [A]
E [V] vs. OCP
-1V
-1.1V
-1.2 V
CVs @25 mV/s_NEGATIVE
1.00E-05
0.00E+00
-1.00E-05
-2.00E-05
-3.00E-05
-4.00E-05
-2.5
-2
-1.5
-1
-0.5
0
I [A]
E [V] vs. OCP
-1V
-1.1V
-1.2 V
-1.4 V
-1.6 V

Figure 60

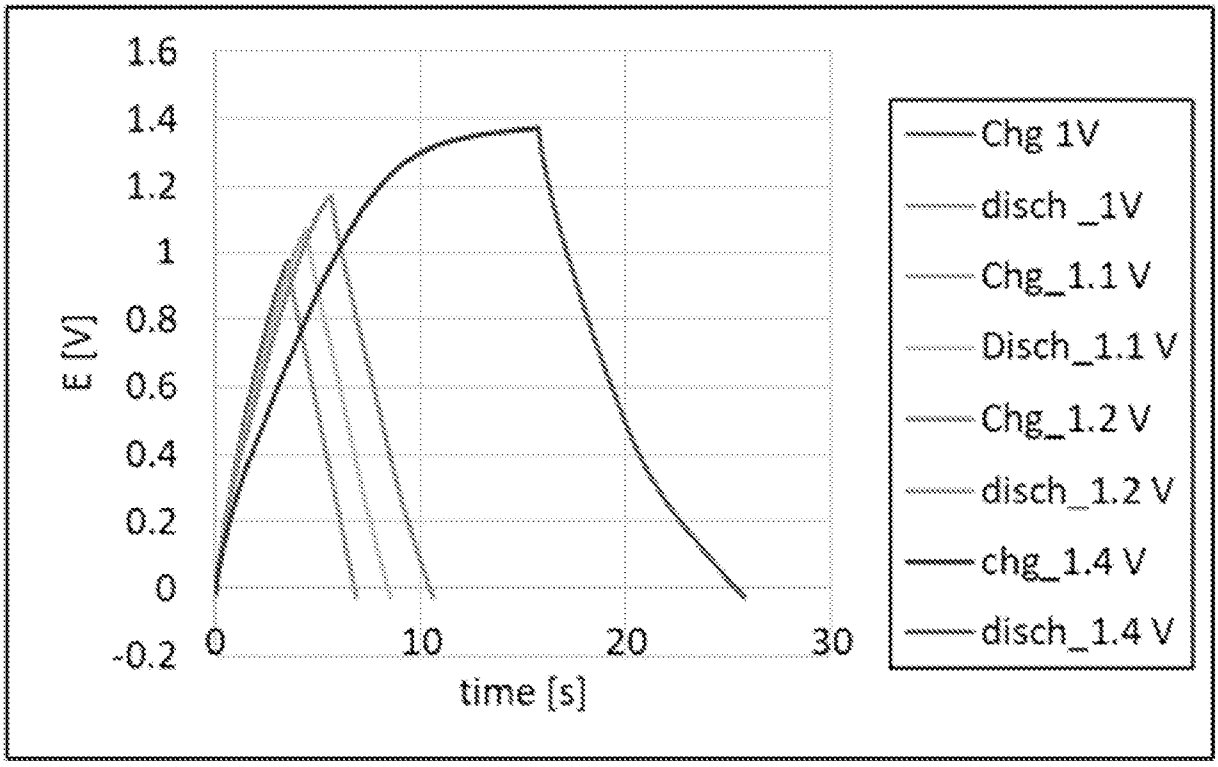


Figure 61

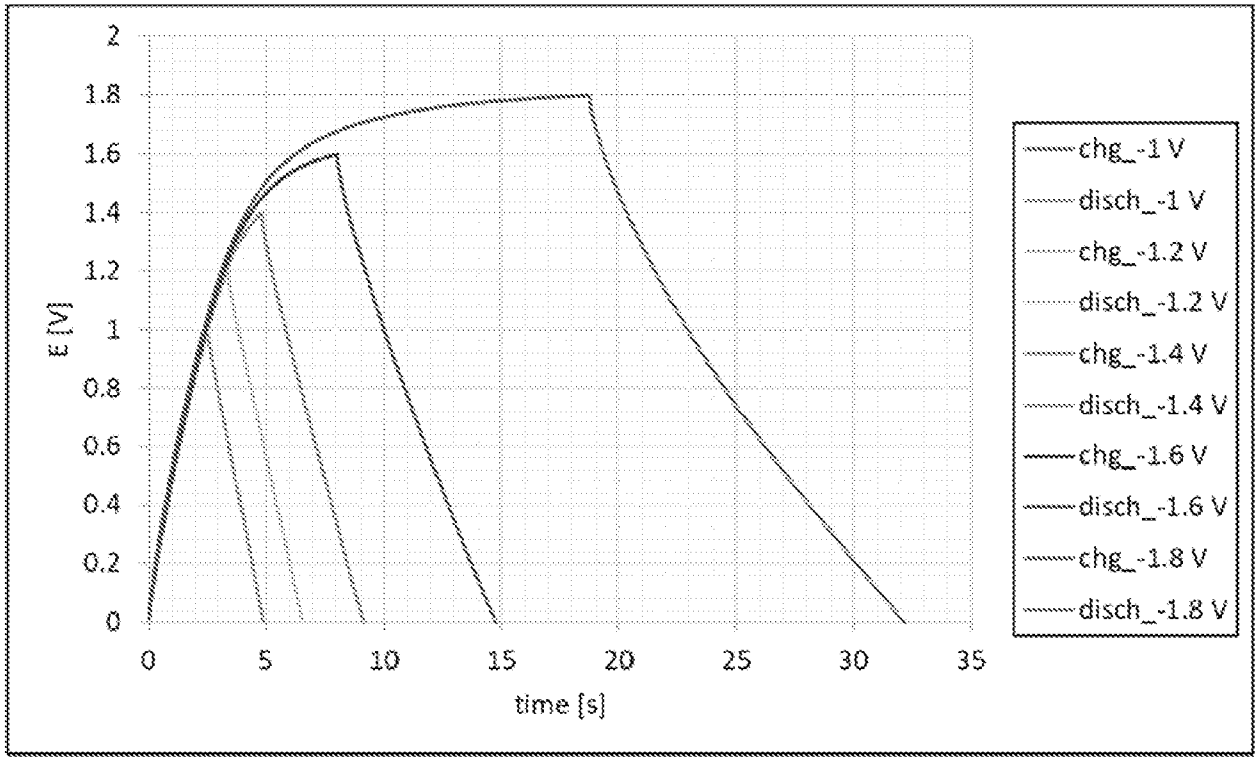


Figure 62

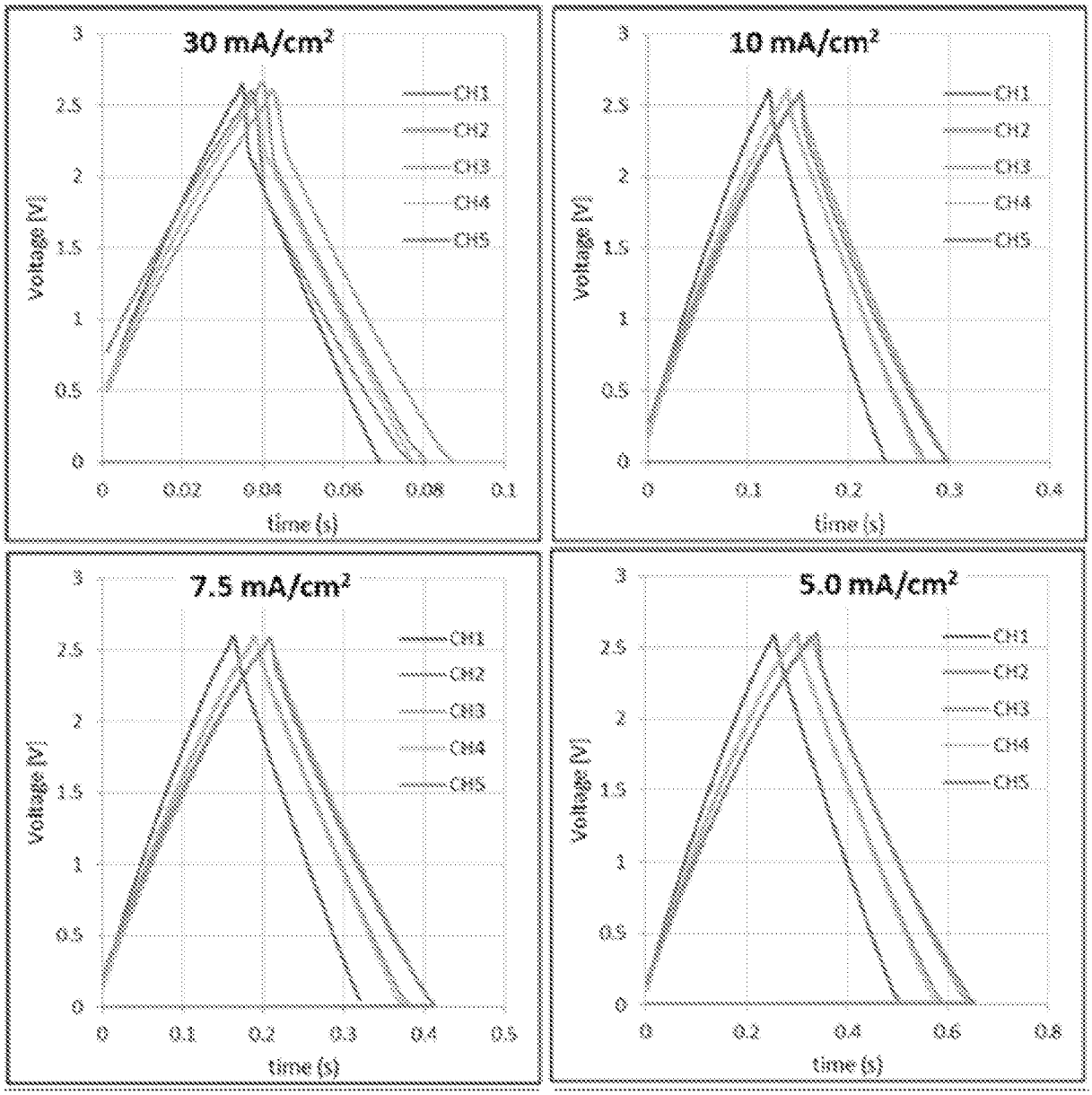

30 mA/cm²
10 mA/cm²
7.5 mA/cm²
5.0 mA/cm²
Voltage [V]
time (s)
CH1
CH2
CH3
CH4
CH5

Figure 63

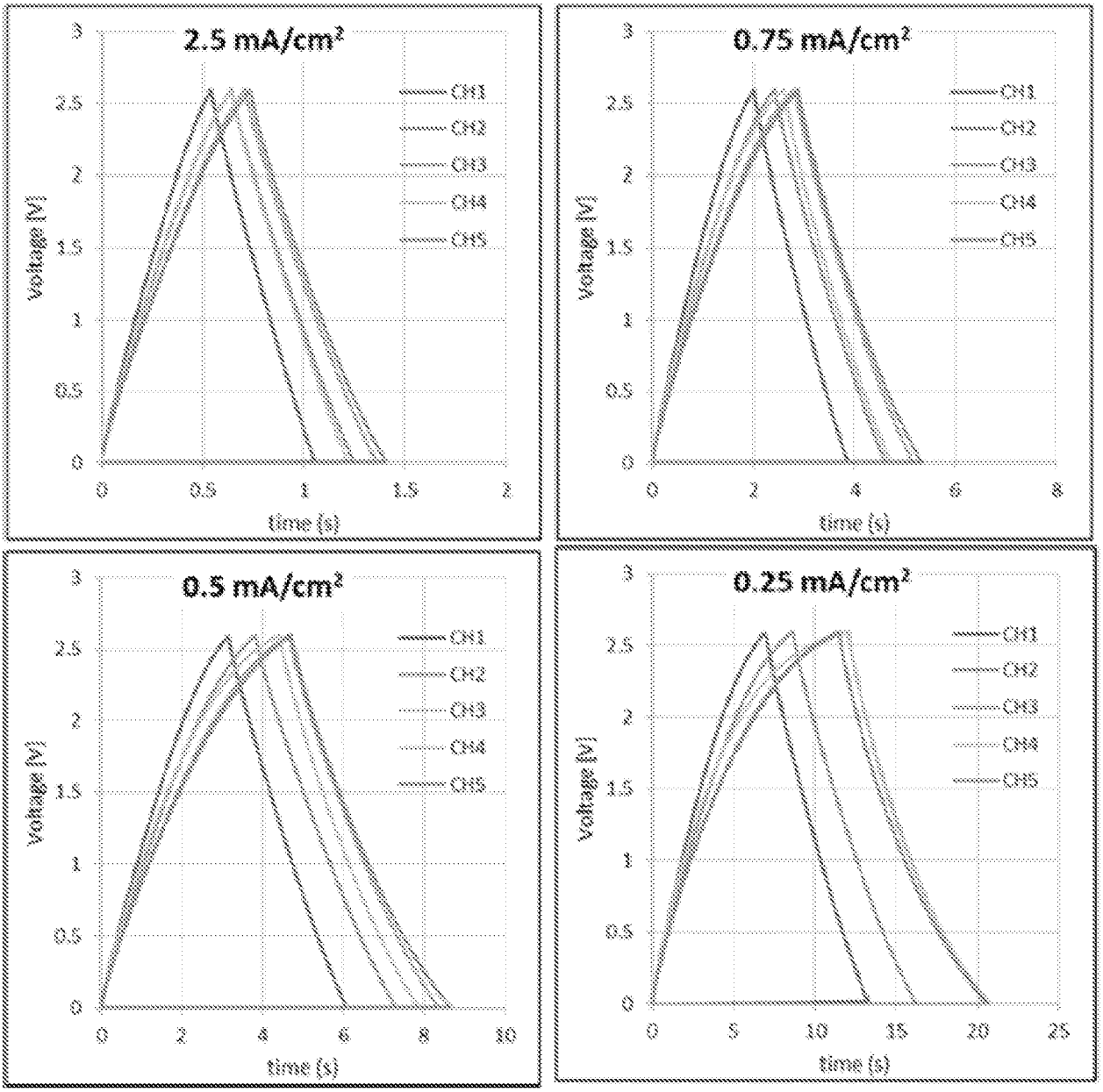

2.5 mA/cm²
0.75 mA/cm²
0.5 mA/cm²
0.25 mA/cm²
Voltage [V]
time (s)
CH1
CH2
CH3
CH4
CH5

Figure 63

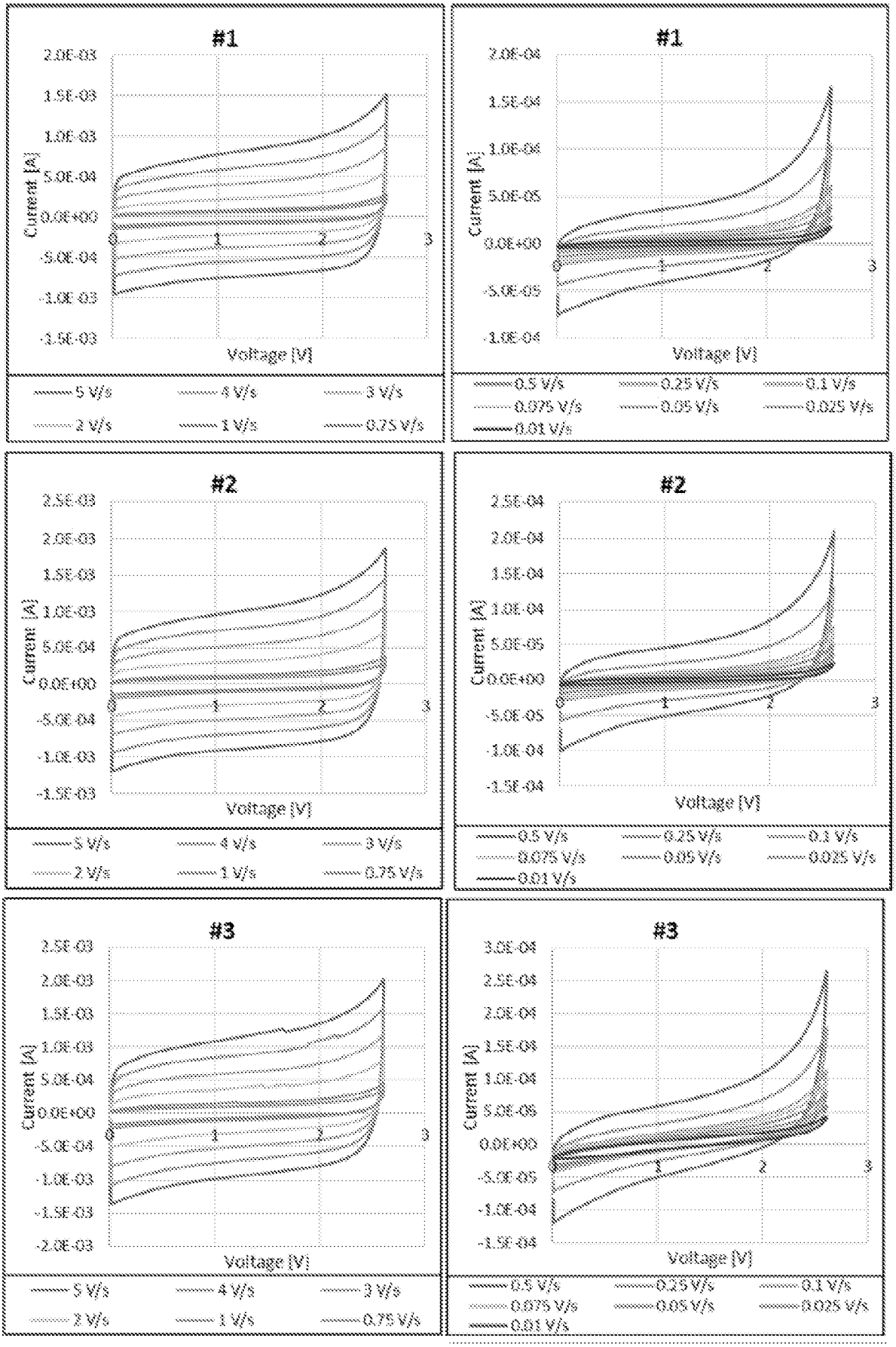
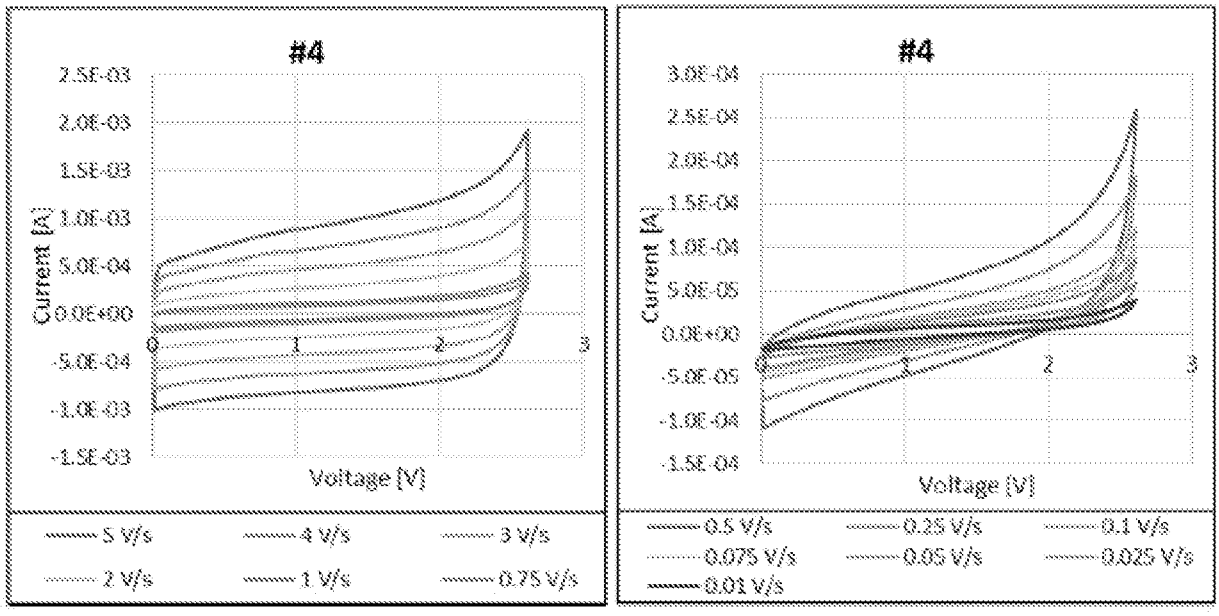

#1
Current [A]
Voltage [V]
5 V/s
4 V/s
3 V/s
2 V/s
1 V/s
0.75 V/s
#1
Current [A]
Voltage [V]
0.5 V/s
0.25 V/s
0.1 V/s
0.075 V/s
0.05 V/s
0.025 V/s
0.01 V/s
#2
Current [A]
Voltage [V]
5 V/s
4 V/s
3 V/s
2 V/s
1 V/s
0.75 V/s
#2
Current [A]
Voltage [V]
0.5 V/s
0.25 V/s
0.1 V/s
0.075 V/s
0.05 V/s
0.025 V/s
0.01 V/s
#3
Current [A]
Voltage [V]
5 V/s
4 V/s
3 V/s
2 V/s
1 V/s
0.75 V/s
#3
Current [A]
Voltage [V]
0.5 V/s
0.25 V/s
0.1 V/s
0.075 V/s
0.05 V/s
0.025 V/s
0.01 V/s

Figure 64


#4
Current [A]
Voltage [V]
5 V/s
4 V/s
3 V/s
2 V/s
1 V/s
0.75 V/s
#4
Current [A]
Voltage [V]
0.5 V/s
0.25 V/s
0.1 V/s
0.075 V/s
0.05 V/s
0.025 V/s
0.01 V/s

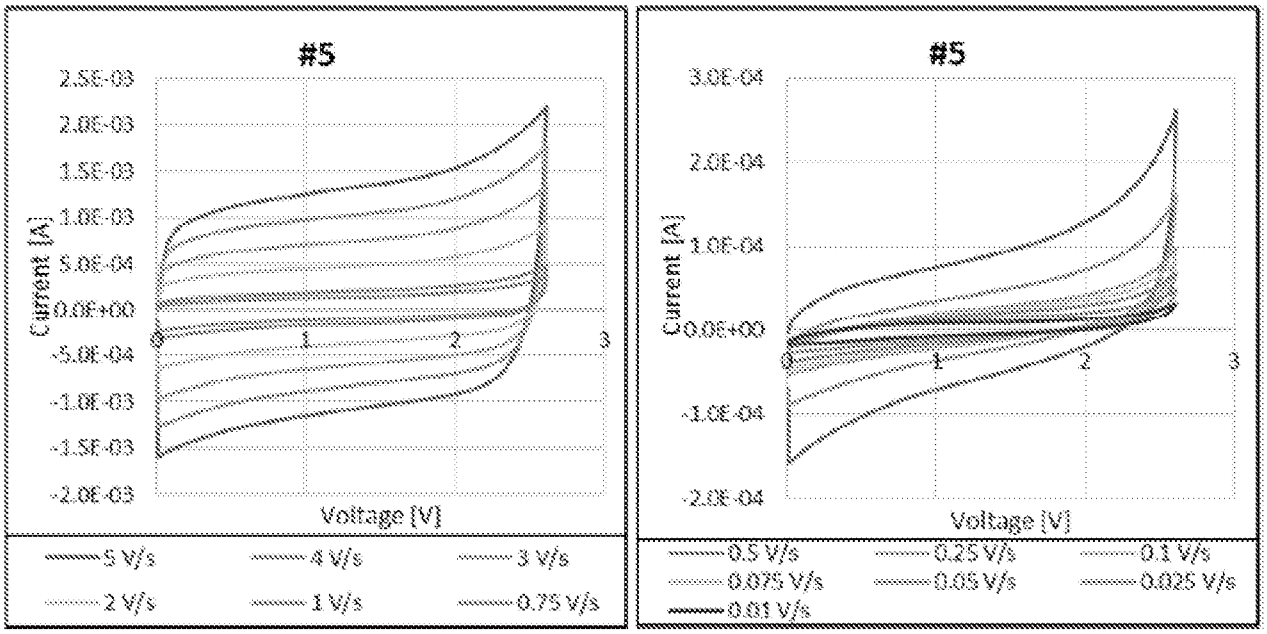
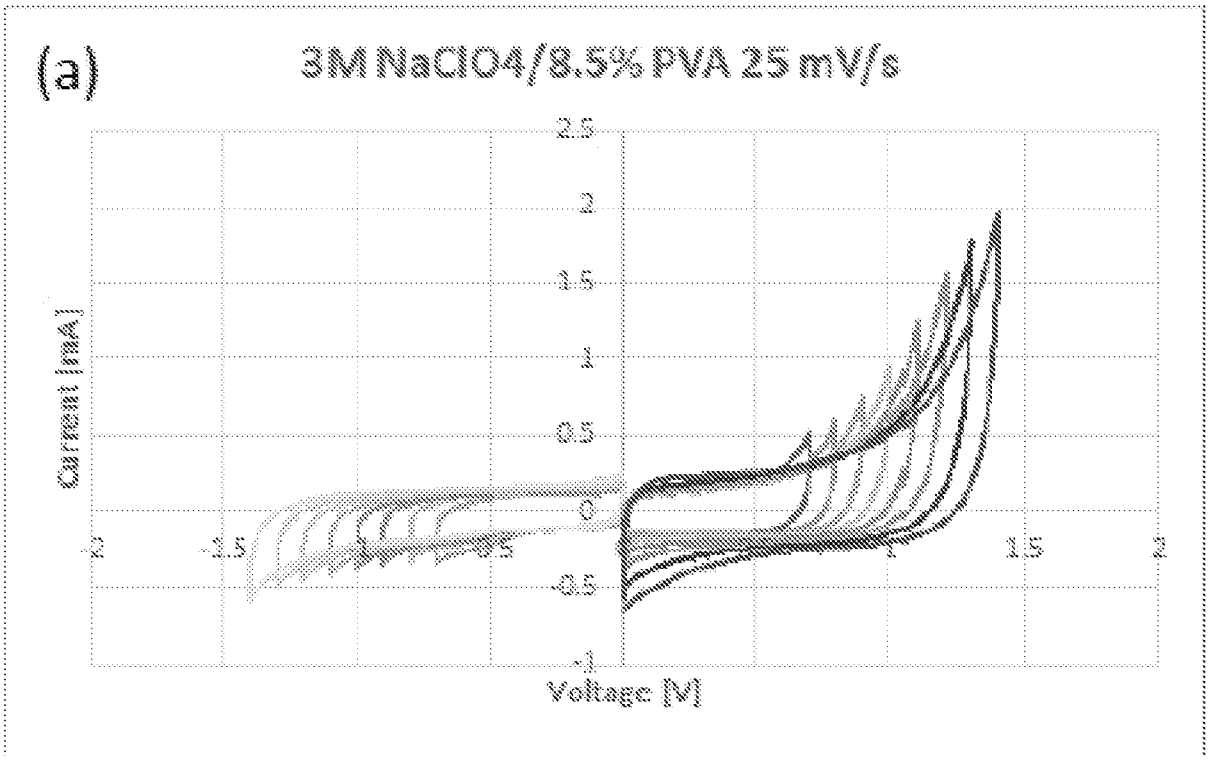

#5
Current [A]
Voltage [V]
5 V/s
4 V/s
3 V/s
2 V/s
1 V/s
0.75 V/s
#5
Current [A]
Voltage [V]
0.5 V/s
0.25 V/s
0.1 V/s
0.075 V/s
0.05 V/s
0.025 V/s
0.01 V/s

Figure 64


(a)
3M NaClO4/8.5% PVA 25 mV/s
Current [mA]
Voltage [V]
2.5
2
1.5
1
0.5
0
-0.5
-1
-2
-1.5
-1
-0.5
0.5
1
1.5
2

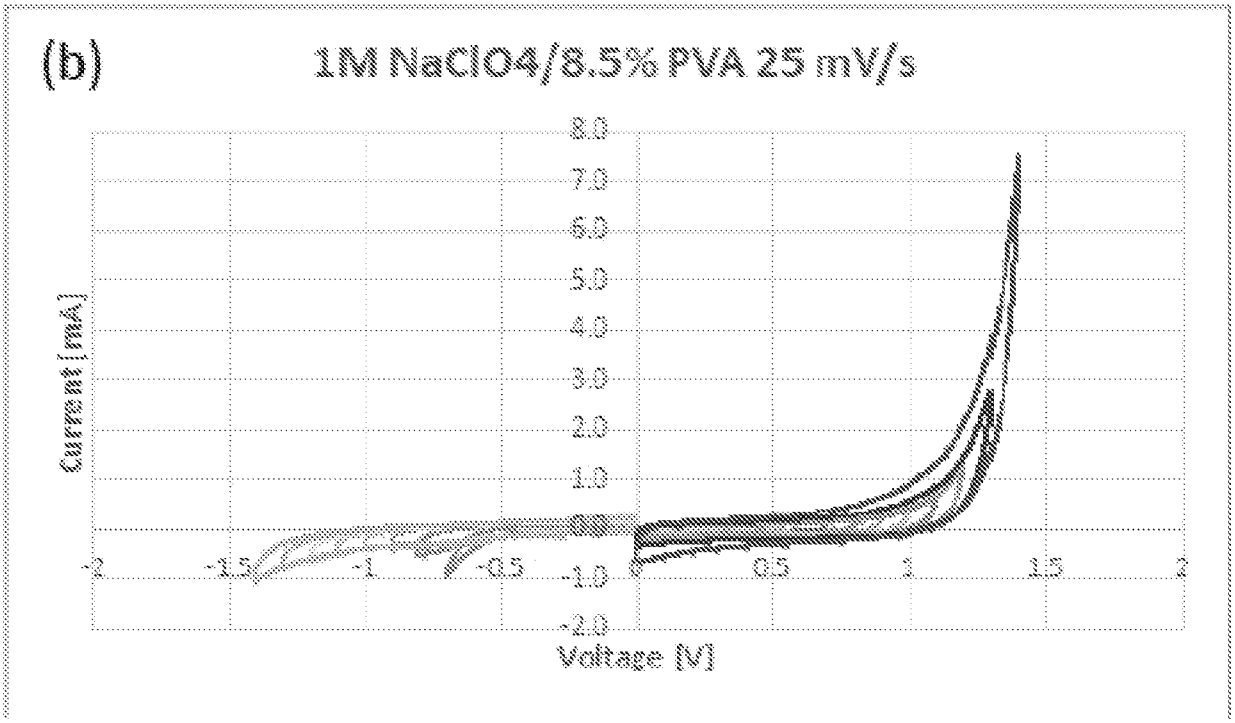
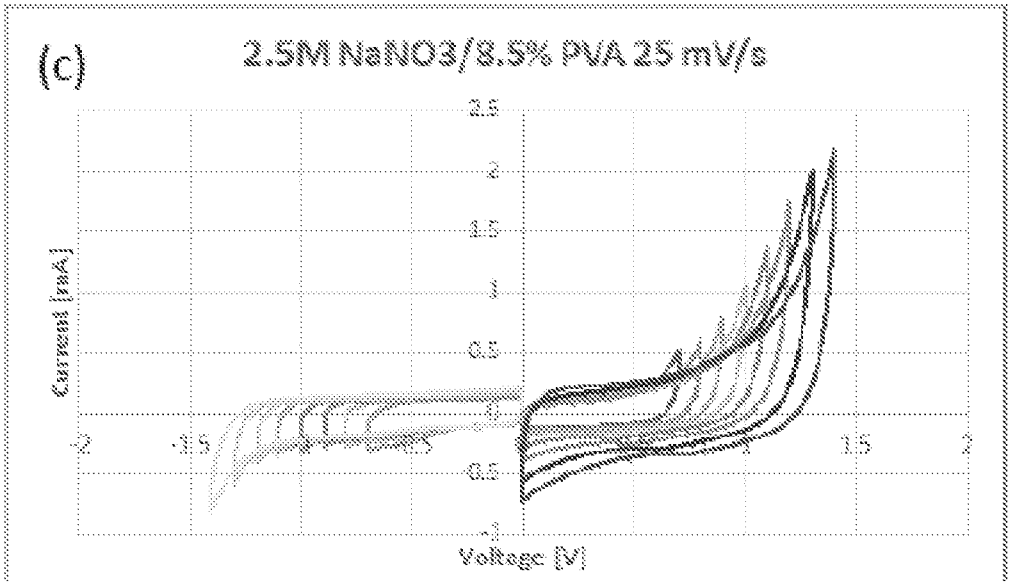
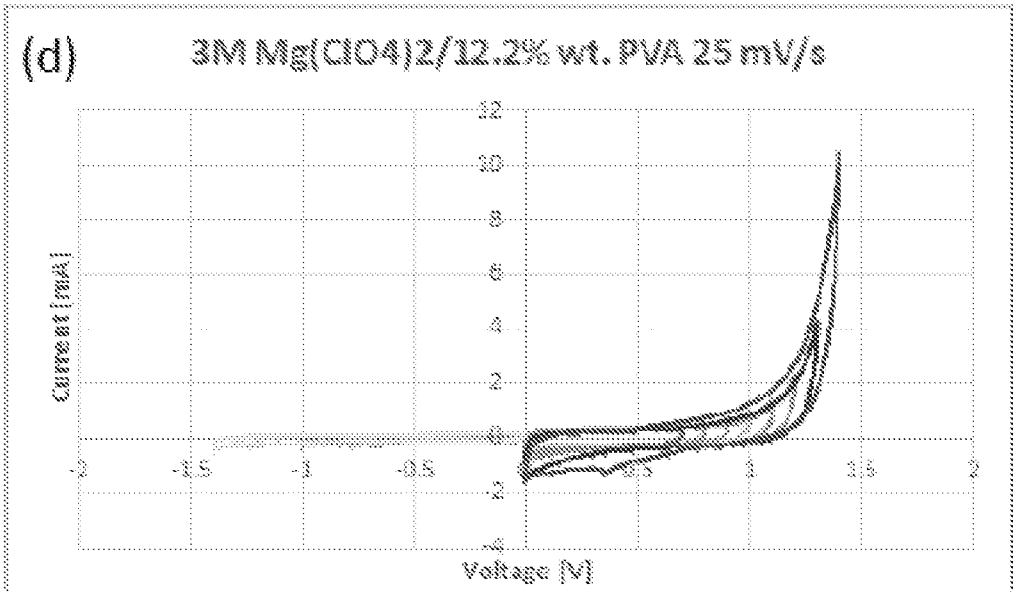

(b)
1M NaClO4/8.5% PVA 25 mV/s
Current [mA]
Voltage [V]
8.0
7.0
6.0
5.0
4.0
3.0
2.0
1.0
-1.0
-2.0
-2
-1.5
-1
-0.5
0.5
1
1.5
2

Figure 65


(c)
2.5M NaNO3/8.5% PVA 25 mV/s
Current [mA]
Voltage [V]


(d)
3M Mg(ClO4)2/12.2% wt. PVA 25 mV/s
Current [mA]
Voltage [V]

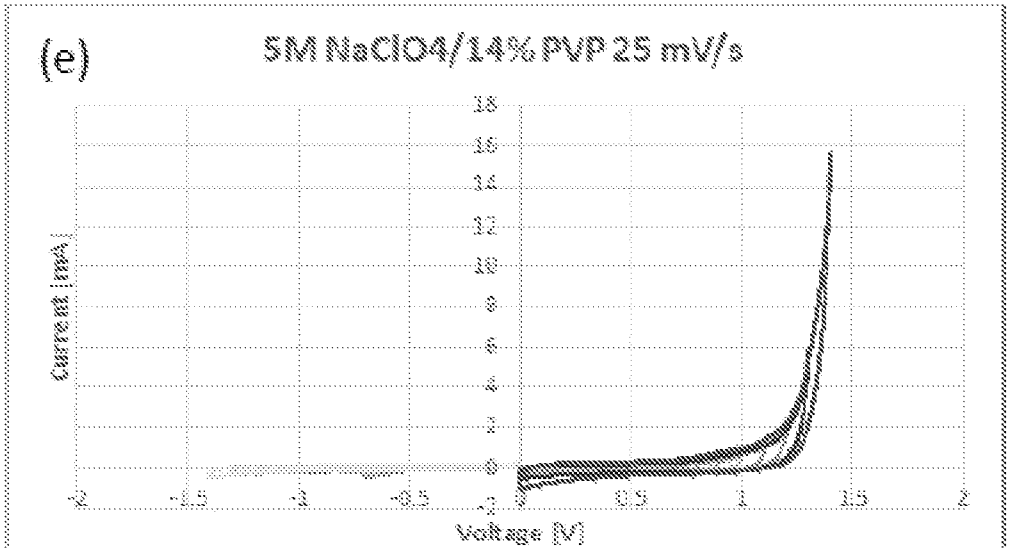

(e)
5M NaClO4/14% PVP 25 mV/s
Current [mA]
Voltage [V]

Figure 65

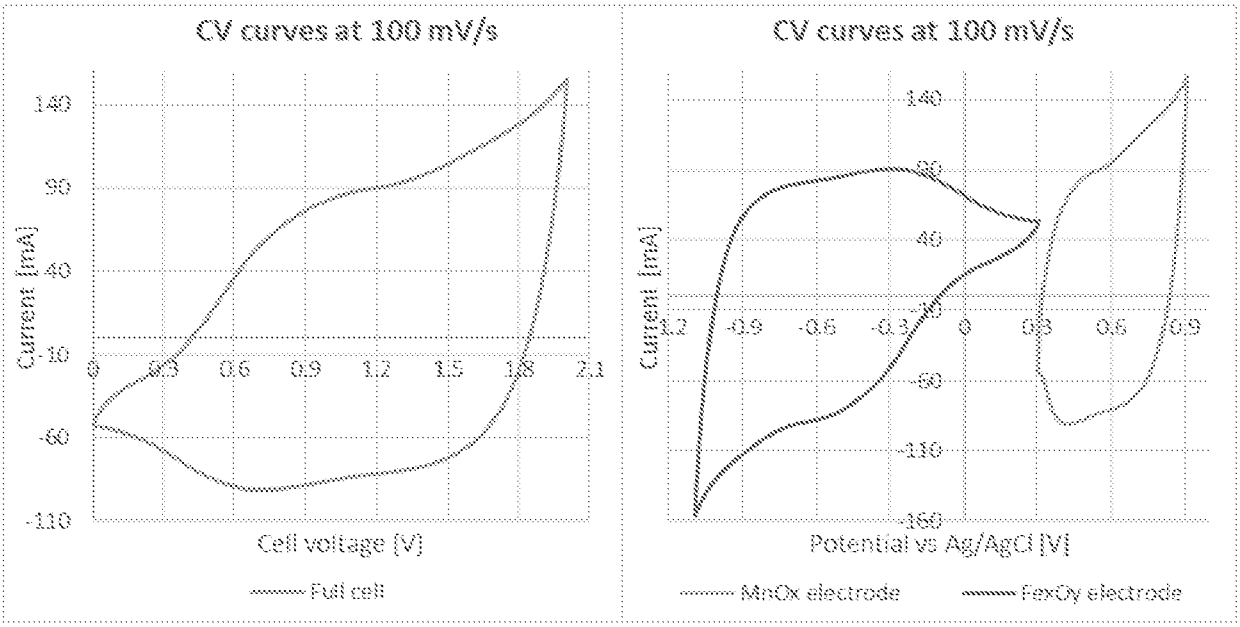


Figure 66

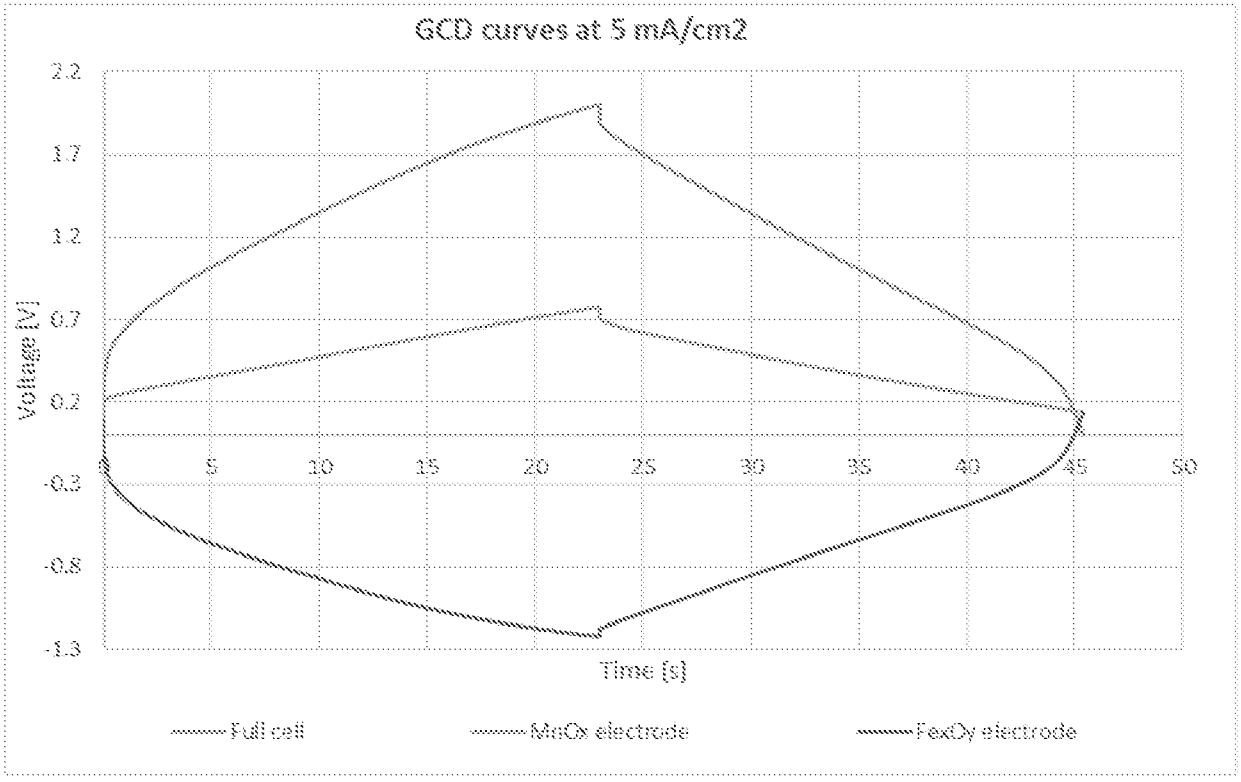


Figure 67

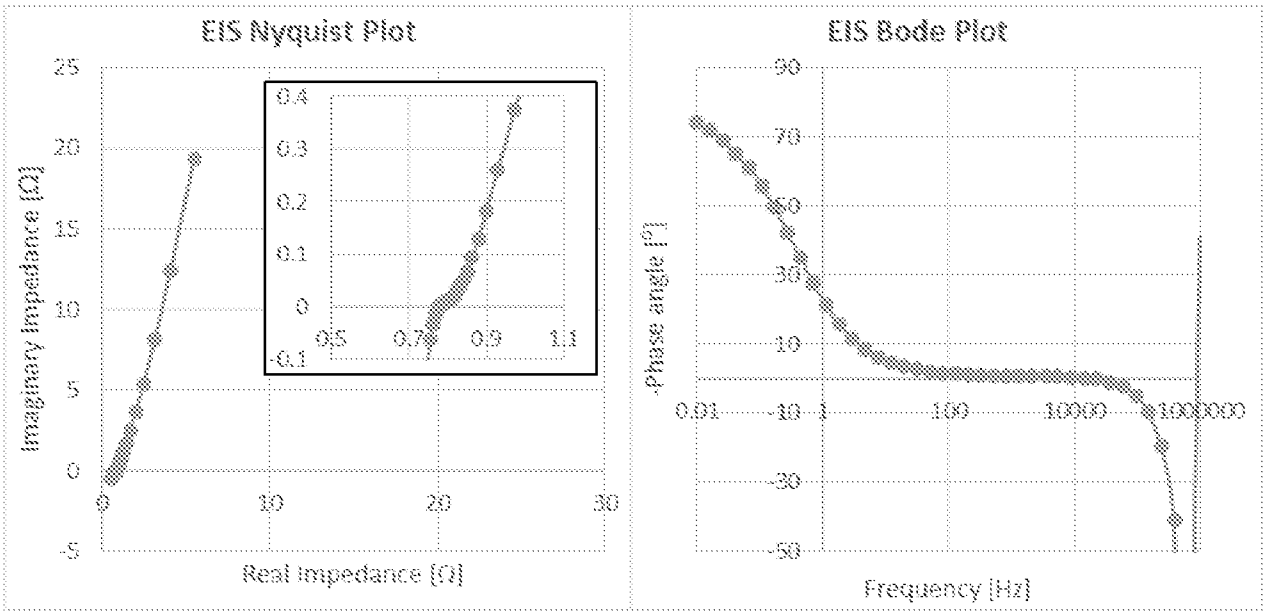


Figure 68

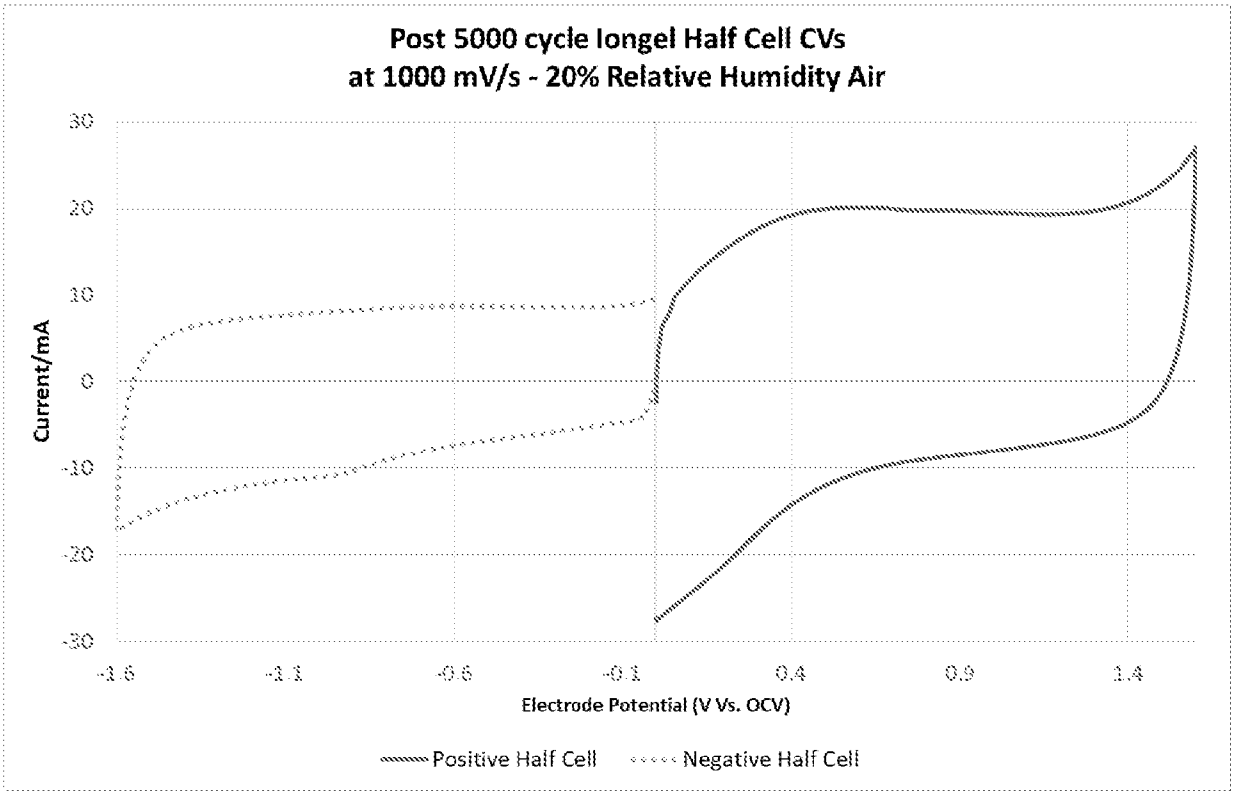


Figure 69

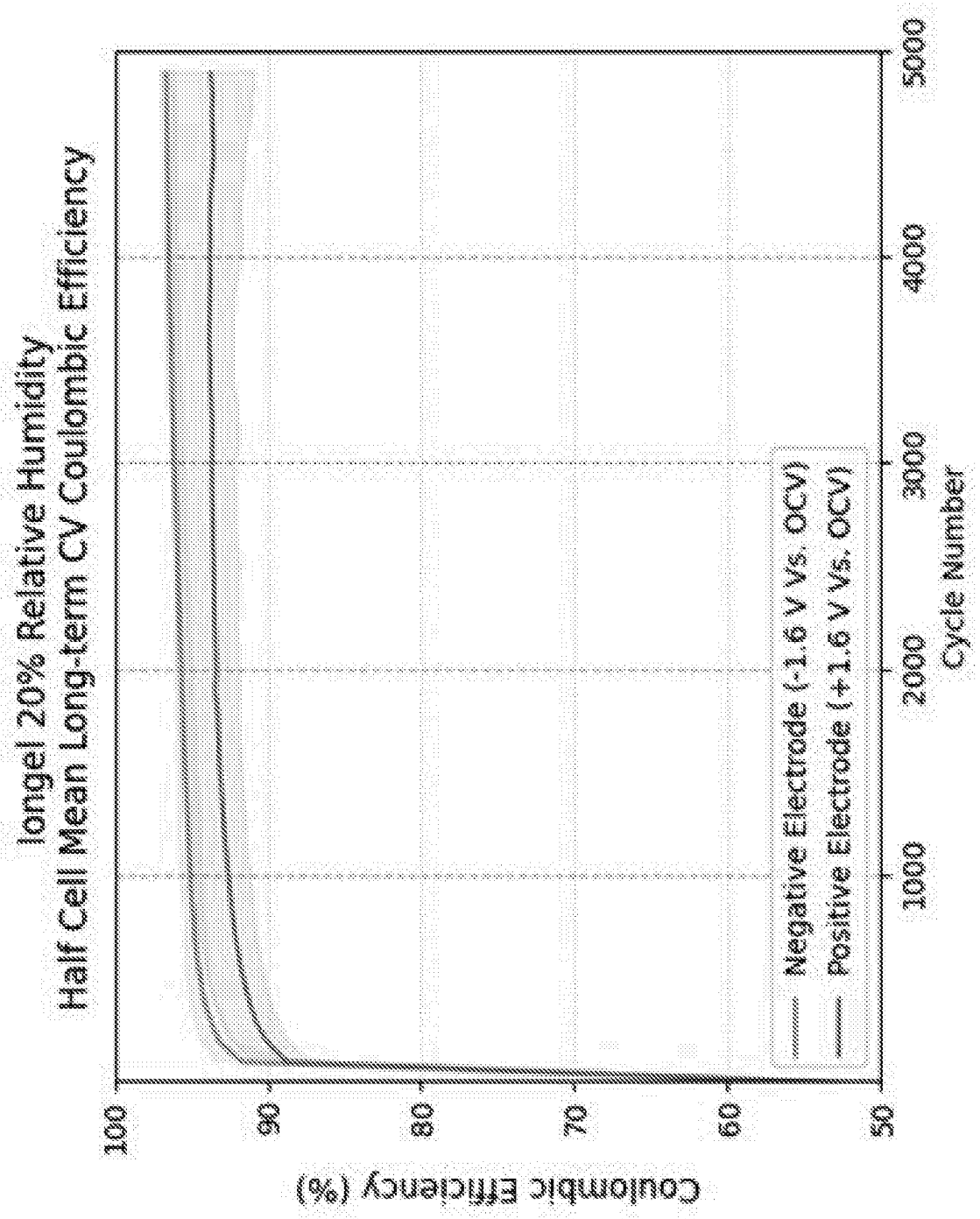

Iongel 20% Relative Humidity
Half Cell Mean Long-term CV Coulombic Efficiency
Coulombic Efficiency (%)
100
90
80
70
60
50
1000
2000
3000
4000
5000
Cycle Number
Negative Electrode (-1.6 V Vs. OCV)
Positive Electrode (+1.6 V Vs. OCV)

Figure 70

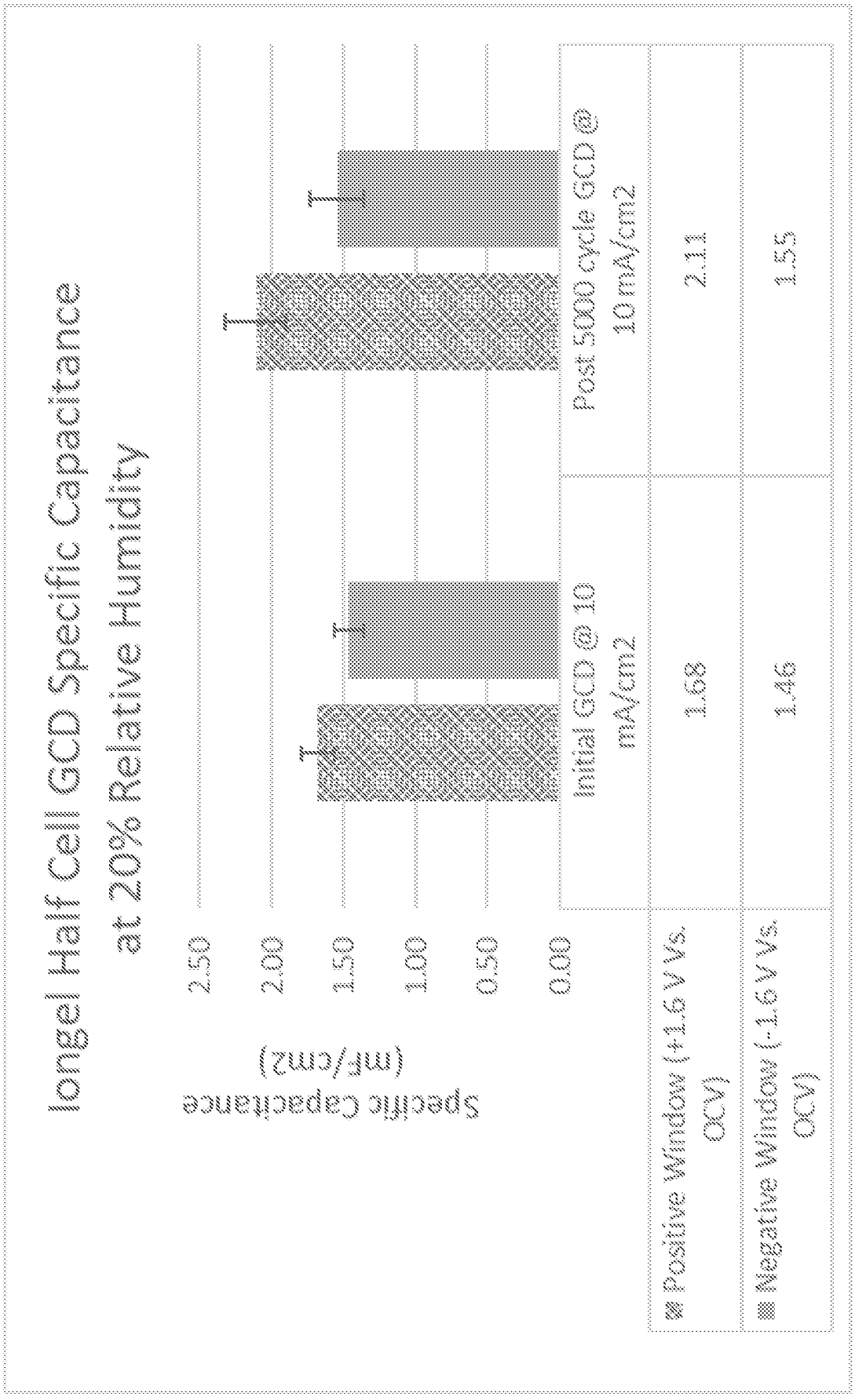

Iongel Half Cell GCD Specific Capacitance
at 20% Relative Humidity
Specific Capacitance (mF/cm2)
2.50
2.00
1.50
1.00
0.50
0.00
Initial GCD @ 10 mA/cm2
Post 5000 cycle GCD @ 10 mA/cm2
Positive Window (+1.6 V Vs. OCV)
1.68
2.11
Negative Window (-1.6 V Vs. OCV)
1.46
1.55

Figure 71

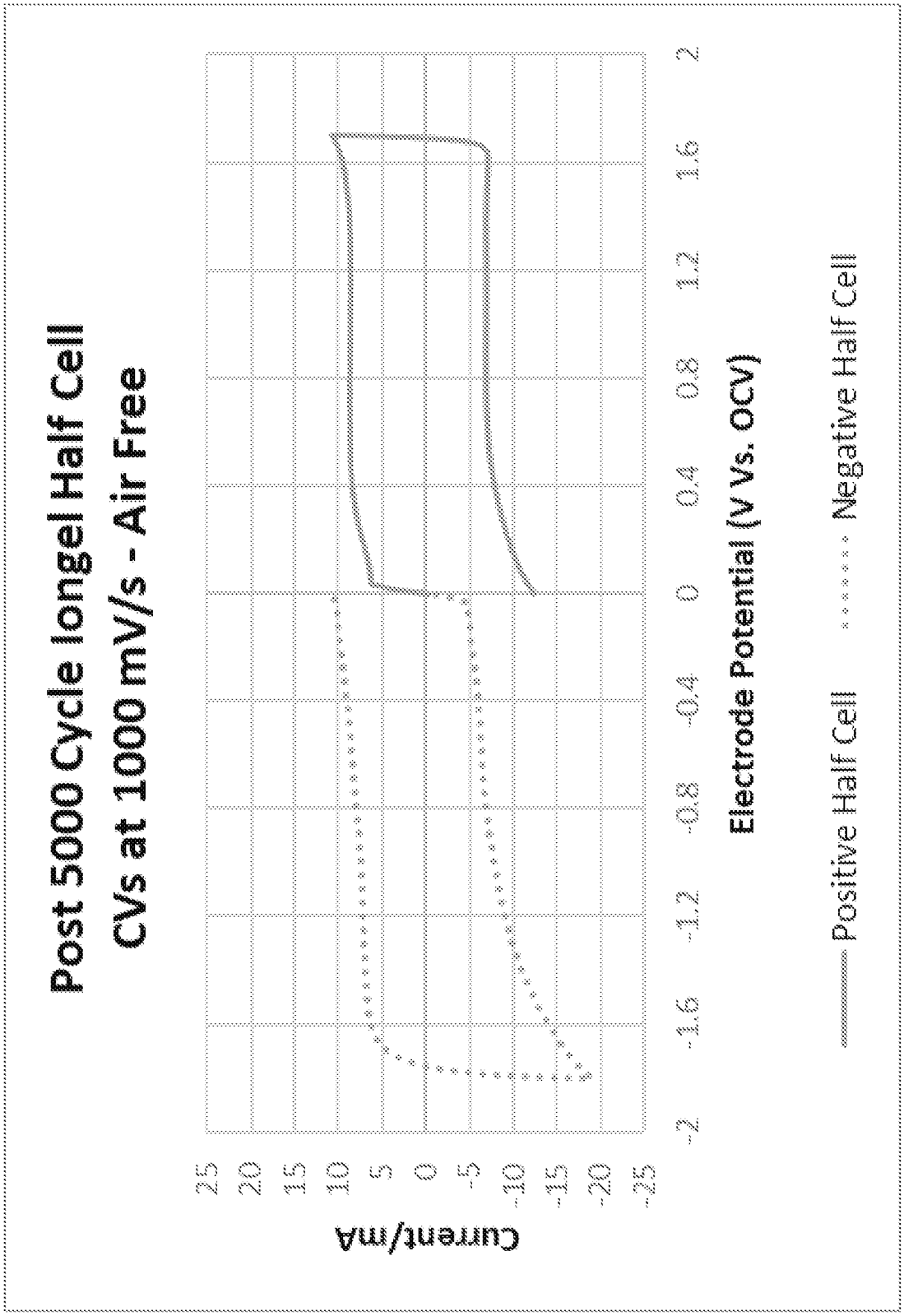

Post 5000 Cycle Iongel Half Cell
CVs at 1000 mV/s - Air Free
Current/mA
25
20
15
10
5
0
-5
-10
-15
-20
-25
-2
-1.6
-1.2
-0.8
-0.4
0
0.4
0.8
1.2
1.6
2
Electrode Potential (V Vs. OCV)
Positive Half Cell
Negative Half Cell

Figure 72

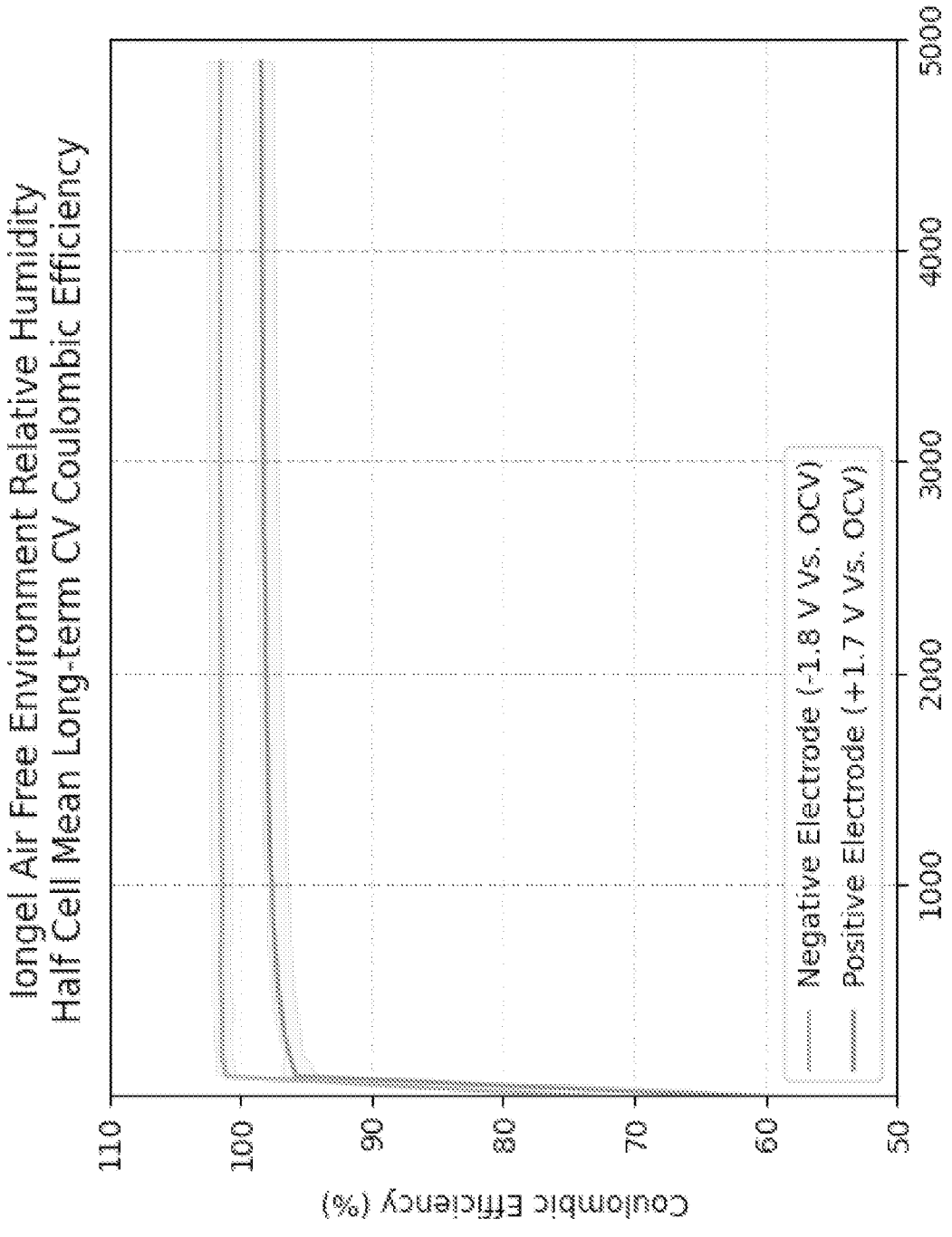

Iongel Air Free Enviroment Relative Humidity
Half Cell Mean Long-term CV Coulombic Efficiency
Coulombic Efficiency (%)
110
100
90
80
70
60
50
1000
2000
3000
4000
5000
Cycle Number
Negative Electrode (-1.8 V Vs. OCV)
Positive Electrode (+1.7 V Vs. OCV)

Figure 73

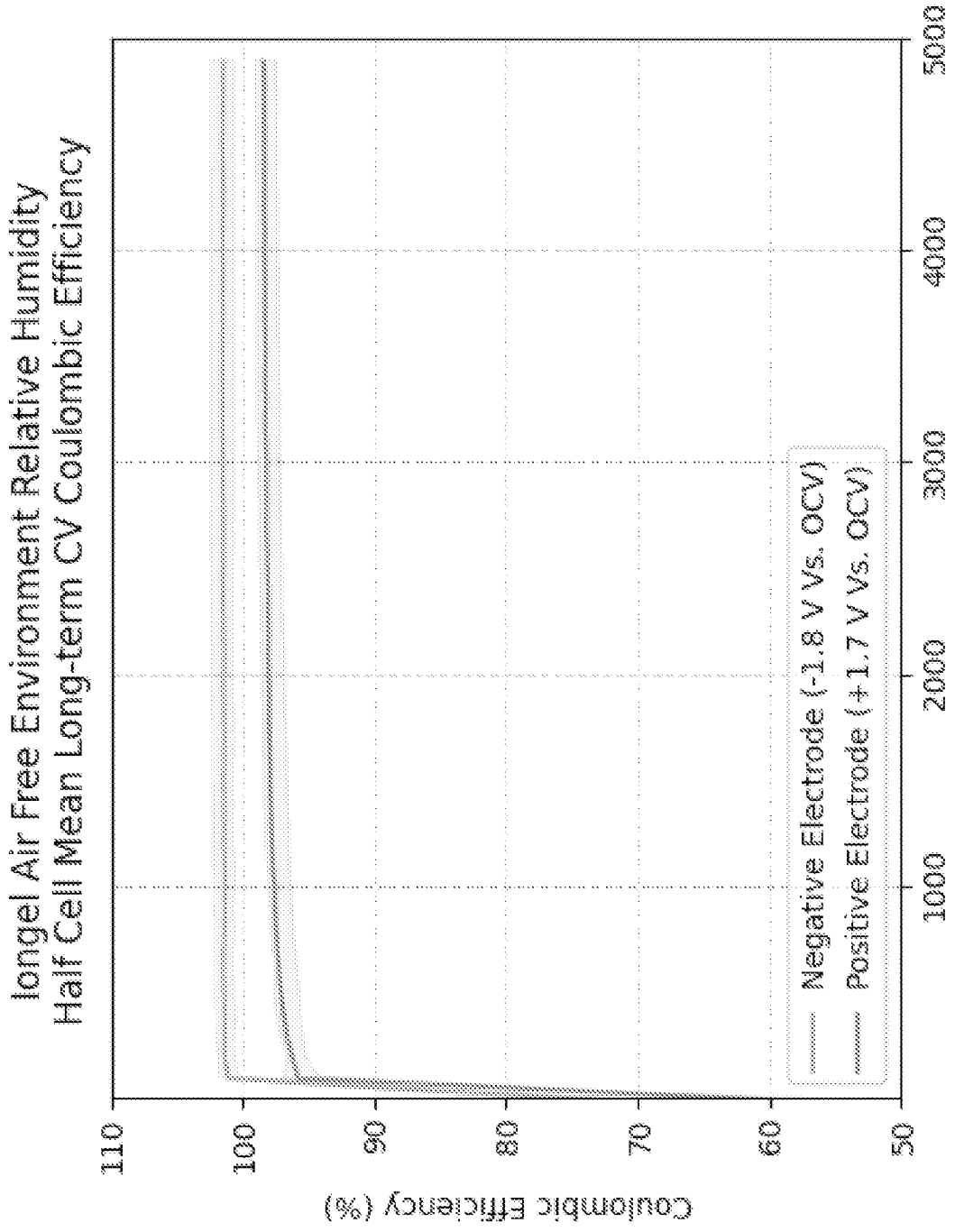

Iongel Air Free Enviroment Relative Humidity
Half Cell Mean Long-term CV Coulombic Efficiency
Coulombic Efficiency (%)
110
100
90
80
70
60
50
1000
2000
3000
4000
5000
Cycle Number
Negative Electrode (-1.8 V Vs. OCV)
Positive Electrode (+1.7 V Vs. OCV)

Figure 74

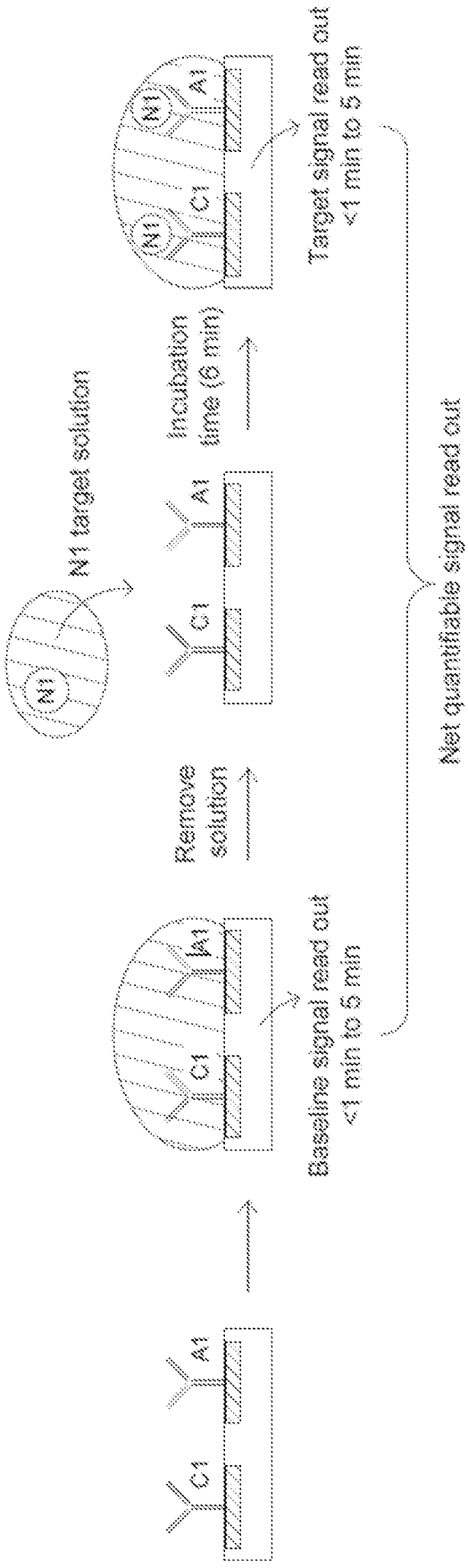

A1
C1
N1 target solution
N1
Incubation time (6 min)
Remove solution
Baseline signal read out <1 min to 5 min
Target signal read out <1 min to 5 min
Net quantifiable signal read out

Figure 75

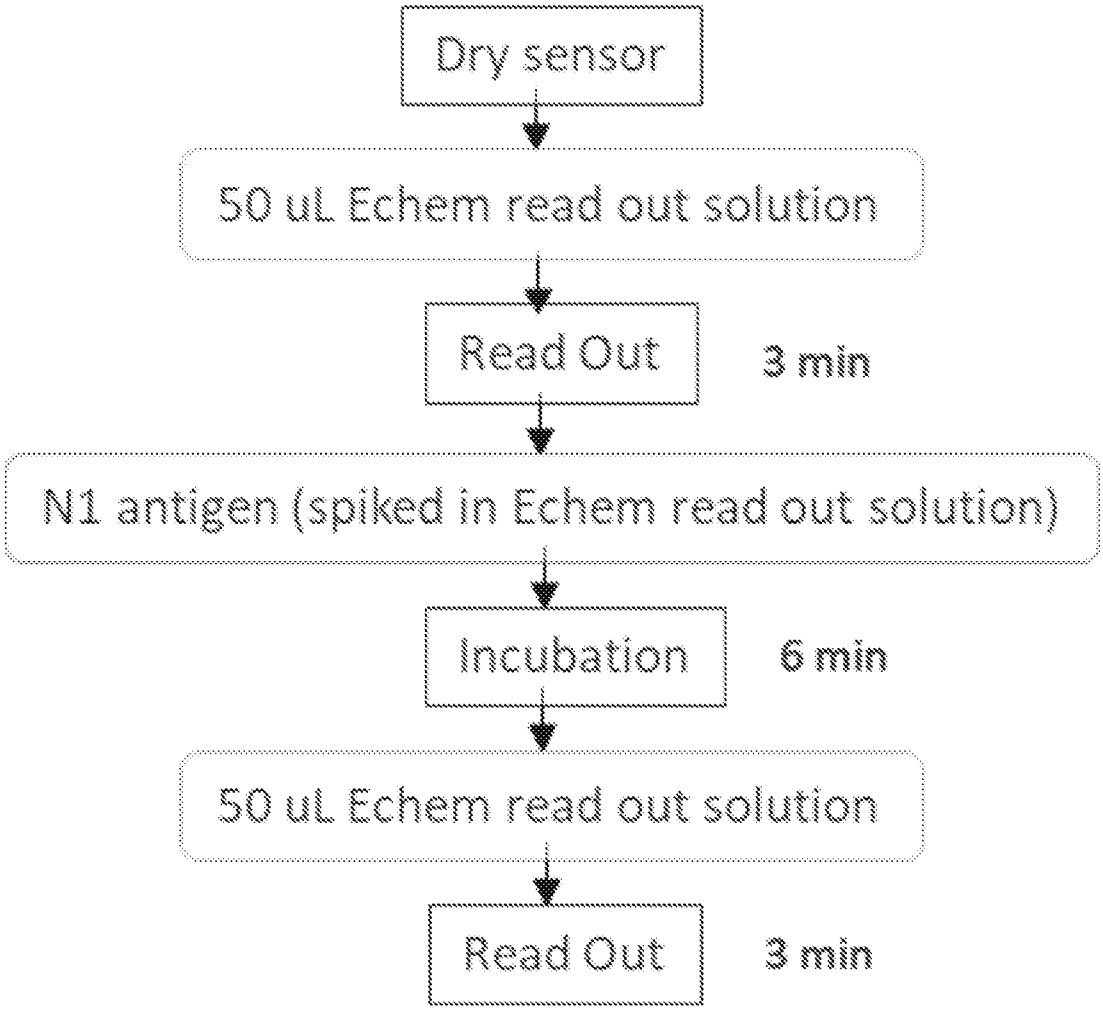

Dry sensor
50 uL Echem read out solution
Read Out
3 min
N1 antigen (spiked in Echem read out solution)
Incubation
6 min
50 uL Echem read out solution
Read Out
3 min

Figure 76

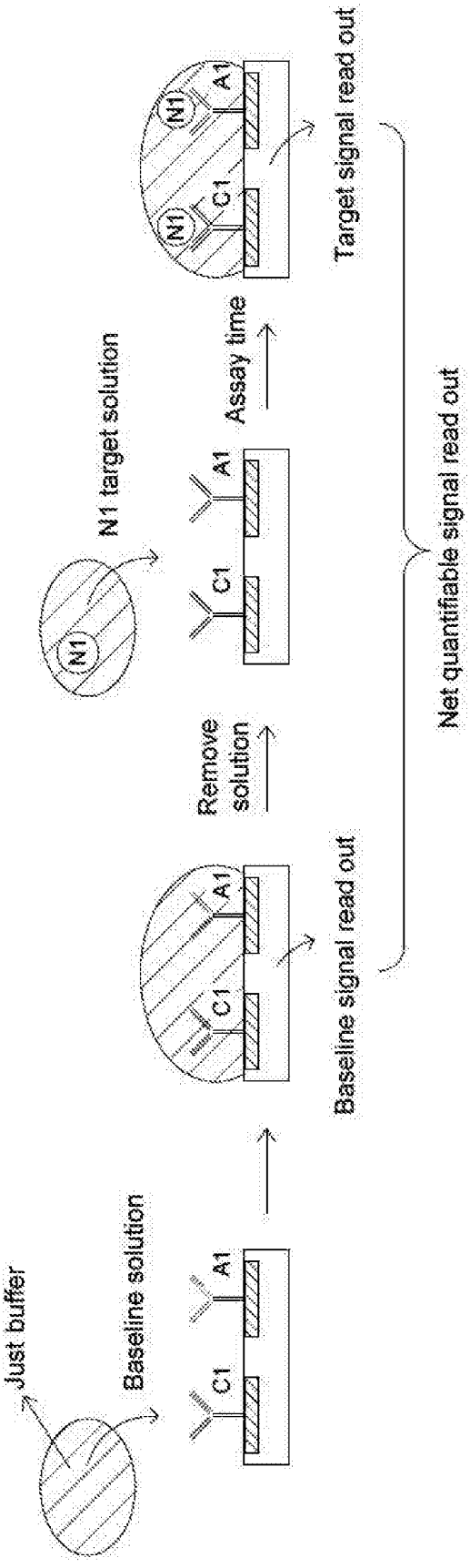

Just buffer
Baseline solution
C1
A1
Baseline signal read out
Remove solution
N1 target solution
N1
Assay time
Target signal read out
Net quantifiable signal read out

Figure 77

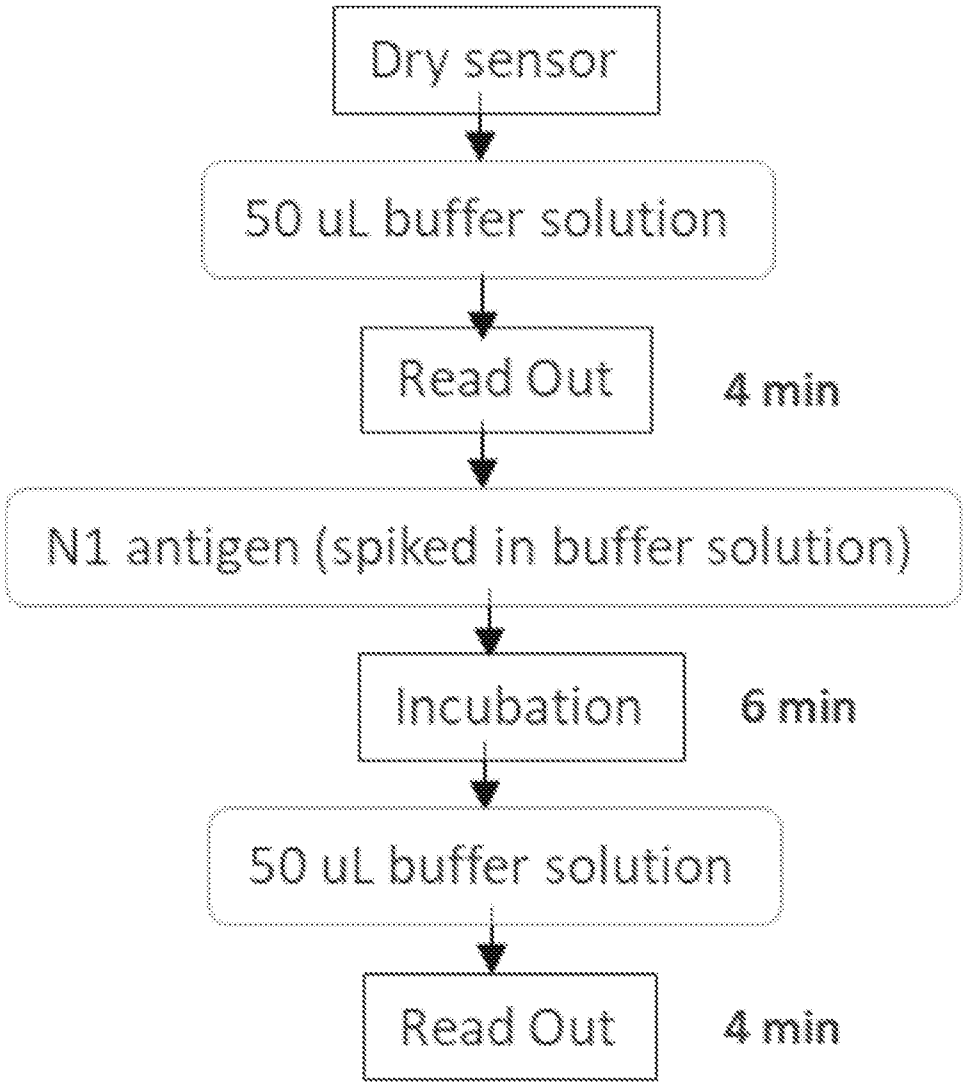

Dry sensor
50 uL buffer solution
Read Out
4 min
N1 antigen (spiked in buffer solution)
Incubation
6 min
50 uL buffer solution
Read Out
4 min

Figure 78

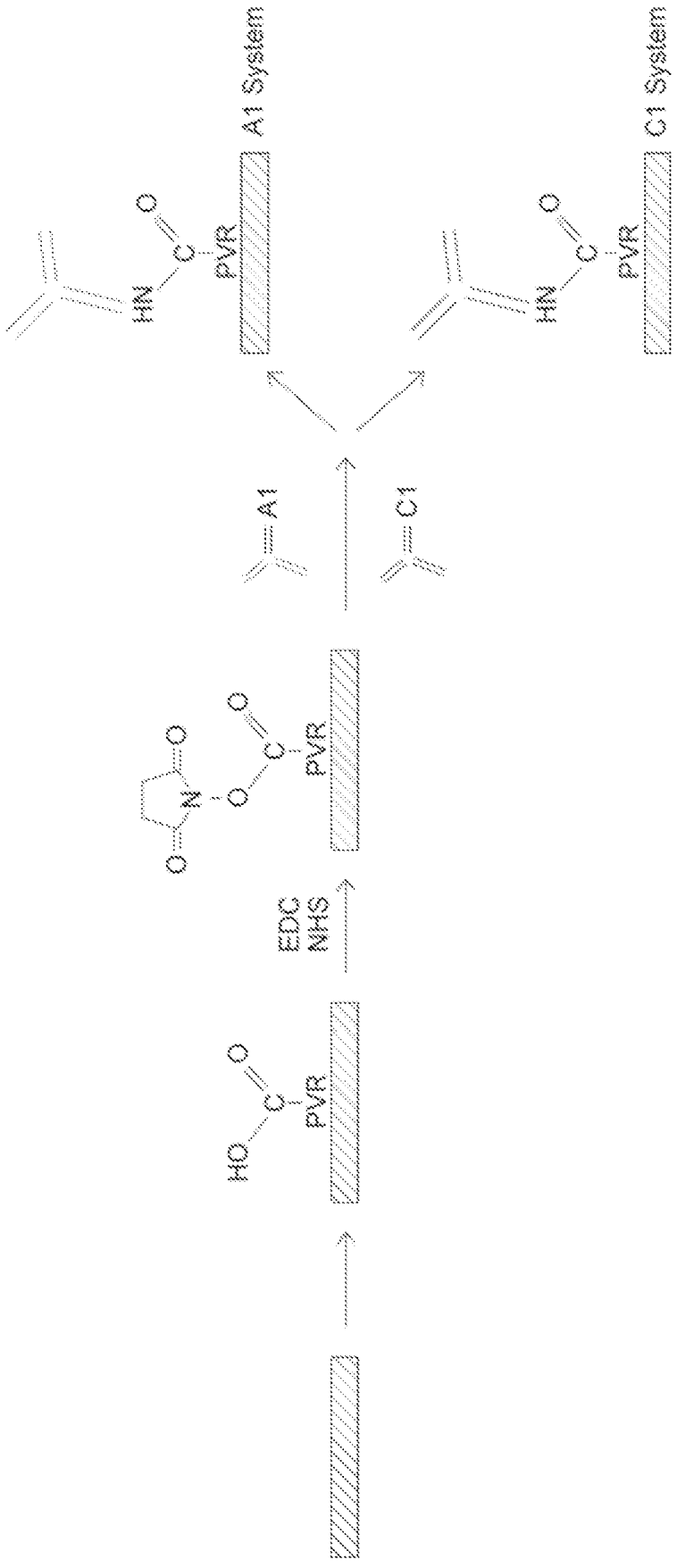


Figure 79

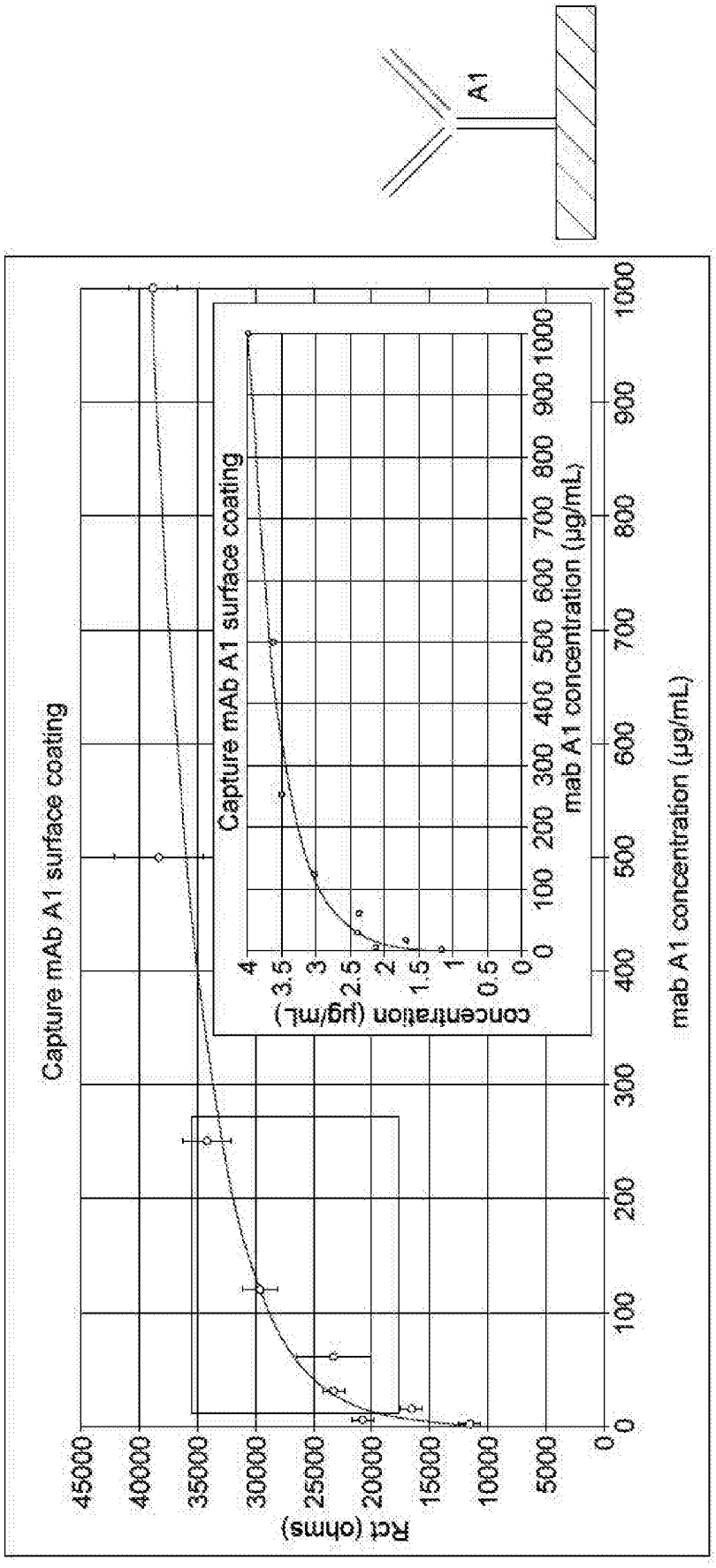

A1
Capture mAb A1 surface coating
Rct (ohms)
mab A1 concentration (µg/mL)
Capture mAb A1 surface coating
concentration (µg/mL)
mab A1 concentration (µg/mL)

Figure 80

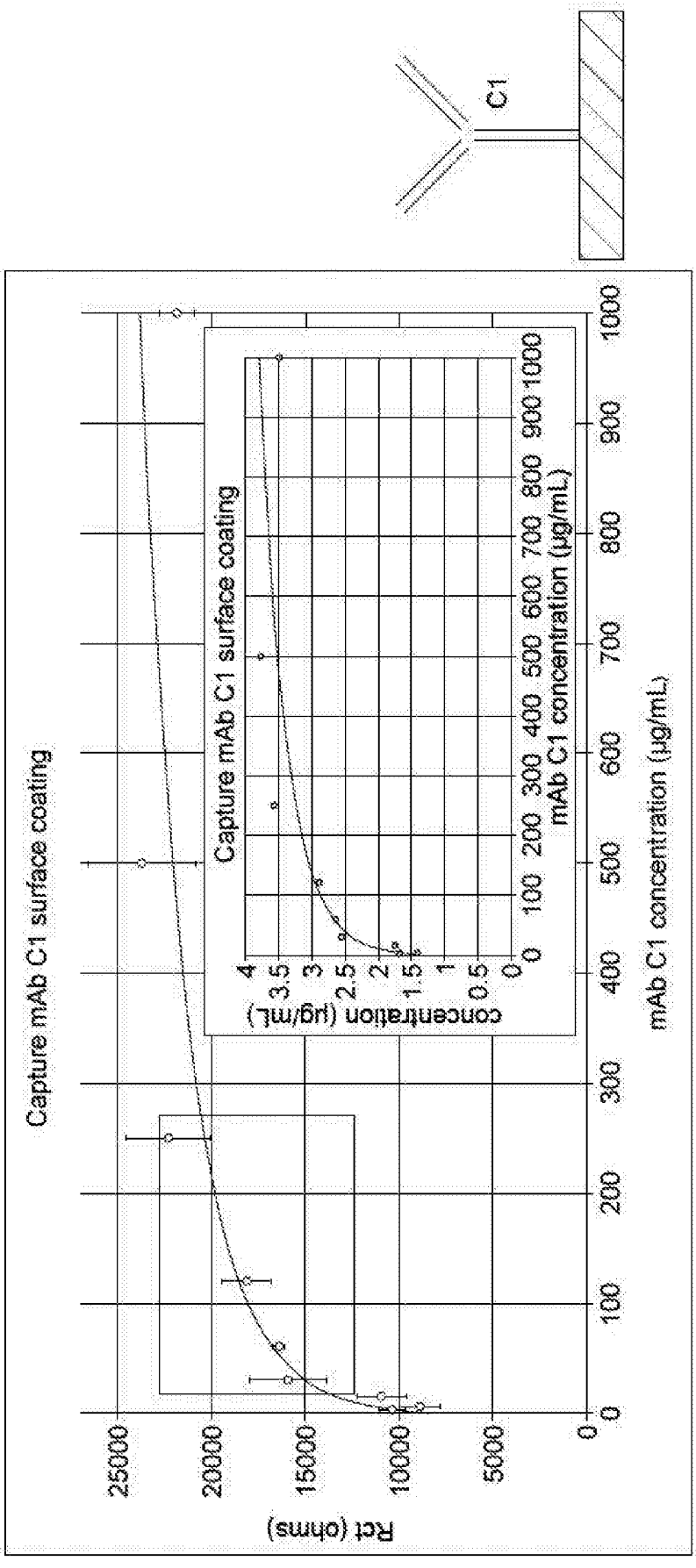

C1
Capture mAb C1 surface coating
Rct (ohms)
25000
20000
15000
10000
5000
0
0
100
200
300
400
500
600
700
800
900
1000
mAb C1 concentration (µg/mL)
Capture mAb C1 surface coating
concentration (µg/mL)
4
3.5
3
2.5
2
1.5
1
0.5
0
0
100
200
300
400
500
600
700
800
900
1000
mAb C1 concentration (µg/mL)

Figure 81

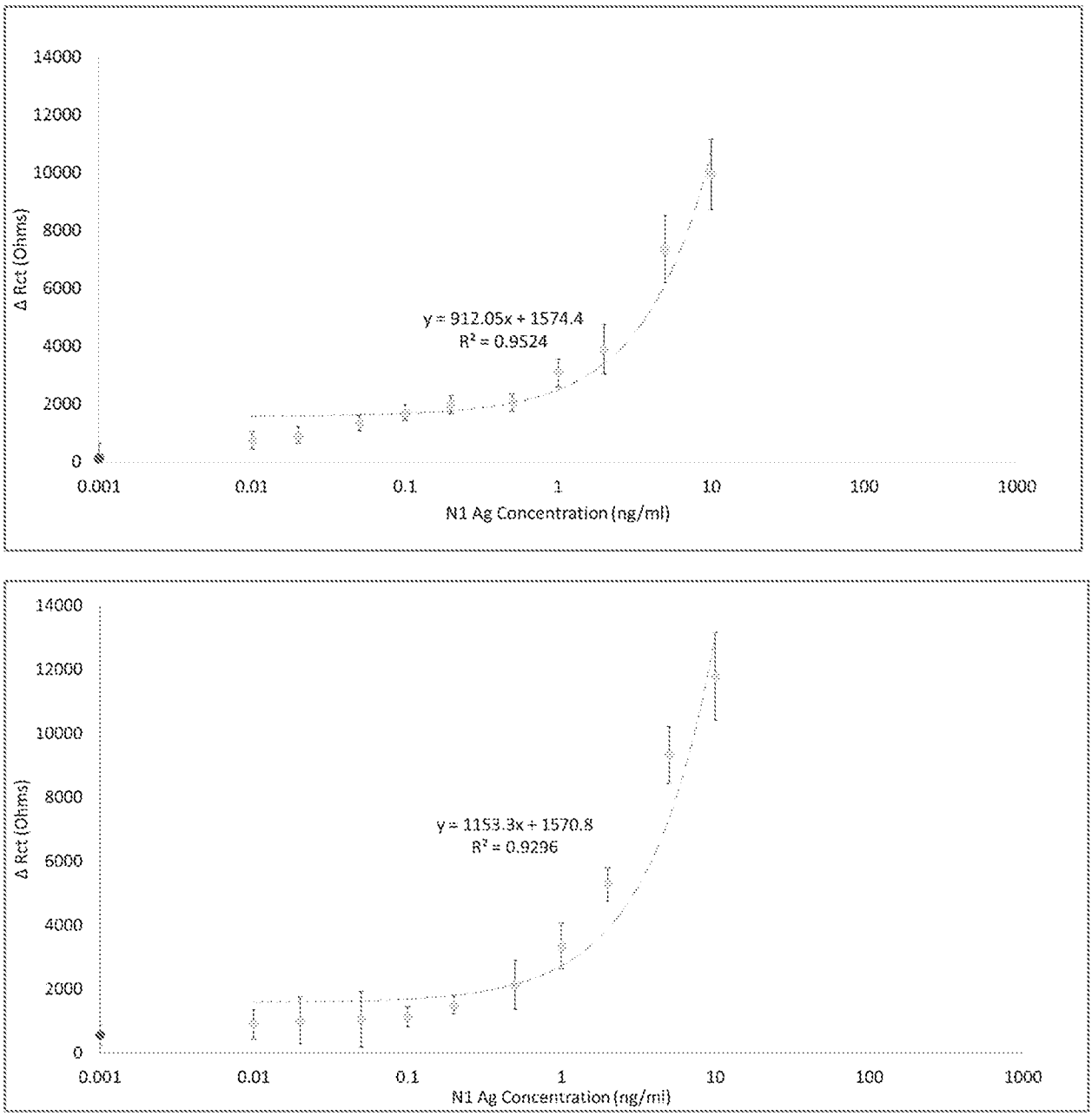
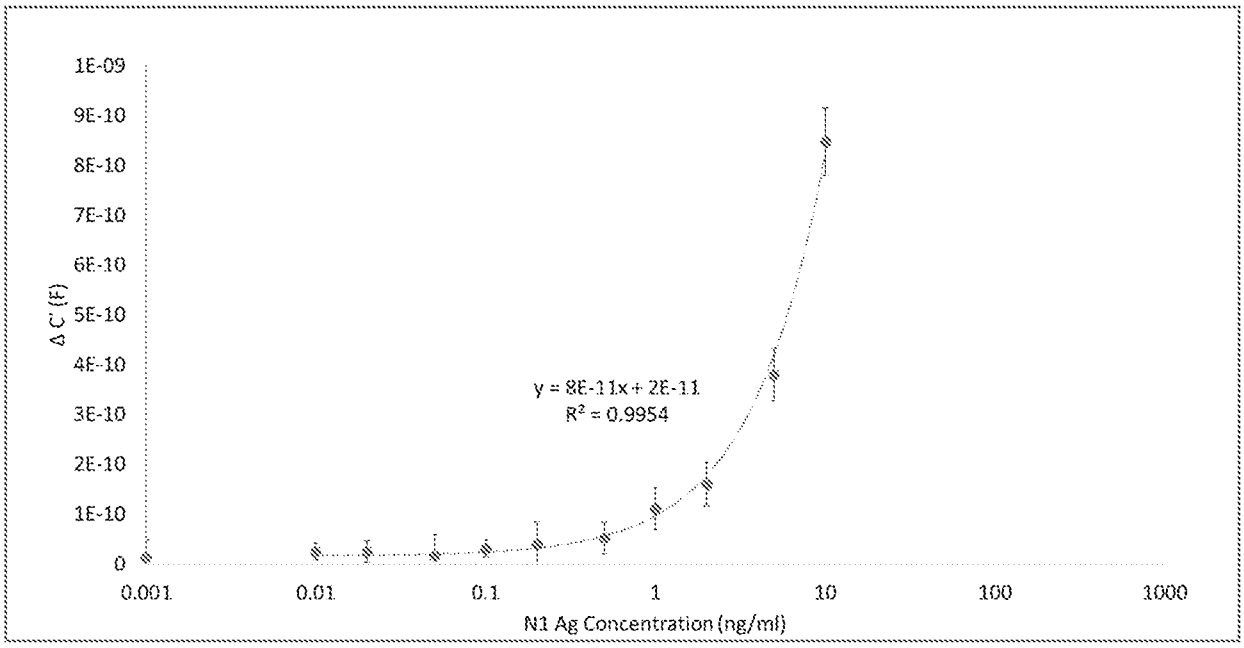

14000
12000
10000
8000
6000
4000
2000
0
Δ Rct (Ohms)
y = 912.05x + 1574.4
R² = 0.9524
0.001
0.01
0.1
1
10
100
1000
N1 Ag Concentration (ng/ml)
14000
12000
10000
8000
6000
4000
2000
0
Δ Rct (Ohms)
y = 1153.3x + 1570.8
R² = 0.9296
0.001
0.01
0.1
1
10
100
1000
N1 Ag Concentration (ng/ml)

Figure 82


1E-09
9E-10
8E-10
7E-10
6E-10
5E-10
4E-10
3E-10
2E-10
1E-10
0
Δ C' (F)
y = 8E-11x + 2E-11
R² = 0.9954
0.001
0.01
0.1
1
10
100
1000
N1 Ag Concentration (ng/ml)

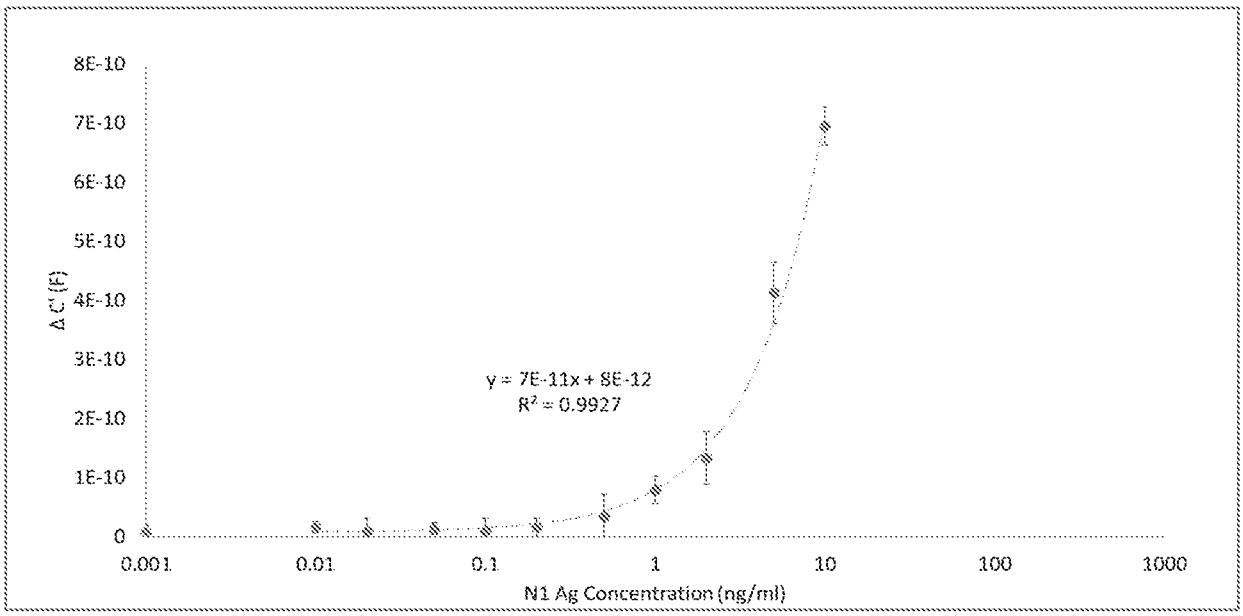

8E-10
7E-10
6E-10
5E-10
4E-10
3E-10
2E-10
1E-10
0
Δ C' (F)
y = 7E-11x + 8E-12
R² = 0.9927
0.001
0.01
0.1
1
10
100
1000
N1 Ag Concentration (ng/ml)

Figure 83

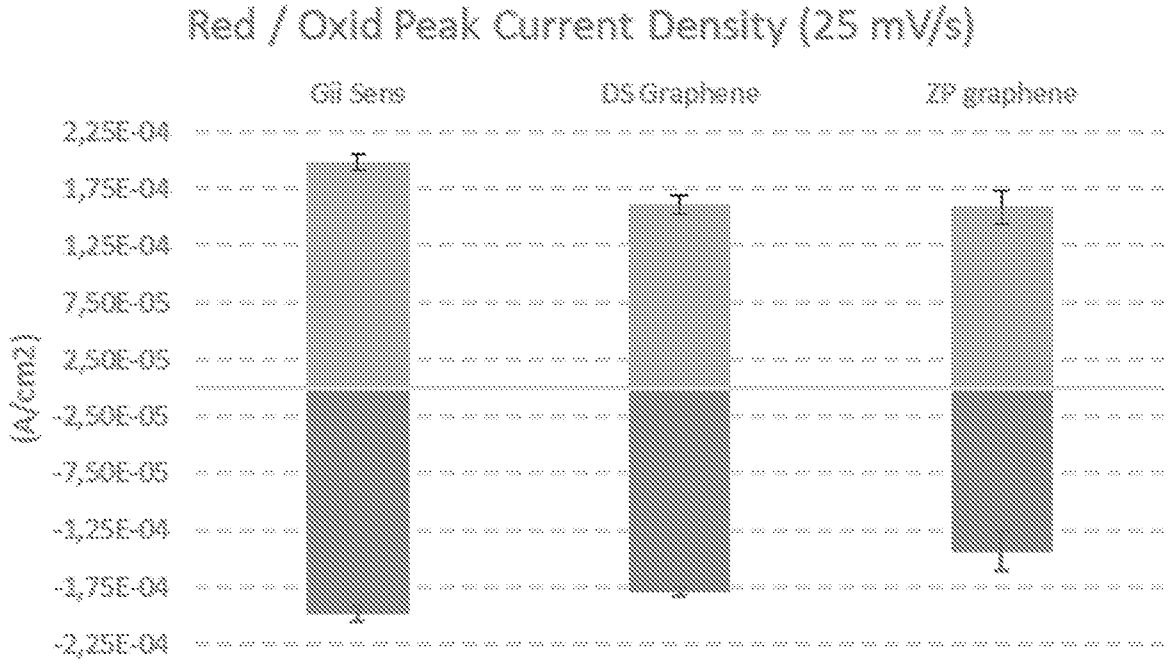


Figure 84

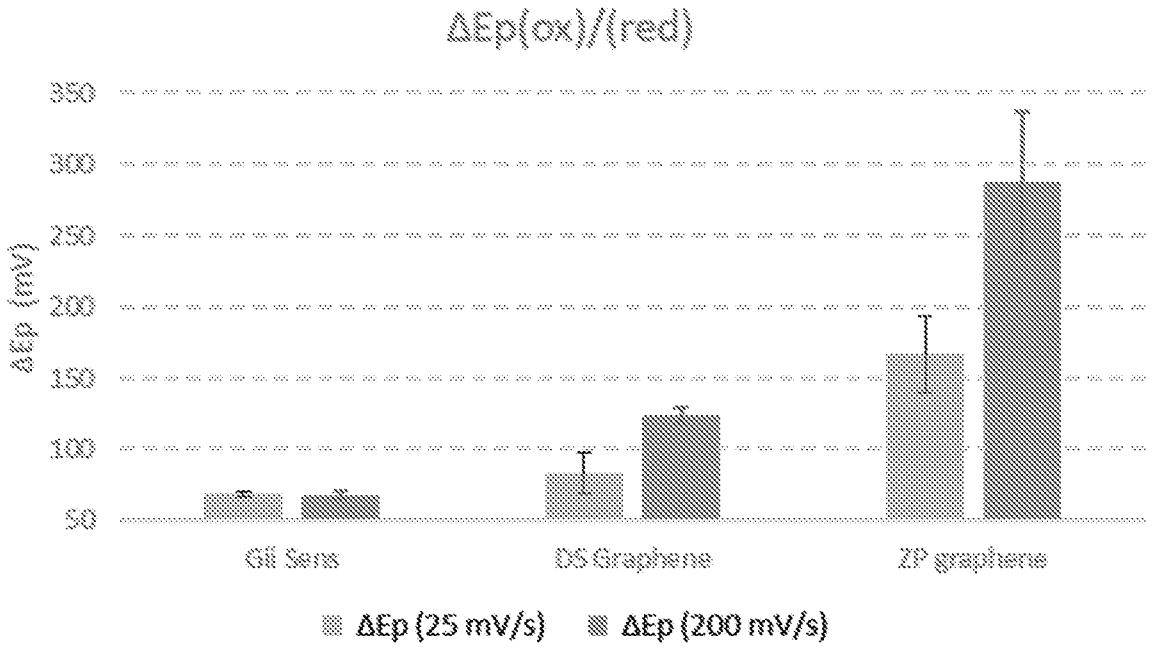


Figure 85

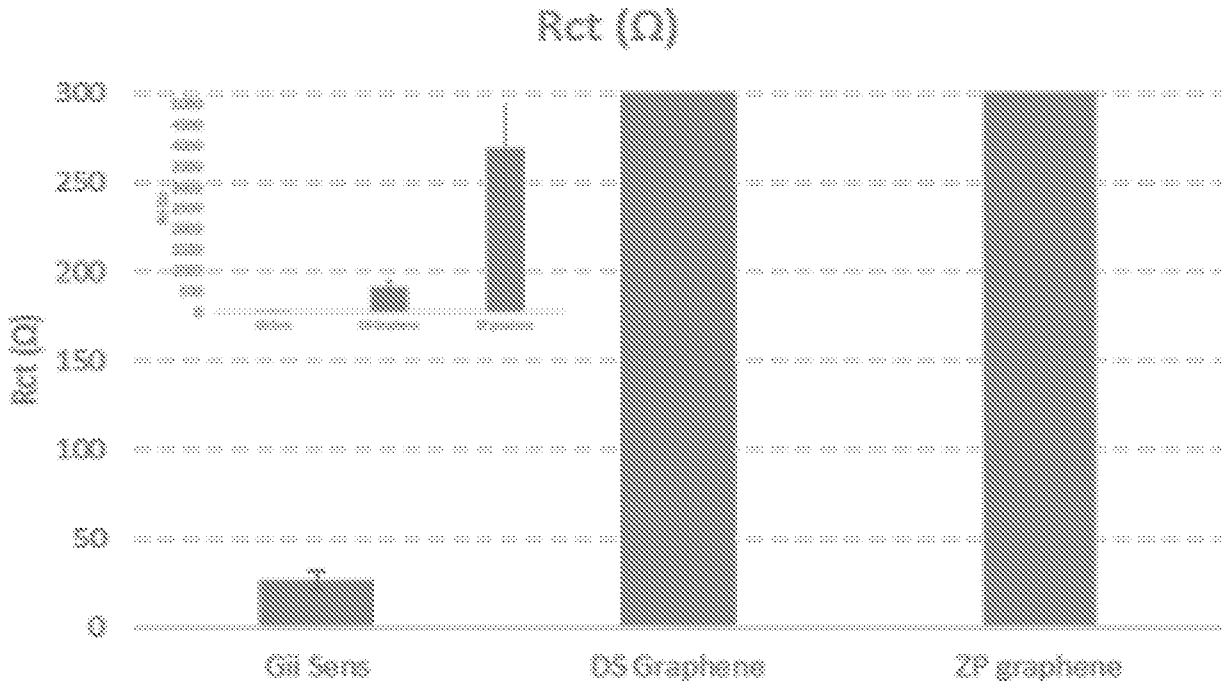


Figure 86

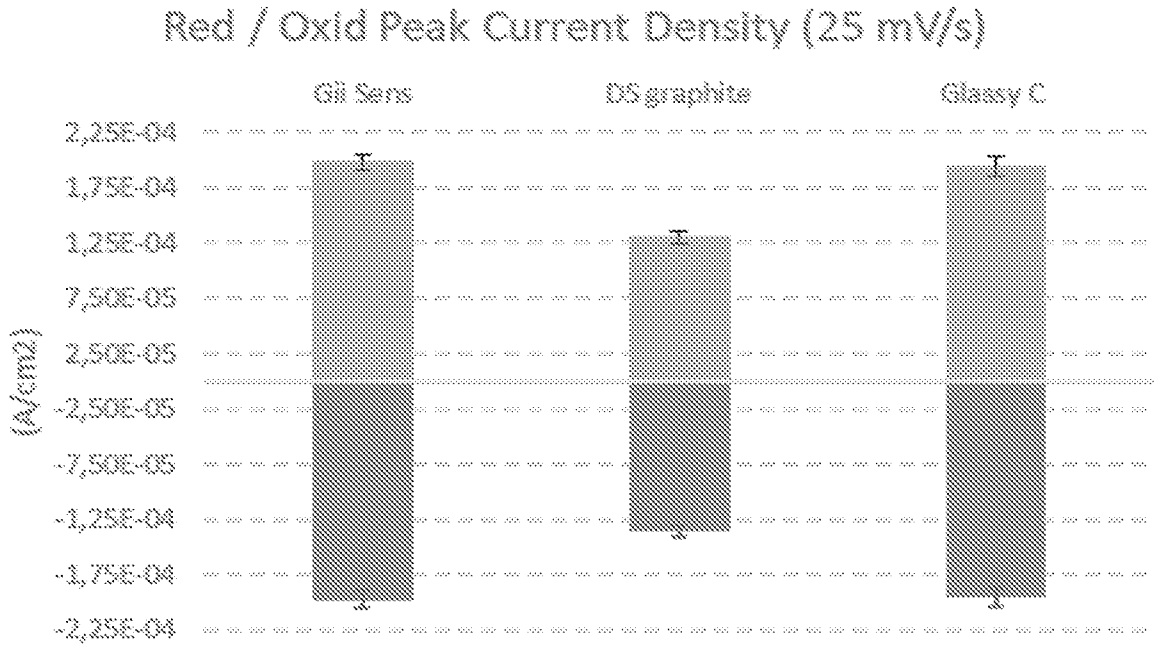


Figure 87

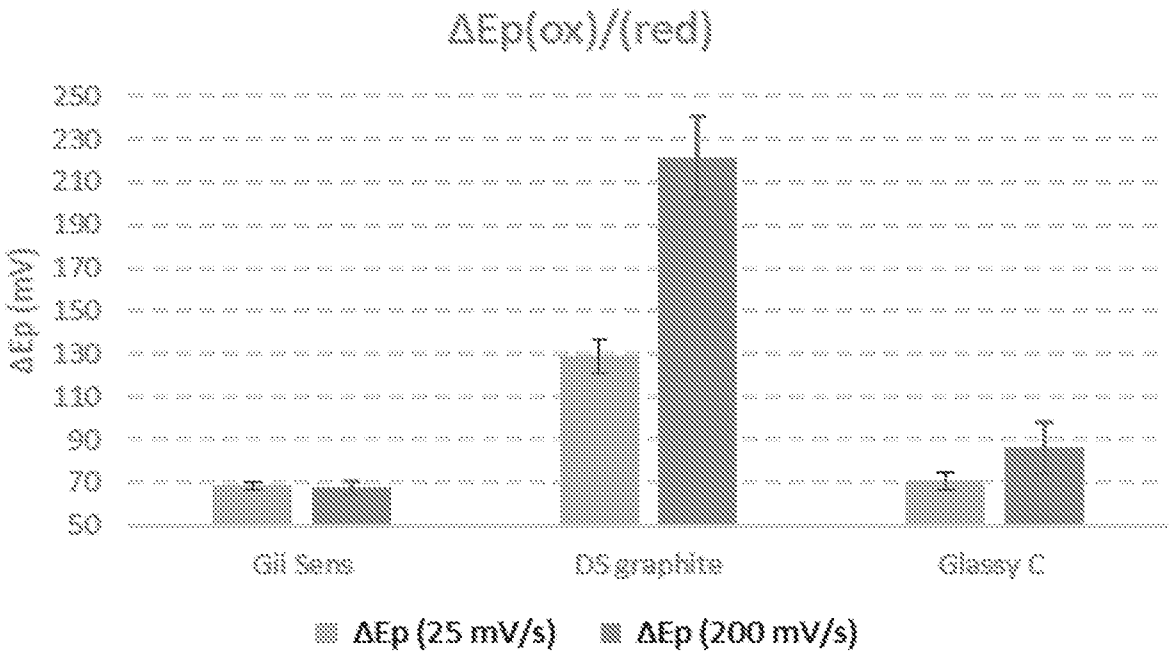


Figure 88

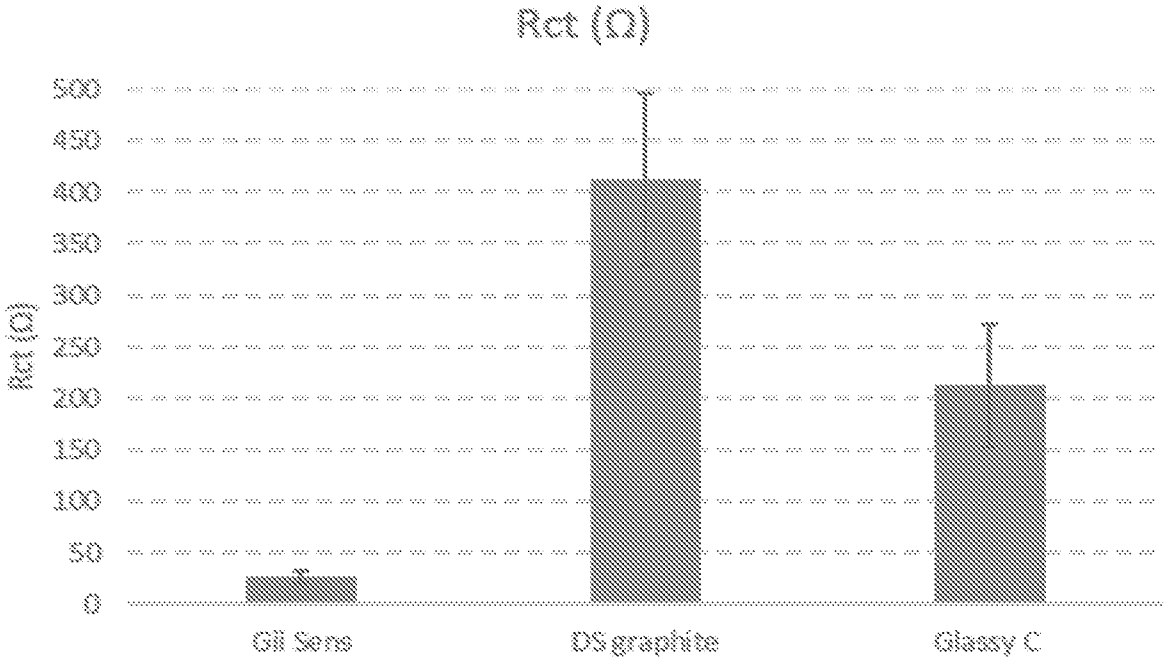


Figure 89

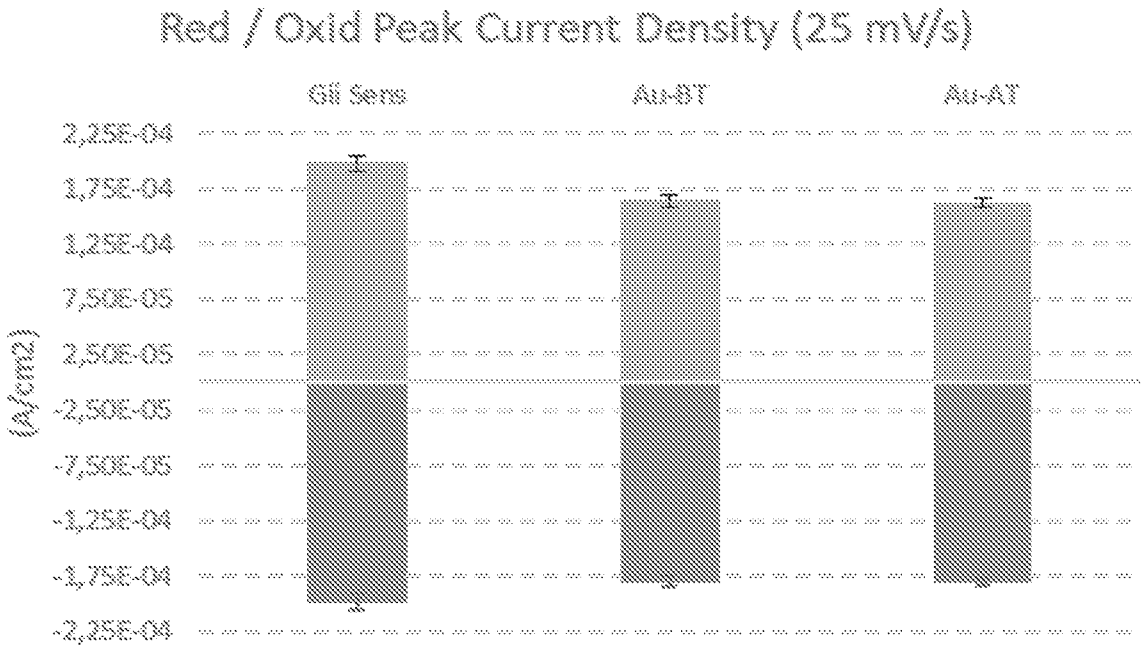


Figure 90

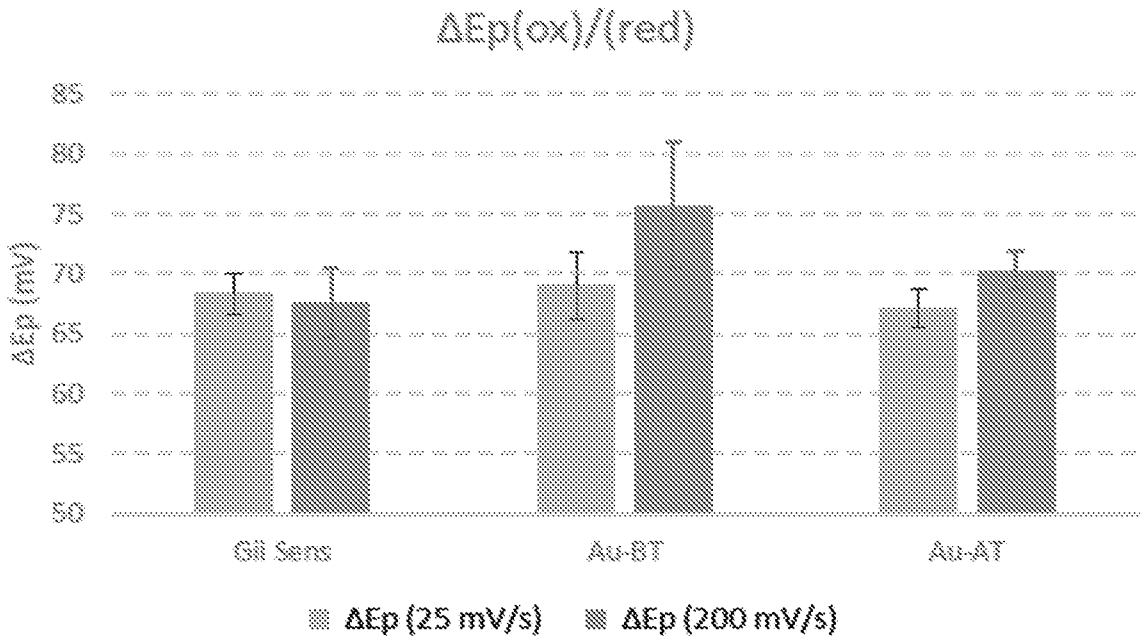


Figure 91

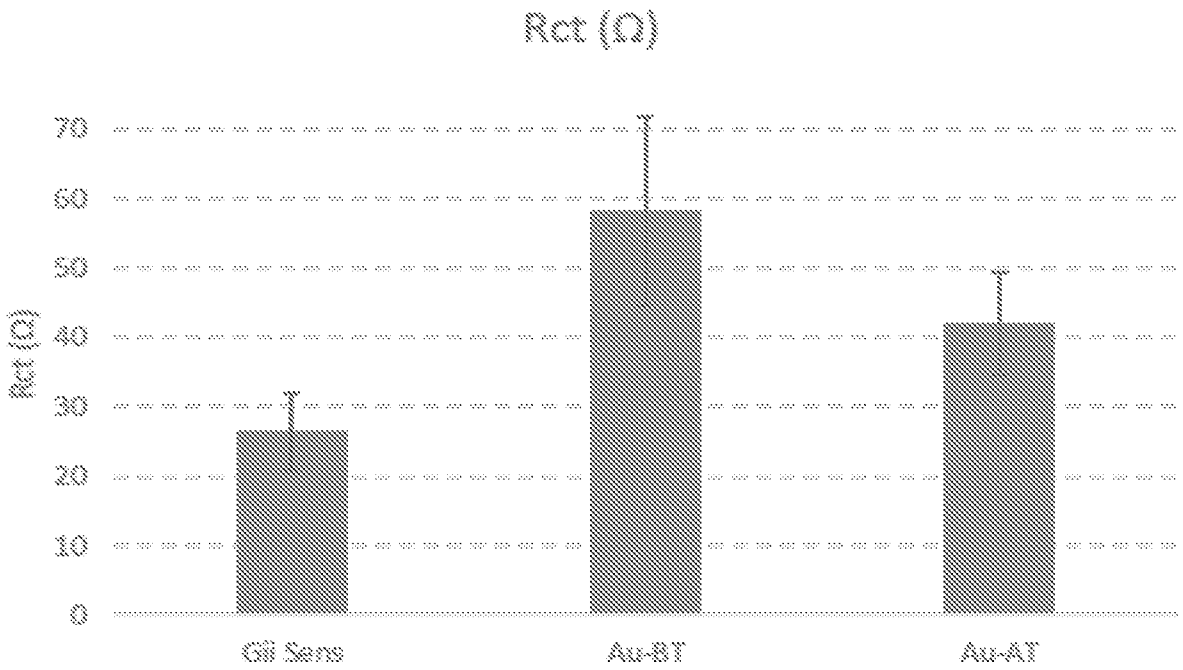


Figure 92

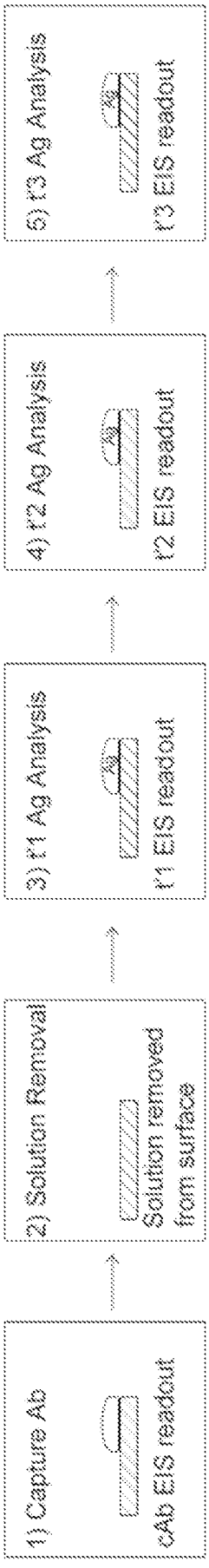

1) Capture Ab
cAb EIS readout
2) Solution Removal
Solution removed from surface
3) t1 Ag Analysis
t1 EIS readout
4) t2 Ag Analysis
t2 EIS readout
5) t3 Ag Analysis
t3 EIS readout

Figure 93

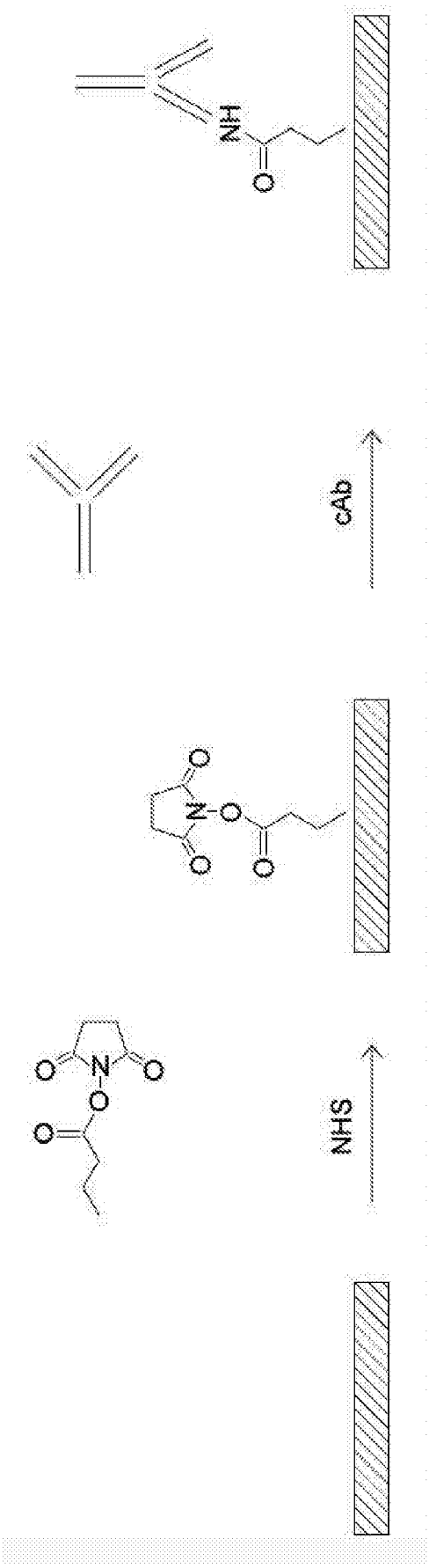


Figure 94

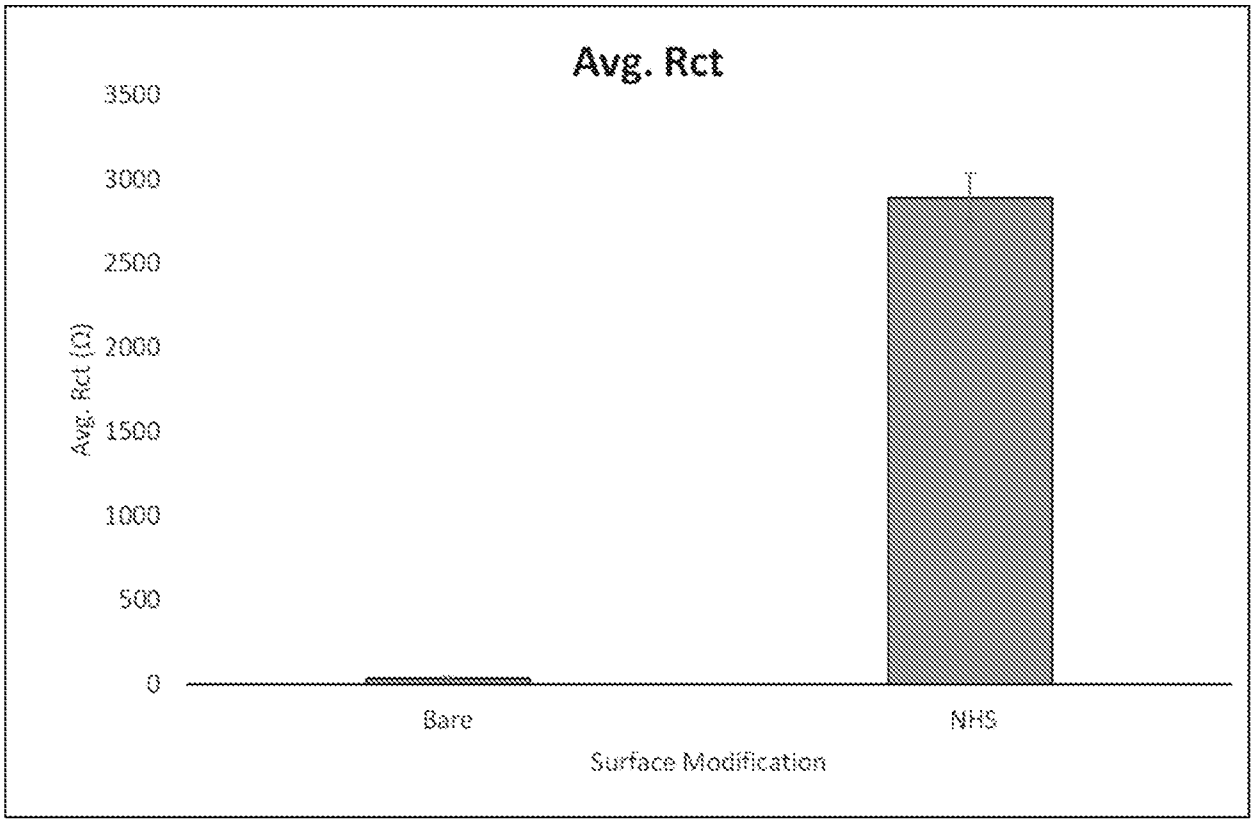

Avg. Rct
3500
3000
2500
2000
1500
1000
500
0
Avg. Rct (Ω)
Bare
NHS
Surface Modification

Figure 95

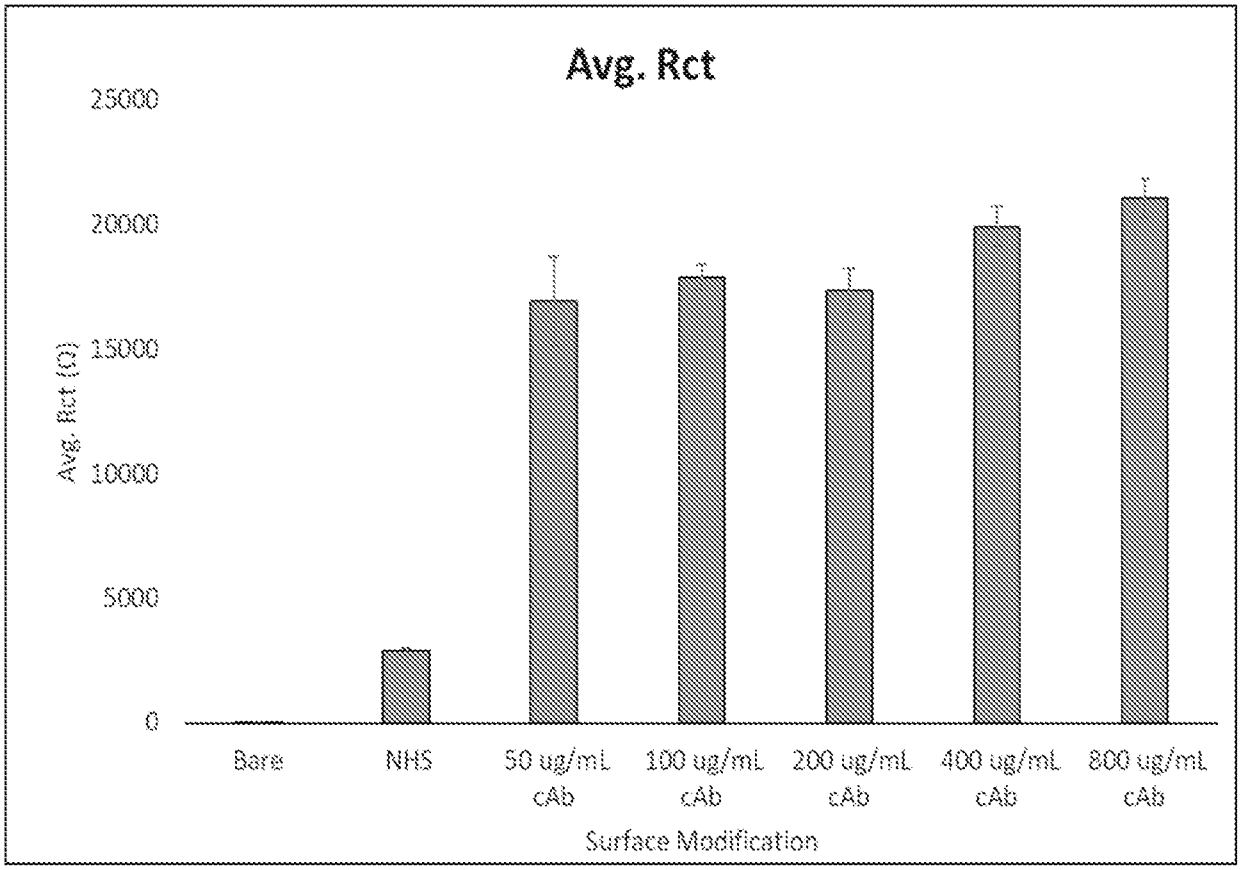
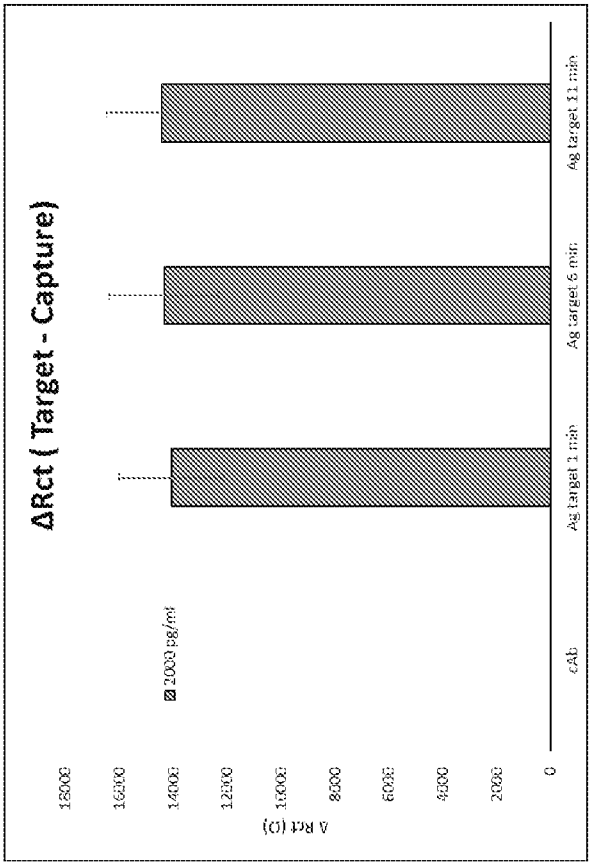

Avg. Rct
25000
20000
15000
10000
5000
0
Avg. Rct (Ω)
Bare
NHS
50 ug/mL cAb
100 ug/mL cAb
200 ug/mL cAb
400 ug/mL cAb
800 ug/mL cAb
Surface Modification

Figure 96


ΔRct (Target - Capture)
Δ Rct (Ω)
18000
16000
14000
12000
10000
8000
6000
4000
2000
0
2000 pg/ml
cAb
Ag target 1 min
Ag target 6 min
Ag target 11 min

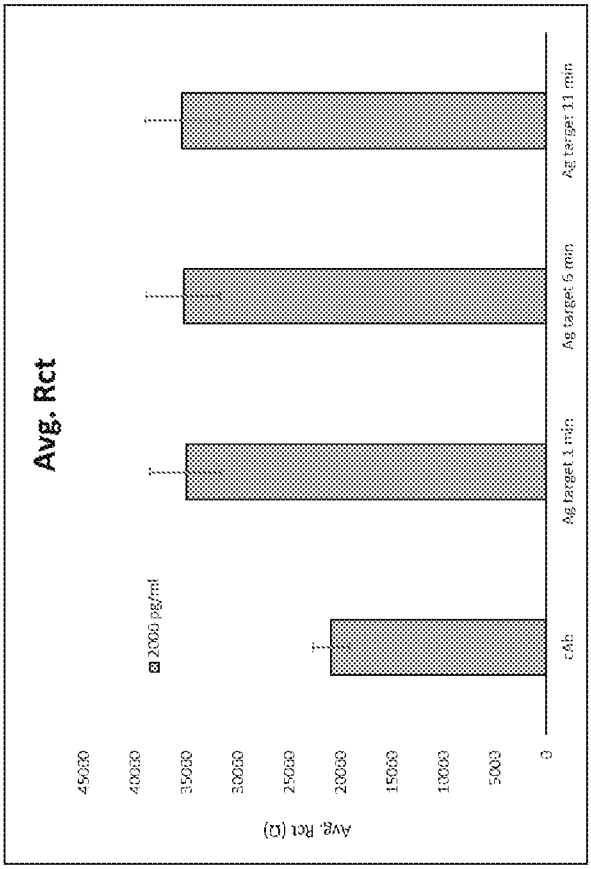

Avg. Rct
Avg. Rct (Ω)
45000
40000
35000
30000
25000
20000
15000
10000
5000
0
2000 pg/ml
cAb
Ag target 1 min
Ag target 6 min
Ag target 11 min

Figure 97

INTERNATIONAL SEARCH REPORT

International application No
PCT/GB2022/053345

A. CLASSIFICATION OF SUBJECT MATTER
INV. C01B32/15 C01B32/05 C01B32/152 C01B32/18 C01B32/182
ADD.

According to International Patent Classification (IPC) or to both national classification and IPC

B. FIELDS SEARCHED

Minimum documentation searched (classification system followed by classification symbols)
C01B

Documentation searched other than minimum documentation to the extent that such documents are included in the fields searched

Electronic data base consulted during the international search (name of data base and, where practicable, search terms used)
EPO-Internal, WPI Data

C. DOCUMENTS CONSIDERED TO BE RELEVANT

Category*	Citation of document, with indication, where appropriate, of the relevant passages	Relevant to claim No.
X	RODE A V ET AL: "Formation of cluster-assembled carbon nano-foam by high-repetition-rate laser ablation", APPLIED PHYSICS A, SPRINGER BERLIN HEIDELBERG, BERLIN/HEIDELBERG, vol. A70, no. 2, 21 January 2000 (2000-01-21), pages 135-144, XP002314578, ISSN: 0947-8396, DOI: 10.1007/S003390050025 1.2 Carbon foam formation in AS ambient the whole document	175-187
X	EP 2 769 967 A1 (ENVIRONMENT ENERGY NANO TECHNICAL RES INST [JP]) 27 August 2014 (2014-08-27) paragraph [0026] the whole document	175-187

-/--

[x] Further documents are listed in the continuation of Box C.

[x] See patent family annex.

* Special categories of cited documents :

"A" document defining the general state of the art which is not considered to be of particular relevance

"E" earlier application or patent but published on or after the international filing date

"L" document which may throw doubts on priority claim(s) or which is cited to establish the publication date of another citation or other special reason (as specified)

"O" document referring to an oral disclosure, use, exhibition or other means

"P" document published prior to the international filing date but later than the priority date claimed

"T" later document published after the international filing date or priority date and not in conflict with the application but cited to understand the principle or theory underlying the invention

"X" document of particular relevance;; the claimed invention cannot be considered novel or cannot be considered to involve an inventive step when the document is taken alone

"Y" document of particular relevance;; the claimed invention cannot be considered to involve an inventive step when the document is combined with one or more other such documents, such combination being obvious to a person skilled in the art

"&" document member of the same patent family

Date of the actual completion of the international search	Date of mailing of the international search report
9 March 2023	20/03/2023

Name and mailing address of the ISA/	Authorized officer
European Patent Office, P.B. 5818 Patentlaan 2 NL - 2280 HV Rijswijk Tel. (+31-70) 340-2040, Fax: (+31-70) 340-3016	Straub, Thomas

1

Form PCT/ISA/210 (second sheet) (April 2005)

INTERNATIONAL SEARCH REPORT

International application No
PCT/GB2022/053345

C(Continuation). DOCUMENTS CONSIDERED TO BE RELEVANT

Category*	Citation of document, with indication, where appropriate, of the relevant passages	Relevant to claim No.
X	RO 135 060 A2 (INSTITUTUL NAT DE CERCETARE DEZVOLTARE PENTRU FIZICA LASERILOR PLASMEI) 30 June 2021 (2021-06-30) paragraphs [0027], [0028] the whole document	175-187
X	LIN JIAN ET AL: "Laser-induced porous graphene films from commercial polymers", NATURE COMMUNICATIONS, vol. 5, no. 1, 1 December 2014 (2014-12-01), XP055878437, DOI: 10.1038/ncomms6714 Retrieved from the Internet: URL:http://www.nature.com/articles/ncomms6714> abstract the whole document Methods	175-187
Y	US 2019/308880 A1 (TOUR JAMES M [US] ET AL) 10 October 2019 (2019-10-10) claims 1,3, 6, 7, 18 the whole document	1-174
Y	GB 2 585 842 A (PARAGRAF LTD [GB]) 27 January 2021 (2021-01-27) page 18, line 20 - page 19, line 11 the whole document	1-174

1

INTERNATIONAL SEARCH REPORT

Information on patent family members

International application No
PCT/GB2022/053345

Patent document cited in search report	Publication date	Patent family member(s)	Publication date
EP 2769967 A1	27-08-2014	CN 104010990 A	27-08-2014
		EP 2769967 A1	27-08-2014
		JP 6263387 B2	17-01-2018
		JP WO2013058382 A1	02-04-2015
		US 2014329076 A1	06-11-2014
		WO 2013058382 A1	25-04-2013
RO 135060 A2	30-06-2021	NONE	
US 2019308880 A1	10-10-2019	US 2019308880 A1	10-10-2019
		WO 2018017369 A2	25-01-2018
GB 2585842 A	27-01-2021	GB 2585842 A	27-01-2021
		TW 202108502 A	01-03-2021
		US 2022267896 A1	25-08-2022
		WO 2021008937 A1	21-01-2021

(19)国家知识产权局

(12)发明专利申请

(10)申请公布号 CN 118742511 A
(43)申请公布日 2024.10.01

(21)申请号 202280085628.9

(22)申请日 2022.12.21

(30)优先权数据
2118948.5 2021.12.23 GB
2202353.5 2022.02.22 GB
2202356.8 2022.02.22 GB
2202357.6 2022.02.22 GB
2202360.0 2022.02.22 GB
2202362.6 2022.02.22 GB
2202364.2 2022.02.22 GB
2202366.7 2022.02.22 GB
2202369.1 2022.02.22 GB
2202372.5 2022.02.22 GB
2202375.8 2022.02.22 GB
2202376.6 2022.02.22 GB
2202380.8 2022.02.22 GB
2202382.4 2022.02.22 GB
2202384.0 2022.02.22 GB
2202387.3 2022.02.22 GB
2202388.1 2022.02.22 GB
2202389.9 2022.02.22 GB

(85)PCT国际申请进入国家阶段日
2024.06.24

(86)PCT国际申请的申请数据
PCT/GB2022/053345 2022.12.21

(87)PCT国际申请的公布数据
WO2023/118866 EN 2023.06.29

(71)申请人 集成石墨烯控股有限公司
地址 英国

(72)发明人 M·卡菲奥 O·森普尔 D·凯恩斯

(74)专利代理机构 北京连和连知识产权代理有限公司 11278
专利代理师 刘小峰 杨帆

(51)Int.Cl.
C01B 32/15(2006.01)
C01B 32/05(2006.01)
C01B 32/152(2006.01)
C01B 32/18(2006.01)
C01B 32/182(2006.01)

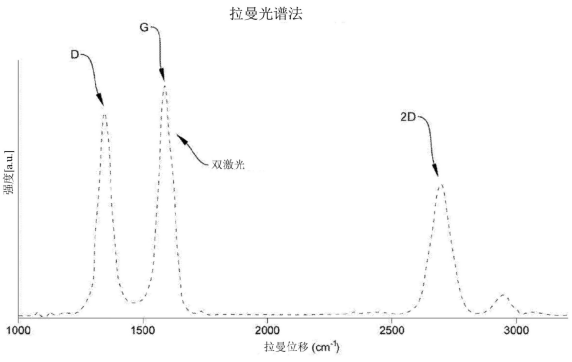
权利要求书13页 说明书87页 附图103页

(54)发明名称

激光诱导的碳纳米结构

(57)摘要

公开了一种制造碳纳米结构、诸如碳泡沫材料的方法。所述方法包括以下步骤:(a)使用第一激光束照射碳前体材料的、在所述材料的表面下方的封装区域或表面下区域,以在所述表面下区域中产生碳泡沫并且在所述碳泡沫上方产生无序无定形非石墨烯材料,然后(b)使用第二激光束去除或烧蚀位于所述碳泡沫上方的所述无序无定形非石墨烯材料,以暴露所述碳泡沫中的至少一些。所得碳泡沫材料显示出显著的D峰;2D峰显著小于G峰;并且D峰:G峰的比率显著高于零。在外观和拉曼特征签名方面,所述碳泡沫材料似乎类似于碳纳米洋葱材料。所述碳泡沫材料可以用于生物传感器、超级电容器和赝电容器中。



CN 118742511 A

1.一种碳泡沫材料的制造方法,包括以下步骤:

(a)使用第一激光束照射碳前体材料的、在所述材料的表面下方的封装区域或表面下区域,以在所述表面下区域中产生碳泡沫并且在所述碳泡沫上方产生无序无定形非石墨烯材料,然后

(b)使用第二激光束去除或烧蚀位于所述碳泡沫上方的所述无序无定形非石墨烯材料,以暴露所述碳泡沫中的至少一些。

第一激光束参数和控制方案

2.如权利要求1所述的方法,其中所述第一激光束在第一波段下操作,并且所述第二激光束在第二波段下操作。

3.如前述权利要求中任一项所述的方法,其中所述第一激光束和所述第二激光束通过不同的激光系统产生。

4.如前述权利要求中任一项所述的方法,其中所述第一激光束和所述第二激光束通过同一激光系统产生。

5.如前述权利要求中任一项所述的方法,其中照射所述表面下区域或封装区域的所述第一激光束的参数包括以下中的一者或多者:强度、波长、脉冲频率、脉冲持续时间、脉冲轮廓、扫描速度、焦距、在所述表面下区域或封装区域产生的热。

6.如前述权利要求中任一项所述的方法,其中改变所述第一激光束的激光参数使所述碳泡沫材料的性质改变,从而能够生产出具有针对不同应用而优化的性质的碳泡沫。

7.如前述权利要求中任一项所述的方法,其中改变所述第一激光束的激光参数使以下碳泡沫材料性质或参数中的一者或多者改变:存在的碳纳米结构的类型、缺陷的大小、缺陷的分布、缺陷的程度、缺陷的类型、拉曼D和2D峰、拉曼D和2D峰的相对大小、厚度或深度、柔韧性、粘附性、孔隙率、电导率、电容、有机溶剂和水基溶液的吸收、亲水性、EMI屏蔽、电极质量、可润湿性、接触角、防污性。

8.如前述权利要求中任一项所述的方法,其中通过所述第一激光束未产生通向所述前体材料的表面的实质气体逸出通道。

9.如前述权利要求中任一项所述的方法,其中所述第一激光束在所述表面下区域或封装区域产生高于500℃的温度以形成碳泡沫。

10.如前述权利要求中任一项所述的方法,其中所述第一激光束的脉冲持续时间在1ns与10μs之间,从而给出在约5×10^{7}℃/s与2×10^{12}℃/s之间的加热速率。

11.如前述权利要求中任一项所述的方法,其中所述第一激光束的功率在8瓦特至20瓦特的典型工作范围,最佳为12W。

12.如前述权利要求中任一项所述的方法,其中所述第一激光束的焦距在50mm-400mm的典型工作范围。

13.如前述权利要求中任一项所述的方法,其中所述第一激光束的脉冲频率在50kHz与500kHz之间。

14.如前述权利要求中任一项所述的方法,其中所述第一激光束的脉冲频率在1kHz与2MHz之间。

15.如前述权利要求中任一项所述的方法,其中所述第一激光束的波长在0.7μm-2.5μm之间。

16.如前述权利要求中任一项所述的方法,其中所述第一激光以在9cm/s与40cm/s之间的范围或这些范围的±50%扫描。

17.如前述权利要求中任一项所述的方法,其中所述第一激光束的参数包括焦点参数。

18.如前述权利要求中任一项所述的方法,其中所述第一激光束的参数包括衍射参数。

19.如前述权利要求中任一项所述的方法,其中所述第一激光束的参数包括干涉图案参数。

20.如前述权利要求中任一项所述的方法,其中所述第一激光束的焦点移动穿过所述碳前体材料的深度,以在所述碳前体的所述表面下区域或封装区域中产生碳泡沫。

21.如前述权利要求中任一项所述的方法,其中所述第一激光束的焦点移动穿过所述碳前体材料的深度至少约50μm,以在所述碳前体的所述表面下区域或封装区域中产生碳泡沫。

22.如前述权利要求中任一项所述的方法,其中所述第一激光束的焦点移动穿过所述碳前体材料的深度至少100μm,以在所述碳前体的所述表面下区域或封装区域中产生碳泡沫。

23.如前述权利要求中任一项所述的方法,其中所述第一激光束在所述碳前体材料上扫描、例如光栅扫描,或侧向移动,以形成所需图案。

24.如前述权利要求中任一项所述的方法,其中所述第一激光束在所述碳前体材料上扫描或侧向移动,以形成包括非重叠区域或线的所需图案。

25.如前述权利要求中任一项所述的方法,其中所述第一激光束在所述碳前体材料上重复地扫描(例如,光栅扫描)或侧向移动,其中焦点或强度最大值被布置在所述碳前体材料内的多个不同深度,直到产生具有所需图案和深度的碳泡沫。

26.如前述权利要求中任一项所述的方法,其中所述第一激光束以在1.7mm/s与3550m/s之间或更通常在35mm/s与350mm/s之间的扫描速率下扫描,并且所述扫描可以使得每英寸脉冲数(PPI)在100与10000之间(与生产个别近似于大小为220mm×180mm的聚酰亚胺片材有关)。

27.如前述权利要求中任一项所述的方法,其中所述第一激光束具有基本上不被所述碳前体材料吸收或者被所述碳前体材料以极低的吸收率吸收的波长。

28.如前述权利要求中任一项所述的方法,其中所述第一激光束具有被所述碳前体材料以极低的吸收率吸收的波长。

29.如前述权利要求中任一项所述的方法,其中所述碳前体材料的每厘米辐射吸收率(10进制)低于50、或低于20、或低于10。

30.如前述权利要求中任一项所述的方法,其中所述第一激光束是IR激光。

31.如前述权利要求中任一项所述的方法,其中所述第一激光束是具有在0.7μm-2.5μm之间的波长的IR激光。

32.如前述权利要求中任一项所述的方法,其中所述第一激光束是具有在0.75μm-1.40μm之间的波长的IR激光。

表面下区域或封装区域的属性

33.如前述权利要求中任一项所述的方法,其中所述碳前体材料中所述表面下区域或封装区域的所需深度通过将所述第一激光束的焦点移动穿过所述深度来实现。

34.如前述权利要求中任一项所述的方法,其中所述表面下区域或封装区域在所述碳前体材料的所述表面下方至少10μm。

35.如前述权利要求中任一项所述的方法,其中所述表面下区域或封装区域在所述碳前体材料的所述表面下方至少20μm。

36.如前述权利要求中任一项所述的方法,其中所述表面下区域或封装区域在所述碳前体材料的所述表面下方至少30μm。

37.如前述权利要求中任一项所述的方法,其中所述表面下区域或封装区域在所述碳前体材料的所述表面下方至少40μm。

38.如前述权利要求中任一项所述的方法,其中所述表面下区域或封装区域在所述碳前体材料的所述表面下方至少50μm。

39.如前述权利要求中任一项所述的方法,其中与常规石墨烯泡沫不同,所述表面下区域或封装区域的厚度能够超过约50μm。

40.如前述权利要求中任一项所述的方法,其中所述表面下区域或封装区域具有在10μm与200μm之间的厚度。

41.如前述权利要求中任一项所述的方法,其中所述表面下区域或封装区域能够面向入射激光在所述碳前体材料的所述表面下方的不同深度;并且所述表面下区域或封装区域所在的确切深度是各种因素的函数,所述因素诸如激光强度或其他激光参数以及对所使用的碳前体材料的选择。

42.如前述权利要求中任一项所述的方法,其中所述表面下区域或封装区域在所述碳前体材料的所述表面下方的距离是所述碳前体材料的总厚度的至少1%、或所述碳前体材料的总厚度的至少10%、或所述碳前体材料的总厚度的至少20%、或所述碳前体材料的总厚度的至少30%、或所述碳前体材料的总厚度的至少40%。

43.如前述权利要求中任一项所述的方法,其中所述表面下区域或封装区域是以所述第一激光束的最小横截面的中心为中心的一定体积的空间,并且所述体积在所述中心的500微米内、或在所述中心的100微米内、或在所述中心的1微米内。

碳前体材料

44.如前述权利要求中任一项所述的方法,其中所述碳前体材料基本上由热固性材料制成。

45.如前述权利要求中任一项所述的方法,其中所述碳前体材料基本上由非热塑性材料制成。

46.如前述权利要求中任一项所述的方法,其中所述碳前体材料是热固性膜。

47.如前述权利要求中任一项所述的方法,其中所述热固性膜是聚酰亚胺膜。

48.如前述权利要求中任一项所述的方法,其中所述碳前体是聚酰亚胺膜。

49.如前述权利要求中任一项所述的方法,其中所述碳前体是聚酰亚胺膜,并且所述第一激光的波长在0.7μm至2.5μm的范围内。

50.如前述权利要求中任一项所述的方法,其中所述碳前体是至少50质量%碳、或至少75质量%碳、或至少90质量%碳。

51.如前述权利要求中任一项所述的方法,其中所述碳前体是膜或片材。

52.如前述权利要求中任一项所述的方法,其中所述碳前体材料是柔性的。

53.如前述权利要求中任一项所述的方法,其中所述碳前体材料是印刷层,诸如丝网印刷层。

54.如前述权利要求中任一项所述的方法,其中所述碳前体材料的厚度大于5μm、或在5μm与120μm之间、或大于120μm。

55.如前述权利要求中任一项所述的方法,其中所述碳前体材料是基本上平面或平坦的,并且垂直于所述第一激光束取向。

56.如前述权利要求中任一项所述的方法,其中所述碳前体材料是均质的。

57.如前述权利要求中任一项所述的方法,其中所述碳前体材料是异质的,并且包含若干不同的材料。

58.如前述权利要求中任一项所述的方法,其中所述碳前体被支撑在基板上,所述基板不是由碳前体制成。

59.如前述权利要求中任一项所述的方法,其中所述碳前体材料在所述第一激光束波长下具有低吸收系数。

60.如前述权利要求中任一项所述的方法,其中所述碳前体材料对于所述第一激光束的吸收系数低于$50cm^{-1}$、或低于$20cm^{-1}$、或低于$10cm^{-1}$。

61.如前述权利要求中任一项所述的方法,其中所述碳前体材料对于所述第二或烧蚀激光束的吸收系数低于$300cm^{-1}$。

62.如前述权利要求中任一项所述的方法,其中所述碳前体材料对于所述第二或烧蚀激光束的吸收系数为$300\pm50cm^{-1}$。

63.如前述权利要求中任一项所述的方法,其中所述碳前体材料的热导率小于1.0W/mK(使用根据ASTM D5470的方法)。

64.如前述权利要求中任一项所述的方法,其中所述碳前体材料的热导率小于0.5W/mK(使用根据ASTM D5470的方法)。

65.如前述权利要求中任一项所述的方法,其中所述碳前体材料安装在基板上,所述基板在所述激光束的一个或多个波长下是基本上光学透明的。

66.如前述权利要求中任一项所述的方法,其中所述碳前体材料的碳源包含一种或多种聚合物或由其形成。

67.如前述权利要求中任一项所述的方法,其中所述碳前体材料包含以下材料中的一者或多者:聚酰亚胺类(例如,聚(4,4'-氧二亚苯基-均苯四甲酸二胺),另外还称为聚酰亚胺)、聚醚酰亚胺类(PEI)、聚(甲基丙烯酸甲酯)类(PMMA)(例如,喷涂的PMMA)、聚氨酯类(PU)、聚酯类、乙烯基聚合物类、碳化聚合物类、光阻聚合物类、醇酸树脂类、脲醛。

68.如前述权利要求中任一项所述的方法,其中所述碳前体包含以下材料中的一者或多者:聚(酰胺酸)类(例如,含芳基的聚(酰胺酸))(例如,聚(均苯四甲酸二酐-共-4,4'-氧二苯胺),酰胺酸,另外还称为聚酰胺酸);二酐类(例如,芳基二酐)(例如,均苯四甲酸二酐);所述聚(酰胺酸)类的衍生物;所述二酐类的衍生物(例如,均苯四甲酸二酐的衍生物)。

69.如前述权利要求中任一项所述的方法,其中所述碳前体包含以下材料中的一者或多者:芳香族材料(例如,芳香族聚合物);杂芳香族材料(例如,杂芳香族聚合物);含有芳香族部分的聚合物;环状材料(例如,含有环状部分的聚合物);杂环材料(例如,含有杂环部分的聚合物);杂芳香族材料(例如,含有杂芳香族部分的聚合物)。

70.如前述权利要求中任一项所述的方法,其中所述碳前体包含含有芳香键、或杂芳香键、或杂键(例如,酰亚胺键)中的一者或多者的材料。

支撑碳前体材料的基板

71.如前述权利要求中任一项所述的方法,其中所述碳前体被定位在基板上或与基板相邻。

72.如前述权利要求中任一项所述的方法,其中所述碳前体被定位在所述基板“上方”(例如,所述碳前体被定位成比所述基板更靠近激光源)。

73.如前述权利要求中任一项所述的方法,其中所述碳前体被定位在所述基板“下方”(例如,所述碳前体被定位成比所述基板更远离激光源)。

74.如前述权利要求中任一项所述的方法,其中所述基板是塑料主体、膜或箔。

75.如前述权利要求中任一项所述的方法,其中所述基板是柔性的。

76.如前述权利要求中任一项所述的方法,其中所述基板是聚酰亚胺电路板。

77.如前述权利要求中任一项所述的方法,其中所述基板对所述第一激光束具有极低的吸收率。

78.如前述权利要求中任一项所述的方法,其中所述基板在所述第一激光束的一个或多个波长下是基本上光学透明的。

79.如前述权利要求中任一项所述的方法,其中所述基板对所述第一激光束具有高的吸收率,吸收大于60%的所述第一激光束。

80.如前述权利要求中任一项所述的方法,其中所述基板对所述第一激光束具有高的吸收率,吸收大于60%的所述第一激光束,并且具有至少10W/mK的热导率。

81.如前述权利要求中任一项所述的方法,其中所述碳前体材料的所述表面通过所述激光束转化为无序无定形非石墨烯物质,并且所述无序无定形非石墨烯物质粘附或粘合至基板,并且因此将所述3D碳材料泡沫间接地附接至所述基板。

82.如前述权利要求中任一项所述的方法,其中所述基板由以下中的一者或多者形成:硅(Si)、二氧化硅(SiO_2)、氮化镓(GaN)、砷化镓(GaAs)、氧化锌(ZnO)。

83.如前述权利要求中任一项所述的方法,其中所述基板是硅晶圆。

84.如前述权利要求中任一项所述的方法,其中所述基板是二氧化硅晶圆。

85.如前述权利要求中任一项所述的方法,其中所述基板是包含硅和二氧化硅二者的晶圆。

86.如前述权利要求中任一项所述的方法,其中所述基板是碳源。

87.如前述权利要求中任一项所述的方法,其中所述基板不是碳源,例如,金属、电介质材料、丝网印刷电介质材料。

在激光束入射的表面处的碳化

88.如前述权利要求中任一项所述的方法,其中所述碳前体材料的所述表面通过所述第一激光束转化为无序无定形非石墨烯物质。

89.如前述权利要求中任一项所述的方法,其中所述无序无定形非石墨烯物质占据自所述碳前体材料的所述表面起所述碳前体材料的总厚度的约1%、或小于约1%、或小于约5%、或小于约10%的厚度。

90.如前述权利要求中任一项所述的方法,其中所述无序无定形非石墨烯物质占据自

所述碳前体材料的所述表面起至少10μm的厚度。

91.如前述权利要求中任一项所述的方法,其中所述无序无定形非石墨烯物质从其外表面向所述碳前体材料的主体中延伸至10μm或更小的深度、或20μm或更小的深度、或30μm或更小的深度、或40μm或更小的深度、或50μm或更小的深度、或100μm或更小的深度。

在与支撑碳前体材料的基板的物理界面处的碳化

92.如前述权利要求中任一项所述的方法,其中所述碳前体被定位在基板上或与基板相邻。

93.如前述权利要求中任一项所述的方法,其中所述碳前体材料在与所述基板的物理界面处通过所述激光束转化为无序无定形非石墨烯物质至由所述激光束的参数限定的深度。

94.如前述权利要求中任一项所述的方法,其中所述无序无定形非石墨烯物质处于粘附或以其他方式附接至所述碳泡沫的一个区域和粘附或以其他方式附接至所述基板的另一区域,因此为所述碳泡沫提供稳定性。

95.如前述权利要求中任一项所述的方法,其中所述无序无定形非石墨烯物质所占据的从所述碳前体材料与所述基板的界面测量的厚度为所述碳前体材料的总厚度的约1%、或小于约1%、或小于约5%、或小于约10%。

96.如前述权利要求中任一项所述的方法,其中所述无序无定形非石墨烯物质所占据的自所述碳前体材料与所述基板的界面起的厚度为至少10μm。

97.如前述权利要求中任一项所述的方法,其中所述无序无定形非石墨烯物质从所述碳前体材料与所述基板的界面延伸至10μm或更小的深度、或20μm或更小的深度、或30μm或更小的深度、或40μm或更小的深度、或50μm或更小的深度、或100μm或更小的深度。

烧蚀激光束或第二激光束

98.如前述权利要求中任一项所述的方法,其中所述第二激光束的参数包括以下中的一者或多者:强度、波长、脉冲频率、脉冲持续时间、脉冲轮廓、扫描速度、焦距、在所述表面下区域或封装区域产生的热。

99.如前述权利要求中任一项所述的方法,其中改变所述第二激光参数使所述碳泡沫材料的性质改变,从而能够生产出具有针对不同应用而优化的性质的碳泡沫。

100.如前述权利要求中任一项所述的方法,其中改变所述第二激光束的所述激光参数使以下碳泡沫材料的性质或参数中的一者或多者改变:存在的碳纳米结构的类型、缺陷的大小、缺陷的分布、缺陷的程度、缺陷的类型、拉曼D和2D峰、拉曼D和2D峰的相对大小、厚度或深度、柔韧性、粘附性、孔隙率、电导率、电容、有机溶剂和水基溶液的吸收、亲水性、EMI屏蔽、电极质量、可润湿性、接触角、防污性。

101.如前述权利要求中任一项所述的方法,其中所述第二激光束是CO_2激光。

102.如前述权利要求中任一项所述的方法,其中所述第二激光束改变所述碳泡沫,作为使其暴露的工艺的一部分。

103.如前述权利要求中任一项所述的方法,其中所述第二激光束改变所述碳泡沫的形态,作为使其暴露的工艺的一部分。

104.如前述权利要求中任一项所述的方法,其中所述第二激光束被自动控制以在相同区域、和/或重叠区域、和/或非重叠区域上扫描。

105.如前述权利要求中任一项所述的方法,其中烧蚀所述无定形非石墨烯物质的所述第二激光束的波长在8μm-15μm之间。

106.如前述权利要求中任一项所述的方法,其中所述第二激光束是长IR激光、或UV激光、或可见光激光。

107.如前述权利要求中任一项所述的方法,其中所述第二激光束的脉冲频率在50kHz与500kHz之间,并且扫描速度在9cm/s与40cm/s之间。

108.如前述权利要求中任一项所述的方法,其中所述碳前体材料对于所述第二激光束的吸收系数高于100cm^{-1},或对于所述第二激光束的吸收系数高于200cm^{-1}。

109.如前述权利要求中任一项所述的方法,其中所述碳前体材料对于所述第二激光束的吸收系数为300±50cm^{-1}。

110.如前述权利要求中任一项所述的方法,其中所述激光功率在8瓦特至20瓦特的典型工作范围内,最佳为12W。

111.如前述权利要求中任一项所述的方法,其中所述第二激光焦距在50mm-400mm的典型工作范围内。

112.如前述权利要求中任一项所述的方法,其中所述第二激光束以包括非重叠区域或线的图案(例如,光栅)扫描。

113.如前述权利要求中任一项所述的方法,其中所述第二激光束以与所述第一激光束的扫描图案匹配的图案扫描。

114.如前述权利要求中任一项所述的方法,其中所述第二激光束是散焦的。

115.如前述权利要求中任一项所述的方法,其中所述第二激光束与照射碳前体材料的所述封装区域或表面下区域的所述激光束相同,以在所述封装区域或表面下区域中产生碳泡沫。

116.如前述权利要求中任一项所述的方法,其中所述制造工艺是三阶段工艺,其包括以下步骤:(a)所述第一激光束在制造场所照射碳前体材料的表面下区域,以产生未完成的碳泡沫产品;(b)将所述未完成的碳泡沫产品转移至客户控制的制造场所;以及(c)在所述客户控制的制造场所进行激光烧蚀或处理。

碳泡沫

117.如前述权利要求中任一项所述的方法,其中所述碳泡沫是多层扭转或乱层碳泡沫,或包括多层扭转或乱层碳泡沫。

118.如前述权利要求中任一项所述的方法,其中所述碳泡沫是非石墨烯碳泡沫,或包括非石墨烯碳泡沫。

119.如前述权利要求中任一项所述的方法,其中所述碳泡沫包括碳质纳米结构,诸如碳纳米洋葱、碳纳米角、碳纳米管、碳纳米点、纳米金刚石和富勒烯、或其任何组合。

120.如前述权利要求中任一项所述的方法,其中所述碳泡沫的厚度为至少约50μm。

121.如前述权利要求中任一项所述的方法,其中所述碳泡沫的厚度在约50μm至300μm之间。

122.如前述权利要求中任一项所述的方法,其中所述碳泡沫是或包括具有导致高电化学反应性的缺陷的空间分布的碳泡沫。

123.如前述权利要求中任一项所述的方法,其中所述碳泡沫是或包括具有导致高电化

学反应性的空位基面缺陷的碳泡沫。

124.如前述权利要求中任一项所述的方法,其中所述碳泡沫的碳:氧比率在25:1与50:1之间。

125.如前述权利要求中任一项所述的方法,其中所述碳泡沫具有快速电子转移常数。

126.如前述权利要求中任一项所述的方法,其中与使用常规激光工艺制成的常规石墨烯泡沫相比,所述碳泡沫具有以下性质中的一者或多者:厚度或深度更容易控制;与使用常规激光工艺制成的高脆性石墨烯相比,柔韧性更大;对下层柔性基板的粘附性更强;孔隙率更高;电导率更高;电容或电荷存储增加;对有机溶剂和水基溶液的吸收更快;亲水性更高;接触角低于约20°;防污性能增强;EMI屏蔽更高;电极质量增强。

生物传感器用例

127.如前述权利要求中任一项所述的方法,其中所述碳泡沫被功能化为生物传感器。

128.如前述权利要求中任一项所述的方法,其中所述碳泡沫通过添加对目标或分析物具有特异性的受体而被功能化为生物传感器。

129.如前述权利要求中任一项所述的方法,其中所述碳泡沫被功能化为具有可逆聚合物位移传感器机构的生物传感器,用于电化学葡萄糖监测。

130.如前述权利要求中任一项所述的方法,其中所述可逆聚合物位移传感器包括针对被吸附到包括所述碳泡沫的电极上的葡萄糖的芘衍生硼酸化学受体。

131.如前述权利要求中任一项所述的方法,其中通过添加对目标或分析物具有特异性的受体以及使所述受体能够附接至所述碳泡沫的接头来将所述碳泡沫功能化为生物传感器。

132.如前述权利要求中任一项所述的方法,其中所述接头选自纳米颗粒、聚合物、聚合物刷、配体、包含一个或多个官能团的有机化合物、共价或非共价键合至所述碳泡沫的分子、或其混合物。

133.如前述权利要求中任一项所述的方法,其中所述接头选自:聚合物,优选(甲基)丙烯酸酯聚合物;包含一个或多个官能团的有机化合物;碳二亚胺;重氮化合物;或其混合物。

134.如前述权利要求中任一项所述的方法,其中所述一个或多个官能团独立地选自:氧、氮、硫、卤化物、羟基、羰基、羧基、胺、氨基、酰胺、亲水性聚合物或其混合物,任选地其与线性、支链或环状烷基、烯基、炔基、芳基残基、丙烯酰基、酰基、酰氧基、烷氧基、亚烷氧基或其混合物组合。

135.如前述权利要求中任一项所述的方法,其中所述有机化合物还包含一个或多个任选地包含一个或多个杂原子的环状部分,并且所述环状部分中的至少一个直接或间接地连接至所述官能团中的至少一个,或者所述接头是作为所述有机化合物的酯或盐的衍生物,或者是在与所述碳泡沫反应中释放所述有机化合物的化合物。

136.如前述权利要求中任一项所述的方法,其中所述接头选自1-芘丁酸、N-羟基琥珀酰亚胺(NHS)、芘-1-羧酸琥珀酰亚胺酯、1-氨基芘、N-(1-芘)马来酰亚胺或其混合物。

137.如前述权利要求中任一项所述的方法,其中所述接头通过π-π相互作用键合至所述碳泡沫。

138.如前述权利要求中任一项所述的方法,其中所述受体是以下中的一者:电化学受体、化学受体、生物受体、光学受体、物理或机械受体,优选生物受体。

139.如前述权利要求中任一项所述的方法,其中所述受体选自冠醚、催化剂、硼酸、概念、配体、适体、蛋白质、酶、抗体、抗原、微生物、核酸、脂肪酸、脂肪酸酯、分子印迹聚合物、金属有机骨架、能够形成配体结合的多肽或寡肽、细胞、细胞器或其他细胞组分或其混合物,优选地选自蛋白质、核酸、抗体、酶或其混合物。

140.如前述权利要求中任一项所述的方法,其中所述受体选自免疫球蛋白A(IgA)、葡萄糖脱氢酶、链霉亲和素或其混合物。

141.如前述权利要求中任一项所述的方法,其中所述受体以物理、生物和/或化学方式键合至所述接头,优选以化学方式键合,更优选共价键合。

超级电容器用例

142.如前述权利要求中任一项所述的方法,其中所述碳泡沫形成储能装置中的电极,所述储能装置诸如电化学电容器、超级电容器、赝电容器或电容器。

143.如前述权利要求中任一项所述的方法,其中所述碳泡沫用金属氧化物膜或其他赝电容材料处理以提供赝电容。

144.如前述权利要求中任一项所述的方法,其中所述碳泡沫形成储能装置中的至少一个电极,所述储能装置诸如电化学电容器、超级电容器、赝电容器或电容器,并且水凝胶电解质包封活性区域中的所述电极或每个电极,以产生增强的操作电压窗口。

145.如前述权利要求中任一项所述的方法,其中所述碳泡沫形成电池中的电极。

146.如前述权利要求中任一项所述的方法,其中所述碳泡沫形成电导体。

制造工艺细节

147.如前述权利要求中任一项所述的方法,其包括在使用所述第一激光束之前将电接触件丝网印刷至所述碳前体材料上或所述碳前体材料中的步骤。

148.如前述权利要求中任一项所述的方法,其包括在使用所述第一激光束和所述第二激光束之后将电接触件丝网印刷至所述碳前体材料上或所述碳前体材料中的步骤。

149.如前述权利要求中任一项所述的方法,其中所述制造方法是室温工艺。

150.如前述权利要求中任一项所述的方法,其中所述制造方法是环境压力工艺。

151.如前述权利要求中任一项所述的方法,其中所述制造方法能够在塑料基板上完成。

152.如前述权利要求中任一项所述的方法,其中所述制造方法使得能够在柔性基板上产生3D碳泡沫。

153.如前述权利要求中任一项所述的方法,其中所述制造方法仅在所述碳前体材料的所述封装表面下区域中产生碳泡沫材料,并且不在所述碳前体材料的任何表面产生碳泡沫材料。

154.如前述权利要求中任一项所述的方法,其中所述制造方法使用行业标准、低成本和可扩展的(i)丝网印刷技术和(ii)计算机控制的激光扫描技术的组合。

155.如前述权利要求中任一项所述的方法,其中所述制造方法使用高速、大批量卷对卷或卷对片生产。

156.如前述权利要求中任一项所述的方法,其中如权利要求1所述的步骤(a)在一个制造设施中进行,并且如权利要求1所述的步骤(b)在不同的设施中进行。

157.如前述权利要求中任一项所述的方法,其包括以下步骤:(a)将电接触件丝网印刷

至碳前体材料上或中;(b)使用在第一波段下操作的激光束在碳前体材料的表面下方照射所述材料的封装区域或表面下区域,以在所述封装区域或表面下区域中产生碳泡沫,并且其中步骤(a)和(b)可以按照(a)然后(b)或(b)然后(a)的顺序进行;然后(c)使用在第二波段下操作的激光束去除或烧蚀位于所述碳泡沫与所述碳前体材料的所述表面之间的材料,以暴露与所述电接触件连接的所述碳泡沫中的至少一些。

应用

158.如前述权利要求中任一项所述的方法,其用于制造包括感测电极的生物传感器,所述感测电极包括至少部分地通过如前述制造方法权利要求中任一项所述的方法制成的碳泡沫。

159.如前述权利要求中任一项所述的方法,其用于制造包括传感器电极诸如工作电极、对电极的生物传感器,每个所述传感器电极包括至少部分地通过如前述制造方法权利要求中任一项所述的方法制成的碳泡沫,并且所述方法包括在每个电极上方丝网印刷电连接轨迹,并且用丝网印刷电介质至少部分地覆盖所述电极和连接轨迹。

160.如前述权利要求中任一项所述的方法,其用于在一个制造设施中制造包括传感器电极诸如工作电极、对电极的生物传感器,每个所述传感器电极包括至少部分地通过如前述制造方法权利要求中任一项所述的方法制成的碳泡沫,并且所述方法包括在不同的制造设施将功能化基团添加至所述工作电极的另一步骤。

161.如前述权利要求中任一项所述的方法,其用于在一个制造设施中制造包括传感器电极诸如工作电极、对电极的生物传感器,每个所述传感器电极包括至少部分地通过如前述制造方法权利要求中任一项所述的方法制成的碳泡沫,并且所述方法包括在所述制造设施将功能化基团添加至所述工作电极的另一步骤。

162.如前述权利要求中任一项所述的方法,其用于制造包括传感器电极诸如工作电极和对电极的生物传感器,每个所述传感器电极包括至少部分地通过如前述制造方法权利要求中任一项所述的方法制成的碳,并且所述方法包括以下步骤:(a)在所述基板上丝网印刷碳层;(b)丝网印刷电连接轨迹和参比电极;(c)在所述碳和所述电连接轨迹以及所述参比电极上方丝网印刷电介质层;然后(d)使用如前述制造方法权利要求中任一项所述的方法产生碳泡沫传感器电极。

163.如前述权利要求中任一项所述的方法,其用于制造储能装置诸如超级电容器或赝电容器,其中储能电极包括至少部分地通过如前述制造方法权利要求中任一项所述的方法制成的碳泡沫材料。

164.如前述权利要求中任一项所述的方法,其用于制造储能装置诸如超级电容器或赝电容器,其中储能电极包括至少部分地通过如前述制造方法权利要求中任一项所述的方法制成的碳泡沫材料;

并且所述方法包括在每个电极的至少一部分上方丝网印刷电连接轨迹以及用丝网印刷电介质层至少部分地覆盖所述电极和连接轨迹的步骤。

165.如前述权利要求中任一项所述的方法,其用于制造储能装置诸如超级电容器或赝电容器,其中储能电极包括至少部分地通过如前述制造方法权利要求中任一项所述的方法制成的碳泡沫材料并且以叉指图案布置;

并且所述方法包括在每个电极的至少一部分上方丝网印刷电连接轨迹的步骤,其中单

个电连接轨迹连接至从所述电连接轨迹的两侧垂直延伸的下层指位。

166.如前述权利要求中任一项所述的方法,其用于制造储能装置诸如超级电容器或赝电容器;

并且所述方法包括以下步骤:(a)将电连接器丝网印刷至基板上;(b)在所述电集电极上方丝网印刷碳层;(c)在所述碳层的至少一些上方丝网印刷电介质;然后(d)至少部分地通过如前述制造方法权利要求中任一项所述的方法产生碳泡沫储能电极。

167.如前述权利要求中任一项所述的方法,其用于制造储能装置诸如超级电容器或赝电容器,其中储能电极包括至少部分地通过如前述制造方法权利要求中任一项所述的方法制成的碳泡沫材料;

并且所述方法包括应用赝电容材料、诸如金属氧化物向所述储能电极的电化学沉积工艺的步骤。

168.如前述权利要求中任一项所述的方法,其用于制造储能装置,诸如超级电容器或赝电容器,其中储能电极包括至少部分地通过如前述制造方法权利要求中任一项所述的方法制成的碳泡沫材料;

并且所述方法包括在低湿度但非惰性的环境中应用离子凝胶的步骤,其中测量并控制所述环境中O_2和H_20的水平以优化所述储能装置的电容。

169.如前述权利要求中任一项所述的方法,其用于制造电导体,其中所述电导体包括至少部分地通过如前述制造方法权利要求中任一项所述的方法制成的碳泡沫。

170.如前述权利要求中任一项所述的方法,其用于制造包括传感器和储能装置二者的装置,所述储能装置诸如超级电容器,其中所述传感器和所述储能装置均包括至少部分地通过如前述制造方法权利要求中任一项所述的方法制成的碳泡沫材料。

171.如前述权利要求中任一项所述的方法,其用于制造包括电池和超级电容器的集成装置,所述电池提供长期功率,并且所述超级电容器在高于所述电池的水平下提供短期功率,其中所述超级电容器包括至少部分地通过如前述制造方法权利要求中任一项所述的方法制成的碳泡沫材料。

172.如前述权利要求中任一项所述的方法,其用于制造包括天线和超级电容器的集成装置,其中所述超级电容器为所述天线提供功率并且包括至少部分地通过如前述制造方法权利要求中任一项所述的方法制成的碳泡沫材料。

173.如前述权利要求中任一项所述的方法,其用于制造包括一个或多个电极的装置,每个电极都包括碳泡沫材料;

其中所述方法包括使碳前体膜的连续卷轴通过制造至少部分地通过如前述制造方法权利要求中任一项所述的方法制成的碳泡沫材料所需的一系列操作。

装置

174.一种装置,其包括至少部分地通过如前述制造方法权利要求中任一项所述的方法制成的碳泡沫材料。

175.如前述装置权利要求中任一项所述的装置,其为包括能量采集器系统和超级电容器的数据记录装置,其中所述超级电容器为天线提供功率并且包括至少部分地通过如前述制造方法权利要求中任一项所述的方法制成的碳泡沫材料。

176.如前述装置权利要求中任一项所述的装置,其为储能装置,诸如超级电容器,其包

括:

(i)碳前体膜;

(ii)丝网印刷导电浆料或油墨层,其在所述碳前体膜的所述表面上;

(iii)丝网印刷集电极层,其在所述丝网印刷导电浆料或油墨层上方;

(iv)丝网印刷电介质层,其在所述集电极层上方;以及

(v)储能电极,其包括至少部分地通过如前述制造方法权利要求中任一项所述的方法由所述碳前体膜制成的碳泡沫材料,并且其中导电通路形成为经由所述导电浆料或油墨层从所述碳泡沫材料至所述集电极层。

177.如前述装置权利要求中任一项所述的装置,其为包括电池和超级电容器的智能标签,所述电池提供长期功率,并且所述超级电容器在高于所述电池的水平下提供短期功率,其中所述超级电容器包括至少部分地通过如前述制造方法权利要求中任一项所述的方法制成的碳泡沫材料;

并且所述智能标签包括由电池提供功率的电子器件、诸如传感器电子器件以及由所述超级电容器提供功率的数据发送器。

178.如前述装置权利要求中任一项所述的装置,其为包括电池和超级电容器的智能标签,所述电池提供长期功率,并且所述超级电容器在高于所述电池的水平下提供短期功率,其中所述超级电容器包括至少部分地通过如前述制造方法权利要求中任一项所述的方法制成的碳泡沫材料;

并且所述智能标签包括由所述电池提供功率的电子器件、诸如传感器电子器件以及由所述超级电容器提供功率的数据发送器,其中所述超级电容器为所述数据发送器提供足够的功率,以使得所述数据发送器能够与基站或集线器建立数据连接,并且一旦建立了数据连接就传输数据有效载荷。

179.如前述装置权利要求中任一项所述的装置,其为储能装置,诸如超级电容器,其包括子组件,所述子组件包括:

(i)碳前体膜;

(ii)丝网印刷导电浆料或油墨层,其在所述碳前体膜的所述表面上;

(iii)丝网印刷集电极层,其在所述丝网印刷导电浆料或油墨层上方;

(iv)丝网印刷电介质层,其在所述集电极层上方;

(v)储能电极,其包括至少部分地通过如前述制造方法权利要求中任一项所述的方法由所述碳前体膜制成的碳泡沫材料,并且其中导电通路形成为经由所述导电浆料或油墨层从所述碳泡沫材料至所述集电极层;

并且其中多个子组件形成为堆叠,并且其中相邻的储能电极通过离子凝胶电解质分开。

180.如前述装置权利要求中任一项所述的装置,其为包括定位于所述装置的上表面上的样品孔的微流体诊断装置,参比电极、工作电极和对电极至少部分地通过如前述制造方法权利要求中任一项所述的方法由碳前体膜制成且在所述样品孔下方的层中,并且参比电极连接件、工作电极连接件和对电极连接件在所述参比电极、工作电极和对电极下方的层中。

181.如前述装置权利要求中任一项所述的装置,其为芯片实验室装置,包括子组件,所

述子组件包括：

(i)碳前体膜；

(ii)丝网印刷导电浆料或油墨层,其在所述碳前体膜的所述表面上；

(iii)丝网印刷导电层,其在所述丝网印刷导电浆料或油墨层上方；

(iv)丝网印刷参比电极；

(v)丝网印刷电介质层,其在所述集电极层上方；

(vi)传感器电极,其包括至少部分地通过如前述制造方法权利要求中任一项所述的方法由所述碳前体膜制成的碳泡沫材料,并且其中导电通路形成为经由所述导电浆料或油墨层从所述碳泡沫材料至所述导电层形成。

182.如前述装置权利要求中任一项所述的装置,其为包括激光诱导碳泡沫材料的装置,所述激光诱导碳泡沫材料通过以下制造：

(a)使用在第一波段下操作的激光束照射碳前体材料的、在所述材料的表面下方的封装区域或表面下区域,以在所述表面下区域中产生碳泡沫,然后

(b)使用在第二波段下操作的激光束去除或烧蚀位于所述碳泡沫与所述碳前体材料的所述表面之间的材料,以暴露所述碳泡沫中的至少一些。

183.如前述装置权利要求中任一项所述的装置,其为包括激光诱导碳泡沫材料的装置,所述激光诱导碳泡沫材料通过以下制造：

(a)使用在第一波段下操作的激光束照射碳前体材料的、在所述材料的表面下方的封装区域或表面下区域,以在所述表面下区域中产生碳泡沫,然后

(b)使用在第二波段下操作的激光束去除或烧蚀位于所述碳泡沫与所述碳前体材料的所述表面之间的材料,以暴露所述碳泡沫中的至少一些;其中所述装置是或包括以下中的一者:霍尔效应传感器;用于例如机器人学的触觉传感器;感染性疾病传感器;生物传感器;持续监测化学传感器;葡萄糖监测传感器;乳酸传感器;气体检测传感器;自充电混合能源产生装置;绿色气体转化装置;燃料电池,例如氢燃料电池;过滤器,包括透气过滤器;加热装置。

碳泡沫

184.一种激光诱导碳泡沫,其通过以下制成：

(a)使用在第一波段下操作的激光束照射碳前体材料的、在所述材料的表面下方的封装区域或表面下区域,以在所述表面下区域中产生碳泡沫,然后

(b)使用在第二波段下操作的激光束去除或烧蚀位于所述碳泡沫与所述碳前体材料的所述表面之间的材料,以暴露所述碳泡沫中的至少一些。

185.一种激光诱导碳泡沫,其使用如前述制造方法权利要求中任一项所述的方法制成。

186.一种激光诱导碳泡沫,其使用如前述制造方法权利要求中任一项所述的方法制成,所述碳泡沫包括一种或多种碳质纳米结构,诸如碳纳米洋葱、碳纳米角、碳纳米管、碳纳米点、纳米金刚石和富勒烯、或其任何组合。

激光诱导的碳纳米结构

技术领域

[0001] 本发明涉及激光诱导生产碳纳米结构,包括乱层扭转的多层碳泡沫。

背景技术

[0002] 碳纳米结构既极具吸引力,又是热点研究主题。碳纳米洋葱(也称为多层富勒烯)例证了这一点。参见“Raman spectroscopy of polyhedral carbon nano-onions”,DOI:10.1007/s00339-015-9315-9以及“Carbon nano-onions:unique carbon nano-structures with fascinating properties and their potential applications”,DOI:10.1016/j.ica.2017.07.021,其内容以引用的方式并入。

[0003] 作为另一种碳纳米结构,石墨烯多年来由于包括生物传感器、电化学传感系统、超级电容器、电极和燃料电池的应用而受到广泛关注。已知的生产3D石墨烯的方法包括WO 2019/038558中所述的激光诱导生产石墨烯;当将合适的碳前体材料(诸如聚酰亚胺膜)定位在支撑基板上并且用CO_2激光照射时,在暴露的聚酰亚胺膜的表面形成3D石墨烯。经验表明,通过这种方法生产的3D石墨烯的厚度小于50μm;此外,3D石墨烯本身可能很脆,并且与下层(underlying)基板的粘附较差,因此可能会从所述基板剥落。因此3D石墨烯不适合许多应用。

[0004] 关于碳纳米结构领域中使用的术语的说明:如果我们仅采用术语“石墨烯”,则“石墨烯”有许多不同的形式;例如,文献描述了单层石墨烯、双层石墨烯、乱层石墨烯、石墨烯超晶格、石墨烯纤维、3D石墨烯、石墨烯气凝胶、褶皱石墨烯和许多其他形式。这提出了定义上的挑战,因为使用特定术语(例如,“3D石墨烯”)可能意味着仅限于所述特定形式的石墨烯。此外,IUPAC(国际纯化学和应用化学联合会(International Union for Pure and Applied Chemistry))建议针对三维材料使用名称“石墨”,而仅当讨论个别层的反应、结构关系或其他特性时使用“石墨烯”。

[0005] 因此,在本说明书中,我们使用术语“碳泡沫”作为概括性术语,并且此术语应被广泛解释为覆盖任何碳纳米结构,诸如3D碳材料泡沫,包括乱层扭转的多层3D碳材料泡沫。

[0006] 术语“碳泡沫”的一个实例是指使用本说明书中描述的方法制造的材料;这种材料的特性与常规石墨烯或常规石墨烯泡沫略有不同。例如,石墨烯泡沫具有若干特征:它是疏水性的,可润湿性低。对典型的石墨烯泡沫的拉曼分析揭示了以下特征签名(signature):不存在D峰;2D峰高于G峰;D峰:G峰的比率接近于零。正如我们将在下文中更详细地描述的,在本发明的具体实施中产生的碳泡沫不具有这些特征;它是亲水性的,接触角低于20°;它缺乏石墨烯指示性的拉曼特征签名:它显示出明显的D峰;2D峰明显小于G峰;D峰:G峰的比率明显高于零。在外观和拉曼特征签名方面,它似乎更接近碳纳米洋葱材料。因此,术语“碳泡沫”在其范围内还包括作为碳质纳米结构的材料,诸如碳纳米洋葱、碳纳米角、碳纳米管、碳纳米点、纳米金刚石和富勒烯或其任何组合。

发明内容

[0007] 在本说明书中,我们描述了一种方法,其中碳前体的表面根本不转化为石墨烯;而是通过聚焦的激光束将碳前体的表面下区域或封装区域转化为碳泡沫。

[0008] 我们概括出如权利要求1中所述的发明,即一种制造碳泡沫材料的方法,其包括以下步骤:

[0009] (a)使用第一激光束在碳前体材料的表面下方照射所述材料的封装或表面下(sub-surface)区域,以在所述表面下区域中产生碳泡沫并且在所述碳泡沫上方产生无序的无定形非石墨烯材料,然后

[0010] (b)使用第二激光束去除或烧蚀位于所述碳泡沫上方的所述无序的无定形非石墨烯材料,以暴露所述碳泡沫中的至少一些。

[0011] 无定形非石墨烯材料在碳泡沫“上方”,因为它比碳泡沫更靠近产生激光束的激光。本发明的一个具体实施被描述为“双激光”工艺,因为在生产碳泡沫材料中使用了两种单独的激光。碳泡沫材料显示出显著的D峰;2D峰显著小于G峰;并且D峰:G峰的比率显著高于零。在外观和拉曼特征签名方面,它似乎更类似于碳纳米洋葱材料。它可以用于生物传感器、超级电容器和赝电容器。在一个具体实施中,碳泡沫被称为“Gii”碳泡沫。

附图说明

[0012] 将参考以下附图所示的本发明的具体实施来描述本发明。

[0013] 图1-图6示意性地显示了用于当将聚酰亚胺(PI)膜(其充当碳前体)定位在基板上时产生碳泡沫的双激光工艺。

[0014] 图7是扫描电子图像,其显示了使用双激光方法实现的碳泡沫的独特表面形态(x250)。

[0015] 图8是扫描电子图像,其显示了常规激光诱导石墨烯的表面。

[0016] 图9-图14B示意性地显示了用于当不将PI膜(其充当碳前体)定位在基板上时产生碳泡沫的双激光工艺。

[0017] 图15是使用双激光方法生产的碳泡沫电极的循环伏安法(CV)图。

[0018] 图16A是显示使用双激光方法生产的碳泡沫电极的峰分离ΔE_p作为扫描速率函数的图。

[0019] 图16B为显示常规制造的石墨烯电极的峰分离ΔE_p作为扫描速率函数的图。

[0020] 图17是使用双激光方法生产的碳泡沫电极与另外常规制造的石墨烯电极的电化学阻抗谱结果的比较。

[0021] 图18A和图B是通过双激光工艺制成的碳泡沫样品的拉曼分析。

[0022] 图18C是碳纳米洋葱材料的拉曼分析。

[0023] 图19是显示双激光碳泡沫和常规石墨烯的扫描电子图像。

[0024] 图20是包括双激光碳泡沫(碳泡沫的这种具体实施称为Gii-Sens)的生物传感器的示意性图像。

[0025] 图21-图23是双激光碳泡沫(称为Gii-Sens、Gii-Sens+和PPC Gii-Sens变体)的详细加工流程图。

[0026] 图24-图27是包括双激光碳泡沫(碳泡沫的这种具体实施称为Gii-Cap)的超级电

容器的示意性图像。

[0027] 图28-图29是双激光碳泡沫(称为Gii-Cap和Gii-Cap+变体)的详细加工流程图。

[0028] 图30是集成芯片实验室(LoC)装置的示意性横截面,所述装置包括使用双激光碳泡沫制成的生物传感器和超级电容器。

[0029] 图31是完全集成LoC装置的分解图。

[0030] 图32显示在其显示器上展示定量结果的LoC装置。

[0031] 图33是包括Gii-Sens传感器的环境监测装置的分解图。

[0032] 图34是组装的环境监测装置的视图。

[0033] 图35是具有电池(例如,印刷电池或常规电池)和Gii-Cap超级电容器的装置的示意性横截面。

[0034] 图36是智能标签的示意图;它具有电池(例如,印刷电池或常规电池)和Gii-Cap超级电容器。

[0035] 图37是显示Gii-Thru变体中不同材料的基本分层的示意性横截面,所述变体是碳泡沫的三维结构。

[0036] 图38-图42是各种Gii-Thru Gii-Cap/Gii-Cap+三维超级电容器装置的示意图。

[0037] 图43A和图43B是双激光碳泡沫Gii-Thru Cap三维超级电容器装置的详细加工流程图。

[0038] 图44A和图44B是在三样品阵列微流体诊断装置中使用的Gii-Thru传感器的示意图。

[0039] 图45A和图45B是在八样品阵列微流体诊断装置中使用的Gii-Thru传感器的示意图。

[0040] 图46A显示完全组装的多样品阵列微流体诊断装置的透视图。

[0041] 图46B是多样品阵列微流体诊断装置的俯视图。

[0042] 图47和图48是微流体诊断装置的视图。

[0043] 图49是高灵敏度低成本Gii-Thru变体的详细制造工艺流程。

[0044] 图50是Gii碳泡沫的高速卷对卷或卷对片制造系统的示意图。

[0045] 图51显示图50系统的详细工艺流程。

[0046] 图52-图57A是显示双激光碳泡沫在不同放大倍数下的扫描电子图像。

[0047] 图57B是使用常规工艺制成的碳纳米洋葱材料的扫描电子图像。

[0048] 图58显示使用双激光工艺制成的八个碳泡沫片材的拉曼位移。

[0049] 附录1使用水凝胶电解质的超级电容器具体实施

[0050] 图59呈现在25mV/s下测量的针对阳极电压的碳泡沫循环伏安图。

[0051] 图60显示在25mV/s下测量的针对阴极电压的碳泡沫循环伏安图。

[0052] 图61显示在0.5mA/cm^2下测量的针对阳极电压窗口的碳泡沫恒电流充电放电(galvanostatic charge discharge,GCD)曲线。

[0053] 图62显示在0.5mA/cm^2下测量的针对阴极电压窗口的碳泡沫恒电流充电放电(GCD)曲线。

[0054] 图63显示从五个双电极装置取得的碳泡沫恒电流充电放电(GCD)数据。

[0055] 图64显示在高(左)和低(右)扫描速率下从五个不同的双电极装置记录的碳泡沫

循环伏安图。

[0056] 图65显示五个其他系统的碳泡沫循环伏安图数据,所述系统因为水凝胶电解质的性质而有所不同:(a)3M $NaClO_4$和PVA;(b)1M $NaClO_4$和PVA;(c)2.5M $NaNO_3$和PVA;(d)3M $Mg(ClO_4)_2$和PVA;以及(e)5M $NaClO_4$和PVP。

[0057] 附录2:Gii-Cap+水凝胶

[0058] 图66是Gii-Cap+水凝胶装置的典型CV曲线。

[0059] 图67是调节后Gii-Cap+水凝胶装置的典型GCD曲线。

[0060] 图68显示Gii-Cap+装置的后调节奈奎斯特(Nyquist)(左)和伯德(Bode)(右)曲线图。

[0061] 附录3GiiCap离子凝胶

[0062] 图69-图74是GiiCap离子凝胶装置的结果。

[0063] 附录4 3个月Gii-Sens测定可行性提议

[0064] 图75-图78是Gii-Sens 3D碳泡沫测定系统的测定程序的示意图。

[0065] 图79-图81显示Gii-Sens 3D碳泡沫的表面化学。

[0066] 图82-图83显示Gii-Sens 3D碳泡沫的无标签测定探究。

[0067] 附录6基准实验条件

[0068] 图84-图86是比较Gii-Sens碳泡沫与石墨烯电极材料的性能的图。

[0069] 图87-图89是比较Gii-Sens碳泡沫与碳基电极材料的性能的图。

[0070] 图90-图92是比较Gii-Sens碳泡沫与丝网印刷金的性能的图。

[0071] 附录7:抗人原降钙素(cAb)的表面固定的优化

[0072] 图93显示抗人原降钙素(cAb)的表面固定的优化的直接测定程序。

[0073] 图94是表面固定反应示意图。

[0074] 图95显示Gii-Sens电极的NHS功能化的Rct和ΔEp信号响应。

[0075] 图96显示GiiSens电极上的cAb固定。

[0076] 图97显示使用100μg/ml cAb表面涂层的直接测定形式中来自2000pg/ml的信号响应。

[0077] 需注意,Gii、Gii-Sens、Gii-Sens+、Gii-Cap、Gii-Cap+、Gii-Thru和PPC Gii是专利所有者的商标。“Gii”通常指代使用双激光工艺制成的碳泡沫。“Gii-Sens”是指在传感器(诸如,生物传感器)中使用的Gii碳泡沫。“Gii-Cap”是指在超级电容器中使用的Gii碳泡沫。+后缀是指用金属氧化物层或膜改性的Gii碳泡沫。“Gii-Thru”是指被布置成特定的三维结构的Gii碳泡沫。“PPC”是指特定的制造工艺,即“印刷后转化”,其中在已完成各种丝网印刷步骤后产生Gii碳泡沫。

[0078] 附图标记

[0079] 双激光工艺

[0080] 11 IR激光

[0081] 12 IR激光束

[0082] 13 PI膜的内部

[0083] 14 PI膜

[0084] 15 基板

[0085] 16 表面下碳泡沫区域

[0086] 17在表面下碳泡沫区域下方的无序的无定形非石墨烯材料

[0087] 18在表面下碳泡沫区域上方的无序的无定形非石墨烯材料的扩展区域

[0088] 20CO2激光

[0089] 21暴露碳泡沫区域的独特表面形态

[0090] 生物传感器

[0091] 201 聚酰亚胺基板

[0092] 202 碳泡沫工作电极

[0093] 203 碳泡沫对电极

[0094] 204 碳泡沫参比电极

[0095] 205 丝网印刷银连接轨迹

[0096] 206 电介质层

[0097] 207银连接轨迹与电极重叠的区域

[0098] Gii-Cap超级电容器

[0099] 241 碳泡沫电极的阵列

[0100] 242 丝网印刷银连接器

[0101] 243 电介质层

[0102] 244 聚酰亚胺基底层

[0103] 245 铜连接插片

[0104] 246 电解质层

[0105] 247 铝层压热封袋

[0106] 250 碳泡沫指位(digit)的圆形边缘

[0107] 组合的传感器和超级电容器

[0108] 301 上部聚酰亚胺层

[0109] 302 Gii-Sens生物传感器

[0110] 303 下部聚酰亚胺层

[0111] 304 超级电容器

[0112] 305 塑料件

[0113] 306 微通道

[0114] 307 连接器轨迹

[0115] 308 柔性电子器件

[0116] 310 感应功率回路

[0117] 312 Gii-Cap超级电容器

[0118] 313 Gii-Sens生物传感器

[0119] 314 具有微电子器件的装置层

[0120] 315 顶部面板

[0121] 316 显示器

[0122] 317 圆形分析物孔

[0123] 环境监测器

[0124] 330 Gii-Sens碳泡沫传感器

[0125] 331 控制电子器件

[0126] 332 PV太阳能电池

[0127] 333 Gii-Cap碳泡沫超级电容器

[0128] 334 可剥离的背部

[0129] 组合的超级电容器和电池

[0130] 351 第一聚酰亚胺层

[0131] 352 超级电容器

[0132] 353 第二聚酰亚胺层

[0133] 354 电池

[0134] 355BMS(电池管理系统)

[0135] 356 柔性电子器件

[0136] 357 电连接件

[0137] 智能标签

[0138] 360 柔性电池

[0139] 361 超级电容器

[0140] 362 电子器件模块

[0141] 363 暴露的标签表面364粘性离型衬垫364Gii-Thru Cap

[0142] 371PI膜

[0143] 372丝网印刷导电油墨或浆料层

[0144] 373 丝网印刷集电极

[0145] 374 电介质隔离器

[0146] 375 封装碳泡沫层376在碳泡沫层下的无序无定形非石墨烯层377 独特的表面形态层

[0147] 390 水凝胶电解质层

[0148] 391具有独特的表面形态的碳泡沫层

[0149] 392 PI膜

[0150] 393 丝网印刷碳浆料层

[0151] 394 丝网印刷银连接器层

[0152] 395 银连接器层的酮插片

[0153] 396 分配的电介质隔离层

[0154] 397 具有独特的表面形态的第二碳泡沫层

[0155] 398 PI膜

[0156] 399 水凝胶电解质层

[0157] 400 电介质隔离层

[0158] 401 丝网印刷银集电极层

[0159] 402 铜插片

[0160] 403 丝网印刷碳浆料层

[0161] 404 碳泡沫层

[0162] 405 PI膜

[0163] Gii-Thru Sens

[0164] 三点阵列微流体诊断装置

[0165] 440 分析物样品孔

[0166] 441 层压孔间隔件层

[0167] 442 聚酰亚胺膜

[0168] 443 丝网印刷导电碳层

[0169] 444A 参比电极连接件

[0170] 444B 工作电极连接件

[0171] 444C 对电极连接件

[0172] 447 丝网印刷电介质层

[0173] 448A 参比电极

[0174] 448B 工作电极

[0175] 448C 对电极

[0176] 449 参比电极丝网印刷碳层

[0177] 八点阵列微流体诊断装置

[0178] 451 层压孔间隔件

[0179] 452 八个分析物孔的阵列

[0180] 453 对电极的孔

[0181] 454 参比电极的孔

[0182] 455 聚酰亚胺层

[0183] 456 聚酰亚胺层

[0184] 457 八个工作电极

[0185] 458 对电极

[0186] 459 参比电极

[0187] 460 丝网印刷碳连接界面层

[0188] 461 丝网印刷银连接轨迹

[0189] 462 丝网印刷电介质层

[0190] 470 顶层微流体箔

[0191] 471 中间层微流体箔

[0192] 472印刷或模制微流体流体通道

[0193] 473具有粘合剂的底层微流体箔

[0194] 474Gii-Thru传感器

[0195] 475连接器

[0196] 481透明树脂倒钩(barb)连接器

[0197] 482 顶部箔

[0198] 483 透明树脂模制微流体卡

[0199] 484 微流体通道

[0200] 485 孔单元

[0201] 486Gii-Thru传感器

具体实施方式

[0202] 我们将从本发明的具体实施的简化的、示意性演示(walk-through)开始。我们给出了两个演示;第一个演示(图1-6)将在高层次上描述将碳前体(例如,聚酰亚胺(PI)膜,在这种情况下诸如Kapton®膜)安装在基板上的情况下的碳泡沫生产工艺;第二个演示(图9-14)覆盖了未将聚酰亚胺膜安装在基板上的情况下的碳泡沫生产工艺。在每种情况下,我们均使用双激光工艺;我们将在下文解释术语的含义。

[0203] 在第一阶段,(参见图1),波长为A的激光11使用激光束12照射聚酰亚胺膜14的内部13,所述聚酰亚胺膜被定位在适于末端应用的基板15上。此激光可以是脉冲IR激光,其递送波长为1064nm的IR辐射。

[0204] 如图2所示,对波长为A的激光11进行调谐,使得表面下区域16转化为碳泡沫。激光A的焦点逐渐移动穿过聚酰亚胺膜14的内部13,以产生整个碳泡沫区域16。碳泡沫区域16的深度或高度可以是约50μm或更大,比其他方法可能实现的高得多。需注意,任何时候在聚酰亚胺膜14的暴露表面(即,激光束入射在该表面上)上都不产生碳泡沫。在碳泡沫16上方(即,比碳泡沫区域16更靠近激光)的区域不转化为碳泡沫。在碳泡沫区域16下方的区域17(即,PI膜的下表面)也不转化为碳泡沫,而是转化为粘附至下层基板15的无序无定形非石墨烯材料。

[0205] 图3显示,由于气体滞留(trapped),波长为A的激光11在内部碳泡沫区域16上方(即,比碳泡沫区域16更靠近激光)的区域18导致物理膨胀。此区域18不是3D石墨烯,也不是聚合物;它是无序无定形材料。

[0206] 在第二阶段中,现在在碳泡沫区域16上方的无序无定形材料区域18上对波长为B的激光20进行调谐,如图4所示。这可以是波长为10.6μm的CO_2激光。

[0207] 如图5所示,波长为B的激光20烧蚀碳泡沫区域16上方的区域18中的一些或全部,暴露出下层碳泡沫区域16中的至少一些。

[0208] 波长为B的激光20还给出具有独特的表面形态21的下层碳泡沫区域,如图6所示。

[0209] 我们将图1-6中描述的工艺称为“双激光工艺”。

[0210] 图7是扫描电子图像,其显示了使用双激光方法实现的独特的表面形态(x250)。在这种情况下,首先用来自脉冲IR激光的波长为1064nm的IR辐射照射碳源,辐射聚焦至碳源中并逐渐深入碳源内,然后用来自CO_2激光的波长为10.6μm的激光束照射碳源。此图像中碳泡沫层的厚度为约220μm。

[0211] 如图8所示,与使用常规LIG方法实现的表面形态(x250)的对比明显:具有清晰的光栅线,并且折叠不那么旋绕。此碳泡沫层的厚度小于50μm。

[0212] 根据图7图像,我们可以推断,使用双激光工艺产生的材料不具有与常规石墨烯泡沫相似的表面形态;虽然它看起来是具有泡沫状结构的乱层扭转多层3D碳基材料,但它不必然是常规意义上通常描述为“石墨烯”的材料。更多详情在下文特点R中。

[0213] 在前述演示(图1-6)中,我们研究了将碳前体材料(聚酰亚胺膜)安装在基板上的双激光工艺。在下面的图9-14中,我们将研究不将聚酰亚胺膜安装在基板上的双激光工艺。我们稍后详细描述称为Gii-Cap(超级电容器)和Gii-Sens(传感器)的两种具体实施的制造

工艺,所述工艺使用聚酰亚胺膜的标准220mm×180mm片材,其不安装在基板上;标准激光扫描装置中可以考虑这种大小,所述装置通常用于激光雕刻、激光切割和激光绘图(其可以描绘出由标准CAD程序定义的路径)。所述制造工艺还使用标准平板丝网印刷装置和标准传送带式干燥机,以便轻松兼容不同大小的薄PI膜。可以考虑其他大小的聚酰亚胺片材。

[0214] 如前所述,波长为A的激光11(例如,IR激光)照射PI膜14的内部13;膜14现在未安装在基板上,如图9所示。它可以是其边缘被支撑或者暂时搁置在表面上、或者在使用连续制造(例如,卷对卷或卷对片)系统时形成PI膜卷轴的一部分的片材(参见下面的特点P)。

[0215] 对波长为A的激光11进行调谐,使得表面下区域16转化为碳泡沫,如图10所示。焦点逐渐移动穿过膜14,以产生整个碳泡沫区域16。碳泡沫区域16的高度可以是约50μm或更大,比用其他方法可能实现的更深得多或高得多。

[0216] 在任何时候,聚合物膜的暴露表面上都不产生3D石墨烯。碳泡沫上方的区域不转化为3D石墨烯。

[0217] 如图11所示,由于气体滞留,内部碳泡沫区域16上方的区域18发生物理膨胀。此区域不是3D石墨烯,也不是聚合物;它是无序无定形材料。

[0218] 现在在碳泡沫上方的区域18上对波长为B的激光20(例如,CO_2)进行调谐,如图12所示。波长为B的激光20烧蚀碳泡沫区域16上方的区域18,暴露出下层碳泡沫16中的至少一些,如图13所示。

[0219] 正如将聚酰亚胺膜14安装在基板上的情况一样,波长为B的激光20还赋予下层碳泡沫16以独特的表面形态21,如图14所示。

[0220] 生产碳泡沫的这种双激光方法的一些具体实施的细节如下:在一个实例中,Nd:YAG固态激光是波长A激光,并且其被定位成使得通过固态激光产生的IR激光辐射束(波长为1064nm)垂直撞击聚酰亚胺层。光学器件将IR激光辐射激光束聚焦至聚酰亚胺层内一定体积的最小射束会聚。

[0221] 在最小射束会聚周围的封装区域或表面下区域或位置中,激光和聚酰亚胺的相互作用导致碳源的碳化。这种碳化导致在封装区域或表面下区域中产生碳泡沫,诸如扭转或乱层多层碳泡沫,并且导致在聚酰亚胺膜的表面产生无序无定形非石墨烯物质层。

[0222] 在维持激光束聚焦在聚酰亚胺层内的特定深度的同时,激光在聚酰亚胺层上方侧向扫描。以这种方式,完全在聚酰亚胺碳源内的路径被追踪并转化为碳泡沫。因此,聚酰亚胺以与由扫描、聚焦的IR激光束追踪的路径对应的图案碳化为碳泡沫。

[0223] 在一种设置中,Nd:YAG IR激光的脉冲频率为80kHz,并且激光束以9.4cm/s的速度在表面上扫描。其他实施方案利用了不同的参数。例如,还利用了50kHz的脉冲频率和35.5cm/s的扫描速度来成功地产生碳泡沫。激光功率在8-20瓦特的典型工作范围内,最佳为12W;激光焦距在50mm-400mm的典型工作范围内。

[0224] 一旦聚酰亚胺层内的预定区域以上述方式被聚焦IR激光束照射,聚酰亚胺中封装区域或表面下区域或位置的深度就被改变,并且IR激光束再次扫描某一区域,在这种情况下扫描同一个预定区域。可以使用标准的计算机控制激光扫描系统,所述系统控制激光在聚酰亚胺膜上的X-Y位置。可能需要使聚焦IR激光辐射多于一次地通过同一区域,以产生碳泡沫。在此具体实施中,聚焦IR激光还照射相邻但不实质上重叠的区域。重复这种使用聚焦IR激光辐射以不同的焦点深度照射碳源的工艺,直到所需深度的聚酰亚胺层暴露于IR激光

辐射并且在封装区域或表面下区域中形成碳泡沫。然而,表面层是无序无定形非石墨烯物质。

[0225] 在第二步中,将聚酰亚胺层暴露于来自CO_2激光的辐射以进行烧蚀步骤,暴露下层碳泡沫中的至少一些并得到具有特定表面形态的暴露碳泡沫。来自CO_2激光的辐射以19cm/s的速度在处理的碳源的表面上扫描,以匹配已使用IR激光照射的图案或区域。其他实施方案利用了不同的参数。例如,还利用了50kHz的脉冲频率和35.5cm/s的扫描速度来成功地显露下层碳泡沫。激光功率在8-20瓦特的典型工作范围内,最佳为12W;激光焦距在50mm-400mm的典型工作范围内。

[0226] 如上所述,CO_2激光烧蚀表面层无序无定形非石墨烯物质,从而暴露下层碳泡沫并改变所述碳泡沫的表面形态,以产生与标准激光诱导的石墨烯相比具有更多数量的缺陷的暴露碳泡沫;如前所述,这样赋予碳泡沫以优于标准激光诱导的石墨烯的极其有用的性质。

[0227] 改变任一或两种激光(例如,IR激光和CO_2激光)的激光参数,诸如功率、焦点、波长、扫描速度,则改变碳泡沫材料的性质,使得能够生产出具有针对不同应用而优化的性质的碳泡沫。

[0228] 通过双激光工艺制成的暴露碳泡沫的一种有用的性质是高度的可润湿性:接触角可以小于20°,从而使得这种碳泡沫是亲水的,相比之下,常规石墨烯泡沫的接触角在70°与150°之间,从而使得其是疏水的。通过双激光工艺生产的碳泡沫的亲水性对于两种关键应用来说是高度相关的,即生物传感器(称为Gii-Sens的具体实施)和超级电容器(称为Gii-Cap的具体实施)。对于生物传感器,可润湿性高导致被测试的液体(例如,液体分析物)在整个工作电极上快速且均匀地蔓延,从而导致灵敏度、一致性和速度更高。对于超级电容器,可润湿性高意味着电解质更好地润湿超级电容器电极,从而导致性能更高。常规石墨烯泡沫可以被加工成使其更易润湿,但该碳泡沫具体实施不需要这样额外的加工步骤。

[0229] 通过双激光工艺制成的暴露碳泡沫的另一有用的性质是高度防污:这可以导致生物传感器的灵敏度增强以及寿命延长。碳泡沫可以用于污染物或残留物的累积可能损害元件(例如,过滤器、电子烟中的加热元件;电极)的性能或寿命的应用中;通过双激光工艺制成的暴露碳泡沫可以用于所述元件,从而导致性能或寿命增强。

[0230] 已经通过循环伏安法(CV)探索了使用这种双激光方法生产的碳泡沫电极的性能,如图15所示。利用使用上文所述的方法制备的电极并且利用使用已知的常规CO_2激光辐射方法制备的电极,对已充分表征的铁氰化物/亚铁氰化物氧化还原反应进行了循环伏安图绘制。图15显示以扫描速率10mV/s、25mV/s、50mV/s、75mV/s、100mV/s和150mV/s取得的CV曲线图。每个曲线图都显示了利用使用本发明双激光方法生产的碳泡沫电极(浅色线)以及利用使用已知的CO_2激光照射方法生产的3D石墨烯电极(深色线)记录的数据。在阴极电流方向上在约0.22V的峰对应于铁氰化物向亚铁氰化物的还原;并且在阳极电流方向上在约0.28V的峰对应于亚铁氰化物向铁氰化物的氧化。

[0231] 远离突出的氧化还原峰,根据这些图定性地看出,使用了使用本说明书中公开的双激光方法生产的碳泡沫电极记录的CV曲线图的外观比使用通过已知方法生产的3D石墨烯电极记录的曲线图更呈矩形。这在电压范围的高点(约0.6V)和较高的扫描速率(参见例如100mV/s)下最为明显。这种增加的矩形外观指示使用本发明双激光方法制备的电极的电容行为增加,从而反映通过这种方法生产的扭转或乱层多层碳泡沫的表面积非常高。

[0232] 根据CV曲线图还明显看出,与使用通过常规的已知方法生产的3D石墨烯电极进行的那些测量相比,对于使用通过双激光方法生产的碳泡沫电极进行的测量,分离氧化峰和还原峰的电压始终较小。使用根据本发明公开的方法生产的碳泡沫电极取得的CV测量结果的作为扫描速率的函数的峰分离ΔE_p绘制在图16(a)中,并且使用根据已知方法生产的3D石墨烯电极取得的CV测量结果的作为扫描速率函数的峰分离ΔE_p绘制在图16(b)中。

[0233] 此数据显示,当根据双激光方法制备电极时,ΔE_p变窄。可逆系统(诸如,铁氰化物/亚铁氰化物可逆氧化还原反应)的理论峰分离参数为57mV,但实际上这对电极结构对电化学的影响敏感。显然,循环伏安曲线图中氧化峰和还原峰的电压分离接近理论值。这证明了通过已知方法和双激光方法生产的电极的质量。此外,使用通过双激光方法生产的碳泡沫电极记录的结果显示分离减少,表明以这种方式生产的电极的孔隙率相比于通过常规方法生产的电极有所改善。

[0234] 图17显示包括使用双激光方法生产的碳泡沫电极的系统(正方形)和包括使用已知方法生产的3D石墨烯电极的系统(圆形)的电化学阻抗谱结果的比较。伯德曲线图显示相位角作为频率的函数的变化。两个系统的频率响应明显不同。具体而言,使用了使用双激光方法生产的碳泡沫电极记录的测量结果缺少使用了使用常规方法生产的3D石墨烯电极记录的测量结果中在约1kHz观察到的相位角信号的峰。来自使用双激光方法制备的电极的响应指示电子转移响应快速。所述差异进一步清楚地证明,通过双激光方法生产的碳泡沫与通过常规方法生产的3D石墨烯不同并且是可区分的。

[0235] 从图18A可以清楚地看到另外的细节。通过双激光工艺制成的碳泡沫的拉曼光谱示于图18A中,其具有三个主峰。具体来说,在约1344cm^{-1}的D峰是存在晶格缺陷的特征,并且在约1577cm^{-1}的G峰是存在sp^2碳杂化的特征,存在扭曲的六员(six-fold)碳环。在约2685cm^{-1}的2D峰是3D石墨烯中二级转变的特征,并且这里不存在双峰结构指示缺乏在多层2D石墨烯或石墨中可以发现的平面AB堆积。将2D峰与以2685cm^{-1}为中心的单个Lorentzian峰(其半极大处全宽度为67cm^{-1})拟合,指示在用这两种方法形成的3D碳中仅存在一个或几个碳泡沫样层。对双激光工艺的D/G峰值比(0.85)的分析指示,与使用单激光步骤的常规激光诱导石墨烯工艺(0.67)相比,缺陷密度更高,如以下表1所示。

[0236]

工艺	D/G	2D/G	D/D'
双激光	0.85±0.1	0.95±0.12	3.7±1.3
常规单激光	0.67±0.13	0.75±0.05	2.6±0.22

[0237] 表1

[0238] 正如我们之前说明的,对典型的石墨烯泡沫的拉曼分析揭示了以下特征签名:不存在D峰;2D峰高于G峰;D峰:G峰的比率接近于零。本发明的具体实施中产生的碳泡沫不具有这些特征;它是高度亲水的,接触角低于20°;它缺乏石墨烯指示性的拉曼特征签名:图18A显示通过双激光工艺制成的材料:存在D峰;2D峰低于G峰;D峰:G峰的比率高于零。图18B是通过双激光工艺制成的碳泡沫的另一拉曼分析,再次显示存在D峰;2D峰低于G峰;D峰:G峰的比率高于零。图18C是碳纳米洋葱材料的拉曼分析,参见“Raman spectroscopy of polyhedral carbon nano-onions”,DOI:10.1007/s00339-015-9315-9,并且与通过双激光工艺制成的碳泡沫的拉曼的相似性显而易见。一个合理的解释是,通过双激光工艺制成的碳泡沫是或包含碳纳米洋葱材料。还可参见下文的图57A和图57B。

[0239] 双激光碳泡沫和通过单激光工艺制成的常规石墨烯均显示出微孔结构,如图19SEM图像所示。低放大倍数的图像显示表面形态的明显差异。单激光表面显示更光滑、线纹状且边缘粗糙的表面,而通过双激光工艺制成的碳泡沫显示粗糙表面。下面的特点R再述这个区域。

[0240] 关键特点

[0241] 在本节中,我们概述了本发明的具体实施的关键特点A-R。这些特点限定了早先描述的双激光制造工艺中碳纤维泡沫的生产;这种工艺相比于常规CVD具有许多优势:我们可以比较表2中向塑料基板(或实际上许多其他类型的基板)上生产1cm^{2}约50μm厚的碳泡沫。

[0242]

工艺	步骤数量	时间	温度	压力	成本
CVD	6	300min	800C	真空	$50
双激光工艺	1	2min	20C	环境	低于$1

[0243] 表2

[0244] 特点A-R限定了碳泡沫制造工艺的各个方面,所述工艺是高度可扩展的、产量高、可再现性高,并且可以容易地适应于许多不同的应用,这些应用全部都使用相同工艺。例如,双激光碳泡沫特别适合于生物传感器和电化学电容器(例如,超级电容器和赝电容器应用)。

[0245] 对于生物传感器应用,双激光碳泡沫相比于常规石墨烯泡沫具有以下优势:电子传输速率更高;检测灵敏度更高;电化学有效区域更大;可再现性高大;成本更低;可润湿性更高;防污性更高。生物传感器的一种具体实施称为Gii-Cap,我们将在下面对其进行更详细的描述。

[0246] 对于超级电容器和其他电子应用,碳泡沫相比于常规石墨烯泡沫具有以下优势:表面积更大;多孔结构更多;质量更高;片材电阻更低;可润湿性更高;防污性更高。超级电容器的一种具体实施称为Gii-Cap,我们将在下面对其进行更详细的描述。

[0247] 特点A-R被组织为以下四组:

[0248] 第1组:表面下碳泡沫

[0249] 第2组:双激光加工

[0250] 第3组:产品

[0251] 第4组:其他方面。

[0252] 我们可以对这种组织进行如下扩展:

[0253] 第1组:表面下碳泡沫

[0254] 特点A:在碳前体材料的表面下区域中产生的碳泡沫

[0255] 特点B:在碳前体材料的封装区域中产生的碳泡沫

[0256] 特点C:在碳前体材料的区域中产生的碳泡沫,其中所述区域不具有实质气体逸出通道

[0257] 特点D:粘附至基板的无定形非石墨烯材料。

[0258] 第2组:双激光加工

[0259] 特点E:通过激光烧蚀表面下碳泡沫区域所产生的碳泡沫

[0260] 特点F:通过激光烧蚀表面下碳泡沫区域所产生的非石墨烯碳泡沫

[0261] 特点G:在不同频带下操作的双激光

[0262] 特点H:定位在通过激光烧蚀表面下碳泡沫区域所产生的碳泡沫中的电接触件

[0263] 特点I:在聚酰亚胺膜上印刷电接触件,然后产生暴露碳泡沫

[0264] 特点J:在碳泡沫中制成的高轨迹

[0265] 特点K:在不同的制造设施中应用第一激光和第二激光

[0266] 第3组:产品

[0267] 特点L1:生物传感器

[0268] 特点L2:使用丝网印刷技术以可扩展、低成本的方式制造碳泡沫生物传感器

[0269] 特点L3:在不同的制造设施中向生物传感器添加功能化基团

[0270] 特点L4:向生物传感器添加功能化基团,作为生物传感器生产工艺的一部分

[0271] 特点L5:使用PPC制造生物传感器:印刷后转化

[0272] 特点M1:储能装置

[0273] 特点M2:丝网印刷的碳泡沫超级电容器层

[0274] 特点M3:碳泡沫超级电容器:共集电极

[0275] 特点M4:碳泡沫超级电容器:PPC制造工艺

[0276] 特点M5:碳泡沫赝电容器:金属氧化物变体

[0277] 特点M6:碳泡沫超级电容器:在低湿度环境中使用离子凝胶

[0278] 特点N1:电导体

[0279] 特点N2:组合的传感器和超级电容器

[0280] 特点N3:组合的超级电容器和电池

[0281] 特点N4:智能标签

[0282] 特点N5:组合的超级电容器和天线

[0283] 特点N6:组合的能量采集器(Energy Scavenger)+超级电容器。

[0284] 特点O1:3D碳泡沫结构:用于Gii-Cap的Gii-Thru

[0285] 特点O2:3D碳泡沫结构:Gii-Thru可堆叠Gii-Cap/Gii-Cap+

[0286] 特点O3:3D碳泡沫结构:用于Gii-Sens的Gii-Thru:HISLOC

[0287] 特点O4 3D碳泡沫结构:用于Gii-Sens的Gii-Thru:HISLOC制造工艺

[0288] 第4组:其他方面

[0289] 特点P:碳泡沫的可扩展制造:Gii 3

[0290] 特点Q:各种其他碳泡沫应用

[0291] 特点R:非石墨烯碳泡沫

[0292] 现在来看第1组:

[0293] 第1组:表面下碳泡沫

[0294] 特点A:在碳前体材料的表面下区域中产生的碳泡沫

[0295] 在现有技术部分中,我们已经描述了早先激光诱导石墨烯方法如何将碳前体的表面层转化为3D石墨烯。然而,所得3D石墨烯可能有点脆,可能从下层基板剥落,并且通常不适合于许多现实生活应用;此外,3D石墨烯通常相对薄,深度小于50μm。

[0296] 在本说明书中,我们描述了一种替代方法,其中碳前体的表面根本不被转化为石墨烯;而是仅碳前体的表面下区域14通过聚焦激光束12转化为碳泡沫16;在一个具体实施中,聚焦IR射束12在极短的时间内,在1ns与10μs之间(即,速率在约5×10^{7}℃/s与2×10^{12}

℃/s之间),在聚酰亚胺膜14内部的表面下区域或封装区域产生高于500℃的温度;这种短暂而强烈的加热足以在此表面下区域或封装区域中形成碳泡沫16。此表面下区域或封装区域16没有实质气体逸出通道;将气态产物限制在表面下区域或封装区域内有利地影响在所述表面下区域中形成的碳泡沫16的结构。仅在表面下区域中形成碳泡沫16是意外的发现;意外的原因有以下几点,包括聚酰亚胺碳前体材料对1064nm IR辐射的吸收率极低,每厘米的辐射吸收率(10进制)低于50或低至低于10。

[0297] 在激光照射下,表面(例如,垂直并面向激光的碳前体材料与碳前体材料周围的气体环境之间的界面)膨胀,并且从碳前体材料转化为无序无定形非石墨烯物质18。这种无序无定形非石墨烯物质18形成层,其通常是碳前体材料的总厚度的至少1%;对于500μm厚的聚酰亚胺膜,则通常顶部1μm-10μm被转化为无序无定形非石墨烯物质18;在此上部表面层下方,在碳前体材料的主体中,我们得到转化为碳泡沫16的区域。

[0298] 这种碳泡沫16的厚度通过逐渐移动激光束的焦点,穿过碳前体材料来控制;异常厚的碳泡沫结构可以使用这种工艺制成:已经实现了50μm-200μm(约)厚的碳泡沫轨迹。

[0299] 如果激光照射碳膜前体材料,诸如如图9-14B中所示悬浮在空间中(即,未安装在基板上)的聚酰亚胺膜,则在照射后,当我们逐渐移动穿过材料时,我们在上表面(即,面向激光的表面)得到无序无定形非石墨烯物质18;然后我们得到碳泡沫区域16。激光束12通常不接近碳前体材料的下表面,使得碳泡沫区域16位于尚未转化为碳泡沫的碳前体材料上方。如果激光接近碳前体材料的下表面,则靠近和位于下表面的碳前体转化为无序无定形非石墨烯物质。

[0300] 类似地,如果激光照射碳前体膜,诸如安装在基板上的聚酰亚胺(PI)膜,如图1-6所示,则我们得到相同的材料次序;此外,激光通常将接近靠在基板上的碳前体材料的下表面:然后靠近和位于下表面的碳前体转化为无序无定形非石墨烯物质17。此无序无定形非石墨烯物质17粘附至基板15;由于碳泡沫区域16粘合至此无序无定形非石墨烯物质17,因此碳泡沫区域16本身不直接结合至基板15,而是经由中间无序无定形非石墨烯物质17牢固地附接至基板15。

[0301] 这种方法实现了比使用将石墨烯泡沫形成限制于表面区域的先前方法可能获得的厚度显著更厚的碳泡沫结构。此外,这种方法实现了更稳健地(但不直接)粘附至下层基板的碳泡沫结构。需注意,使用这种方法,碳前体材料的任何表面都不产生碳泡沫。而是仅在碳前体材料内部的表面下区域中产生碳泡沫。

[0302] 我们可以概括为:

[0303] 一种制造碳泡沫材料的方法,其包括以下步骤:照射碳前体材料的表面下区域,激光束的参数被选择用于在所述表面下区域中产生碳泡沫。

[0304] 特点B:在碳前体材料的封装区域中产生的碳泡沫

[0305] 在上文特点A中,我们将通过激光照射而产生碳泡沫的区域定义为“表面下”区域。描述所述区域的另一种方式是将它定性为“封装”;这体现了碳泡沫与其周围环境的三维关系;碳泡沫16被原始碳前体材料并且被通过在碳前体材料14的上表面进行激光照射所产生的无序无定形非石墨烯物质18“封装”。

[0306] 我们可以概括为:

[0307] 一种制造碳泡沫材料的方法,其包括以下步骤:照射碳前体材料的封装区域,激光

束的参数被选择用于在所述封装区域中产生碳泡沫。

[0308] 特点C:在碳前体材料的区域中产生的碳泡沫,其中所述区域不具有实质气体逸出通道。

[0309] 在上文我们已经看到,碳前体的表面下区域或封装区域被转化为碳泡沫,并且此表面下区域或封装区域没有实质气体逸出通道;将气态产物限制在表面下区域或封装区域内影响在所述区域中形成的碳泡沫16的结构。

[0310] 我们可以概括为:

[0311] 一种制造碳泡沫材料的方法,其包括以下步骤:照射碳前体材料的封装、表面下区域,激光束的参数被选择用于在所述区域中产生碳泡沫,并且其中激光束不产生通向前体材料的表面的实质气体逸出通道。

[0312] 特点D:粘附至基板的无定形非石墨烯材料

[0313] 我们早先已经看到,如果激光11照射安装在基板15上的碳膜14,则激光使相邻于基板15的碳膜的表面碳化,以相邻于基板15形成无序无定形非石墨烯物质17;这种无序无定形非石墨烯物质17粘附至基板15;由于内部或表面下或封装碳泡沫区域16本身粘合至这种无序无定形非石墨烯物质17,因此碳泡沫区域16本身不直接附接至基板15,而是经由中间无序无定形非石墨烯物质17牢固地定位在基板15上。与常规激光诱导石墨烯相比,碳泡沫区域16粘合得更牢固,并且即使基板是柔性的,也不太可能剥落,从而实现了例如其中基板通常是薄且柔性结构的生物传感器应用。

[0314] 我们可以概括为:

[0315] 一种制造碳泡沫材料的方法,其包括以下步骤:照射定位于基板上的碳前体材料的内部区域,激光束的参数被选择用于在所述区域中产生碳泡沫并在碳泡沫区域与基板之间产生无序无定形非石墨烯材料;其中所述无序无定形非石墨烯材料粘附或以其他方式直接附接至基板。

[0316] 第2组:双激光加工

[0317] 特点E:通过激光烧蚀表面下碳泡沫区域所产生的碳泡沫

[0318] 先前的特点A-D覆盖了在碳前体材料的表面下区域或封装区域中产生碳泡沫。因为碳泡沫不在暴露表面上形成,而许多应用需要暴露碳泡沫(例如,用于生物医学传感应用或超级电容器而功能化),所以我们可以进行额外的步骤来暴露表面下或封装碳泡沫中的至少一些。

[0319] 我们早先已经看到,使用IR激光11进行激光照射,在表面下或封装碳泡沫16上方形成无序无定形非石墨烯材料18:我们现在使用激光(通常是长IR CO_2激光20)来烧蚀或以其他方式处理这种无序无定形非石墨烯材料18,并且因此暴露下层碳泡沫16。与初始激光不同,此第二激光20通常是散焦的。

[0320] 如前所述,我们使用标准220mm×180mm聚酰亚胺片材(但也可以考虑其他大小的聚酰亚胺片材);通常用于激光雕刻、激光切割和激光绘图(其可以描绘出由标准CAD程序定义的路径)的标准激光扫描装置以及标准平板丝网印刷装置和标准传送带式干燥机中可以考虑这种大小。可以考虑其他大小的聚酰亚胺片材。

[0321] 我们已发现,这种二次激光照射步骤以令人惊讶且有利的方式改变了下层碳泡沫的形态和其他特征,从而产生了先前未观察到的扭转或乱层多层碳泡沫。改变CO_2激光20参

数可以改变所述碳泡沫材料的性质,使得能够生产出具有针对不同应用而优化的性质的碳泡沫。

[0322] 这种新的暴露碳泡沫具有以下性质中的一者或多者:

[0323] • 厚度或深度易于控制

[0324] • 与使用常规激光工艺制成的高脆性石墨烯相比,柔韧性更大。

[0325] • 对任何下层柔性基板具有强粘附性

[0326] • 孔隙率高

[0327] • 电导率高

[0328] • 电容或电荷存储增加

[0329] • 对有机溶剂和水基溶液的吸收快速

[0330] • 亲水性更高

[0331] • EMI屏蔽高

[0332] • 电极质量增强

[0333] • 可润湿性高

[0334] • 防污。

[0335] 需注意,通过改变双激光工艺中使用的任一或两种激光的激光参数,可以改变这些性质中的一者或多者,以及缺陷的大小和程度及拉曼D峰和2D峰的大小(包括相对大小)。以这种方式,可以生产出具有针对不同应用而调谐或特别适合于不同应用的碳泡沫。令人惊讶的是,第二烧蚀激光的操作可以使得能够产生可用的暴露碳泡沫区域,特别是具有可以通过改变第一激光和/或第二激光的参数来调整的性质的那些暴露碳泡沫区域。

[0336] 我们可以概括为:

[0337] 一种制造碳泡沫材料的方法,其包括以下步骤:(a)激光束照射碳前体材料的封装区域或表面下区域,以在封装区域或表面下区域中产生碳泡沫并且在碳泡沫上方产生无序无定形非石墨烯物质,然后(b)进行激光烧蚀或处理,以去除无序无定形非石墨烯物质并暴露碳泡沫中的至少一些。

[0338] 特点F:通过激光烧蚀表面下碳泡沫区域所产生的碳泡沫

[0339] 在前述特点E中,我们描述了通过使用激光11(例如,IR激光)照射碳前体的封装区域或表面下区域而在所述区域中形成碳泡沫16;所述照射导致上层(在激光方向上)碳前体材料14膨胀为无序无定形非石墨烯物质18;然后,我们通过使用第二激光20(例如,CO_2激光)烧蚀上层无序无定形非石墨烯物质18来暴露或显露所述碳泡沫16。此第二辐射步骤不仅烧蚀了上层无序无定形非石墨烯物质18并且因此暴露下层碳泡沫16,而且还给予此下层碳泡沫具有非常理想的特征的意外且不寻常的表面形态21;这种所得碳泡沫可能是扭转或乱层多层碳泡沫。

[0340] 然而,由于这种泡沫可能具有与石墨烯泡沫不相关的特征(诸如广泛的缺陷、外观、可润湿性和拉曼光谱(参见以下特点R),所以在特点F中,我们明确将这种泡沫描述为“非石墨烯碳泡沫”。因此,术语“非石墨烯碳泡沫”(与术语“碳泡沫”不同)明确排除了石墨烯泡沫,包括扭转或乱层多层石墨烯泡沫,但延伸到覆盖任何其他3D碳材料泡沫。

[0341] 我们可以概括为:

[0342] 一种制造非石墨烯碳泡沫的方法,其包括以下步骤:

[0343] (a)激光束照射碳前体材料的封装区域或表面下区域,以在封装区域或表面下区域中产生碳泡沫并且在碳泡沫上方产生无序无定形非石墨烯物质,然后

[0344] (b)进行激光烧蚀或处理,以去除无序无定形非石墨烯物质并暴露下层碳泡沫中的至少一些,并且将下层碳泡沫中的至少一些转变成非石墨烯碳泡沫。

[0345] 特点G:在不同波段下的双激光

[0346] 我们在前面的特点E和F中看到,我们可以使用两个单独的激光照射步骤。这些步骤通常使用两个单独的激光进行:第一步,产生表面下或封装碳泡沫,通常使用聚焦IR激光11完成;以及第二步,涉及使用散焦CO_2激光20在较长波长下进行激光照射,但也可以使用其他波长(例如,UV和可见光)。

[0347] 第二激光20烧蚀位于碳泡沫16与表面之间的材料18(例如,无序无定形非石墨烯材料)并且暴露下层碳泡沫16。暴露碳泡沫16还可以通过第二激光来改变(例如,在其表面形态21方面),即,术语‘暴露’应被广泛解释为不仅包括显露预先存在的碳泡沫中的至少一些,而且还包括将预先存在的碳泡沫中的至少一些转变或改变为特征与预先存在的石墨烯泡沫的特征不同的3D碳材料泡沫。

[0348] 我们可以概括为:

[0349] 一种制造碳泡沫材料的方法,其包括以下步骤:

[0350] (a)使用在第一波段下操作的激光束照射碳前体材料的、在所述材料的表面下方的封装区域或表面下区域,以在所述封装区域或表面下区域中产生碳泡沫,然后

[0351] (b)使用在第二波段下操作的激光束去除或烧蚀位于碳泡沫上方的材料,以暴露所述碳泡沫中的至少一些。

[0352] 特点H:定位在通过激光烧蚀表面下碳泡沫区域所产生的碳泡沫中的电接触件

[0353] 我们早先已经看到我们如何产生碳泡沫,所述碳泡沫可以是扭转或乱层多层碳泡沫:因为这种材料具有特别的电性质(例如,电导率、电容),我们可以将一个或多个电接触件(还包括诸如柔性电子器件、微处理器、天线、IoT装置、电接口等电物件)附接或定位至碳泡沫中。对于印刷轨迹(例如,丝网印刷银轨迹),将这些轨迹丝网印刷至聚酰亚胺膜(或其他合适的基板)上以及预先存在的3D碳材料泡沫上方和内部,使得轨迹与泡沫以及泡沫上形成的任何结构诸如功能化层形成良好的电接触件(例如,参见下面的特点L,其中我们描述了如何将碳泡沫功能化以形成具有分析物特异性受体层的生物传感器)。

[0354] 我们可以概括为:

[0355] 一种制造碳泡沫材料的方法,其包括以下步骤:

[0356] (a)使用在第一波段下操作的激光束照射碳前体材料的、在所述材料的表面下方的封装区域或表面下区域,以在所述封装区域或表面下区域中产生碳泡沫,然后

[0357] (b)使用在第二波段下操作的激光束去除或烧蚀位于碳泡沫上方的材料,以暴露所述碳泡沫中的至少一些;以及

[0358] (c)将一个或多个电接触件附接、打印或定位至碳泡沫中。

[0359] 特点I:在聚酰亚胺膜上印刷电接触件并且然后产生暴露碳泡沫

[0360] 在特点H中,我们看到,一旦双激光工艺完成,便添加电接触件或电路以接触预先存在的碳泡沫,例如,可以将简单的银电接触件丝网印刷至碳泡沫上。在此特点I中,我们描述了通过首先将电接触件丝网印刷至聚酰亚胺膜上来开始工艺,然后通过使用双激光工艺

的第二个激光烧蚀步骤产生暴露碳泡沫来完成工艺。这具有一些优点,因为丝网印刷工艺可以干扰或破坏碳泡沫。我们将这种工艺称为“PPC”(“印刷后转化”的缩写),其中丝网印刷步骤在双激光工艺之前完成,以产生碳泡沫。在特点L5中,我们在下文描述了一种使用PPC工艺制造的生物传感器。

[0361] 因此对于丝网印刷轨迹(例如,丝网印刷银轨迹),这些轨迹被丝网印刷至聚酰亚胺膜(或其他合适的基板)上,使得碳泡沫随后在印刷轨迹的一端周围形成,从而提供了具有大表面并且因此具有非常好的电连接性的接触区域。与上文特点H中描述的替代工艺一样,印刷轨迹还与泡沫上形成的任何结构(诸如,功能化层)形成良好的电接触(例如,参见下面的特点L,其中我们描述了如何将碳泡沫功能化以形成具有分析物特异性受体层的生物传感器)。

[0362] 另选的顺序涉及使用第一激光束产生表面下碳泡沫,然后丝网印刷电接触件,然后使用第二激光束产生碳泡沫,使得形成与电接触件的良好电接触。

[0363] 我们可以概括为:

[0364] 一种制造碳泡沫材料的方法,其包括以下步骤:

[0365] (a)将电接触件丝网印刷至碳前体材料上或碳前体材料中;

[0366] (b)使用在第一波段下操作的激光束照射碳前体材料的、在所述材料的表面下方的封装区域或表面下区域,以在所述封装区域或表面下区域中产生碳泡沫,并且其中步骤(a)和(b)可以按(a)然后(b)或(b)然后(a)的顺序进行;以及

[0367] (c)使用在第二波段下操作的激光束去除或烧蚀位于碳泡沫上方的材料,以暴露碳泡沫中的至少一些,其与电接触件连接。

[0368] 特点J:在碳泡沫中制成的高轨迹

[0369] 我们早先已经看到,表面下或封装碳泡沫区域的厚度可以远远超过局限于表面层的常规石墨烯泡沫的厚度:第一激光束的激光焦点可以逐渐向下移动穿过碳前体材料,以产生深或厚的表面下或封装碳泡沫层。然后,我们展开第二激光照射步骤,烧蚀位于碳泡沫与碳前体材料的表面之间的材料,得到碳泡沫的暴露区域。此现在暴露的碳泡沫区域的厚度或深度为至少50μm;已经生产出厚度为300μm的碳泡沫。增加的厚度是有益的,因为它可以导致更好的电导率、更大的电容和更高的机械完整性。

[0370] 我们可以概括为:

[0371] 一种制造碳泡沫材料的方法,其包括以下步骤:

[0372] (a)使用在第一波段下操作的激光束照射碳前体材料的、在所述材料的表面下方的封装区域或表面下区域,以在所述封装区域或表面下区域中产生碳泡沫,然后

[0373] (b)使用在第二波段下操作的激光束去除或烧蚀位于碳泡沫上方的材料,以暴露所述碳泡沫中的至少一些;

[0374] 并且其中碳泡沫的厚度或深度为至少50μm。

[0375] 特点K:在不同的制造设施中应用第一激光和第二激光

[0376] 由第二激光束产生的碳泡沫的具体性质或结构可以被视为敏感信息,因为它们限定最终产品的特点;对于第一激光束工艺,期望由碳泡沫的供应商在供应商的制造设施进行,然后供应商将碳泡沫供应给客户,客户再在它们自己的制造设施使用第二激光束进行最后阶段。如我们早先说明的那样,通过改变第一激光和第二激光的参数,有可能改变碳泡

沫材料性质,使得能够生产出具有针对不同应用而优化的性质的碳泡沫。可以以这种方式改变或调谐的典型参数包括:强度、波长、脉冲频率、脉冲持续时间、脉冲轮廓、扫描速度、焦距、在表面下区域或封装区域产生的热。

[0377] 通过以这种方式分割制造工艺,供应商无需了解客户用作第二激光烧蚀工艺的一部分的特定制造工艺(例如,他们如何改变第二激光束的参数以给予暴露碳泡沫以他们需要的性质);客户可以对他们如何生产成品的细节保密。

[0378] 所以,制造工艺是一种三阶段工艺,其涉及以下步骤:(a)所述第一激光束在制造场所照射碳前体材料的表面下区域,以产生未完成的碳泡沫产品;(b)将所述未完成的碳泡沫产品转移至客户控制的制造场所;以及(c)在所述客户控制的制造场所进行所述激光烧蚀或处理。

[0379] 此外,这种方法实现了仅通过第一激光工艺来大规模制造(例如参见特点P)碳泡沫,从而降低了这种材料的成本,其可以用于许多不同的应用和客户。使用第二激光束产生的更专业的产品的制造量可能比仅通过第一激光工艺生产的碳泡沫的量低得多。所以,这种方法实现了更有效且更低成本地制造基础材料,即仅通过第一激光工艺生产的碳泡沫。

[0380] 我们可以概括为:

[0381] 一种制造装置的方法,其包括以下步骤:

[0382] (a)使用在第一波段下操作的激光束照射碳前体材料的、在所述材料的表面下方的封装区域或表面下区域,以在所述封装区域或表面下区域中产生碳泡沫,然后

[0383] (b)使用在第二波段下操作的激光束去除或烧蚀位于碳泡沫上方的材料,以暴露所述碳泡沫中的至少一些;

[0384] 其中步骤(a)在一个制造设施中进行,并且步骤(b)在不同的制造设施中进行。

[0385] 对于特点A-K,以下任选特点是尤其相关的。需注意,以下任选特点中的任何一者或多者各自都可以与一个或多个其他兼容的任选特点以及与特点A-K中的一者或多者组合:

[0386] 我们将覆盖以下领域:

[0387] 制造工艺

[0388] 第一激光束参数和控制方案

[0389] 表面下区域或封装区域的属性

[0390] 碳前体材料

[0391] 支撑碳前体材料的基板

[0392] 在激光束入射的表面处的碳化

[0393] 烧蚀激光束或第二激光束

[0394] 碳泡沫。

[0395] 需注意,以下任选特点中的任何一者或多者各自都可以与一个或多个其他兼容的任选特点以及与本说明书列出的其他“特点”中的任何一者或多者(例如,特点A-R)组合:

[0396] 上文所述的基于激光的制造工艺与常规CVD工艺相比具有许多优势;我们可以将这些列为以下任选特点:

[0397] 是室温工艺。

[0398] 是环境压力工艺。

[0399] 可以在塑料基板上进行(与任何制造工艺兼容,不仅仅是硅芯片制造)。

[0400] 可以在没有催化剂的情况下完成。

[0401] 向塑料基板上制造1cm^{2}约为50μm厚的碳泡沫约需要约2分钟或更短时间。

[0402] 实现了在柔性基板上形成3D碳泡沫。

[0403] 不需要石墨烯或氧化石墨烯前体。

[0404] 仅在碳前体材料的封装区域或表面下区域中产生碳泡沫材料,并且不在碳前体材料的任何表面产生碳泡沫材料。

[0405] 使用行业标准、低成本和可扩展的(i)丝网印刷技术和(ii)计算机控制的激光扫描技术的组合。

[0406] 可以适于高速、大批量卷对卷或卷对片生产。

[0407] 第一激光束参数和控制方案对于碳泡沫的生产非常重要;我们在此定义相关任选特点:

[0408] • 照射表面下区域或封装区域的激光束的参数包括以下中的一者或多者:

[0409] 强度、波长、脉冲频率、脉冲持续时间、脉冲轮廓、扫描速度、焦距、在表面下区域或封装区域产生的热。

[0410] • 改变激光参数使碳泡沫材料的性质改变,使得能够生产出具有针对不同应用而优化的性质的碳泡沫。

[0411] • 改变激光参数使以下碳泡沫材料性质或参数中的一者或多者改变:缺陷的大小、缺陷的分布、缺陷的程度、缺陷的类型、拉曼D和2D峰、拉曼D和2D峰的相对大小、厚度或深度、柔韧性、粘附性、孔隙率、电导率、电容、有机溶剂和水基溶液的吸收、亲水性、EMI屏蔽、电极质量、可润湿性、接触角、防污性。

[0412] • 激光束在表面下区域或封装区域中产生高于500℃的温度以形成碳泡沫。

[0413] • 激光束在表面下区域或封装区域中产生超过约500℃的温度以形成碳泡沫。

[0414] • 激光束的脉冲持续时间在约1ns与10μs之间,得到在约5×10^7℃/s

[0415] 与2×10^{12}℃/s之间的加热速率。

[0416] • 激光功率在8-20瓦特的典型工作范围内,最佳为12W。

[0417] • 激光焦距在50mm-400mm的典型工作范围内。

[0418] • 激光脉冲频率在约50kHz与500kHz之间。

[0419] • 激光脉冲频率在约1kHz与2MHz之间。

[0420] • 激光波长在约0.7μm-2.5μm之间。

[0421] • 激光在约9cm/s与40cm/s之间扫描。

[0422] • 激光束的参数包括焦点参数。

[0423] • 激光束的参数包括衍射参数。

[0424] • 激光束的参数包括干涉图案参数。

[0425] • 激光束的焦点移动穿过碳前体材料的深度,以在焦点通过的碳前体的表面下区域或封装区域中产生碳泡沫。

[0426] • 激光束的焦点移动穿过碳前体材料的深度至少约50μm,以在碳前体的厚度至少50μm的表面下区域或封装区域中产生碳泡沫。

[0427] • 激光束的焦点移动穿过碳前体材料的深度至少约100μm,以在碳前体的厚度为

至少100μm的表面下区域或封装区域中产生碳泡沫。

[0428] • 激光束在碳前体材料上扫描(例如,光栅扫描)或侧向移动,以形成所需的图案。

[0429] • 激光束在碳前体材料上扫描或侧向移动,以形成包括非重叠区域或线的所需图案。

[0430] • 激光束在碳前体材料上重复地扫描(例如,光栅扫描)或侧向移动,其焦点或强度最大值被布置在碳前体材料内的多个不同深度,直到产生具有所需图案和深度的碳泡沫。

[0431] • 激光束以在1.7mm/s与3550m/s之间,或更通常在35mm/s与350mm/s之间的扫描速率下扫描,并且扫描可以使得每英寸脉冲数(PPI)在100与10000之间(与生产个别近似于为220mm×180mm的聚酰亚胺片材有关)。

[0432] • 激光束的波长基本上不被碳前体材料吸收。

[0433] • 碳前体材料对激光束的波长的吸收率极低,其中每厘米辐射吸收率(10进制)低于50、或低于20、或低于10。

[0434] • 激光束是IR激光。

[0435] • 激光束是波长在约0.7μm-2.5μm之间的IR激光。

[0436] • 激光束是波长在约0.75μm-1.40μm之间的IR激光。

[0437] 可以通过以下任选特点来定义其中产生有碳泡沫的表面下区域或封装区域的属性:

[0438] • 与常规石墨烯泡沫不同,表面下区域或封装区域的厚度可以超过约50μm。

[0439] • 碳前体材料中表面下区域或封装区域的所需深度通过将第一激光束的焦点移动穿过深度来实现。

[0440] • 表面下区域或封装区域可以面向入射激光在碳前体材料的表面下方的不同深度;并且表面下区域或封装区域所在的确切深度是各种因素的函数,诸如激光强度、对所使用的碳前体材料的选择等。例如,表面下区域或封装区域可以低于碳前体材料的表面至少约10μm、20μm、30μm、40μm、50μm或更多。

[0441] • 表面下区域或封装区域的厚度可以在约10μm与200μm之间。

[0442] • 表面下区域或封装区域在低于碳前驱体材料的表面的一定距离处,该距离是各种因素的函数,所述因素诸如激光强度、其他激光参数、对所使用的碳前驱体材料的选择等。例如,表面下区域或封装区域的顶部可以低于表面碳前驱体材料的总厚度的至少1%、10%、20%、30%、40%。

[0443] • 表面下区域或封装区域是以第一激光束的最小横截面的中点为中心的一定体积的空间,并且所述体积在此中点的500或100微米、或1微米内。

[0444] 碳前体材料可以通过以下任选特点来定义:

[0445] • 碳前体材料基本上由热固性材料制成。

[0446] • 碳前体材料基本上由非热塑性材料制成。

[0447] • 碳前体材料是热固性膜。

[0448] • 热固性膜是聚酰亚胺膜。

[0449] • 碳前体是聚酰亚胺膜。

[0450] • 碳前体是聚酰亚胺膜,第一激光的波长在0.7μm至2.5μm的范围内。

[0451] • 碳前体是至少50质量％碳、或至少75质量％碳、或至少90质量％碳。

[0452] • 碳前体是膜或片材。

[0453] • 碳前体材料是柔性的。

[0454] • 碳前体材料是印刷层,诸如丝网印刷层。

[0455] • 碳前体材料的厚度大于5μm、或在5μm与120μm之间、或大于120μm。

[0456] • 碳前体材料是基本上平面或平坦的,并且垂直于第一激光束取向。

[0457] • 碳前体材料是均质的。

[0458] • 碳前体材料是异质的并且包含若干不同的材料。

[0459] • 碳前体被支撑在基板上,所述基板不由碳前体制成。

[0460] • 碳前体材料在第一激光束波长下的吸收系数低。

[0461] • 碳前体材料对于第一激光束的吸收系数低于50cm^{-1}、或低于20cm^{-1}、或低于10cm^{-1}。

[0462] • 碳前体材料对第二或烧蚀激光束的吸收系数(参见下文第3组特点)低于300cm^{-1}。

[0463] • 碳前体材料对于第二或烧蚀激光束的吸收系数为300±50cm^{-1}。

[0464] • 碳前体材料的热导率小于1.0W/mK(使用根据ASTM D5470的方法)。

[0465] • 碳前体材料的热导率小于0.5W/mK(使用根据ASTM D5470的方法)。

[0466] • 碳前体材料安装在基板上,所述基板在第一和/或第二激光束的一个或多个波长下是基本上光学透明的。

[0467] • 碳前体材料的碳源包含一种或多种聚合物或由其形成。

[0468] • 碳前体材料包含以下材料中的一者或多者:聚酰亚胺类(例如,聚(4,4'-氧二亚苯基-均苯四甲酸二胺),另外还称为聚酰亚胺)、聚醚酰亚胺类(PEI)、聚(甲基丙烯酸甲酯)类(PMMA)(例如,喷涂的PMMA)、聚氨酯类(PU)、聚酯类、乙烯基聚合物类、碳化聚合物类、光阻聚合物类、醇酸树脂类、脲醛。

[0469] • 碳前体包含以下材料中的一者或多者:聚(酰胺酸)类(例如,含芳基的聚(酰胺酸))(例如,聚(均苯四甲酸二酐-共-4,4'-氧二苯胺),酰胺酸,另外还称为聚酰胺酸);二酐类(例如,芳基二酐)(例如,均苯四甲酸二酐);所述聚(酰胺酸)类的衍生物;所述二酐类的衍生物(例如,均苯四甲酸二酐的衍生物)。

[0470] • 碳前体包含以下材料中的一者或多者:芳香族材料(例如,芳香族聚合物);杂芳香族材料(例如,杂芳香族聚合物);含有芳香族部分的聚合物;环状材料(例如,含有环状部分的聚合物);杂环材料(例如,含有杂环部分的聚合物);杂芳香族材料(例如,含有杂芳香族部分的聚合物)。

[0471] • 碳前体包含含有芳香键、或杂芳香键、或杂键(例如,酰亚胺键)中的一者或多者的材料。

[0472] 基板可以被认为是具有其上定位有碳前体的表面的材料;基板的具体材料、厚度和性质通过应用确定:例如,对于一些传感器,基板可以是薄的柔性塑料膜;对于其他应用,基板可以是其上可以安装有电子电路的刚性聚酰亚胺板。IR激光可以直接照射碳源;替代地,来自IR激光的辐射可以首先穿过基板,之后到达碳源,在这种情况下有两种替代情形:首先,基板对IR辐射是基本上透明的,并且碳泡沫形成的机制如上文所述。但在第二种情形

下,基板对IR辐射是基本上不透明的:然后,从基板至碳前体材料中的快速热传递首先在与基板的界面层产生无序无定形非石墨烯层,然后在碳前体材料内部的表面下区域或封装区域中形成碳泡沫。

[0473] 碳前体材料可以定位并支撑在基板上,所述基板可以通过以下任选特点来定义:

[0474] 基板是塑料主体、膜或箔。

[0475] 基板是柔性的。

[0476] 基板是聚酰亚胺电路板。

[0477] 基板对第一激光束的吸收率极低。

[0478] 基板在第一激光束的一个或多个波长下是基本上光学透明的。

[0479] 基板对第一激光束的吸收率高,吸收大于60%的第一激光束。

[0480] 基板对第一激光束的吸收率高,吸收大于60%的第一激光束,并且其热导率为至少10W/mK。

[0481] 碳前体材料的表面通过激光束转化为无序无定形非石墨烯物质,并且无序无定形非石墨烯物质粘附或粘合至基板,并且因此间接地将3D碳材料泡沫附接至基板。

[0482] 基板由以下中的一者或多者形成:硅(Si)、二氧化硅(SiO2)、氮化镓(GaN)、砷化镓(GaAs)、氧化锌(ZnO)。

[0483] 基板是硅晶圆。

[0484] 基板是二氧化硅晶圆。

[0485] 基板是包含硅和二氧化硅的晶圆。

[0486] 基板是碳源。

[0487] 基板不是碳源,例如,是金属、电介质材料、丝网印刷电介质材料。

[0488] 碳前体被定位在基板“上方”(例如,碳前体被定位成比基板更靠近激光源)。

[0489] 碳前体被定位在基板“下方”(例如,碳前体被定位成比基板更远离激光源)。

[0490] 在激光束入射的表面处的碳化可以通过以下任选特点定义:

[0491] 碳前体材料的表面由第一激光束转化为无序无定形非石墨烯物质。

[0492] 无序无定形非石墨烯物质占据低于相邻碳前体材料的表面的厚度,为碳前体材料的总厚度的约1%、或小于约1%、或小于约5%、或小于约10%。

[0493] 无序无定形非石墨烯物质延伸至低于碳前体材料的表面的距离,所述距离为至少10μm。

[0494] 无序无定形非石墨烯物质从外表面向碳前体材料的主体中延伸至10μm或更小的深度、或20μm或更小的深度、或30μm或更小的深度、或40μm或更小的深度、或50μm或更小的深度、或100μm或更小的深度。

[0495] 烧蚀激光束或第二激光束可以通过以下任选特点来定义:

[0496] 激光束的参数包括以下中的一者或多者:强度、波长、脉冲持续时间、脉冲轮廓、扫描速度、在表面下区域或封装区域产生的热。

[0497] 改变激光参数使碳泡沫材料的性质改变,从而能够生产出具有针对不同应用而优化的性质的碳泡沫。

[0498] 改变激光参数使以下碳泡沫材料的性质或参数中的一者或多者改变:存在的碳纳米结构的类型(例如,碳纳米洋葱等)、缺陷的大小、缺陷的分布、缺陷的程度、缺陷的类型、

拉曼D和2D峰、拉曼D和2D峰的相对大小、厚度或深度、柔韧性、粘附性、孔隙率、电导率、电容、有机溶剂和水基溶液的吸收、亲水性、EMI屏蔽、电极质量、可润湿性、接触角、防污性。

[0499] 烧蚀在碳前体中封装区域或表面下区域上方形成的无定形非石墨烯物质的激光束(“第二激光束”)是CO_2激光。

[0500] 第二激光束改变碳泡沫,作为使其暴露的工艺的一部分。

[0501] 第二激光束改变碳泡沫的形态,作为使其暴露的工艺的一部分。

[0502] 第二激光束被自动控制,以在相同区域、和/或重叠区域、和/或非重叠区域上扫描(例如,光栅扫描)。

[0503] 烧蚀无定形非石墨烯物质的激光束的波长在8μm-15μm之间。

[0504] 第二激光束是长IR激光、或UV激光、或可见光激光。

[0505] 第二激光束的脉冲频率在50kHz与500kHz之间,并且扫描速度在9cm/s与40cm/s之间。

[0506] 碳前体材料对于第二激光束的吸收系数高于$100cm^{-1}$,或对于第二激光束的吸收系数高于$200cm^{-1}$。

[0507] 碳前体材料对于第二激光束的吸收系数为$300\pm50cm^{-1}$。

[0508] 激光功率在8-20瓦特的典型工作范围内,最佳为12W。

[0509] 激光焦距在50mm-400mm的典型工作范围内。

[0510] 第二激光束以包括非重叠区域或线的图案扫描。

[0511] 第二激光束以与第一激光束的扫描图案匹配的图案扫描。

[0512] 第二激光束是散焦的。

[0513] 制造工艺是一种三阶段工艺,其涉及以下步骤:(a)所述第一激光束在制造场所照射碳前体材料的表面下区域,以产生未完成的碳泡沫产品;(b)将所述未完成的碳泡沫产品转移至客户控制的制造场所;以及(c)在所述客户控制的制造场所进行所述激光烧蚀或处理。

[0514] 碳泡沫可以通过以下任选特点来定义:

[0515] 碳泡沫的厚度为至少50μm。

[0516] 碳泡沫的厚度在50μm至300μm之间。

[0517] 碳泡沫是或包括多层扭转或乱层多层泡沫。

[0518] 碳泡沫是或包括具有缺陷的空间分布的碳泡沫,从而导致高电化学反应性。

[0519] 碳泡沫是或包括具有空位基面缺陷的碳泡沫,从而导致高电化学反应性。

[0520] 碳泡沫的碳:氧比率在25:1与50:1之间。

[0521] 碳泡沫具有快速电子转移常数。

[0522] 碳泡沫具有以下性质中的一者或多者:

[0523] o厚度或深度易于控制

[0524] o与使用常规激光工艺制成的高脆性石墨烯相比,柔韧性更大。

[0525] o对下层柔性基板具有强粘附性

[0526] o孔隙率高

[0527] o电导率高

[0528] o电容或电荷存储增加

[0529] o对有机溶剂和水基溶液的吸收快速

[0530] o亲水性更高

[0531] oEMI屏蔽高

[0532] o电极质量增强

[0533] o接触角为约20°或更小。

[0534] 碳泡沫的性质通过选择特定的激光参数来选择,以生成具有以下所需性质或参数中的一者或多者的碳泡沫材料:缺陷的大小、缺陷的分布、缺陷的程度、缺陷的类型、拉曼D和2D峰、拉曼D和2D峰的相对大小、厚度或深度、柔韧性、粘附性、孔隙率、电导率、电容、有机溶剂和水基溶液的吸收、亲水性、EMI屏蔽、电极质量、可润湿性、接触角、防污性。

[0535] 第3组:产品

[0536] 特点L1:生物传感器

[0537] 通过上文所述的双激光方法制成的碳泡沫在许多不同类型的传感器上具有广泛的应用。为简单起见,我们将在此特点L中使用短语“碳泡沫”指代通过本说明书中描述的方法制成的任何碳泡沫或3D碳材料泡沫。附录1包括有关此领域的更多细节,更详细地描述了一种生物传感器,其包括通过添加特异于目标或分析物的受体来功能化的碳泡沫,以及使受体能够间接附接至碳泡沫的接头;(一些受体不可以直接附接至碳泡沫,因为其与表面接触时稳定性较差;而是必须使用接头作为碳泡沫与受体之间的中介。在制造期间,首先将接头添加至碳泡沫,然后将受体添加至接头。)。

[0538] 对于生物传感器应用,功能化碳泡沫相比于常规石墨烯泡沫具有以下优势:电子传输速率更高;检测灵敏度更高;电化学有效区域更大;可再现性更高;成本更低;可润湿性增强;接触角为约20°或更小。

[0539] 在高层次上,功能化碳泡沫可用于传感器,因为它能够产生可检测的状态变化;它的高灵敏度是其大的表面积的函数。它可以用于检测特定化学物质、特定气体、机械应力和温度以及其他变量。我们将简要地查看每个类别。

[0540] 首先,化学传感器:化学检测系统依赖于检测当目标化学物质存在时碳泡沫的电响应;可以使用许多不同的检测原理,诸如电容、电阻、伏安法、氧化还原电势和电荷转移电阻的变化。

[0541] 例如,当特定的分析物或目标与碳泡沫结合时,可以检测到所述结合,因为其改变了碳泡沫的表面。将生物分子添加至碳泡沫,诸如特定抗体或适体(适体是短的单链DNA或RNA分子,其可以选择性地结合特定目标,包括蛋白质、肽、碳水化合物、小分子、毒素和活细胞)。当目标存在并与适体结合时,适体的形态就发生改变(例如,减少表面积),并且组合的碳泡沫和适体系统的电容以可测量的方式降低。

[0542] 使用这种原理,可以建立高灵敏度且高选择性的传感器;由于存在可测量变量(例如,电容)的定量减少,可以建立LOC(芯片实验室),其不仅包括碳泡沫和适体生物传感器,还包括LOC上的功率源,诸如超级电容器或使用碳泡沫作为其电极的其他储能器,以及测量变量、计算生物传感器输出并在LOC屏幕上展示所述输出(例如,目标存在或不存在;目标的浓度)的电路;特点O3(对于Gii-Sens的Gii-Thru:HISLOC)对此进行了进一步描述。

[0543] 碳泡沫传感器还可以测量目标的氧化还原电势;例如,当目标化学物质的氧化被添加至碳泡沫的特定催化剂催化时,可以检测到电流峰值;由于电流通常是目标化学物质

浓度的函数,所以有可能定量测量目标浓度。

[0544] 已应用于常规石墨烯传感器的其他技术,诸如检测特定化学物质的热导率测量,推断温度、物理变形或在存在特定化学物质的情况下的转变的电阻测量,检测运动的压阻变形,全部都可以应用于通过上文所述的双激光方法制成的碳泡沫传感器。

[0545] 利用通过双激光方法产生的碳泡沫的极大电化学有效区域和快速的电子传输速率的重要应用是针对生物传感而优化的电分析感测电极(称为"Gii-Sens"的具体实施)。

[0546] 例如,所述电分析感测电极可以用于即时诊断装置;所述感测电极具有极高的灵敏度、可靠性、纯度、可润湿性和电导率。

[0547] 图20A是称为Gii-Sens的生物传感器的透视图。所述组件由以下组成:聚酰亚胺基板201;工作电极202,其由Gii碳泡沫制成;对电极203,由Gii碳泡沫制成;参比电极204,其由丝网印刷银-氯化银制成;三个丝网印刷银连接轨迹205;和丝网印刷电介质层206。

[0548] 图20B-20D显示了四个主要制造阶段。图20B显示了步骤1,其中双激光工艺使用聚酰亚胺基板201作为前体产生Gii碳泡沫工作电极202(面积为18.94mm^2)和对电极203(面积为20.84mm^2)。

[0549] 图20C显示了步骤2,其中银-氯化银参比电极204(面积为8.99mm^2)被丝网印刷至聚酰亚胺基板201上。

[0550] 图20D显示了步骤3,其中银连接轨迹205被丝网印刷至聚酰亚胺基板201上;这些与电接触区域207处的碳泡沫电极重叠。银轨迹面积为1x18.85mm^2,并且三条银轨迹面积为3x 56.55mm^2。与下层碳泡沫电极重叠的面积为1x 2.21mm^2,并且与三个碳泡沫电极重叠的面积为3x 6.63mm^2。

[0551] 图20E显示了步骤4,其中电介质层206被丝网印刷在碳泡沫电极202、203、204和银连接轨迹205上方。电极的活性区域如下:工作电极202:12.64mm^2;对电极203:14.18mm^2;参比电极204:2.59mm^2。银连接轨迹205的暴露面积为1x 7.15mm^2和2x 21.45mm^2。

[0552] 图20F显示了单个聚酰亚胺片材,已使用上文所述的步骤1双激光工艺在所述单个聚酰亚胺片材上产生了100个碳泡沫工作电极和对电极的阵列。所述片材是标准类型的聚酰亚胺片材,220mm×180mm,使得能够使用标准丝网印刷和激光扫描设备进行处理;它可以是A5大小或任何其他合适的大小。

[0553] 图20G和20H显示了步骤4完成后片材的最终形式。100个单独的单元可以被切割并组装到100个成品Gii-Sens生物传感器中。

[0554] Gii-Sens感测电极的一个具体用例是用于电化学葡萄糖监测的可逆聚合物位移传感器机构。用于这种用例的石墨烯传感器已被提出:参见Polymer indicator displacement assay:electrochemical glucose monitoring based on boronic acid receptors and graphene foam competitively binding with poly-nordihydroguaiaretic acid",Wikeley等人,DOI:10.1039/d1an01991k。这篇论文描述了葡萄糖的芘衍生的硼酸化学受体被吸附至石墨烯泡沫电极上。去甲二氢愈创木酸(NHG)向石墨烯泡沫电极上的自发氧化聚合得到与硼酸受体共价附接的氧化还原活性膜(poly-NHG)。poly-NHG的氧化释放了硼酸受体,以与溶液相的葡萄糖相互作用,其由于还原的poly-NHG与硼酸官能团重新结合时的竞争性结合而被检测到。所述传感器显示出预期的硼酸对果糖葡萄糖的选择性。采用poly-NHG未结合和结合的伏安峰下的电荷比进行葡萄糖感

测,在pH 7水性缓冲液中,大致线性的分析范围为1至50mM葡萄糖。

[0555] Gii-Sens感测电极具体实施相比于诸如石墨烯传感器的电流感测电极具有许多优势:

[0556] 使用无扩增、无酶、无标记的电化学生物传感而检测限较低。

[0557] 可再现性增强。

[0558] 优化可用的动态范围。

[0559] 使背景噪音最小化。

[0560] 减少方案时间和操作。

[0561] 对于低成本制造来说可扩展。

[0562] 灵敏度和选择性高。

[0563] 给出定量的数字结果。

[0564] 可以被印刷成特定图案,例如叉指图案(interdigitated pattern),实现微型化集成装置。

[0565] 可以将现有的生物识别和测试格式(例如,ELISA、PCR、RT-PCR)翻译为电化学微流体POC,而不影响性能质量。

[0566] 可以进行基于阻抗的测量,具有极高的灵敏度、可靠性和极低的背景信号干扰。

[0567] 代替昂贵的大规模实验室测试和低灵敏度的侧向流测试。

[0568] 可以在微流体分析(单目标或多目标)和芯片实验室(LOC)装置中实现。

[0569] 可以用于用户旨在固定感兴趣的(生物)分子的任何传感器应用(例如,可以将羧基/n-羟基琥珀酰亚胺部分添加至传感器表面,以为后续的固定缀合化学反应提供平台)。

[0570] 可以用于多种诊断:POC(即时)人和动物健康、食品安全、就地环境健康和安全、农业健康和安全,由于其纯度和高比表面积,所有这些都具有增强的生物传感灵敏度、选择性和可再现性。

[0571] 可润湿性增强(例如,接触角低于约20°)。

[0572] 防污性增强。

[0573] 我们可以概括为:

[0574] 一种制造生物传感器的方法,其包括感测电极,所述感测电极包括至少部分地通过如上文特点A-K中任一项所定义的方法制成的碳泡沫。

[0575] L2:使用丝网印刷技术以可扩展、低成本的方式制造碳泡沫生物传感器

[0576] 我们已经在上文看到了丝网印刷如何广泛地用于制造工艺:这是一种众所周知的、可扩展的、可预测的且低成本的技术。Gii-Sens碳泡沫生物传感器的详细制造工艺示于图21中。

[0577] 我们可以概括如下:

[0578] 一种制造包括传感器电极诸如工作电极、对电极的生物传感器的方法,每个传感器电极包括至少部分地通过如上文特点A-K中任一项所定义的方法制成的碳泡沫,并且所述方法包括在每个电极上方丝网印刷电连接轨迹,并且用丝网印刷电介质至少部分地覆盖电极和连接轨迹。

[0579] 任选特点包括以下:

[0580] 上文所定义的方法,其中在步骤1中,双激光工艺使用PI基板作为前体产生碳泡沫

工作电极和对电极。

[0581] 上文所定义的方法,其中在步骤2中,参比电极,诸如银-氯化银电极,被丝网印刷至PI基板上。

[0582] 上文所定义的方法,其中在步骤3中,连接轨迹,诸如银轨迹,被丝网印刷至PI基板上以与碳泡沫电极重叠。NB:步骤2和3的顺序可以颠倒。

[0583] 上文所定义的方法,其中在步骤4中,电介质层被丝网印刷在碳泡沫电极和银连接轨迹中的至少一些上方。

[0584] 其他方面是:

[0585] 一种生物传感器,其包括传感器电极,诸如工作电极和对电极,每个传感器电极都包括至少部分地通过如上文特点A-K中任一项所定义的方法制成的碳泡沫,并且每个传感器电极都电连接至丝网印刷轨迹并且还至少部分地被丝网印刷电解质覆盖。

[0586] 一种即时诊断装置,其包括如上所定义的生物传感器。

[0587] L3:在不同的制造设施处向生物传感器添加功能化基团

[0588] 对于Gii-Sens生物传感器,在一个设施中制造了生物传感器,但客户在另一个设施(通常是他们自己的设施)中添加生物分子可以附接的功能化基团,因此加快了这些功能化基团的开发和测试,并且还保护了他们在这些功能化基团和生物传感器的最终设计方面的商业秘密和专有技术。

[0589] 我们可以概括为:

[0590] 一种在一个制造设施中制造包括传感器电极诸如工作电极、对电极的生物传感器的方法,每个传感器电极包括至少部分地通过如上文特点A-K中任一项所定义的方法制成的碳泡沫,并且所述方法包括在不同的制造设施将功能化基团添加至工作电极的另一步骤。

[0591] L4:向生物传感器添加功能化基团是生物传感器生产工艺的一部分

[0592] 对于Gii-Sens+生物传感器,制造工艺包括添加功能化基团。图22显示了Gii-Sens+的详细制造工艺。

[0593] 我们可以概括为:

[0594] 一种在一个制造设施中制造包括传感器电极诸如工作电极、对电极的生物传感器的方法,每个传感器电极包括至少部分地通过如上文特点A-K中任一项所定义的方法制成的碳泡沫,并且所述方法包括在所述制造设施将功能化基团添加至工作电极的另一步骤。

[0595] L5:使用PPC制造生物传感器:印刷后转化

[0596] Gii-Sens制造工艺的PPC变体示于图23中。PPC是“印刷后转化”的缩写,其中丝网印刷步骤在双激光工艺之前完成,以产生碳泡沫。具体步骤如下:

[0597] 1.在基底(例如,聚酰亚胺)上丝网印刷碳层

[0598] 2.丝网印刷Ag/AgCl参比电极

[0599] 3.丝网印刷Ag电连接轨迹

[0600] 4.丝网印刷电介质

[0601] 4.使用双激光工艺在基板中产生碳泡沫。

[0602] 所有丝网印刷步骤(1-3)都可以使用卷对卷或卷对片工艺完成,然后使用双激光工艺产生碳泡沫,并且然后将材料保持平整堆叠。

[0603] 另外,仅第一激光工艺(表面下泡沫产生)可以在设施中完成,然后将片材运送给客户,并且客户进行双激光工艺的第二阶段(激光烧蚀);客户可以在自己的制造设施中添加功能化基团,所述设施不同于进行双激光工艺中的第一激光工艺步骤(或两个激光工艺步骤)的设施。替代地,功能化可以在进行双激光工艺的设施中进行。

[0604] 在制造碳泡沫之前进行丝网印刷具有优势:因为我们没有对碳泡沫进行干燥,所以它不那么疏水。碳层充当聚酰亚胺中形成的碳泡沫(例如,碳泡沫和非石墨烯无序无定形泡沫)与银连接件之间的桥梁。

[0605] 我们可以概括为:

[0606] 一种制造包括传感器电极诸如工作电极和对电极的生物传感器的方法,每个传感器电极包括至少部分地通过如上文特点A-K中任一项所定义的方法制成的碳泡沫,并且所述方法包括以下步骤:(a)在所述基板上丝网印刷碳层;(b)丝网印刷电连接轨迹和参比电极;(c)在所述碳和所述电连接轨迹以及所述参比电极上方丝网印刷电介质层;然后(d)使用如上文特点A-K中任一项所定义的方法产生碳泡沫传感器电极。

[0607] 特点M1:储能装置:超级电容器

[0608] 因为使用特点A-K中任一项制造的碳泡沫具有非常大的电化学活性区域和快速的电子传输速率,所以它是电容器或超级电容器或赝电容器电极的理想材料。

[0609] 一种重要的应用是超级电容器(具体实施称为“Gii-Cap”)或其他储能设备(例如,锂离子电池)。对于超级电容器和其他电子应用,碳泡沫相比于常规石墨烯泡沫具有以下优势:表面积更大;多孔结构更多;质量更高;片材电阻更低;可润湿性更高。

[0610] 碳泡沫可以用金属氧化物或用于赝电容的其他赝电容材料(我们称为Gii-Cap+的变体)(例如,以产生金属氧化物层或膜)进行处理,并且所述金属氧化物膜具有极其大的表面积和快速的表面法拉第机制。

[0611] 需注意,当我们使用术语Gii-Cap时,我们包括Gii-Cap+变体,除非上下文明确表明了我们特别排除Gii-Cap+变体。还需注意,我们使用术语“超级电容器”来包括(i)电双层(EDLC)电容器,其中电荷以静电方式存储,电极与电解质离子之间没有相互作用,以及(ii)赝电容器,其中电极与电解质以及使用电双层电容和赝电容的组合的任何储能装置之间存在电子电荷转移。最后需注意,术语“超级电容器”应广泛解释为覆盖任何电化学电容器,包括EDLC超级电容器、赝电容器和这些的混合。Gii-Cap+变体主要是赝电容器,但我们仍然将其称为“超级电容器”。

[0612] 与常规超级电容器相比,Gii-Cap超级电容器中的碳泡沫电极增强了静电双层电容和电化学赝电容二者。附录2提供了有关超级电容器的更多细节,并且描述了一种具体实施,其中水凝胶电解质(例如,高摩尔浓度的盐)包封活性区域中的叉指碳泡沫电极以产生增强的操作电压窗口。

[0613] EDLC超级电容器Gii-Cap和赝电容器Gii-Cap+具体实施相比于常规可充电电池具有许多优势:

[0614] 充电快速

[0615] 功率高

[0616] 可回收

[0617] 不易爆炸

[0618] 柔性的形式和形状

[0619] 可以使用固体凝胶电解质或聚合物电解质(例如,离子凝胶或水凝胶),所述电解质在室温下为固体,具有远超过正常使用温度(例如90℃)的高转变温度;这样大大降低了电解质渗漏的风险。

[0620] 它可用于非常广泛的装置和功率存储需求,诸如芯片实验室(LOC)、IoT装置、电动汽车、UAV、EV应用。

[0621] 我们可以概括为:

[0622] 一种储能装置,诸如超级电容器,其中储能电极包括至少部分地通过如上文特点A-K中任一项所定义的方法制成的碳泡沫材料。

[0623] 特点M2:丝网印刷碳泡沫超级电容器层

[0624] 图24是Gii-Cap超级电容器的分解透视图。它由一系列碳泡沫电极241组成,所述碳泡沫电极连接至丝网印刷银连接器242对,使用上文所述的双激光工艺制成。电介质层243被丝网印刷在碳泡沫电极241和丝网印刷银连接器242上方。碳泡沫电极241形成在聚酰亚胺基层244上。铜连接插片245对连接至所述丝网印刷银连接器242对。电解质层246覆盖碳泡沫电极241(例如,离子凝胶电解质,诸如聚合物水凝胶电解质,其在室温下为凝胶或半固体,以使泄漏风险最少,并且在高于90℃时可逆地液化,因此可以在制造期间以液体形式应用)。所述组件被密封在铝层压热封袋247内。

[0625] 图25是超级电容器组件的分解透视图:它由形成超级电容器的碳泡沫电极241的叉指阵列组成;丝网印刷银连接器轨迹242为碳泡沫电极241提供电流,并且被电绝缘的电介质层243覆盖。聚酰亚胺片材244形成组件的基部。

[0626] 图26A-H显示了制造顺序。图26A显示了步骤1,使用双激光工艺产生叉指碳泡沫电极。图26B中的放大区域更详细地显示了叉指碳泡沫电极;A组电极形成电极集合,并且B组电极形成另一电极集合;两组电极之间的电容耦合储存能量。碳泡沫电极的厚度为约20-30μm。

[0627] 图26C显示了步骤2,丝网印刷银集电极。一个银连接器A'为A组电极提供电流,并且银连接器B'为B组电极提供电流。银层的厚度为约20-40μm,并且可以应用若干层。

[0628] 我们使用"共集电极"布局:典型的叉指超级电容器具有两个长的银集电极,石墨烯指位从每个长的银集电极的一侧延伸。长的银集电极由于其长度较长而电阻较大,并且使用显著量的银。此外,印刷集电极的弯曲部分也很困难。示于图26D中的"共集电极"方法中,我们具有从共享集电极242的两侧延伸的碳泡沫指位C:这样使指位的空间利用最大,并且因此使电容最大,减少了所需的集电极材料的量并消除了困难的弯曲集电极部分。

[0629] 连接至共集电极的碳泡沫指位的区域250具有圆形边缘;这些圆形边缘减少了应力断裂形成的机会并且增加了电连接的可靠性。

[0630] 图26F显示了步骤3,将电介质层243丝网印刷在银集电极上方以使它们电绝缘;大致厚度为10-30μm。

[0631] 图26G显示了步骤4,添加铜连接插片245(其由导电金属条带制成)以连接至银集电极242。图26H显示了步骤5,将电解质层246沉积在叉指碳泡沫指位上方。电解质可以是水凝胶和盐的组合(参见附录2)。图26I显示了步骤6,将整个组件包装至铝层压热封袋247中,仅留下铜连接插片245被暴露。还需注意,步骤4,添加铜连接插片245,可以在步骤2(丝网印

刷银集电极)之前以及在步骤5(将电解质层246沉积在叉指碳泡沫指位上方)之后完成。

[0632] 图27显示了单个聚酰亚胺片材将如何容纳6个220mm×180mm大小的这些Gii-Cap组件;其他大小(例如,A4、A5、A6或不同于A系列标准大小)也是可能的。

[0633] 详细的Gii-Cap制造工艺示于图28中。

[0634] 使用水凝胶电解质一次生产运行Gii-Cap超级电容器的规格示于以下表3中。

[0635]

描述	EDL 超级电容器
格式	A7 V4
电压窗口	2.5 V
电容	4.06±0.10 mF（在 65 mA 下测量）
等效串联电阻	0.77±0.04 Ohm
时间常数	0.016±0.001 s
能量	0.0033±0.0001 mWh（在 65 mA 下测量）
功率	355.77±9.11 mW（在 390 mA 下测量）
峰值功率	2.03 W
N	6

[0636] 表3

[0637] 我们可以概括为:

[0638] 一种储能装置,诸如超级电容器,其中储能电极包括至少部分地通过如上文特点A-K中任一项所定义的方法制成的碳泡沫材料;

[0639] 并且其中丝网印刷电连接轨迹形成在每个电极的至少一部分上方,并且丝网印刷电介质层至少部分覆盖电极和连接轨迹。

[0640] 特点M3:碳泡沫超级电容器:共集电极

[0641] 我们在上文看到了如何使用“共集电极”。

[0642] 我们可以概括为:

[0643] 一种储能装置,诸如超级电容器,其中储能电极包括至少部分地通过如上文特点A-K中任一项所定义的方法制成的碳泡沫材料并且以叉指图案布置;

[0644] 并且其中丝网印刷电连接轨迹形成在每个电极的至少一部分上方,并且其中单个电连接轨迹连接至从电连接轨迹两侧垂直延伸的下层指位。

[0645] 特点M4:碳泡沫超级电容器:PPC制造工艺

[0646] PPC(印刷后转化)示于图29中。步骤如下:

[0647] 1.将银集电极丝网印刷至基板(例如,聚酰亚胺)上。

[0648] 2.将碳丝网印刷在银集电器上方,然后干燥。

[0649] 3.将电介质丝网印刷在碳层上方,然后干燥。

[0650] 4.使用双激光工艺在碳层中产生碳泡沫;碳泡沫经由非石墨烯中间层附接至下层聚酰亚胺基板。

[0651] 5.分配电解质。

[0652] 6.添加铜/铝等插片以与银集电极接触(也可以是步骤1)。

[0653] 7.添加封盖/小袋。

[0654] 所有丝网印刷步骤(1-3)都可以使用卷对卷工艺完成,然后使用双激光工艺产生碳泡沫,并且然后将材料保持平整堆叠。另外,仅第一激光工艺(表面下碳材料泡沫产生)可以在设施中完成,然后将片材运送给客户,并且客户进行双激光工艺的第二阶段(激光烧蚀)和步骤5-7。

[0655] 在制造碳泡沫之前进行丝网印刷具有优势:如果首先制成碳泡沫,则它可能具有锋利边缘;在这些锋利的边缘上方施加的银丝网印刷层可能会在这些锋利边缘处破裂。但是通过在产生碳泡沫之前进行丝网印刷,我们就没有这种问题。另外,因为我们没有对碳泡沫进行干燥,所以它不具有疏水性。

[0656] 我们可以概括为:

[0657] 一种制造储能装置诸如超级电容器或赝电容器的方法;

[0658] 并且所述方法包括以下步骤:(a)将电连接器丝网印刷至基板上;(b)在所述电集电极上方丝网印刷碳层;(c)在所述碳层的至少一些上方丝网印刷电介质;然后(d)至少部分地通过如上文特点A-K中任一项所定义的方法产生碳泡沫储能电极。

[0659] 特点M5:碳泡沫赝电容器:金属氧化物变体

[0660] 使用金属氧化物电化学沉积工艺(例如,+ve为MnO_x;-ve为Fe_xO_x)产生Gii-Cap+变体;与标准Gii-Cap装置相比,其电容高得多(参见表4)。

[0661]

描述	赝电容器
格式	A7 V4
电压窗口	2 V
电容	856±120 mF(在65 mA下测量)
等效串联电阻	0.81±0.03 Ohm
时间常数	4.0±0.8 s
能量	0.48±0.07 mWh(在65mA下测量)
功率	277.91±13.94 mW(在390 mA下测量)
峰值功率	1.23 W
N	12

[0662] 表4

[0663] 这种金属氧化物电化学沉积工艺可以应用于Gii-Cap Supercap制造工艺以及PPC工艺,并且因此所有Gii-Cap产品也可以是Gii-Cap+产品。详细工艺流程图如图29所示。

[0664] 我们可以概括为:

[0665] 一种制造储能装置诸如超级电容器或赝电容器的方法,其中储能电极包括至少部分地通过如上文特点A-K中任一项所定义的方法制成的碳泡沫材料;

[0666] 并且所述方法包括应用赝电容材料诸如金属氧化物向所述储能电极进行电化学沉积工艺的步骤。

[0667] 特点M6:碳泡沫超级电容器:在低湿度环境中使用离子凝胶

[0668] 我们使用给出3V-6V的电压离子凝胶(具有气相二氧化硅SiO_2的离子液体)。它在低于90℃时为固态,所以在运输和正常使用期间不泄漏,并且因此特别可用于智能标签和IoT装置;在高于90℃时,其液化,并且因此可以进行印刷,其中在超过90℃的温度下进行电

化学印刷。离子凝胶通常由离子液体(例如,1-乙基-3-甲基咪唑鎓四氟硼酸盐(EMIMBF4)加上凝胶形成剂(例如,气相二氧化硅SiO_2))制成。

[0669] 通常,在惰性(例如,氩气)气氛下进行制造,因为O_2和H_2O的存在可能导致电压和稳定性降低。

[0670] 我们获得增加的电容与降低的电压之间的最佳平衡的O_2和H_2O水平的最佳位点在附录3(GiiCap Iongel)中进行更详细的描述。

[0671] 我们可以概括为:

[0672] 一种制造储能装置诸如超级电容器的方法,其中储能电极包括至少部分地通过如上文特点A-K中任一项所定义的方法制成的碳泡沫材料;

[0673] 并且所述方法包括在低湿度但非惰性的环境中应用离子凝胶的步骤,其中测量并控制所述环境中O_2和H_2O的水平以优化所述储能装置的电容。

[0674] 在覆盖特点M1-M6的前述章节中,我们关注了Gii-Cap碳泡沫超级电容器的一些一般特点。在覆盖特点N-S的以下章节中,我们关注实现Gii-Cap的一些更具体的产品。

[0675] 特点N1:电导体

[0676] 对于如上文所述的生物传感器的装置,有可能并且期望制造提供来自由双激光方法制成的碳泡沫材料的测量信号连接的电导体:因为这些电导体的电阻极低,所以灵敏度被最大化。电极(例如,被功能化的生物传感器工作电极,以及在上文被描述为被丝网印刷的参比电极;电容器板电极)是本特点N1覆盖的电导体的实例。另外,此特点N1还覆盖了主要功能是仅承载信号和电流的电极,例如,以替代常规的银连接轨迹,诸如我们在上文描述的生物传感器中的丝网印刷Ag电连接轨迹。

[0677] 我们可以概括为:

[0678] 一种制造电导体的方法,其中电导体包括至少部分地通过如上文特点A-K中任一项所定义的方法制成的碳泡沫。

[0679] 一种电导体,其包括至少部分地通过如上文特点A-K中任一项所定义的方法制成的碳泡沫。

[0680] 特点N2:组合的传感器和超级电容器

[0681] 上文特点L1-L4描述了在其传感器电极中使用通过双激光方法制成的碳泡沫的生物传感器;特点M1-M6描述了在其电极中使用通过双激光方法制成的碳泡沫的超级电容器和赝电容器。

[0682] 可以建立高灵敏度且高选择性的生物传感器,将此生物传感器和此超级电容器组合成单个集成装置,所述装置还包括测量被检测或测量的变量、计算生物传感器输出并将所述输出发送到POC诊断装置或将所述输出显示在装置的显示屏上(例如,目标存在或不存在;目标的浓度)的电子电路。

[0683] 图30是此集成LOC装置的示意性横截面:有两个独立的聚酰亚胺膜层,上层301包括功能化碳泡沫生物传感器(Giii-Sens)302,如特点L所述;下层303包括超级电容器304(Giii-Cap),如特点M所述。尽管示出了背靠背的聚酰亚胺层,但它们也可以并排的;此外,还可以有单个聚酰亚胺膜,其将生物传感器302和超级电容器304一起集成到单个物件上。

[0684] 具有微通道306的塑料件305提供了将测试流体分配在生物传感器302上方的微流体系统;如特点O中所述的表面下碳泡沫电极或常规连接器轨迹307从生物传感器指引至柔

性电子器件308(例如,在存在目标分析物的情况下测量生物传感器的电化学性质的变化的微控制器;显示诊断结果的显示面板;控制从超级电容器304到电子器件308的功率的功率管理系统)。超级电容器304(Gii-Cap)被充电(例如,通过由微控制器控制的无线感应过程(未示出))并为生物传感器测量过程和显示定量测量结果的集成显示器提供功率。替代地,可充电二次电池(未示出)或不可充电一次电池(未示出)可以对超级电容器304充电,然后超级电容器304为生物传感器测量过程提供功率。另一变体是使用可充电二次电池(未示出)或不可充电一次电池(未示出),其为超级电容器304充电,并且还为生物传感器测量过程提供功率。然后,超级电容器304被保留用于为高功率过程(诸如无线数据传输)提供功率,使得LOC成为独立成套的LOC装置,其可以进行诊断过程,并且还可以无线传输结果数据,而无需用户接近LOC,而如果LOC使用常规NFC(近场通信),则需要这样做。从超级电容器304到柔性电子器件308的电连接器轨迹未示出。

[0685] 完全集成LoC装置的分解图示于图31。从最底层向上,我们有(i)感应功率回路310;(ii)Gii-Cap超级电容器312,其由感应回路310无线提供功率;(iii)Gii-Sens生物传感器313;(iv)层314,其具有由超级电容器312提供功率的用于生物传感器的电子器件以及微流体通道;(v)顶部面板315,其包括同样由超级电容器提供功率的显示器316,以及环形孔317,样品被递送到所述环形孔中。

[0686] 图32显示在其显示器上展示定量结果的LOC。

[0687] 图33显示环境监测装置的分解图,所述环境监测装置包括Gii-Sens传感器330,其被配置用于检测环境参数,诸如CO_2水平、挥发性有机化合物和其他大气污染物。Gii-Sens不限于作为生物传感器,还可以检测碳泡沫传感器电极可以被功能化以检测的任何分子。环境监测装置包括Gii-Sens传感器330以及相关的控制和无线传输(例如,LoRaWAN)电子器件331,以及PV太阳能电池332和Gii-Cap超级电容器333。电子器件331中包括二次或一次电池(其可以是印刷电池),并且与PV太阳能电池332一起工作,为那些电子器件提供功率并为Gii-Cap超级电容器333充电。Gii-Sens传感器还可以被配置用于测量温度、湿度和压力。所述装置具有背部334,其可以被剥离,以显露粘性表面,使得可以将装置粘在墙上等。PV太阳能电池与电子器件331上的二次或一次电池结合,提供功率以为Gii-Cap超级电容器333充电,并且超级电容器333继而提供数据传输所需的峰值突发功率。与当前的环境监测装置不同,所述装置可以永久地安装并且就地保持多年,根本不需要更换电池。它可以检测大气污染物,其信噪比优于常规装置。组装的装置示于图34。

[0688] 可以使用组合的碳泡沫传感器和碳泡沫超级电容器实现许多其他类型的装置;例如:

[0689] 受益于能够(例如,无线)传输数据的任何生物传感器,其中数据传输由超级电容器提供功率,例如可穿戴健康监测装置,诸如连续血糖监测器、感测电解质、钾、钠、乳糖水平的其他可穿戴监测器。

[0690] 受益于能够(例如,无线)传输数据的任何传感器装置(即,不一定是生物传感器),其中数据传输由超级电容器提供功率。

[0691] 受益于能够(例如,无线)传输数据的任何IoT装置,其中数据传输由超级电容器提供功率。

[0692] 所述装置可以包括由超级电容器提供功率的电子器件。

[0693] 所述装置可以包括电池,以为储能装置和/或功率装置电子器件充电。

[0694] 所述装置可以包括PV电池,以为储能装置和/或装置和/或功率装置电子器件中的二次电池充电。

[0695] 我们可以概括为:

[0696] 一种制造包括传感器和储能装置诸如超级电容器二者的装置的方法,其中传感器和储能装置二者包括至少部分地通过如上文特点A-K中任一项所定义的方法制成的碳泡沫材料。

[0697] 一种传感器装置,诸如生物传感器,其包括(a)感测电极,其包括至少部分地通过如上文特点A-K中任一项所定义的方法制成的碳泡沫材料,以及(b)储能装置,诸如超级电容器,其中储能装置包括至少部分地通过如上文特点A-K中任一项所定义的方法制成的碳泡沫材料。

[0698] 一种即时诊断装置,其包括(a)感测电极,其包括至少部分地通过如上文特点A-K中任一项所定义的方法制成的碳泡沫材料,以及(b)储能装置,诸如超级电容器,其中储能装置包括至少部分地通过如上文特点A-K中任一项所定义的方法制成的碳泡沫材料。

[0699] 特点N3:组合的超级电容器和电池

[0700] 在此实例中,我们将两个不同的功率源组合到单个装置中,以形成合并或混合的功率源:所述装置具有电池(例如,印刷电池或常规电池)和超级电容器,所述超级电容器在其电极中使用通过双激光方法制成的碳泡沫;它们以互补的方式一起工作。电池可以是一次性使用的不可充电电池(“一次”电池),或者它可以是可充电电池(“二次”电池)。

[0701] 功率源具有互补的作用:电池可以为超级电容器提供缓慢而长期的充电,或为消耗功率水平相对较低的电子器件提供功率;超级电容器可以提供快速而高功率的放电并且为需要更高水平功率的功能(例如无线数据连接功能和数据有效载荷传输功能)提供功率。需注意,超级电容器可以是EDL超级电容器或赝电容器,或者任何其他形式的储能装置。所述装置可以用于偶尔需要高功率的情况(例如,为发送器提供功率以连接至数据网络并发送数据有效载荷),但所述装置需要是独立成套的并且在现场持续使用数月或数年:所述装置可以是高价值资产跟踪标签,其仅偶尔需要播送其信息,但需要以比常规印刷电池所能提供的更高的功率进行播送。

[0702] 示意图示于图35中。有两个单独的聚酰亚胺膜层,一个层351包括如特点M中所述的超级电容器(Gii-Cap)352,并且一个层353包括电池354,诸如印刷电池;这可以包括使用双激光工艺制造的碳泡沫或常规工艺制成的电极。还可能在同一片聚酰亚胺上制造印刷电池354和超级电容器352,但是由于印刷柔性电池或超级电容器中的任何缺陷将导致设备报废,因此产量可能会受到影响。

[0703] 如上文所述的表面下碳泡沫电极(或常规印刷电极)从超级电容器(Gii-Cap)352以及印刷电池354引导至BMS(电池管理系统)355;BMS 355为柔性电子器件356提供功率;表面下碳泡沫电极或常规连接器轨迹357连接柔性电子器件356的不同部分。BMS 355控制功率从电池354流向电子器件356;电池354可以对超级电容器352进行涓流充电。(超级电容器也可以是主功率源,其被设计为在设施充电一次,随后无需重新充电。)

[0704] 电池354可以是印刷电池,并且可以是可充电的二次印刷电池或一次性不可充电的一次电池;电池354可以对超级电容器352进行涓流充电并且为传感器或其他装置电子器

件356提供功率;然后,超级电容器352为对相对高的突发功率有短暂需求的电路(诸如,数据发送器)提供功率(例如,瞬时峰值功率)。如上所述,印刷电池、超级电容器、电子器件全部都可以是单个集成装置的一部分,例如全部在单个基板上,或者在单独但附接的基板上。

[0705] 尽管示出了背靠背的聚酰亚胺层,但它们也可以并排的;此外,还可以有单个聚酰亚胺膜,其将电池354和超级电容器352集成到单个物件上。

[0706] 电池354、超级电容器352、电子器件356全部可以作为连续或批量制造工艺的一部分在一个或多个基板上形成(例如,你不使用先前制造的电池并将其与超级电容器组合)。这使得互连件被构造为制造工艺的整体部分,导致较低的成本、较快的制造和较高的性能(例如,互连件更短)。

[0707] 所述装置可以用于智能标签(见下文),或IoT环境监测装置(例如,温度或湿度传感器)、火车座位占用传感器、医疗监测装置(例如连续血液葡萄糖监测器)。更一般地,装置可以包括由电池提供功率的电子器件;装置可以包括由超级电容器提供功率的电子器件;装置可以包括由超级电容器提供功率的数据发送器;电池可以是印刷电池;电池可以是一次电池或二次电池。

[0708] 我们可以概括为:

[0709] 一种制造包括电池和超级电容器的集成装置的方法,所述电池提供长期功率,并且所述超级电容器以高于所述电池的水平提供短期功率,其中所述超级电容器包括至少部分地通过如上文特点A-K中任一项所定义的方法制成的碳泡沫材料。

[0710] 一种包括电池和超级电容器的集成装置,所述电池提供长期功率,并且所述超级电容器以高于所述电池的水平提供短期功率,其中所述超级电容器包括至少部分地通过如上文特点A-K中任一项所定义的方法制成的碳泡沫材料。

[0711] 特点N4:智能标签

[0712] 一种重要的应用是智能标签,示于图36,底部表面示于左侧,具有人可读文本的暴露标签表面363示于右侧;标签包括粘性离型衬垫364,以便可以将底部表面附接至包装、部件等。标签包括薄的柔性电池360,其被印刷至聚酰亚胺膜,然后Gii-cap超级电容器361在同一聚酰亚胺层(或与印刷电池聚酰亚胺摸连接的不同的聚酰亚胺层)上形成。所述薄的柔性电池可以是不可充电的一次电池,或可充电的二次电池。超级电容器为数据发送器提供功率;印刷电池为智能标签电子器件(包括传感器)和功率管理电子器件提供功率。智能标签的一个表面上包括人可读的印刷信息363;背侧。

[0713] 智能标签包括电子器件模块362,其具有功率管理、传感器(例如,固态振动、温度、压力、GPS等传感器)和数据传输电子器件(诸如,LTE发送器或超低成本的LoRaWan发送器)。一旦建立了数据连接,超级电容器361便提供足够的峰值功率来发送有用的数据包,所以无需简单地将此数据包包括在“通告(advertising)”信号中;而是智能标签可以与数据接收器建立数据连接,然后一旦建立连接,便发送数据有效载荷;因此可以合理地确保其数据已被接收。更一般地,装置可以包括由电池提供功率的电子器件;装置可以包括由超级电容器提供功率的电子器件;装置可以包括由超级电容器提供功率的数据发送器;电池可以是印刷电池;电池可以是一次电池或二次电池。

[0714] 对于可扩展的制造(例如,以低成本生产数百万个智能标签),卷对片制造智能标签是理想的(参见下文特点P:Gii 3)。

[0715] 我们可以概括为:

[0716] 一种包括电池和超级电容器智能标签,所述电池提供长期功率,并且所述超级电容器以高于所述电池的水平提供短期功率,其中所述超级电容器包括至少部分地通过如上文特点A-K中任一项所定义的方法制成的碳泡沫材料;

[0717] 并且智能标签包括由电池提供功率的电子器件诸如传感器电子器件,以及由超级电容器提供功率的数据发送器。

[0718] 特点N5:组合的超级电容器和天线

[0719] 特点M中前述实例的超级电容器可以为天线提供功率,但不与电池集成:例如,它可以从太阳能电池提供功率或从本地WiFi或无线充电器(例如,Qi标准)提取功率。

[0720] 我们可以概括为:

[0721] 一种制造包括天线和超级电容器的集成装置的方法,其中超级电容器为天线提供功率并且包括至少部分地通过如上文特点A-K中任一项所定义的方法制成的碳泡沫材料。

[0722] 一种集成装置,其包括天线和超级电容器,其中超级电容器为天线提供功率并且包括至少部分地通过如上文特点A-K中任一项所定义的方法制成的碳泡沫材料。

[0723] 特点N6:组合的能量采集器+超级电容器

[0724] 一个有用的特点是将能量采集器与碳泡沫超级电容器组合成装置。能量收集器可以是固态能量收集器诸如太阳能电池,或振动能量收集器(例如,基于压电纤维),或热电发电机(例如,Seebeck发电机)。超级电容器可以为对相对高的突发功率有短暂需求的电路(诸如,数据发射器和天线)提供功率(例如,瞬时功率)。所述装置还可以包括一次电池(例如,不可充电的印刷电池)或二次可充电电池。

[0725] 能量采集器可以与超级电容器在同一基板上,或在单独但相连的基板上;超级电容器可以与能量采集器在基板的同一侧,或在相反侧。

[0726] 当装置中包括电池(例如,印刷可充电二次电池)时,能量收集器向电池充电,并且电池为低功率子系统(例如,传感器)提供功率,并且还向超级电容器充电;超级电容器为数据传输提供瞬时高功率。替代地,能量收集器可以直接向超级电容器充电。

[0727] 这种方法可以用于智能标签,或IoT环境监测装置(例如温度或湿度传感器)、火车座位占用传感器、可穿戴装置、医疗监测装置(例如连续血液葡萄糖监测器)。这种方法在需要持续(或高度规律地)为装置提供功率的情况下特别有用,例如,在需要持续监测环境或个人健康状况的情况下。

[0728] 所述装置可以包括LoRaWan或其他超低功率发送器。一旦建立了数据连接,超级电容器便可以提供足够的峰值功率来发送有用的数据包,所以无需简单地将此数据包包括在通告信号中;而是智能标签可以与数据接收器建立数据连接,并且因此可以确保其数据已被接收。

[0729] 更一般地,能量收集器可以是固态能量收集器,诸如太阳能电池、或振动能量收集器(例如,基于压电纤维)或热电发电机(例如,Seebeck发电机);所述装置可以包括由能量收集器提供功率的一个或多个传感器;能量收集器可以向超级电容器充电;所述装置可以包括一次电池或二次电池;所述装置可以是智能标签、或IoT环境监测装置(例如,温度或湿度传感器)、火车座位占用传感器、可穿戴装置或医疗监测装置。

[0730] 我们可以概括为:

[0731] 一种数据记录装置,其包括能量采集器系统和超级电容器,其中超级电容器为天线提供功率并且包括至少部分地通过如上文特点A-K中任一项所定义的方法制成的碳泡沫材料。

[0732] 特点O1:3D碳泡沫结构:用于Gii-Cap的Gii-Thru

[0733] 在早先的章节中,Gii-Cap超级电容器中的碳泡沫形成为单个平面叉指指位层。在本节中,我们描述了碳泡沫的三维结构,所述结构能够使碳泡沫超级电容器电极形成为平行板的3D结构,其储能潜在地大于单层叉指石墨烯泡沫指位。

[0734] 图37显示了核心结构中不同材料的基本分层。在PI聚酰亚胺膜371片材上进行多个丝网印刷步骤。首先,将导体(诸如,碳墨水或碳浆料层372)丝网印刷至聚酰亚胺膜371的下表面上。然后,将集电极373(例如,丝网印刷银集电极)丝网印刷在碳层372上方。然后,将电介质层374丝网印刷在集电极上方。

[0735] 图38显示了使用上文双激光工艺在聚酰亚胺膜371中形成的碳泡沫层:更具体地说,IR激光在PI膜371中形成封装碳泡沫层375;在此碳泡沫层下方,是在PI膜371的下表面形成的无序无定形非石墨烯层376。CO2烧蚀激光使先前封装的碳泡沫层370暴露,从而给予暴露表面层377以独特的形态。

[0736] 这种结构提供了从集电极层373、穿过导电墨水或浆料层372、穿过无序无定形非石墨烯层376、然后到碳泡沫层375的导电通路。以这种方式,就可以提高大面积碳泡沫375的电势,使其能够充当电容板;所述结构形成半电池的一部分。

[0737] 典型的厚度如下:聚酰亚胺膜371:127μm;碳墨水层:20μm;银集电极层373:30μm;电介质层:40μm;碳泡沫层375和无序无定形非石墨烯层376:127μm;独特的表面形态层377:25μm。

[0738] 需注意,Gii-Cap+(使用金属氧化物电化学沉积工艺(例如,+ve为MnO_x;-ve为Fe_xO_x,参见上文特点M2))并且比标准Gii-Cap装置递送显著更高的电容的变体)可用于Gii-Thru。

[0739] 我们可以概括为

[0740] 一种储能装置,诸如超级电容器,其包括:

[0741] (i)碳前体膜;

[0742] (ii)丝网印刷导电浆料或油墨层,其在所述碳前体膜的表面上;

[0743] (iii)丝网印刷集电极层,其在所述丝网印刷导电浆料或油墨层上方;

[0744] (iv)丝网印刷电介质层,其在所述集电极层上方;

[0745] (v)储能电极,其包括由至少部分地通过如上文特点A-K中任一项所定义的碳前体膜制成的碳泡沫材料,并且其中导电路径形成为经由所述导电浆料或油墨层从所述碳泡沫材料至所述集电极层。

[0746] 特点O2:3D碳泡沫结构:Gii-Thru可堆叠Gii-Cap/Gii-Cap+

[0747] 可以将图38中描述的多个结构彼此堆叠在一起;由于碳泡沫层的表面积可以很大(显著大于前面描述的平面叉指超级电容器中指位的表面积),这使得能够生产高性能超级电容器。

[0748] 半电池图示于图39中。它包括(逐渐向下移动穿过结构):水凝胶电解质层390;PI膜392中具有独特的表面形态的碳泡沫层391;丝网印刷碳浆料层393;带有外部铜插片395

连接点的丝网印刷银连接器层394;丝网印刷电介质隔离层396;PI膜398中具有独特的表面形态的第二碳泡沫层397;以及在堆叠基部的水凝胶电解质层399。将此结构与图38示意图相关联可能会有帮助:在图40A中,我们将图38所示的四个主要层分组在A处,即沿着堆叠向下移动,碳泡沫层,然后是碳墨水层,然后是银集电极层,然后是电介质层。图40B是图40A结构的横截面,显示了A组特点。图40B是相同的横截面,但这次标记了图39中的所有元件。

[0749] 全单元示于图41A和41B中。在图41A中,我们仅标记了图39中也存在的特点(使用相同的编号)。所以它包括:水凝胶电解质层390;PI膜392中具有独特的表面形态的碳泡沫层391;丝网印刷碳浆料层393;具有外部铜插片395连接点的丝网印刷银连接器层394;以及丝网印刷电介质隔离层396。

[0750] 在图41B中,我们现在增加了额外的层;逐渐向下移动穿过结构,我们具有丝网印刷电介质隔离层400,然后是具有铜插片402的丝网印刷银集电极层401,然后是丝网印刷碳浆料层403,然后是PI膜405中具有独特的表面形态的碳泡沫层404。

[0751] 在图41C中,我们将图38所示的四个主要层一起分组在A处;四个顶层的顺序相反,我们将它们一起分组在B处。A组和B组通过水凝胶(例如,聚合物水凝胶)电解质层399分开,使用常规电解质分配系统进行分配。

[0752] 图41D是此结构的横截面,显示了通过水凝胶(例如,聚合物水凝胶)电解质层399分开的A组层和B组层。图41E是同一横截面,但这次各个层按照图38的示意图进行编号。

[0753] 图41F是组装的超级电容器的透视图。

[0754] 图42显示了4个全单元超级电容器的堆叠;碳泡沫层示于A,并且聚合物水凝胶电解质示于B。可以向堆叠增加另外的单元,以得到所需的性能。

[0755] 图43A显示了Gii-Thru超级电容器的详细制造流程,并且图43B显示了Gii-Thru多堆叠超级电容器的详细制造流程。

[0756] 我们可以概括为:

[0757] 一种储能装置,诸如超级电容器,其包括子组件,所述子组件包括:

[0758] (i)碳前体膜;

[0759] (ii)丝网印刷导电浆料或油墨层,其在所述碳前体膜的表面上;

[0760] (iii)丝网印刷集电极层,其在所述丝网印刷导电浆料或油墨层上方;

[0761] (iv)丝网印刷电介质层,其在所述集电极层上方;

[0762] (v)储能电极,其包括至少部分地通过如上文特征A-K中任一项所定义的方法由所述碳前体膜制成的碳泡沫材料,并且其中导电通路形成为经由所述导电浆料或油墨层从所述碳泡沫材料至所述集电极层;

[0763] 并且其中多个子组件形成为堆叠,并且其中相邻的储能电极通过离子凝胶电解质分开。

[0764] 特点03:3D碳泡沫结构:用于Gii-Sens的Gii-Thru:HISLOC

[0765] 图38中描述的Gii-Thru结构不仅可以用于超级电容器,还可以用于Gii-Sens传感器,诸如生物传感器。

[0766] 对于微流体,Gii-Thru HISLOC(高灵敏度低成本)平台方法使液体和碳泡沫传感器能够在生物传感器装置的上表面上,并且连接至碳泡沫传感器的电连接件能够在生物传感器装置的下表面上。微流体技术常规使用功能化金电极,其中连接至功能化金电极的电

连接器全部是共面的;相比于这些功能化金电极,Gii-Thru生物传感器具有成本、产量和性能优势。并且将电连接件移动至生物传感器的底部或基部能够实现更大的小型化和与POC(即时)系统的兼容性。

[0767] 图44A是在三样品阵列微流体诊断装置中使用的Gii-Thru传感器的横截面示意图。顶层有三个样品孔440;待分析的流体流动至这些样品440中的每一个中。孔440形成为位于聚酰亚胺膜层442上方的层压孔间隔层441中的小孔。

[0768] 在聚酰亚胺膜层442中形成三个功能化碳泡沫区域,它们形成参比电极448A、工作电极448B和对电极448C;每个电极448A-448C的上表面暴露于孔440中存在的分析物流体。

[0769] 参比电极448A的基部可以包括Ag-AgCl层(或丝网印刷碳层)449;工作电极448B的基部是丝网印刷导电碳层443;对电极448C的基部是另一丝网印刷导电碳层443。以这种方式,参比电极448A与参比电极连接件444A电接触;工作电极448B与工作电极连接件444B电接触;并且对电极448C与对电极连接件444C电接触。

[0770] 丝网印刷电介质层447形成结构的基部。

[0771] 所以这种结构的有趣之处在于,电极连接件444A-C不与功能化碳泡沫电极448A-C共面,这与常规丝网印刷传感器不同。而是,它们在功能化碳泡沫电极448A-C下方的平面中,在与孔440的相反侧。这种结构使得能够实现更大的小型化和与POC(即时)系统的兼容性。

[0772] 图44B显示了图44A微流体诊断装置的等距分解图。三个样品孔440位于层压孔间隔层441中,所述层压孔间隔层位于聚酰亚胺膜层442上方。示出了参比电极448A、工作电极448B和对电极448C;参比电极448A的末端被Ag-AgCl层或丝网印刷碳层449覆盖;工作电极448B和对电极448C被丝网印刷导电碳层443覆盖。如上文所指出,参比电极448A与参比电极连接件444A电接触;工作电极448B与工作电极连接件444B电接触;并且对电极448C与对电极连接件444C电接触。

[0773] 需注意,三个功能化碳泡沫区域448A-C显示为位于不同平面的平面正方形;然而,这仅是用于创建附图的CAD的人为产物,并且碳泡沫区域448A-C更好地呈现于图44A中。丝网印刷电介质层447形成结构的基部。

[0774] 上文图44A和44B显示了三点阵列微流体诊断装置。在图45A和图45B中,我们展示了八点阵列微流体诊断装置。在等距图45A中,层压孔间隔件451包括用于工作电极的八个分析物孔452阵列,加上用于对电极的孔453和用于参比电极的孔454;层压孔间隔件451位于聚酰亚胺层455上方。聚酰亚胺层456中的Gii碳泡沫形成八个工作电极457和对电极458,并且使用双激光工艺制成。还需注意,碳泡沫电极457、458显示为位于三个不同平面的平面正方形;然而,这只是CAD的人为产物,并且碳泡沫在聚酰亚胺层455中形成连续区域。

[0775] 参比电极459用薄的丝网印刷Ag-AgCl层覆盖。薄的丝网印刷碳连接界面层460位于工作电极457和对电极458下方;丝网印刷银连接轨迹461形成与所有电极457、458和459的电连接。然后,丝网印刷电介质层462形成装置的壳体。图45B是图45A装置的一对俯视图;下图显示了下层连接轨迹路径。

[0776] 图46A显示完全组装的多样品阵列微流体诊断装置的透视图;图46B是俯视图。

[0777] 我们可以概括为

[0778] 一种微流体诊断装置,其包括定位于装置的上表面的样品孔,参比电极、工作电极

和对电极至少部分地通过由上文特点A-K中任一项所定义的方法由碳前体膜制成,在样品孔下方的层中,并且参比电极连接件、工作电极连接件和对电极连接件在所述参比电极、工作电极和对电极下方的层中。

[0779] 图47A显示了包括多个层压层的微流体诊断装置的分解图;它包括实现Gii-Thru的三点阵列(3SA)微流体生物传感器,如图44A所示。装置的顶层470是微流体箔;中间层471是具有粘合剂的微流体箔,并且包括印刷或模制微流体通道472,并且底层473是具有粘合剂的微流体箔。Gii-Thru传感器474是三点阵列(3SA)生物传感器并且包括连接器475。图47B是显示内部结构的俯视图。Gii-Thru传感器473可以用不同的生物传感器(例如,8SA)替代,以实现更大的灵活性。

[0780] 图48B显示了包含印刷或模制微流体卡的微流体诊断装置的分解图,并且它包括实现Gii-Thru的三点阵列(3SA)微流体生物传感器,如图44A所示。此装置包括透明树脂倒钩连接器481、顶部箔482、具有微流体通道484的透明树脂模制微流体卡483、由具有粘合剂的微流体箔制成的孔单元485和Gii-Thru传感器486。同样,Gii-Thru传感器486可以用不同的生物传感器(例如,8SA)替代,以实现更大的灵活性,并且模制微流体卡483可以用不同的微流体特点设计替代,以允许用于不同的测定平台。图45B是俯视图和侧视图。

[0781] 特点04:3D碳泡沫结构:用于Gii-Sens的Gii-Thru:HISLOC制造工艺

[0782] HISLOC制造工艺可以汇总如下:

[0783] 1.将弹层丝网印刷在聚酰亚胺膜的下侧。

[0784] 2.丝网印刷银连接件。

[0785] 3.丝网印刷银/氯化银参比电极(步骤3和4可以重新排序为4然后3)。

[0786] 4.丝网印刷电介质。

[0787] 5.使用双激光工艺在聚酰亚胺膜中产生Gii碳泡沫传感器电极。

[0788] 详细的制造工艺流程示于图49中。

[0789] 我们可以概括为:

[0790] 一种芯片实验室装置,其包括子组件,所述子组件包括:

[0791] (i)碳前体膜;

[0792] (ii)丝网印刷导电浆料或油墨层,其在所述碳前体膜的表面上;

[0793] (iii)丝网印刷导电层,其在所述丝网印刷导电浆料或油墨层上方;

[0794] (iv)丝网印刷参比电极;

[0795] (v)丝网印刷电介质层,其在所述集电极层上方;

[0796] (vi)传感器电极,其包括由至少部分地通过如上文特点A-K中任一项所定义的方法由碳前体膜制成的碳泡沫材料,并且其中导电路径经由所述导电浆料或油墨层从所述碳泡沫材料至所述导电层形成。

[0797] 第4组

[0798] 特点P:可扩展的制造:G-ii 3

[0799] Gii-3是卷对卷或卷对片生产上文所述的全部的基于Gii的材料的可扩展的制造设施。关键的商业优势在于,Gii 3制造不需要定制设备,它使用现成的计算机控制激光进行双激光碳泡沫制造以及常规丝网印刷和干燥技术:这些是众所周知的、易于理解的制造加工步骤和设备,实现了可再现性和可靠性。

[0800] 图50是总体制造工艺的示意图,并且图51显示了详细的工艺流程。

[0801] 我们可以概括为:

[0802] 一种制造包括一个或多个电极的装置的方法,每个电极都包括碳泡沫材料;

[0803] 其中所述方法包括使碳前体膜的连续卷轴通过制造至少部分地通过如上文特点A-K中任一项所定义的方法制成的碳泡沫材料所需的一系列操作。

[0804] 特点Q:各种其他Gii应用

[0805] 本说明书中描述的Gii碳泡沫可以用于各种各样的应用,包括常规石墨烯泡沫被认为适用的许多应用。

[0806] 我们可以概括为:

[0807] 一种装置,其包括至少部分地通过如上文特点A-K中任一项所定义的方法制成的碳泡沫材料,其中所述装置是以下类型的装置之一:

[0808] 霍尔效应传感器:碳泡沫显示出对磁场的响应。

[0809] 例如用于机器人的触觉传感器;显示了原型传感器,其使用聚二甲基硅氧烷(PDMS)嵌入至结构中和上方的Gii碳泡沫作为基于压阻的压力传感器中的活性层,以用于机器人触摸感应应用:几个碳泡沫层能够对压力呈现灵敏度,在0至>50kPa范围内,灵敏度为0.0418mV/kPa。参见DOI:10.4028/p-oy94hj.和DOI:1109/CDE52135.2021.9455738。这些内容在允许的最大范围内以引用的方式并入。

[0810] 感染性疾病传感器。

[0811] 生物传感器,其中Gii碳泡沫用芘羧酸(PCA)进行π-π非共价官能化,以用于白介素10阻抗检测。参见DOI:10.1016/j.bios.2022.114954,其内容在允许的最大范围内以引用的方式并入。

[0812] 持续监测化学传感器。

[0813] 葡萄糖监测传感器:显示了一种用于电化学葡萄糖监测的可逆聚合物位移传感器机构;葡萄糖的芘衍生的硼酸化学受体被吸附至碳泡沫电极上,与聚去甲二氢愈创木酸竞争性结合。参见DOI:10.1039/D1AN01991K,其内容在允许的最大范围内以引用的方式并入。

[0814] 乳酸传感器:采用合成有机受体分子,其基于将硼酸附接至碳泡沫,以在竞争性分析物结合中提供功能性和选择性,其中使用表面氧化还原聚合物指示剂置换。参见DOI:10.1016/j.snb2022.133089,其内容在允许的最大范围内以引用的方式并入。

[0815] 气体检测传感器,诸如过氧化氢和氧气检测,使用浸入pH 7的磷酸盐缓冲溶液中的Gii碳泡沫和自具微孔纳米颗粒聚合物(PIM-1)。参见DOI:10.1016/j.elecom.2022.107394,其内容在允许的最大范围内以引用的方式并入。

[0816] 光学检测器。

[0817] 自充电混合能源产生装置。

[0818] 绿色气体转化为有用的化学物质。

[0819] 燃料电池,例如氢燃料电池。

[0820] 过滤器,包括透气过滤器。

[0821] 加热装置。

[0822] 特点R:非石墨烯碳材料泡沫

[0823] 在扫描电子显微镜下,常规石墨烯泡沫看起来具有大的开放环状结构,通常大小

为500μm。使用双激光工艺生成的碳泡沫看起来非常不同;图52-图57A是这种Gii碳泡沫的SEM图像。

[0824] 图57B是碳纳米洋葱的SEM,参见“Raman spectroscopy of polyhedral carbon nano-onions”,DOI:10.1007/s00339-015-9315-9以及“Carbon nano-onions:unique carbon nano-structures with fascinating properties and their potential applications”,DOI:10.1016/j.ica.2017.07.021。它与Gii碳泡沫的相似性显而易见。

[0825] 如前所述,石墨烯泡沫具有许多特征:它是疏水性的,可润湿性低。对典型的石墨烯泡沫的拉曼分析揭示了以下特征签名:不存在D峰;2D峰高于G峰;D峰:G峰的比率接近于零。然而,使用双激光工艺生成的碳泡沫不具有这些特征;它是亲水性的,接触角低于20°;它缺乏石墨烯指示性的拉曼光谱特征签名:它显示出明显的D峰;2D峰明显小于G峰;D峰:G峰的比率明显高于零。图58显示使用双激光工艺制成的八个碳泡沫片材的拉曼位移,显示了拉曼特征签名的一致性。它还显示出显著的D峰;2D峰小于G峰;D峰:G峰的比率显著高于零。正如我们早先说明的,此拉曼光谱与碳纳米洋葱有很多共同之处。还可参见图18C,同样来自“Raman spectroscopy of polyhedral carbon nano-onions”,DOI:10.1007/s00339-015-9315-9。用于产生Gii碳泡沫的这种低电阻碳纳米洋葱变体的具体双激光参数在以下表5中:

[0826]

	第一激光	第二激光
激光机器	S300	S300
激光波长（nm）	Flexx - IR 1064nm	CO2 10600nm
功率（瓦特）	11	36
速度（mm/s）	810.11	188.15
PPI（每英寸脉冲）	n/a	1000
频率（Hz）	80000	n/a
DPI（点/英寸）	1000	1000
偏离（mm）	0	15
程数	1	1

[0827] 表5

[0828] 我们可以概括如下:

[0829] 一种碳泡沫材料,其至少部分地通过如上文特点A-K中任一项所定义的方法制成,并且其是亲水性的,接触角低于20°。

[0830] 一种碳泡沫材料,其至少部分地通过如上文特点A-K中任一项所定义的方法制成,并且其拉曼光谱表现出显著的D峰;2D峰小于G峰;D峰:G峰的比率高于零。

[0831] 一种碳纳米洋葱材料,其至少部分地通过如上文特点A-K中任一项所定义的方法制成。

[0832] 需注意,前面描述的任何装置,例如传感器、压力传感器、生物传感器、霍尔效应传感器、超级电容器、氢燃料电池、过滤器,都可以通过使用这些材料来表征,并且因此我们可以概括如下:

[0833] 一种装置,其包括至少部分地通过如上文特点A-K中任一项所定义的方法制成的碳泡沫材料,并且所述碳泡沫材料是亲水性的,接触角低于20°。

[0834] 一种装置,其包括至少部分地通过如上文特点A-K中任一项所定义的方法制成的碳泡沫材料,并且所述碳泡沫材料的拉曼光谱表现出显著的D峰;2D峰小于G峰;D峰:G峰的比率高于零。

[0835] 一种装置,其包括至少部分地通过如上文特点A-K中任一项所定义的方法制成的碳纳米洋葱材料。

[0836] 附录1使用水凝胶电解质的超级电容器具体实施

[0837] 附录2Gii-Cap+水凝胶

[0838] 附录3GiiCap离子凝胶

[0839] 附录4 3个月Gii-Sens®测定可行性提议

[0840] 附录5受体通过接头粘合至3D碳泡沫材料的传感器具体实施

[0841] 附录6基准实验条件

[0842] 附录7抗人原降钙素(cAb)的表面固定的优化

[0843] 需注意,附录1-7描述了Gii碳泡沫的特定具体实施。

[0844] 附录8特点和任选特点的合并列表

[0845] 附录1使用水凝胶电解质的超级电容器具体实施

[0846] 背景

[0847] 超级电容器是储存电荷的装置。根据构成和功能,超级电容器介于电解电容器与可充电电池之间。

[0848] 超级电容器的性质使其在需要短充电时间的应用中并且在使用许多充电/放电循环的应用中优于可充电电池。相比于电池,超级电容器的缺点包括在长时间段内储存能量的能力较弱。

[0849] 超级电容器的操作限制由部件的材料性质决定。具体来说,超级电容器可以操作(即其可以被充电)的最大电压取决于电解质和/或电极的稳定性。电容器的最大电压是一个重要参数,特别是因为电容器所存储的能量与电压的平方成正比。具有有机电解质的超级电容器通常比具有水性电解质的超级电容器支持更高的电压。通过利用有机电解质,超级电容器设计者可以生产出工作范围为2.5至2.7V的装置。相比之下,水性电解质虽然常常由于成本低和毒性小而优选,但通常产生的装置的工作电压范围较低。已知的对称型水性超级电容器通常不能支持高于1.3-1.5V的电压。如果使用不同材料的电极,则此电压限制可能达到1.8-2.0V。水基超级电容器的局限性归因于水的电解,原则上,当水暴露于1.23V的电势差时发生电解。但实际上,为了克服过电势的影响,在发生电解之前需要更大的电势差。

[0850] 基于碳的电极自其开发初期以来,便与超级电容器相关联。最初,碳作为电极材料受到关注,因为它提供了制造具有大表面积的电极的可能性。在超级电容器装置开发后期,人们才意识到电极表面所谓的双层的重要性。这种复杂且常常难以理解的现象与使用碳作为电极材料有关,是与超级电容器相关联的高电容值的核心。包括碳基电极的超级电容器装置被认为涉及在电极表面的双层,并且能量以静电方式存储。此类超级电容器被称为静电双层电容器或EDLC。

[0851] 还存在其他类别的超级电容器。电化学赝电容器利用金属氧化物电极或导电聚合物电极。与EDLC的静电荷存储机制相比,赝电容器中的电荷存储主要是电化学的。第三种类型的超级电容器是混合电容器。混合电容器具有不对称电极。一个电极通常由碳制成并且具有静电荷存储特性;另一个电极通常是含锂或掺杂锂的材料,其主要表现出电化学电荷存储特性。

[0852] 常规上,超级电容器可以被认为是并被建模为两个电容器的串联连接,每个电极与一个电容器相关联。每个电容器都定位于电极与电解质之间的界面处,并且由超级电容器电极、由电解质中存在的溶剂分子形成的电介质层(称为内亥姆霍兹平面)和由电解质提供的作为反电荷在电极上充电的电荷载体层(称为外亥姆霍兹平面)形成。在每个电极处形成电容系统的电极、内亥姆霍兹平面和外亥姆霍兹平面的这种三重结构被称为双层或电双层。

[0853] 本附录1特点的汇总

[0854] 所述特点的第一方面提供了一种对称型超级电容器装置,其包括:两个电极,其中每个电极包括如本说明书所述的碳泡沫(例如,参见附录8中的特点A-K);和在活性区域中包封电极的离子凝胶或水凝胶电解质。

[0855] 我们发现,根据上文特点的组合的对称型超级电容器装置产生增强的操作电压窗口。将所述装置称为对称型意指电极包括相同的材料,并且可能由相同的材料构成。

[0856] 超级电容器的操作电压窗口或操作窗口是这种装置的关键参数,并且由电解质的击穿电压决定。对于基于水性电解质的超级电容器,水的分解通常导致对操作电压窗口的限制。

[0857] 尽管尚未详细理解使用本发明公开的装置观察到的出乎意料的大操作窗口的原因,但是不受任何理论的约束,显而易见,所述特殊性质是碳泡沫电极和电解质的组合的结果,并且特别是这些元件之间的界面的结果。

[0858] 在电化学方面,本发明装置的大操作窗口等同于电极上出乎意料地大的过电势。过电势是超过特定还原/氧化反应的发生所述反应所需的热力学氧化还原电势的电势差。过电势通常是一种难以理解的现象,部分因为有很多因素会导致过电势。例如,过电势取决于电极材料、电极形态和电解质的性质。在本发明的特点中,碳泡沫电极提供给电解质的大的表面积被认为可能在装置性能中发挥作用。已知离子如何从电解质本体扩散到电极表面以及电极表面电荷载体的关联消耗对过电势产生影响。这可能在本发明的装置中发挥作用。电解质中电荷载体的扩散速率可能受到比非水合离子的大小更大的水合离子的存在的影响。电荷载体与碳泡沫电极的形态之间的相互作用也可能对过电势产生影响。离子凝胶或水凝胶聚合物的存在也被认为对电荷载体向电极表面的扩散有影响,可能是空间影响,并且与碳泡沫形态有关。

[0859] 水凝胶是一种液体成分为水并且可以由聚合物链网络形成的凝胶。由水凝胶电解质形成电介质的超级电容器将预期具有与基于水性电解质的超级电容器相关联的性能特征。然而针对此预期,本发明人发现,根据第一方面的超级电容器(即,对称型装置,其中电极由相同材料制成,这些电极包括碳泡沫并且被包封在水凝胶电解质中)的性能胜过水基装置的预期性能。相比于基于水性电解质的装置,所述装置的操作电压窗口出乎意料地得到了增强。操作窗口更类似于基于有机溶剂的超级电容器。

[0860] 具有大量亲水基团的聚乙烯醇(PVA)、聚乙烯吡咯烷酮(PVP)、聚丙烯酸钠、丙烯酸酯聚合物和共聚物是可以在水凝胶中利用的聚合物的实例。可以使用氟化水凝胶。水凝胶和离子电荷载体的组合有助于实现通过本发明系统实现的令人惊讶的大操作窗口。

[0861] 本发明公开的装置的电极位于基板上,并且电解质以密封电极结构的至少一部分的方式存在于电极顶部,因此形成活性区域。超级电容器的活性区域是包括电解质和电极的超级电容器中存储电荷的区域。

[0862] 所述装置的电极可以具有叉指(interdigitated)几何形状,即,它们可以是叉指的。叉指电极几何形状有助于最大化超级电容器的电容。叉指电极的几何形状还实现了不具有隔板(sepatator)的装置。超级电容器通常在相背对的电极之间包括隔板,以防止电极之间的短路。不存在隔板便于构造超级电容器装置。隔板也可能对装置性能产生负面影响,例如抑制电荷流动,导致充电/放电速率降低。不存在隔板避免了这些负面性能影响。

[0863] 叉指电极几何形状非常适合于对称型装置。在相反电极的材料不同的情况下构建叉指电极几何形状结构显然比在电极具有相同材料的情况下更为复杂。如果电极具有相同的材料,那么可以通过一个方法步骤就地制造电极。如果使用不同的电极材料,那么需要多个制造步骤,大大增加了制造工艺的复杂性。

[0864] 另外,不存在隔板还去除了隔板可能对装置性能产生的任何负面影响,例如抑制电荷流动,导致充电/放电速率降低。

[0865] 水凝胶电解质可以包含足够高以产生所述增强的操作电压窗口的电荷载体浓度。

[0866] 增强的操作电压窗口可能取决于电荷载体的浓度。

[0867] 电荷载体可以具有支持增强的操作电压窗口的氧化还原电势。

[0868] 电荷载体可以由酸的水溶液、碱的水溶液或盐的水溶液提供。可以使用的酸包括硫酸。可以使用的碱包括氢氧化钾。

[0869] 水凝胶电解质可以包括水凝胶和盐的混合物。电解质可以由水凝胶构成,其水凝胶聚合物可以例如是PVA或PVP。所述盐可以是,例如$NaClO_4$、或$NaNO_3$、或$Mg(ClO_4)_2$。盐的摩尔浓度可以是例如0.5M或更大,例如1M或更大,例如2M或更大,例如2.5M或更大,例如3M或更大,例如约5M。盐的摩尔浓度可以例如在1M与10M之间,或者它可以例如在2.5M与7.5M之间。

[0870] 可以使用的盐包括磷盐、高氯酸盐、硝酸盐和砷酸盐。盐的实例包括硫酸钠、硫酸氢钠、过硫酸钠、高氯酸钠、高氯酸锂、高氯酸镁、硝酸钠、六氟砷酸锂。这些盐的水溶液可以用于电解质中以提供离子载体。

[0871] 电荷载体可以是离子。电荷载体可以是水合离子。

[0872] 水合离子是水环境中的离子。极性水分子自身围绕离子布置,形成以离子为中心的水合球体。以本发明的特点观察到的令人惊讶的宽增强操作电压窗口背后的机制的细节难以理解,并且本发明人不希望受理论的束缚。然而,本发明的装置的令人惊讶的有利性质是电极与电介质材料之间协同作用的结果。增强的性能是在本领域技术人员预期发生电解的电压条件下缺乏水分解的表现。预期电极与电解质之间的界面是其性能的起源。电荷载体(可能是水合物)的大小与电极中存在的孔隙的大小之间可能存在协同相互作用。水凝胶包含聚合物链网络,并且水凝胶的这种链网络还可能具有物理(空间)效应,其限制了水分子暴露于可能导致其分解的电势差。

[0873] 水合离子大小的增加被认为与碳泡沫电极的多孔结构组合以阻碍靠近电极表面的扩散,导致过电势增加。

[0874] 对称型超级电容器装置的电极可以包括多孔碳泡沫。任选地,电极可以不包括额外的粘合剂材料。

[0875] 多孔碳泡沫电极被认为与电解质中的电荷载体组合以增加过电势,从而增强超级电容器的操作窗口。

[0876] 碳泡沫由一个或多个2D碳片材(每个片材是一层sp2键合碳)组成,它们彼此背向折叠,形成三维结构而不是平面片材。碳泡沫缺乏石墨或多层2D碳中发现的平面碳片材的规则AB堆叠。碳泡沫材料通常是多孔的。碳泡沫具有高表面积。通过改变生长方法的参数,可以控制碳泡沫的孔隙率,并且因此控制泡沫的表面积。这样的优势在于,可以在电极的制造工艺期间控制装置电极的孔隙率。

[0877] 碳泡沫电极可以在基板上。碳泡沫电极可以在聚酰亚胺基板上。聚酰亚胺基板可以是聚酰亚胺。基板可以形成超级电容器装置的基板。基板可以足够薄以便是柔性的,从而产生柔性的超级电容器装置。基板可以包含以下材料中的一者或多者(例如,由其形成):聚酰亚胺类(例如,聚(4,4'-氧二亚苯基-均苯四甲酸二胺),另外还称为聚酰亚胺)、聚醚酰亚胺类(PEI)、聚(甲基丙烯酸甲酯)类(PMMA)(例如,喷涂的PMMA)、聚氨酯类(PU)、聚酯类、乙烯基聚合物类、碳化聚合物类、光阻聚合物类、醇酸树脂类、脲醛。

[0878] 这些基板材料可以用作碳源,使用上文所述的双激光工艺将其转变为碳泡沫。可以通过用辐射(例如,激光辐射)照射聚酰亚胺基板(例如)来以这种方式生产碳泡沫。这样产生的碳泡沫经由直接附接至基板的无定形非石墨烯物质的中间层以化学方式间接固定至基板(参见本说明书前面的部分),从而得到稳固的结构。因此,通过使用基板的一部分作为碳源,即作为生产碳泡沫的试剂,可以原位生产电极。所述结构在稳固的同时又是柔性的。柔性装置在许多方面都有优势。柔性装置可以例如通过将其卷起来而方便地包装。例如,柔性装置还可以附接至弯曲结构的表面。

[0879] 基板可以基本上是平面的。基板可以是膜,例如薄膜。基板的厚度可以大于5μm。基板的厚度可以小于120μm。基板的厚度可以在5μm与120μm之间。基板的厚度在基板的表面上可以是基本上均匀的。基板可以是柔性的。基板可以是柔韧的。

[0880] 基板可以是具有第一表面和第二表面的聚酰亚胺条带(例如,聚酰亚胺条带)。

[0881] 电极可以进行质量平衡以优化操作电压窗口。

[0882] 超级电容器可以被视为两个串联在一起的电容器。为了使超级电容器的容量最大,两个组成性电容器的容量应相等。这可以通过调整各个电极的表面积来工程化,从而补偿影响容量的其他因素,诸如溶剂化离子的性质。调整各个电极的这种过程称为质量平衡。电极的质量平衡具有以下优势:可以最大化超导装置的容量,并可以延长超级电容器的寿命。

[0883] 在第二方面,有一种制造根据第一方面的对称型超级电容器装置的方法,其中:

[0884] 在基板上形成电极;

[0885] 将包含电荷载体和水凝胶的电解质前体应用至电极;

[0886] 电解质由前体形成,使得电极嵌入活性区域中的电解质中。

[0887] 碳泡沫电极可以通过以下制成:将基板的一部分(如果所述基板是或包括碳源)转

化为碳泡沫;或者使用化学或物理沉积方法,诸如物理气相沉积(PVD)、化学气相沉积(CVD)、分子束外延(MBE)、溅射、激光诱导生长、脉冲激光沉积、阴极电弧沉积、旋涂、浸涂或溶胶-凝胶法。以这种方式,在基板上原位生产电极。

[0888] 可以通过制备电荷载体的水溶液并且通过将此水溶液与水凝胶混合来制备电解质前体。可以使用激光辐射形成电极。

[0889] 在制备电解质前体时,应牢记不期望电解质中盐的沉淀或结晶。电解质中盐或任何固体的沉淀都可能导致装置破裂,或装置的其他缺陷,或装置性能的缺陷。这为盐溶液的浓度设置了上限。避免使用过饱和的盐溶液可能是有利的。精确的浓度上限可能取决于所存在的化学物质的具体情况。对于高氯酸钠,本发明人发现,浓度为5M所产生的电解质避免了盐的沉淀或结晶,同时结合其他特征,使得超级电容器装置的操作窗口超出根据对各个部件的考量所预期的范围。电解质可以包括浓度大于4M的盐溶液。电解质可以包括浓度大于3M,或大于2M,或大于1M,或大于0.5M的盐溶液。

[0890] 在较高的浓度下,观察到盐容易从电解质凝胶中沉淀出来,并且速度太快,导致装置无法正常使用。这种沉淀可能由水的蒸发造成。水解失水可能是另一个原因。在任何情况下,本发明人发现,尽管电解质凝胶可以使用浓度高达16.5M的高氯酸钠来形成,但是在所有高于10M的浓度下都观察到沉淀的问题。

[0891] 在制造水凝胶电解质时,可以使用高摩尔盐溶液。

[0892] 出于成本原因,较低浓度的盐溶液通常是有利的。

[0893] 碳泡沫层的厚度可在10μm与100μm之间。这有利于装置的柔韧性。可以将装置卷起来以变得更加紧凑。

[0894] 100μm与1000μm之间的间隙可以将电极彼此分开。装置的容量取决于电极之间的间隙,并且因此调控这个间隙会影响可以存储的电荷量。

[0895] 本发明的装置的操作窗口可以大于1.5V,或者它可以大于2V,或者它可以大于2.5V。

[0896] 系统的任一个方面的任选和优选特点都可以是系统的任何其他方面的特点。

[0897] 附录1附图说明

[0898] 我们参考了以下附图,在附图中:

[0899] 图59呈现在25mV/s下测量的针对正电压的碳泡沫循环伏安图。

[0900] 图60呈现在25mV/s下测量的针对负电压的碳泡沫循环伏安图。

[0901] 图61呈现在0.5mA/cm^2下测量的针对正电压窗口的碳泡沫恒电流充电放电(GCD)曲线。

[0902] 图62呈现在0.5mA/cm^2下测量的针对负电压窗口的碳泡沫恒电流充电放电(GCD)曲线。

[0903] 图63呈现从五个双电极装置取得的碳泡沫恒电流充电放电(GCD)数据。

[0904] 图64呈现在高(左)和低(右)扫描速率下从五个不同的双电极装置记录的碳泡沫循环伏安图。

[0905] 图65呈现五个其他系统的碳泡沫循环伏安图数据,所述系统因为水凝胶电解质的性质而有所不同:(a)3M $NaClO_4$和PVA;(b)1M $NaClO_4$和PVA;(c)2.5M $NaNO_3$和PVA;(d)3M $Mg(ClO_4)_2$和PVA;以及(e)5M $NaClO_4$和PVP。

[0906] 附录1详细描述

[0907] 双电极超级电容器

[0908] 根据此特点的典型碳泡沫超级电容器装置具有叉指碳泡沫电极，如图26所示。重新总结，聚酰亚胺基板支撑超级电容器电极，在此实例中，超级电容器电极由碳泡沫构成并且以叉指梳状几何形状布置，并且其形成叉指电极结构。银电流集电极沿着装置的每一侧延伸，使每个相反电极在电气上成为一体。叉指电极结构的非基板侧包封在水凝胶中。可以添加聚酰亚胺盖来容纳水凝胶，或者另外以其他合适的方式包装装置。

[0909] 如前文所解释，碳泡沫电极可以在聚酰亚胺基板上形成。通过将合适的基板(即提供碳源的基板，在此实例中为聚酰亚胺基板)暴露于激光束，在基板上方形成碳泡沫。以这种方式生产的碳泡沫从基板生长，并且间接粘附至基板。基板和以这种方式原位形成的碳泡沫电极形成一个主体。

[0910] 碳泡沫电极在环境条件下使用红外CO_2激光生产。基板是商用聚酰亚胺膜，标称厚度为127微米。一个实例是每个电极有十一个平行的碳泡沫条带。这个数字显然可以变化。正电极的碳泡沫条相对于第二电极的碳泡沫条偏移，从而形成叉指结构。

[0911] 电极尺寸如表6所示：

[0912]

质量平衡比	1.18
正极半电池“电极指”	
长度(cm)	0.4
宽度(cm)	0.0472
厚度(cm)	0.005
指的数量	11
暴露的总面积(cm^2)	0.20768
负极半电池“电极指”	
长度(cm)	0.4
宽度(cm)	0.04
厚度(cm)	0.005
指的数量	11
暴露的总面积(cm^2)	0.176
指间距离(cm)	0.04
总活性电极表面积(cm^2)	0.38368
总活性电极体积(cm^3)	0.0019184

[0913] 表6

[0914] 三电极装置

[0915] 除双电极超级电容器装置之外，还制造了另外包括参比电极的三电极测试装置。三电极装置包括工作电极、对电极和Ag/AgCl参比电极。工作电极和对电极中的每一者均由碳泡沫制成，在此具体实施方案中，碳泡沫通过聚酰亚胺基板的双激光照射而产生，如前所述。此装置用于确定$NaClO_4$水凝胶电解质稳定的电压范围。使三电极装置在制造后在进行任何测量之前稳定至少一小时。

[0916] 水凝胶电解质的制备

[0917] 所公开的双电极和三电极装置中的每一者均基于5M高氯酸钠溶液,并且电解质以现在描述的方式制备。通过将高氯酸钠(纯度98%,来自Sigma-Aldrich)溶解于去离子水中(用量:将3.061g $NaClO_4$溶解于5ml去离子H_2O中),制备5M高氯酸钠溶液。然后在120℃的热板上用磁力搅拌器搅拌高氯酸钠溶液,同时添加聚乙烯醇(PVA,99%水解,Sigma-Aldrich)。每10mL溶液溶解1.5g PVA。将高氯酸钠溶液和PVA的混合物从热板上移开并使其冷却,随后其形成白色不透明的凝胶状溶液。然后将凝胶溶液加热至120℃,直到它液化并变得透明。然后将它沉积至石墨烯电极上。沉积在电极表面后,液化水凝胶电解质材料在室温下在约5分钟内凝固。沉积在电极上的电解质的量取决于待覆盖的表面积。对于测试装置,沉积150μL电解质。

[0918] 三电极装置的实验结果

[0919] 可从超级电容器获得的性能最终受到电解质稳定性的限制。

[0920] 为了测试本发明系统中的电解质稳定性,使用本文所述的三电极装置进行了几项实验。最初使用差分脉冲伏安法(DPV)来选择通过循环伏安法(CV)和恒电流充电放电(GCD)测量来调查哪些电压窗口。

[0921] i循环伏安法

[0922] 进行循环伏安测量以确定电解质的稳定性。在标准的三电极测量中,工作电极与参比电极之间的电势以恒定速率从开放电路电势(OCP;标称0V)扫描至预定上限,之后再次向下扫描。在此期间监测工作电极的电流响应。

[0923] 这些测量的结果示于图59和图60中。图59显示从OCP以正方向扫描电压的结果。

[0924] 上部结果集合显示最大电势为1V、1.2V、1.3V和1.4V的四个伏安图。下部结果集合另外包括最大电势为1.6V的伏安图。当电压上限增加超过1.2V时,循环伏安图的形状变得不那么“正方形样”。随着最终扫描电压变大,尾部变得越来越明显,指示电解质降解,这可能归因于水的电解。这些伏安图指示,电解质在高达+1.2V下是稳定的。

[0925] 图60显示了类似的结果集合,但是针对的是负极电压。这些数据表明电解质直到-1.4V都是稳定的。

[0926] 综合起来,图59和60中的数据为装置提供了2.6V的工作窗口。这比使用水基电解质的预期情况高得多。

[0927] ii恒电流充放电(GCD)数据

[0928] 进行了恒电流充放电(GCD)测量,以根据充电和放电时间确定库仑效率。在这些测量中,在计数器与工作电极之间施加电流,并且测量工作电极的电压响应(相对于参比电极)。对于正极电压,针对选定的电压窗口使用2×10^{-5}A(0.5mA/cm^2)的放电电流所测量的GCD曲线示于图61中。曲线在超过1.2V后趋于平稳,这指示电解质降解。选定负极电压窗口的GCD曲线示于图62中。

[0929] 对于高达-1.6V和-1.8V的电压窗口看到显著的趋于平稳,指示电解质降解。-1.4V的电压窗口具有三角形GCD曲线,指示了稳定性。

[0930] 对三电极系统的循环伏安法测量和恒电流充电放电测量的结果汇总于下表。

[0931] 第一个表格(表7)总结了正极电压窗口的平均库仑效率、面积放电电容和放电能量数据。

[0932]

EW	平均库仑效率	标准偏差	平均放电面积电容	标准偏差	来自 GCD 的放电能量
[V]	[%]	[%]	[mF/cm²]	[mF/cm²]	[J]
1	93.9	0.91	1.59	5.66E-02	3.12E-05
1.1	91.7	1.32	1.69	6.23E-02	4.02E-05
1.2	**87.8**	**1.30**	**1.82**	**7.53E-02**	**5.17E-05**
1.4	54.9	7.04	2.95	3.56E-01	1.14E-04
1.6	25.3	2.71	9.60	1.32E+00	4.05E-04

[0933] 表7

[0934] 第二个表格(表8)总结了负极电压窗口的平均库仑效率、面积放电电容和放电能量数据。

[0935]

EW [V]	平均库仑效率	标准偏差	平均放电面积电容	标准偏差	来自 GCD 的放电能量[J]
-1	87.86	9.911	1.2970	0.311	2.65E-05
-1.2	87.98	7.354	1.5103	0.577	3.84E-05
-1.4	**87.04**	**5.636**	**1.8482**	**1.012**	**5.72E-05**
-1.6	82.21	5.419	3.1486	2.598	1.30E-04
-1.8	67.16	17.728	5.3844	4.637	2.88E-04

[0936] 表8

[0937] 在这些汇总表中,库仑效率是在第二个GCD循环中测量的存储能量和递送能量的比率;以mF/cm²为单位的面积电容通过以下公式计算:

[0938] 面积电容 $$\left[\frac{mF}{cm^2}\right] = \frac{2 * E_{\text{充/放电}}\ [J]}{A_{\text{几何}}\ [cm^2] * (EW)^2\ [V^2]} * 1000$$

[0939] 并且放电能量是GCD曲线的充电部分和放电部分随时间推移的积分。

[0940] GCD曲线指示+1.2V和-1.4V是实际的正极电压和负极电压极限。

[0941] 这些电压极限和面积电容的值允许根据以下公式计算质量平衡:

[0942] $$\frac{m^+}{m^-} = \frac{C^-\Delta E^-}{C^+\Delta E^+}$$

[0943] 其中,m^+=正电极的质量,m^-=负电极的质量,C^+=正电极的电容(F),C^-=负电极的电容(F),ΔE^+=正极电压窗口极限,ΔE^-=负极电压窗口极限。

[0944] 双电极装置的实验结果——超级电容器性能

[0945] 针对双电极超级电容器装置,在0.25mA/cm²至30mA/cm²的施加电流密度的范围内,收集了恒电流充放电(GCD)数据。图63绘制了从五个不同装置(CH1-CH5)取得的GCD结果。利用2.6V的电压窗口来收集这些数据,在较高的电流密度下观察到更大的电解质稳定性。双电极超级电容器的另外的性能数据呈现于图64中,显示了在0.01V/s至5V/s的扫描速率下,

从根据本发明具体实施的五个不同装置(装置#1至#5)记录的循环伏安图。

[0946] 右栏中的循环伏安图是在低扫描速率(0.01V/s、0.025V/s、0.05V/s、0.075V/s、0.1V/s、0.25V/s和0.5V/s)下记录的,并且左栏中的循环伏安图是在高扫描速率(0.75V/s、1V/s、2V/s、3V/s、4V/s和5V/s)下记录的。这些数据中显示的趋势是,扫描速率越高,电解质稳定性越高。在图64所示的每个循环伏安图集合中,较快的扫描电压导致电压上升与电压下降之间的电流响应的差异较大。

[0947] 除上文公开的装置之外,还以类似的方式但使用包含以下的水凝胶电解质构造了装置:(a)3M $NaClO_4$和PVA,(b)1M $NaClO_4$和PVA,(c)2.5M $NaNO_3$和PVA,(d)3M $Mg(ClO_4)_2$和PVA,以及(e)5M $NaClO_4$和PVP。

[0948] 这些额外装置的循环伏安测量结果如图[.]10所示。对于每种电解质,在0V与0.7V之间、0V与0.8V之间、0V与0.9V之间、0V与1.0V之间、0V与1.2V之间、0V与1.3V之间以及0V与1.4V之间运行循环伏安图。相似地,对于每种电解质,在0V与-0.7V之间、0V与-0.8V之间、0V与-0.9V之间、0V与-1.0V之间、0V与-1.2V之间、0V与-1.3V之间以及0V与-1.4V之间运行循环伏安图。这些数据示于图65中。

[0949] 数据指示,在每个装置中,对于(d)3M $Mg(ClO_4)_2$和PVA以及(e)5M $NaClO_4$和PVP中的每一者,电解质直到极限-1.4V和+1.1V以及直到+1.2V都是稳定的。

[0950] 可以在本公开的范围内做出进一步的变化和修改。

[0951] 附录1概念

[0952] 1.一种对称型超级电容器装置,其包括:

[0953] 两个电极,其中每个电极包括碳泡沫材料;以及

[0954] 水凝胶电解质,其包封活性区域中的电极。

[0955] 2.根据概念1所述的对称型超级电容器装置,其中所述水凝胶电解质包含水凝胶和盐的混合物。

[0956] 3.根据概念1或概念2所述的对称型超级电容器装置,其包括离子电荷载体。

[0957] 4.根据概念3所述的对称型超级电容器装置,其中所述离子电荷载体是水合的。

[0958] 5.根据前述概念中任一项所述的对称型超级电容器装置,其中所述电极包括碳泡沫。

[0959] 6.根据前述概念中任一项所述的对称型超级电容器装置,其中所述电极包括碳泡沫材料。

[0960] 7.根据概念1、5和6中任一项所述的对称型超级电容器装置,其中所述碳泡沫材料形成在基板上。

[0961] 8.根据概念7所述的对称型超级电容器装置,其中所述基板为聚酰亚胺基板。

[0962] 9.根据概念7或概念8所述的对称型超级电容器装置,其中所述基板形成所述装置的基板。

[0963] 10.根据前述概念中任一项所述的对称型超级电容器装置,其中所述对称超级电容器装置是柔性的。

[0964] 11.一种制造根据概念1至10中任一项所述的对称型超级电容器装置的方法,其中:

[0965] 在基板上形成电极;

[0966] 将包含电荷载体和水凝胶的电解质前体施加至电极;

[0967] 电解质由前体形成,使得电极嵌入有效区域中的电解质中。

[0968] 12.根据概念11所述的制造对称型超级电容器装置的方法,其中通过制备电荷载体的水溶液并且通过将所述水溶液与水凝胶混合来制备所述电解质前体。

[0969] 13.根据概念11或概念12所述的制造对称型超级电容器装置的方法,其中所述电极原位形成。

[0970] 14.根据概念11至权利要求13中任一项所述的制造对称型超级电容器装置的方法,其中所述电极通过用激光辐射照射所述基板来形成。

[0971] 附录2:Gii-Cap+水凝胶

[0972] 在此附录2部分中,我们证明了Gii碳泡沫作为其上可以沉积赝电容材料的理想基板的有效性,与使用Gii碳泡沫作为唯一电极材料相比,产生了极大增强的电容。就上下文而言,这些仅碳泡沫的装置显示在0.25-0.4mF/cm^2区域内的全电池比电容。

[0973] 样品制备

[0974] 对A7大小的Gii-Cap进行电沉积,以便在其上铸造赝电容材料层。v4和v5设计均适用于电沉积,得到类似的性能。v4样品的结果将在本文档中详细说明。

[0975] 首先将含有6个Gii-Cap装置(2行、3列)的片材切成两半,得到两个3装置半片材。将两个半片材安装在内部制作的夹具上并放置在电沉积槽MiniPlant 3的内部。首先将样品沉积MnOx,用去离子水冲洗,随后再沉积FexOy。FexOy沉积后,将其再次冲洗并在40℃的空气中干燥至少2小时。

[0976] 沉积的详情如下。氧化锰前体溶液含有乙酸锰四水合物(40mM)和表面活性剂(Tween20,0.1重量%)的混合物。沉积通过恒定电流脉冲进行。开启时间为0.5秒,关闭时间为2秒。施加的开启电流为744mA(19.14mA/cm^2,基于电极的标称几何面积)。关闭电流为0mA,即开放电路。MnOx沉积共计390个循环(每个电极3.7C/cm^2)。FexOy前体溶液包含40mM Fe-TEA复合物(TEA是三乙醇胺)。它含有$FeCl_3$、TEA和NaOH。沉积同样通过恒定电流脉冲进行。开启时间为1s,关闭时间为2s。施加的开启电流为233mA(6mA/cm^2),关闭电流设定为0mA。沉积过程进行了1,000个循环,得到每个电极6C/cm^2。

[0977] 沉积完成且将样品干燥后,将它们分割成各个装置。在工作区域外部,沿着装置边缘之一固定包含丝网印刷Ag/AgCl油墨的准参比电极(RE)(用于在测试期间监测各个电极电势)。然后将电解质应用至装置的的工作区域,并延伸至RE上。所用的电解质是水性水凝胶,其含有作为盐的$NaClO_4$和作为胶凝剂的PVA(聚乙烯醇)。水凝胶储备液批含有199.5g NaClO4一水合物、256.9ml去离子水和42.4g PVA。混合物在室温下是固体,在接近水的沸点的温度下变成液体。为了分配水凝胶,将其加热至94℃以使其液化。通过将液体电解质滴加至有效区域和RE上来进行分配,通常每个装置3-4ml。然后使样品上的水凝胶冷却,约10分钟后重新凝固。凝固后,通过向装置上应用聚酰亚胺膜来防止电解质过度蒸发。一旦施加了盖子,装置即可进行测试。

[0978] 电化学测试参数

[0979] 使用Biologic VMP-3稳压器/稳流器对样品进行电化学测试。对它们进行初始性能表征,然后进行500次充电-放电循环(调节方案(conditioning protocol)),并完成最终表征。报告的标称值是在第二个表征步骤中获得的值。应用调节方案以使样品的性能更加

稳定和一致。

[0980] 测试期间,将电压控制在电池水平(正电极与负电极之间的绝对差),最小值为0V,最大值为2V。还测量了每个电极与共同RE之间的电势差,使得能够计算出各个电极性能度量。

[0981] 这两个表征步骤称为Ragone测试。它们是相同的,并且包括以下:

[0982] a)循环伏安法(CV)。使用了三种扫描速率:50、100和250mV/s。每个扫描速率五个循环。

[0983] b)恒电流充电-放电(GCD)。测试了七种电流密度:1、2.5、5、7.5、10、20和30mA/cm^2(基于总装置几何面积=12.96cm^2)。每个电流密度下进行五个循环。

[0984] c)电化学阻抗谱(EIS)。电压控制,使用1V DC施加电压和10mV AC信号。在1MHz-10mHz区域内测量。

[0985] 调节步骤通过以10mA/cm^2进行500个GCD来实现。

[0986] 标称电容值是在5mA/cm^2下调节后根据GCD计算的。ESR(等效串联电阻)根据GCD中放电半循环开始时的电压降计算。报告的ESR值也来自5mA/cm^2下的最终GCD。ESR还可以根据从EIS获得的奈奎斯特曲线图来计算。获得的结果几乎相同。

[0987] 结果和结论

[0988] 对总计48个装置计算平均值。采用来自第3258和3259批的样品。典型的CV曲线示于图66中。全电池响应(左图)显示准矩形的形状,指示存储机构不是纯电容的。这是可以预料到的,因为MnOx和FexOy都是氧化还原活性材料。装置的大部分电容都集中在高于0.5V的电池电压下,如通过0-0.5V区域中的全电池曲线的小包络(envelope)可以看出。低电池电压下电容较小的解释可以在半电池曲线上看出,示于图66的右图。根据此图可以看到,MnOx用作正电极,而FexOy是负电极。MnOx是近乎理想的赝电容材料,如其CV大致呈矩形(灰色轨迹)所证明。

[0989] 同时,FexOy电极对电势的响应更加不对称。其电容大部分集中在低于0V vs Ag/AgCl的电势。当电势大于0V vs Ag/AgCl时,FexOy显示出很小的电容,如通过在这些电势下蓝色轨迹的小包络所示。因此,这种不对称的FexOy响应解释了在全电池中获得的在低电压下的较小电容。

[0990] 图66显示来自样品3258-1#4的在100mV/s下获得的后调节CV曲线。左图显示全电池CV,而右图显示在全电池测量期间获得的半电池曲线。

[0991] 使用GCD曲线进行电容计算,因为它们提供更准确的值。调节后的典型GCD曲线示于图67,显示了全电池和半电池测量结果。所述装置显示出良好的电容响应,具有准三角曲线。全电池呈现从最大电压降至约0.5V的线性放电,指示MnOx和FexOy的赝电容实现了近乎理想的电容行为。如在CV曲线中看到的那样,FexOy显示出不对称的电容与电势关系,这解释了在低于0.5V的电池电压下放电更快。

[0992] 图67显示来自样品3258-1#4的在5mA/cm^2下获得的后调节GCD曲线。全电池和对应的半电池响应分别示于在顶部线、中部线和底部线中。

[0993] 除相对于电势的不同赝电容行为之外,MnOx和FexOy电极还显示不同水平的电容。两个电极在装置中占据相同的几何面积,但MnOx电极在装置内经历小得多的电化学窗口(参见图66和图67中最大电极电势与最小电极电势之间的差)。MnOx窗口较小(0.65±

0.06V)的原因是,与FexOy(1.35±0.06V窗口)相比,它的比电容较大。对于本研究中所评估的装置,调节后的MnOx电容达到246.8±36.0mF/cm^2,而FexOy电极的调节后电容为171.4±38.4mF/cm^2。因此,这些Gii-Cap+装置在电极尺寸方面是对称的,但在电极组成和电势分裂(potential split)方面是不对称的。

[0994] 由于全电池实际上是两个串联的电容器(由电极与电解质抗衡离子之间的双层形成),因此总电池电容将低于单个电极的电容。调节后的平均全电池电容为52.5±9.4mF/cm^2。在与报告标称电容相同的电流密度(64.8mA,5mA/cm^2,电池水平)下,根据放电开始时的电压降计算的ESR为0.85±0.12Ω。

[0995] EIS测量进一步证实了这些装置良好的电容响应,如图68所示。根据奈奎斯特曲线图,可以通过定位曲线与y轴的交点来估算ESR。就图68所示的样品而言,根据EIS计算的ESR为0.78Ω,与针对同一样品根据GCD计算的0.73Ω非常匹配。伯德曲线图提供了有关装置在不同频率下的行为的信息。在高频率下,例如100-10000Hz,装置的功能基本上类似于电阻器,相位角为0°。随着频率下降,相位角增加,指示电容贡献更大(理想电容器的相位角为-90°)。当相位角超过45°标记时,装置被认为本质上主要是电容性的。因此,45°相移发生的时间可以被视为装置的特征时间常数。对于本研究中的样品,平均时间常数为4.48±1.18秒。此时间常数可以理解为有效电容响应的循环时间阈值。当循环时间低于时间常数时,装置将无法完全充分操作。

[0996] 图68显示来自样品3258-1#4的通过在1V DC(全电池)下的恒电势EIS获得的调节后奈奎斯特(左)和伯德(右)曲线图。左图的插图显示了高频率响应的放大视图。

[0997] 考虑到利用Gii作为唯一电极材料的装置显示0.25-0.4mF/cm^2的比电容,添加赝电容材料使这些Gii-Cap的能量存储容量增强多于100倍。此外,添加这些金属氧化物不会显著增加这些装置的ESR,从而保持其在高功率应用中的有用性。电沉积工艺是可控的,如果需要的话,可以制造沉积材料较少,从而总电容较少的电池。所得到的装置本质上是不对称的,其中MnOx为主要正电极,而FexOy为负电极。

[0998] 附录3GiiCap离子凝胶

[0999] 目的:为了展示电解质制剂的比电容和电化学稳定窗口(ESW),所述制剂包含室温熔融盐1-乙基-3-甲基咪唑鎓四氟硼酸盐(EMIMBF4)和气相二氧化硅,称为Iongel,结合了GiiCap®A7装置,在“低”湿度和“无空气”氩气环境下进行。

[1000] 实验条件:

[1001] 所有电化学测试都在“3电极”设置下进行,其中制造了规则的叉指A7装置,“工作”电极和“对”电极面积比为1:2,并且第三准参比电极包括丝网印刷AgCl墨,用于在测试期间监测各个电极电势。

[1002] 制备了电解质Iongel并将其储存在无空气的环境中。

[1003] 在应用至A7装置上以便测试之前,将Iongel加热至90℃,然后通过“刮墨刀”向A7上分配薄而均匀的层。使电解质冷却,之后将装置准备用于测试和连接。对于无空气装置,在存储并分配有电解质的相同无空气环境中进行测试,其中装置连接至电化学测试仪器:Biologic VMP-3稳压器。

[1004] 对于低湿度环境,将装置转移至相对湿度设定为20%的湿度受控的室中,并且密封并连接至仪器。

[1005] 对于每种湿度,测试了接近净电解质的标称文献值[1]的一系列最大电极电势(Emax)(单位为伏特(V))。它们是:

[1006] 正极:2.0、1.9、1.8、1.7、1.6、1.5

[1007] 负极:-2.0、-1.9、-1.8、-1.7、-1.6。

[1008] 对于每种湿度和电极电势组合,从头开始制作N=8个样品。

[1009] 电化学测试参数:

[1010] 使用了标准方案,其中测试窗口为0.0-Emax V vs OCV。OCV定量为0.25V vs AgCl Qref。

[1011] 电化学测试分为3个阶段:a)Ragone表征;b)长期(LT)循环;c)Ragone表征(后)。

[1012] LT循环之前和之后的Ragone表征包括:OCV,1小时;循环伏安法(CV),在100、1000mV/s下,每个进行5个循环;恒电流充电-放电(GCD),在5、10mA/cm^2下,每个进行10个循环;电位电阻抗谱(PEIS),在10MHz-0.01Hz之间。

[1013] LT循环包括:CV,在750mV/s下,5000个循环。

[1014] 电化学稳定性的确定通过对电极损坏和电解质变色进行事后目视分析,以及对跨LT循环期的库仑效率变化的评估来进行。装置性能的确定根据5000个LT循环后通过GCD的比电容来确定。

[1015] 结论:

[1016] 通过对LT CV循环的库仑效率相对于循环次数作图来确定ESW。当库仑效率在整个5000个循环中保持一致时,可以确定循环Emax在给定的环境条件下是稳定的。根据此分析发现,在相对湿度为20%的空气中,Iongel-A7装置在负电极电势和正电极电势分别为-1.6和+1.6V时是稳定的。在无空气环境的情况下,正极和负极ESW分别确定为-1.8和+1.7V。

[1017] 关于性能评估,发现在正极窗口下,20%相对湿度和无空气的装置的比电容分别为2.11和1.60mF/cm^2。在20%和无空气环境下的负极窗口比电容为1.55和2.11mF/cm^2。

[1018] 图69、图70和图71是相关结果。

[1019] 图72、图73和图74是另外的相关结果。

[1020] 附录4 3个月Gii-Sens测定可行性提议

[1021] 目标:

[1022] 使用对Gii-Sens 3D碳泡沫分析系统来说关键的试剂证明项目的可行性。

[1023] 第1阶段:表面固定

[1024] 目的:最大化mAb(2)表面固定。评估将mAb固定至表面上的最方便的表面化学。

[1025] 可交付成果:支持最大表面覆盖率和所选程序的数据。

[1026] 第3阶段:目标分析物感应范围和LOD

[1027] 目的:电化学免疫测定程序和结果。建立电化学免疫测定步骤(孵育时间、浓度、体积)并建立产生最灵敏的分析测定的参数。

[1028] 可交付成果:支持电分析免疫测定性能的数据。

[1029] 实验部分

[1030] 溶液组成

[1031] 表面化学

[1032] 10mM在DMF中的芘丁酸

[1033] 4mM EDC/10mM SulfoNHS

[1034] PBS 0.1M pH 7.2

[1035] 读出

[1036] 在0.02M KCl中的1mM $K_3Fe(CN)_6$+1mM $K_4Fe(CN)_6$

[1037] 0,02M PBS

[1038] 传感器修饰程序

[1039] 10μL PyrBuOOH在传感器表面上,在湿室中孵育2h,之后使溶剂自发蒸发

[1040] 15μL EDC/NHS,持续30min

[1041] 10μL在PBS中的A1或C1 mAb,持续1h

[1042] 电化学技术

[1043] 电化学阻抗

[1044] 施加电压＝0V

[1045] 幅度＝0.01VRMS

[1046] 频率范围-5000-0.1Hz

[1047] 测定程序

[1048] 直接测定:无标记:参见图75和图76。

[1049] 直接测定:无标记和无试剂:参见图77和图78。

[1050] 校准曲线图

[1051] 每个点重复,n＝5(最小值)不同的一次性传感器(单次读出,传感器被处置)

[1052] 每个校准曲线图含有随后几天由不同操作员获得的数据(测定间和测定内变化性)

[1053] 第1阶段:表面化学

[1054] 根据图79方案,选择的表面化学是Pyr-COOH修饰的石墨烯和捕获mAb(A1和C1)的EDC/NHS缀合物,所述图显示表面固定反应示意图。

[1055] 使用电化学阻抗谱筛选表面固定mAb(A1和C1)的浓度。(参见实验部分)。参见图80(在Gii-Sens®表面上的mAb A1固定。插图归一化信号)和图81(在Gii-Sens®表面上的mAb C1固定。插图归一化信号)。

[1056] A1和C1都显示合乎逻辑的表面覆盖趋势。基于归一化曲线,A1显示出略大的表面覆盖。筛选出的最佳覆盖范围为15至250μg/mL之间。估计所述浓度范围足以提供传感器的最佳性能。

[1057] 第3阶段:测定和目标分析物探究

[1058] 对使用Gii-Sens®作为传感电化学平台的测定潜力和益处的更深入的评估一直是在无标记测定形式下进行的。

[1059] 与此同时,还探究了无试剂形式,其中用于孵育和产生读出信号的溶液仅仅是缓冲液,如实验部分所述。还在高浓度下探究了测定的动态范围,还期望鉴定扩大所述浓度范围的潜力。

[1060] 由于在上文所述的调查期间获得的有趣结果和一般的时间限制,探究了低至10pg/mL的测定灵敏度,并且目的是探究高达1000ng/mL的高浓度范围。

[1061] 无标记测定探究

[1062] 如先前所述的无标记测定包括不需要二抗的测定,但使用特定的电化学读出溶液。在此项研究期间,电化学溶液也被用作载体溶液,因此消除了对洗涤步骤的需要或任何其他测定复杂情况。

[1063] 对于A1和C1修饰传感器二者,探究的第一个浓度范围是10ng/mL至10pg/mL。参见图82,其显示了A1(顶部)和C1(底部)传感器相比于不同N1抗原浓度的无标记剂量响应曲线。对于所有情况,表面涂布>60μg/mL,并且测定孵育时间为6分钟。

[1064] 对于研究的浓度范围,A1和C1均显示相似的响应并且实现了良好的初步剂量响应曲线特征。

[1065] 为了进一步研究如何增强测定性能,对总体浓度范围进行了划分,并且使用获得的相同数据在不同的灵敏度范围内进行了探究。

[1066] 无标记和无试剂测定探究

[1067] 如前所述,无标记测定包括不需要二抗的测定。在无试剂的情况下,也不需要存在电化学读出溶液,因为所有的孵育和测量都仅在缓冲溶液中完成,缓冲溶液还充当载体溶液,进一步消除了对额外洗涤步骤的需要。

[1068] 对于A1和C1修饰传感器二者,探究的第一个浓度范围是10ng/mL至10pg/mL。参见图83,其显示了A1(顶部)和C1(底部)传感器相比于不同N1抗原浓度的无标记和无试剂剂量响应曲线。对于所有情况,表面涂布>60μg/mL,并且测定孵育时间为6分钟。

[1069] 对于研究的浓度范围,A1和C1均显示相似的响应并且实现了良好的初步剂量响应曲线特征。

[1070] 附录5受体通过接头键合至3D碳泡沫材料的传感器具体实施

[1071] 背景

[1072] 传感器是检测变化或反应并且对来自环境的某种输入做出响应的分析装置。近年来,由于传感器具有特异性和灵敏度高、结果快速且可靠、易于处理和即时诊断的优势,其使用日益增多。由于这些优势,传感器已经进入多种技术领域,诸如化学和医学诊断、环境影响分析、食品工业和海洋部门。

[1073] 不同形式的石墨烯及其衍生物已被用于传感器(特别是生物传感器)的生产和开发。石墨烯的电化学、物理和化学性质使其成为这些应用感兴趣的材料。然而,常规石墨烯(例如,2D石墨烯)在实际应用中难以处理,因为其具有超薄的结构和柔韧性,这使得其容易卷曲、起折痕和起皱。这显著降低了传感器的分析性能,尤其是其灵敏度。迄今为止,已经实施了许多策略和技术来制造不同类型的石墨烯(例如,不同的形态、不同的表面性质、不同的功能化衍生物,诸如石墨烯量子点、氧化石墨烯或还原氧化石墨烯),并且这些导致了传感器之间的传感性能差异。

[1074] E.A.Obaje,G.Cummins,H.Schulze,S.Mahmood,M.P.Y.Desmulliez和T.T.Bachmann,Journal of Interdisciplinary Nanomedicine,2016;0(0),doi:10.1002/jin2.16研究了新制造的传感器与其下层复合材料的功能有关的电化学性能,并且通过表征如表面粗糙度、润湿性和非特异性DNA结合的易感性的性质评估了碳和介电质浆料的选择。

[1075] L.H.Hess,A.Lyuleeva,B.M.Blaschke,M.Sachsenhauser,M.Seifert和J.A.Garrido,ACS Appl.Materials&Interfaces,2014,6,9705-9710描述了基于聚合物修

饰的CVD生长石墨烯电晶体的生物传感应用的平台。

[1076] C.Fenzl,P.Nayak,T.Hirsch,O.S.Wolfbeis,H.N.Alshareef和A.J.Baeumner,ACS Sensors,2017,2,616-620描述了在血清分析中作为高灵敏度且可靠的生物传感器换能器的激光刻划石墨烯(LSG)电极。

[1077] S.Singal,A.K.Srivastava,S.Dhakate,A.M.Biradar和Rajesh,RSC Advances,2015,5,74994-75003描述了用于检测人心脏肌钙蛋白-I的电活性石墨烯-多壁碳纳米管混合负载的阻抗免疫传感器。

[1078] 不管存在所有现有技术,但仍持续需要改进那些基于石墨烯的传感器的传感活性。此外,仍然希望改进所述传感器的灵敏度,而不损害那些传感器的其他方面中的至少一者,诸如它们的稳健性、稳定性、耐用性、功能化的便利性和/或制造的简易性。

[1079] 本附录5特点的汇总

[1080] 在第一方面,提供了一种传感器,其包括:(i)碳泡沫电极,(ii)接头,和(iii)受体,其中所述受体通过所述接头键合至所述碳泡沫电极。碳泡沫电极至少部分地通过上述特点A-K中任一项所定义的方法制成。

[1081] 在第二方面,提供了一种制造根据第一方面的传感器的方法,其包括按顺序的以下步骤:(i)提供如第一方面所述的碳泡沫电极;(ii)用接头处理所述碳泡沫电极;以及(iii)用受体处理步骤(ii)中获得的所述接头修饰的碳泡沫电极。

[1082] 在第三方面,提供了一种感测目标的方法,其包括按顺序的以下步骤:(i)提供根据第一方面的传感器;(ii)将所述传感器与含有或怀疑含有所述目标的样品接触;(iii)测量所述传感器的响应;以及任选地(iv)将所述响应与所述样品中的所述目标的水平相关联。

[1083] 碳泡沫材料通常具有折叠结构,这使得碳泡沫具有多孔形态和高比表面积。不希望受任何理论的束缚,据信,传感器的分析性能受碳泡沫的形态以及可及表面积的影响。3D结构导致可用表面积增加,使得接头和受体(诸如,酶、蛋白质、核酸和抗体)能够有效地键合至碳泡沫,从而关于灵敏度提高传感器性能。

[1084] 另外,还期望用非常厚的碳泡沫层构建传感器。优选地,碳泡沫的层厚度大于50μm。由于碳泡沫可以是多孔的,因此这种厚的碳泡沫层预期提供更大的表面积,与其他常规的基于石墨烯的传感器相比,其有利于增强分析性能,特别是传感性质。

[1085] 接头

[1086] 在本发明特点的上下文中,碳泡沫被接头修饰,作为形成所需传感器的工艺的一部分。上文所述的碳泡沫(例如,具有折叠结构的厚的多孔碳泡沫)提供了改进的修饰基础,因为增加的表面积可用于与接头的相互作用,导致传感器的灵敏度改善。

[1087] 然后通过受体处理改性碳泡沫以获得传感器。因此,接头充当碳泡沫与受体之间的中间体。有可能接头的至少一部分被设置(例如,分配)在碳泡沫内。有可能整个接头被设置(例如,分配)在碳泡沫内。

[1088] 接头可以选自纳米颗粒、聚合物、聚合物刷、配体、包含一个或多个官能团的有机化合物、共价或非共价键合至所述碳泡沫的分子或其混合物。通常,接头选自聚合物(例如,(甲基)丙烯酸酯聚合物);包含一个或多个官能团的有机化合物;碳二亚胺;重氮化合物;或其混合物。

[1089] 通常,上文所述的有机化合物包含一个或多个功能团,其独立地选自氧、氮、硫、卤化物、羟基、羰基、羧基、胺、氨基、酰胺、亲水性聚合物或其混合物,其任选地与线性、支链或环状烷基、烯基、炔基、芳基残基、丙烯酰基、酰基、酰氧基、烷氧基、亚烷氧基或其混合物组合。在相同的实施方案中,所述任选结构可以是C1-C20直链、支链或环状烷基、烯基、炔基、芳基残基、丙烯酰基、酰基、酰氧基、烷氧基、亚烷氧基或其混合物。仍在相同的实施方案中,任选地,具有上文所述的官能团的有机化合物还可以包含一个或多个任选地包含一个或多个杂原子的环状部分,并且环状部分中的至少一个直接或间接地连接至所述官能团中的至少一个,或者接头是作为这种有机化合物的酯或盐的衍生物,或者是在与所需的3D碳泡沫反应中释放这种有机化合物的化合物。代表性地,接头选自本段中上述有机化合物。

[1090] 代表性地,接头选自1-芘丁酸、N-羟基琥珀酰亚胺(NHS)、芘-1-羧酸琥珀酰亚胺酯、1-氨基芘、N-(1-芘)马来酰亚胺或其混合物。

[1091] 接头可以共价或非共价地键合至碳泡沫。例如,重氮化合物(例如,重氮盐)可以共价键合至碳泡沫。对于非共价键合,接头可以通过以下中的至少一者键合至碳泡沫:π-π相互作用、离子键合、氢键合、疏水或亲水效应、静电相互作用、聚合物包裹、吸附、接枝(例如,光接枝)。例如,包含一个或多个如上所述的环状部分(例如,1-芘丁酸、N-羟基琥珀酰亚胺(NHS)、芘-1-羧酸琥珀酰亚胺酯、1-氨基芘、N-(1-芘)马来酰亚胺或其混合物)的接头可以通过π-π相互作用键合至碳泡沫。

[1092] 在本特点的上下文中,受体通过接头键合至碳泡沫。因此受体是间接键合的。当接头的至少一部分或优选整个接头设置(例如,分散)在碳泡沫内时,受体的至少一部分或整个受体也可以设置(例如,分散)在碳泡沫内。

[1093] 本文中的“受体”意指涵盖能够对待分析样品中存在的目标材料(即目标)有响应的任何分子。样品可以是生物、化学、光学、物理或机械样品,通常是生物样品。因此,目标意指涵盖但不限于生物材料、化学物质或混合物、光学物体、物理或机械物品等,通常是生物材料。术语“响应”可以包括但不限于生物、和/或化学、和/或光学、和/或物理、和/或机械相互作用,通常是生物和/或化学相互作用。这些典型的相互作用可以包括但不限于受体与目标之间的键合、或杂交、或疏水效应。

[1094] 因此,受体可以包括但不限于以下之一:电化学受体、化学受体、生物受体、光学受体、物理或机械受体。受体可以选自但不限于冠醚、配体、催化剂、硼酸、碳水化合物、适体、蛋白质、酶、抗体、抗原、微生物、核酸、脂肪酸、脂肪酸酯、分子印迹聚合物、金属-有机骨架、能够形成配体结合的多肽或寡肽、细胞、细胞器或其他细胞组分、或其混合物。

[1095] 通常,受体是生物受体(即,传感器是生物传感器)。通常,受体选自适体、蛋白质、酶、抗体、抗原、微生物、核酸、能够形成配体结合的多肽或寡肽、细胞、细胞器、或其他细胞组分、或其混合物。更通常,受体选自蛋白质(例如,免疫蛋白、非免疫蛋白、免疫球蛋白结合蛋白、糖结合蛋白)、核酸、抗体、酶(例如,氧化还原酶(优选葡萄糖氧化酶、酒精氧化酶或乳酸氧化酶)、脱氢酶)或其混合物。代表性地,受体选自免疫球蛋白A(IgA)、葡萄糖脱氢酶、链霉亲和素或其混合物。

[1096] 通常,目标是生物材料。生物材料可以包括但不限于脱氧核糖核酸(DNA)、核糖核酸(RNA)、肽、蛋白质、蛋白质复合物、核酸、抗体、抗原、脂质、脂肪酸、脂肪酸酯、维生素、微生物、胶束、细胞、细胞器、或其他细胞组分、病毒、酶或其混合物。通常,生物材料选自脱氧

核糖核酸(DNA)、核糖核酸(RNA)、肽、蛋白质、核酸、抗体、抗原、酶或其混合物。更通常,生物材料选自蛋白质、核酸、抗体、酶或其混合物。还应当理解,在本特点的上下文中,生物受体和生物材料都可以是天然存在的或合成产生的。

[1097] 受体可以附接至接头。受体可以通过物理、生物和/或化学方式键合至接头。通常,受体化学键合至接头。本文,化学键可以包括但不限于共价键、非共价键(例如,离子键)、金属键、氢键、螯合键,以及非共价相互作用,诸如范德华力、π-π相互作用、疏水或亲水效应和静电相互作用。通常,受体(例如,生物受体)共价键合至接头。通常,受体(例如,生物受体)键合(例如,共价)接头中包含的一个或多个官能团(例如,如先前所述的有机化合物的官能团)。例如,生物受体可以共价键合至接头(例如,1-芘丁酸、N-羟基琥珀酰亚胺(NHS)、芘-1-羧酸琥珀酰亚胺酯、1-氨基芘、N-(1-芘)马来酰亚胺)的羧基、氨基或胺、或酰胺基。

[1098] 传感器

[1099] 根据本特点的传感器通常包括碳泡沫层,其可以通过先前公开的双激光处理方法生产。通常,碳泡沫的层厚度大于50μm,优选大于100μm,更优选大于200μm,并且更优选大于300μm。通常,接头的至少一部分或整个接头被设置(例如,分散)在碳泡沫内。任选地,受体的至少一部分或整个受体也设置(例如,分散)在碳泡沫内(即,当接头的至少一部分或优选地整个接头被设置(例如,分散)在碳泡沫内时)。通常,接头的至少一部分和任选地受体的一部分被设置(例如,分散)在碳泡沫(例如,碳泡沫层)表面下方的一定深度,所述深度大于所述碳泡沫的总深度的1%,优选大于总深度的5%,更优选大于10%,甚至更优选大于15%,更优选大于20%。通常,接头的至少一部分和任选地受体的至少一部分被设置(例如,分散)在碳泡沫(例如,碳泡沫层)表面下方的一定深度,所述深度在所述碳泡沫表面下方大于1μm,优选大于5μm,更优选大于10μm,甚至更优选大于15μm,最优选大于20μm。整个接头和任选地整个受体可以被设置(例如,分散)在碳泡沫(例如,碳泡沫层)表面下方的一定深度处,所述深度大于所述碳泡沫的总深度的1%。碳泡沫层的厚度可以是上文所述的任何范围(例如,至少大于50μm)。本文中的"分散"意指至少部分地被设置在碳泡沫内的接头(任选地,和受体)分子分布在其中以形成除单个簇之外的多个离散结构域。所述结构域可以均匀和/或连续地分布(例如,分布为均匀和/或连续的层)在所述碳泡沫内。不希望受任何理论的束缚,据信接头(任选地,和受体)的置换导致碳泡沫的改善功能化,从而增强传感器的传感活性(即,灵敏度)。

[1100] 此外并且任选地,接头和受体均不被设置(例如,分散)在遍及碳泡沫(例如,碳泡沫层)的整个深度。换句话说,所述碳泡沫的芯未被接头或受体修饰。

[1101] 接头可以选自1-芘丁酸、N-羟基琥珀酰亚胺(NHS)、芘-1-羧酸琥珀酰亚胺酯、1-氨基芘、N-(1-芘)马来酰亚胺或其混合物,并且受体可以选自免疫球蛋白A(IgA)、葡萄糖脱氢酶、链霉亲和素或其混合物。

[1102] 传感器还可以包括基板。在获得碳泡沫的第一种方法中,如果在基板上或相邻于基板提供碳源,则最终的传感器可以包括所述基板作为组成部分。在需要使用基板的第二种方法中,最终的传感器也可以包括所述基板作为组成部分。无论通过哪种方法获得,碳泡沫都可以任选地粘附至传感器内的基板。因此传感器中所包括的基板可以具有根据先前针对碳泡沫生产中所用的基板所描述的特点之一和/或这些特点的可能组合之一的特征。替代地,传感器不必包括基板。换句话说,即使碳泡沫被生产为粘附至基板,也可以将其从基

板去除,作为后续修饰的准备的一部分。

[1103] 通常,根据本发明特点的传感器是化学、物理或机械、生物或光学传感器,优选地是生物传感器(即,当受体是生物受体时)。通常,传感器(例如,生物传感器)采用电极或电极装置的形式。传感器(例如,生物传感器)可以包括多电极平台,例如,包括对电极(CE)、工作电极(WE)和参比电极(E或RE)的三电极平台。电极(例如,WE)可以由本发明特点的经修饰碳泡沫(即,通过接头由受体修饰的碳泡沫)制成。其他电极(例如,CE和/或RE)也可以是基于碳泡沫的,优选是基于碳泡沫的,更优选是基于没有任何修饰的相同碳泡沫。所有电极可以具有相同或不同的尺寸。

[1104] 传感器(例如,生物传感器)可以作为产品提供,其中所述传感器被容纳在包装内,并且产品优选地包括使用说明。通常,包装包括其中容纳传感器的初级包装。传感器可以被提供在容纳于初级包装内的适配器上。初级包装的合适实例是护盖、口袋、文件夹、信封、盒子、容器、纸盒、壳体等。任选地,包装还包括次级包装。此类次级包装通常是使一个或多个传感器保持在一起的包装。次级包装的合适实例是塑料纸盒、硬纸板纸盒、泡罩包装、盒子(例如,硬纸板或塑料盒子)、壳体、容器、硬纸板或塑料板条箱、托盘、具有或不具有一个或多个气袋的包装捆包等。仍任选地,包装可以包括三级包装,其可以选自盒子、壳体、纸盒、容器等。合适地,上文所述的包装中的至少一种可以保护传感器免受光(例如,直射阳光)、湿气、物理和/或化学损害和污染。说明书可以给出使用根据特点的第三方面的传感器的步骤的详细信息。说明书可以以印刷形式的标签、小册子、手册或传单提供。说明书还可以印刷在产品包装上。

[1105] 传感器的制造

[1106] 第二方面,提供了一种制造根据第一方面的传感器的方法,其中步骤包括:(i)提供碳泡沫;(ii)用接头处理碳泡沫;以及(iii)用受体处理接头修饰的碳泡沫。

[1107] 所述方法可以包括在提供碳泡沫并用接头处理碳泡沫之前制造碳泡沫的步骤。因此,碳泡沫是通过本文公开的激光处理方法之一生产的,通常是第一种方法或第二种方法,更通常是第一种方法。如此生产的碳泡沫可以粘附至基板、附接至基板或提供在基板上。通常,可以在步骤(ii)中处理接头之前将所述碳泡沫从所述基板去除。换句话说,步骤(i)中的碳泡沫是在没有基板的情况下提供的。替代地,不需要去除所述碳泡沫(例如,所述碳泡沫仍然粘附至所述基板)。换句话说,步骤(i)中的碳泡沫设置有基板。

[1108] 碳泡沫可以与接头一起孵育。孵育可以发生在缓冲液中,优选在缓冲溶液中。此外或任选地,通过接头的修饰可能需要以下条件中的至少一种:光(紫外线、可见光或红外辐射)或热。孵育后,可以清洗接头修饰的碳泡沫。

[1109] 接头修饰的碳泡沫可以与受体一起孵育。孵育后,可在使用前清洗如此获得的传感器。清洗后,传感器可能会被钝化。钝化被理解为封闭未被受体功能化的剩余活化位点。

[1110] 所述受体用于处理步骤(iii)中的接头修饰的碳泡沫。

[1111] 传感器可以是电极或者包括多电极平台的电极装置。因此,上文所述的制造步骤可以适用于电极的制造。当传感器为包括多电极平台的电极装置时,上文所述的制造步骤适用于生产工作电极(WE),并且所述方法还包括以下额外步骤:生产对电极(CE)和参比电极(E或RE)。

[1112] 传感器的使用

[1113] 在第三方面,提供了一种使用传感器的方法,其包括按顺序的以下步骤:(i)提供根据第一方面的传感器;(ii)将传感器与含有或怀疑含有目标的样品接触;(iii)测量传感器的响应;以及(iv)任选地,将响应与样品中的目标水平相关联。

[1114] 目标可以是本文公开的目标,通常是本文公开的生物材料。样品可以是本文公开的样品,通常是本文公开的生物样品。

[1115] 在使用之前,传感器(例如,生物传感器)可以适当地储存在环境条件下(例如,约20℃的室温和1个大气压)。通常,传感器储存在干燥条件下。使用后,可以将传感器进行适当处置(即,传感器是一次性传感器)。

[1116] 可以将传感器浸入样品中。样品可以含有磷酸盐缓冲盐水(PBS)。样品中目标的浓度可以为至少1ppm。平衡时间可以为至少0.5分钟,或至少1分钟,或至少10分钟,或至少30分钟,通常不超过2小时,或不超过1小时,或不超过40分钟。可以在接触样品后,对传感器进行清洁,之后测量响应。可以通过使用PBS冲洗来清洁传感器。可以在清洁后将传感器干燥(例如,通过气流,或者通过自然干燥)。

[1117] 可以通过差分脉冲伏安图和/或阻抗谱来测量响应。测量的响应可能与样品中的目标水平进一步相关。所述方法可以包括如上文所述的步骤(i)、(ii)和(iii),并且另外包括按顺序的以下步骤:(iv)使传感器与含有已知水平的目标的一个或多个样品(即,对照样品)接触;(v)测量传感器对一个或多个对照样品的响应;(vi)将对含有或怀疑含有目标的样品的响应与对一个或多个对照样品的响应相比较;以及(vii)将对含有或怀疑含有目标的样品的响应与所述样品中所述目标的水平相关联。

[1118] 附录5概念

[1119] 1.一种传感器,其包括:(i)碳泡沫,(ii)接头,和(iii)受体,其中所述受体通过所述接头键合至所述碳泡沫。

[1120] 2.根据概念1所述的传感器,其中所述碳泡沫可通过在碳源内的至少一个位置集中红外辐射,从而在所述至少一个位置产生碳泡沫的方法获得,并且所述红外辐射由激光束提供,所述激光束是红外激光束。

[1121] 3.根据概念2所述的传感器,其中集中红外辐射包括衍射所述红外辐射以形成干涉图案,干涉图案的每个条纹在所述碳源内的位置内。

[1122] 4.根据概念2或概念3所述的传感器,其中所述至少一个位置在所述碳源内侧向移动并且/或者所述至少一个位置在所述碳源的深度内移动。

[1123] 5.根据概念2至4中任一项所述的传感器,其中所述红外辐射直接照射所述碳源,或者所述红外辐射在照射所述碳源之前穿过基板,其中所述碳源设置在所述基板的表面上或相邻于所述基板的表面。

[1124] 6.根据概念2至5中任一项所述的传感器,其中所述碳源另外用额外的辐射照射,并且所述额外的辐射在将红外辐射集中在所述碳源内的至少一个位置的步骤之前、同时或之后进行。

[1125] 7.根据概念6所述的传感器,其中所述额外的辐射在所述碳源的所述表面上光栅化。

[1126] 8.根据概念6或概念7所述的传感器,其中所述额外的辐射直接照射所述碳源,或在照射所述碳源之前穿过如概念5所述的基板。

[1127] 9.根据前述概念中任一项所述的传感器,其中所述接头的至少一部分设置(优选分散)在所述碳泡沫内;并且任选地,所述受体的至少一部分设置(优选分散)在所述碳泡沫内。

[1128] 10.根据概念2至9中任一项所述的传感器,其中所述碳泡沫的层厚度大于50μm,优选大于100μm,更优选大于200μm,并且更优选大于300μm。

[1129] 11.根据概念1所述的传感器,其中所述碳泡沫可通过在基板表面上或相邻于基板表面提供碳源并且将包含含碳材料的所述碳源的至少一部分和/或所述基板的至少一部分暴露于激光束,从而将所述碳源的至少一部分转化为所述碳泡沫的方法获得。

[1130] 12.根据概念5、8或11所述的传感器,其中所述基板包括以下中的一者或多者:硅树脂(silicone)、二氧化硅、氮化镓、砷化镓、氧化锌;或替代地,一种或多种聚合物;或替代地,一种或多种选自铝、铜、金或其他金属的金属,或者所述金属的氧化物、氮化物或砷化物。

[1131] 13.根据前述概念中任一项所述的传感器,其中所述碳泡沫包含原子百分比小于3%、优选小于1.5%的氧,和/或原子百分比小于3%的氮。

[1132] 14.根据前述概念中任一项所述的传感器,其中所述接头选自纳米颗粒、聚合物、聚合物刷、配体、包含一个或多个官能团的有机化合物、共价或非共价键合至所述碳泡沫的分子、或其混合物。

[1133] 15.根据概念14所述的传感器,其中所述接头选自聚合物(优选(甲基)丙烯酸酯聚合物);包含一个或多个官能团的有机化合物;碳二亚胺;重氮化合物;或其混合物。

[1134] 16.根据概念15所述的传感器,其中所述一个或多个官能团独立地选自氧、氮、硫、卤化物、羟基、羰基、羧基、胺、氨基、酰胺、亲水性聚合物或其混合物,其任选地与线性、支链或环状烷基、烯基、炔基、芳基残基、丙烯酰基、酰基、酰氧基、烷氧基、亚烷氧基或其混合物组合。

[1135] 17.根据概念16所述的传感器,其中所述有机化合物还包含一个或多个任选地包含一个或多个杂原子的环状部分,并且所述环状部分中的至少一个直接或间接地连接至所述官能团中的至少一个,或者所述接头是作为所述有机化合物的酯或盐的衍生物,或者是在与所述碳泡沫反应中释放所述有机化合物的化合物。

[1136] 18.根据概念17所述的传感器,其中所述接头选自1-芘丁酸、N-羟基琥珀酰亚胺(NHS)、芘-1-羧酸琥珀酰亚胺酯、1-氨基芘、N-(1-芘)马来酰亚胺或其混合物。

[1137] 19.根据概念17或概念18所述的传感器,其中所述接头通过π-π相互作用键合至所述碳泡沫。

[1138] 20.根据前述概念中任一项所述的传感器,其中所述受体是以下中的一者:电化学受体、化学受体、生物受体、光学受体、物理或机械受体,优选生物受体。

[1139] 21.如权利要求20所述的传感器,其中所述受体选自冠醚、催化剂、硼酸、概念(concept)、配体、适体、蛋白质、酶、抗体、抗原、微生物、核酸、脂肪酸、脂肪酸酯、分子印迹聚合物、金属有机骨架、能够形成配体结合的多肽或寡肽、细胞、细胞器或其他细胞组分、或其混合物,优选地选自蛋白质、核酸、抗体、酶或其混合物。

[1140] 22.根据概念21所述的传感器,其中所述受体选自免疫球蛋白A(IgA)、葡萄糖脱氢酶、链霉亲和素或其混合物。

[1141] 23.根据前述概念中任一项所述的传感器,其中所述受体以物理、生物和/或化学方式键合至所述接头,优选以化学方式键合,更优选共价键合。

[1142] 24.一种制造根据前述概念中任一项所述的传感器的方法,其包括按顺序的以下步骤:(i)提供如概念1至13、19中任一项所述的碳泡沫;(ii)用如概念1、14至19、23中任一项所述的接头处理所述碳泡沫;以及(iii)用如概念1、20至23中任一项所述的受体处理步骤(ii)中获得的接头修饰的碳泡沫。

[1143] 25.一种感测目标的方法,其包括按顺序的以下步骤:(i)提供根据概念1至23中任一项所述的传感器;(ii)将所述传感器与含有或怀疑含有所述目标的样品接触;(iii)测量所述传感器的响应;以及任选地(iv)将所述响应与所述样品中的所述目标的水平相关联。

[1144] 还需注意,此附录5中描述的传感器可以是本说明书前面描述的Gii-Sens碳泡沫传感器。

[1145] 附录6基准实验条件

[1146] 在0.1M硝酸锶中的1mM铁氰化钾/亚铁氰化钾,并随机挑选最少五个重复样。进行在25和200mV/s扫描速率下的循环伏安法,作为比较技术。研究了各种特点并得出结论,以评估差异电极材料的性能。

[1147] 电化学阻抗谱在平衡电势下进行,幅度为5mV,并且频率为0.1至100kHz

[1148] 使用传感器内置或外部银/氯化银参比电极。

[1149] Gii Sens碳泡沫相比于常规石墨烯电极材料

[1150] 对Gii Sens碳泡沫传感器进行了评估,并将其与其他可商购获得的基于石墨烯的传感器相比较。参见图84。

[1151] 记录的获得的还原和氧化峰电流显示,单位几何面积的电流密度方面的效率增大了25%。这清楚地反映了Gii Sens 3D碳泡沫所提供的可用电化学可用面积更大。参见图85。

[1152] 根据循环伏安法,可以将对还原-氧化峰分离的评估解释为表面对电压扫描的电子氧化还原响应率及其有效进行快速氧化还原反应的能力的量度。研究显示,还原-氧化峰分离保持低于70mV,并且从25到200mV/s均未显示分离增加。

[1153] 其他石墨烯电极表面显示从还原到氧化的电压分离较大,指示氧化还原法拉第反应效率较低,并且与较快的扫描速度相关联的有害效应明显。参见图86。

[1154] 不同表面的电荷转移电阻值显示Gii Sens传感器表面有显著的改善。这说明Gii Sens对于实现具有可靠性和很少背景信号干扰的基于阻抗的测量具有巨大的潜力。

[1155] Gii Sens相比于其他碳基材料

[1156] 碳基电极材料在电分析应用中非常常见。碳糊电极是丝网印刷传感器的常见材料。由于其制造灵活性和可负担性,它们是实际即时应用中最广泛使用的电极表面。碳基板料的另一端是玻璃碳表面,预期性能更好,但针对制造灵活性和可负担性的可用性有限。参见图87。

[1157] Gii Sens碳泡沫性能显示与纯玻璃碳材料性能在可用的电化学活性区域方面相匹配,同时同等大小的碳糊电极可用的面积增加了50%。参见图88。

[1158] 从循环伏安法获得的还原-氧化峰分离首先显示,碳糊材料的性能较差,并且其高度依赖慢扫描速率来在其表面实现相对可接受的氧化还原反应。Gii Sens的响应甚至在任

何扫描速率下都优于纯玻璃碳,显示出其结合在制造方面的灵活性和优异性能的巨大潜力。参见图89。

[1159] 表面电荷转移电阻的量度强调了Gii Sens作为优于玻璃碳的基于阻抗的感测表面具有巨大的潜力,并开辟了碳糊电极材料尚不可及的领域。

[1160] Gii Sens相比于丝网印刷金

[1161] 丝网印刷金传感器具有两种最重要的性质,使传感器材料可用于实际电化学感测应用:灵活的制造程序和优异的电化学反应。评估了两种可商购获得的丝网印刷金样品。参见图90。Gii Sens碳泡沫被证明也具有这些性质,同时还具有可负担性。

[1162] 记录的记录还原和氧化峰电流显示,每几何面积单位可用的电化学有效区域增加了至少20%。参见图91。

[1163] 如所预期的那样,丝网印刷金显示出评估批次中最具有响应性的电极表面材料,然而Gii-Sens匹配甚至提高了此性能,特别是在快速扫描速率下。参见图92。

[1164] 比较丝网印刷金和Gii Sens的电极表面的电荷转移电阻也突出了Gii碳泡沫材料的巨大潜力;在所有情况下,它都显示较低的电阻率相关值。

[1165] Gii Sens与丝网印刷金的比较旨在显示在易于制造和卓越性能方面的比较的优胜性,而可负担性和可扩展性无疑是Gii Sens传感器的有益固有特点。

[1166] 结论

[1167] Gii Sens传感器的性能优于市场上任何其他碳基或甚至石墨烯传感器。甚至胜过丝网印刷金表面,这消除了人们对使用Gii Sens表面作为最终电化学传感平台的总体便利性的任何疑虑。Gii Sens首次显示用于电分析应用的制造和可扩展材料的完美选择,同时保持最高性能,确保用于实现大通量和即时诊断应用的最大灵敏度和灵活性。

[1168] 附录7抗人原降钙素(cAb)的表面固定的优化

[1169] 目标:

[1170] 抗人原降钙素(cAb)的表面固定的优化

[1171] 结果汇总

[1172] 选择表面NHS生产方法。匹配现有标准制造工艺

[1173] 使用100μg/ml cAb实现最佳cAb表面覆盖。

[1174] 对于标准裸Gii-Sens®传感器,通常的%CV为7%。对于本报告中所示的实验中的所有传感器,100μg/ml cAb涂层的%CV为10%。

[1175] 使用100μg/ml cAb涂层,以直接测定的方式成功检测出2000pg/ml Ag。信号输出的%CV为10%。

[1176] 实验部分

[1177] 溶液组成

[1178] 表面化学

[1179] NHS修饰

[1180] 花NHS

[1181] 捕获抗体(cAb):

[1182] 产品名称:抗h PCT 4004SPTN-5

[1183] 抗原(Ag):

[1184] 产品名称:重组PCT抗原

[1185] Echem读出溶液

[1186] 在20mM KCl中的1mM $K_3Fe(CN)_6$+1mM $K_4Fe(CN)_6$

[1187] cAb固定溶液

[1188] 在1×PBS(pH 7.2)中的抗h PCT

[1189] 抗原(Ag)检测溶液

[1190] 在20mM KCl中的1mM $K_3Fe(CN)_6$+1mM $K_4Fe(CN)_6$+Ag

[1191] 电化学技术

[1192] 电化学阻抗

[1193] 施加电压:OCP

[1194] 幅度:$0.01V_{RMS}$

[1195] 频率范围:100000-0.1Hz

[1196] 循环伏安法

[1197] 扫描速率:25mV/s

[1198] 起始电势:-0.3V

[1199] 高电势:0.6V

[1200] V低电势:-0.3V

[1201] 测定程序

[1202] NHS固定

[1203] 制备在DMF中的10mM Pyr NHS。

[1204] 将10μL滴涂至每个传感器的工作电极上。

[1205] 将传感器放置在不透气的盒子内,并且使其孵育12至18h。

[1206] 确认PyrNHS/DMF已从表面充分蒸发。

[1207] cAb固定程序

[1208] 将NHS GiiSens+传感器放置于平坦表面上。

[1209] 将10μL cAb滴涂至每个传感器的工作电极上。

[1210] 将传感器放置在密封容器内,水浴2小时。

[1211] 取出传感器,并且用DI水轻轻冲洗掉溶液,之后用N_2气流轻轻干燥。

[1212] 测定程序:直接测定1-参见图93

[1213] 1)cAb读出,将电化学读出溶液施加至传感器表面,之后进行EIS测量。

[1214] 2)溶液去除,从传感器表面去除电化学读出溶液。

[1215] 3)t'1读出,将加有抗原的电化学读出溶液施加到传感器表面,之后进行EIS测量。在添加溶液与测量之间有约1min。

[1216] 4)t'2读出,进行EIS测量。在添加溶液与测量之间有约6min。

[1217] 5)t'3读出,进行EIS测量。在添加溶液与测量之间有约11min。

[1218] 电化学读数程序参见附件

[1219] 1.表征曲线图

[1220] 每个点重复样,n=5个(最小值)不同的一次性传感器(单次读出,传感器被处置)

[1221] 第1阶段:表面化学

[1222] 选择的表面化学是NHS修饰碳泡沫,之后遵循以下方案经由酰胺键形成来缀合cAb。参见图94:表面固定反应示意图。

[1223] 使用电化学阻抗谱和循环伏安法监测碳泡沫表面上的NHS产生。参见图95:GiiSens®电极的NHS功能化的Rct和ΔEp信号响应。

[1224] Rct和ΔEp相对于裸电极的增加证实了碳泡沫电极的NHS功能化。

[1225] 使用电化学阻抗谱法筛选了50-800μg/ml之间的一系列cAb浓度。参见图96:GiiSens®电极上的cAb固定。

[1226] 对于NHS修饰传感器上的固定,观察到Rct随cAb浓度的逻辑增加。估计NHS电极上的最佳覆盖为100μg/ml cAb,估计所述浓度提供传感器的最佳性能,而不会浪费材料来获得很小的收益。在此浓度下观察到优异的可再现性水平(%CV 3%)。

[1227] 第2阶段:电化学信号

[1228] 评价了产生的电化学信号以用于直接测定,这意味着不需要利用二抗来辅助抗原检测。

[1229] 选择2000pg/ml的抗原浓度用于研究直接测定。根据本报告第1阶段的结果,表面抗体涂层固定为100μg/ml。选择Ag-Ab孵育时间作为研究的初步测定参数。参见图97:使用100μg/ml cAb表面涂层的直接测定形式中来自2000pg/ml的信号响应。

[1230] 100μg/ml cAb再次显示出良好的可再现性水平(%CV 8%)。cAb的平均Rct之间的区别很明显,给出了不同的可量化信号输出(ΔRct)。ΔRct信号输出还显示出可接受的可再现性水平,在每次读取时间,%CV≥10%。1、6与11m之间的输出信号的稳定性显示在第一次测量后没有发生额外的Ab-Ag相互作用。测量之间的5分钟时间间隔归因于EIS测量所需的时间长度。对于2000pg/ml Ag样品,最佳测定孵育时间低至1分钟。

[1231]

cAb 浓度(μg/ml)	分析溶液	电化学分析参数	
		循环伏安法	EIS
		扫描速率:25 mV/s	施加电压: OCP
50、100、200、400 和 800	20 mM KCl + 1 mM 铁氰化钾 + 1 mM 亚铁氰化钾	电势窗口: -0.3-0.6 V	幅度: 0.01 V_{RMS}
			频率范围: 100000-0.1 Hz

[1232] 表9:cAb固定的关键实验和电化学参数

	Ag 浓度（pg/ml）	cAb 浓度（μg/ml）	分析溶液	电化学分析参数
[1233]	2000	100	20 mM KCl + 1 mM 铁氰化钾 + 1 mM 亚铁氰化钾	EIS 施加电压：OCP 幅度：0.01 V_{RMS} 频率范围：100000-0.1 Hz

[1234] 表10:Ag检测的关键实验和电化学参数

[1235] 附录8:

[1236] 特点和任选特点的合并列表

[1237] 此附录8是特点和任选特点的合并列表。需注意,特点A-R中的任何一者或多者每个都可以与一个或多个其他兼容的特点A-R以及与任选的特点中的任何一者或多者组合。

[1238] 第1组:表面下碳泡沫

[1239] 特点A:在碳前体材料的表面下区域中产生的碳泡沫

[1240] 特点B:在碳前体材料的封装区域中产生的碳泡沫

[1241] 特点C:在碳前体材料的区域中产生的碳泡沫,其中所述区域不具有实质气体逸出通道

[1242] 特点D:粘附至基板的无定形非石墨烯材料

[1243] 第2组:双激光处理

[1244] 特点E:通过激光烧蚀表面下碳泡沫区域所产生的碳泡沫

[1245] 特点F:通过激光烧蚀表面下碳泡沫区域所产生的非石墨烯碳泡沫

[1246] 特点G:双激光

[1247] 特点H:定位在通过激光烧蚀表面下碳泡沫区域所产生的碳泡沫中的电接触件

[1248] 特点I:在聚酰亚胺膜上印刷电接触件,然后产生暴露碳泡沫

[1249] 特点J:在碳泡沫中制成的高轨迹

[1250] 特点K:在不同的制造设施中应用第一激光和第二激光

[1251] 第3组:产品

[1252] 特点L1:生物传感器

[1253] 特点L2:使用丝网印刷技术以可扩展、低成本的方式制造碳泡沫生物传感器

[1254] 特点L3:在不同的制造设施处向生物传感器添加功能化基团

[1255] 特点L4:向生物传感器添加功能化基团,作为生物传感器生产工艺的一部分

[1256] 特点L5:使用PPC制造生物传感器:印刷后转化

[1257] 特点M1:储能装置:超级电容器

[1258] 特点M2:碳泡沫超级电容器的详情

[1259] 特点M3:碳泡沫超级电容器:共集电极

[1260] 特点M4:碳泡沫超级电容器:PPC制造工艺

[1261] 特点M5:碳泡沫赝电容器:金属氧化物变体

[1262] 特点M6:碳泡沫超级电容器:在低湿度环境中使用离子凝胶

[1263] 特点N1:电导体

[1264] 特点N2:组合的传感器和超级电容器

[1265] 特点N3:组合的超级电容器和电池

[1266] 特点N4:智能标签

[1267] 特点N5:组合的超级电容器和天线

[1268] 特点N6:组合的能量采集器(Energy Scavenger)+超级电容器。

[1269] 特点O1:3D碳泡沫结构:用于Gii-Cap的Gii-Thru

[1270] 特点O2:3D碳泡沫结构:Gii-Thru可堆叠Gii-Cap/Gii-Cap+

[1271] 特点O3:3D碳泡沫结构:用于Gii-Sens的Gii-Thru:HISLOC

[1272] 特点O4 3D碳泡沫结构:用于Gii-Sens的Gii-Thru:HISLOC制造工艺

[1273] 第4组:其他方面

[1274] 特点P:碳泡沫的可扩展制造:Gii 3

[1275] 特点Q:各种其他碳泡沫应用

[1276] 特点R:非石墨烯碳泡沫

[1277] 特点A:在碳前体材料的表面下区域中产生的碳泡沫

[1278] 一种制造碳泡沫材料的方法,其包括以下步骤:照射碳前体材料的表面下区域,激光束的参数被选择用于在所述表面下区域中产生碳泡沫。

[1279] 一种激光诱导碳泡沫材料,其通过被配置为照射碳前体材料的表面下区域的激光束制成,激光束的参数被选择用于在所述表面下区域中产生碳泡沫。

[1280] 一种装置,其包括通过照射碳前体材料的表面下区域制造的激光诱导碳泡沫材料,激光束的参数被选择用于在所述表面下区域中产生碳泡沫。

[1281] 特点B:在碳前体材料的封装区域中产生的碳泡沫

[1282] 一种制造碳泡沫材料的方法,其包括以下步骤:照射碳前体材料的封装区域,激光束的参数被选择用于在所述封装区域中产生碳泡沫。

[1283] 一种激光诱导碳泡沫材料,其通过被配置为照射碳前体材料的封装区域的激光束制成,激光束的参数被选择用于在所述封装区域中产生碳泡沫。

[1284] 一种装置,其包括通过照射碳前体材料的封装区域制造的激光诱导碳泡沫材料,激光束的参数被选择用于在所述封装区域中产生碳泡沫。

[1285] 特点C:在碳前体材料的区域中产生的碳泡沫,其中所述区域不具有实质气体逸出通道

[1286] 一种制造碳泡沫材料的方法,其包括以下步骤:照射碳前体材料的封装、表面下区域,激光束的参数被选择用于在所述区域中产生碳泡沫,并且其中激光束不产生通向前体材料的表面的实质气体逸出通道。

[1287] 一种激光诱导碳泡沫材料,其通过被配置为照射碳前体材料的封装、表面下区域的激光束制造,激光束的参数被选择用于在所述区域中产生碳泡沫,并且其中激光束不产生通向前体材料的表面的实质气体逸出通道。

[1288] 一种装置,其包括通过照射碳前体材料的封装、表面下区域制造的激光诱导碳泡沫材料,激光束的参数被选择用于在所述区域中产生碳泡沫,并且其中激光束不产生通向

前体材料的表面的实质气体逸出通道。

[1289] 特点D:粘附至基板的无定形非石墨烯材料

[1290] 一种制造碳泡沫材料的方法,其包括以下步骤:照射定位于基板上的碳前体材料的内部区域,激光束的参数被选择用于在所述区域中产生碳泡沫并在碳泡沫区域与基板之间产生无序无定形非石墨烯材料;其中所述无序无定形非石墨烯材料粘附或以其他方式直接附接至基板。

[1291] 一种激光诱导碳泡沫材料,其通过被配置为照射定位于基板上的碳前体材料的内部区域的激光束制成,激光束的参数被选择用于在所述区域中产生碳泡沫并在石墨烯区域与基板之间产生无序无定形非石墨烯材料,所述无序无定形非石墨烯材料粘附或以其他方式直接附接至所述基板。

[1292] 一种装置,其包括通过照射定位于基板上的碳前体材料的内部区域制造的激光诱导碳泡沫材料,激光束的参数被选择用于在所述区域中产生碳泡沫并在石墨烯区域与所述基板之间产生无序无定形非石墨烯材料,所述无序无定形非石墨烯材料粘附或以其他方式直接附接至所述基板。

[1293] 特点E:通过激光烧蚀表面下碳泡沫区域所产生的碳泡沫

[1294] 一种制造石墨烯材料的方法,其包括以下步骤:(a)激光束照射碳前体材料的封装区域或表面下区域,以在封装区域或表面下区域中产生碳泡沫并且在碳泡沫上方产生无序无定形非石墨烯物质,然后(b)进行激光烧蚀或处理,以去除所述无序无定形非石墨烯物质中的至少一些并暴露所述碳泡沫中的至少一些。

[1295] 一种激光诱导碳泡沫,其通过以下制成:(a)激光束照射碳前体材料的封装区域或表面下区域,以在封装区域或表面下区域中产生碳泡沫并且在碳泡沫上方产生无序无定形非石墨烯物质,然后(b)进行激光烧蚀或处理,以去除无序无定形非石墨烯物质并暴露碳泡沫中的至少一些。

[1296] 一种装置,其包括通过以下制造的激光诱导碳泡沫材料:(a)激光束照射碳前体材料的封装区域或表面下区域,以在封装区域或表面下区域中产生碳泡沫并且在碳泡沫上方产生无序无定形非石墨烯物质,然后(b)进行激光烧蚀或处理,以去除无序无定形非石墨烯物质并暴露碳泡沫中的至少一些。

[1297] 特点F:通过激光烧蚀表面下碳泡沫区域所产生的非石墨烯碳泡沫

[1298] 一种制造非石墨烯碳泡沫的方法,其包括以下步骤:

[1299] (a)激光束照射碳前体材料的封装区域或表面下区域,以在封装区域或表面下区域中产生碳泡沫并且在碳泡沫上方产生无序无定形非石墨烯物质,然后

[1300] (b)进行激光烧蚀或处理,以去除无序无定形非石墨烯物质并暴露下层碳泡沫中的至少一些,并且将下层碳泡沫中的至少一些转变成非石墨烯碳泡沫。

[1301] 一种激光诱导碳泡沫,其通过以下制成:

[1302] (a)激光束照射碳前体材料的封装区域或表面下区域,以在封装区域或表面下区域中产生碳泡沫并且在碳泡沫上方产生无序无定形非石墨烯物质,然后

[1303] (b)进行激光烧蚀或处理,以去除无序无定形非石墨烯物质并暴露下层碳泡沫中的至少一些,并且将下层碳泡沫中的至少一些转变成非石墨烯碳泡沫。

[1304] 一种装置,其包括通过以下制成的激光诱导碳泡沫:

[1305] (a)激光束照射碳前体材料的封装区域或表面下区域,以在封装区域或表面下区域中产生碳泡沫并且在碳泡沫上方产生无序无定形非石墨烯物质,然后

[1306] (b)进行激光烧蚀或处理,以去除无序无定形非石墨烯物质并暴露下层碳泡沫中的至少一些,并且将下层碳泡沫中的至少一些转变成非石墨烯碳泡沫。

[1307] 特点G:在不同频带下操作的双激光

[1308] 一种制造碳泡沫材料的方法,其包括以下步骤:

[1309] (a)使用在第一波段下操作的激光束照射碳前体材料的、在所述材料的表面下方的封装区域或表面下区域,以在所述封装区域或表面下区域中产生碳泡沫,然后

[1310] (b)使用在第二波段下操作的激光束去除或烧蚀位于碳泡沫上方的材料,以暴露所述碳泡沫中的至少一些。

[1311] 一种激光诱导碳泡沫,其通过以下制成:

[1312] (a)使用在第一波段下操作的激光束照射碳前体材料的、在所述材料的表面下方所述材料的封装区域或表面下区域,以在所述封装区域或表面下区域中产生碳泡沫,然后

[1313] (b)使用在第二波段下操作的激光束去除或烧蚀位于碳泡沫上方的材料,以暴露所述碳泡沫中的至少一些。

[1314] 一种装置,其包括通过以下制造的激光诱导碳泡沫材料:

[1315] (a)使用在第一波段下操作的激光束照射碳前体材料的、在所述材料的表面下方的封装区域或表面下区域,以在所述封装区域或表面下区域中产生碳泡沫,然后

[1316] (b)使用在第二波段下操作的激光束去除或烧蚀位于碳泡沫上方的材料,以暴露所述碳泡沫中的至少一些。

[1317] 特点H:定位在通过激光烧蚀表面下碳泡沫区域所产生的碳泡沫中的电接触件

[1318] 一种制造碳泡沫材料的方法,其包括以下步骤:

[1319] (a)使用在第一波段下操作的激光束照射碳前体材料的、在所述材料的表面下方的封装区域或表面下区域,以在所述封装区域或表面下区域中产生碳泡沫,然后

[1320] (b)使用在第二波段下操作的激光束去除或烧蚀位于碳泡沫上方的材料,以暴露所述碳泡沫中的至少一些;以及

[1321] (c)将一个或多个电接触件附接、打印或定位至碳泡沫中。

[1322] 一种激光诱导碳泡沫,其通过以下制成:

[1323] (a)使用在第一波段下操作的激光束照射碳前体材料的、在所述材料的表面下方的封装区域或表面下区域,以在所述封装区域或表面下区域中产生碳泡沫,然后

[1324] (b)使用在第二波段下操作的激光束去除或烧蚀位于碳泡沫上方的材料,以暴露所述碳泡沫中的至少一些;

[1325] (c)将一个或多个电接触件附接、打印或定位至碳泡沫中。

[1326] 一种装置,其包括通过以下制造的激光诱导碳泡沫材料:

[1327] (a)使用在第一波段下操作的激光束照射碳前体材料的、在所述材料的表面下方的封装区域或表面下区域,以在所述封装区域或表面下区域中产生碳泡沫,然后

[1328] (b)使用在第二波段下操作的激光束去除或烧蚀位于碳泡沫上方的材料,以暴露所述碳泡沫中的至少一些;以及

[1329] (c)将一个或多个电接触件附接、打印或定位至碳泡沫中。

[1330] 特点I:在聚酰亚胺膜上印刷电接触件并然后产生暴露碳泡沫

[1331] 一种制造碳泡沫材料的方法,其包括以下步骤:

[1332] (a)将电接触件丝网印刷至碳前体材料上或中;

[1333] (b)使用在第一波段下操作的激光束照射碳前体材料的、在所述材料的表面下方的封装区域或表面下区域,以在所述封装区域或表面下区域中产生碳泡沫,并且其中步骤(a)和(b)可以按顺序(a)然后(b)或(b)然后(a)进行;以及

[1334] (c)使用在第二波段下操作的激光束去除或烧蚀位于碳泡沫上方的材料,以暴露碳泡沫中的至少一些,其与电接触件连接。

[1335] 一种激光诱导碳泡沫材料,其通过以下制成:

[1336] (a)将电接触件丝网印刷至碳前体材料上或中;

[1337] (b)使用在第一波段下操作的激光束照射碳前体材料的、在所述材料的表面下方的封装区域或表面下区域,以在所述封装区域或表面下区域中产生碳泡沫,并且其中步骤(a)和(b)可以按顺序(a)然后(b)或(b)然后(a)进行;以及

[1338] (c)使用在第二波段下操作的激光束去除或烧蚀位于碳泡沫上方的材料,以暴露碳泡沫中的至少一些,其与电接触件连接。

[1339] 一种装置,其包括通过以下制造的激光诱导碳泡沫材料:

[1340] (a)将电接触件丝网印刷至碳前体材料上或中;

[1341] (b)使用在第一波段下操作的激光束照射碳前体材料的、在所述材料的表面下方的封装区域或表面下区域,以在所述封装区域或表面下区域中产生碳泡沫,并且其中步骤(a)和(b)可以按顺序(a)然后(b)或(b)然后(a)进行;以及

[1342] (c)使用在第二波段下操作的激光束去除或烧蚀位于碳泡沫上方的材料,以暴露碳泡沫中的至少一些,其与电接触件连接。

[1343] 特点J:在碳泡沫中制成的高轨迹

[1344] 一种制造碳泡沫材料的方法,其包括以下步骤:

[1345] (a)使用在第一波段下操作的激光束照射碳前体材料的所述材料的表面下方的封装区域或表面下区域,以在所述封装区域或表面下区域中产生碳泡沫,然后

[1346] (b)使用在第二波段下操作的激光束去除或烧蚀位于碳泡沫上方的材料,以暴露所述碳泡沫中的至少一些;

[1347] 并且其中碳泡沫的厚度或深度为至少50μm。

[1348] 一种激光诱导碳泡沫材料,其通过以下制成:

[1349] (a)使用在第一波段下操作的激光束照射碳前体材料的、在所述材料的表面下方的封装区域或表面下区域,以在所述封装区域或表面下区域中产生碳泡沫,然后

[1350] (b)使用在第二波段下操作的激光束去除或烧蚀位于碳泡沫上方的材料,以暴露所述碳泡沫中的至少一些;

[1351] 并且其中碳泡沫的厚度或深度为至少50μm。

[1352] 一种装置,其包括通过以下制造的激光诱导碳泡沫材料:

[1353] (a)使用在第一波段下操作的激光束照射碳前体材料的、在所述材料的表面下方的封装区域或表面下区域,以在所述封装区域或表面下区域中产生碳泡沫,然后

[1354] (b)使用在第二波段下操作的激光束去除或烧蚀位于碳泡沫上方的材料,以暴露

所述碳泡沫中的至少一些;

[1355] 并且其中碳泡沫的厚度或深度为至少50μm。

[1356] 特点K:在不同的制造设施中应用第一激光和第二激光

[1357] 一种制造装置的方法,其包括以下步骤:

[1358] (a)使用在第一波段下操作的激光束照射碳前体材料的、在所述材料的表面下方的封装区域或表面下区域,以在所述封装区域或表面下区域中产生碳泡沫,然后

[1359] (b)使用在第二波段下操作的激光束去除或烧蚀位于碳泡沫上方的材料,以暴露所述碳泡沫中的至少一些;

[1360] 其中步骤(a)在一个制造设施中进行,并且步骤(b)在不同的制造设施中进行。

[1361] 一种激光诱导碳泡沫材料,其通过以下制成:

[1362] (a)使用在第一波段下操作的激光束照射碳前体材料的、在所述材料的表面下方的封装区域或表面下区域,以在所述封装区域或表面下区域中产生碳泡沫,然后

[1363] (b)使用在第二波段下操作的激光束去除或烧蚀位于碳泡沫上方的材料,以暴露所述碳泡沫中的至少一些;

[1364] 其中步骤(a)在一个制造设施中进行,并且步骤(b)在不同的制造设施中进行。

[1365] 一种装置,其包括通过以下制造的激光诱导碳泡沫材料:

[1366] (a)使用在第一波段下操作的激光束照射碳前体材料的、在所述材料的表面下方的封装区域或表面下区域,以在所述封装区域或表面下区域中产生碳泡沫,然后

[1367] (b)使用在第二波段下操作的激光束去除或烧蚀位于碳泡沫上方的材料,以暴露所述碳泡沫中的至少一些;

[1368] 其中步骤(a)在一个制造设施中进行,并且步骤(b)在不同的设施中进行。

[1369] 特点L1:生物传感器

[1370] 一种制造生物传感器的方法,所述生物传感器包括感测电极,所述感测电极包括至少部分地通过如上文特点A-K中任一项所定义的方法制成的碳泡沫。

[1371] 一种生物传感器,其包括感测电极,所述感测电极包括至少部分地通过如上文特点A-K中任一项所定义的方法制成的碳泡沫。

[1372] 一种即时诊断装置,其包括具有感测电极的生物传感器,所述感测电极包括至少部分地通过如上文特点A-K中任一项所定义的方法制成的碳泡沫。

[1373] 特点L2:使用丝网印刷技术以可扩展、低成本的方式制造碳泡沫生物传感器

[1374] 一种制造包括传感器电极诸如工作电极和对电极的生物传感器的方法,每个电极包括至少部分地通过如上文特点A-K中任一项所定义的方法制成的碳泡沫,并且所述方法包括在每个电极上方丝网印刷电连接轨迹,并且用丝网印刷电介质至少部分地覆盖电极和连接轨迹。

[1375] 一种生物传感器,其包括传感器电极,诸如工作电极和对电极,每个电极包括至少部分地通过如上文特点A-K中任一项所定义的方法制成的碳泡沫,并且其中所述生物传感器包括(i)在每个电极上方丝网印刷的电连接轨迹和(ii)至少部分地覆盖电极和连接轨迹的丝网印刷电介质。

[1376] 特点L3:在不同的制造设施处向生物传感器添加功能化基团

[1377] 一种在一个制造设施中制造包括传感器电极诸如工作电极、对电极的生物传感器

的方法,每个传感器电极包括至少部分地通过如上文特点A-K中任一项所定义的方法制成的碳泡沫,并且所述方法包括在不同的制造设施将功能化基团添加至至少工作电极的另一步骤。

[1378] 一种生物传感器,其包括传感器电极,诸如工作电极和对电极,每个电极包括至少部分地通过如上文特点A-K中任一项所定义的方法在一个制造设施处制成的碳泡沫,并且其中所述生物传感器包括官能化基团,所述官能化基团在不同的制造设施处被添加至至少工作电极。

[1379] 特点L4:向生物传感器添加功能化基团,作为生物传感器生产工艺的一部分

[1380] 一种在一个制造设施中制造包括传感器电极诸如工作电极、对电极的生物传感器的方法,每个传感器电极包括至少部分地通过如上文特点A-K中任一项所定义的方法制成的碳泡沫,并且所述方法包括在所述制造设施将功能化基团添加至工作电极的另一步骤。

[1381] 一种生物传感器,其包括传感器电极,诸如工作电极和对电极,每个电极包括至少部分的通过如上文特点A-K中任一项所定义的方法在一个制造设施处制成的碳泡沫,并且其中所述生物传感器包括官能化基团,所述官能化基团已在同一制造设施处被添加至至少工作电极。

[1382] 特点L5:使用PPC制造生物传感器:印刷后转化

[1383] 一种制造包括传感器电极诸如工作电极和对电极的生物传感器的方法,每个传感器电极包括至少部分地通过如上文特点A-K中任一项所定义的方法制成的碳,并且所述方法包括以下步骤:(a)在碳前体基板上丝网印刷碳层;(b)丝网印刷电连接轨迹和参比电极;(c)在所述碳层和所述电连接轨迹以及所述参比电极上方丝网印刷电介质层;然后(d)使用如上文特点A-K中任一项所定义的方法产生碳泡沫传感器电极。

[1384] 一种生物传感器,其包括传感器电极,诸如工作电极和对电极,其中所述生物传感器包括(a)丝网印刷在碳前体基板上的碳层;(b)丝网印刷电连接轨迹和丝网印刷参比电极;(c)丝网印刷在所述碳层和所述电连接轨迹以及所述参比电极上方的电介质层;以及(d)使用如上文特点A-K中任一项所定义的工艺制成的碳泡沫传感器电极。

[1385] 特点M1:储能装置

[1386] 一种制造储能装置、诸如超级电容器或赝电容器的方法,其中储能电极包括至少部分地通过如上文特点A-K中任一项所定义的方法制成的碳泡沫材料。

[1387] 一种储能装置,诸如超级电容器或赝电容器,其中储能电极包括至少部分地通过如上文特点A-K中任一项所定义的方法制成的碳泡沫材料。

[1388] 特点M2:丝网印刷碳泡沫超级电容器层

[1389] 一种制造储能装置、诸如超级电容器或赝电容器的方法,其中储能电极包括至少部分地通过如上文特点A-K中任一项所定义的方法制成的碳泡沫材料。

[1390] 并且所述方法包括在每个电极的至少一部分上方丝网印刷电连接轨迹以及用丝网印刷电介质层至少部分地覆盖所述电极和连接轨迹的步骤。

[1391] 一种储能装置,诸如超级电容器或赝电容器,其中储能电极包括至少部分地通过如上文特点A-K中任一项所定义的方法制成的碳泡沫材料。

[1392] 包括在每个电极的至少一部分上方形成的丝网印刷电连接轨迹和至少部分覆盖电极和连接轨迹的丝网印刷电介质层。

[1393] 特点M3:碳泡沫超级电容器:共集电极

[1394] 一种制造储能装置、诸如超级电容器或赝电容器的方法,其中储能电极包括至少部分地通过如上文特点A-K中任一项所定义的方法制成的碳泡沫材料并且以叉指图案布置;

[1395] 并且所述方法包括在每个电极的至少一部分上方丝网印刷电连接轨迹的步骤,其中单个电连接轨迹连接至从所述电连接轨迹两侧垂直延伸的下层指位。

[1396] 一种储能装置,诸如超级电容器或赝电容器,其中储能电极包括至少部分地通过如上文特点A-K中任一项所定义的方法制成的碳泡沫材料并且以叉指图案布置;

[1397] 并且其中丝网印刷电连接轨迹形成在每个电极的至少一部分上方,并且其中单个电连接轨迹连接至从电连接轨迹两侧垂直延伸的下层指位。

[1398] 特点M4:碳泡沫超级电容器:PPC制造工艺

[1399] 一种制造储能装置、诸如超级电容器或赝电容器的方法;

[1400] 并且所述方法包括以下步骤:(a)将电连接器丝网印刷至基板上;(b)在所述电集电极上方丝网印刷碳层;(c)在所述碳层的至少一些上方丝网印刷电介质;然后(d)至少部分地通过如上文特点A-K中任一项所定义的方法产生碳泡沫储能电极。

[1401] 一种储能装置,诸如超级电容器或赝电容器;

[1402] 其包括(a)在基板上的丝网印刷电连接器;(b)在所述电集电极上方的丝网印刷碳层;(c)在所述碳层的至少一些上方的丝网印刷电介质;然后(d)至少部分地通过如上文特点A-K中任一项所定义的方法产生的碳泡沫储能电极。

[1403] 特点M5:碳泡沫超级电容器:金属氧化物变体

[1404] 一种制造储能装置、诸如超级电容器或赝电容器的方法,其中储能电极包括至少部分地通过如上文特点A-K中任一项所定义的方法制成的碳泡沫材料;

[1405] 并且所述方法包括应用赝电容材料诸如金属氧化物向所述储能电极电化学沉积的工艺的步骤。

[1406] 一种储能装置,诸如超级电容器或赝电容器;

[1407] 其包括(a)包括碳泡沫材料的储能电极,所述碳泡沫材料至少部分地通过如上文特点A-K中任一项所定义的方法制成;以及(b)施加于所述储能电极的赝电容材料,诸如金属氧化物。

[1408] 特点M6:碳泡沫超级电容器:在低湿度环境中使用离子凝胶

[1409] 一种制造储能装置、诸如超级电容器或赝电容器的方法,其中储能电极包括至少部分地通过如上文特点A-K中任一项所定义的方法制成的碳泡沫材料;

[1410] 并且所述方法包括在低湿度但非惰性的环境中施加离子凝胶电解质的步骤,其中测量并控制所述环境中O2和H2O的水平以优化所述储能装置的电容。

[1411] 一种储能装置,诸如超级电容器或赝电容器;

[1412] 其包括(a)包括碳泡沫材料的储能电极,所述碳泡沫材料至少部分地通过如上文特点A-K中任一项所定义的方法制成;以及(b)已在低湿度但非惰性环境中施加的离子凝胶电解质,其中测量并控制所述环境中O2和H2O的水平以优化所述储能装置的电容。

[1413] 特点N1:电导体

[1414] 一种制造电导体的方法,其中电导体包括至少部分地通过如上文特点A-K中任一

项所定义的方法制成的碳泡沫。

[1415] 一种电导体,其包括至少部分地通过如上文特点A-K中任一项所定义的方法制成的碳泡沫。

[1416] 特点N2:组合的传感器和超级电容器

[1417] 一种制造包括传感器和储能装置诸如超级电容器二者的装置的方法,其中传感器和储能装置二者包括至少部分地通过如上文特点A-K中任一项所定义的方法制成的碳泡沫材料。

[1418] 一种传感器装置,诸如生物传感器,其包括(a)感测电极,其包括至少部分地通过如上文特点A-K中任一项所定义的方法制成的碳泡沫材料,以及(b)储能装置,诸如超级电容器,其中储能装置包括至少部分地通过如上文特点A-K中任一项所定义的方法制成的碳泡沫材料。

[1419] 一种即时诊断装置,其包括(a)感测电极,其包括至少部分地通过如上文特点A-K中任一项所定义的方法制成的碳泡沫材料,以及(b)储能装置,诸如超级电容器,其中储能装置包括至少部分地通过如上文特点A-K中任一项所定义的方法制成的碳泡沫材料。

[1420] 特点N3:组合的超级电容器和电池

[1421] 一种制造包括电池和超级电容器的集成装置的方法,所述电池提供长期功率,并且所述超级电容器在高于所述电池的水平下提供短期功率,其中所述超级电容器包括至少部分地通过如上文特点A-K中任一项所定义的方法制成的碳泡沫材料。

[1422] 一种包括电池和超级电容器的集成装置,所述电池提供长期功率,并且所述超级电容器在高于所述电池的水平下提供短期功率,其中所述超级电容器包括至少部分地通过如上文特点A-K中任一项所定义的方法制成的碳泡沫材料。

[1423] 特点N4:智能标签

[1424] 一种制造智能标签的方法,其包括组合或集成电池和超级电容器的步骤,所述电池提供长期功率,并且所述超级电容器在高于所述电池的水平下提供短期功率,其中所述超级电容器包括至少部分地通过如上文特点A-K中任一项所述的方法制成的碳泡沫材料;

[1425] 并且智能标签包括由电池提供功率的电子器件、诸如传感器电子器件,以及由超级电容器提供功率的数据发送器。

[1426] 一种包括电池和超级电容器智能标签,所述电池提供长期功率,并且所述超级电容器在高于所述电池的水平下提供短期功率,其中所述超级电容器包括至少部分地通过如上文特点A-K中任一项所定义的方法制成的碳泡沫材料;

[1427] 并且智能标签包括由电池提供功率的电子器件、诸如传感器电子器件,以及由超级电容器提供功率的数据发送器。

[1428] 特点N5:组合的超级电容器和天线

[1429] 一种制造包括天线和超级电容器的集成装置的方法,其中超级电容器为天线提供功率并且包括至少部分地通过如上文特点A-K中任一项所定义的方法制成的碳泡沫材料。

[1430] 一种集成装置,其包括天线和超级电容器,其中超级电容器为天线提供功率并且包括至少部分地通过如上文特点A-K中任一项所定义的方法制成的碳泡沫材料。

[1431] 特点N6:组合的能量采集器+超级电容器。

[1432] 一种制造集成装置的方法,其包括组合或集成能量采集器系统和超级电容器的步

骤,其中所述超级电容器为天线提供功率并且包括至少部分地通过如上文特点A-K中任一项所定义的方法制成的碳泡沫材料。

[1433] 一种数据记录装置,其包括能量采集器系统和超级电容器,其中超级电容器为天线提供功率并且包括至少部分地通过如上文特点A-K中任一项所定义的方法制成的碳泡沫材料。

[1434] 特点O1:3D碳泡沫结构:用于Gii-Cap的Gii-Thru

[1435] 一种制造储能装置的方法,其包括以下步骤:

[1436] (i)提供碳前体膜;

[1437] (ii)在所述碳前体膜的表面上丝网印刷导电浆料或油墨层;

[1438] (iii)在所述丝网印刷导电浆料或油墨层上方丝网印刷集电极层;

[1439] (iv)在所述集电极层上方丝网印刷电介质层;

[1440] (v)至少部分地通过上文特点A-K中任一项所定义的方法由所述碳前体膜制备包括碳泡沫材料的储能电极

[1441] 并且其中经由所述导电浆料或油墨层从所述碳泡沫材料至所述集电极层形成导电路径。

[1442] 一种储能装置,诸如超级电容器,其包括:

[1443] (i)碳前体膜;

[1444] (ii)丝网印刷导电浆料或油墨层,其在所述碳前体膜的所述表面上;

[1445] (iii)丝网印刷集电极层,其在所述丝网印刷导电浆料或油墨层上方;

[1446] (iv)丝网印刷电介质层,其在所述集电极层上方;

[1447] (v)储能电极,其包括至少部分地通过如上文特点A-K中任一项所定义的方法由碳前体膜制成的碳泡沫材料,并且其中导电路径形成为经由所述导电浆料或油墨层从所述碳泡沫材料至所述集电极层。

[1448] 特点O2:3D碳泡沫结构:Gii-Thru可堆叠Gii-Cap/Gii-Cap+

[1449] 一种制造储能装置的方法,其包括以下步骤:

[1450] (i)提供碳前体膜;

[1451] (ii)在所述碳前体膜的表面上丝网印刷导电浆料或油墨层;

[1452] (iii)在所述丝网印刷导电浆料或油墨层上方丝网印刷集电极层;

[1453] (iv)在所述集电极层上方丝网印刷电介质层;

[1454] (v)至少部分地通过上文特点A-K中任一项所定义的方法由所述碳前体膜制备包括碳泡沫材料的储能电极;

[1455] 并且其中经由所述导电浆料或油墨层从所述碳泡沫材料至所述集电极层形成导电路径;

[1456] 并且其中多个子组件形成为堆叠,并且其中相邻的储能电极通过离子凝胶电解质分开。

[1457] 一种储能装置,诸如超级电容器,其包括子组件,所述子组件包括:

[1458] (i)碳前体膜;

[1459] (ii)丝网印刷导电浆料或油墨层,其在所述碳前体膜的所述表面上;

[1460] (iii)丝网印刷集电极层,其在所述丝网印刷导电浆料或油墨层上方;

[1461] (iv)丝网印刷电介质层,其在所述集电极层上方;

[1462] (v)储能电极,其包括至少部分地通过如上文特点A-K中任一项所定义的方法由碳前体膜制成的碳泡沫材料,并且其中导电路径形成为经由所述导电浆料或油墨层从所述碳泡沫材料至所述集电极层;

[1463] 并且其中多个子组件形成为堆叠,并且其中相邻的储能电极通过离子凝胶电解质分开。

[1464] 特点O3:3D碳泡沫结构:用于Gii-Sens的Gii-Thru:HISLOC

[1465] 一种微流体诊断装置,其包括定位于装置的上表面的样品孔,参比电极、工作电极和对电极至少部分地通过由上文特点A-K中任一项所定义的方法由碳前体膜制成其在样品孔下方的层中,并且参比电极连接件、工作电极连接件和对电极连接件在所述参比电极、工作电极和对电极下方的层中。

[1466] 特点O4 3D碳泡沫结构:用于Gii-Sens的Gii-Thru:HISLOC制造工艺

[1467] 一种制造芯片实验室装置的方法,其包括以下步骤:

[1468] (i)提供碳前体膜;

[1469] (ii)在所述碳前体膜的表面上丝网印刷导电浆料或油墨层;

[1470] (iii)在所述丝网印刷导电浆料或油墨层上方丝网印刷导电层;

[1471] (iv)丝网印刷参比电极;

[1472] (v)在所述集电极层上方丝网印刷电介质层;

[1473] (vi)至少部分地通过上文特点A-K中任一项所定义的方法由所述碳前体膜制备包括碳泡沫材料的传感器电极;

[1474] 并且其中经由所述导电浆料或油墨层从所述碳泡沫材料至所述导电层形成导电路径。

[1475] 一种芯片实验室装置,其包括子组件,所述子组件包括:

[1476] (i)碳前体膜;

[1477] (ii)丝网印刷导电浆料或油墨层,其在所述碳前体膜的所述表面上;

[1478] (iii)丝网印刷导电层,其在所述丝网印刷导电浆料或油墨层上方;

[1479] (iv)丝网印刷参比电极;

[1480] (v)丝网印刷电介质层,其在所述集电极层上方;

[1481] (vi)传感器电极,其包括至少部分地通过如上文特点A-K中任一项所定义的方法由碳前体膜制成的碳泡沫材料,并且其中导电路径形成为经由所述导电浆料或油墨层从所述碳泡沫材料至所述导电层。

[1482] 特点P:碳泡沫的可扩展制造:Gii 3

[1483] 一种制造包括一个或多个电极的装置的方法,每个电极都包括碳泡沫材料;

[1484] 其中所述方法包括使碳前体膜的连续卷轴通过制造至少部分地通过如上文特点A-K中任一项所定义的方法制成的碳泡沫材料所需的一系列操作。

[1485] 特点Q:各种其他碳泡沫应用

[1486] 一种装置,其包括至少部分地通过如上文特点A-K中任一项所定义的方法制成的碳泡沫材料,其中所述装置是以下类型的装置之一:

[1487] 霍尔效应传感器:碳泡沫显示出对磁场的响应。

[1488] 用于例如机器人的触觉传感器;原型传感器,其使用聚二甲基硅氧烷(PDMS)嵌入至结构中和上方的Gii碳泡沫作为基于压阻的压力传感器中的活性层,以用于机器人触摸感应应用。

[1489] 感染性疾病传感器。

[1490] 生物传感器,其中Gii碳泡沫用芘羧酸(PCA)进行π-π非共价官能化,以用于白介素10阻抗检测。

[1491] 持续监测化学传感器。

[1492] 葡萄糖监测传感器:一种用于电化学葡萄糖监测的可逆聚合物位移传感器机构;葡萄糖的芘衍生的硼酸化学受体被吸附至碳泡沫电极上,与聚去甲二氢愈创木酸竞争结合。

[1493] 乳酸传感器:采用合成有机受体分子,其基于将硼酸附接至碳泡沫,以在竞争性分析物结合中提供功能性和选择性,使用表面氧化还原聚合物指示剂置换。

[1494] 气体检测传感器,诸如过氧化氢和氧气检测,使用浸入pH 7的磷酸盐缓冲溶液中的Gii碳泡沫和自具微孔纳米颗粒聚合物(PIM-1)。

[1495] 光学检测器。

[1496] 自充电混合能源产生装置。

[1497] 绿色气体转化为有用的化学物质。

[1498] 燃料电池,例如氢燃料电池。

[1499] 过滤器,包括透气过滤器。

[1500] 加热装置。

[1501] 特点R:非石墨烯碳材料泡沫

[1502] 一种碳泡沫材料,其至少部分地通过如上文特点A-K中任一项所定义的方法制成,并且其是亲水性的,接触角低于20°。

[1503] 一种碳泡沫材料,其至少部分地通过如上文特点A-K中任一项所定义的方法制成,并且其拉曼光谱表现出显著的D峰;2D峰小于G峰;D峰:G峰的比率高于零。

[1504] 一种碳纳米洋葱材料,其至少部分地通过如上文特点A-K中任一项所定义的方法制成。

[1505] 一种装置,其包括至少部分地通过如上文特点A-K中任一项所定义的方法制成的碳泡沫材料,并且所述碳泡沫材料是亲水性的,接触角低于20°。

[1506] 一种装置,其包括至少部分地通过如上文特点A-K中任一项所定义的方法制成的碳泡沫材料,所述碳泡沫材料的拉曼光谱表现出显著的D峰;2D峰小于G峰;D峰:G峰的比率高于零。

[1507] 一种装置,其包括至少部分地通过如上文特点A-K中任一项所定义的方法制成的碳纳米洋葱材料。

[1508] 任选特点

[1509] 需注意,以下任选特点中的任何一者或多者每个都可以与一个或多个其他兼容的任选特点以及与主要特点A-R中的任何一者或多者组合。

[1510] 制造工艺

[1511] 制造工艺为室温工艺。

[1512] 制造工艺为常压工艺。

[1513] 可以在塑料基板上完成(与任何制造工艺兼容,不仅仅是硅芯片制造)。

[1514] 可以在没有催化剂的情况下完成。

[1515] 所述制造工艺需要约2分钟或更短时间来向塑料基板上制造1cm^{2}约为50μm厚的碳泡沫。

[1516] 所述制造工艺实现了在柔性基板上形成3D碳泡沫。

[1517] 所述制造工艺不需要石墨烯或氧化石墨烯前体。

[1518] 所述制造工艺仅在碳前体材料的封装、表面下区域中产生碳泡沫材料,并且不在碳前体材料的任何表面产生碳泡沫材料。

[1519] 所述制造工艺使用行业标准、低成本和可扩展的(i)丝网印刷技术和(ii)计算机控制的激光扫描技术的组合。

[1520] 所述制造工艺使用或可以适合于高速、大批量卷对卷或卷对片生产。

[1521] 第一激光束参数和控制方案

[1522] • 所述第一激光束和所述第二激光束通过不同的激光系统产生。

[1523] • 所述第一激光束和所述第二激光束通过相同的激光系统产生。

[1524] • 照射表面下区域或封装区域的激光束的参数包括以下中的一者或多者:强度、波长、脉冲频率、脉冲持续时间、脉冲轮廓、扫描速度、焦距、在表面下区域或封装区域产生的热。

[1525] • 改变激光参数使碳泡沫材料的性质改变,使得能够生产出具有针对不同应用而优化的性质的碳泡沫。

[1526] • 改变激光参数使以下碳泡沫材料的性质或参数中的一者或多者改变:存在的碳纳米结构的类型(例如,碳纳米洋葱等)、缺陷的大小、缺陷的分布、缺陷的程度、缺陷的类型、拉曼D和2D峰、拉曼D和2D峰的相对大小、厚度或深度、柔韧性、粘附性、孔隙率、电导率、电容、有机溶剂和水基溶液的吸收、亲水性、EMI屏蔽、电极质量、可润湿性、接触角、防污性。

[1527] • 激光束在表面下区域或封装区域处产生高于500℃的温度以形成碳泡沫。

[1528] • 激光束在表面下区域或封装区域处产生超过500℃的温度以形成碳泡沫。

[1529] • 激光束的脉冲持续时间在1ns与10μs之间,得到在约5×10^7℃/s与2×10^{12}℃/s之间的加热速率。

[1530] • 激光功率在8-20瓦特的典型工作范围内,最佳为12W。

[1531] • 激光焦距在50mm-400mm的典型工作范围内。

[1532] • 激光脉冲频率在50kHz与500kHz之间。

[1533] • 激光脉冲频率在1kHz与2MHz之间。

[1534] • 激光波长在0.7μm-2.5μm之间。

[1535] • 激光以9cm/s与40cm/s之间(或这些范围的±50%)进行扫描。

[1536] • 激光束的参数包括焦点参数。

[1537] • 激光束的参数包括衍射参数。

[1538] • 激光束的参数包括干涉图案参数。

[1539] • 激光束的焦点移动穿过碳前体材料的深度,以在碳前体的表面下区域或封装区域中产生碳泡沫。

[1540] • 激光束的焦点移动穿过碳前体材料的深度至少约50μm,以在碳前体的表面下区域或封装区域中产生碳泡沫。

[1541] • 激光束的焦点移动穿过碳前体材料的深度至少100μm,以在碳前体的表面下区域或封装区域中产生碳泡沫。

[1542] • 激光束在碳前体材料上扫描(例如,光栅扫描)或侧向移动,以形成所需的图案。

[1543] • 激光束在碳前体材料上扫描或侧向移动,以形成包括非重叠区域或线的所需图案。

[1544] • 激光束在碳前体材料上重复地扫描(例如,光栅扫描)或侧向移动,其焦点或强度最大值被布置在碳前体材料内的多个不同深度,直到产生具有所需图案和深度的碳泡沫。

[1545] • 激光束以在1.7mm/s与3550m/s之间,或更通常在35mm/s与350mm/s之间的扫描速率下扫描,并且扫描可以使得每英寸脉冲数(PPI)在100与10000之间(与生产个别近似于大小为220mm×180mm的聚酰亚胺片材有关)。

[1546] • 激光束所具有的波长基本上不被所述碳前体材料吸收,或者吸收率极低。

[1547] • 碳前体材料对激光束所具有的波长的吸收率极低,

[1548] 其中每厘米辐射吸收率(10进制)低于50、或低于20、或低于10。

[1549] • 激光束是IR激光。

[1550] • 激光束是波长在0.7μm-2.5μm之间的IR激光。

[1551] • 激光束是波长在0.75μm-1.40μm之间的IR激光。

[1552] 表面下区域或封装区域的属性

[1553] • 碳前体材料中表面下区域或封装区域的所需深度通过将第一激光束的焦点移动穿过深度来实现。

[1554] • 表面下区域或封装区域在所述碳前体材料的所述表面下方至少10μm。

[1555] • 表面下区域或封装区域在所述碳前体材料的所述表面下方至少20μm。

[1556] • 表面下区域或封装区域在所述碳前体材料的所述表面下方至少30μm。

[1557] • 表面下区域或封装区域在所述碳前体材料的所述表面下方至少40μm。

[1558] • 表面下区域或封装区域在所述碳前体材料的所述表面下方至少50μm。

[1559] • 与常规石墨烯泡沫不同,表面下区域或封装区域的厚度可以超过约50μm。

[1560] • 表面下区域或封装区域的厚度在10μm与200μm之间。

[1561] • 表面下区域或封装区域可以面向入射激光在碳前体材料的表面下方的不同深度;并且表面下区域或封装区域所在的确切深度是各种因素的函数,所述因素诸如激光强度或其他激光参数、对所使用的碳前体材料的选择等。例如,表面下区域或封装区域可以在碳前体材料的表面下方至少约10μm、20μm、30μm、40μm、50μm或更多。

[1562] • 表面下区域或封装区域在所述碳前体材料的所述表面下方的距离是所述碳前体材料的总厚度的至少1%、或所述碳前体材料的总厚度的至少10%、或所述碳前体材料的总厚度的至少20%、或所述碳前体材料的总厚度的至少30%、或所述碳前体材料的总厚度的至少40%。

[1563] • 表面下区域或封装区域是以所述第一激光束的最小横截面的中心为中心的一定体积的空间,并且所述体积在所述中心的500微米内、或在所述中心的100微米内、或在所

述中心的1微米内。

[1564] 碳前体材料

[1565] • 碳前体材料基本上由热固性材料制成。

[1566] • 碳前体材料基本上由非热塑性材料制成。

[1567] • 碳前体材料是热固性膜。

[1568] • 热固性膜是聚酰亚胺膜。

[1569] • 碳前体是聚酰亚胺膜。

[1570] • 碳前体是聚酰亚胺膜,所述第一激光的波长在0.7μm至2.5μm的范围内。

[1571] • 碳前体是至少50质量%碳、或至少75质量%碳、或至少90质量%碳。

[1572] • 碳前体是膜或片材。

[1573] • 碳前体材料是柔性的。

[1574] • 碳前体材料是印刷层,诸如丝网印刷层。

[1575] • 碳前体材料的厚度大于5μm、或在5μm与120μm之间、或大于120μm。

[1576] • 碳前体材料是基本上平面或平坦的,并且垂直于第一激光束取向。

[1577] • 碳前体材料是均质的。

[1578] • 碳前体材料是异质的并且包含若干不同的材料。

[1579] • 碳前体被支撑在基板上,所述基板不由碳前体制成。

[1580] • 碳前体材料在第一激光束波长下的吸收系数低。

[1581] • 碳前体材料对于第一激光束的吸收系数低于$50cm^{-1}$、或低于$20cm^{-1}$、或低于$10cm^{-1}$。

[1582] • 碳前体材料对第二或烧蚀激光束的吸收系数低于$300cm^{-1}$。

[1583] • 碳前体材料对于第二或烧蚀激光束的吸收系数为$300\pm50cm^{-1}$

[1584] • 碳前体材料的热导率小于1.0W/mK(使用根据ASTM D5470的方法)。

[1585] • 碳前体材料的热导率小于0.5W/mK(使用根据ASTM D5470的方法)。

[1586] • 碳前体材料安装在基板上,所述基板在激光束的一个或多个波长下是基本上光学透明的。

[1587] • 碳前体材料的碳源包含一种或多种聚合物或由其形成。

[1588] • 碳前体材料包含以下材料中的一者或多者:聚酰亚胺类(例如,聚(4,4'-氧二亚苯基-均苯四甲酸二胺),另外还称为聚酰亚胺)、聚醚酰亚胺类(PEI)、聚(甲基丙烯酸甲酯)类(PMMA)(例如,喷涂的PMMA)、聚氨酯类(PU)、聚酯类、乙烯基聚合物类、碳化聚合物类、光阻聚合物类、醇酸树脂类、脲醛。

[1589] • 碳前体包含以下材料中的一者或多者:聚(酰胺酸)类(例如,含芳基的聚(酰胺酸))(例如,聚(均苯四甲酸二酐-共-4,4'-氧二苯胺),酰胺酸,另外还称为聚酰胺酸);二酐类(例如,芳基二酐)(例如,均苯四甲酸二酐);所述聚(酰胺酸)类的衍生物;所述二酐类的衍生物(例如,均苯四甲酸二酐的衍生物)。

[1590] • 碳前体包含以下材料中的一者或多者:芳香族材料(例如,芳香族聚合物);杂芳香族材料(例如,杂芳香族聚合物);含有芳香族部分的聚合物;环状材料(例如,含有环状部分的聚合物);杂环材料(例如,含有杂环部分的聚合物);杂芳香族材料(例如,含有杂芳香族部分的聚合物)。

[1591] • 碳前体包含含有芳香键、或杂芳香键、或杂键(例如,酰亚胺键)中的一者或多者的材料。

[1592] 支撑碳前体材料的基板

[1593] • 基板是塑料主体、膜或箔。

[1594] • 基板是柔性的。

[1595] • 基板是聚酰亚胺电路板。

[1596] • 基板对第一激光束的吸收率极低。

[1597] • 基板在第一激光束的一个或多个波长下是基本上光学透明的。

[1598] • 基板对第一激光束的吸收率高,吸收大于60%的第一激光束。

[1599] • 基板对第一激光束的吸收率高,吸收大于60%的第一激光束,并且其热导率为至少10W/mK。

[1600] • 碳前体材料的表面通过激光束转化为无序无定形非石墨烯物质,并且无序无定形非石墨烯物质粘附或粘合至基板,并且因此间接地将3D碳材料泡沫附接至基板。

[1601] • 基板由以下中的一者或多者形成:硅(Si)、二氧化硅(SiO_2)、氮化镓(GaN)、砷化镓(GaAs)、氧化锌(ZnO)。

[1602] • 基板是硅晶圆。

[1603] • 基板是二氧化硅晶圆。

[1604] • 基板是包含硅和二氧化硅二者的晶圆。

[1605] • 基板是碳源。

[1606] • 基板不是碳源,例如,是金属、电介质材料、丝网印刷电介质材料。

[1607] • 碳前体被定位在基板“上方”(例如,碳前体被定位成比基板更靠近激光源)。

[1608] • 碳前体被定位在基板“下方”(例如,碳前体被定位成比基板更远离激光源)。

[1609] 在激光束入射的表面处的碳化

[1610] • 碳前体材料的表面通过激光束转化为无序无定形非石墨烯物质。

[1611] • 无序无定形非石墨烯物质占据自相邻碳前体材料的表面的厚度,其为碳前体材料的总厚度的约1%、或小于约1%、或小于约5%、或小于约10%。

[1612] • 无序无定形非石墨烯物质从其表面延伸至碳前体材料主体内至少10μm的距离。

[1613] • 所述无序无定形非石墨烯物质从其外表面向所述碳前体材料的主体中延伸至10μm或更小的深度、或20μm或更小的深度、或30μm或更小的深度、或40μm或更小的深度、或50μm或更小的深度、或100μm或更小的深度。

[1614] 在与支撑碳前体材料的基板的物理界面处的碳化

[1615] • 所述碳前体材料在与所述基板的物理界面处通过所述激光束转化为无序无定形非石墨烯物质至由所述激光束的参数限定的深度。

[1616] • 所述无序无定形非石墨烯物质在粘附或以其他方式附接至所述碳泡沫的一个区域,并且在粘附或以其他方式附接至所述基板的另一区域,因此为所述碳泡沫提供稳定性。

[1617] • 从所述碳前体材料与所述基板的界面测量的所述无序无定形非石墨烯物质所占据的厚度为所述碳前体材料的总厚度的约1%、或小于约1%、或小于约5%、或小于约10%。

[1618] • 所述无序无定形非石墨烯物质所占据的自所述碳前体材料与所述基板的界面的厚度为至少10μm。

[1619] • 所述无序无定形非石墨烯物质从所述碳前体材料与所述基板的界面延伸至10μm或更小的深度、或20μm或更小的深度、或30μm或更小的深度、或40μm或更小的深度、或50μm或更小的深度、或100μm或更小的深度。

[1620] 烧蚀激光束或第二激光束

[1621] • 激光束的参数包括以下中的一者或多者:强度、波长、脉冲频率、脉冲持续时间、脉冲轮廓、扫描速度、焦距、在所述表面下区域或封装区域产生的热。

[1622] • 改变激光参数使碳泡沫材料的性质改变,使得能够生产出具有针对不同应用而优化的性质的碳泡沫。

[1623] • 改变激光参数使以下碳泡沫材料的性质或参数中的一者或多者改变:存在的碳纳米结构的类型(例如,碳纳米洋葱等)、缺陷的大小、缺陷的分布、缺陷的程度、缺陷的类型、拉曼D和2D峰、拉曼D和2D峰的相对大小、厚度或深度、柔韧性、粘附性、孔隙率、电导率、电容、有机溶剂和水基溶液的吸收、亲水性、EMI屏蔽、电极质量、可润湿性、接触角、防污性。

[1624] • 烧蚀在碳前体中封装区域或表面下区域上方形成的无定形非石墨烯物质的激光束(“第二激光束”)是CO_2激光。

[1625] • 第二激光束改变碳泡沫,作为使其暴露的工艺的一部分。

[1626] • 第二激光束改变碳泡沫的形态,作为使其暴露的工艺的一部分。

[1627] • 第二激光束被自动控制以在相同区域、和/或重叠区域、和/或非重叠区域上扫描。

[1628] • 烧蚀无定形非石墨烯物质的激光束的波长在8μm-15μm之间。

[1629] • 第二激光束是长IR激光、或UV激光、或可见光激光。

[1630] • 第二激光束的脉冲频率在50kHz与500kHz之间,并且扫描速度在9cm/s与40cm/s之间。

[1631] • 碳前体材料对于第二激光束的吸收系数高于$100cm^{-1}$,或对于第二激光束的吸收系数高于$200cm^{-1}$。

[1632] • 碳前体材料对于第二激光束的吸收系数为$300\pm50cm^{-1}$。

[1633] • 激光功率在8-20瓦特的典型工作范围内,最佳为12W。

[1634] • 激光焦距在50mm-400mm的典型工作范围内。

[1635] • 第二激光束以包括非重叠区域或线的图案(例如,光栅)扫描。

[1636] • 第二激光束以与第一激光束的扫描图案匹配的图案扫描。

[1637] • 第二激光束是散焦的。

[1638] • 第二激光束与照射碳前体材料的封装区域或表面下区域的激光束相同,以在封装区域或表面下区域中产生碳泡沫。

[1639] • 制造工艺是一种三阶段工艺,其涉及以下步骤:(a)所述第一激光束在制造场所照射碳前体材料的表面下区域,以产生未完成的碳泡沫产品;(b)将所述未完成的碳泡沫产品转移至客户控制的制造场所;以及(c)在所述客户控制的制造场所进行所述激光烧蚀或处理。

[1640] 碳泡沫

[1641] • 碳泡沫为多层扭转或乱层碳泡沫。

[1642] • 碳泡沫为非石墨烯碳泡沫。

[1643] • 碳泡沫包括碳质纳米结构,诸如碳纳米洋葱、碳纳米角、碳纳米管、碳纳米点、纳米金刚石和富勒烯、或其任何组合。

[1644] • 碳泡沫的厚度为至少约50μm。

[1645] • 碳泡沫的厚度在约50μm至300μm之间。

[1646] • 碳泡沫是或包括多层扭转或乱层多层泡沫。

[1647] • 碳泡沫是或包括具有导致高电化学反应性的缺陷的空间分布的碳泡沫。

[1648] • 碳泡沫是或包括具有导致高电化学反应性的空缺位置基面缺陷的碳泡沫。

[1649] • 碳泡沫的碳:氧比率在25:1与50:1之间。

[1650] • 碳泡沫具有快速电子转移常数。

[1651] • 与使用常规激光工艺制成的常规石墨烯泡沫相比,碳泡沫具有以下性质中的一者或多者:厚度或深度更容易控制;与使用常规激光工艺制成的高脆性石墨烯相比,柔韧性更大;对下层柔性基板的粘附性更强;孔隙率更高;电导率更高;电容或电荷存储增加;对有机溶剂和水基溶液的吸收更快;亲水性更高;接触角低于约20°;防污性能增强;EMI屏蔽更高;电极质量增强。

[1652] 生物传感器用例

[1653] • 碳泡沫被功能化为生物传感器。

[1654] • 碳泡沫通过添加对目标或分析物具有特异性的受体而被功能化为生物传感器。

[1655] • 碳泡沫被功能化为具有可逆聚合物位移传感器机构的生物传感器,用于

[1656] 电化学葡萄糖监测。

[1657] • 可逆聚合物位移传感器包括针对被吸附到包括所述碳泡沫的电极上的葡萄糖的芘衍生硼酸化学受体。

[1658] • 碳泡沫通过添加对目标或分析物具有特异性的受体以及使所述受体能够附接至所述碳泡沫的接头而被功能化为生物传感器。

[1659] • 接头选自纳米颗粒、聚合物、聚合物刷、配体、包含一个或多个官能团的有机化合物、共价或非共价键合至所述碳泡沫的分子、或其混合物。

[1660] • 接头选自聚合物(优选(甲基)丙烯酸酯聚合物)、包含一个或多个官能团的有机化合物、碳二亚胺、重氮化合物、或其混合物。

[1661] • 所述一个或多个官能团独立地选自氧、氮、硫、卤化物、羟基、羰基、羧基、胺、氨基、酰胺、亲水性聚合物或其混合物,其任选地与线性、支链或环状烷基、烯基、炔基、芳基残基、丙烯酰基、酰基、酰氧基、烷氧基、亚烷氧基或其混合物组合。

[1662] • 所述有机化合物还包含一个或多个任选地包含一个或多个杂原子的环状部分,并且所述环状部分中的至少一个直接或间接地连接至所述官能团中的至少一个,或者所述接头是作为所述有机化合物的酯或盐的衍生物,或者是在与所述碳泡沫反应中释放所述有机化合物的化合物。

[1663] • 接头选自1-芘丁酸、N-羟基琥珀酰亚胺(NHS)、芘-1-羧酸琥珀酰亚胺酯、1-氨基芘、N-(1-芘)马来酰亚胺或其混合物。

[1664] • 接头通过π-π相互作用键合至碳泡沫。

[1665] • 所述受体是以下中的一者:电化学受体、化学受体、生物受体、光学受体、物理或机械受体,优选生物受体。

[1666] • 所述受体选自冠醚、催化剂、硼酸、概念、配体、适体、蛋白质、酶、抗体、抗原、微生物、核酸、脂肪酸、脂肪酸酯、分子印迹聚合物、金属有机骨架、能够形成配体结合的多肽或寡肽、细胞、细胞器或其他细胞组分或其混合物,优选地选自蛋白质、核酸、抗体、酶或其混合物。

[1667] • 受体选自免疫球蛋白A(IgA)、葡萄糖脱氢酶、链霉亲和素或其混合物。

[1668] • 所述受体以物理、生物和/或化学方式键合至所述接头,优选以化学方式键合,更优选共价键合。

[1669] 超级电容器用例

[1670] • 所述碳泡沫形成储能装置中的电极,所述储能装置诸如电化学电容器、超级电容器、赝电容器或电容器。

[1671] • 所述碳泡沫用金属氧化膜处理,以提供赝电容。

[1672] • 所述碳泡沫形成储能装置中的至少一个电极,所述储能装置诸如电化学

[1673] 电容器、超级电容器、赝电容器或电容器,并且水凝胶电解质包封活性区域中的所述电极或每个电极,以产生增强的操作电压窗口。

[1674] • 所述碳泡沫形成电池中的电极。

[1675] • 所述碳泡沫形成电导体。

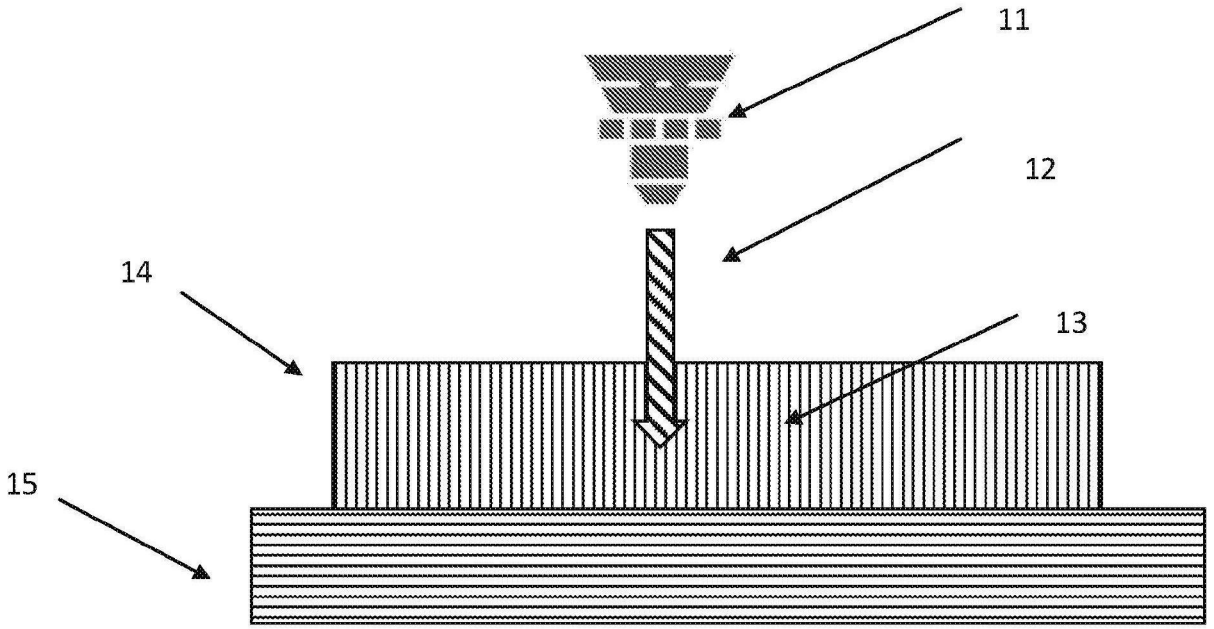


图1

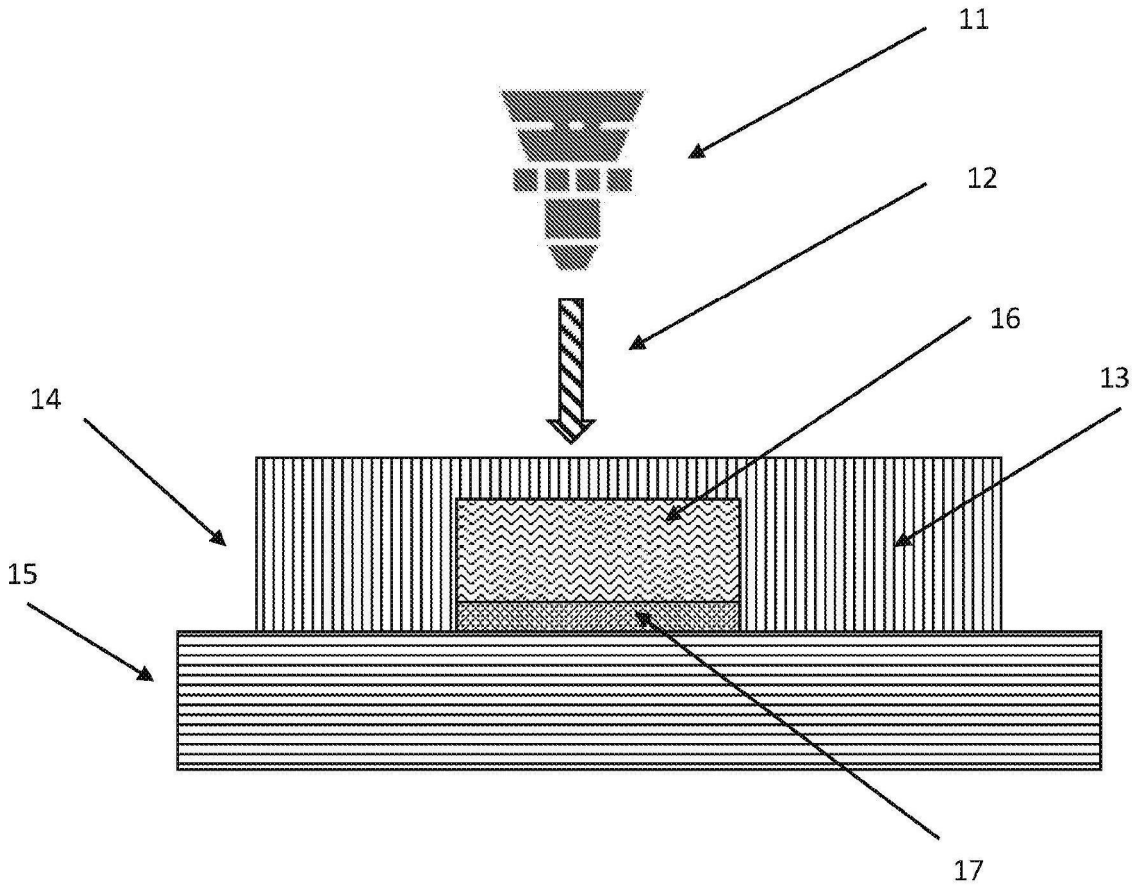


图2

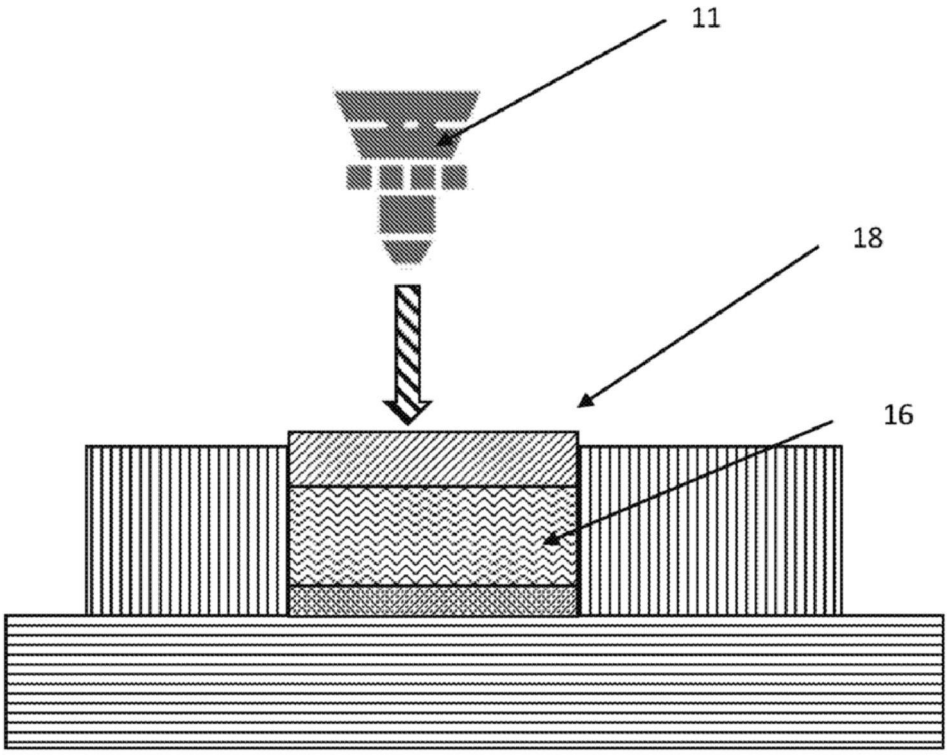


图3

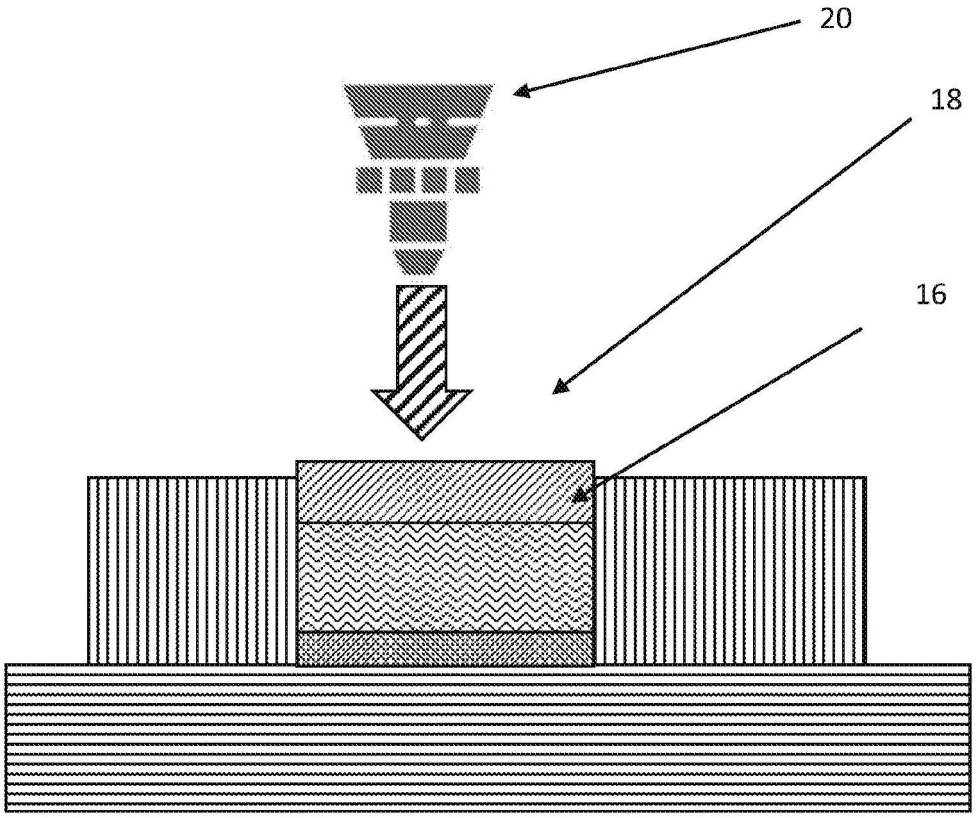


图4

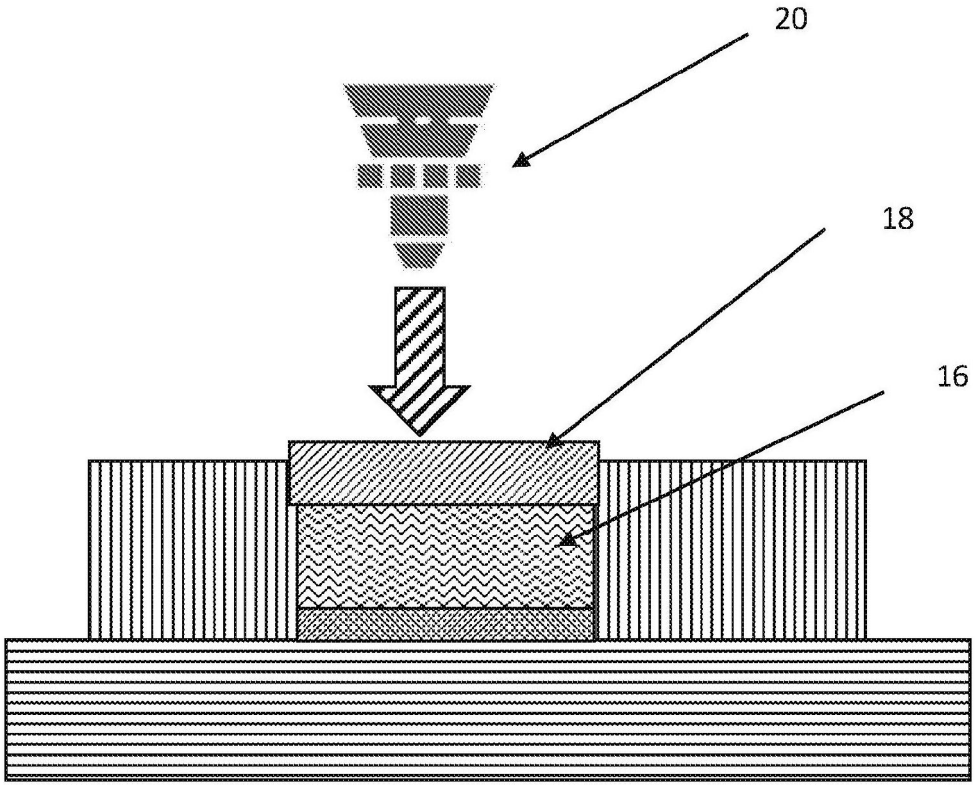


图5

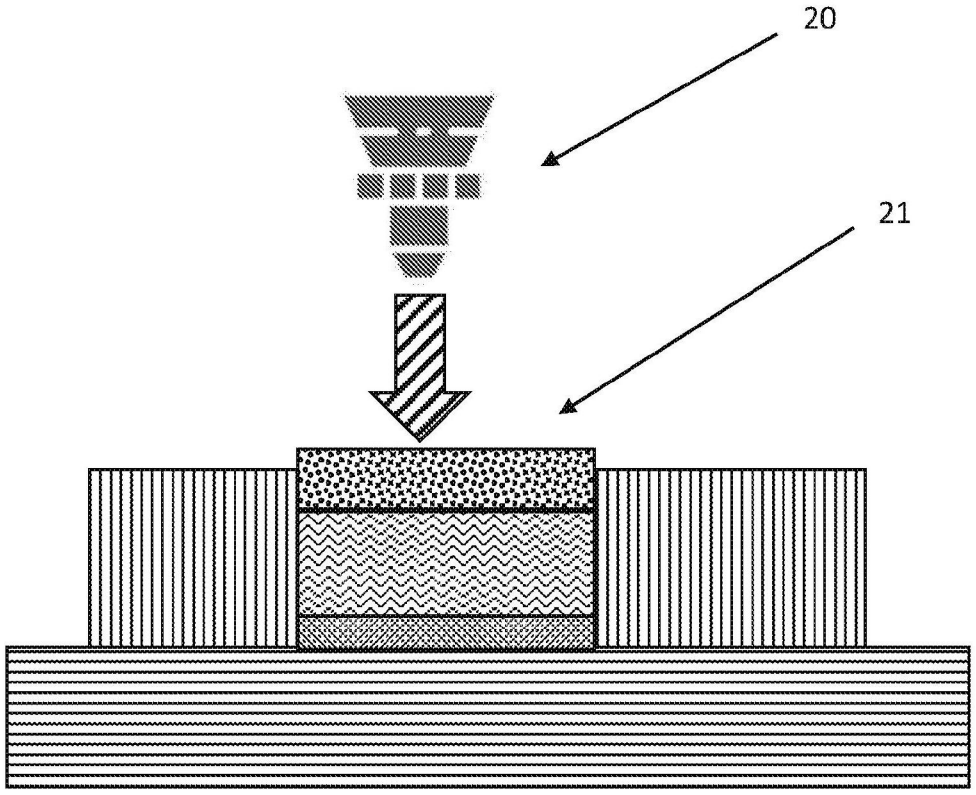


图6

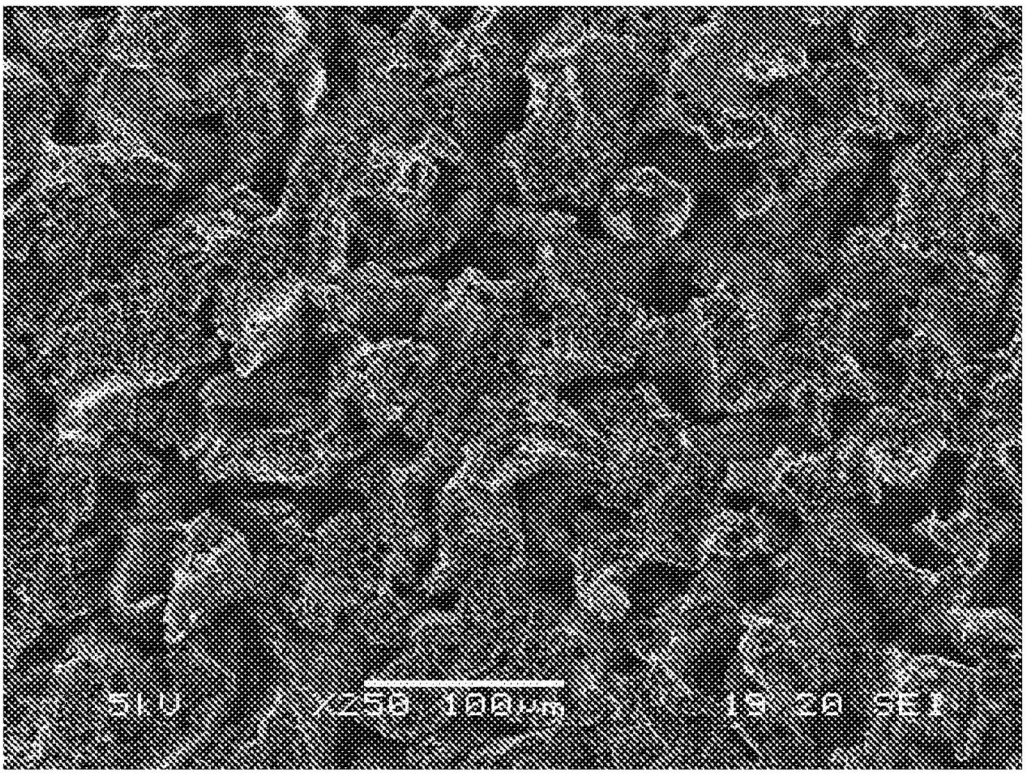


图7

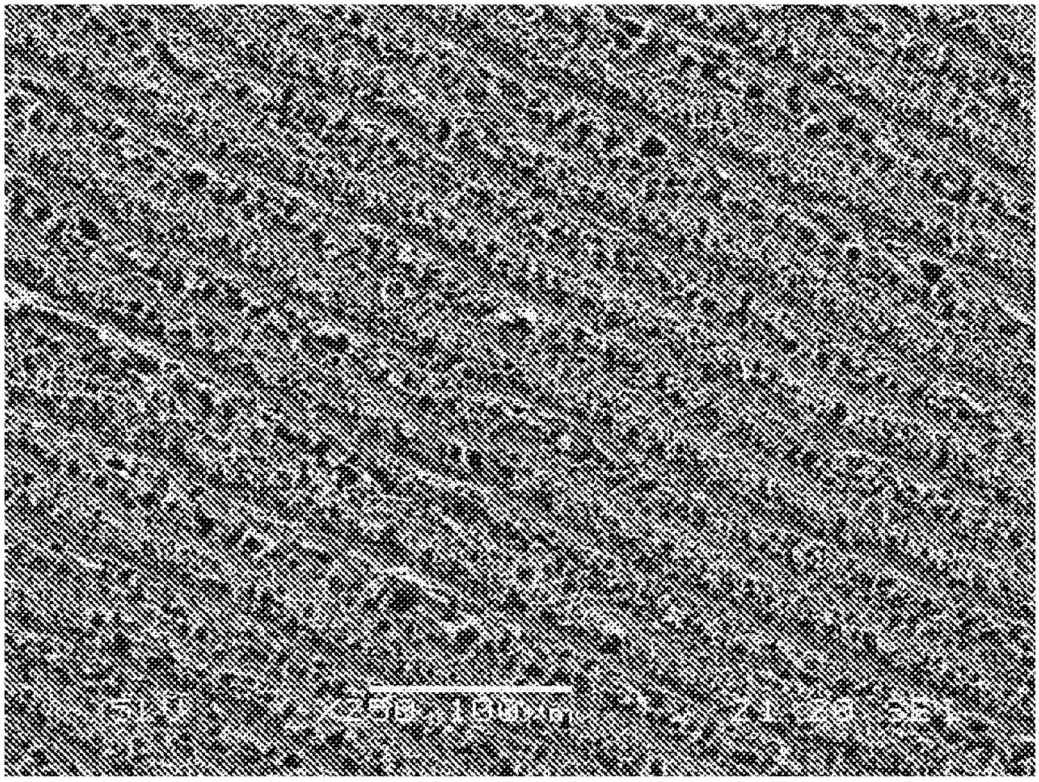


图8

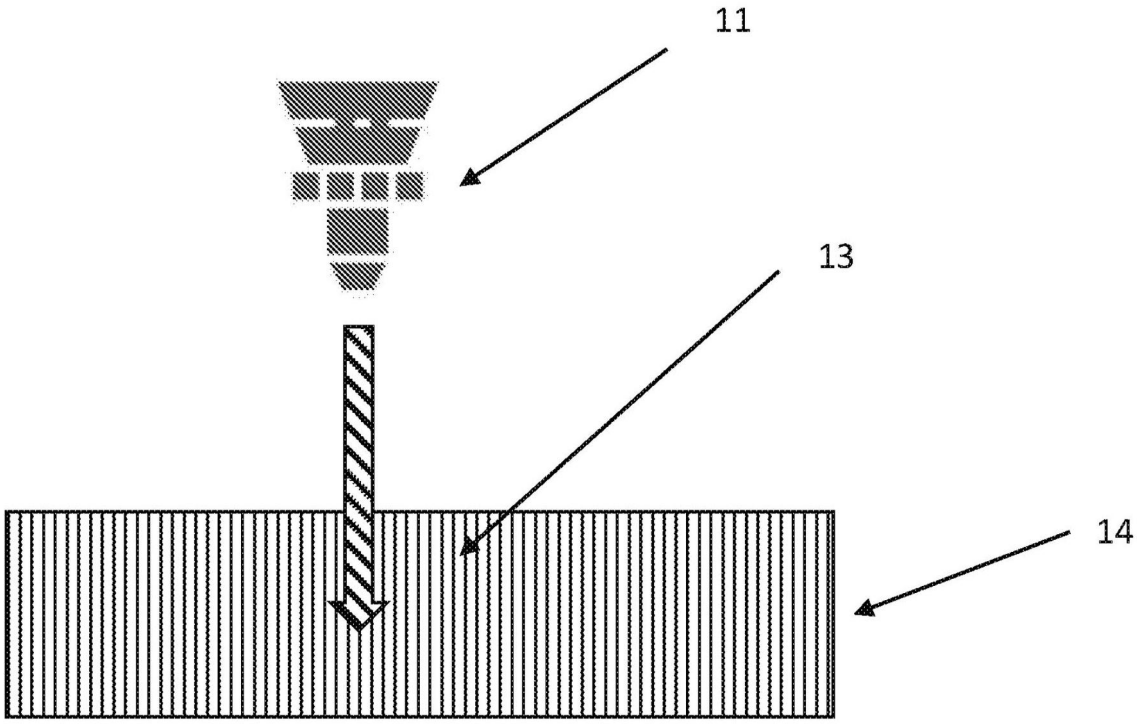


图9

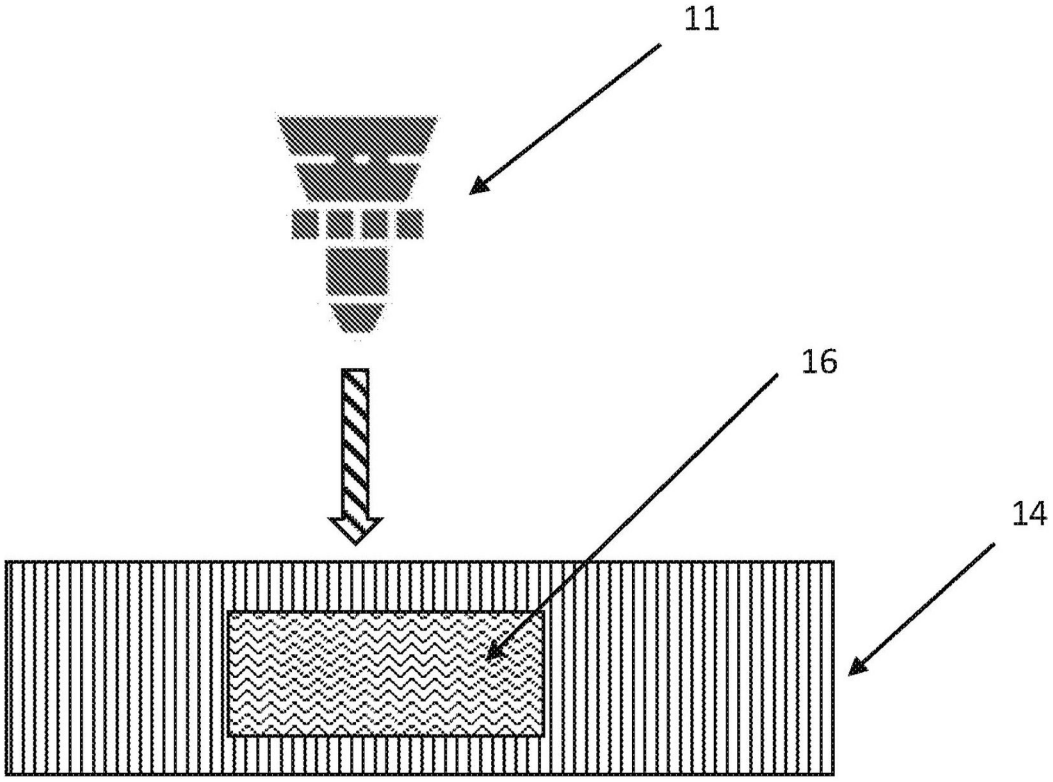


图10

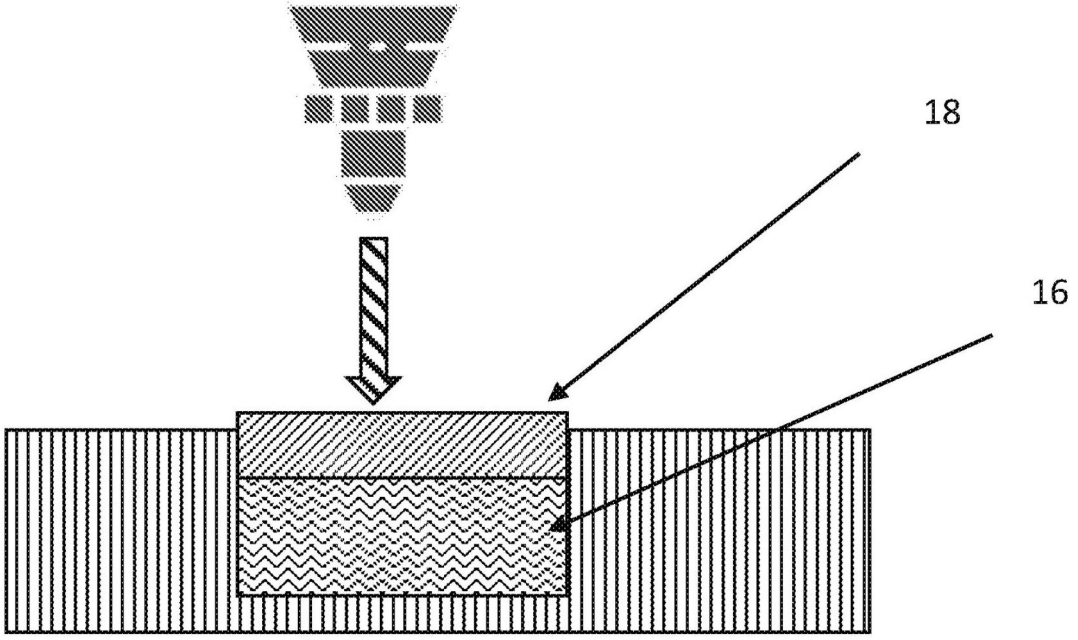


图11

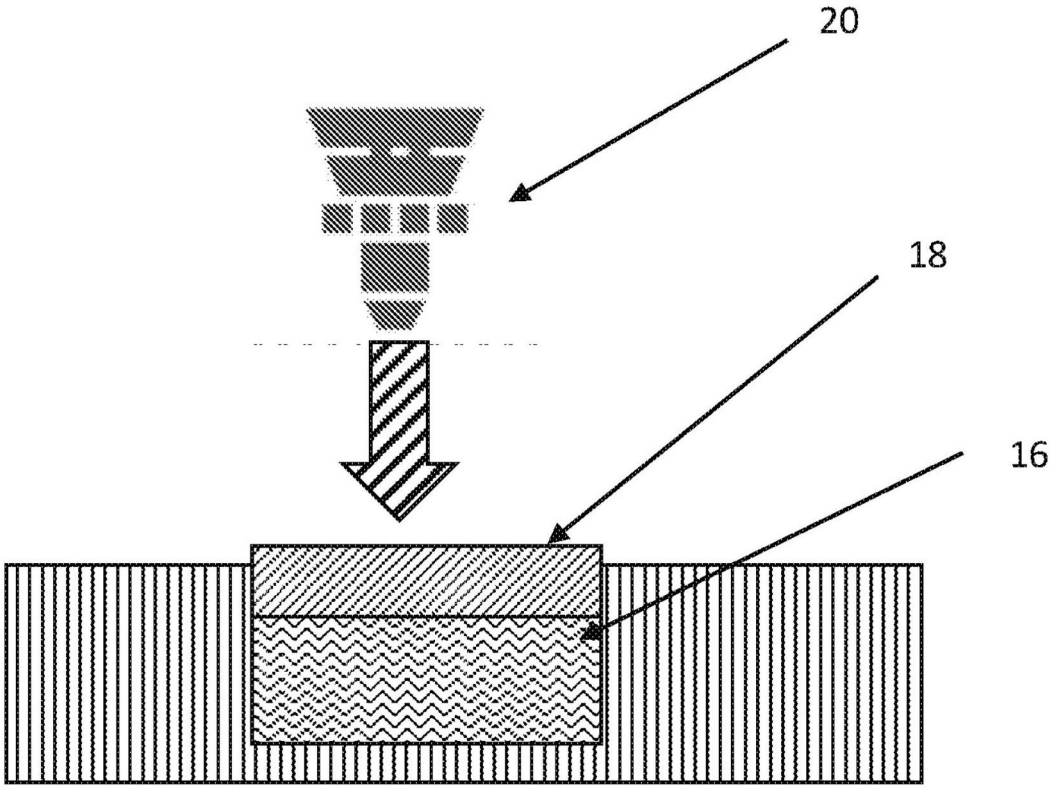


图12

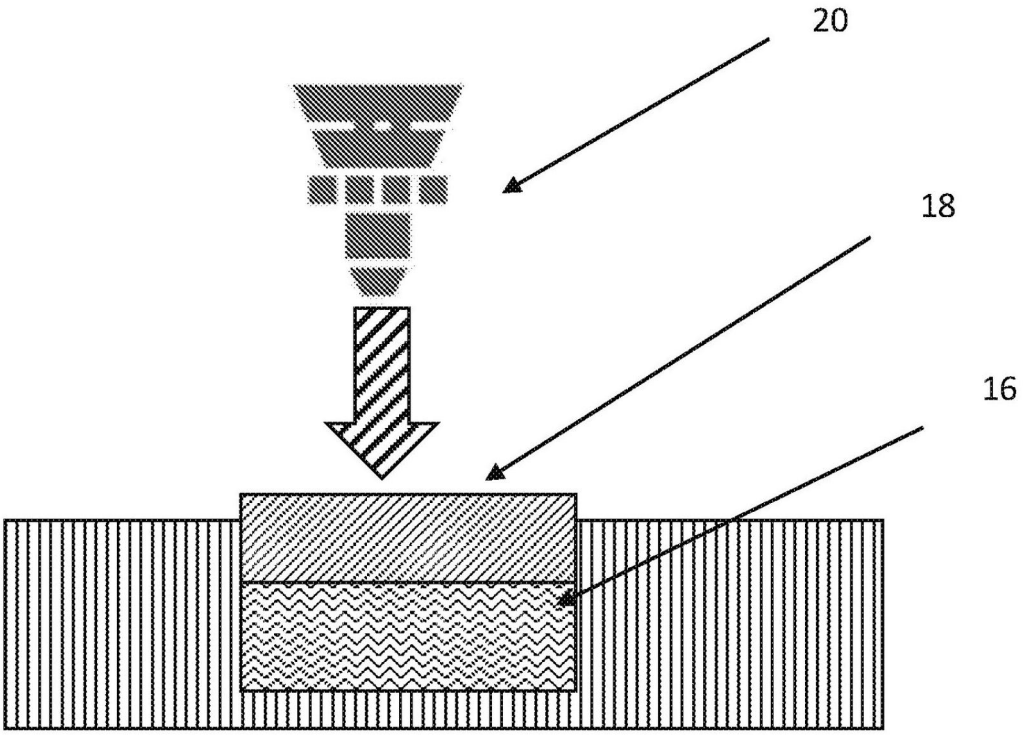


图13

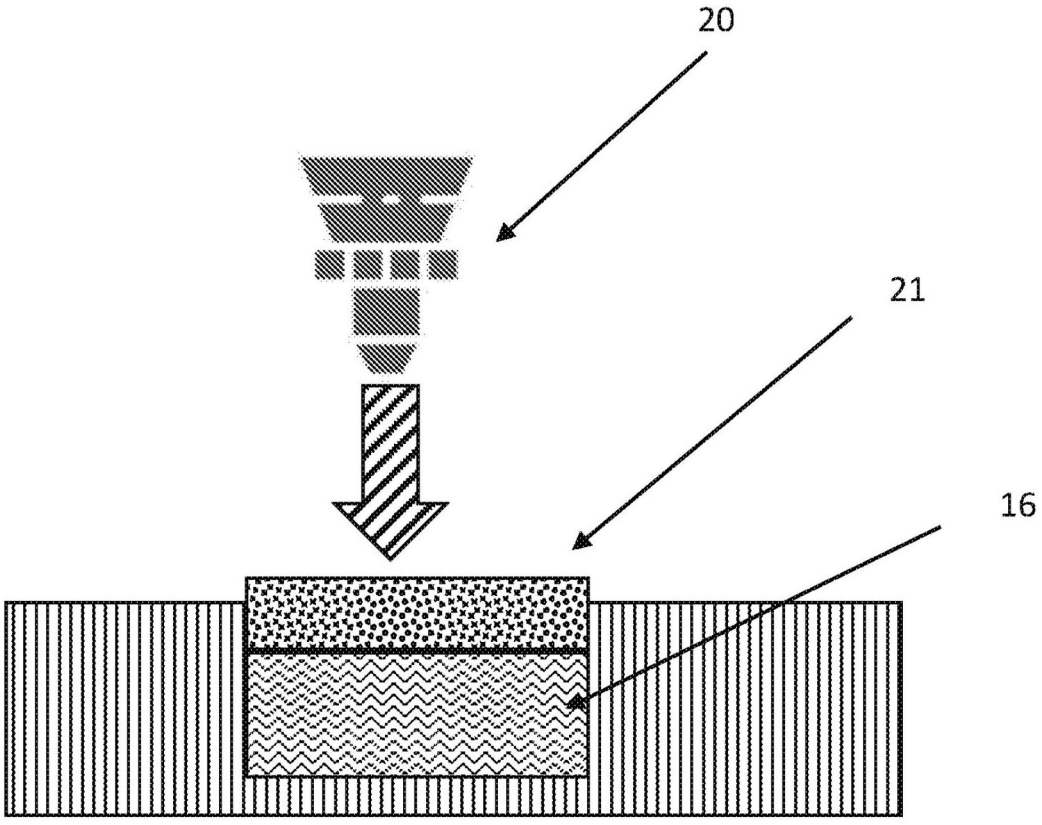


图14A

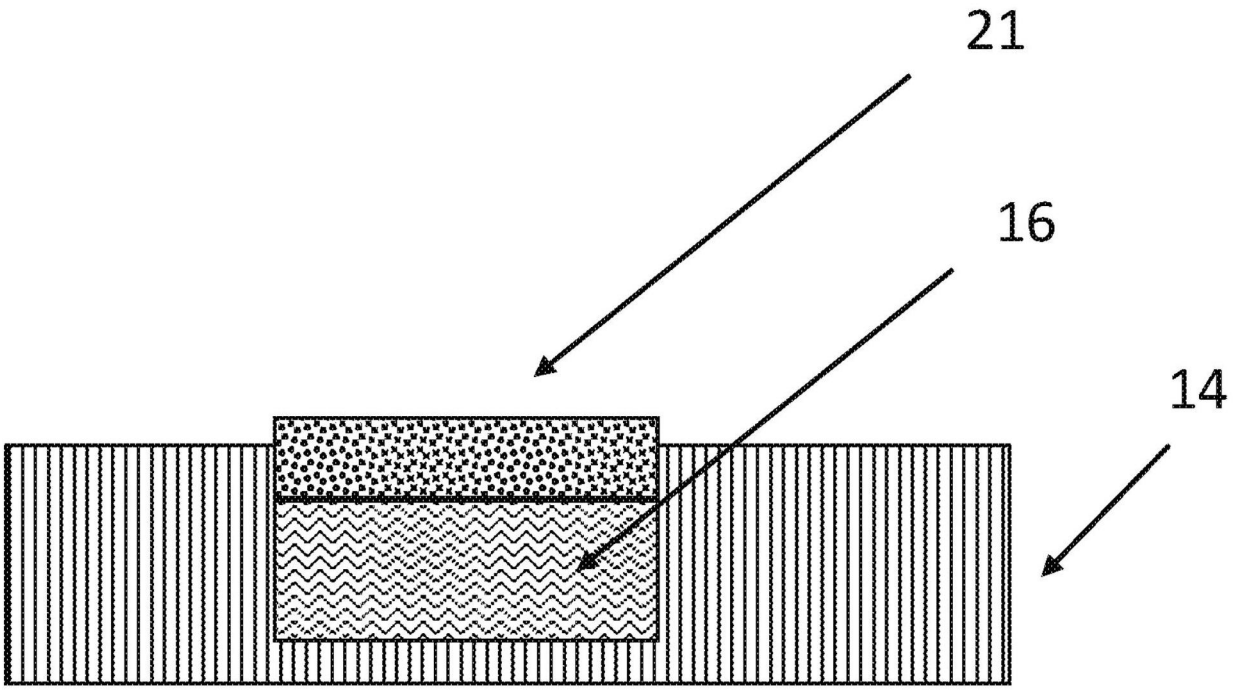


图14B

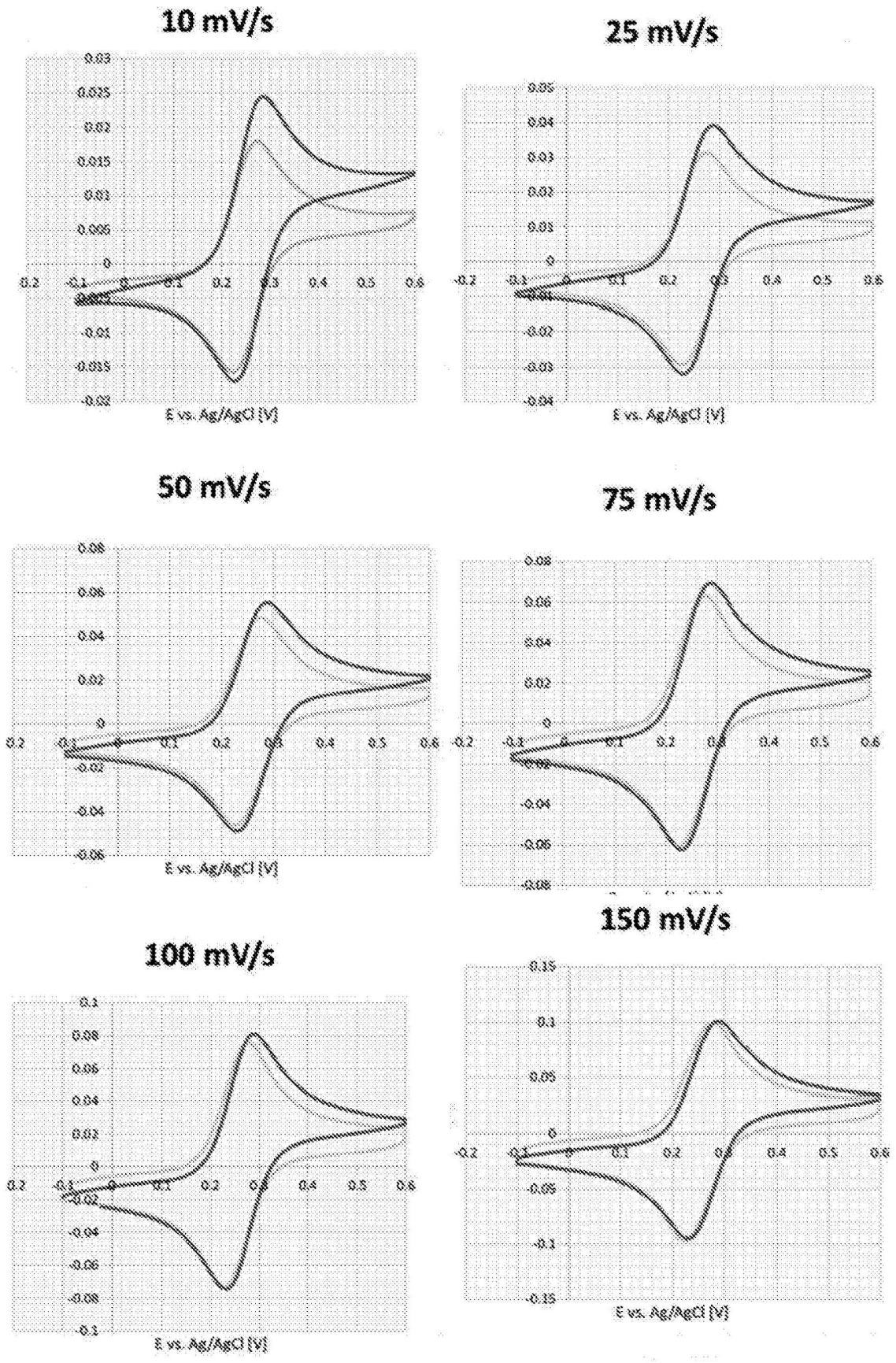

10 mV/s
E vs. Ag/AgCl [V]
25 mV/s
E vs. Ag/AgCl [V]
50 mV/s
E vs. Ag/AgCl [V]
75 mV/s
100 mV/s
E vs. Ag/AgCl [V]
150 mV/s
E vs. Ag/AgCl [V]

图15

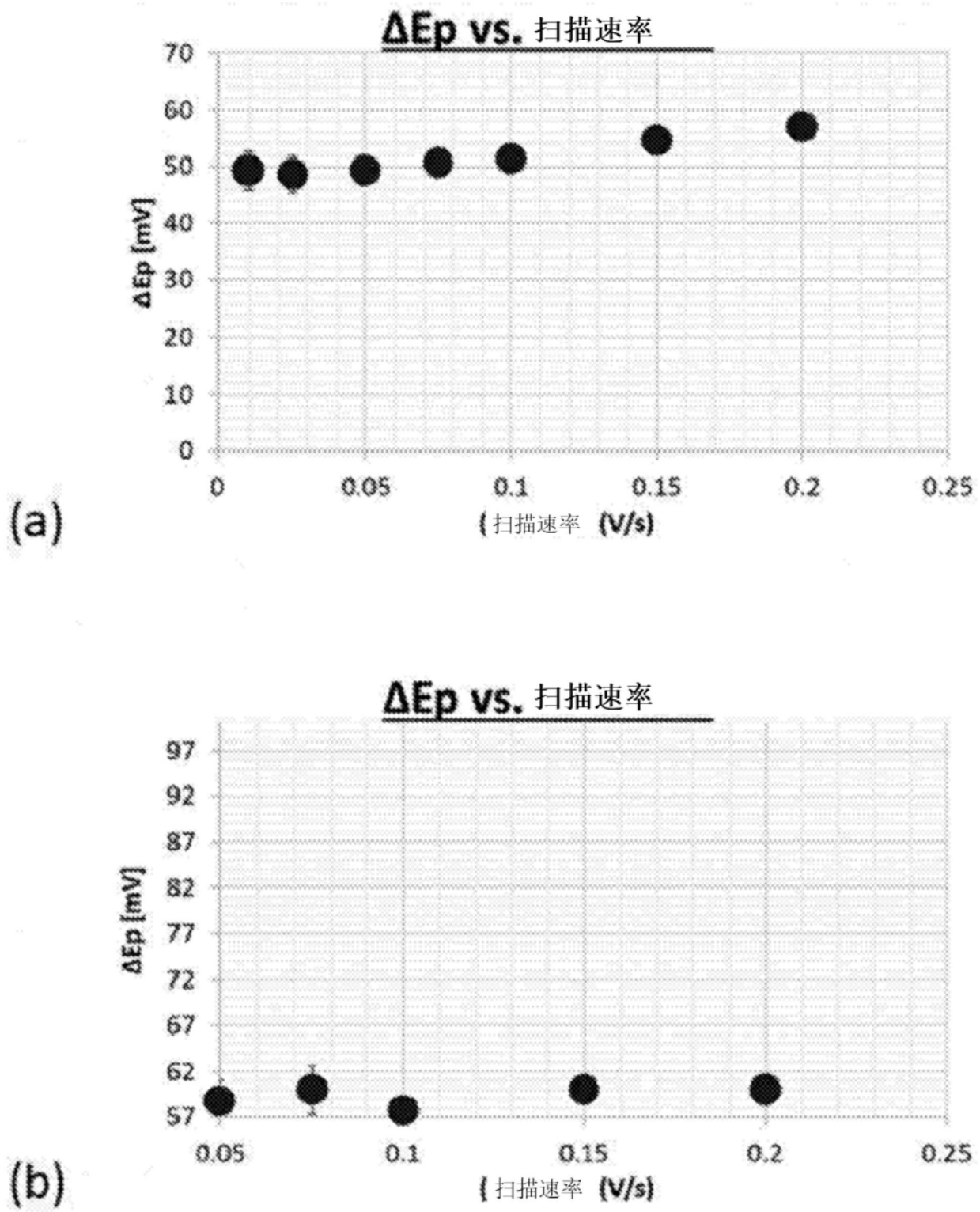

ΔEp vs. 扫描速率
ΔEp [mV]
70
60
50
40
30
20
10
0
0
0.05
0.1
0.15
0.2
0.25
扫描速率 (V/s)
(a)
ΔEp vs. 扫描速率
ΔEp [mV]
97
92
87
82
77
72
67
62
57
0.05
0.1
0.15
0.2
0.25
扫描速率 (V/s)
(b)

图16

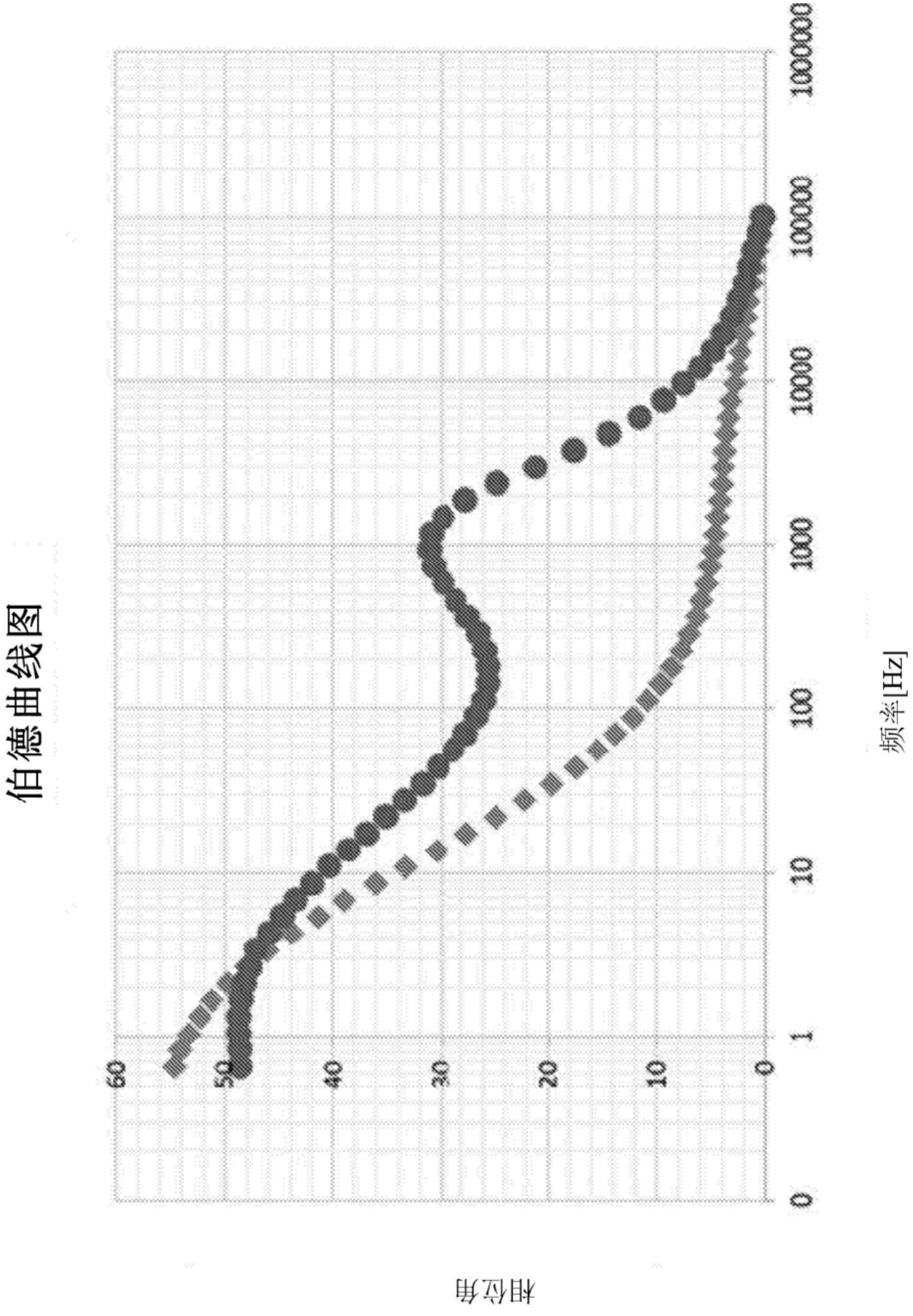

伯德曲线图
相位角
60
50
40
30
20
10
0
0
1
10
100
1000
10000
100000
1000000
频率[Hz]

图17

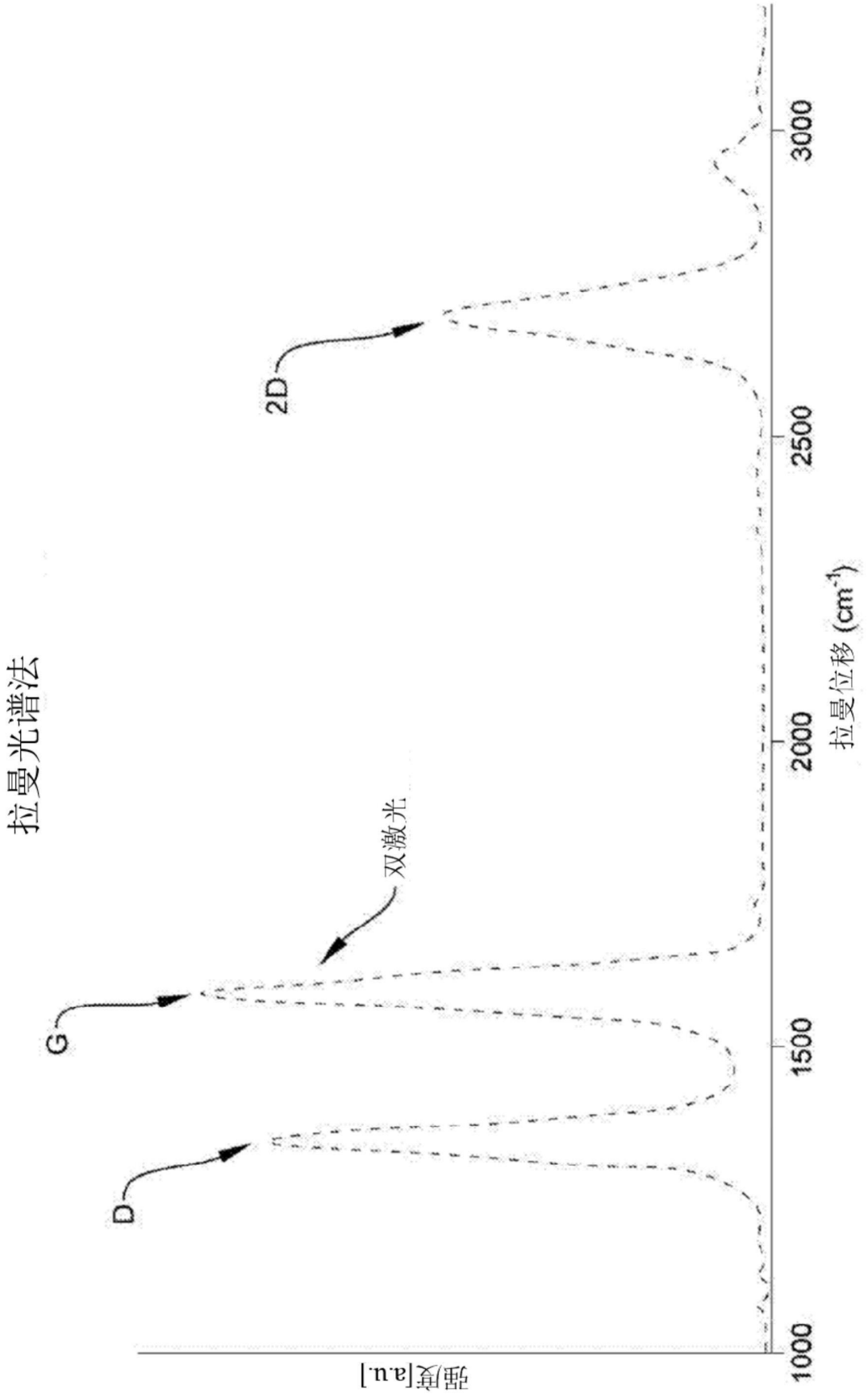


图18

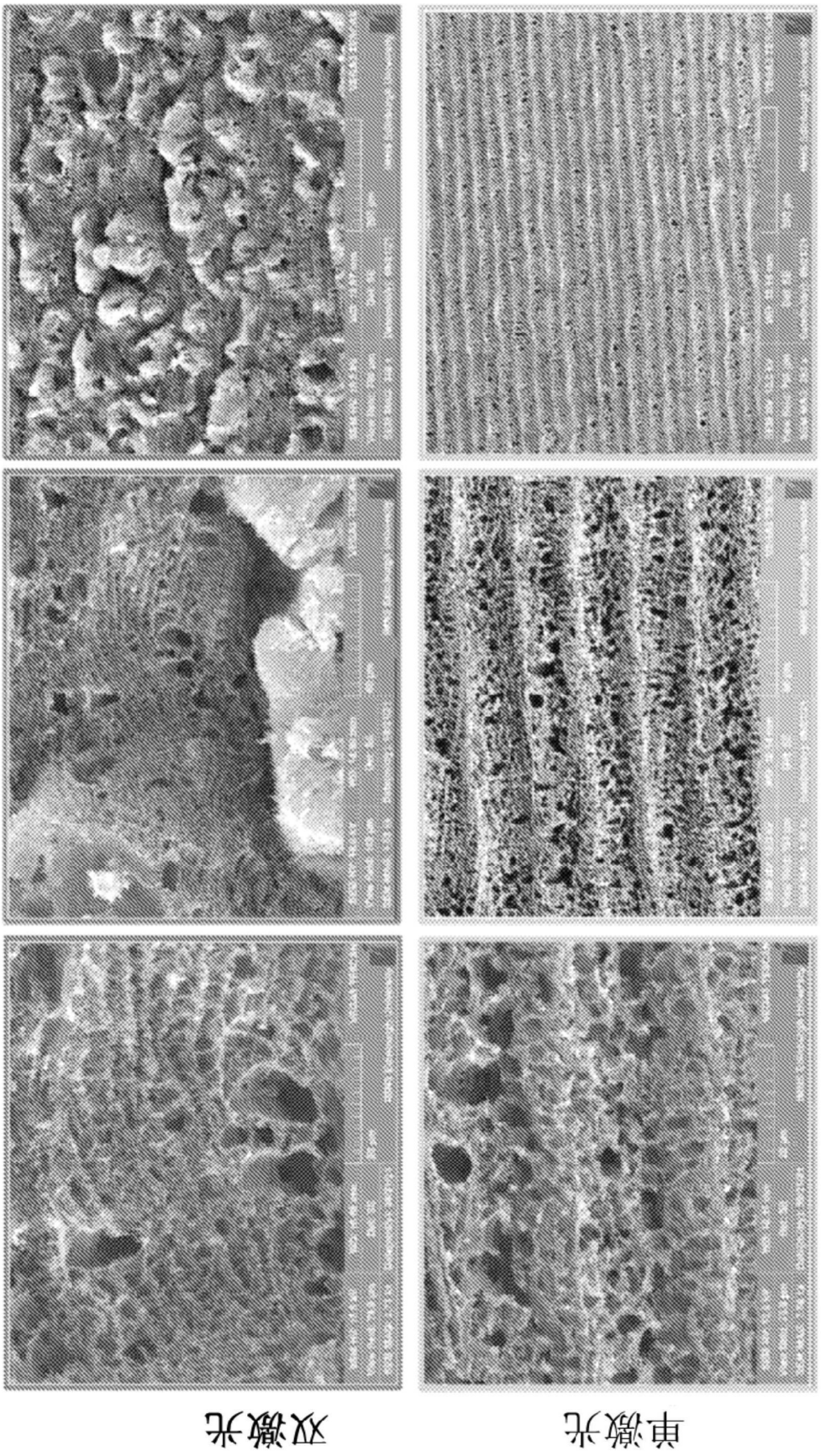


图19

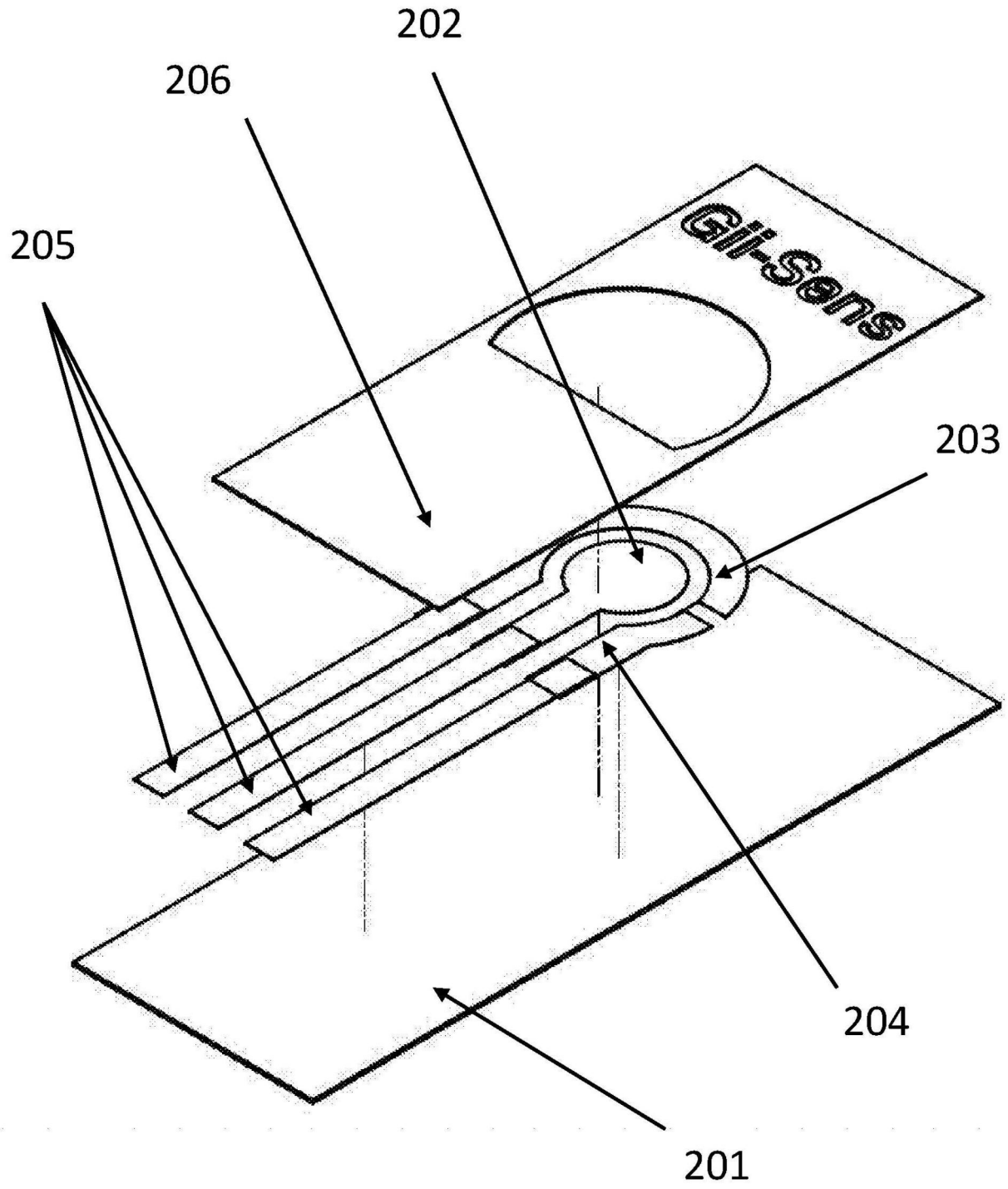


图20A

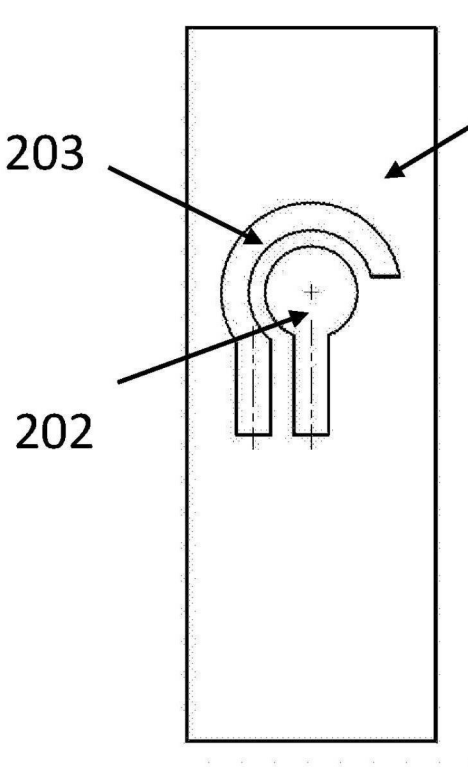


图 20B

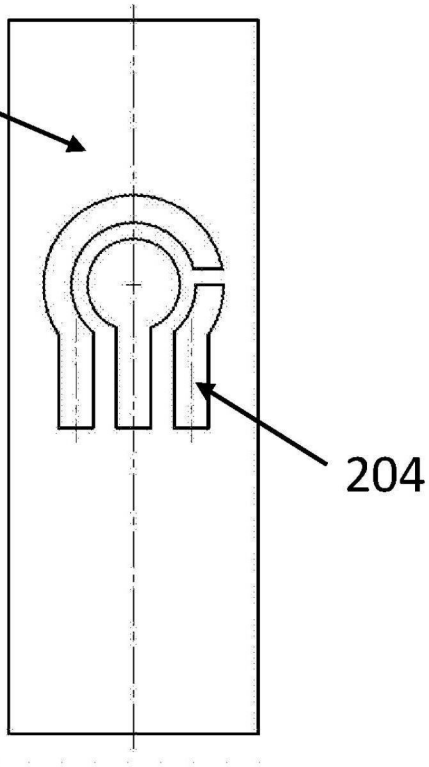


图 20C

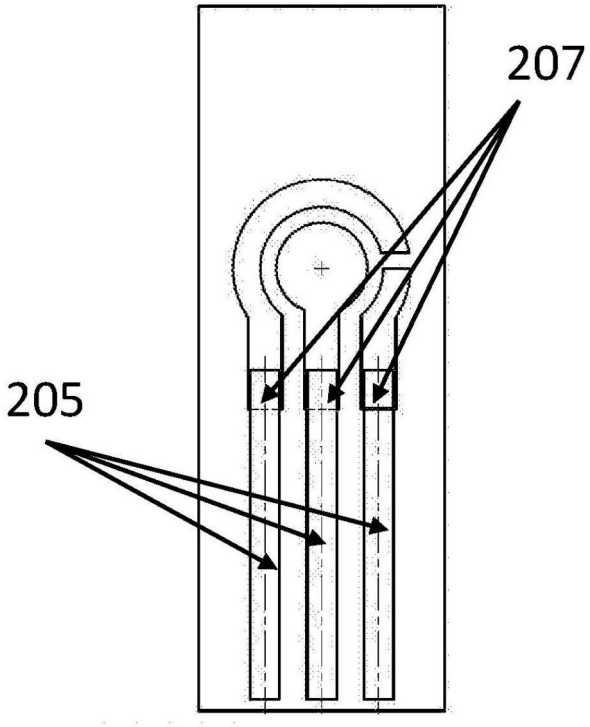


图20D

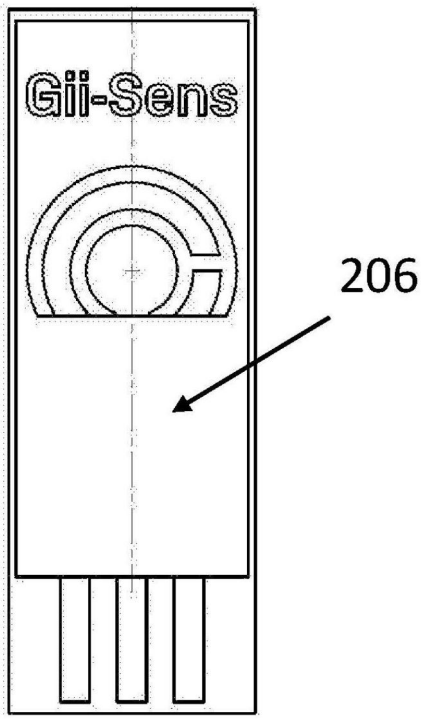


图20E

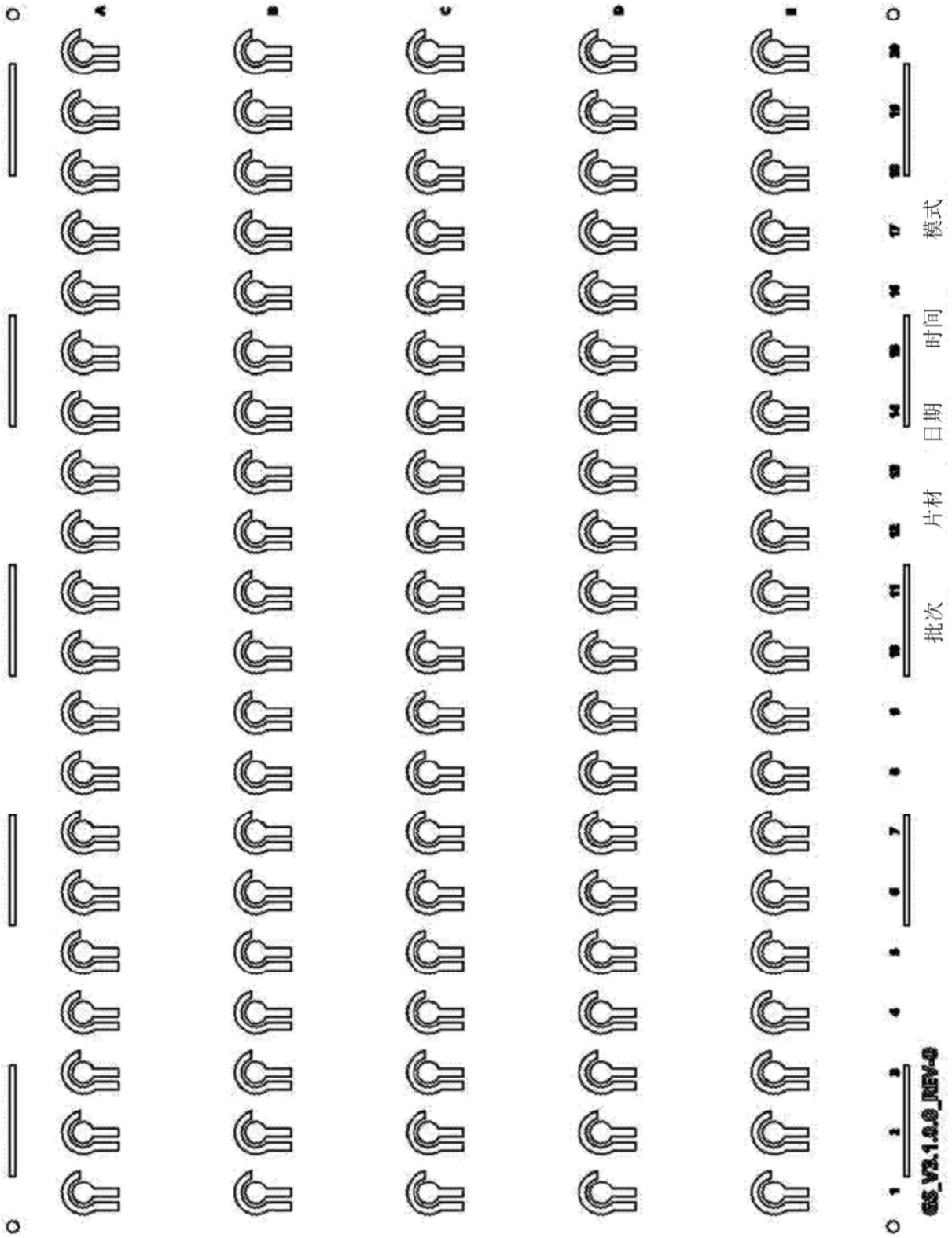


图20F

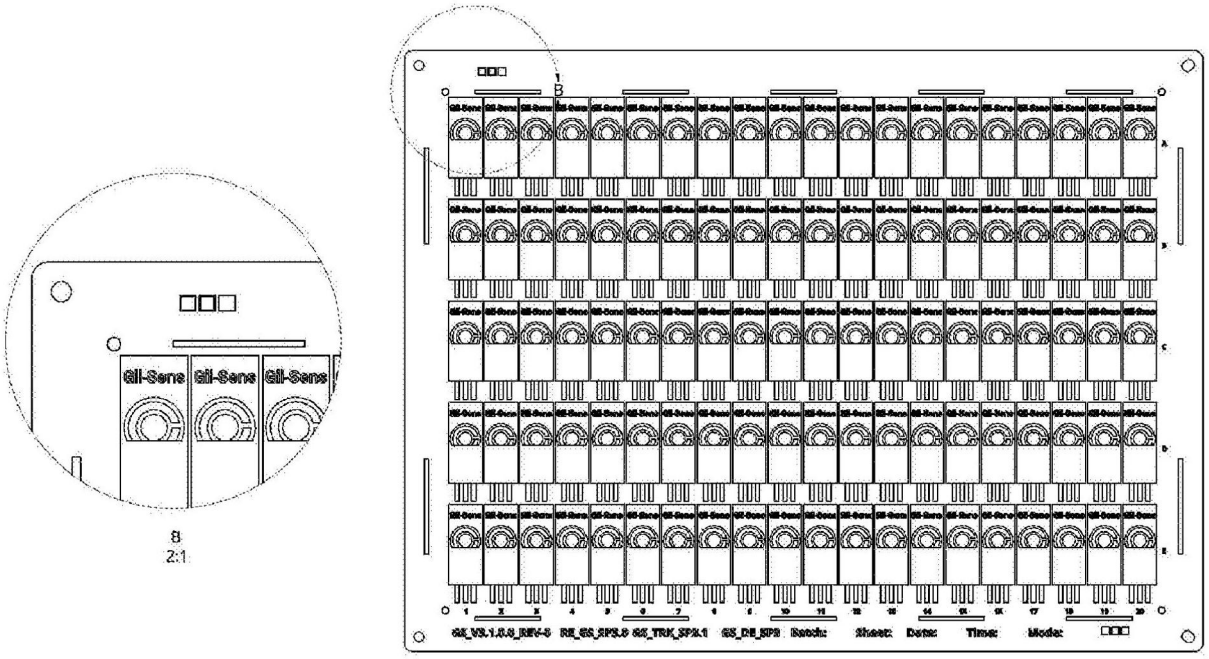


图20G

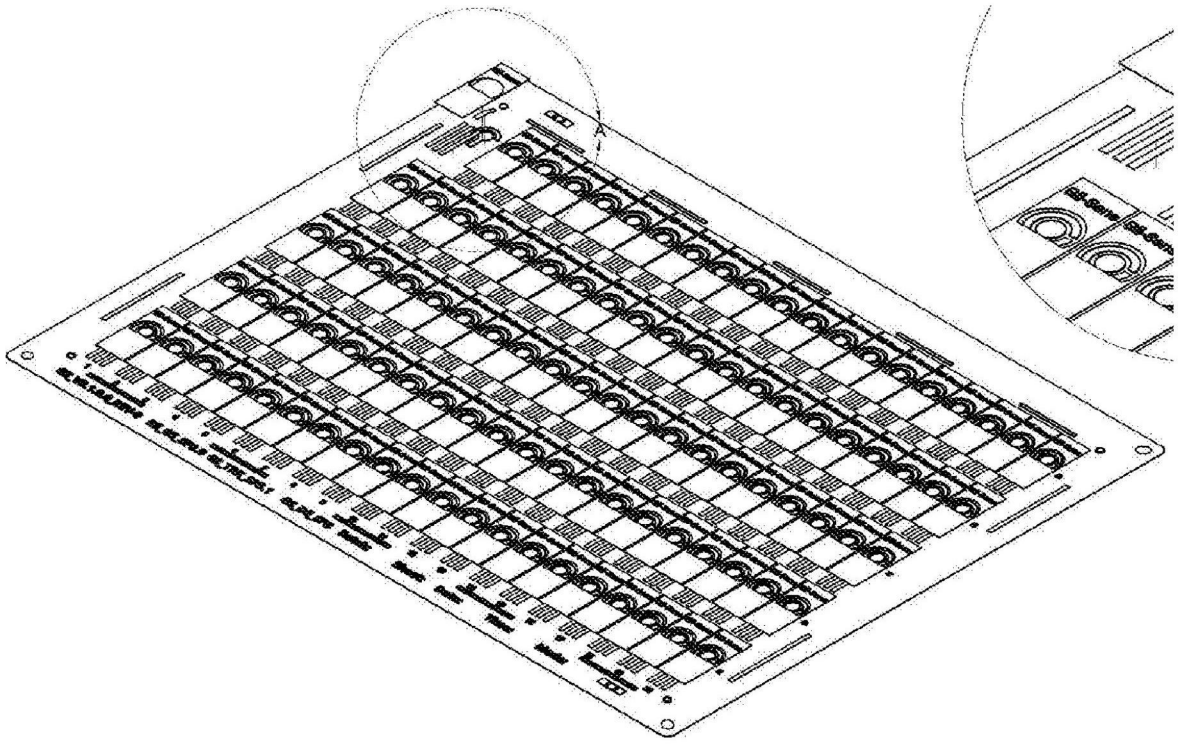


图20H

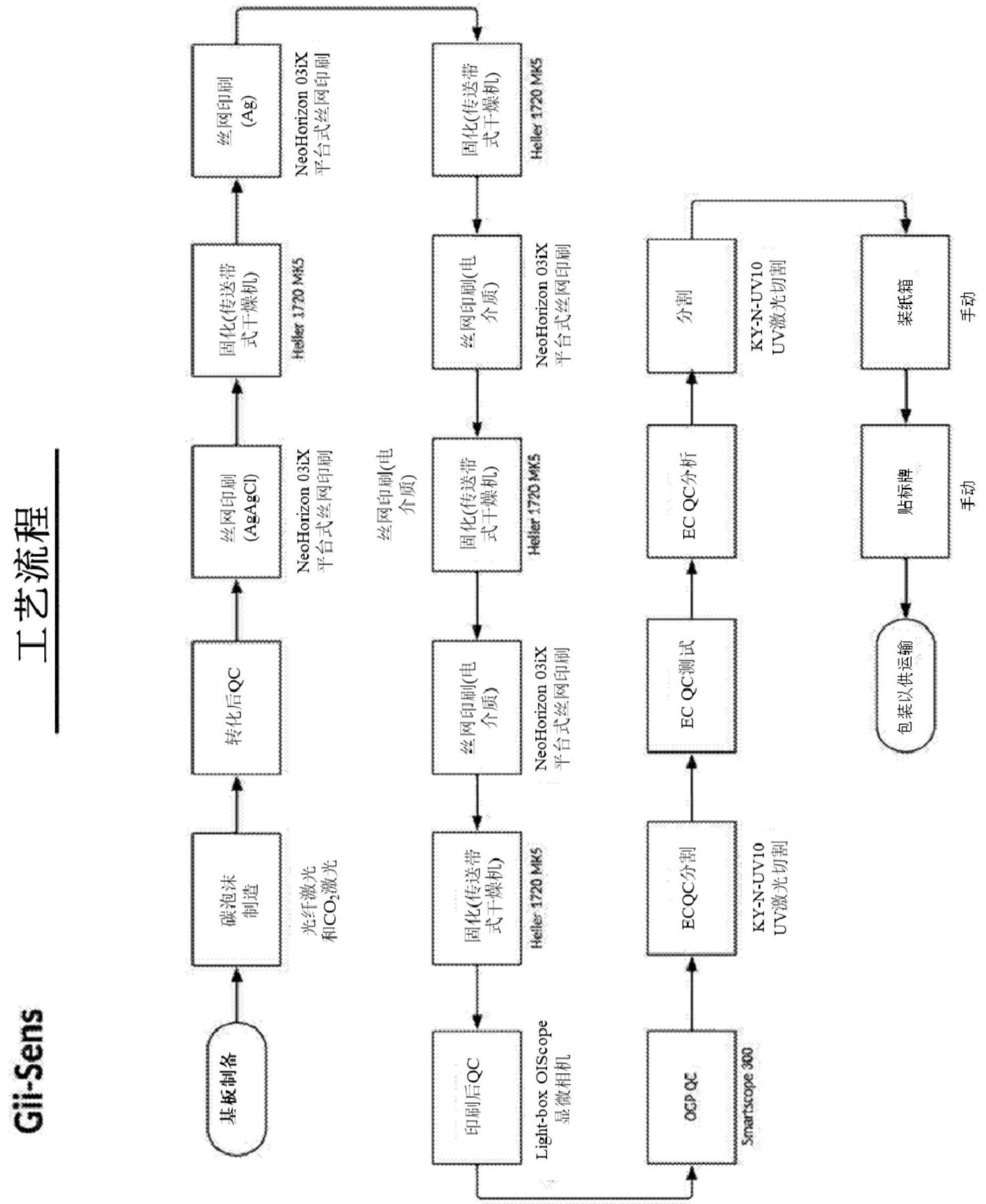

工艺流程
Gii-Sens
基板制备
碳泡沫制造
光纤激光和CO_2激光
转化后QC
丝网印刷(AgAgCl)
NeoHorizon 03iX 平台式丝网印刷
固化(传送带式干燥机)
Heller 1720 MK5
丝网印刷(Ag)
NeoHorizon 03iX 平台式丝网印刷
固化(传送带式干燥机)
Heller 1720 MK5
丝网印刷(电介质)
NeoHorizon 03iX 平台式丝网印刷
固化(传送带式干燥机)
Heller 1720 MK5
丝网印刷(电介质)
NeoHorizon 03iX 平台式丝网印刷
固化(传送带式干燥机)
Heller 1720 MK5
印刷后QC
Light-box OIScope 显微相机
OSP QC
Smartscope 300
ECQC分割
KY-N-UV10 UV激光切割
EC QC测试
EC QC分析
分割
KY-N-UV10 UV激光切割
装纸箱
手动
贴标牌
手动
包装以供运输

图21

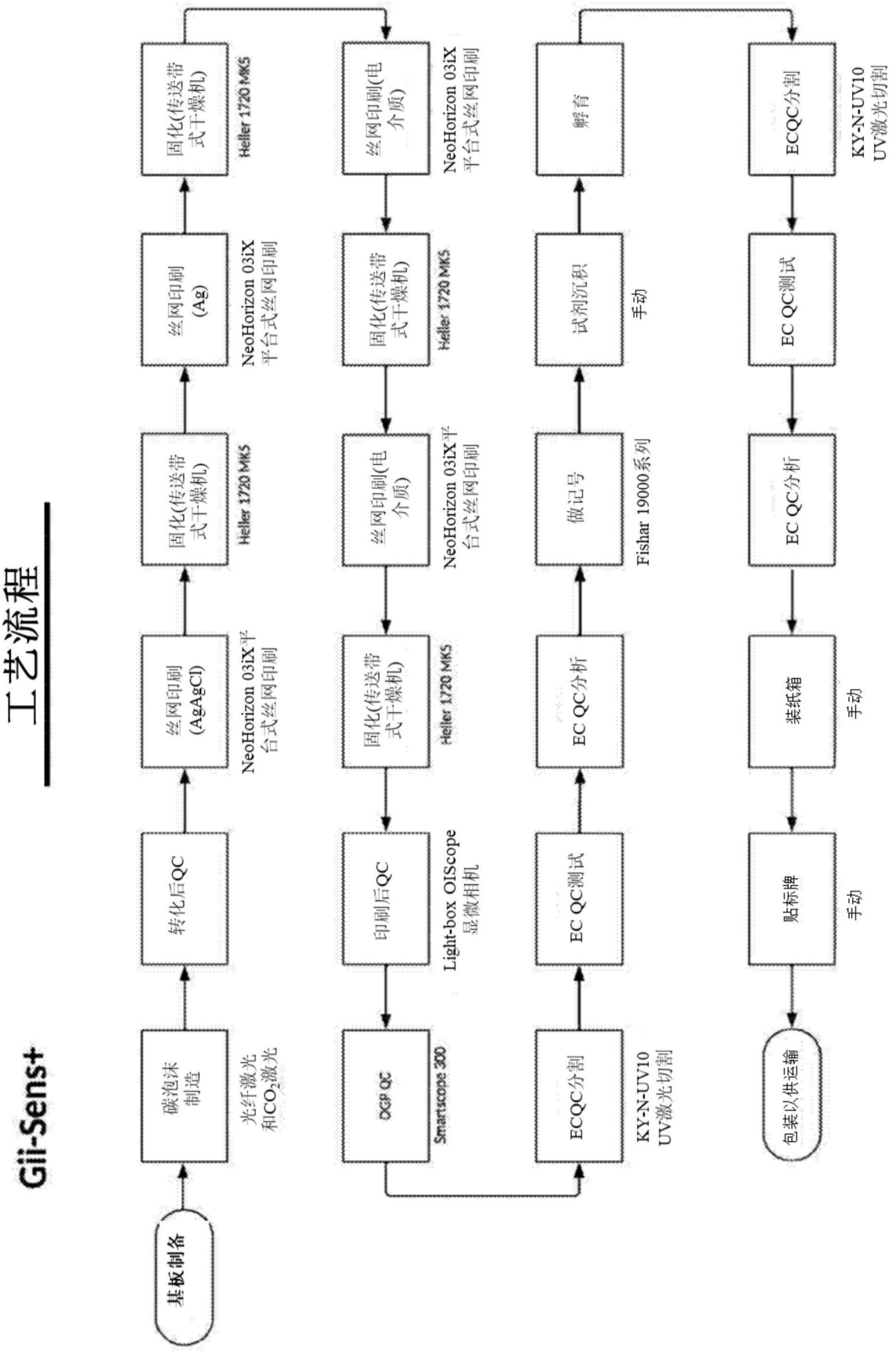

工艺流程
Gii-Sens+
基板制备
碳泡沫制造
光纤激光和CO_2激光
转化后QC
丝网印刷(AgAgCl)
NeoHorizon 03iX平台式丝网印刷
固化(传送带式干燥机)
Heller 1720 MK5
丝网印刷(Ag)
NeoHorizon 03iX平台式丝网印刷
固化(传送带式干燥机)
Heller 1720 MK5
丝网印刷(电介质)
NeoHorizon 03iX平台式丝网印刷
固化(传送带式干燥机)
Heller 1720 MK5
印刷后QC
Light-box OIScope显微相机
DEP QC
Smartscope 300
ECQC分割
KY-N-UV10 UV激光切割
EC QC测试
EC QC分析
做记号
Fishar 19000系列
试剂沉积
手动
孵育
ECQC分割
KY-N-UV10 UV激光切割
EC QC测试
EC QC分析
装纸箱
手动
贴标牌
手动
包装以供运输

图22

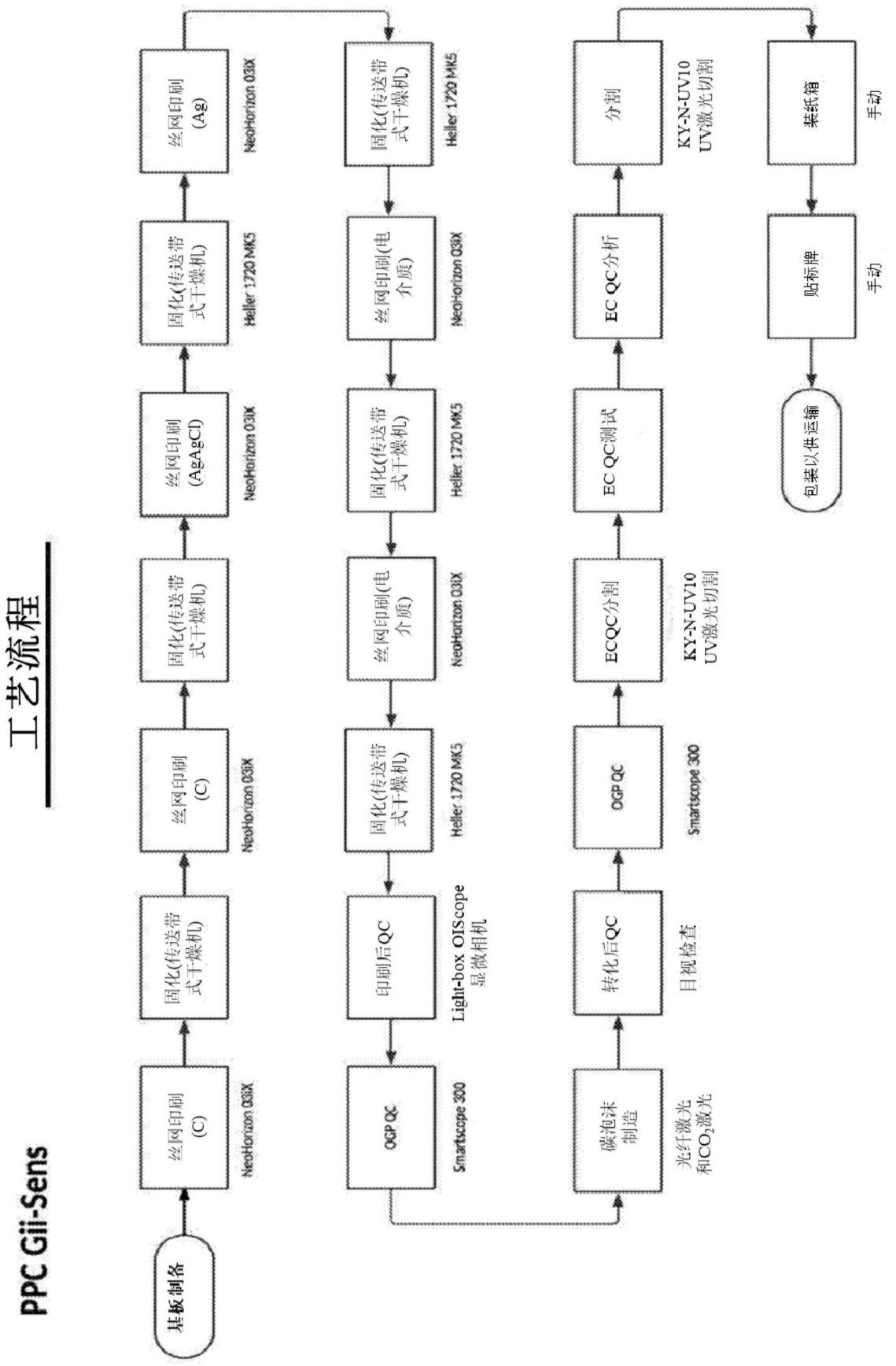

PPC Gii-Sens
工艺流程
基板制备
丝网印刷 (C)
NeoHorizon 03IX
固化(传送带式干燥机)
丝网印刷 (C)
NeoHorizon 03IX
固化(传送带式干燥机)
丝网印刷 (AgAgCl)
NeoHorizon 03IX
固化(传送带式干燥机)
Heller 1720 MK5
丝网印刷 (Ag)
NeoHorizon 03IX
OGP QC
Smartscope 300
印刷后QC
Light-box OIScope 显微相机
固化(传送带式干燥机)
Heller 1720 MK5
丝网印刷(电介质)
NeoHorizon 03IX
固化(传送带式干燥机)
Heller 1720 MK5
丝网印刷(电介质)
NeoHorizon 03IX
固化(传送带式干燥机)
Heller 1720 MK5
碳泡沫制造
光纤激光和CO_2激光
转化后QC
目视检查
OGP QC
Smartscope 300
ECQC分割
KY-N-UV10 UV激光切割
EC QC测试
EC QC分析
分割
KY-N-UV10 UV激光切割
包装以供运输
贴标牌
手动
装纸箱
手动

图23

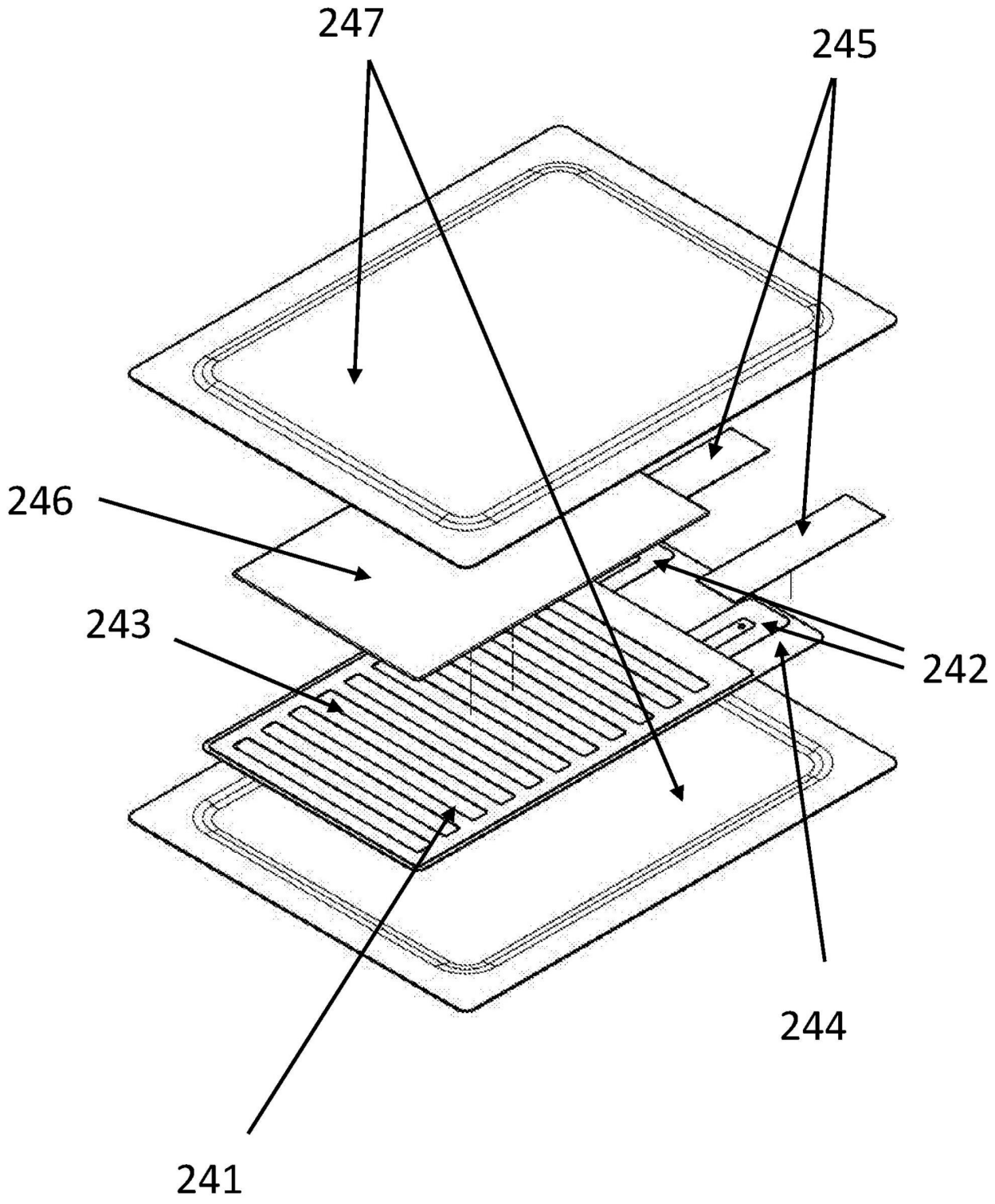


图24

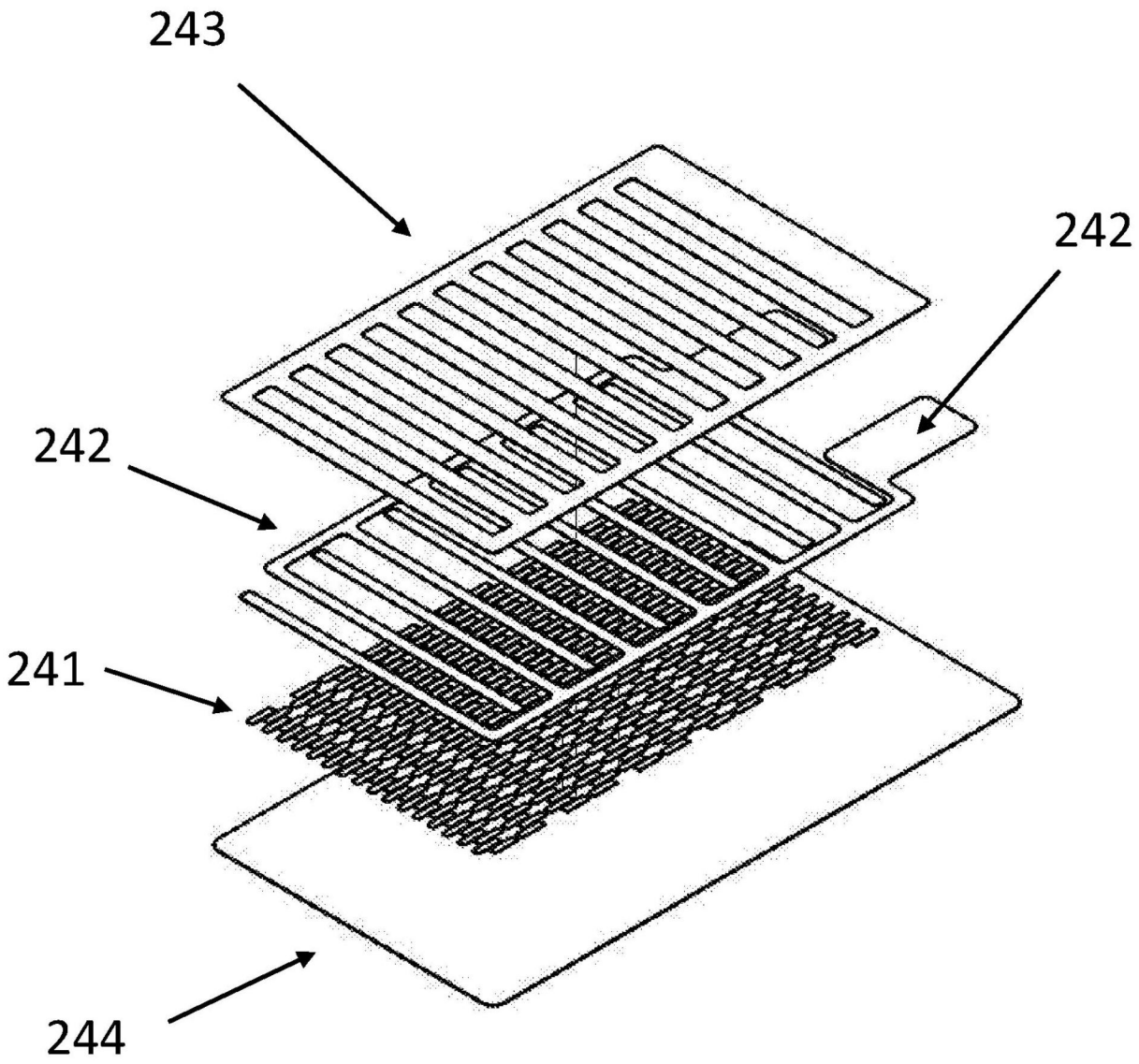


图25



图26A

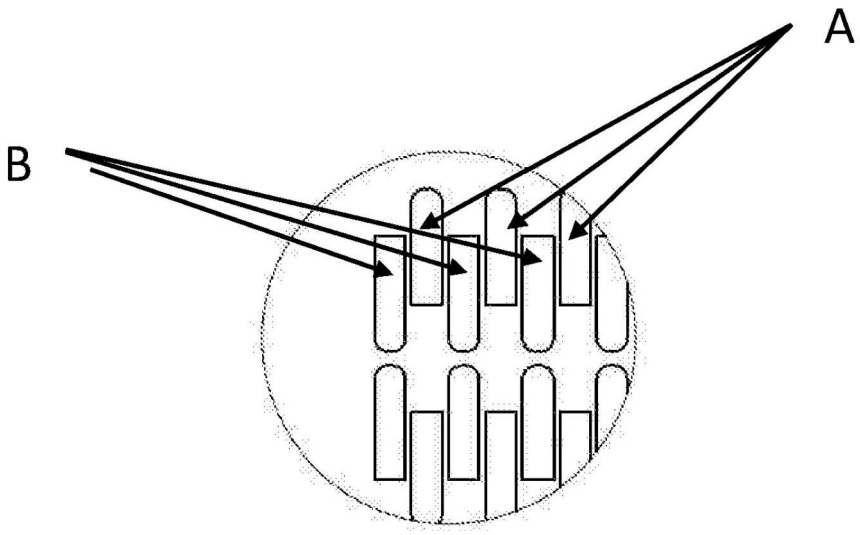


图26B

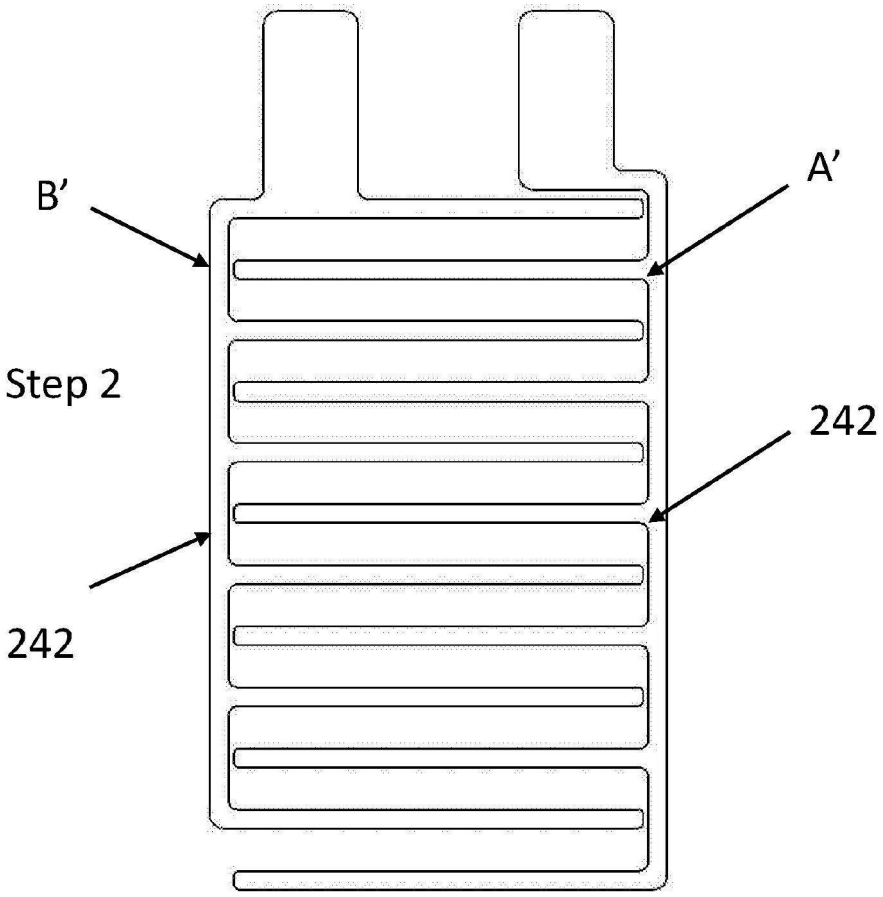


图26C

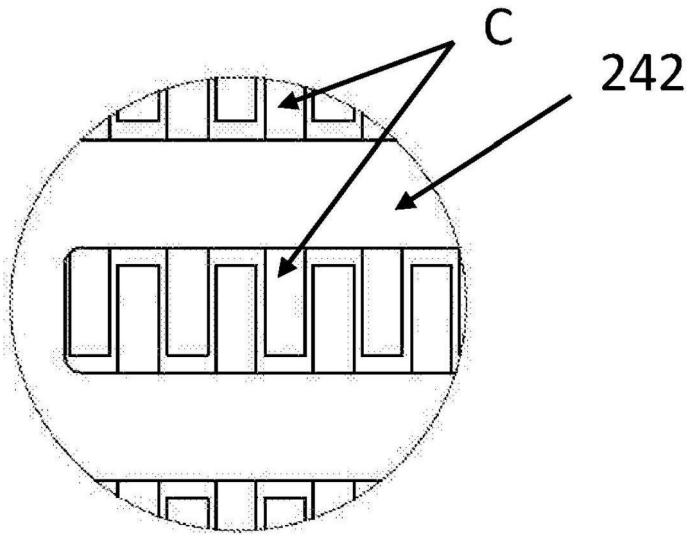


图26D

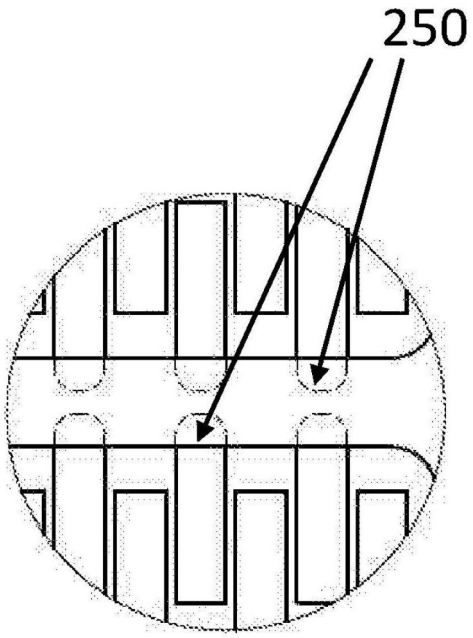


图26E

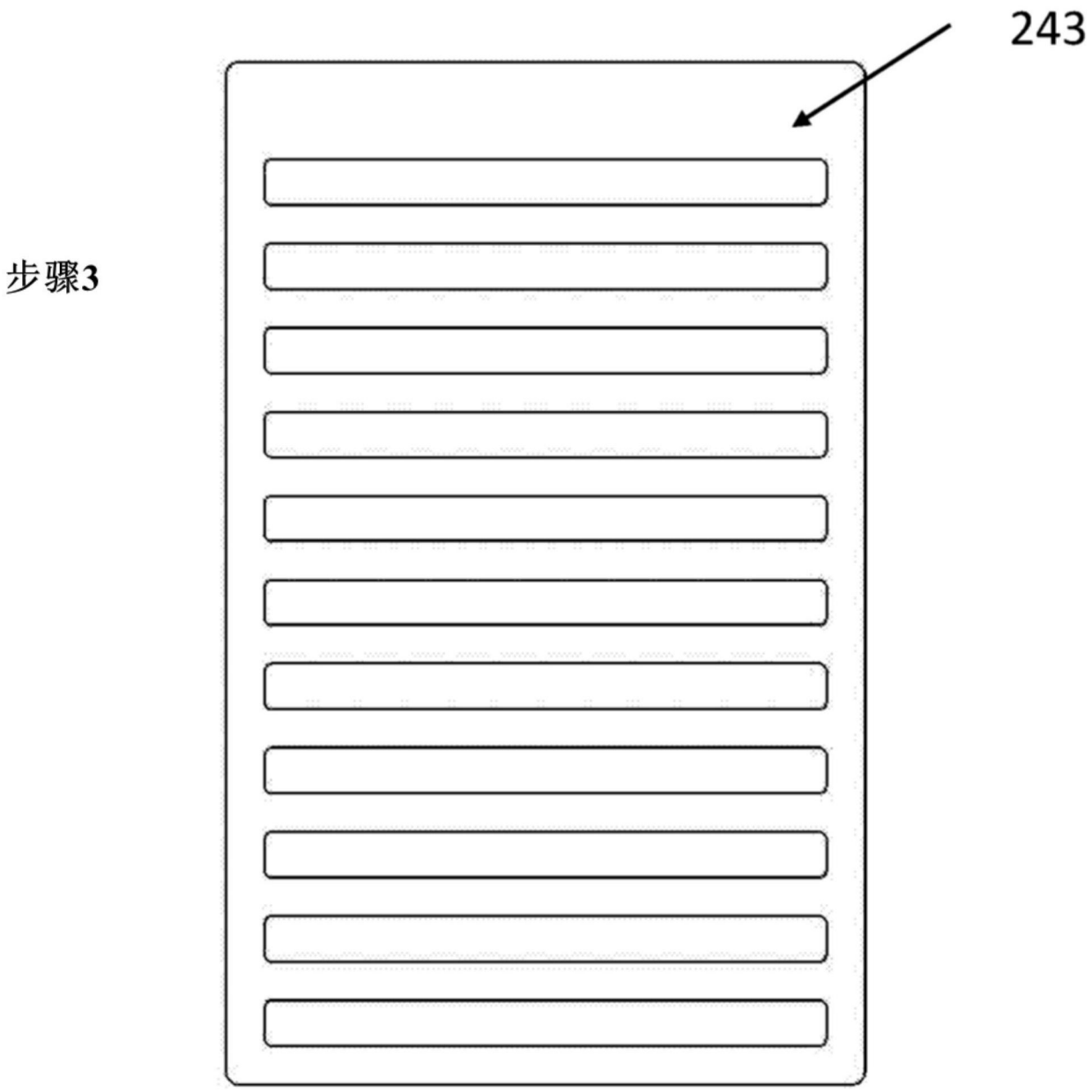


图26F

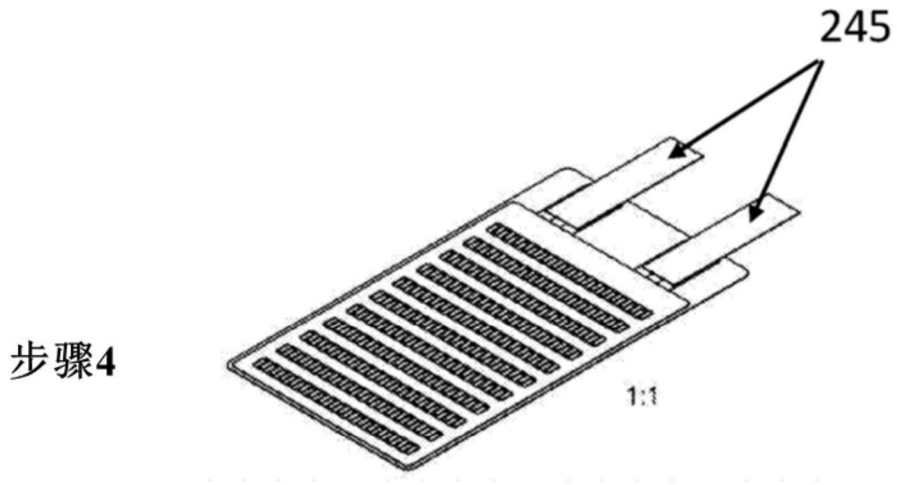


图26G

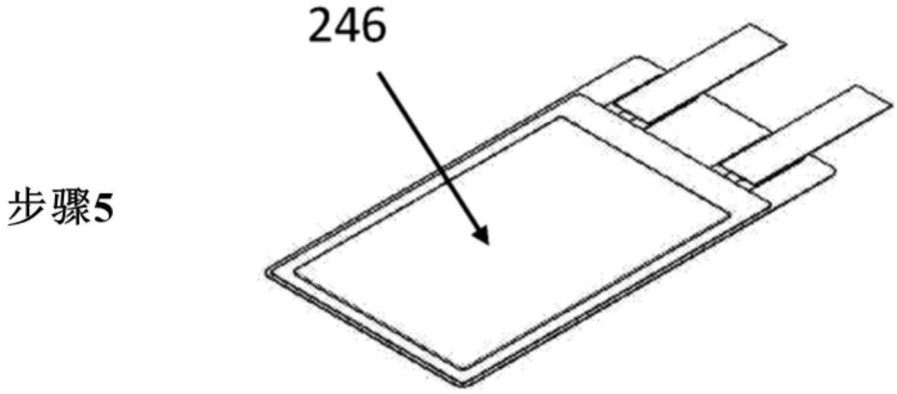


图26H

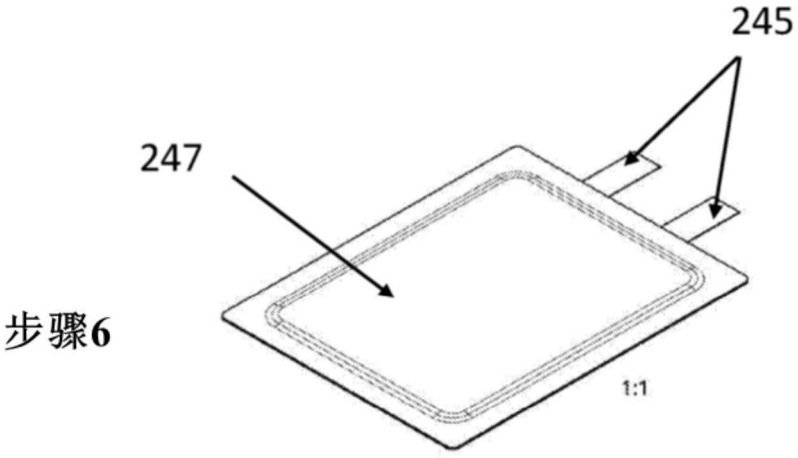


图26I

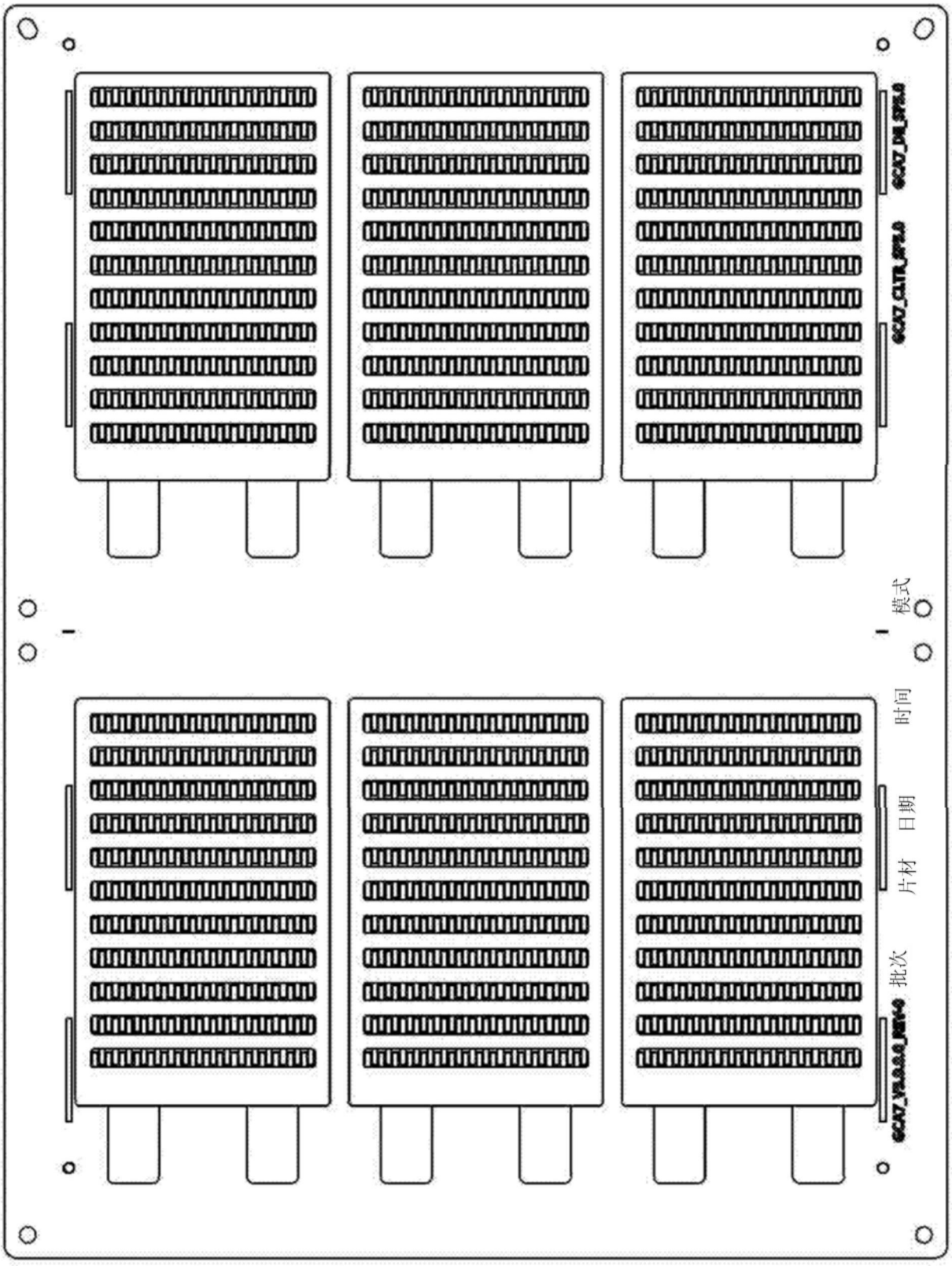


图27

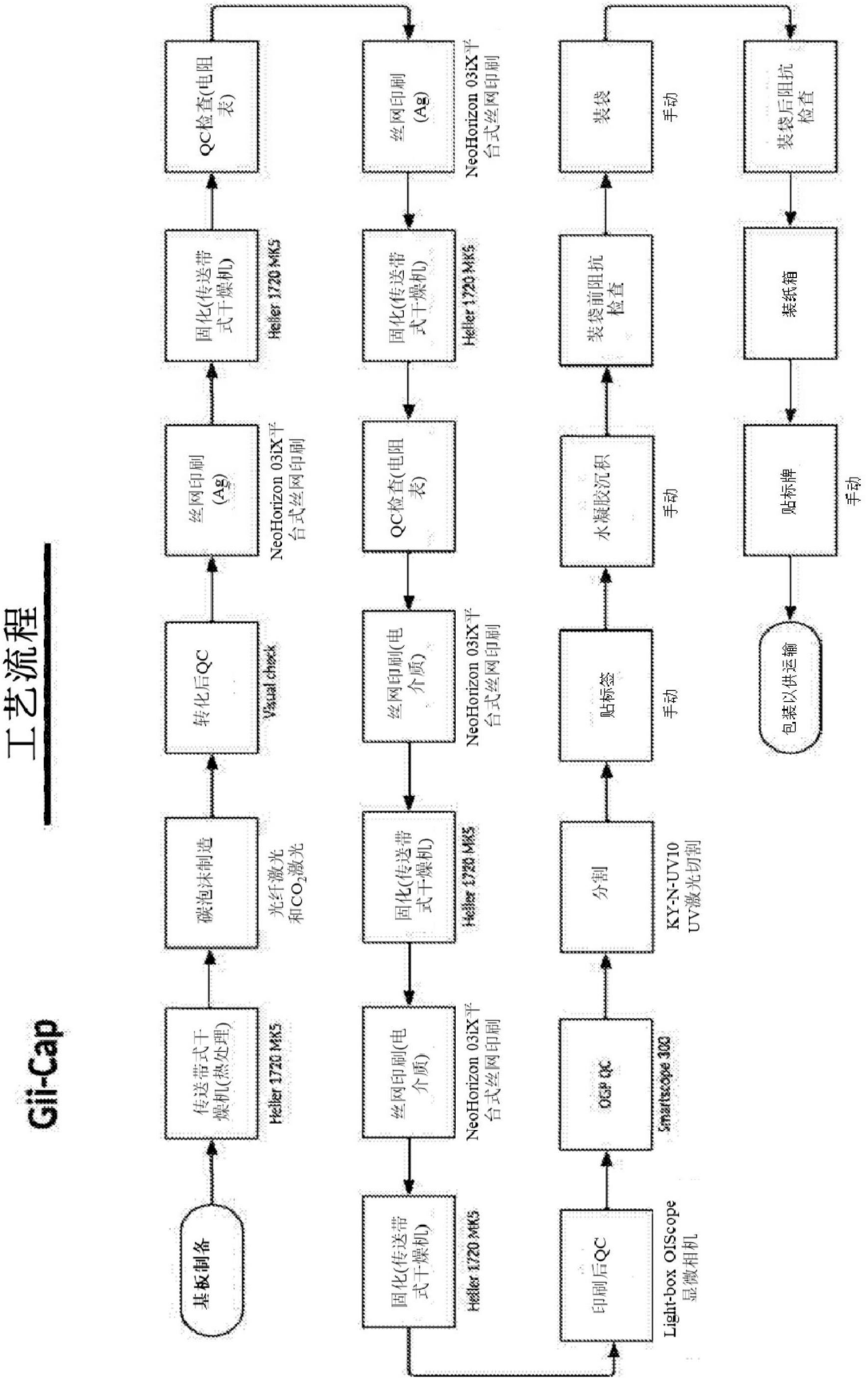

工艺流程
Gii-Cap
基板制备
传送带式干燥机(热处理)
Heller 1720 MK5
碳泡沫制造
光纤激光和CO_2激光
转化后QC
Visual check
丝网印刷(Ag)
NeoHorizon 03iX平台式丝网印刷
固化(传送带式干燥机)
Heller 1720 MK5
QC检查(电阻表)
丝网印刷(电介质)
NeoHorizon 03iX平台式丝网印刷
固化(传送带式干燥机)
Heller 1720 MK5
丝网印刷(电介质)
NeoHorizon 03iX平台式丝网印刷
固化(传送带式干燥机)
Heller 1720 MK5
丝网印刷(Ag)
NeoHorizon 03iX平台式丝网印刷
固化(传送带式干燥机)
Heller 1720 MK5
QC检查(电阻表)
印刷后QC
Light-box OIScope 显微相机
OGP QC
Smartscope 300
分割
KY-N-UV10 UV激光切割
贴标签
手动
水凝胶沉积
手动
装袋前阻抗检查
装袋
手动
贴标牌
手动
装纸箱
装袋后阻抗检查
包装以供运输

图28

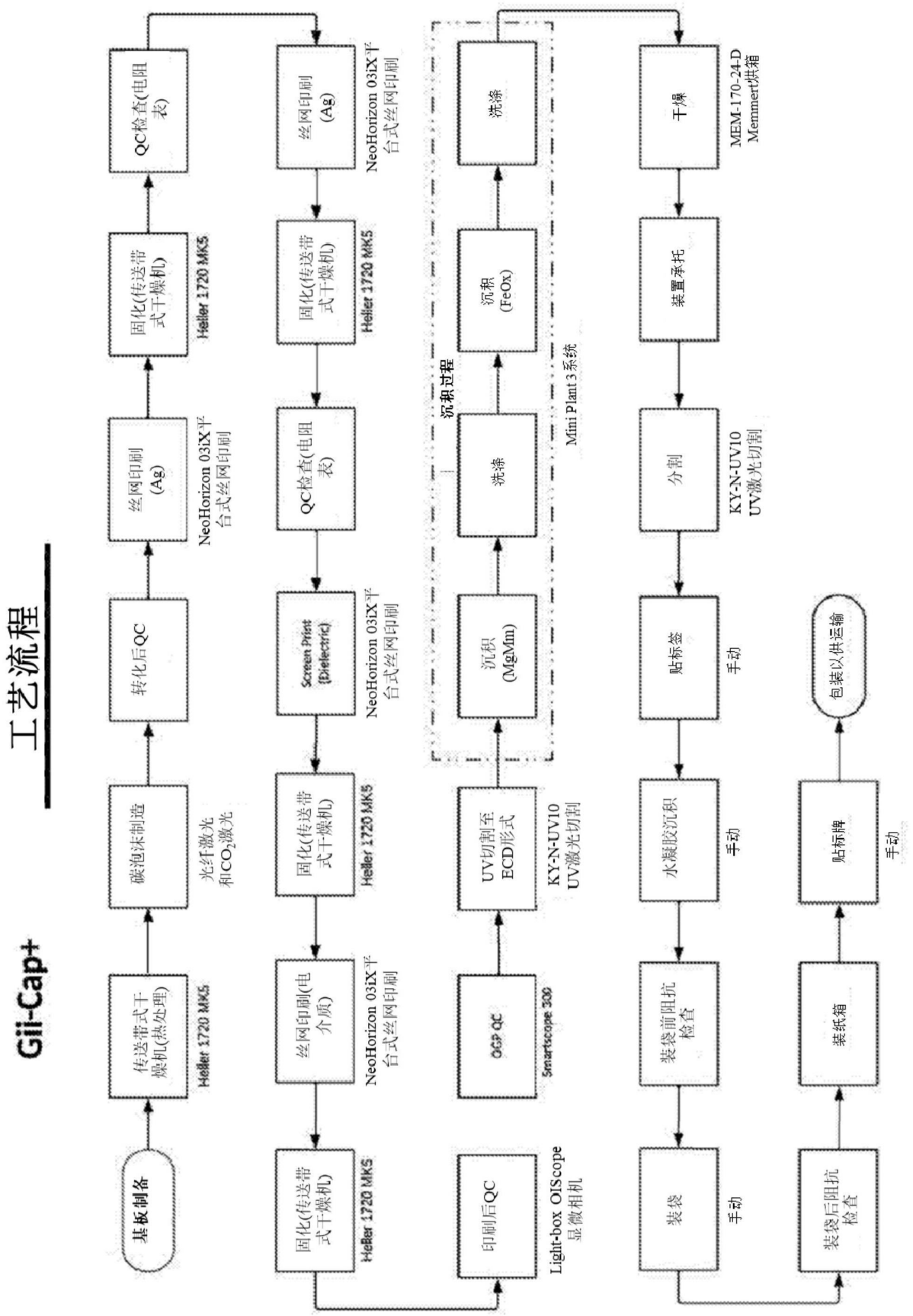

工艺流程
Gii-Cap+
基板制备
传送带式干燥机(热处理)
Heller 1720 MK5
碳泡沫制造
光纤激光和CO_2激光
转化后QC
丝网印刷(Ag)
NeoHorizon 03iX平台式丝网印刷
固化(传送带式干燥机)
Heller 1720 MK5
QC检查(电阻表)
丝网印刷(电介质)
NeoHorizon 03iX平台式丝网印刷
固化(传送带式干燥机)
Heller 1720 MK5
Screen Print (Dielectric)
NeoHorizon 03iX平台式丝网印刷
固化(传送带式干燥机)
Heller 1720 MK5
QC检查(电阻表)
丝网印刷(Ag)
NeoHorizon 03iX平台式丝网印刷
固化(传送带式干燥机)
Heller 1720 MK5
印刷后QC
Light-box OIScope 显微相机
OGP QC
Smartscope 300
UV切割至ECD形式
KY-N-UV10 UV激光切割
沉积过程
沉积(MgMm)
洗涤
沉积(FeOx)
洗涤
Mini Plant 3系统
装袋
手动
装袋前阻抗检查
水凝胶沉积
手动
贴标签
手动
分割
KY-N-UV10 UV激光切割
装置承托
干燥
MEM-170-24-D Memmert烘箱
装袋后阻抗检查
装纸箱
贴标牌
手动
包装以供运输

图29

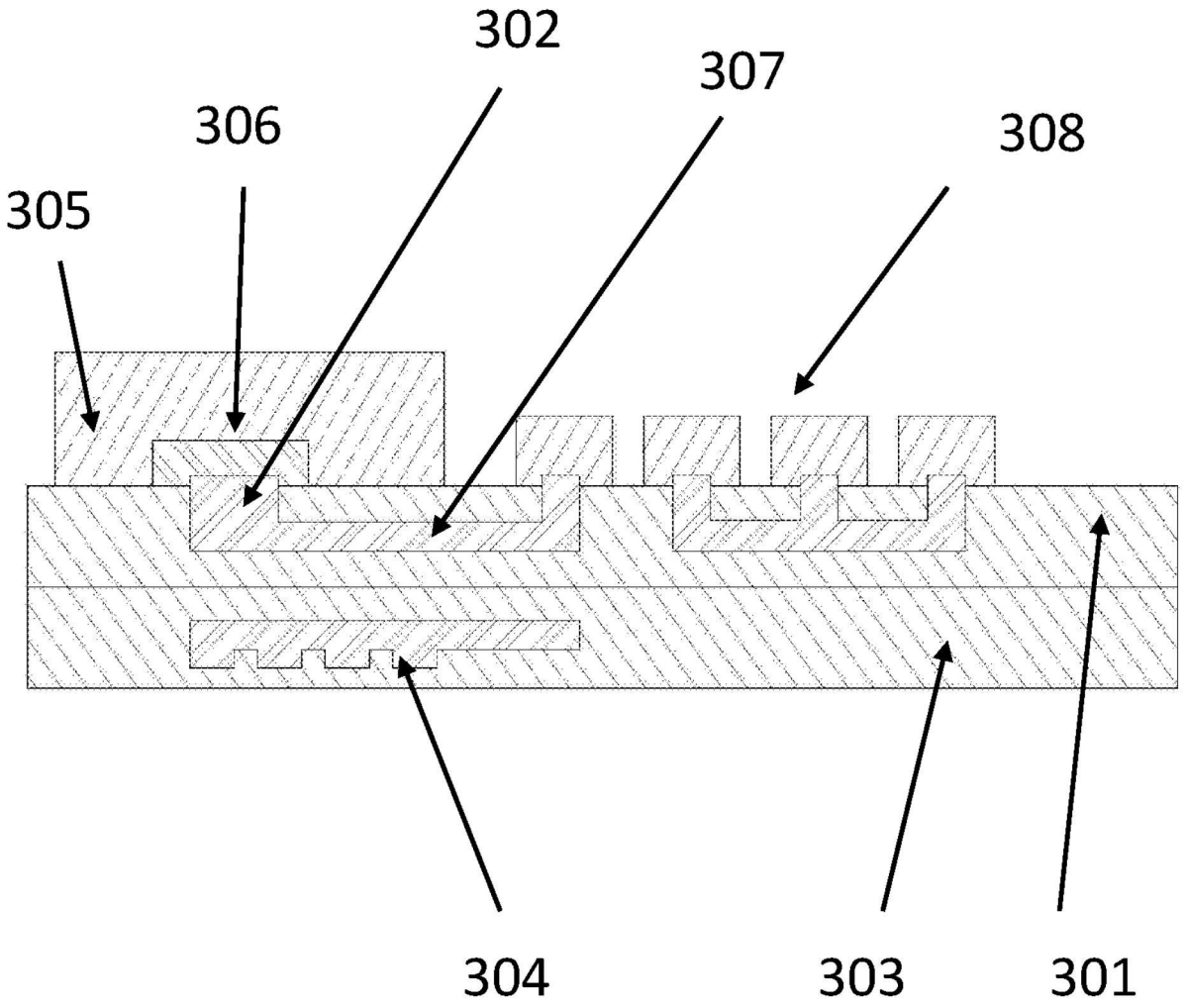


图30

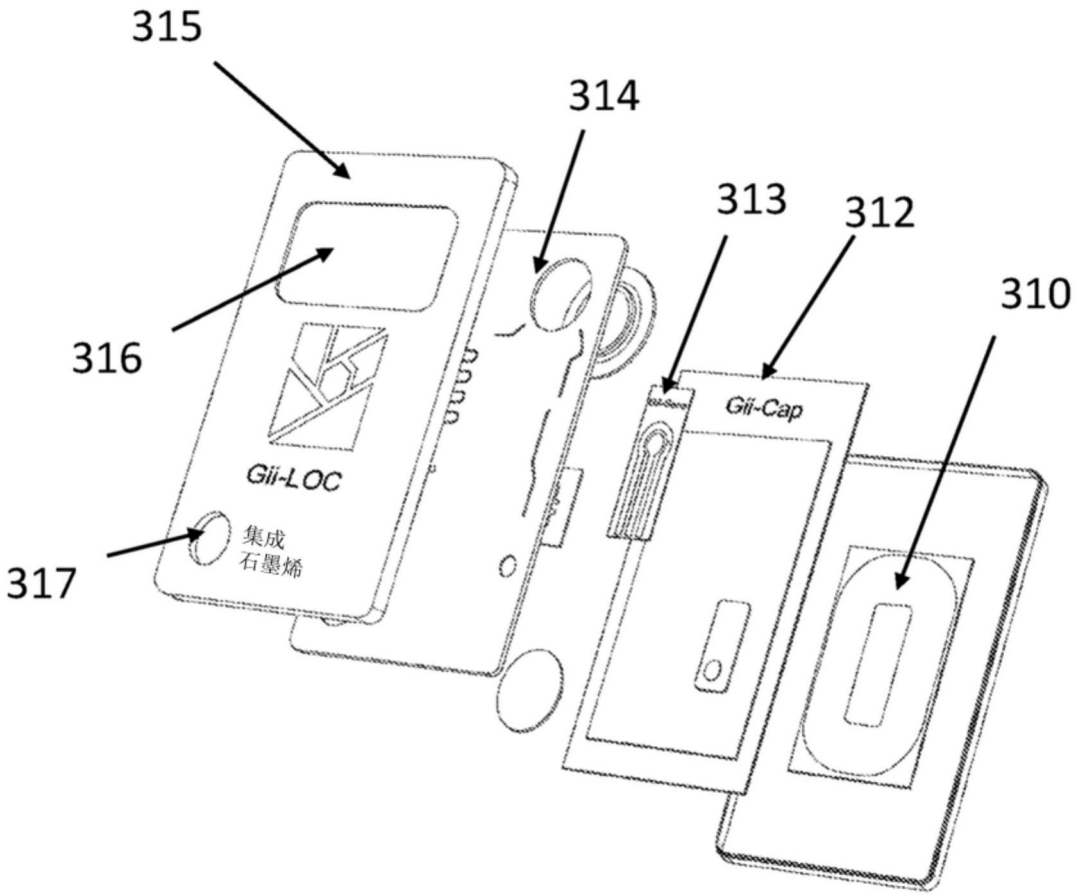

315
314
313
312
310
316
317
Gii-LOC
集成
石墨烯
Gii-Cap

图31


53.02 +
00.94 -
01.75 -
Gii-LOC
集成
石墨烯

图32

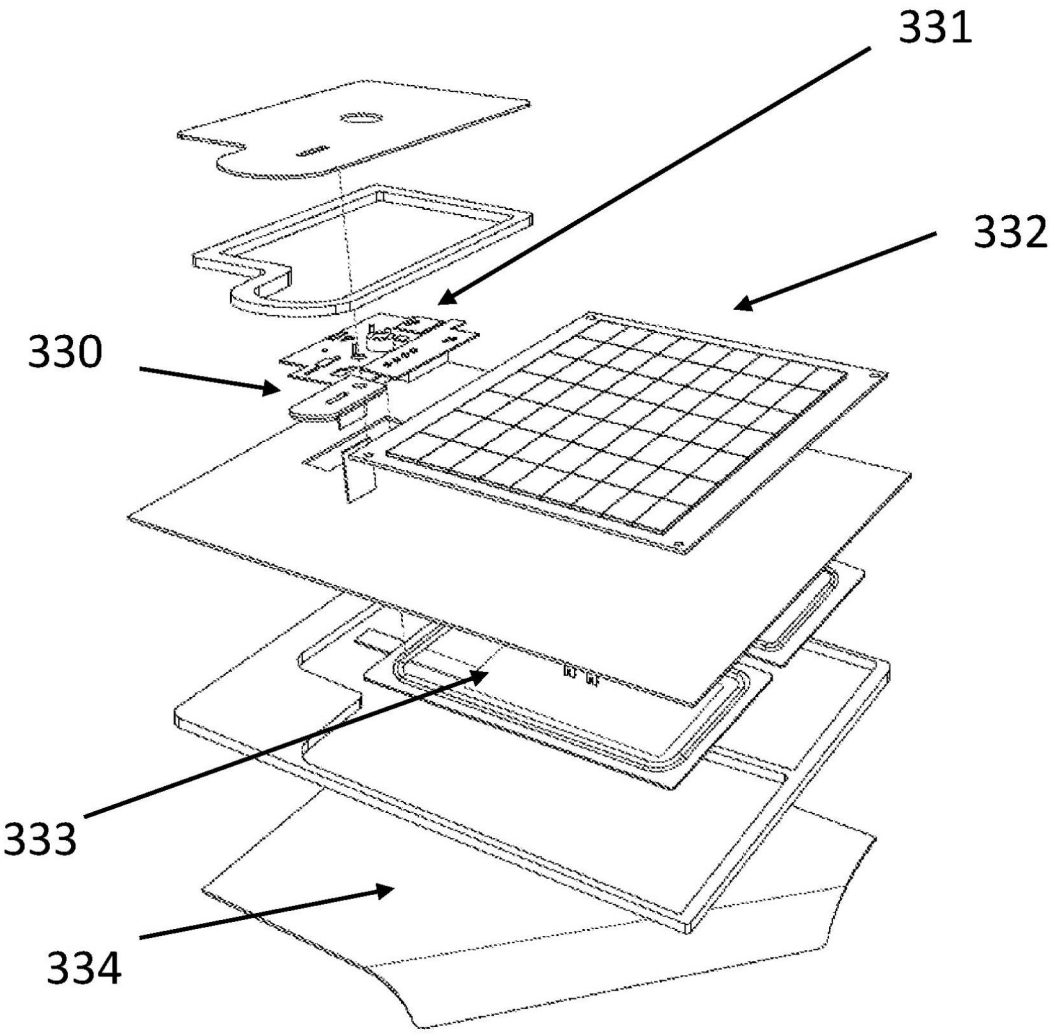


图33

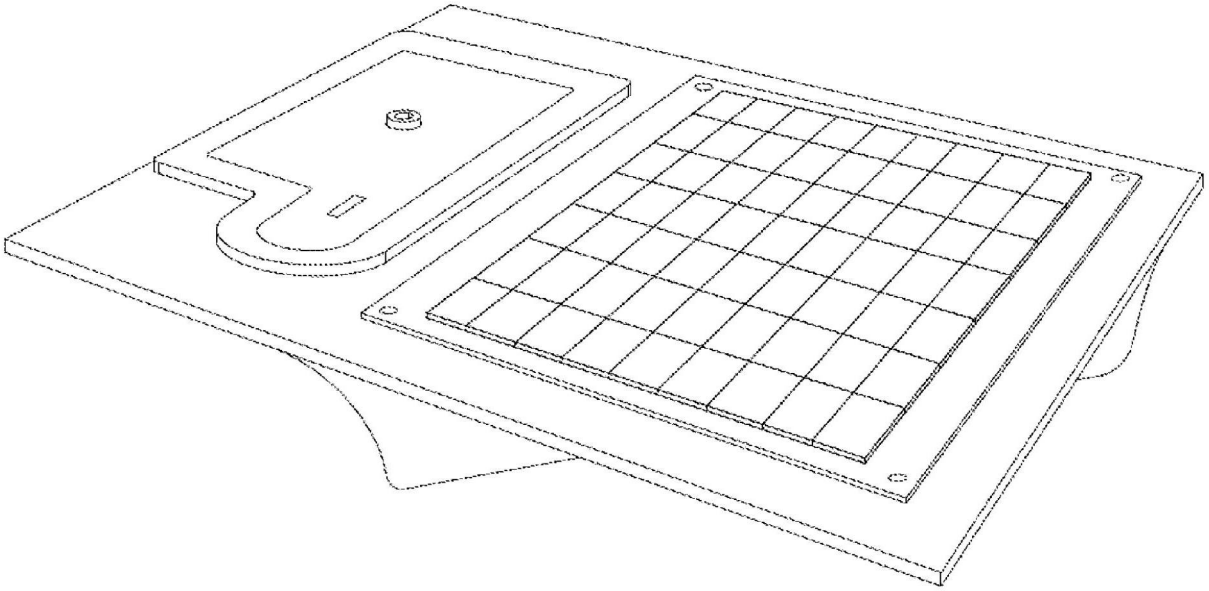


图34

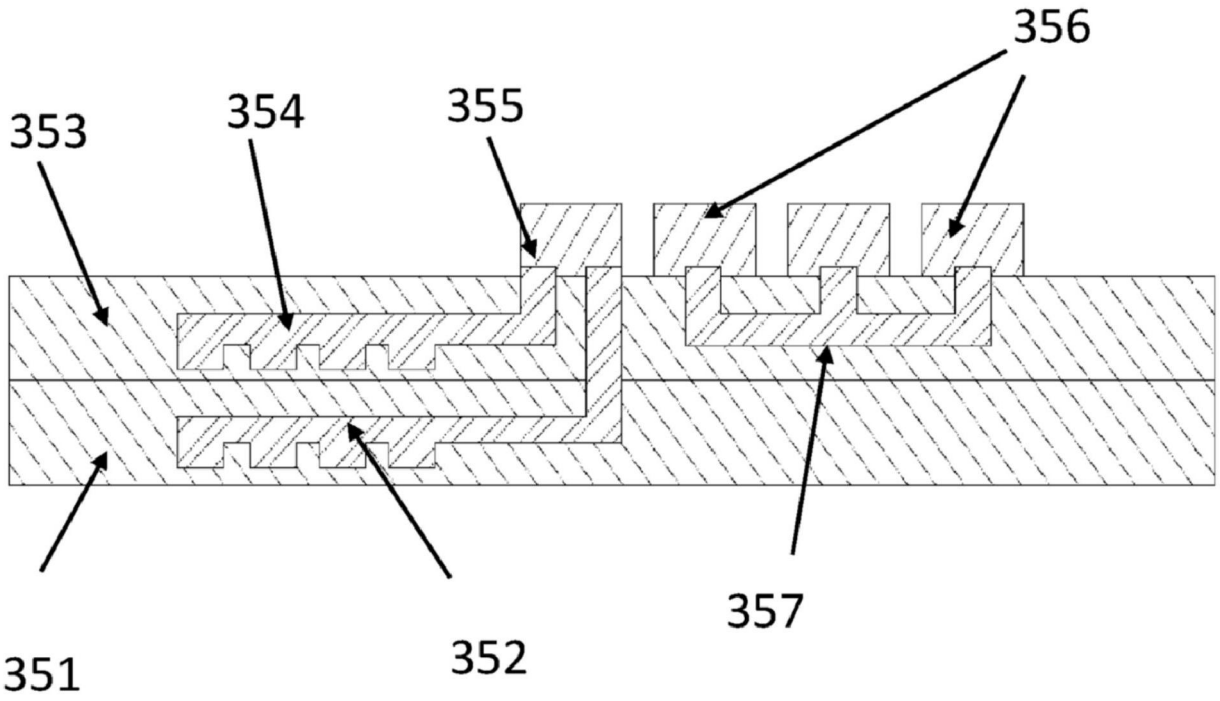


图35

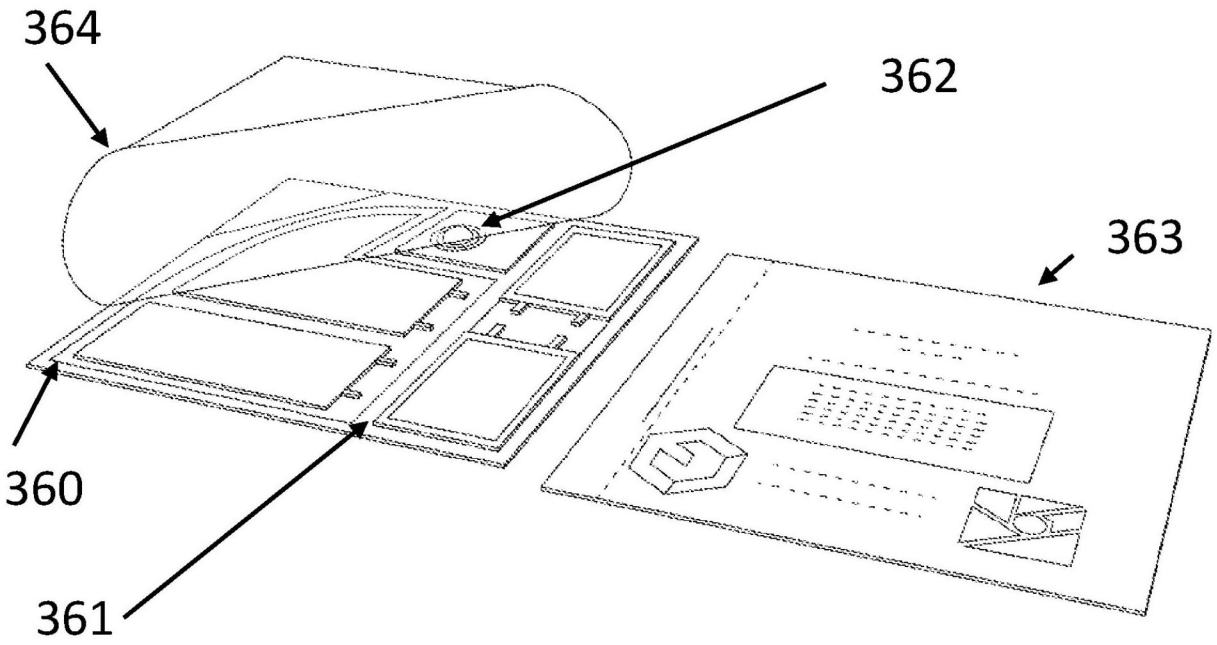


图36

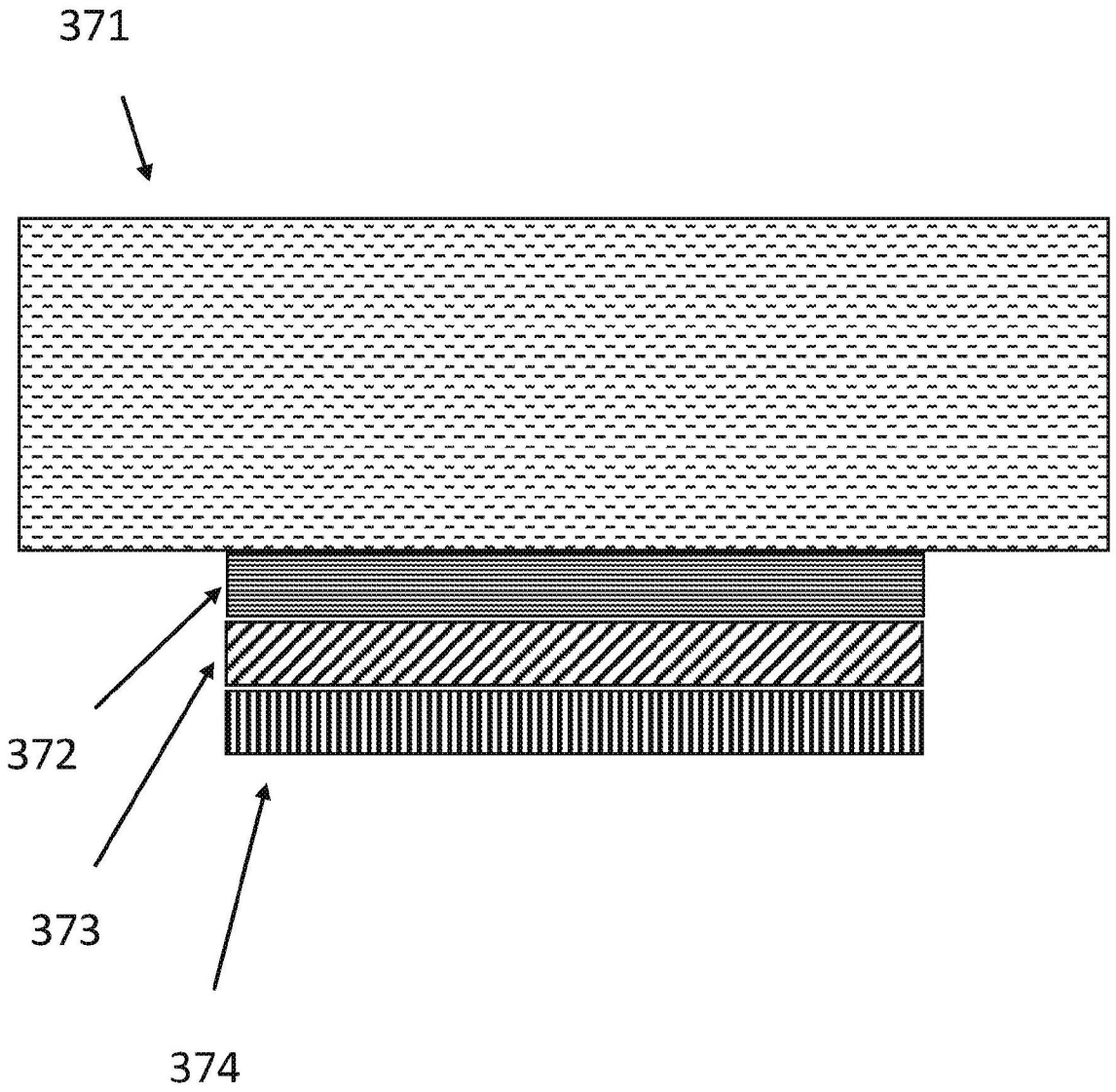


图37

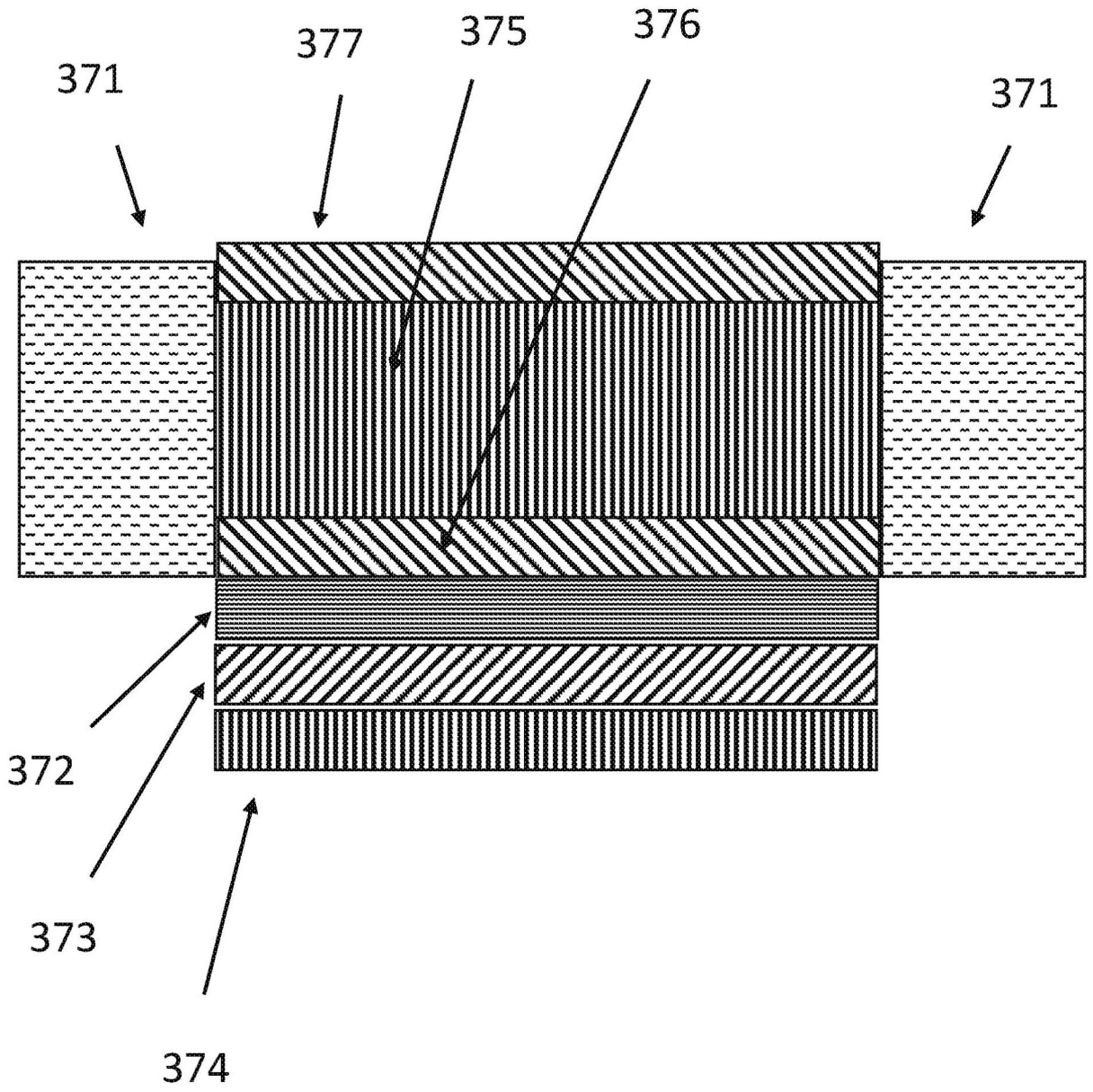


图38

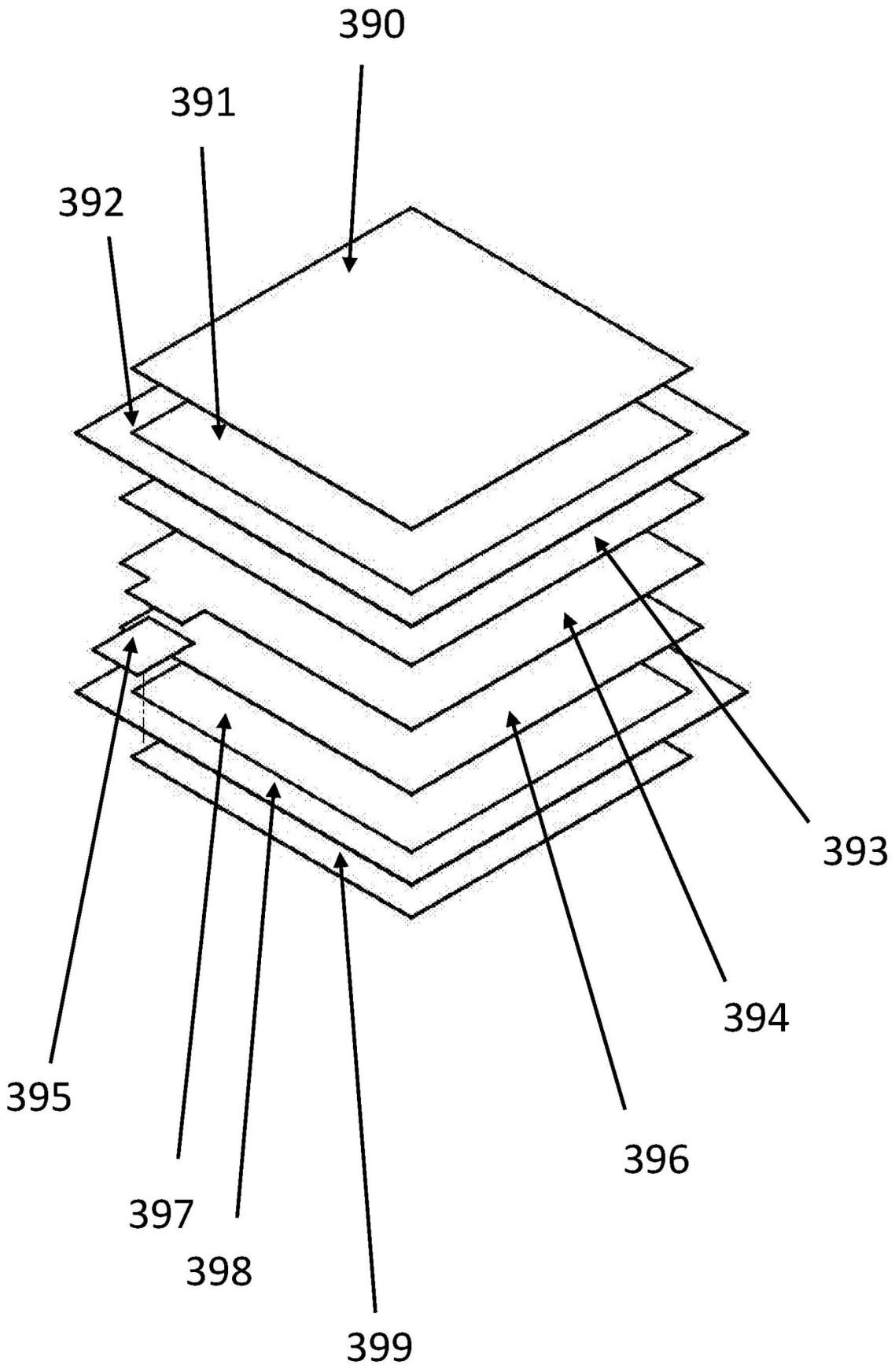


图39

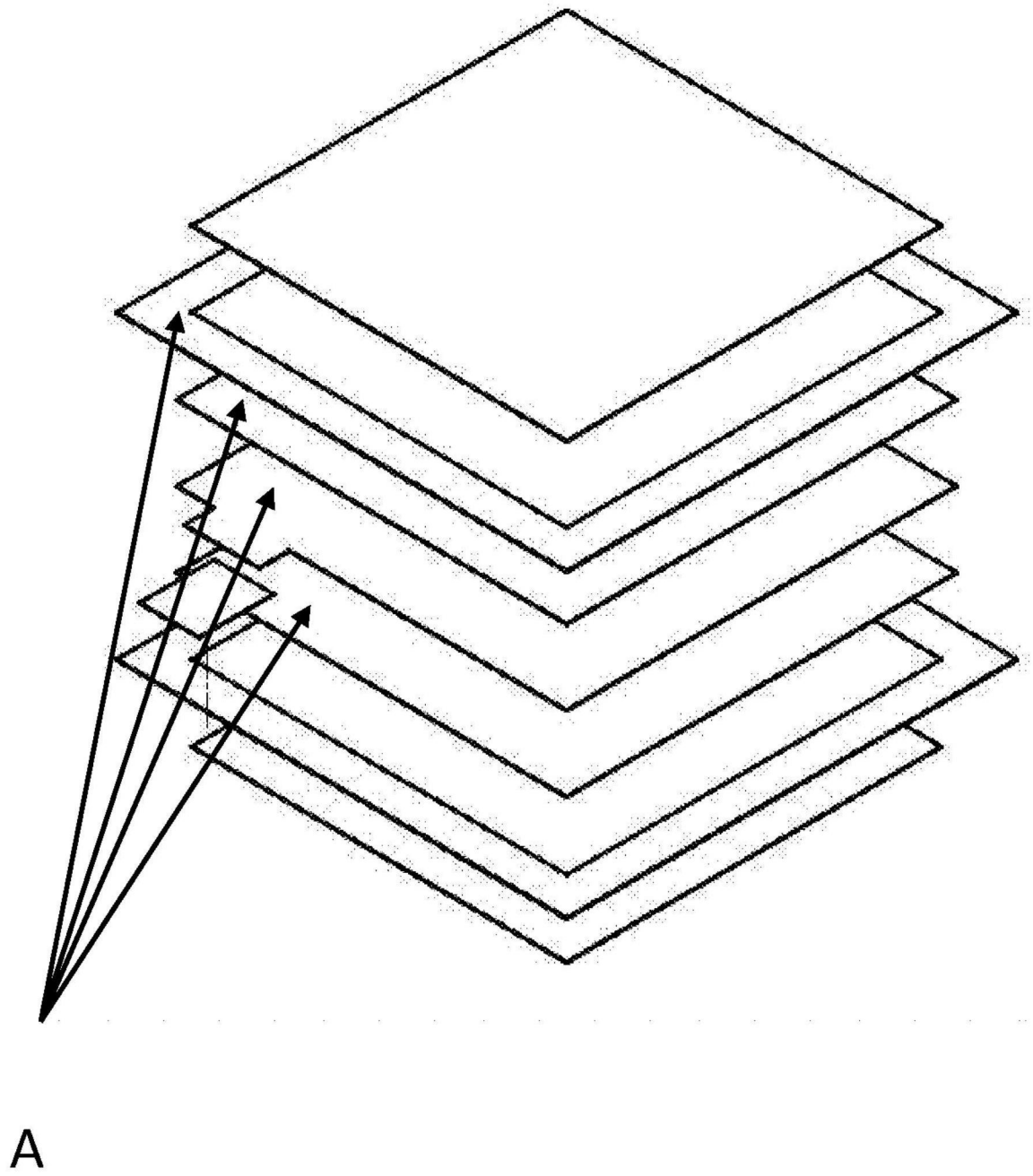


图40A

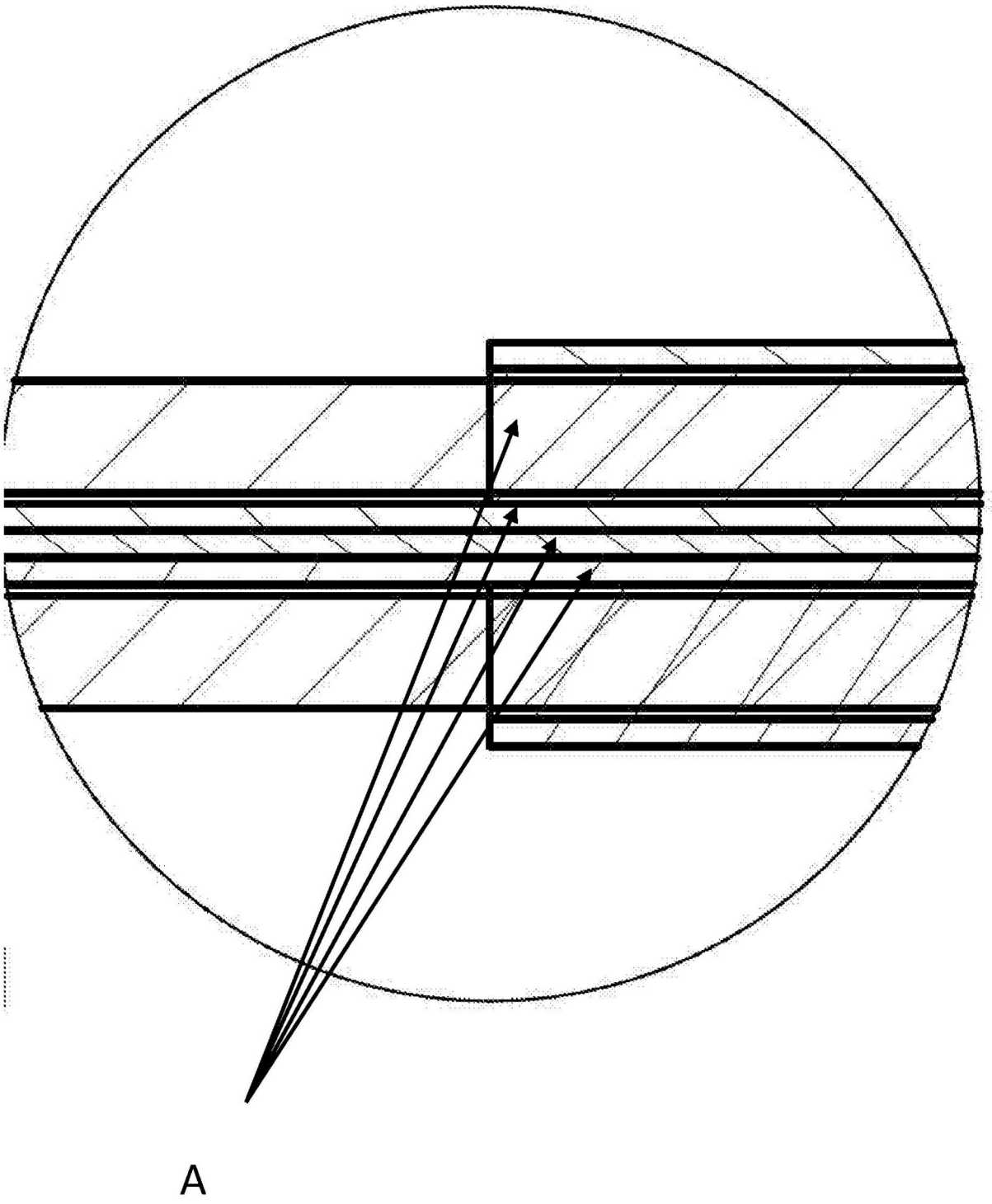


图40B

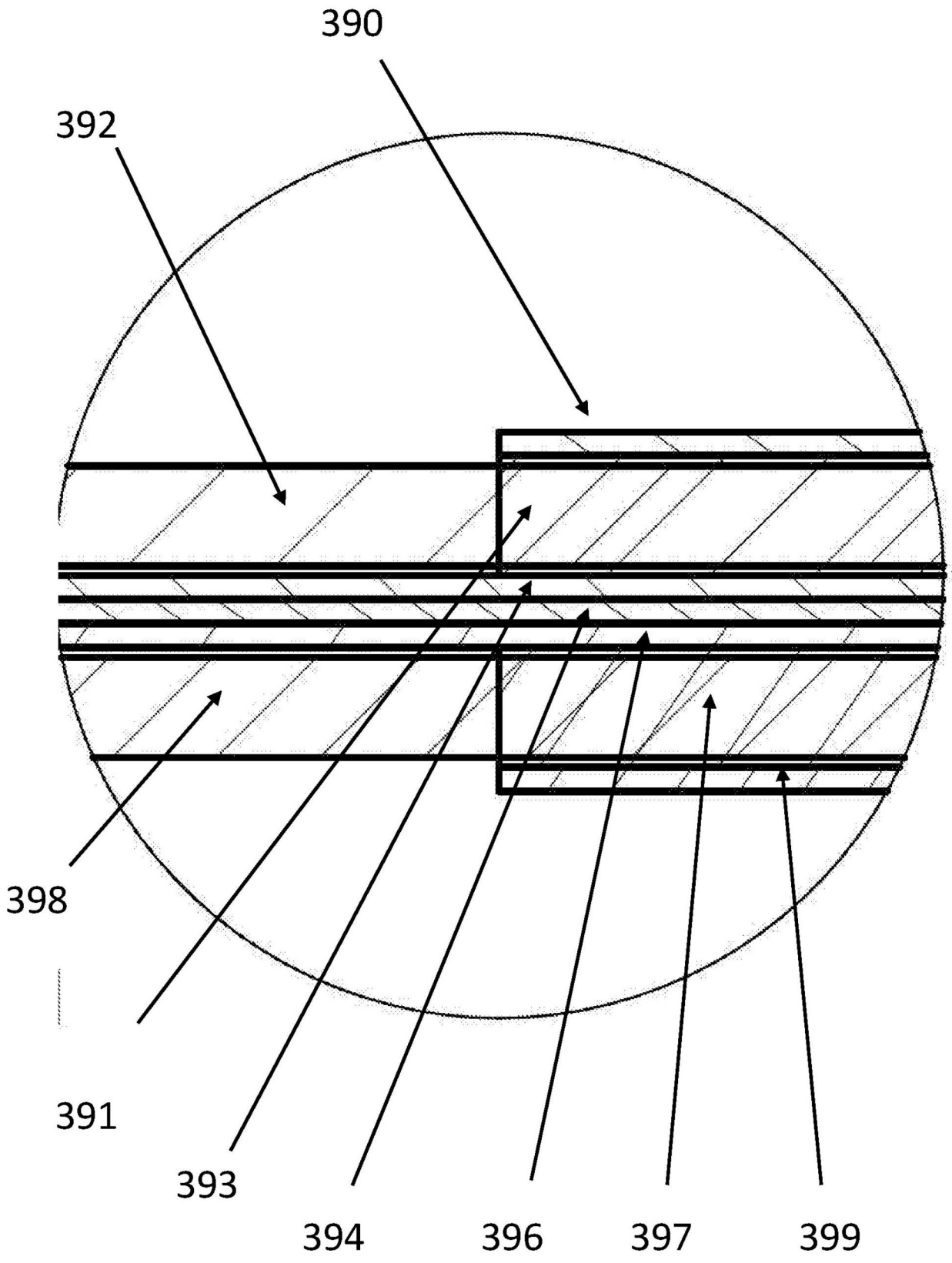


图40C

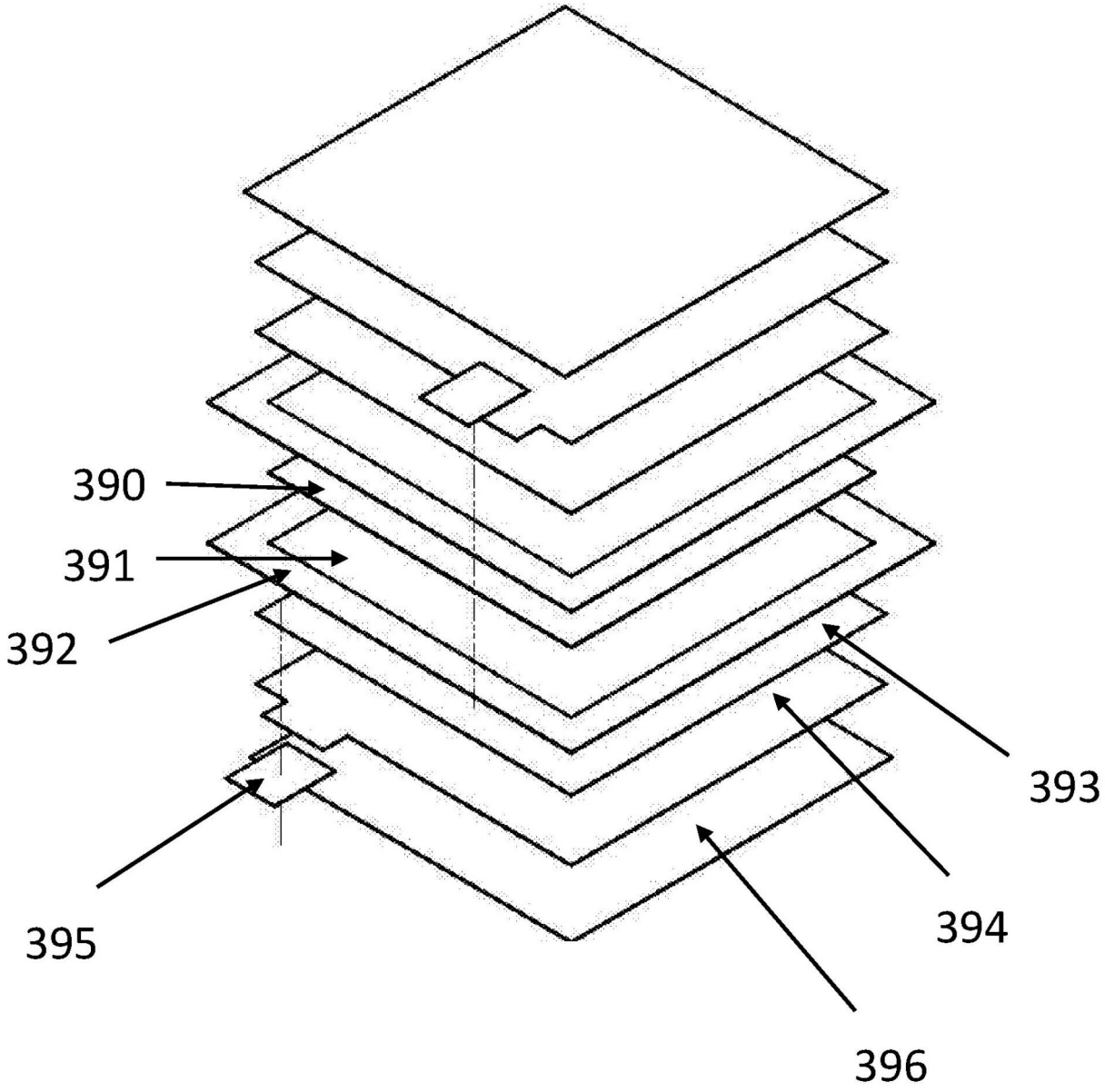


图41A

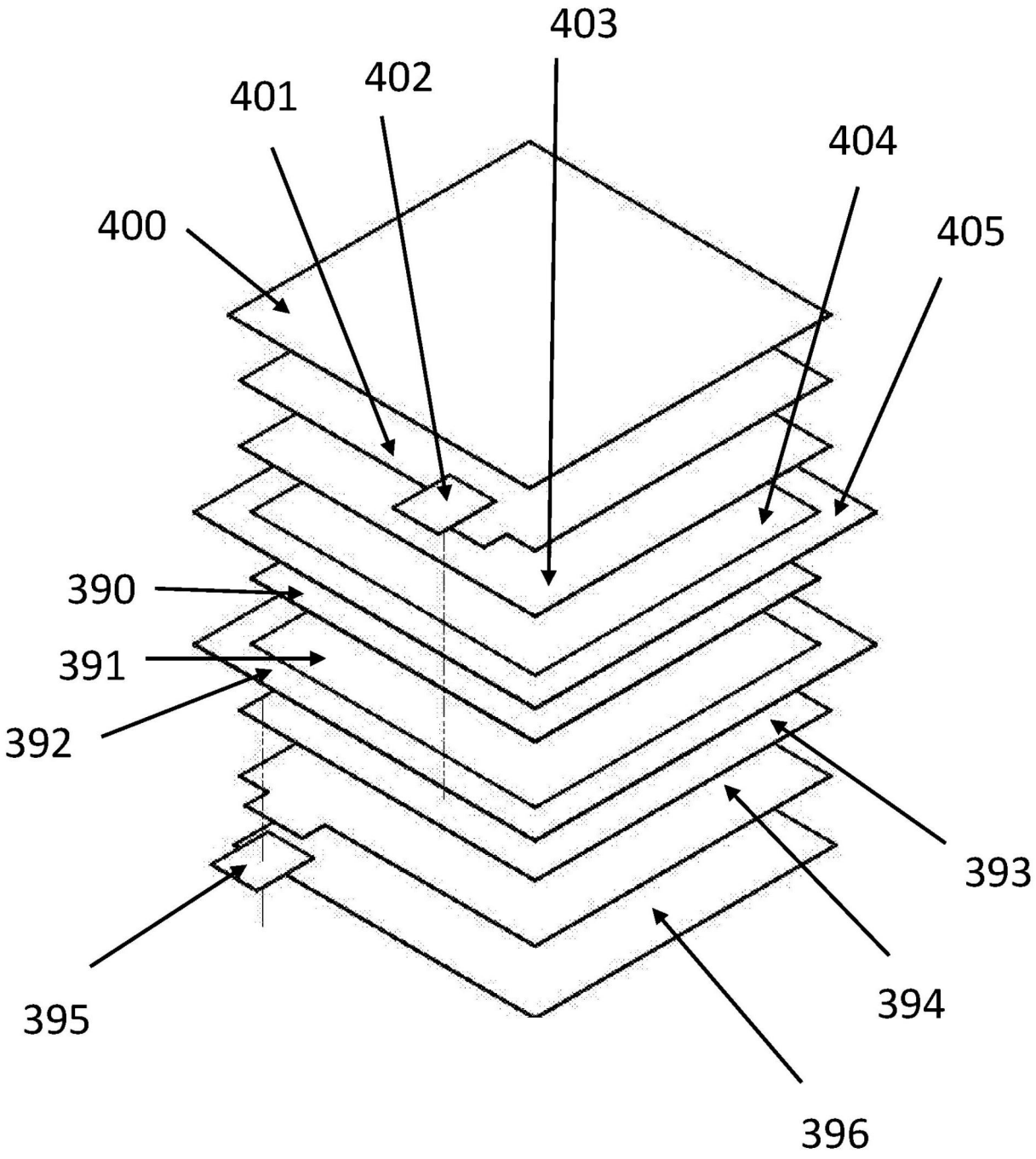


图41B

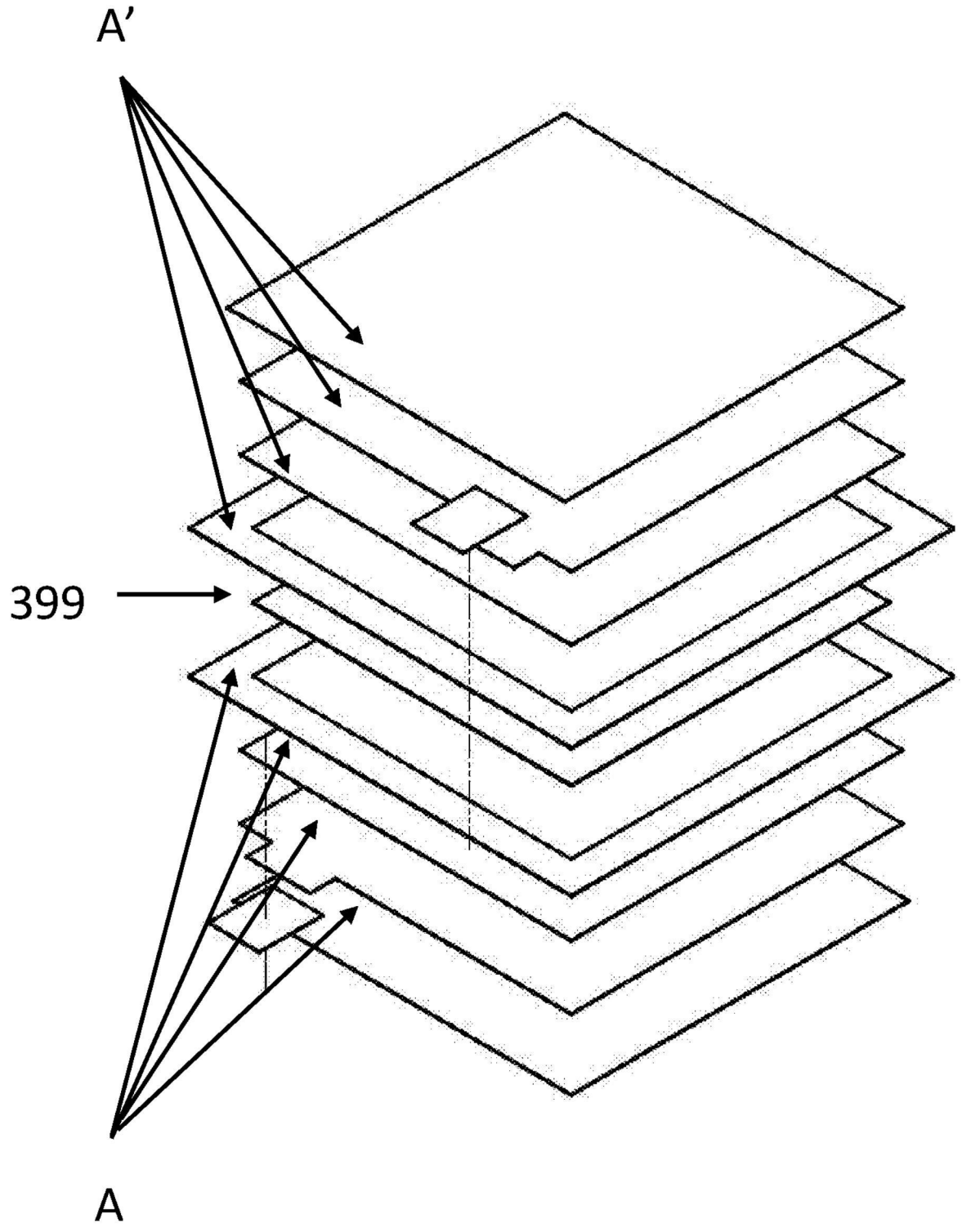


图41C

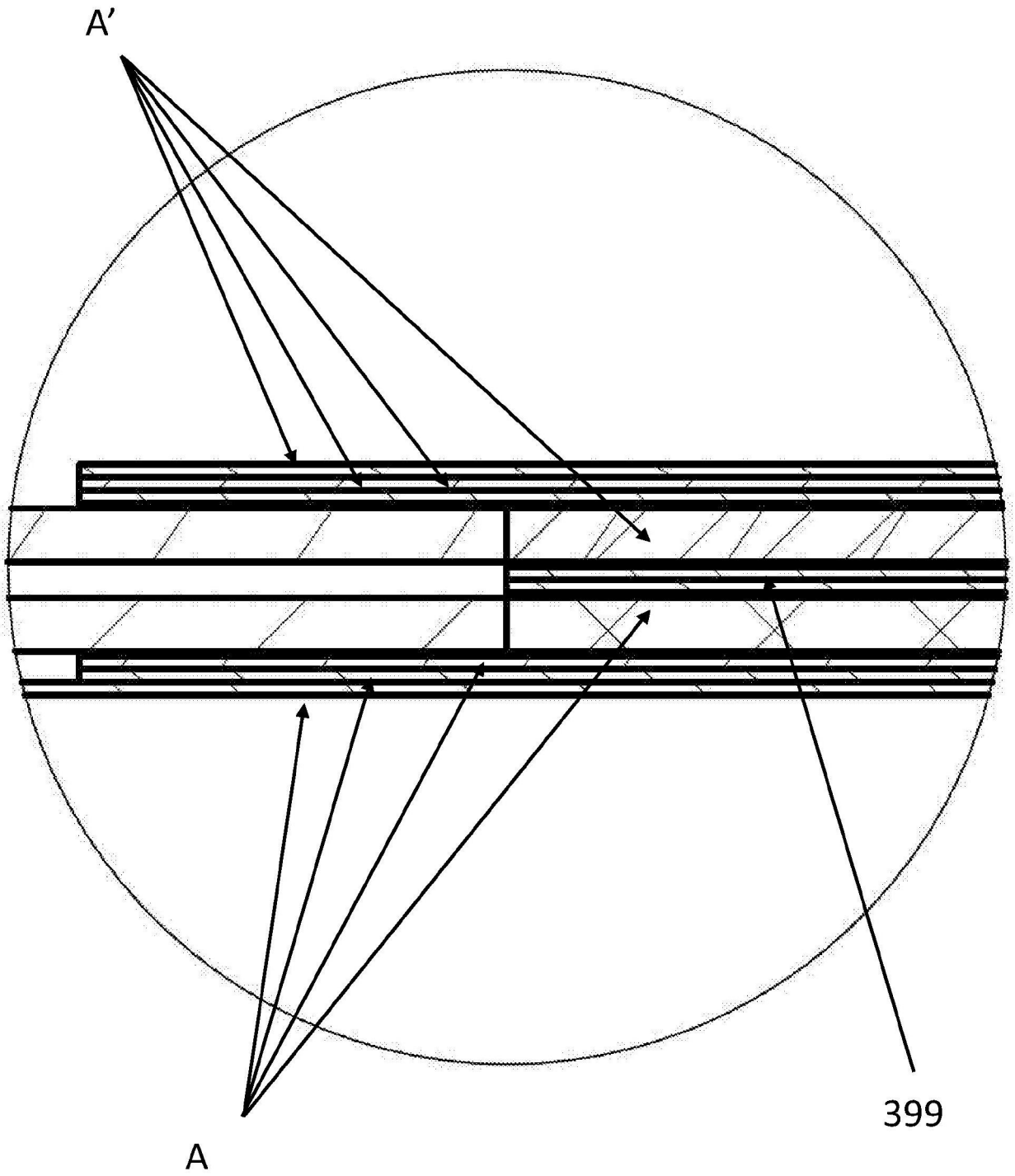


图41D

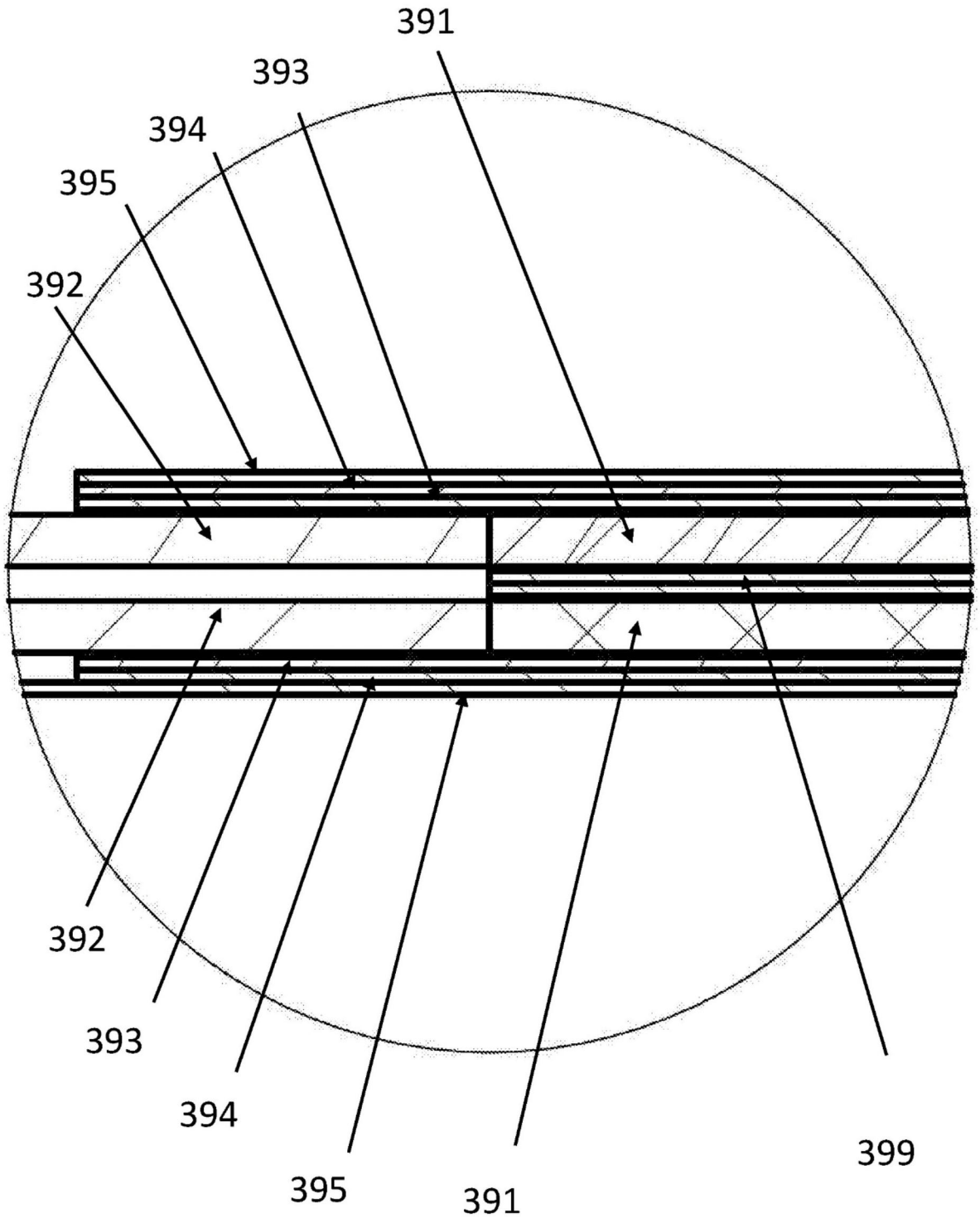


图41E

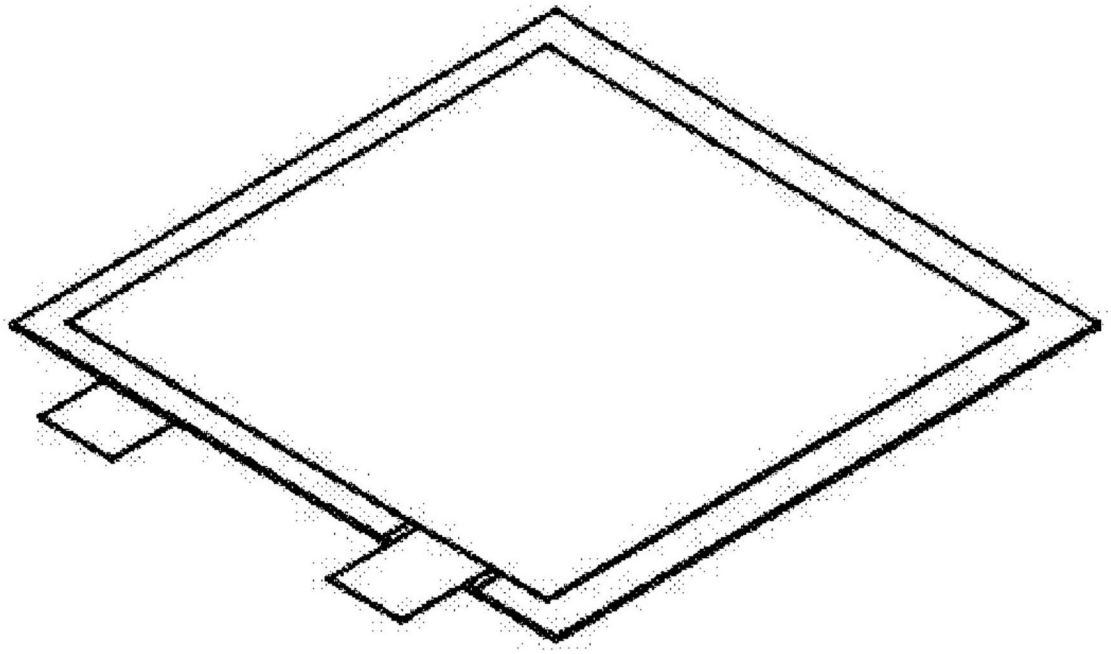


图41F

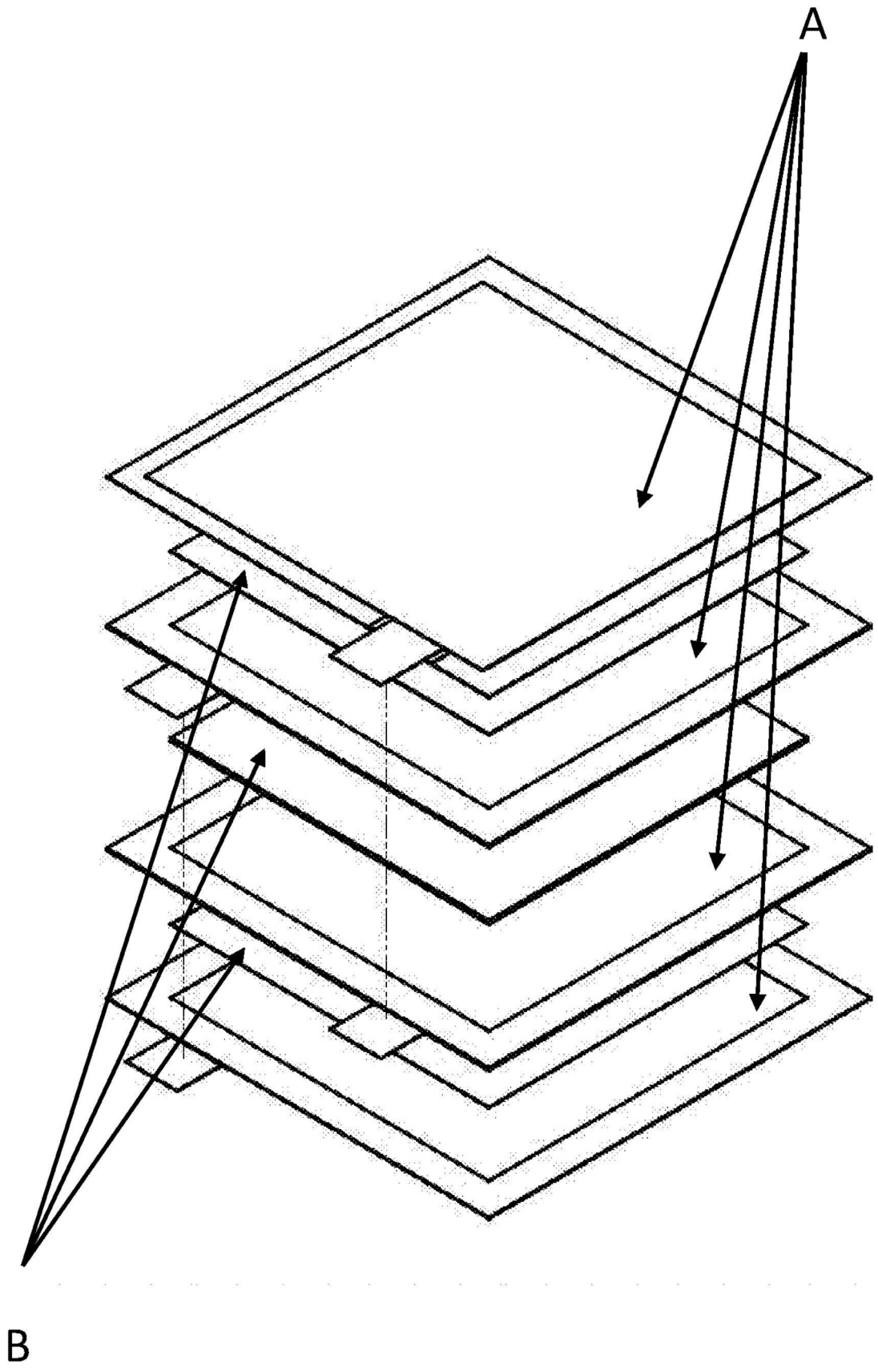


图42

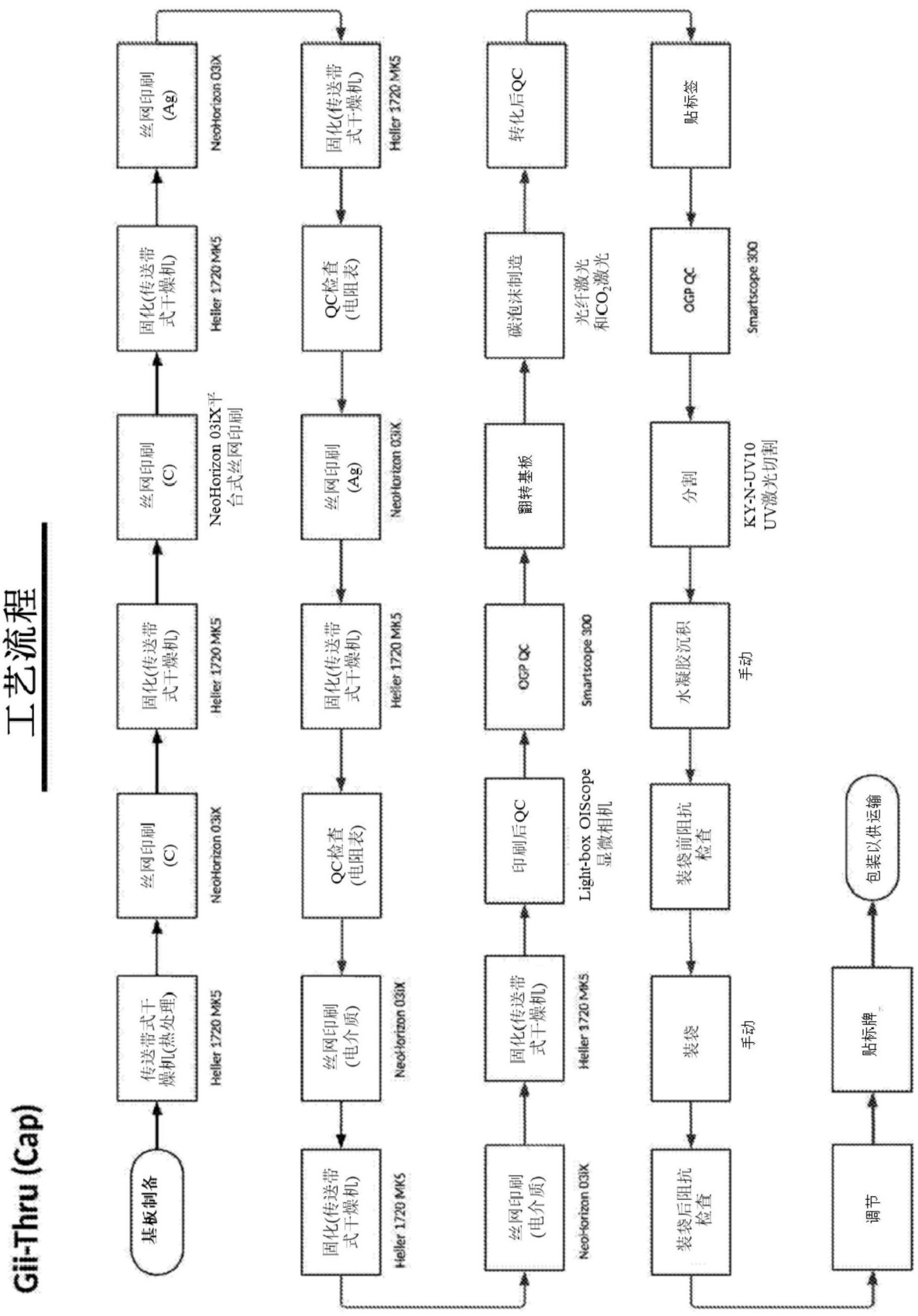

工艺流程
Gii-Thru (Cap)
基板制备
传送带式干燥机(热处理)
Heller 1720 MK5
丝网印刷 (C)
NeoHorizon 03iX
固化(传送带式干燥机)
Heller 1720 MK5
丝网印刷 (C)
NeoHorizon 03iX平台式丝网印刷
固化(传送带式干燥机)
Heller 1720 MK5
丝网印刷 (Ag)
NeoHorizon 03iX
固化(传送带式干燥机)
Heller 1720 MK5
丝网印刷 (电介质)
NeoHorizon 03iX
固化(传送带式干燥机)
Heller 1720 MK5
QC检查 (电阻表)
丝网印刷 (Ag)
NeoHorizon 03iX
固化(传送带式干燥机)
Heller 1720 MK5
QC检查 (电阻表)
丝网印刷 (电介质)
Neo-horizon 03iX
固化(传送带式干燥机)
Heller 1720 MK5
印刷后QC
Light-box OIScope 显微相机
OGP QC
Smartscope 300
翻转基板
碳泡沫制造
光纤激光和CO_2激光
转化后QC
装袋后阻抗检查
装袋
手动
装袋前阻抗检查
水凝胶沉积
手动
分割
KY-N-UV10 UV激光切割
OGP QC
Smartscope 300
贴标签
调节
贴标牌
手动
包装以供运输

图43A

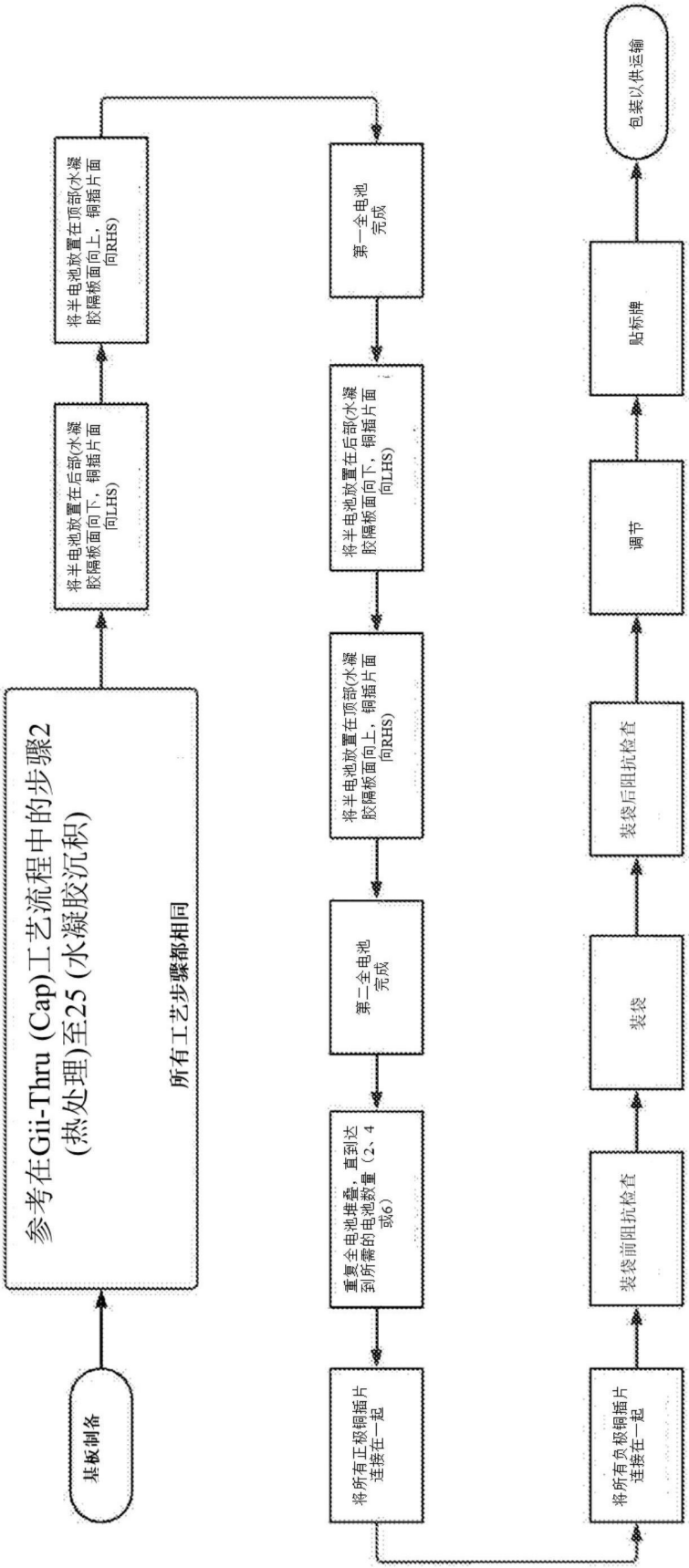

基板制备
参考在Gii-Thru (Cap)工艺流程中的步骤2
(热处理)至25 (水凝胶沉积)
所有工艺步骤都相同
将半电池放置在后部(水凝胶隔板面向下，铜插片面向LHS)
将半电池放置在顶部(水凝胶隔板面向上，铜插片面向RHS)
将所有正极铜插片连接在一起
重复全电池堆叠，直到达到所需的电池数量（2、4或6）
第二全电池完成
将半电池放置在后部(水凝胶隔板面向下，铜插片面向LHS)
将半电池放置在顶部(水凝胶隔板面向上，铜插片面向RHS)
第一全电池完成
将所有负极铜插片连接在一起
装袋前阻抗检查
装袋
装袋后阻抗检查
调节
贴标牌
包装以供运输

图43B

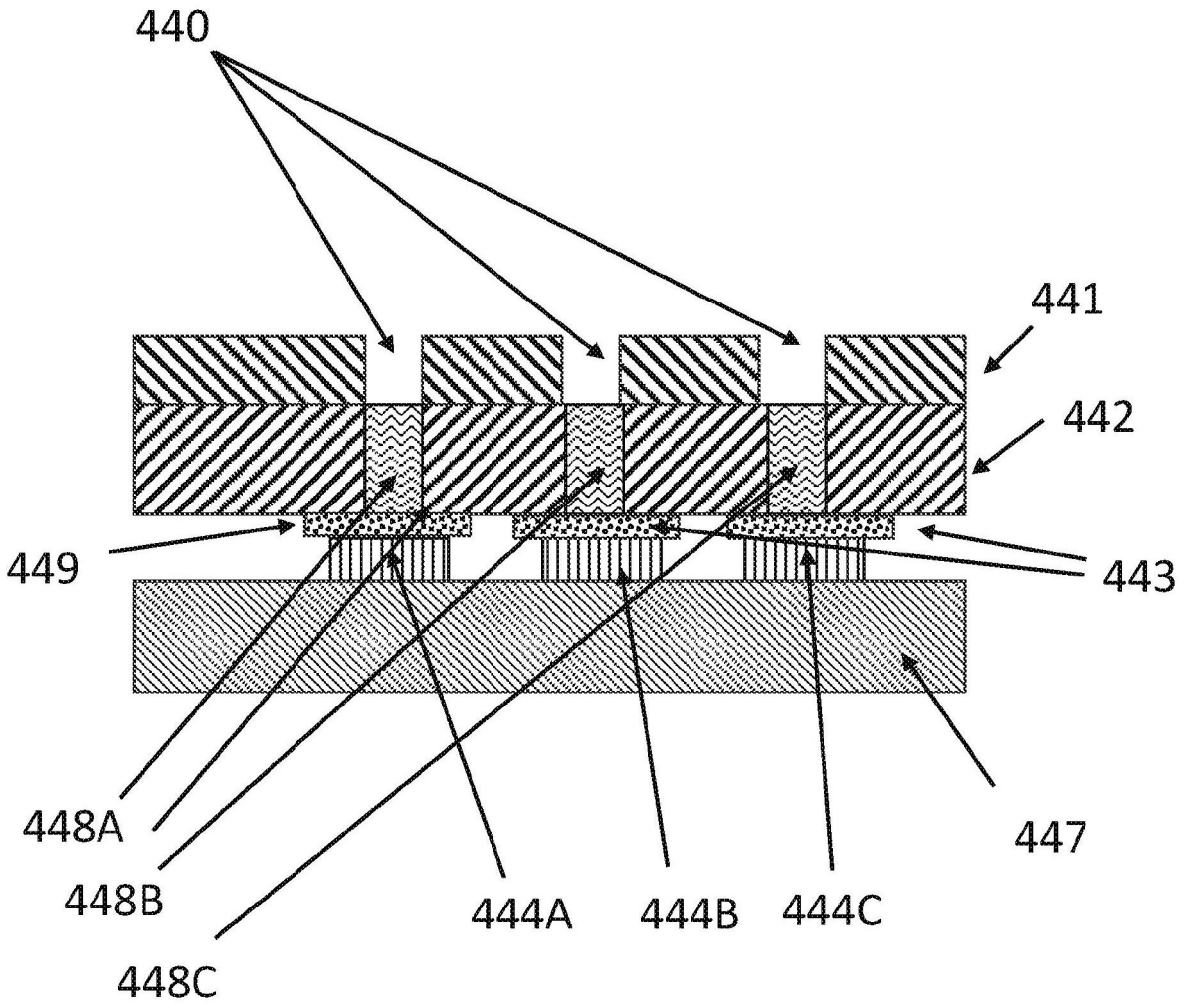


图44A

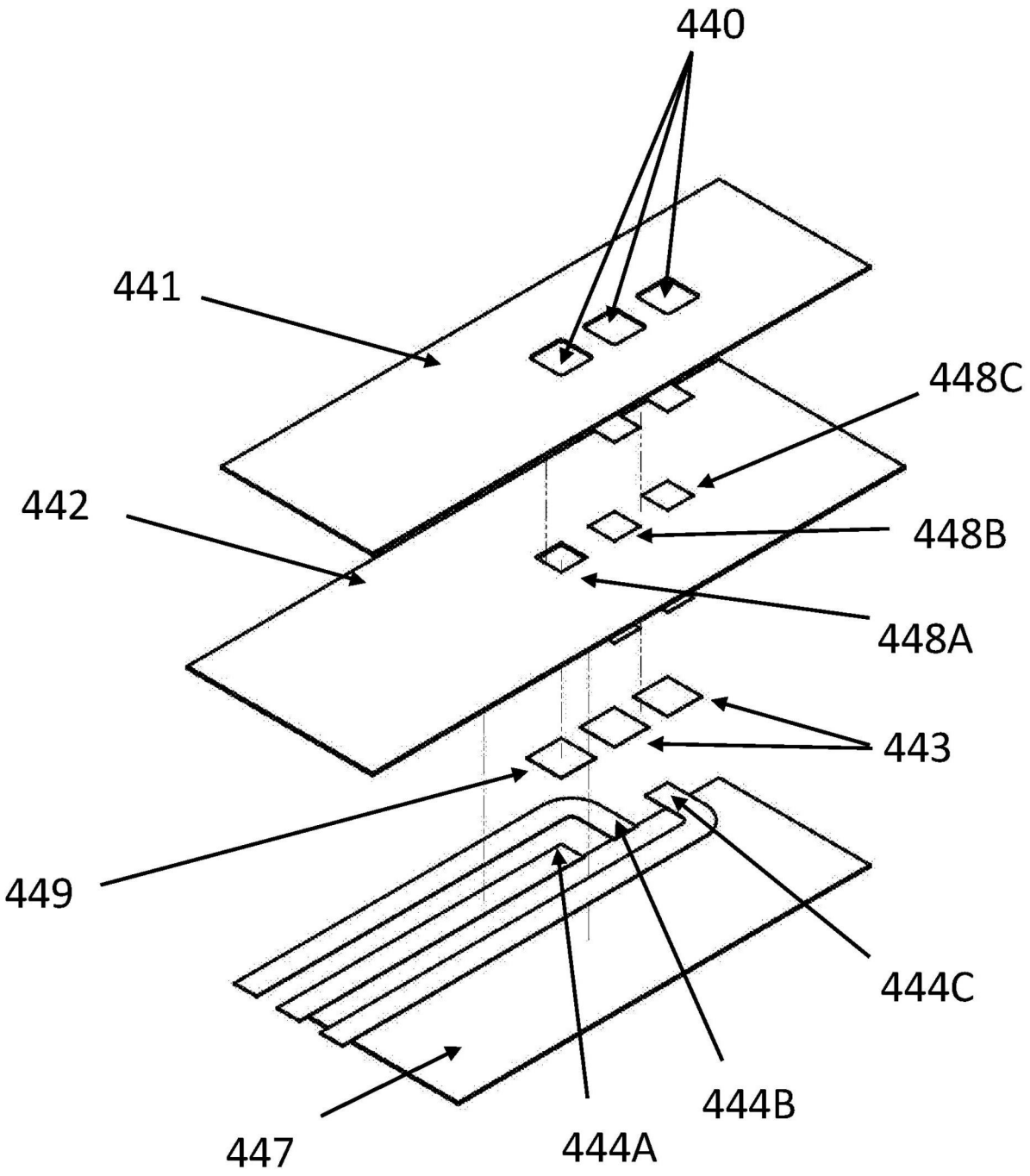


图44B

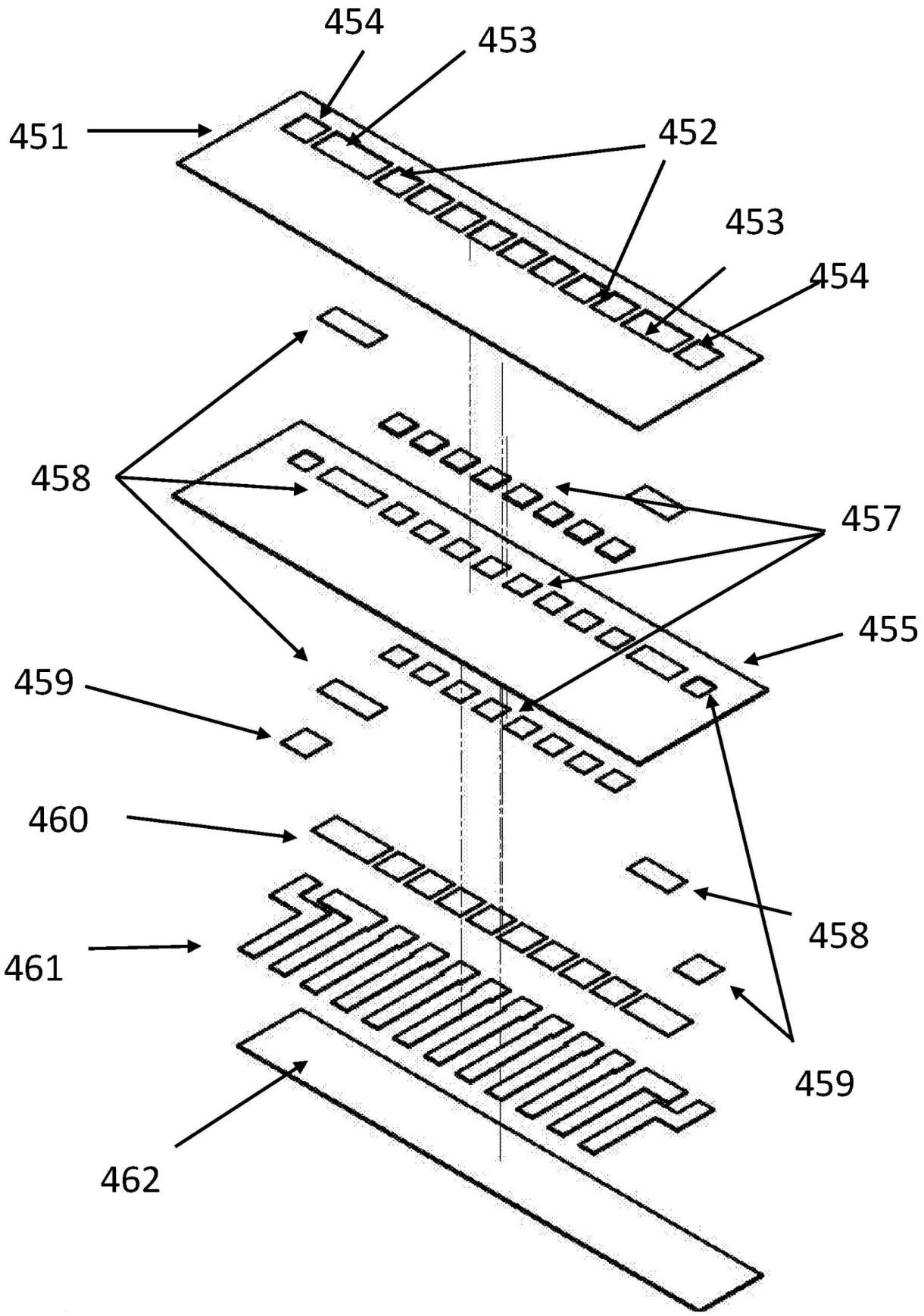
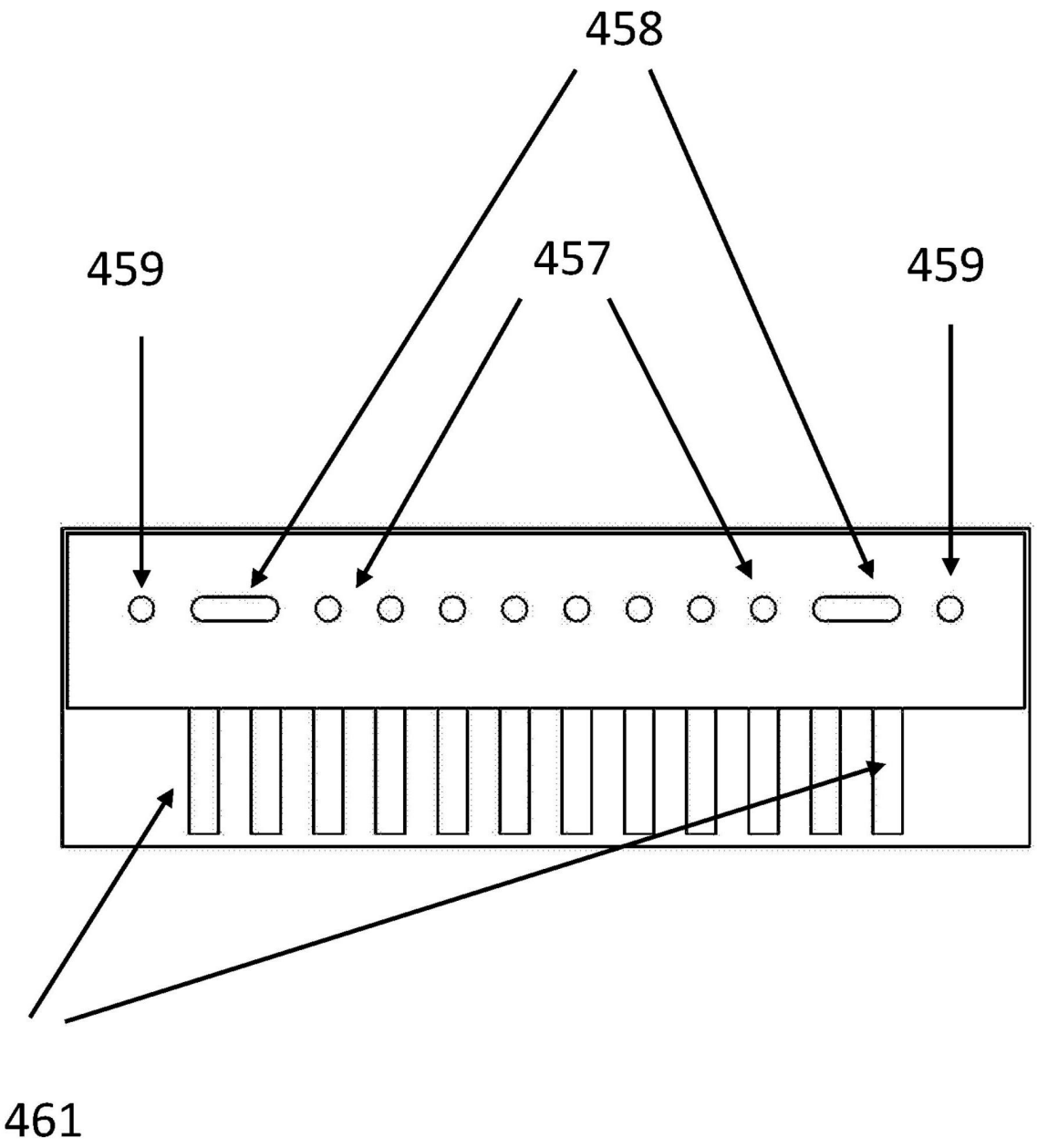


图45A



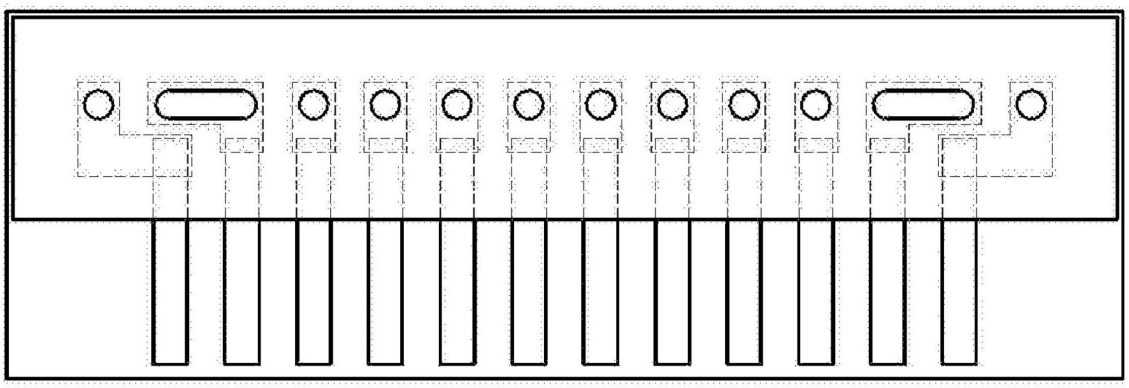


图45B

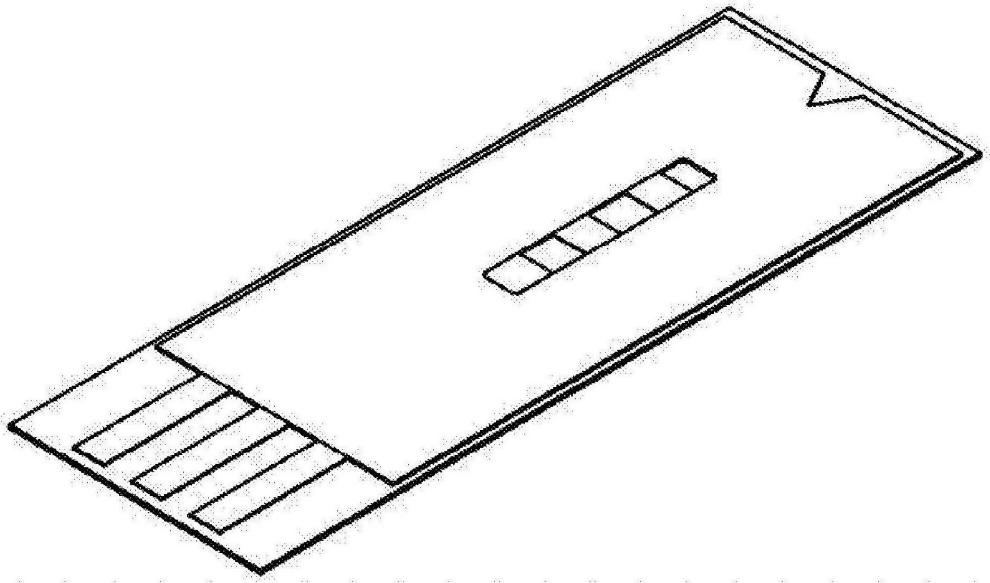


图46A

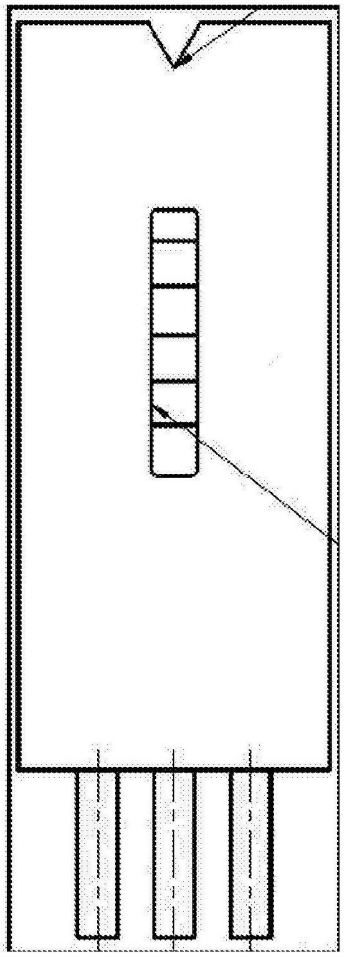


图46B

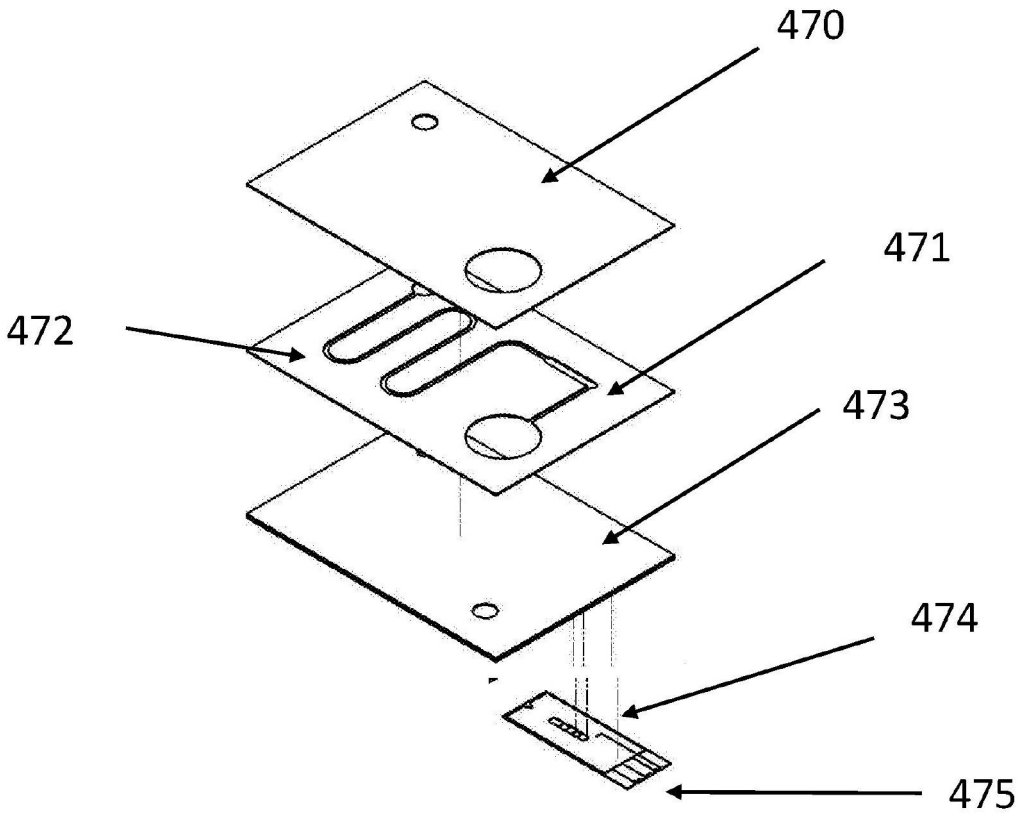


图47A

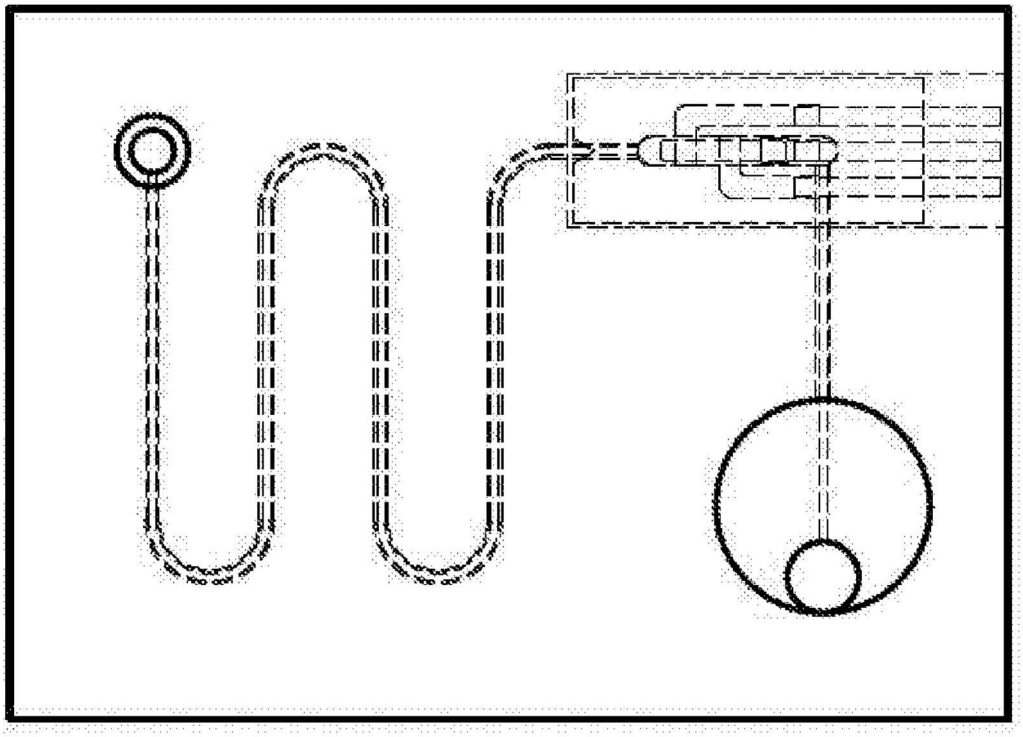


图47B

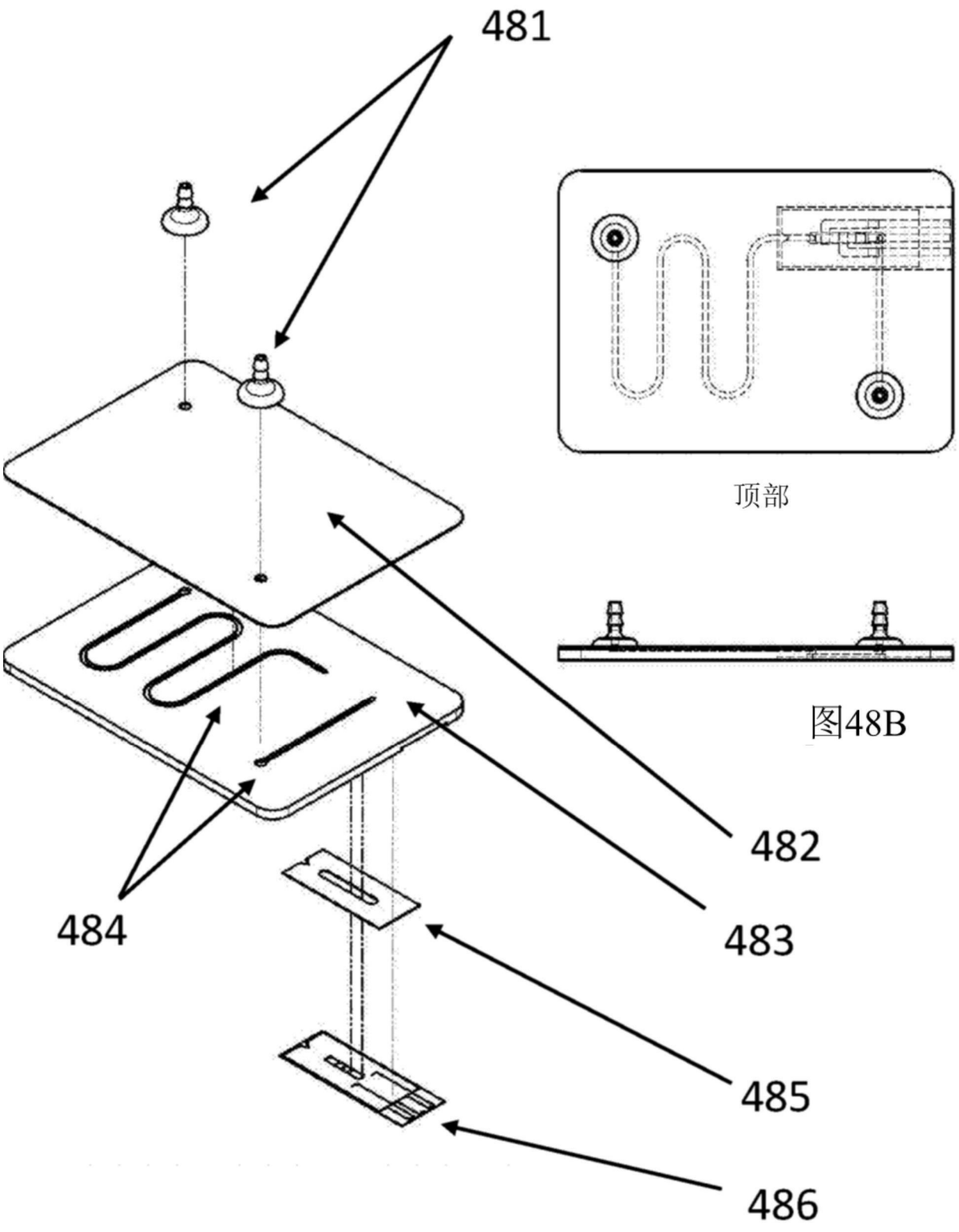


图48B

图 48A

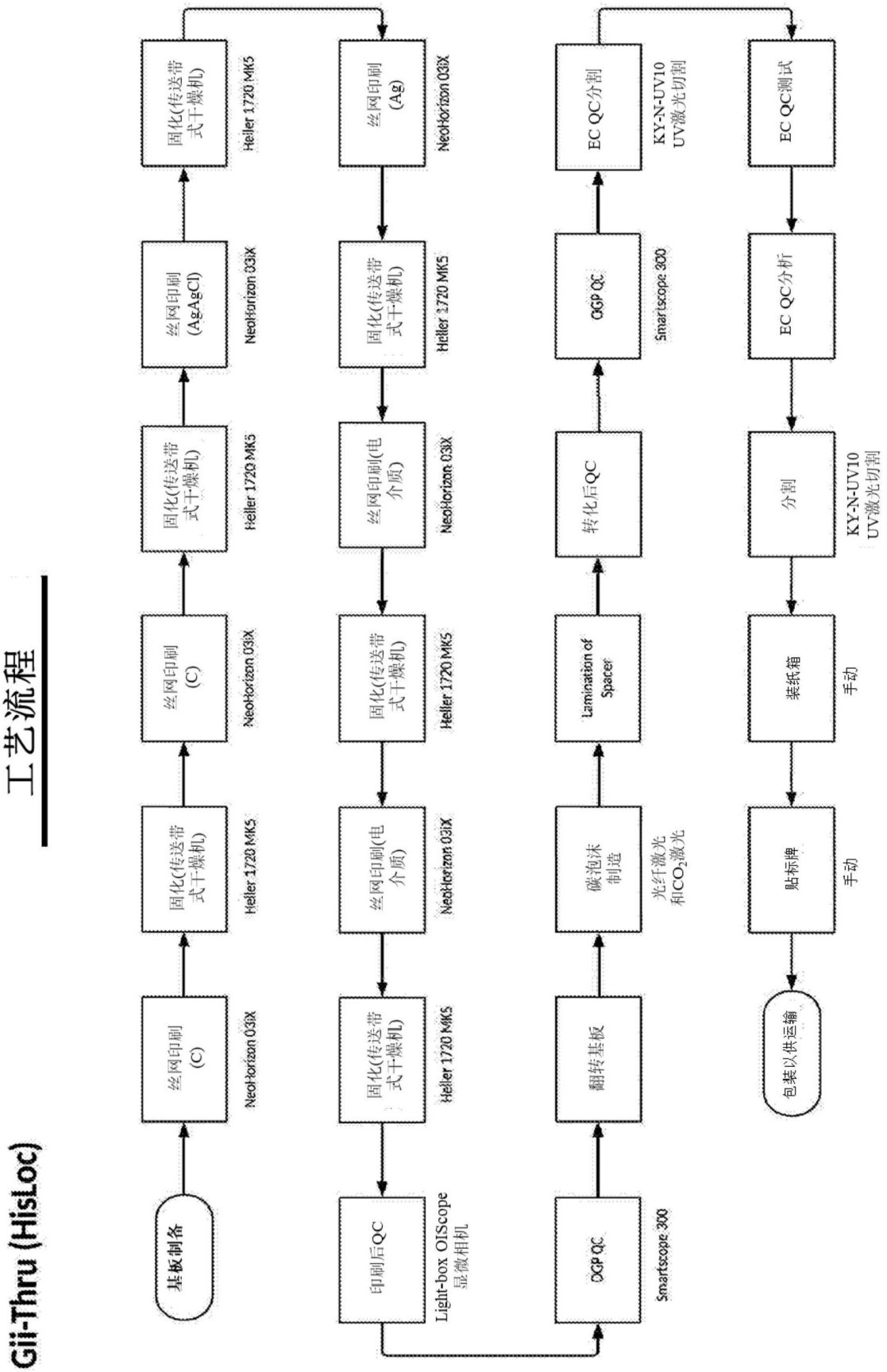

工艺流程
Gii-Thru (HisLoc)
基板制备
丝网印刷 (C)
Neohorizon 03iX
固化(传送带式干燥机)
Heller 1720 MK5
丝网印刷 (C)
Neohorizon 03iX
固化(传送带式干燥机)
Heller 1720 MK5
丝网印刷 (AgAgCl)
Neohorizon 03iX
固化(传送带式干燥机)
Heller 1720 MK5
印刷后QC
Light-box OIScope 显微相机
丝网印刷(电介质)
Neohorizon 03iX
固化(传送带式干燥机)
Heller 1720 MK5
丝网印刷(电介质)
Neohorizon 03iX
固化(传送带式干燥机)
Heller 1720 MK5
丝网印刷 (Ag)
NeoHorizon 03iX
固化(传送带式干燥机)
Heller 1720 MK5
OGP QC
Smartscope 300
翻转基板
碳泡沫制造
光纤激光和CO_2激光
Lamination of Spacer
转化后QC
OGP QC
Smartscope 300
EC QC分割
KY-N-UV10 UV激光切割
EC QC测试
EC QC分析
分割
KY-N-UV10 UV激光切割
装纸箱
手动
贴标牌
手动
包装以供运输

图49

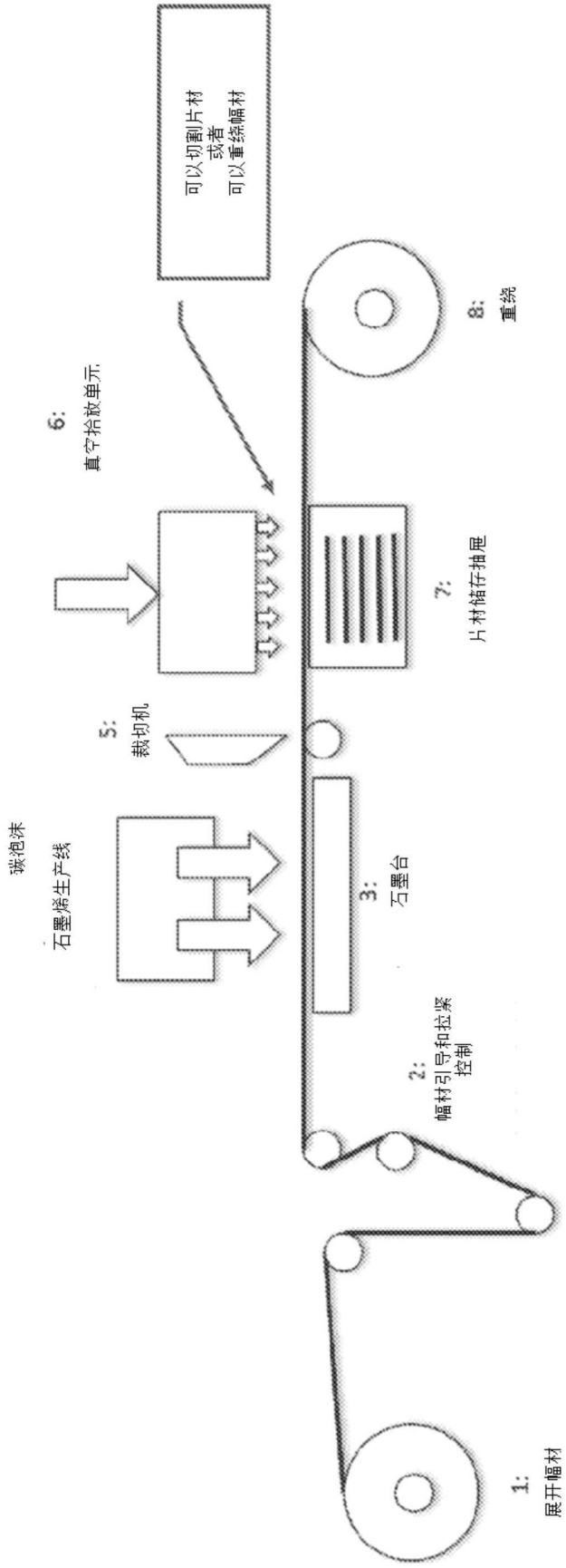

1:
展开幅材
2:
幅材引导和拉紧
控制
3:
石墨台
碳泡沫
石墨烯生产线
5:
裁切机
6:
真空拾放单元
可以切割片材
或者
可以重绕幅材
7:
片材储存抽屉
8:
重绕

图50

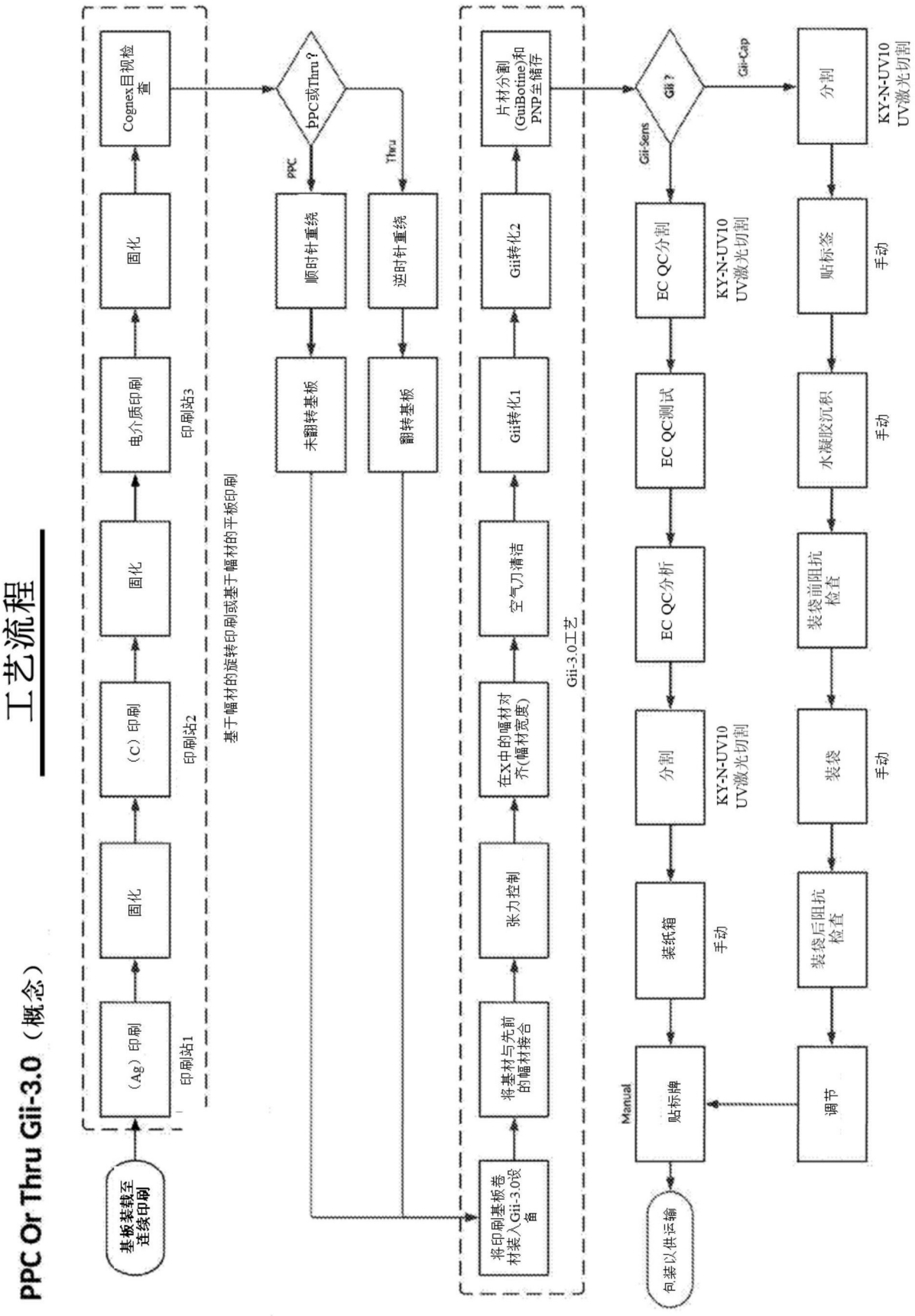
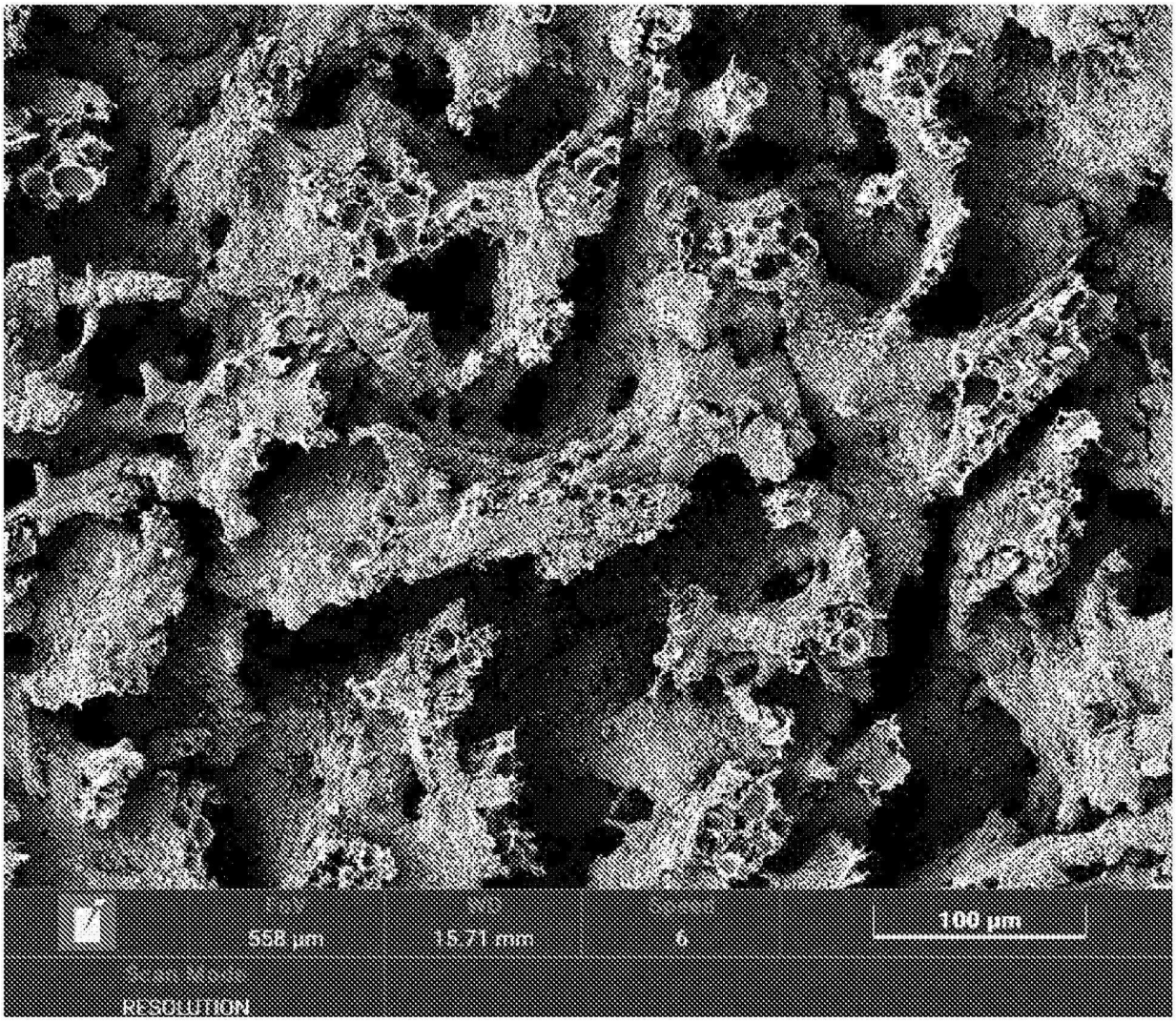

PPC Or Thru Gii-3.0（概念）
工艺流程
基板装载至连续印刷
印刷站1
(Ag) 印刷
固化
印刷站2
(C) 印刷
固化
印刷站3
电介质印刷
固化
Cognex目视检查
基于幅材的旋转印刷或基于幅材的平板印刷
PPC或Thru？
PPC
顺时针重绕
未翻转基板
Thru
逆时针重绕
翻转基板
将印刷基板卷材装入Gii-3.0设备
将基材与先前的幅材接合
张力控制
在X中的幅材对齐(幅材宽度)
空气刀清洁
Gii-3.0工艺
Gii转化1
Gii转化2
片材分割(GuiBotine)和PNP全储存
Gii？
Gii-Sens
Gii-Cap
EC QC分割
KY-N-UV10
UV激光切割
EC QC测试
EC QC分析
分割
KY-N-UV10
UV激光切割
装纸箱
手动
Manual
贴标牌
包装以供运输
调节
装袋后阻抗检查
装袋
手动
装袋前阻抗检查
水凝胶沉积
手动
贴标签
手动
分割
KY-N-UV10
UV激光切割

图51



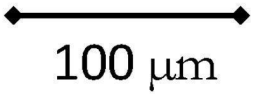
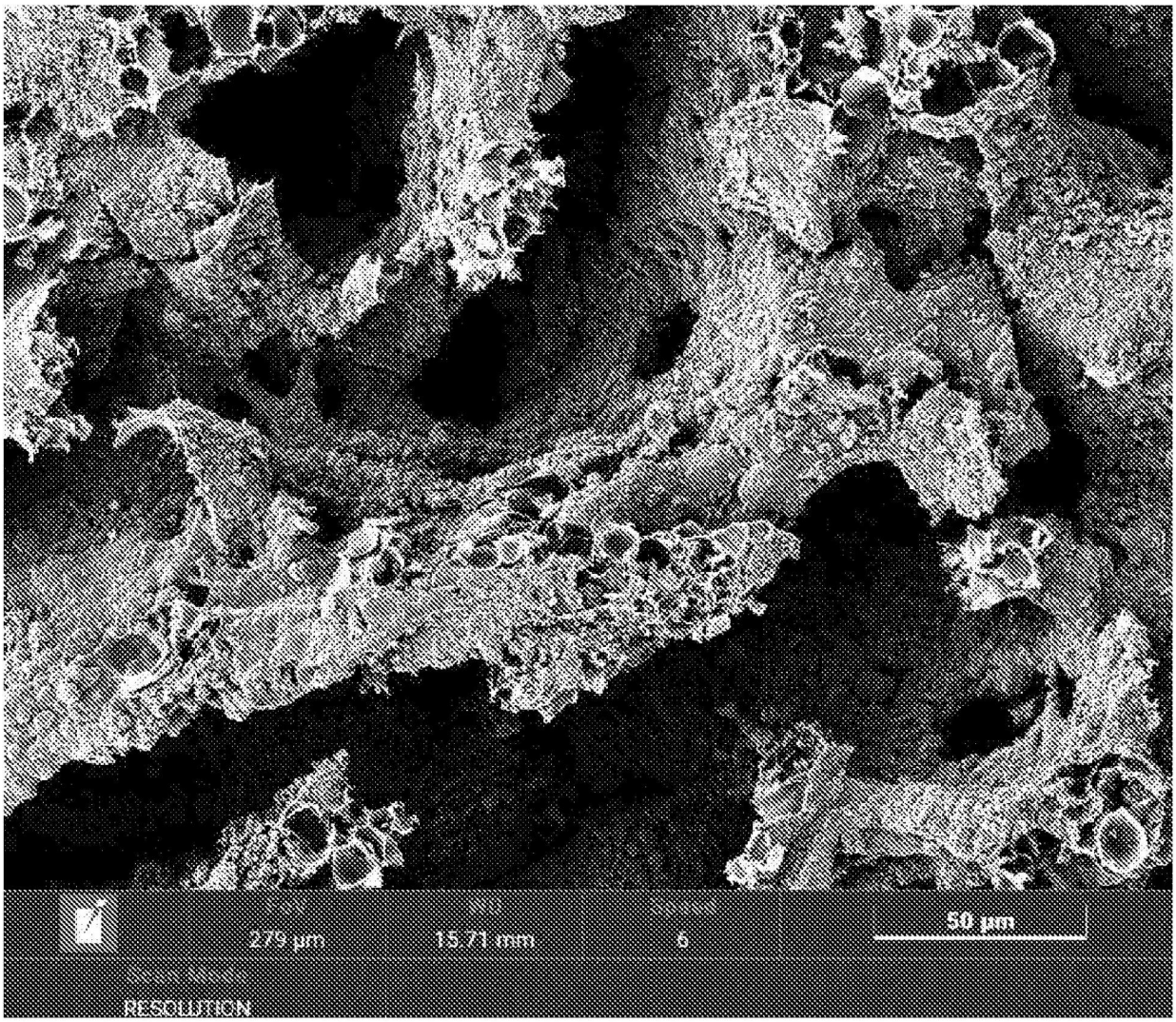
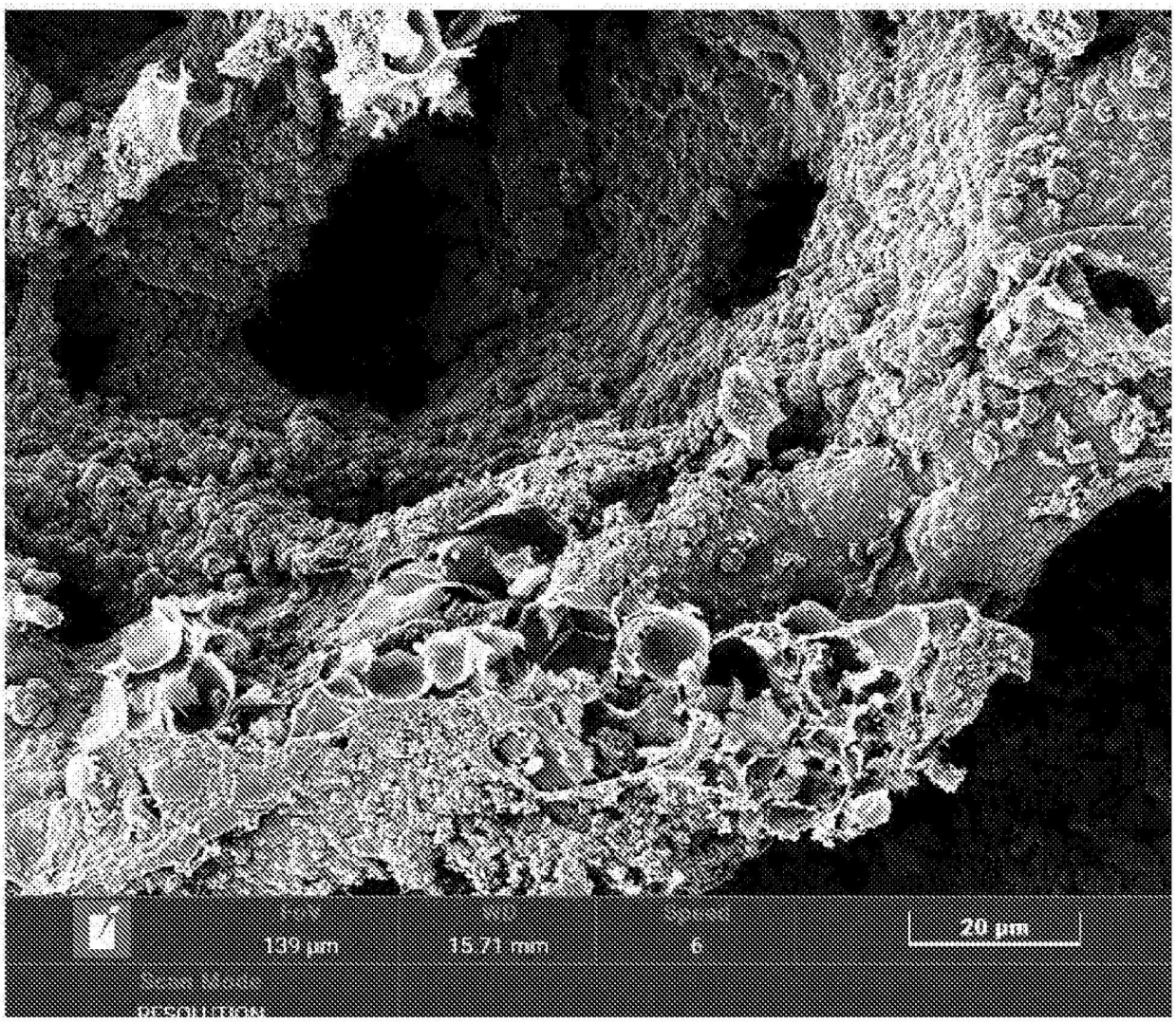


图52



50 µm

图53



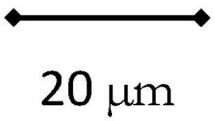


图54

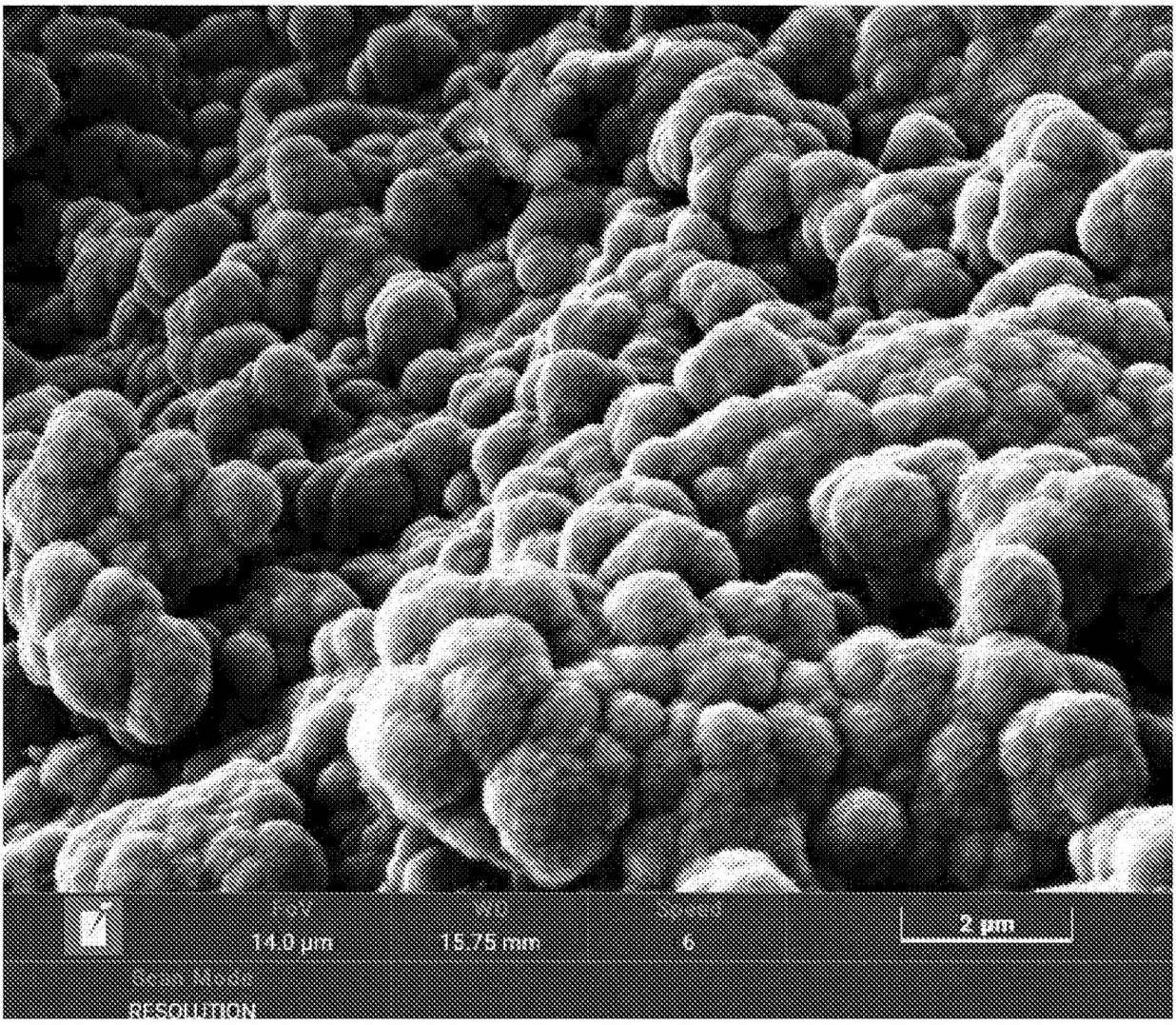
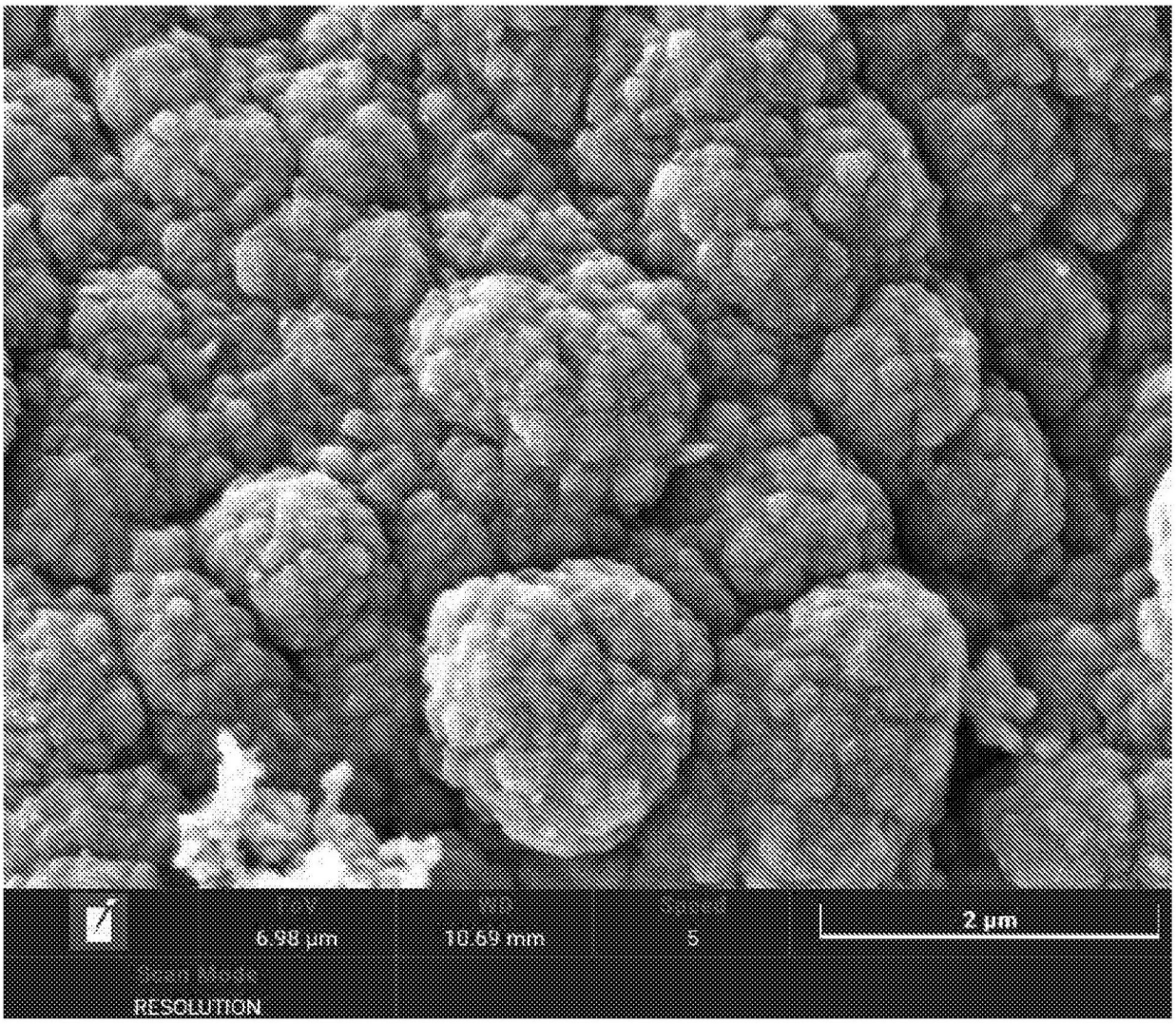


图55



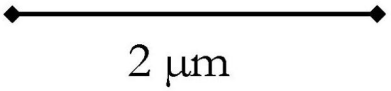
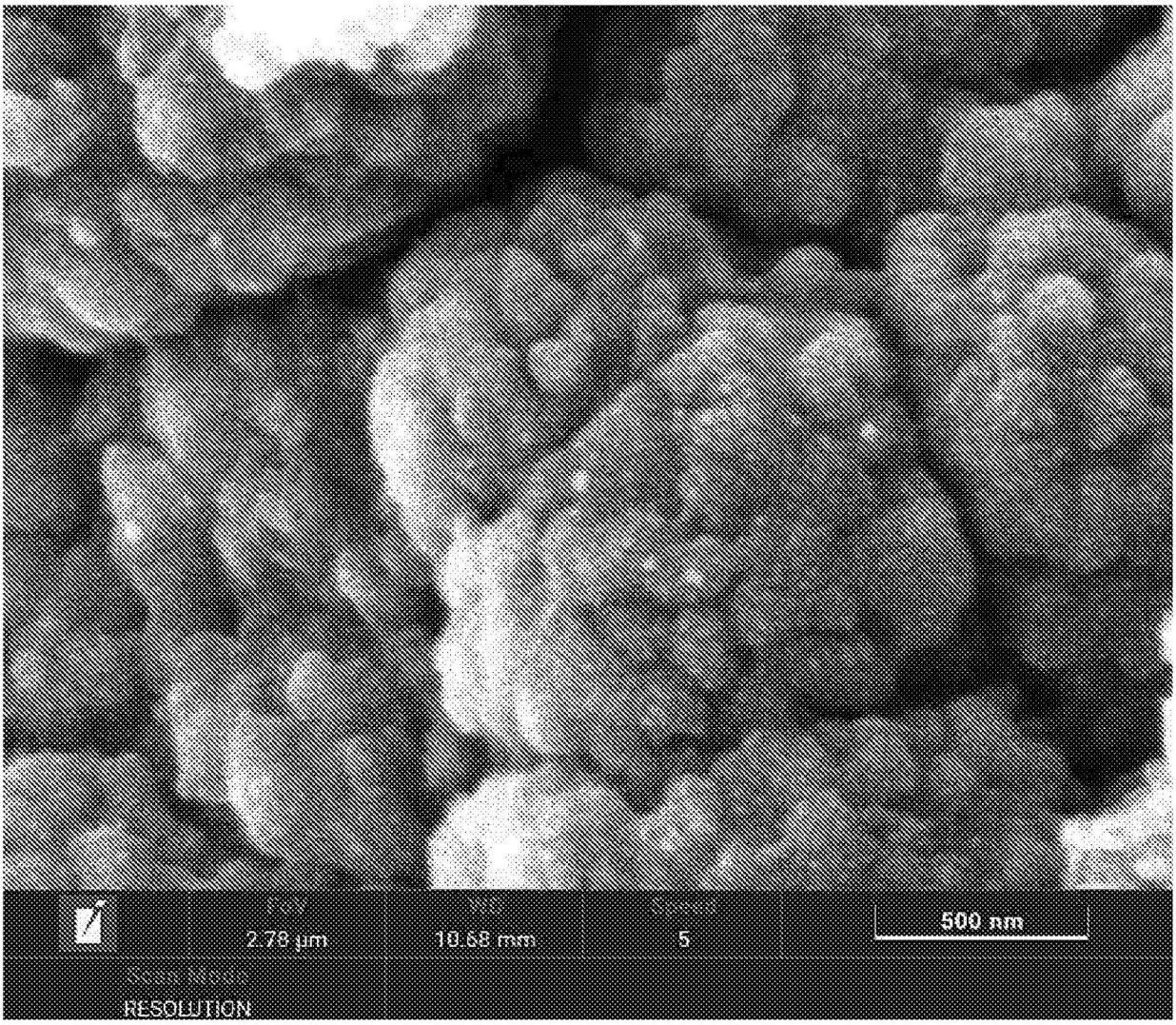


图56



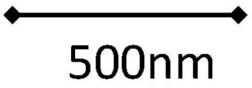


图57

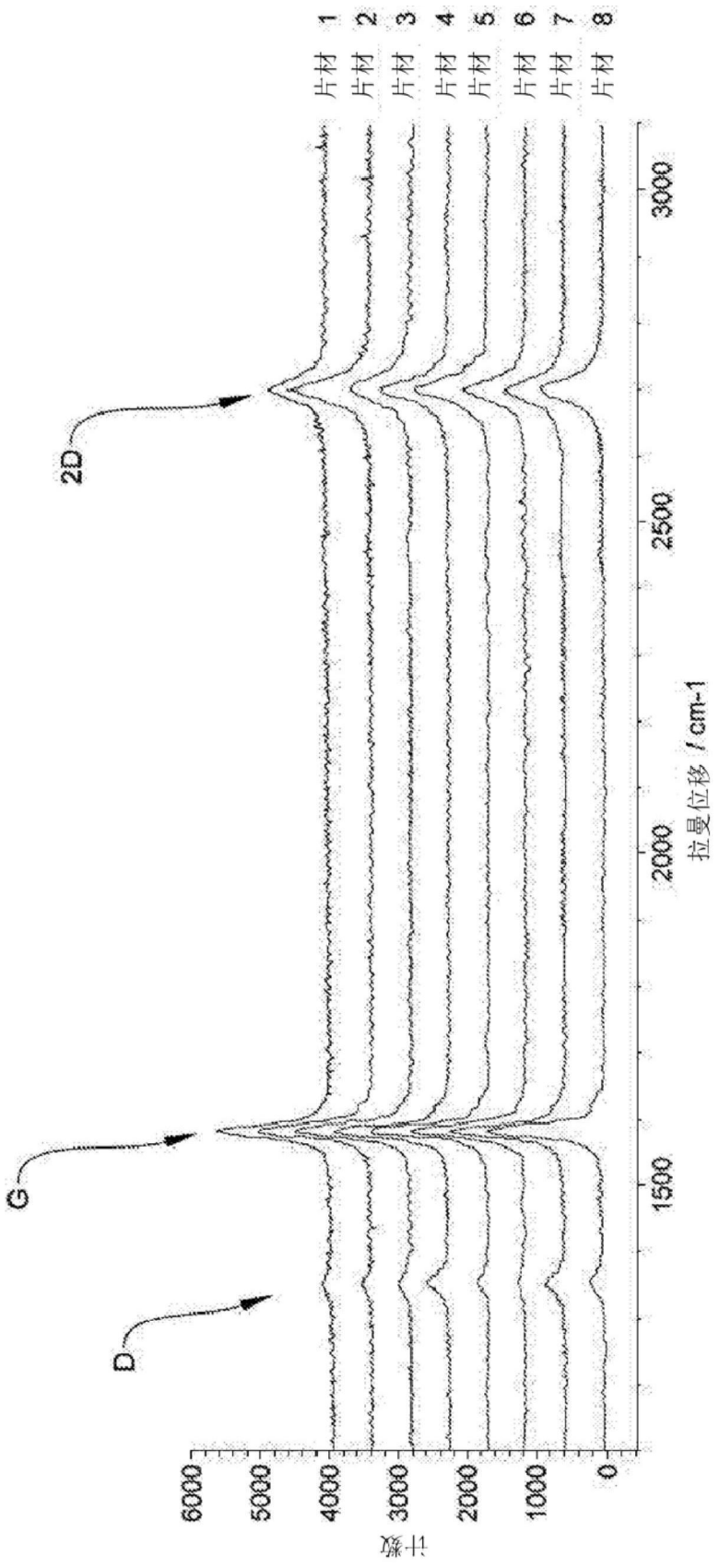

片材 1
片材 2
片材 3
片材 4
片材 5
片材 6
片材 7
片材 8
2D
G
D
计数
拉曼位移 / cm-1
6000
5000
4000
3000
2000
1000
0
1500
2000
2500
3000

图58

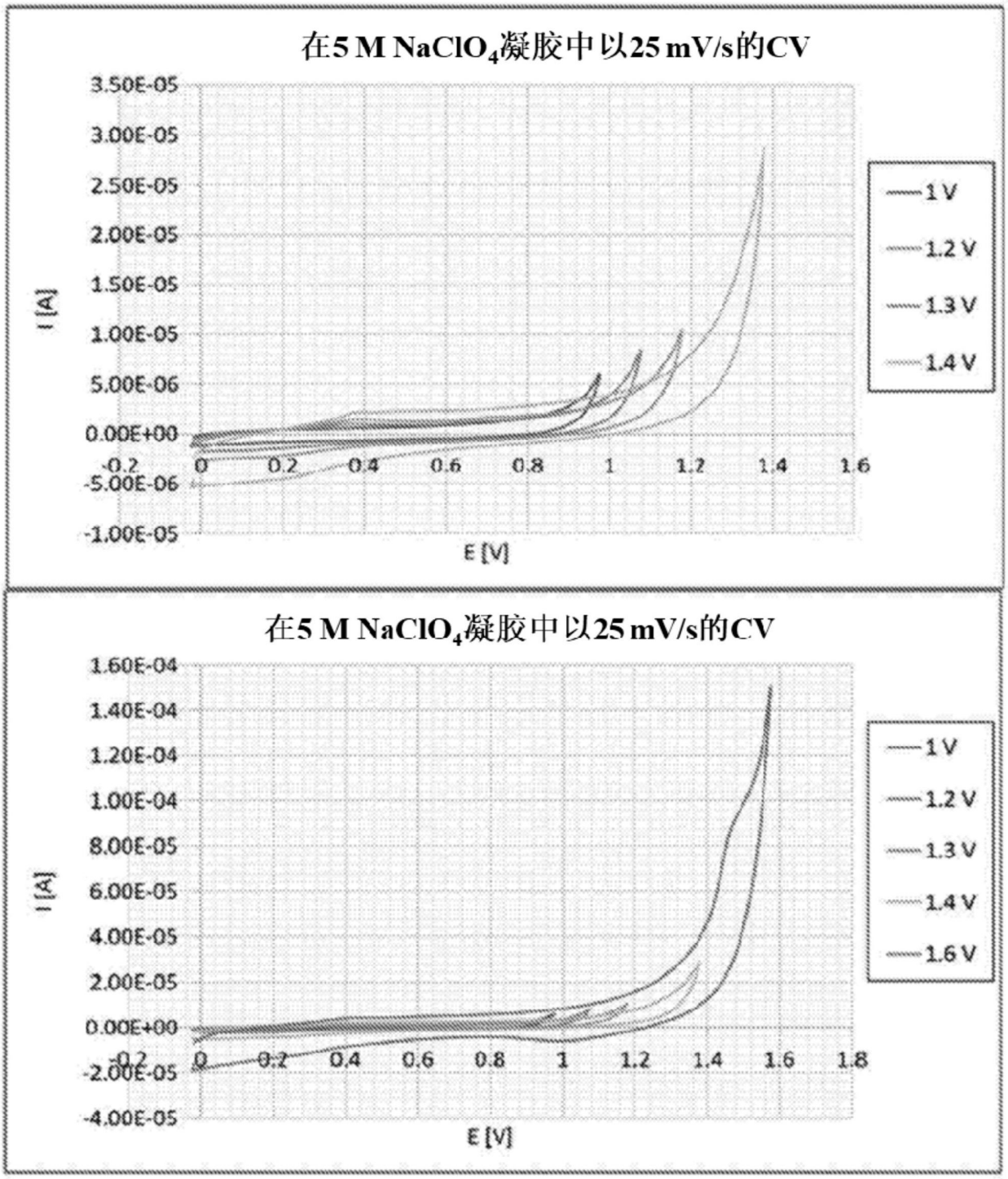

在5 M NaClO4凝胶中以25 mV/s的CV
3.50E-05
3.00E-05
2.50E-05
2.00E-05
1.50E-05
1.00E-05
5.00E-06
0.00E+00
-5.00E-06
-1.00E-05
I [A]
-0.2
0
0.2
0.4
0.6
0.8
1
1.2
1.4
1.6
E [V]
1 V
1.2 V
1.3 V
1.4 V
在5 M NaClO4凝胶中以25 mV/s的CV
1.60E-04
1.40E-04
1.20E-04
1.00E-04
8.00E-05
6.00E-05
4.00E-05
2.00E-05
0.00E+00
-2.00E-05
-4.00E-05
I [A]
-0.2
0
0.2
0.4
0.6
0.8
1
1.2
1.4
1.6
1.8
E [V]
1 V
1.2 V
1.3 V
1.4 V
1.6 V

图59

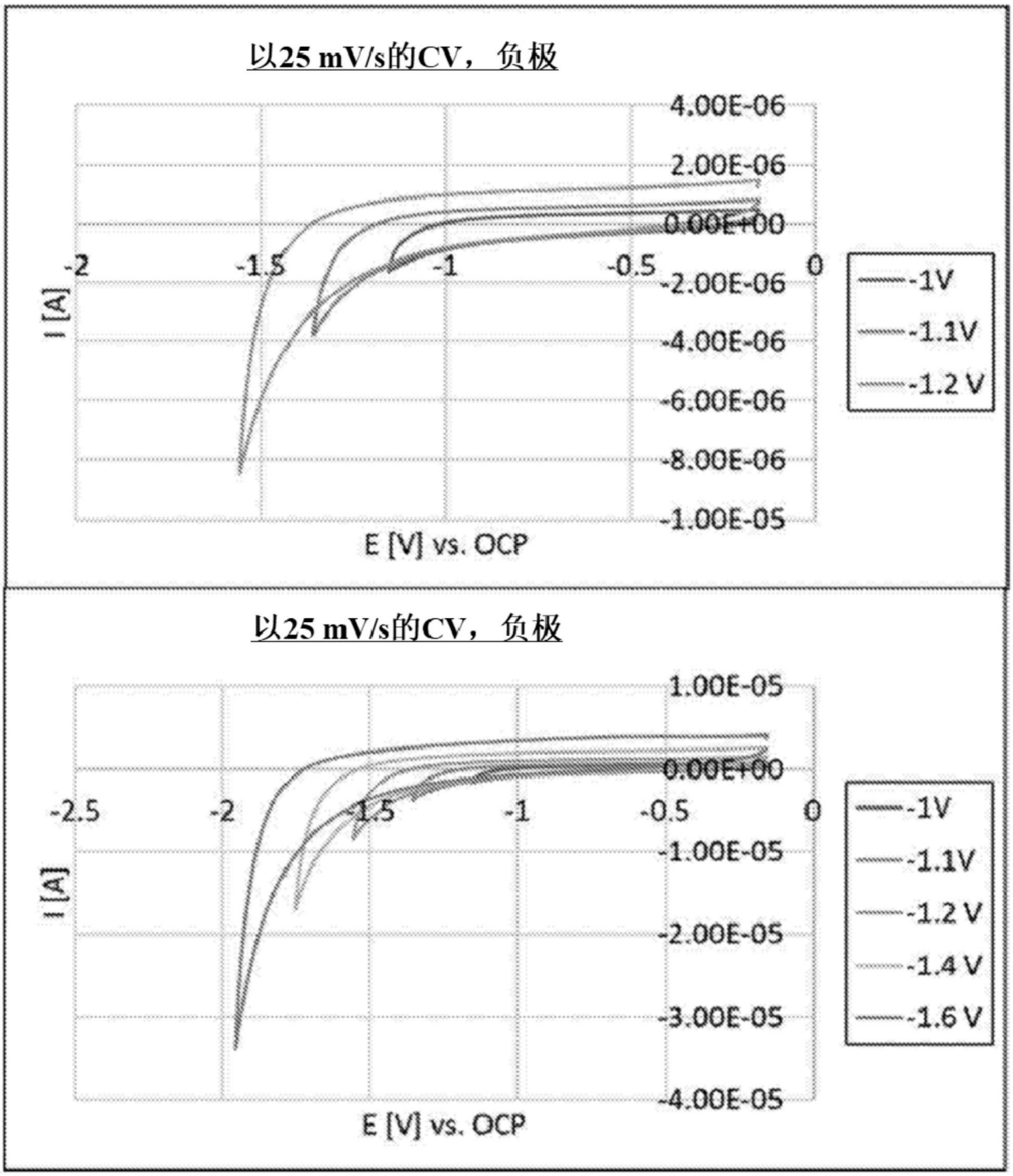

以25 mV/s的CV，负极
4.00E-06
2.00E-06
0.00E+00
-2.00E-06
-4.00E-06
-6.00E-06
-8.00E-06
-1.00E-05
-2
-1.5
-1
-0.5
0
I [A]
E [V] vs. OCP
-1V
-1.1V
-1.2 V
以25 mV/s的CV，负极
1.00E-05
0.00E+00
-1.00E-05
-2.00E-05
-3.00E-05
-4.00E-05
-2.5
-2
-1.5
-1
-0.5
0
I [A]
E [V] vs. OCP
-1V
-1.1V
-1.2 V
-1.4 V
-1.6 V

图60

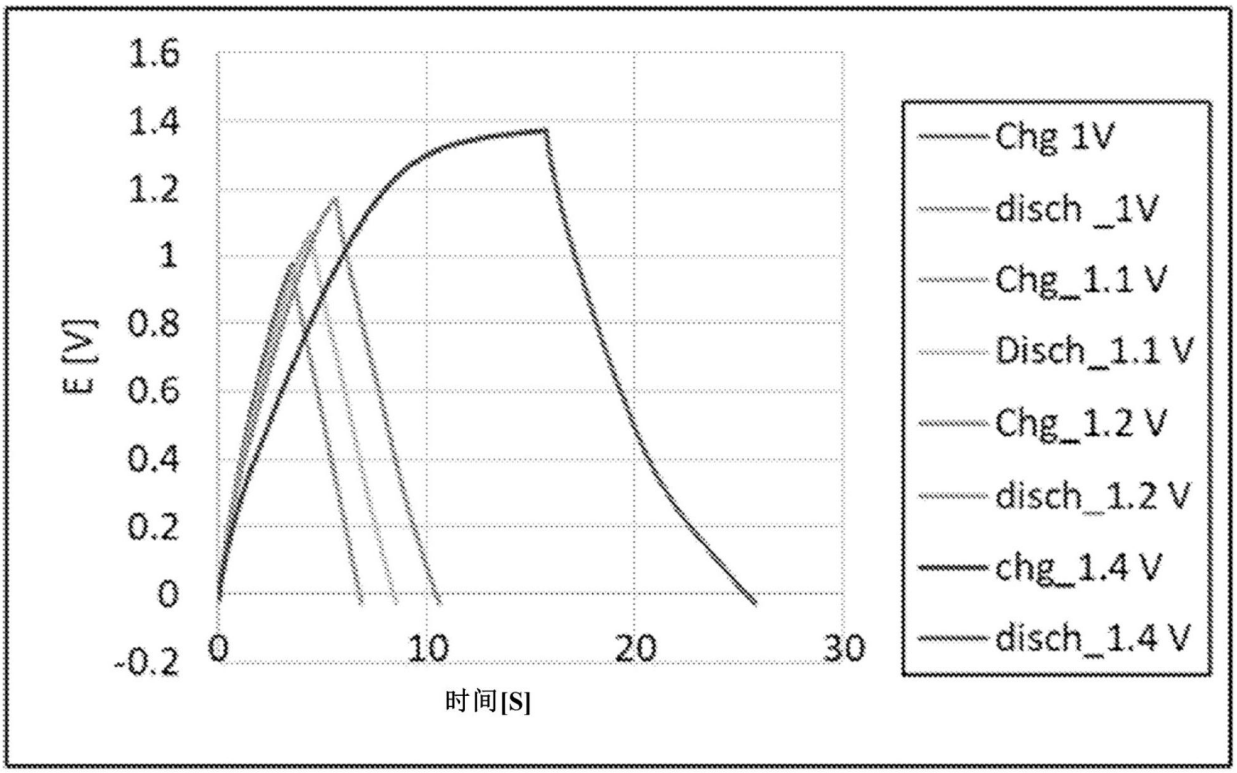

1.6
1.4
1.2
1
0.8
0.6
0.4
0.2
0
-0.2
E [V]
0
10
20
30
时间[S]
Chg 1V
disch _1V
Chg_1.1 V
Disch_1.1 V
Chg_1.2 V
disch_1.2 V
chg_1.4 V
disch_1.4 V

图61

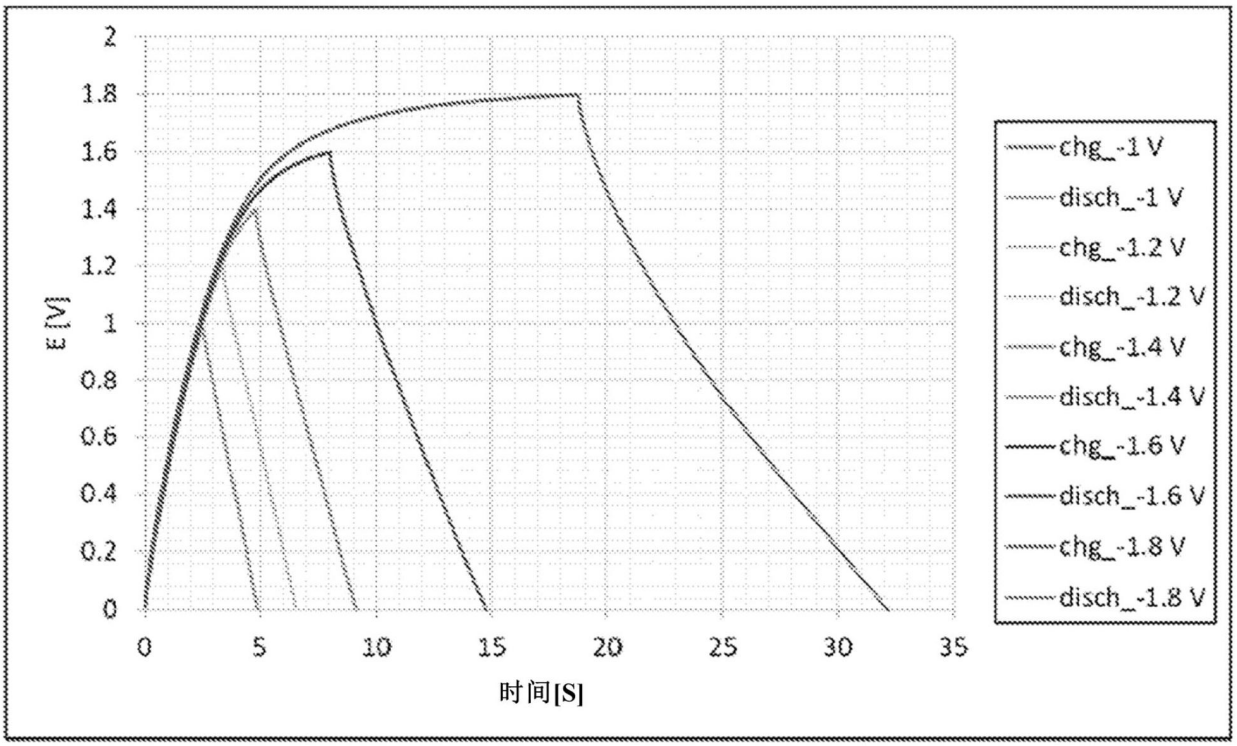

2
1.8
1.6
1.4
1.2
1
0.8
0.6
0.4
0.2
0
E [V]
0
5
10
15
20
25
30
35
时间[S]
chg_-1 V
disch_-1 V
chg_-1.2 V
disch_-1.2 V
chg_-1.4 V
disch_-1.4 V
chg_-1.6 V
disch_-1.6 V
chg_-1.8 V
disch_-1.8 V

图62

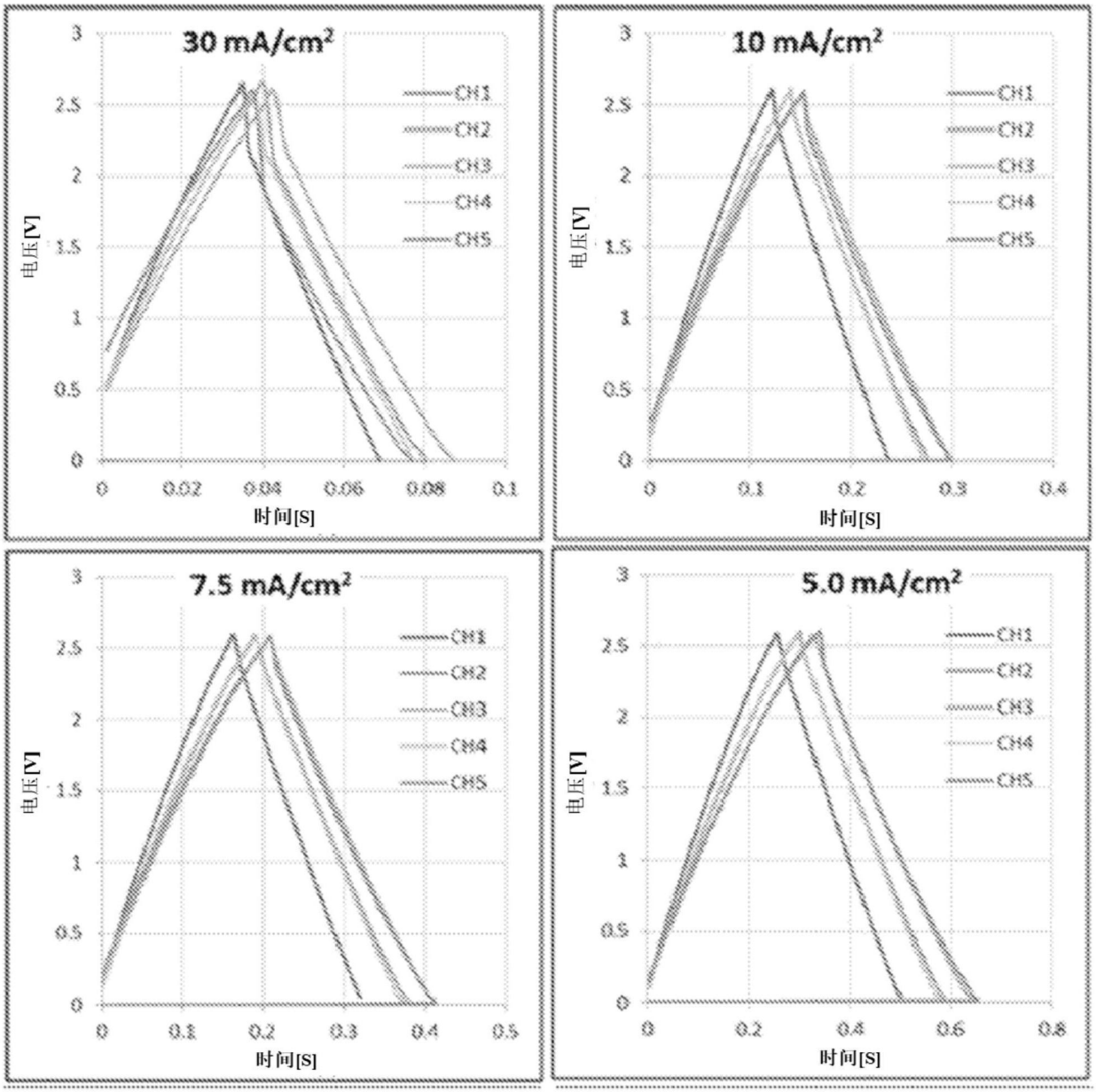


图63

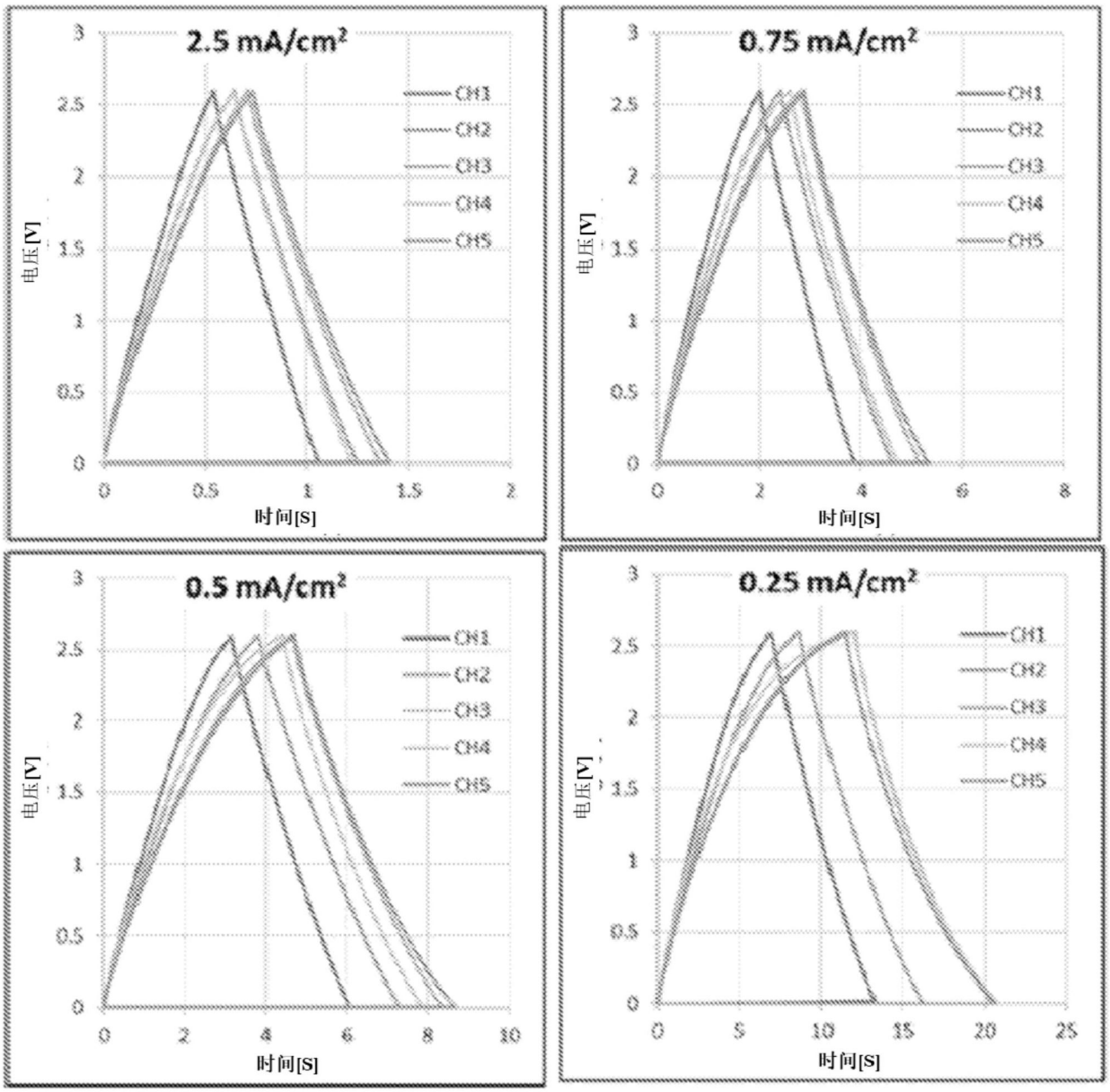

2.5 mA/cm²
0.75 mA/cm²
0.5 mA/cm²
0.25 mA/cm²
电压[V]
时间[S]
CH1
CH2
CH3
CH4
CH5

图63

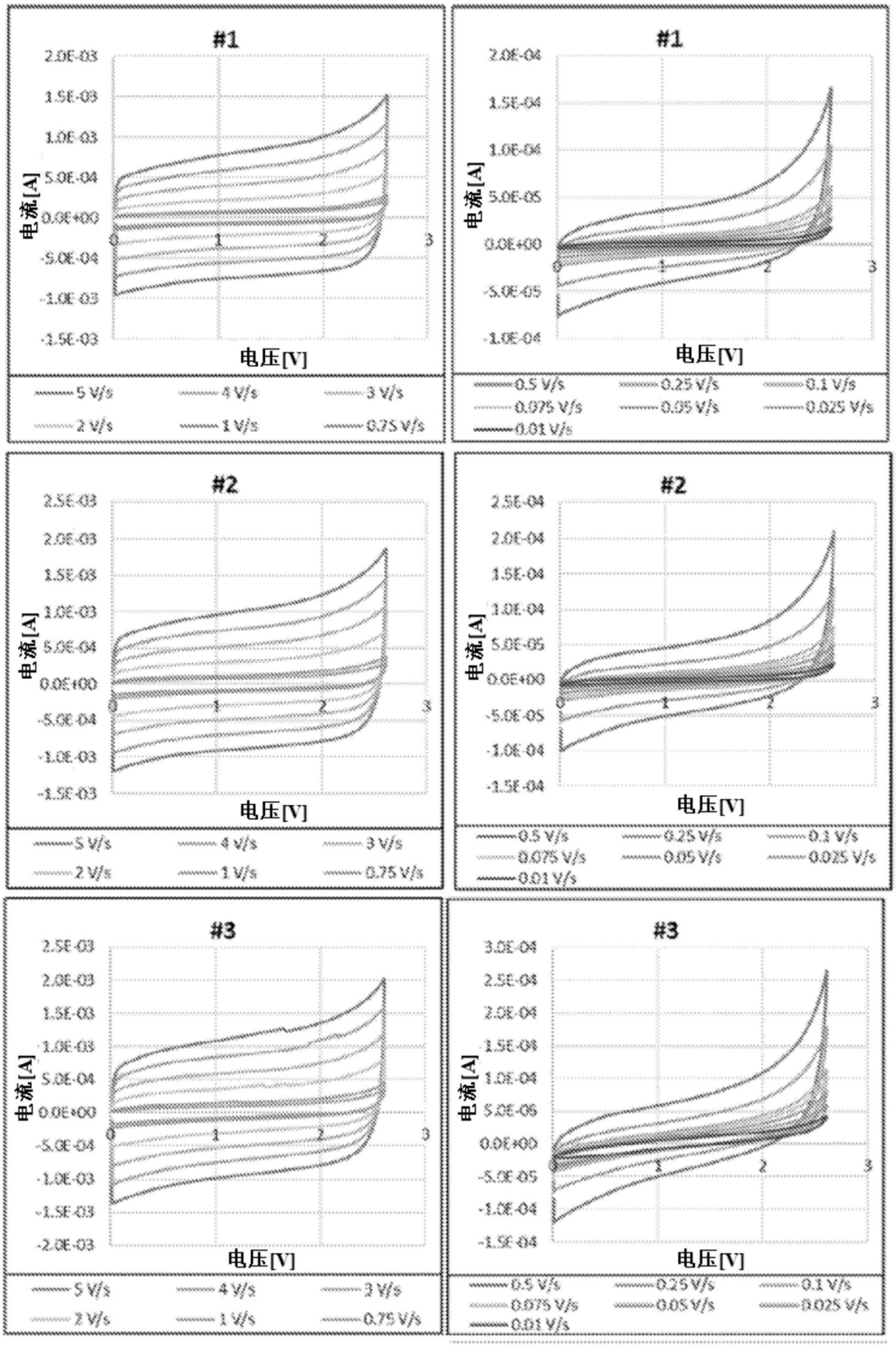
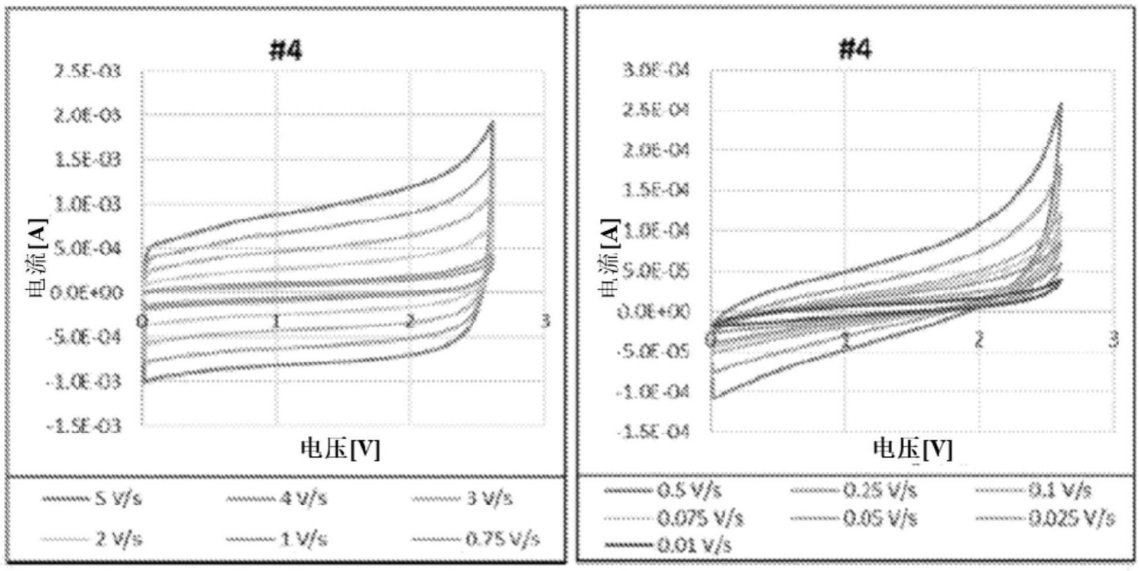

#1
电流[A]
电压[V]
5 V/s
4 V/s
3 V/s
2 V/s
1 V/s
0.75 V/s
#1
电流[A]
电压[V]
0.5 V/s
0.25 V/s
0.1 V/s
0.075 V/s
0.05 V/s
0.025 V/s
0.01 V/s
#2
电流[A]
电压[V]
5 V/s
4 V/s
3 V/s
2 V/s
1 V/s
0.75 V/s
#2
电流[A]
电压[V]
0.5 V/s
0.25 V/s
0.1 V/s
0.075 V/s
0.05 V/s
0.025 V/s
0.01 V/s
#3
电流[A]
电压[V]
5 V/s
4 V/s
3 V/s
2 V/s
1 V/s
0.75 V/s
#3
电流[A]
电压[V]
0.5 V/s
0.25 V/s
0.1 V/s
0.075 V/s
0.05 V/s
0.025 V/s
0.01 V/s

图64


#4
电流[A]
电压[V]
5 V/s
4 V/s
3 V/s
2 V/s
1 V/s
0.75 V/s
#4
电流[A]
电压[V]
0.5 V/s
0.25 V/s
0.1 V/s
0.075 V/s
0.05 V/s
0.025 V/s
0.01 V/s

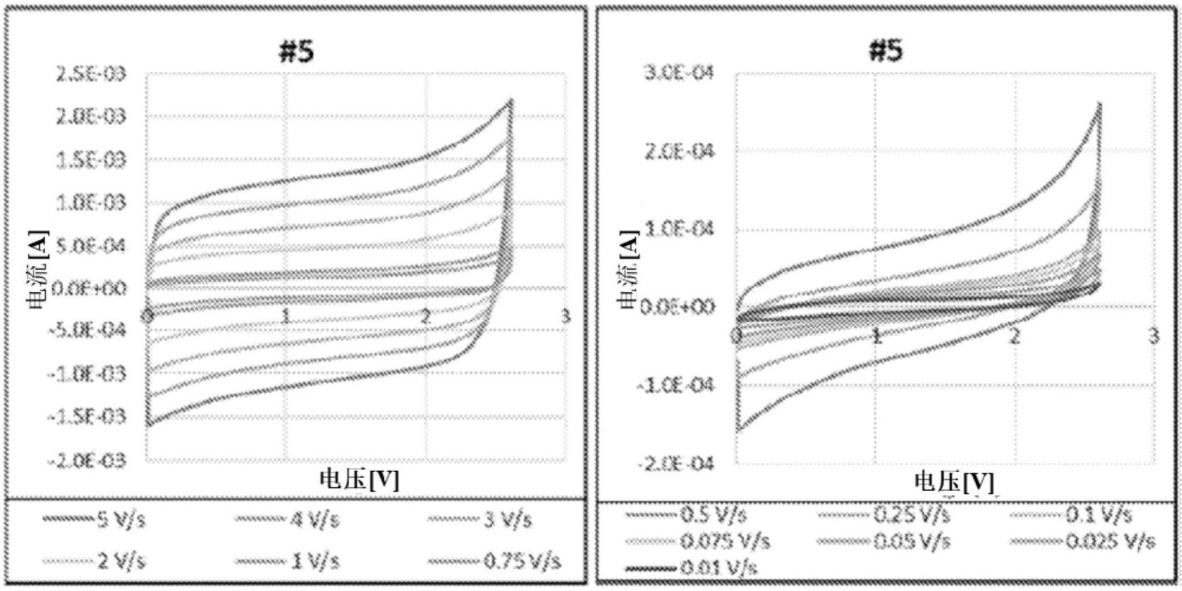
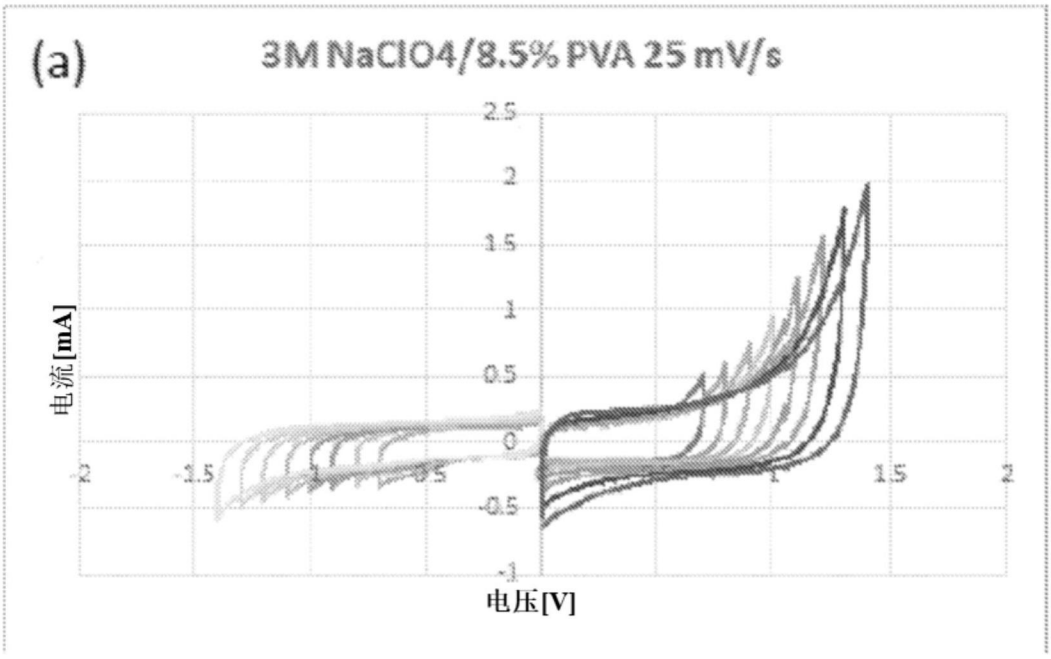

#5
电流[A]
电压[V]
5 V/s
4 V/s
3 V/s
2 V/s
1 V/s
0.75 V/s
#5
电流[A]
电压[V]
0.5 V/s
0.25 V/s
0.1 V/s
0.075 V/s
0.05 V/s
0.025 V/s
0.01 V/s

图64


(a)
3M NaClO4/8.5% PVA 25 mV/s
电流[mA]
电压[V]
2.5
2
1.5
1
0.5
0
-0.5
-1
-2
-1.5
-1
-0.5
0.5
1
1.5
2

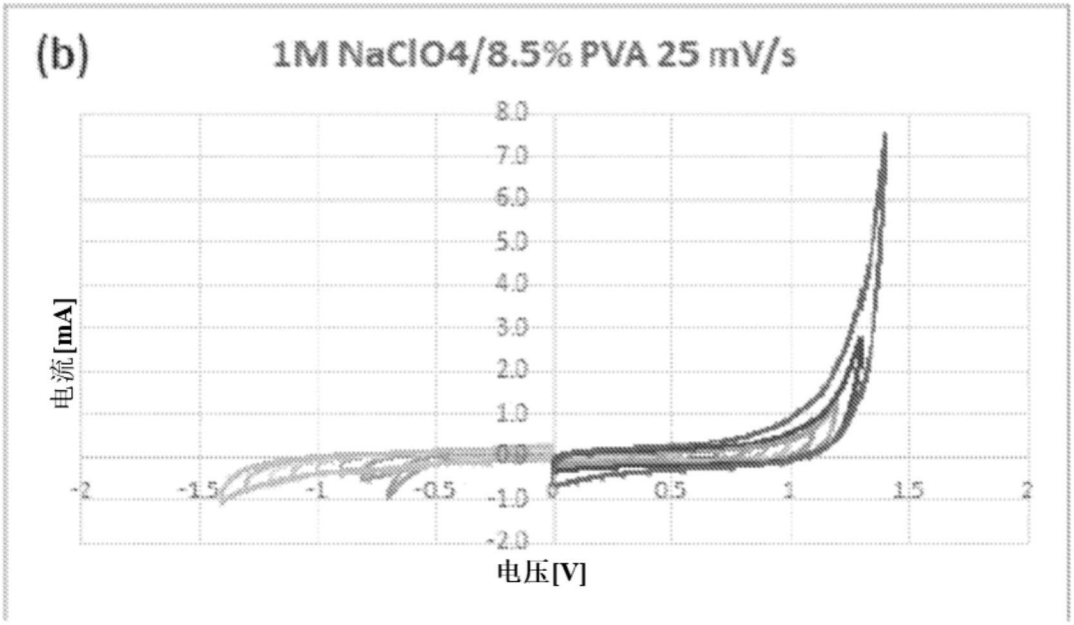

(b)
1M NaClO4/8.5% PVA 25 mV/s
电流[mA]
电压[V]
8.0
7.0
6.0
5.0
4.0
3.0
2.0
1.0
0.0
-1.0
-2.0
-2
-1.5
-1
-0.5
0
0.5
1
1.5
2

图65

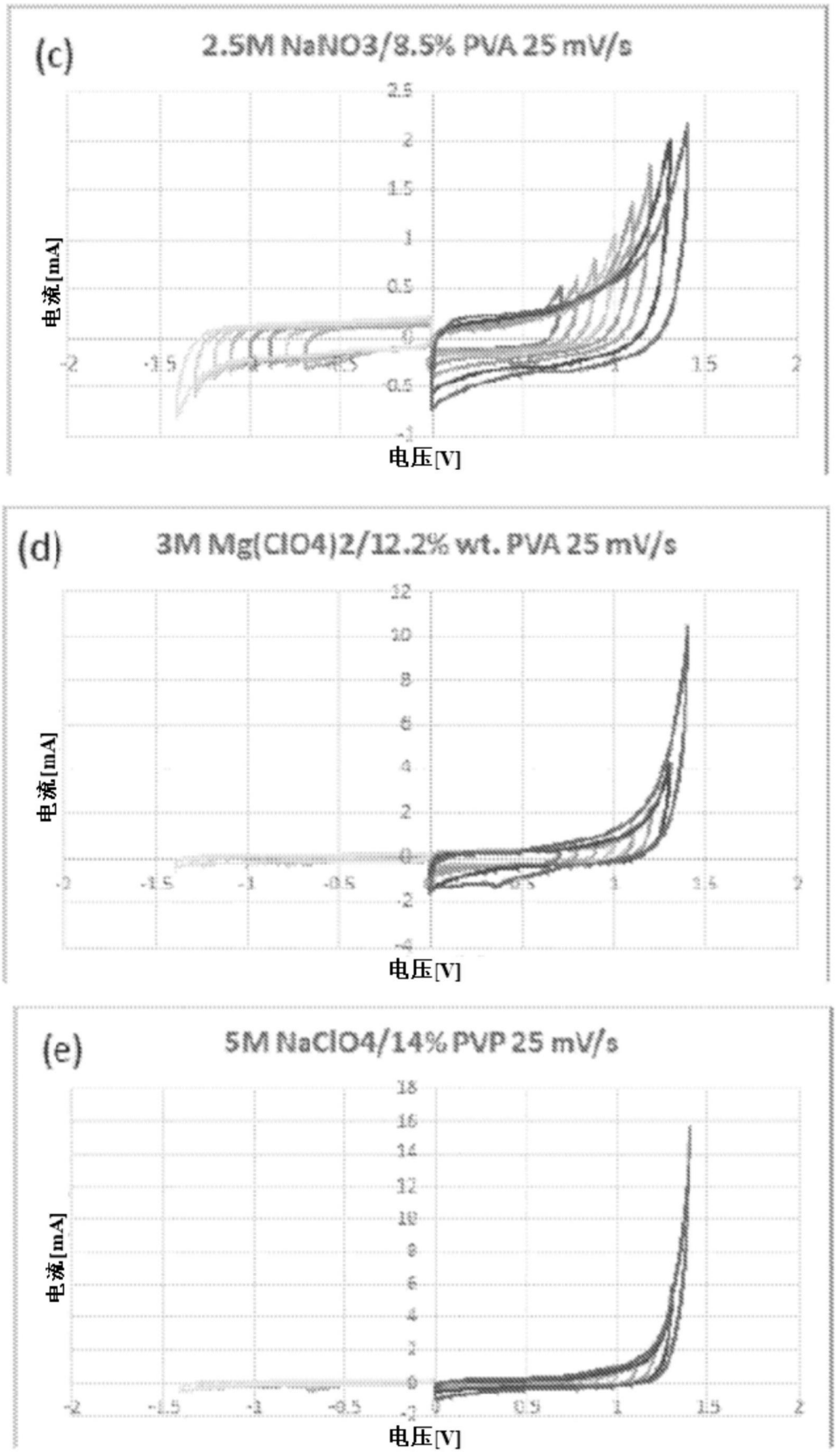

(c)
2.5M NaNO3/8.5% PVA 25 mV/s
电流[mA]
电压[V]
(d)
3M Mg(ClO4)2/12.2% wt. PVA 25 mV/s
电流[mA]
电压[V]
(e)
5M NaClO4/14% PVP 25 mV/s
电流[mA]
电压[V]

图65

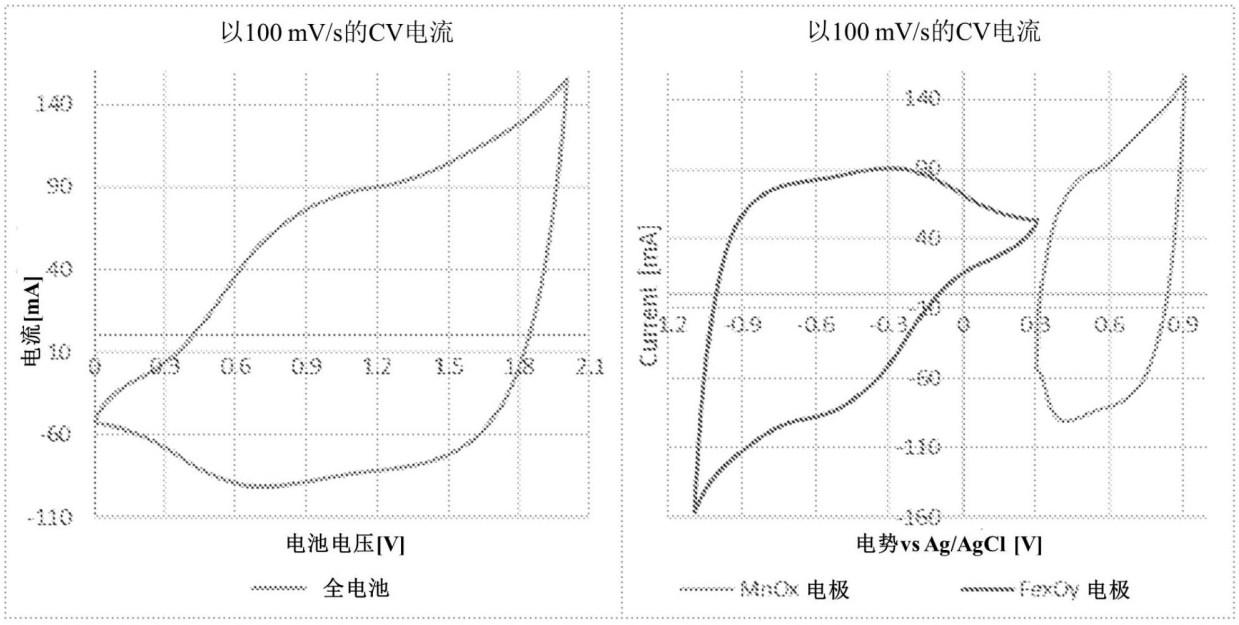

以100 mV/s的CV电流
电流[mA]
电池电压[V]
全电池
以100 mV/s的CV电流
Current [mA]
电势vs Ag/AgCl [V]
MnOx 电极
FexOy 电极

图66

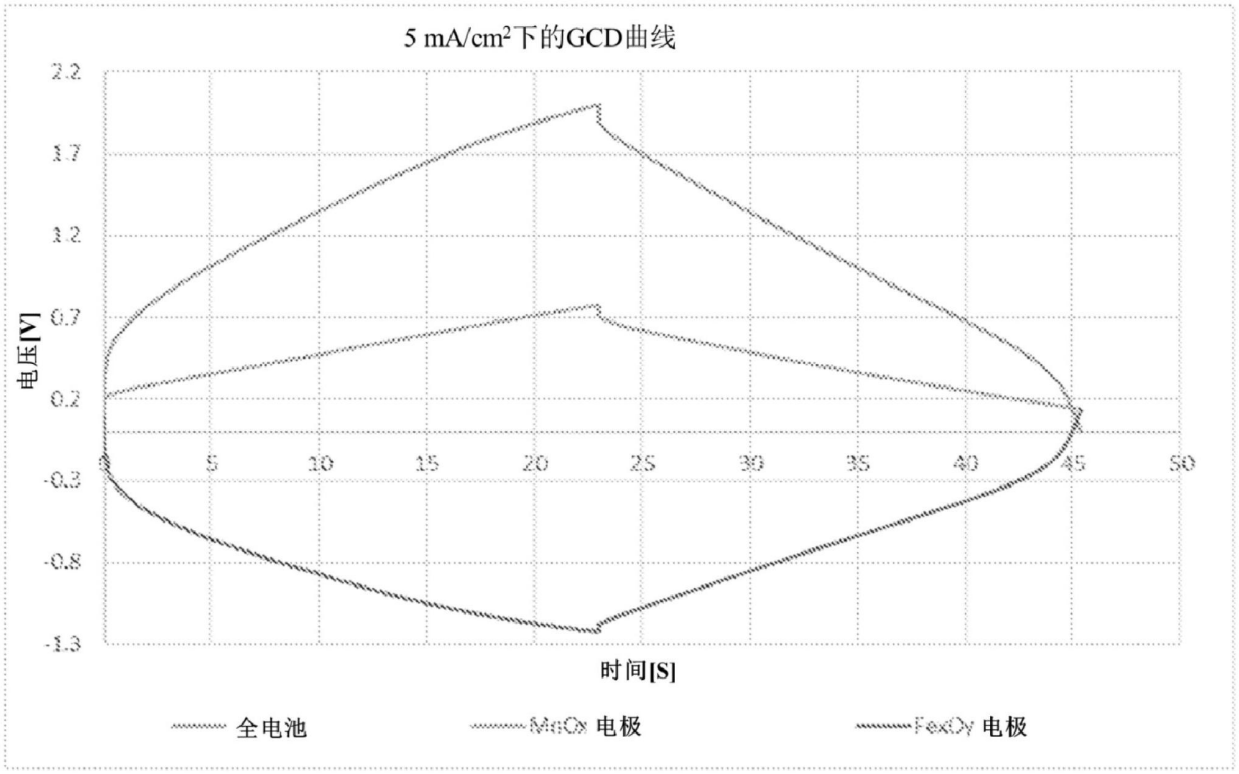

5 mA/cm²下的GCD曲线
电压[V]
时间[S]
全电池
MnOx 电极
FexOy 电极

图67

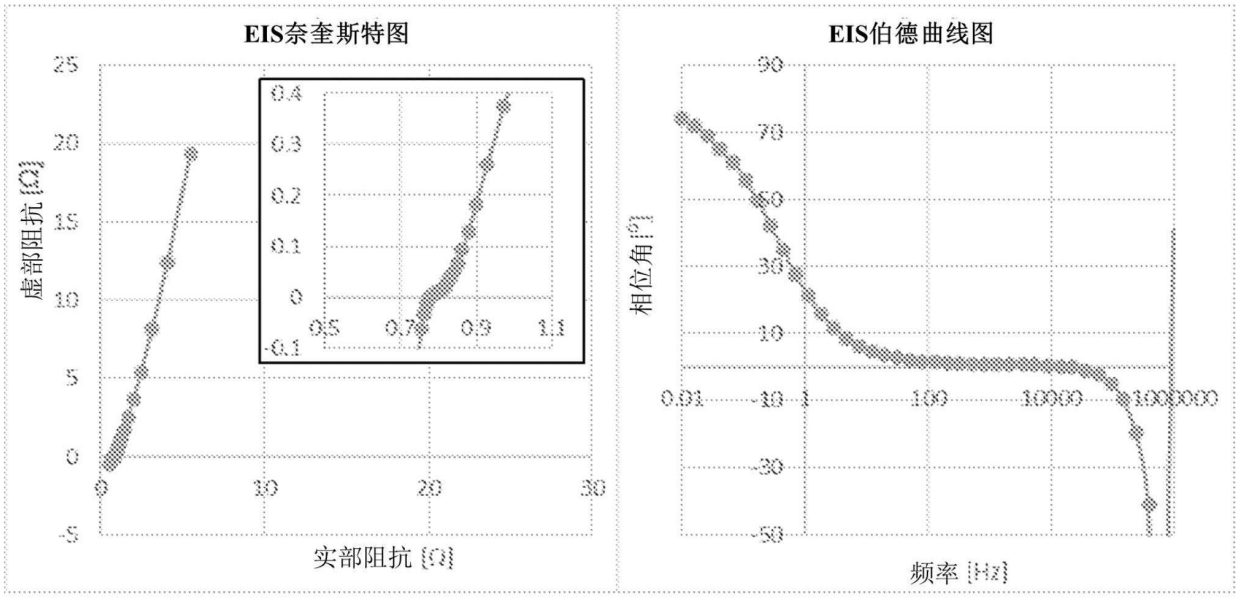

EIS奈奎斯特图
虚部阻抗 [Ω]
实部阻抗 [Ω]
EIS伯德曲线图
相位角 [°]
频率 [Hz]

图68

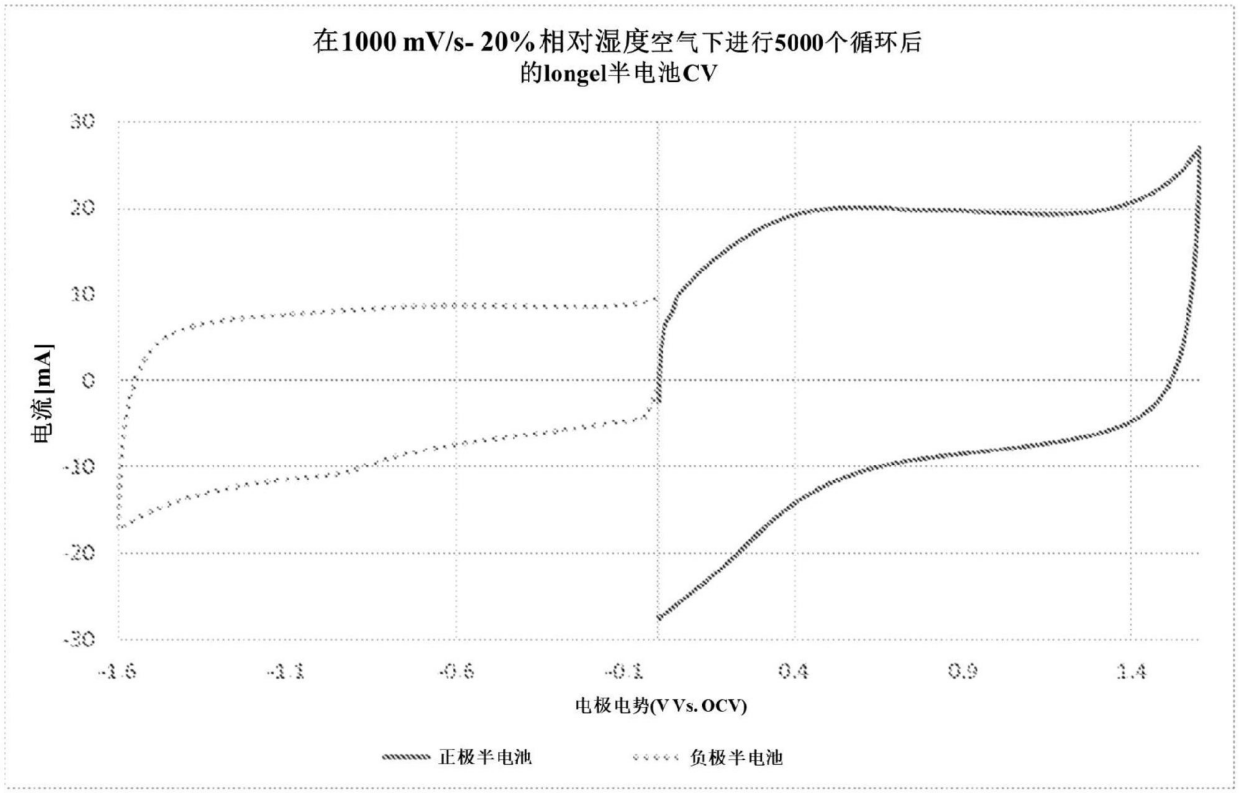

在1000 mV/s- 20%相对湿度空气下进行5000个循环后
的longel半电池CV
电流 [mA]
电极电势(V Vs. OCV)
正极半电池
负极半电池

图69

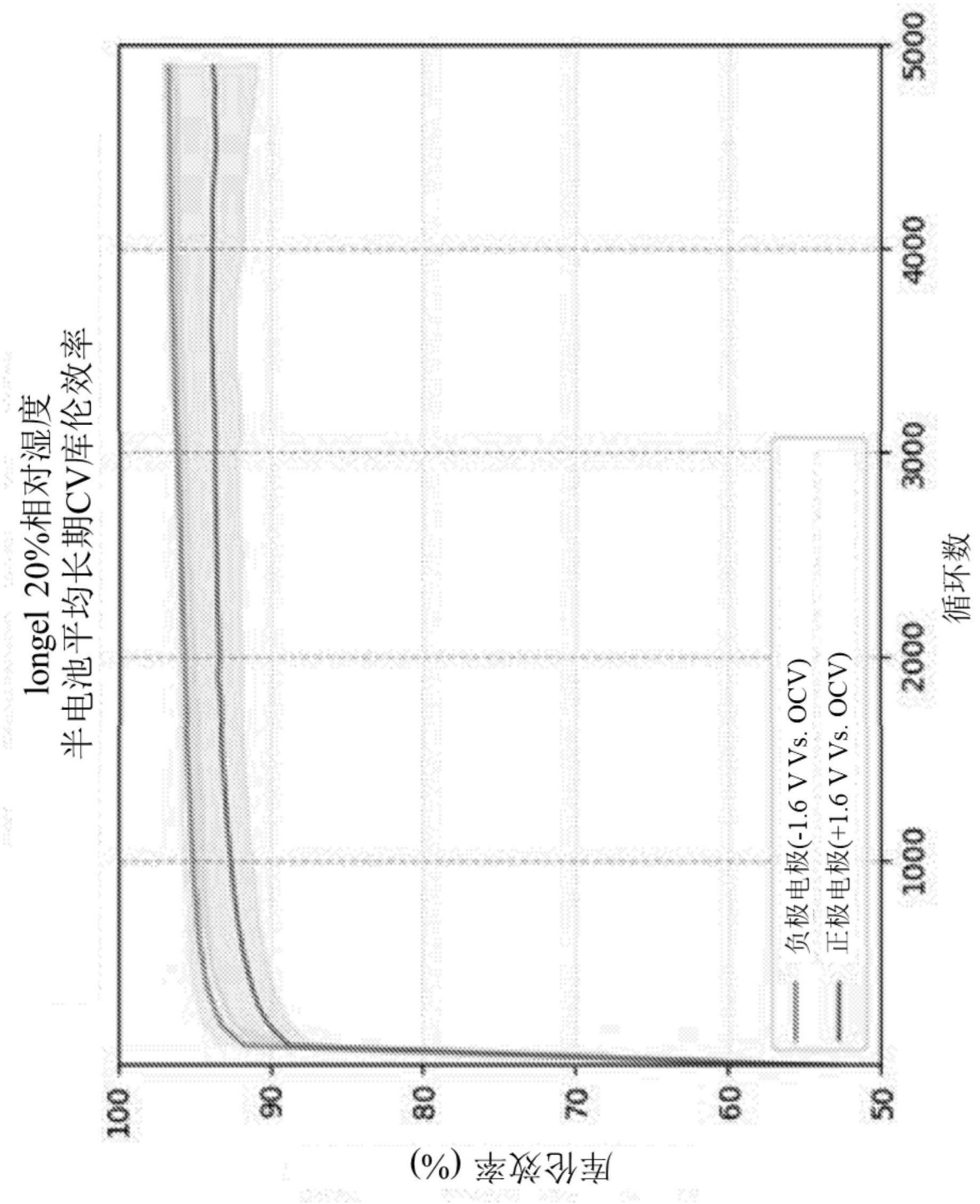

longel 20%相对湿度
半电池平均长期CV库伦效率
库伦效率 (%)
100
90
80
70
60
50
1000
2000
3000
4000
5000
循环数
负极电极(-1.6 V Vs. OCV)
正极电极(+1.6 V Vs. OCV)

图70

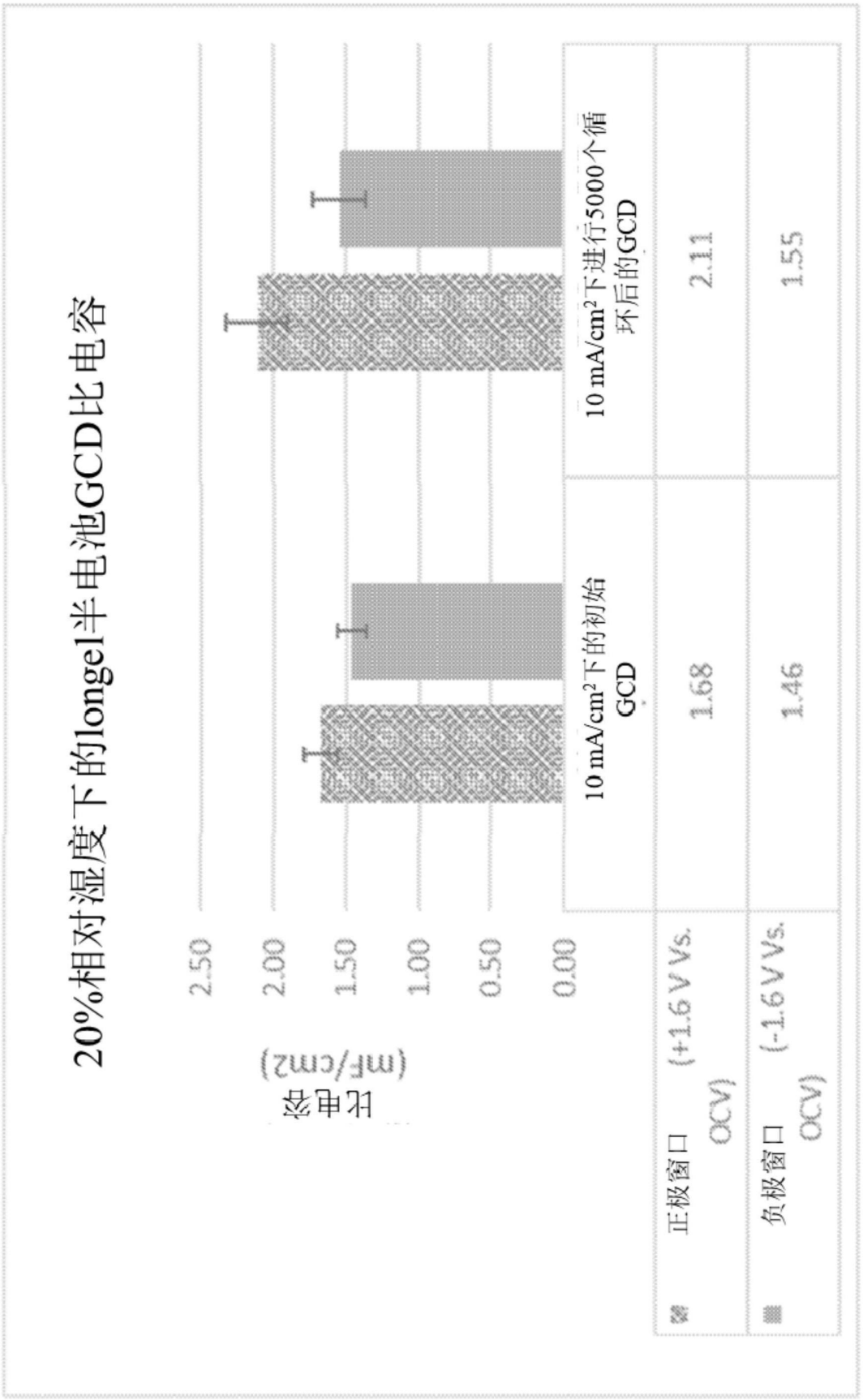

20%相对湿度下的longel半电池GCD比电容
比电容
(mF/cm2)
2.50
2.00
1.50
1.00
0.50
0.00
10 mA/cm² 下的初始 GCD
10 mA/cm² 下进行5000个循环后的GCD
正极窗口 (+1.6 V Vs. OCV)
1.68
2.11
负极窗口 (-1.6 V Vs. OCV)
1.46
1.55

图71

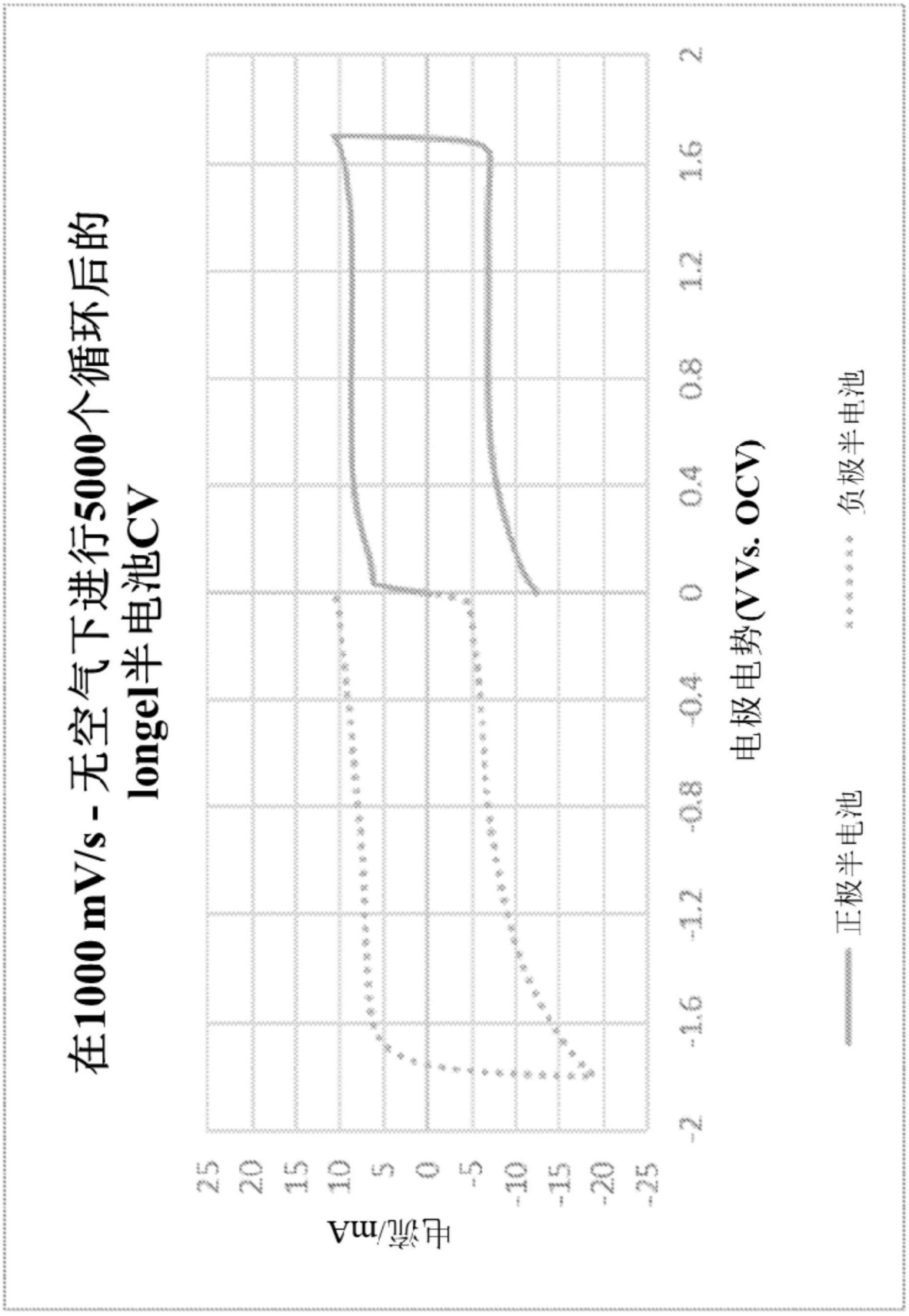

在1000 mV/s - 无空气下进行5000个循环后的
longel半电池CV
电流/mA
25
20
15
10
5
0
-5
-10
-15
-20
-25
-2
-1.6
-1.2
-0.8
-0.4
0
0.4
0.8
1.2
1.6
2
电极电势(V Vs. OCV)
正极半电池
负极半电池

图72

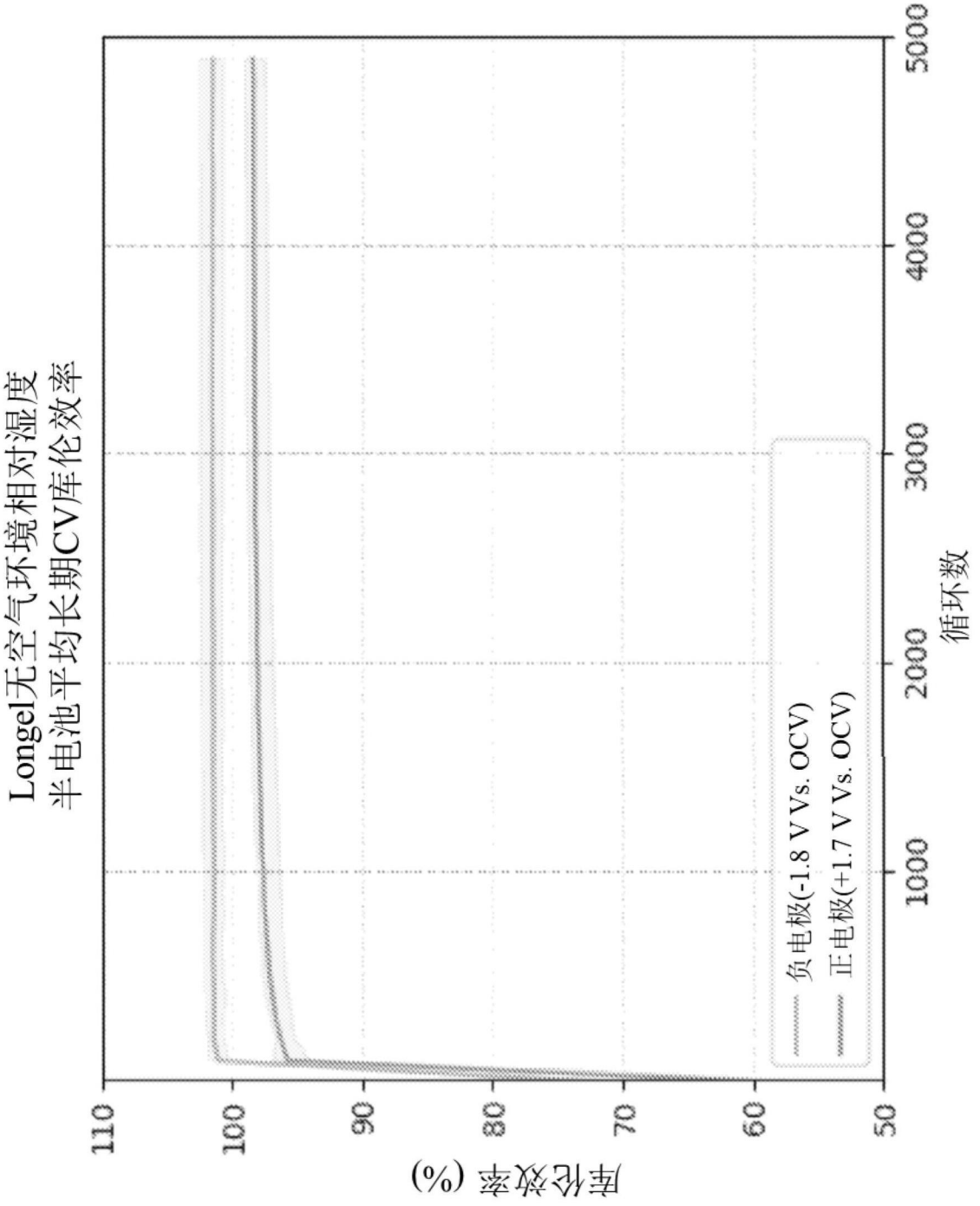

Longel无空气环境相对湿度
半电池平均长期CV库伦效率
库伦效率 (%)
110
100
90
80
70
60
50
1000
2000
3000
4000
5000
循环数
负电极(-1.8 V Vs. OCV)
正电极(+1.7 V Vs. OCV)

图73

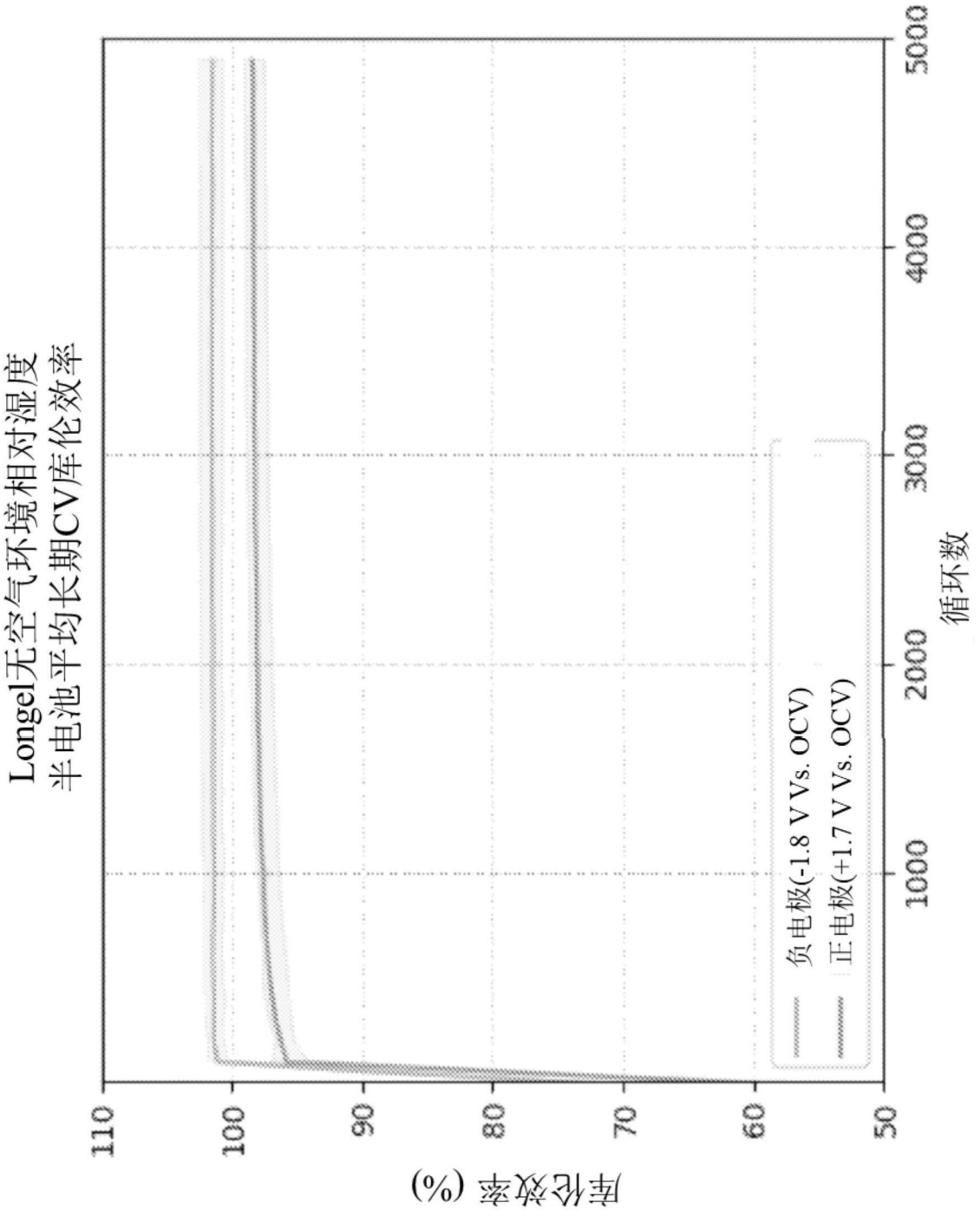

Longel无空气环境相对湿度
半电池平均长期CV库伦效率
库伦效率 (%)
循环数
负电极(-1.8 V Vs. OCV)
正电极(+1.7 V Vs. OCV)
110
100
90
80
70
60
50
1000
2000
3000
4000
5000

图74

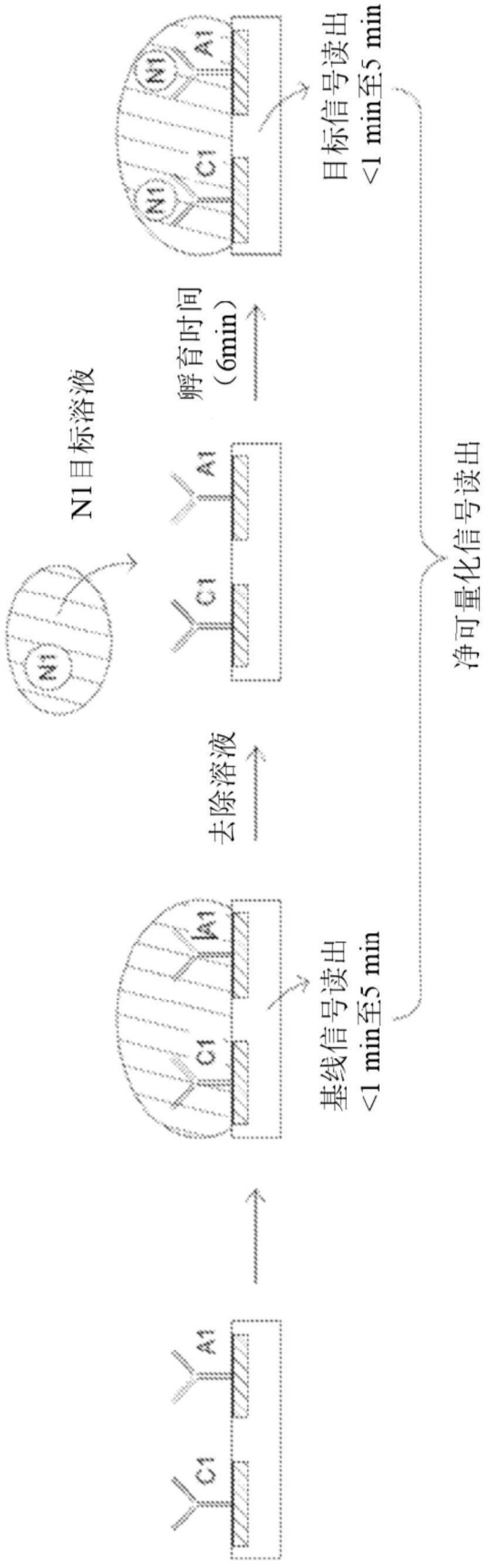

N1目标溶液
孵育时间
（6min）
去除溶液
基线信号读出
<1 min至5 min
目标信号读出
<1 min至5 min
净可量化信号读出
A1
C1
N1

图75


干燥传感器
50 uL Echem读出溶液
读出
3 min
N1抗原(加入Echem读出溶液中)
孵育
6 min
50 uL Echem读出溶液
读出
3 min

图76

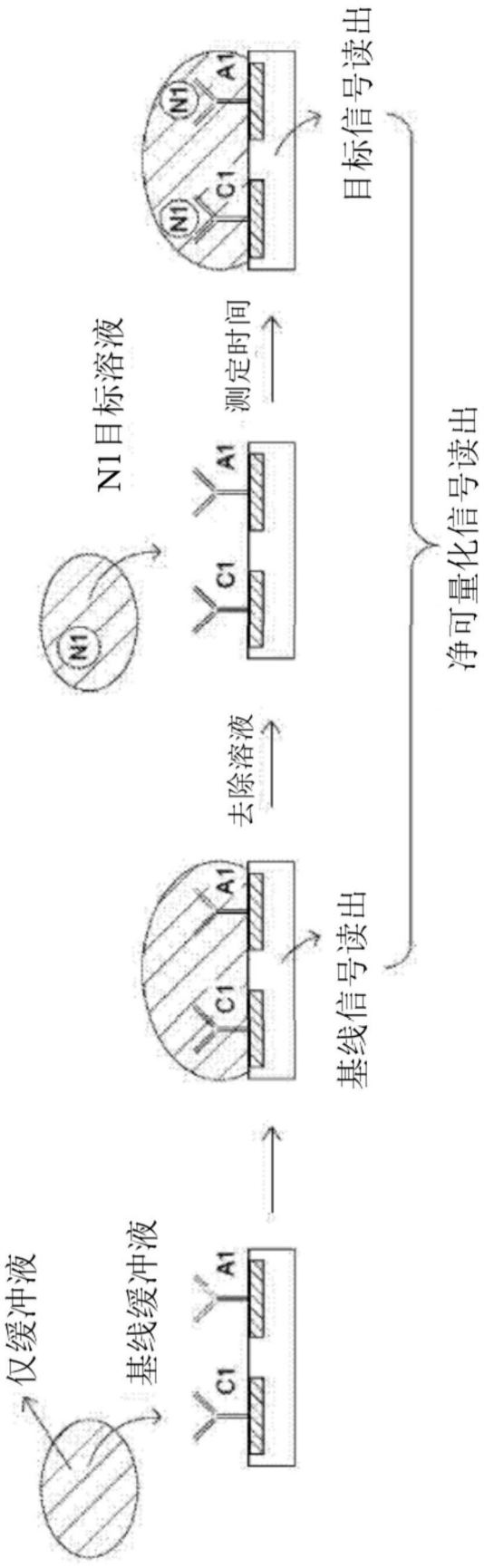


图77

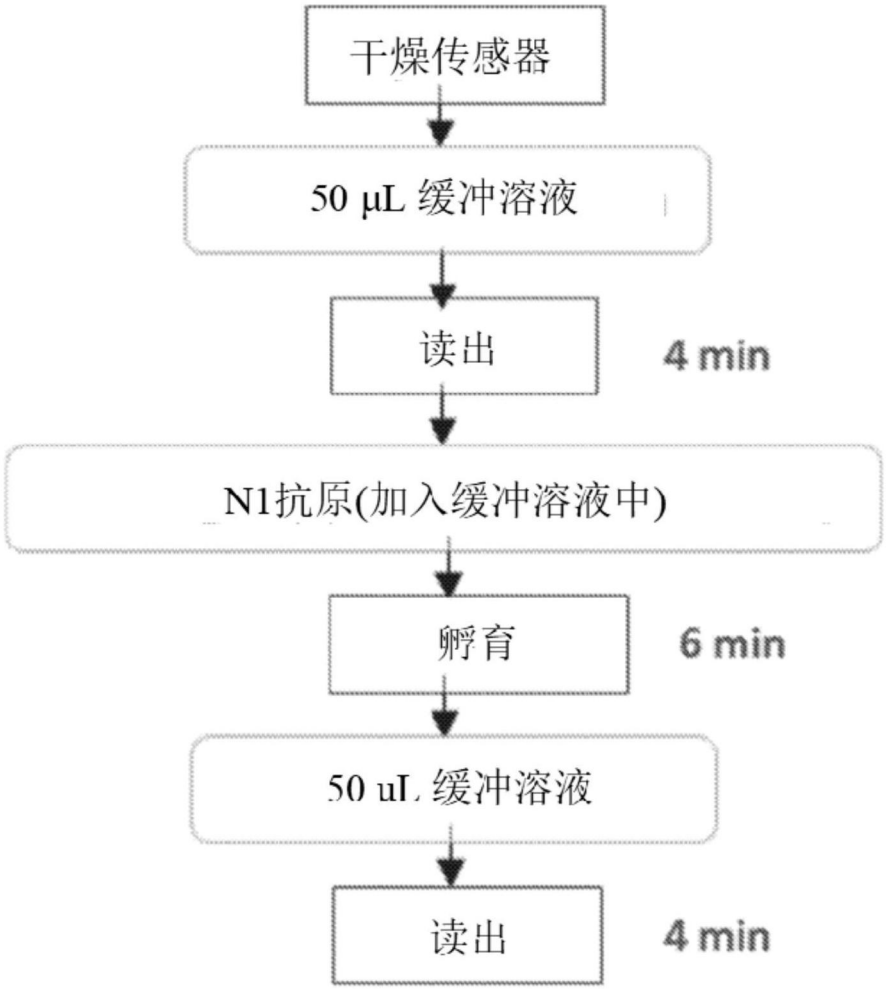

干燥传感器
50 μL 缓冲溶液
读出
4 min
N1抗原(加入缓冲溶液中)
孵育
6 min
50 uL 缓冲溶液
读出
4 min

图78

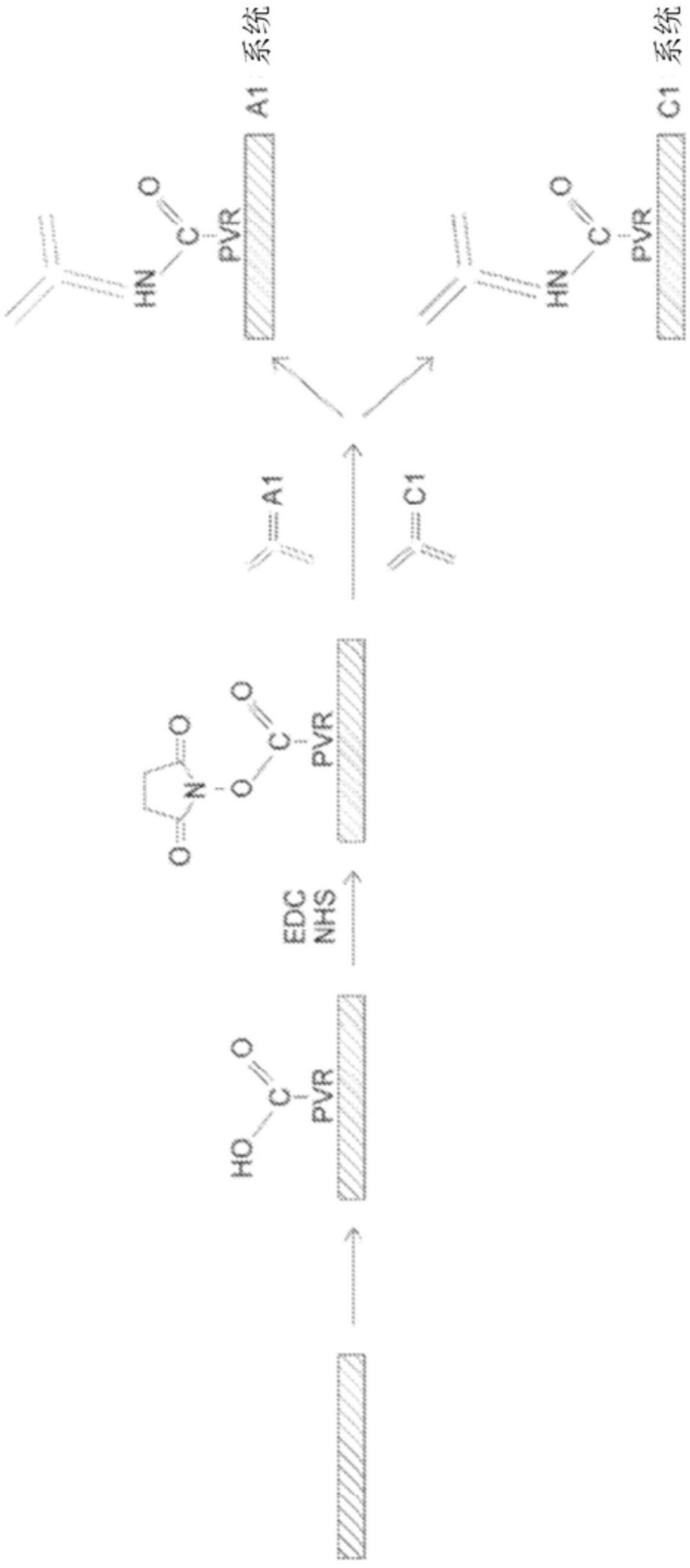


图79

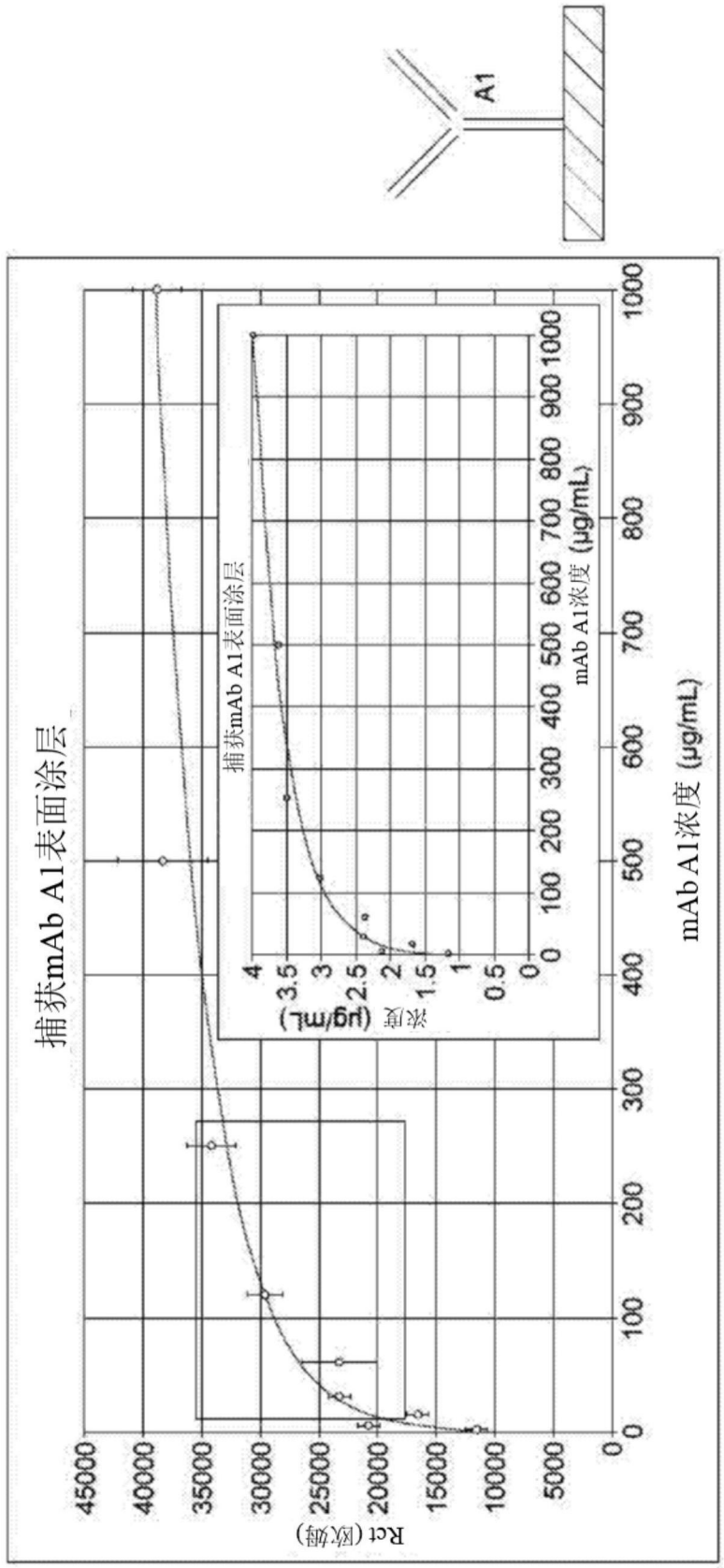

A1
捕获mAb A1表面涂层
Rct (欧姆)
mAb A1浓度 (μg/mL)
捕获mAb A1表面涂层
浓度 (μg/mL)
mAb A1浓度 (μg/mL)

图80

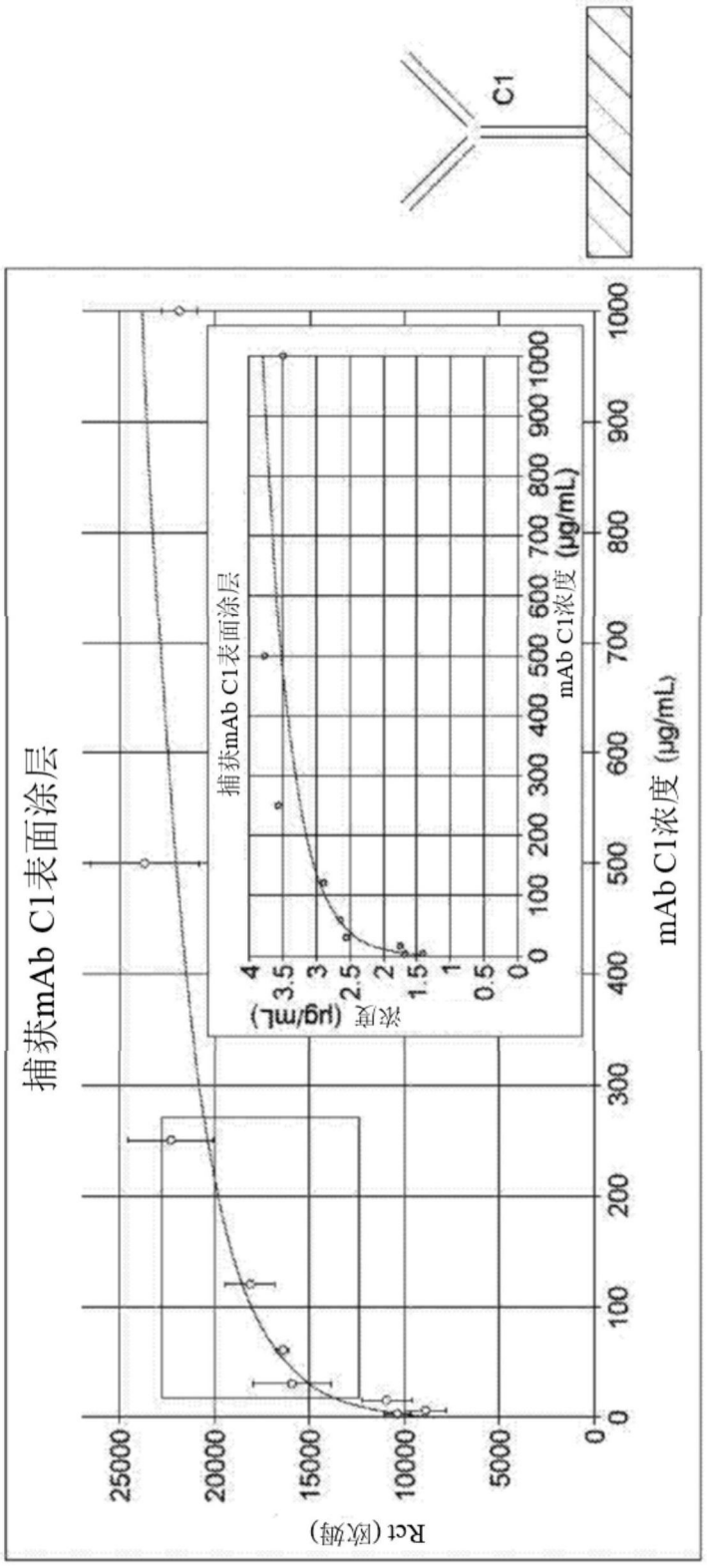

C1
捕获mAb C1表面涂层
Rct (欧姆)
mAb C1浓度 (μg/mL)
捕获mAb C1表面涂层
浓度 (μg/mL)
mAb C1浓度 (μg/mL)

图81

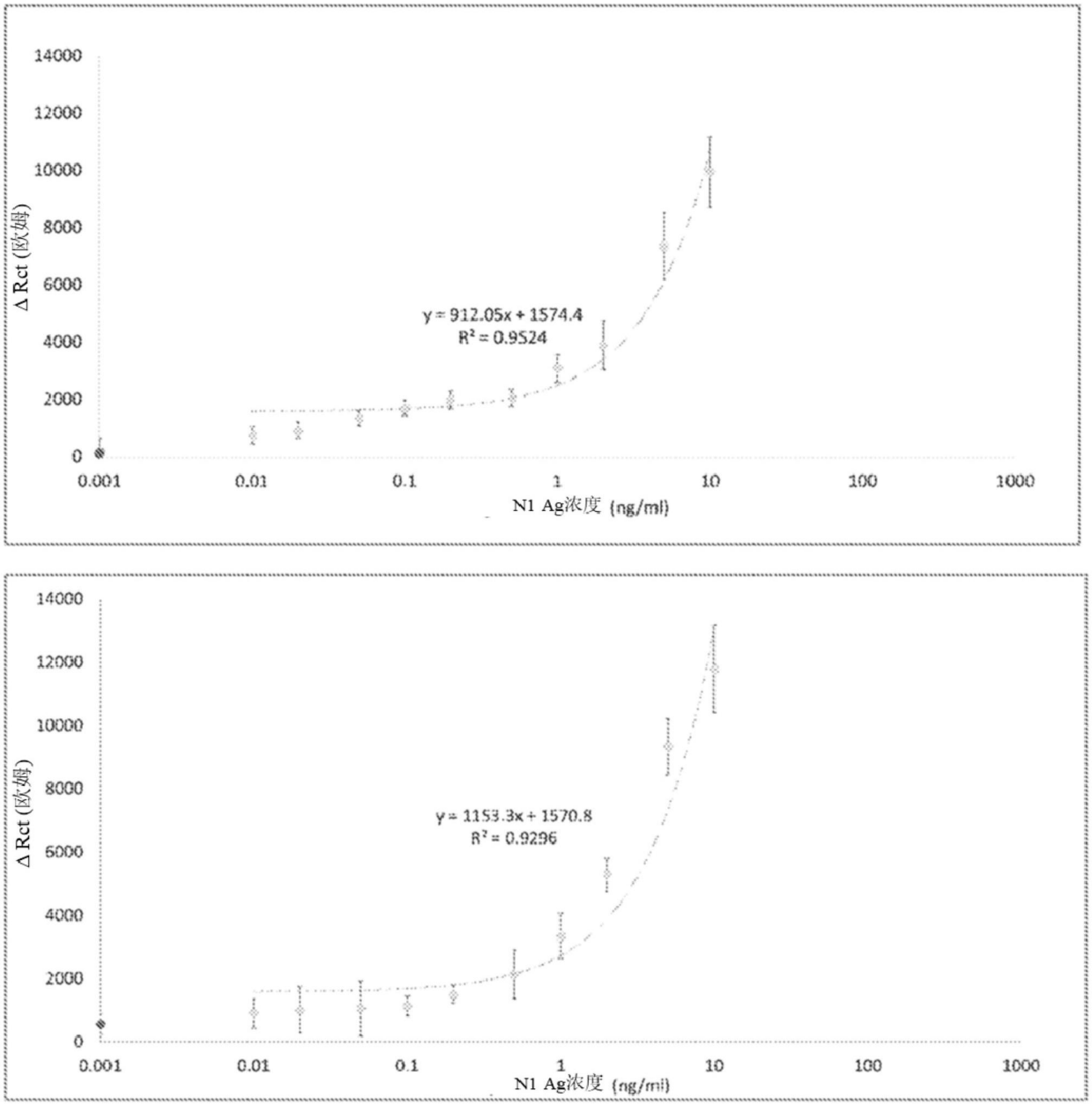

14000
12000
10000
8000
6000
4000
2000
0
Δ Rct (欧姆)
y = 912.05x + 1574.4
R² = 0.9524
0.001
0.01
0.1
1
10
100
1000
N1 Ag浓度 (ng/ml)
14000
12000
10000
8000
6000
4000
2000
0
Δ Rct (欧姆)
y = 1153.3x + 1570.8
R² = 0.9296
0.001
0.01
0.1
1
10
100
1000
N1 Ag浓度 (ng/ml)

图82

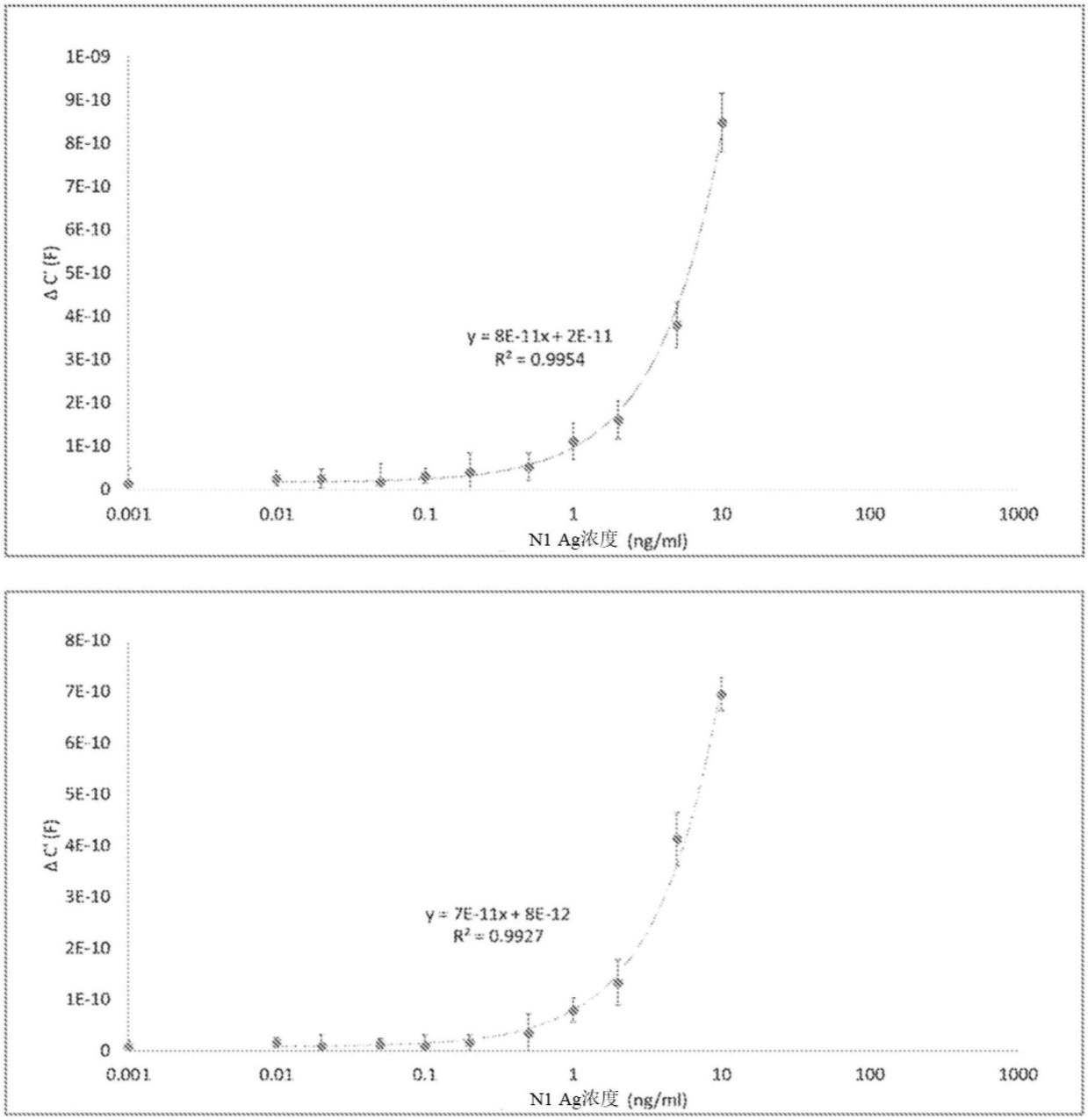

1E-09
9E-10
8E-10
7E-10
6E-10
5E-10
4E-10
3E-10
2E-10
1E-10
0
Δ C' (F)
y = 8E-11x + 2E-11
R² = 0.9954
0.001
0.01
0.1
1
10
100
1000
N1 Ag浓度 (ng/ml)
8E-10
7E-10
6E-10
5E-10
4E-10
3E-10
2E-10
1E-10
0
Δ C' (F)
y = 7E-11x + 8E-12
R² = 0.9927
0.001
0.01
0.1
1
10
100
1000
N1 Ag浓度 (ng/ml)

图83

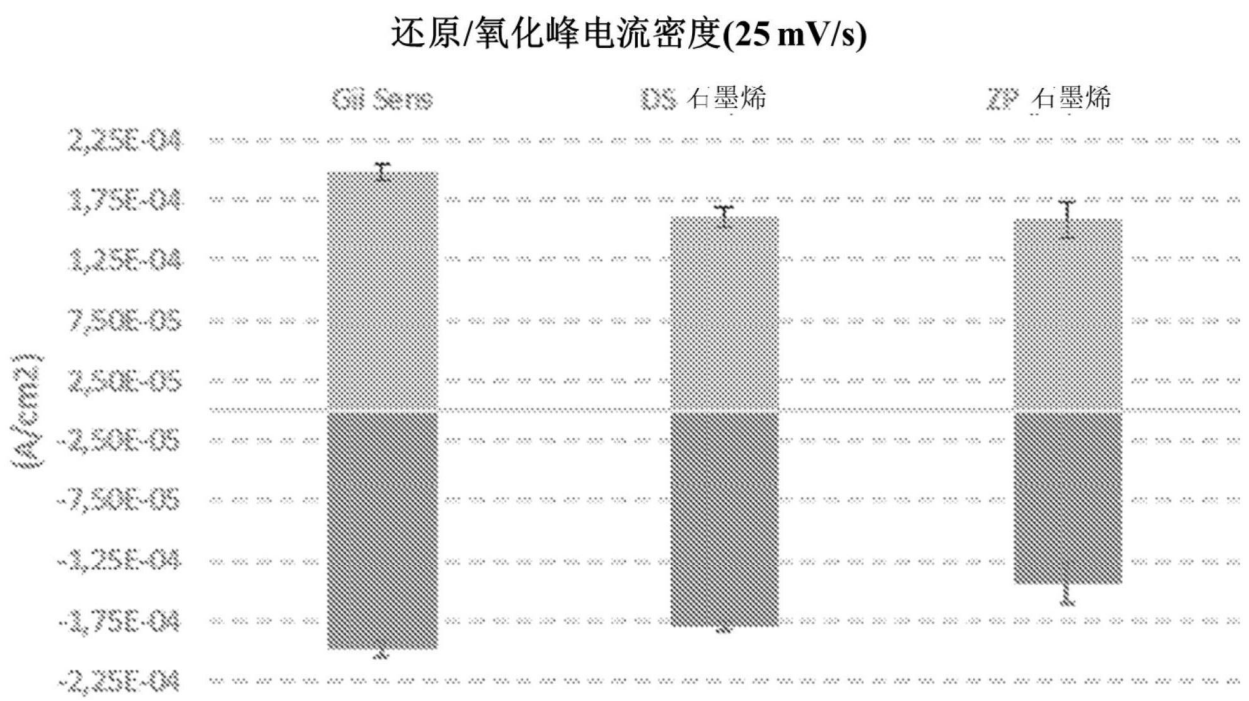

还原/氧化峰电流密度(25 mV/s)
Gil Sens
DS 石墨烯
ZP 石墨烯
2,25E-04
1,75E-04
1,25E-04
7,50E-05
2,50E-05
-2,50E-05
-7,50E-05
-1,25E-04
-1,75E-04
-2,25E-04
(A/cm2)

图84

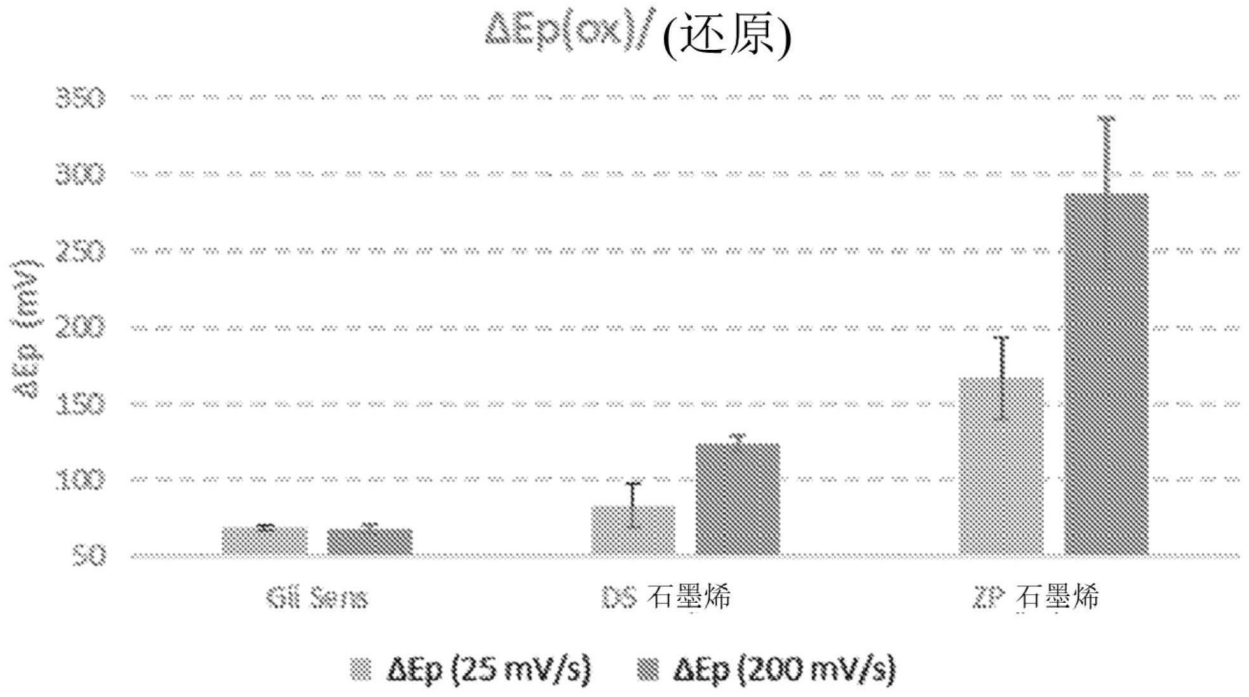

ΔEp(ox)/ (还原)
350
300
250
200
150
100
50
ΔEp (mV)
Gil Sens
DS 石墨烯
ZP 石墨烯
ΔEp (25 mV/s)
ΔEp (200 mV/s)

图85

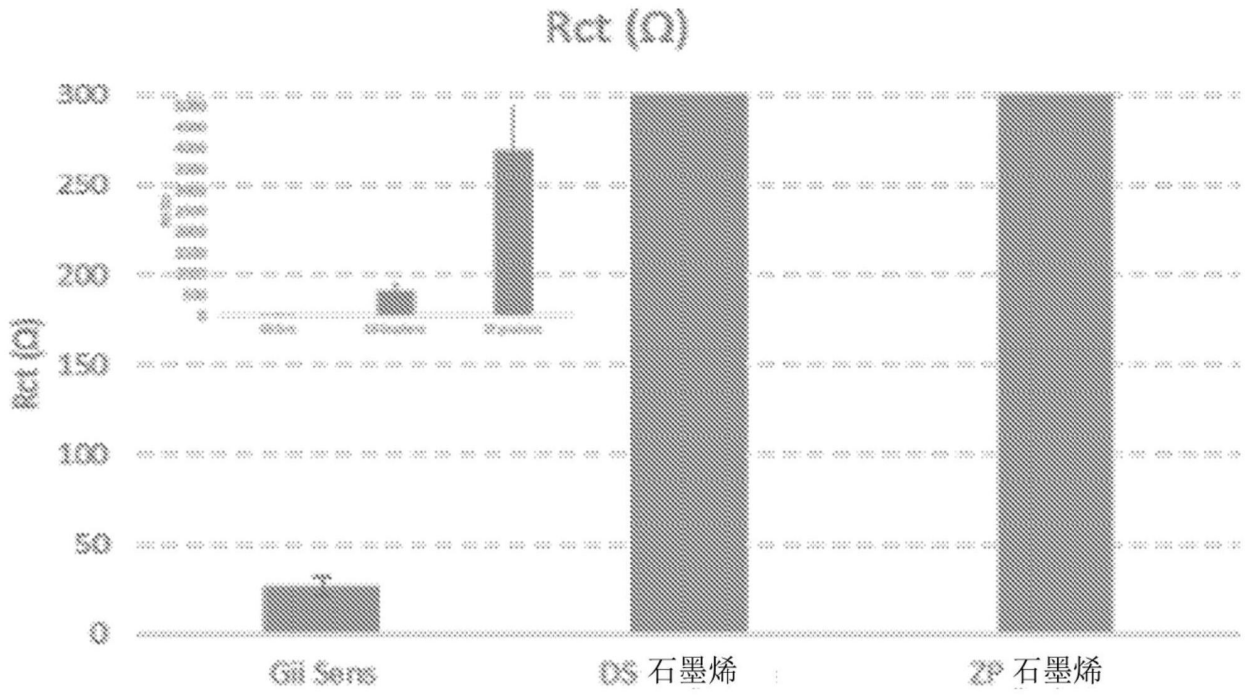

Rct (Ω)
300
250
200
150
100
50
0
Rct (Ω)
Gil Sens
OS 石墨烯
2P 石墨烯

图86

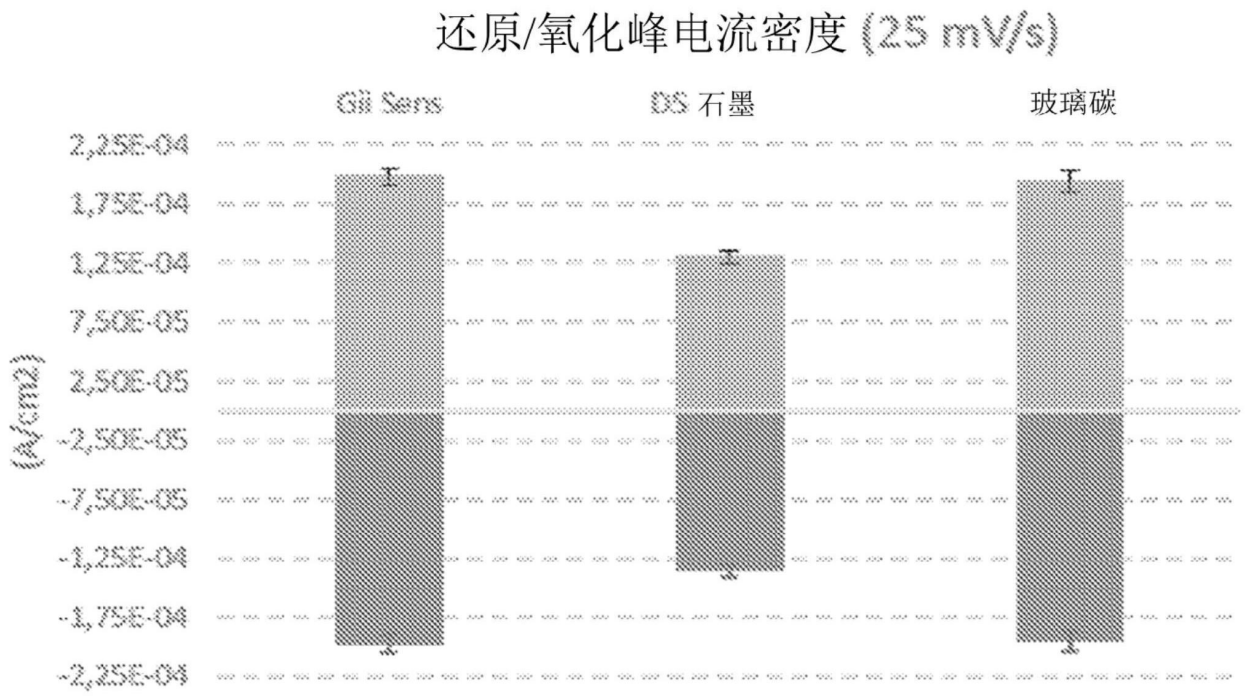

还原/氧化峰电流密度 (25 mV/s)
Gil Sens
OS 石墨
玻璃碳
2,25E-04
1,75E-04
1,25E-04
7,50E-05
2,50E-05
-2,50E-05
-7,50E-05
-1,25E-04
-1,75E-04
-2,25E-04
(A/cm2)

图87

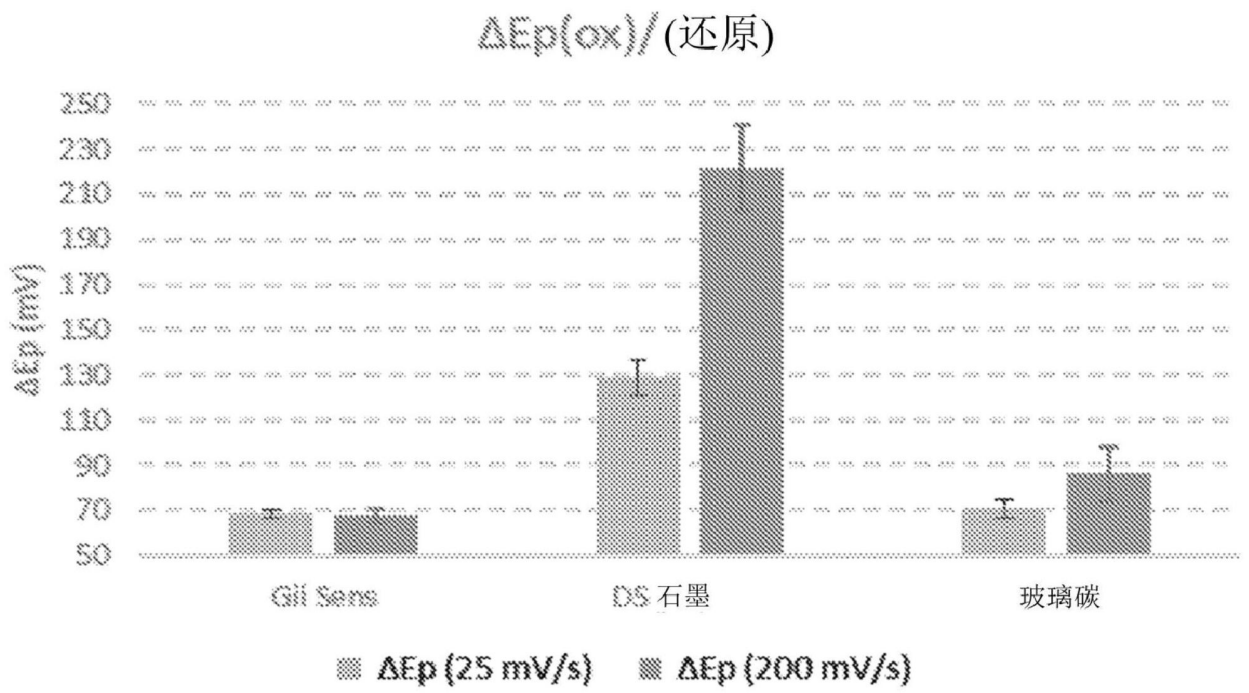

ΔEp(ox)/(还原)
ΔEp (mV)
250
230
210
190
170
150
130
110
90
70
50
Gil Sens
DS 石墨
玻璃碳
ΔEp (25 mV/s)
ΔEp (200 mV/s)

图88

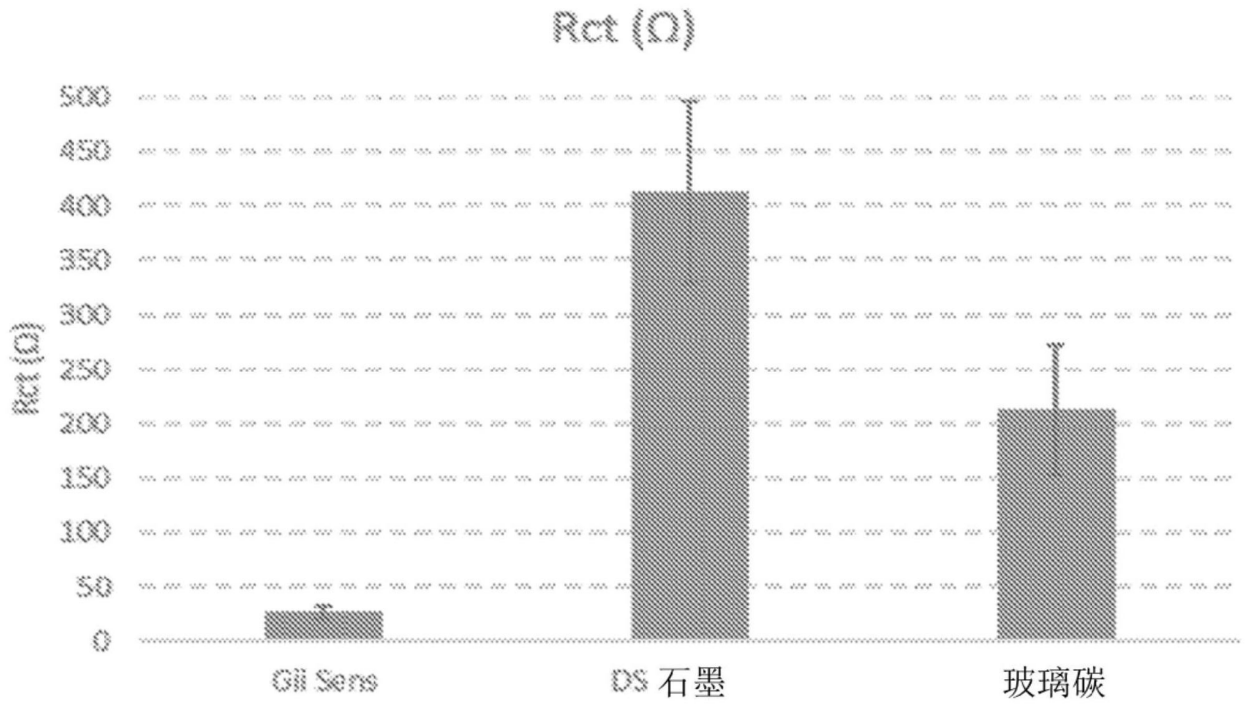

Rct (Ω)
Rct (Ω)
500
450
400
350
300
250
200
150
100
50
0
Gil Sens
DS 石墨
玻璃碳

图89

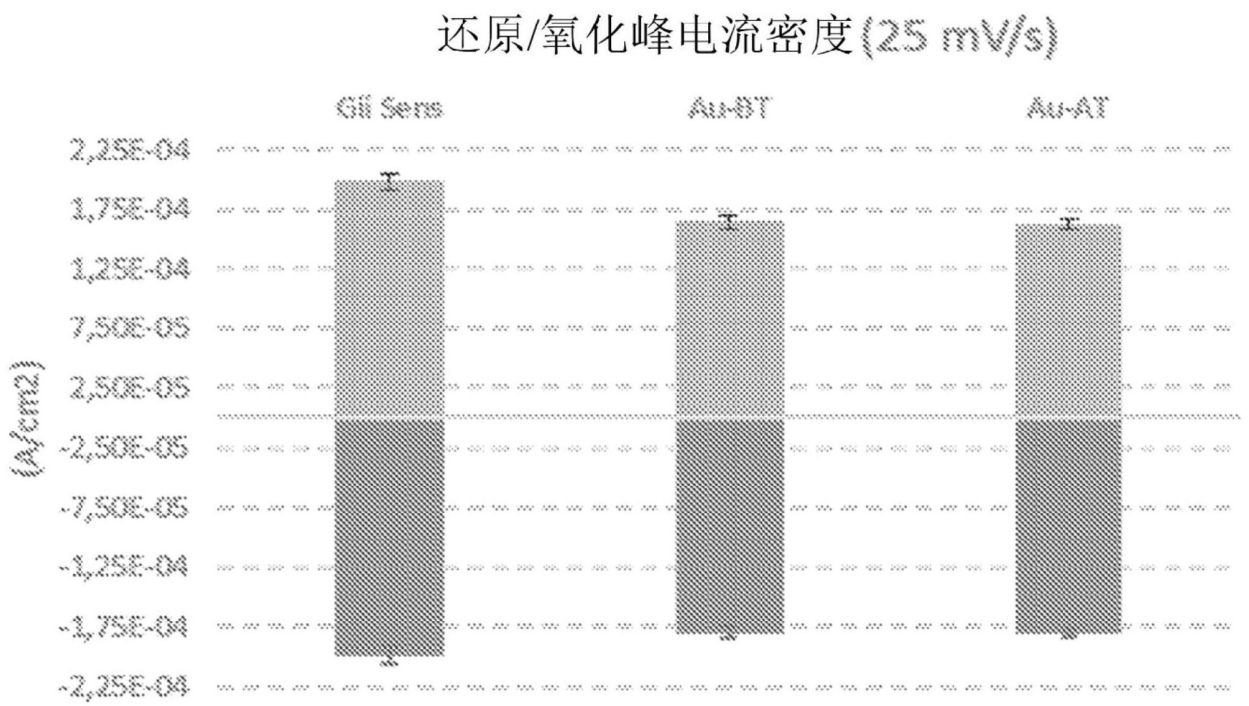

还原/氧化峰电流密度(25 mV/s)
Gil Sens
Au-BT
Au-AT
2,25E-04
1,75E-04
1,25E-04
7,50E-05
2,50E-05
-2,50E-05
-7,50E-05
-1,25E-04
-1,75E-04
-2,25E-04
(A/cm2)

图90

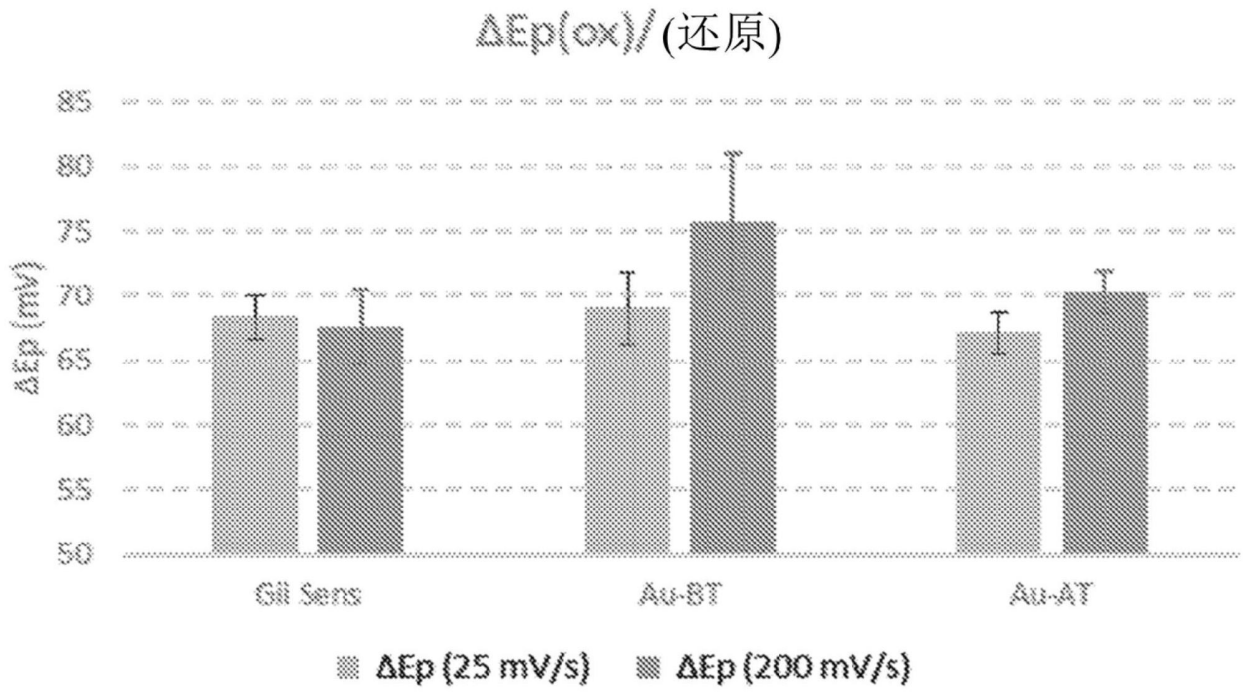

ΔEp(ox)/(还原)
85
80
75
70
65
60
55
50
ΔEp (mV)
Gil Sens
Au-BT
Au-AT
ΔEp (25 mV/s)
ΔEp (200 mV/s)

图91

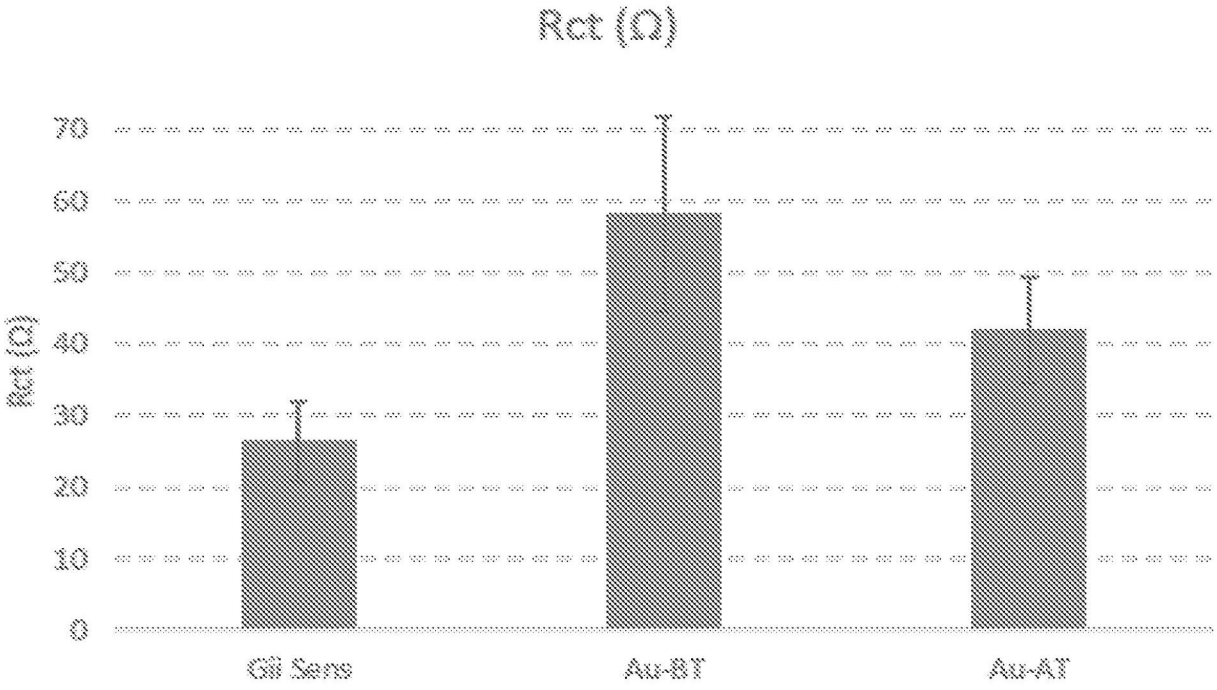


图92

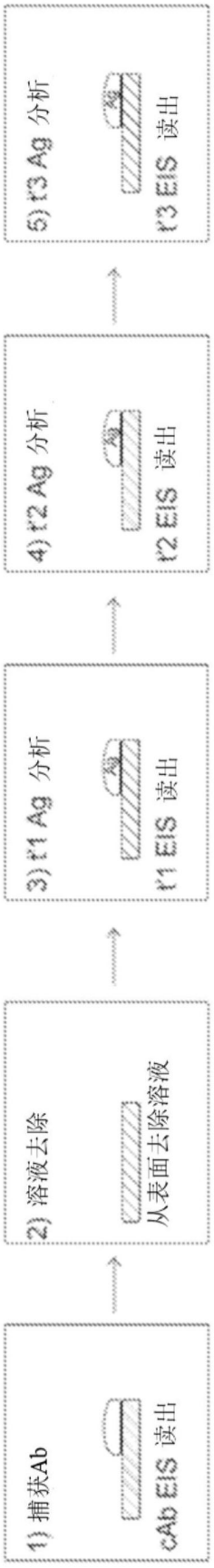

1) 捕获Ab
cAb EIS 读出
2) 溶液去除
从表面去除溶液
3) t'1 Ag 分析
t'1 EIS 读出
4) t'2 Ag 分析
t'2 EIS 读出
5) t'3 Ag 分析
t'3 EIS 读出

图93

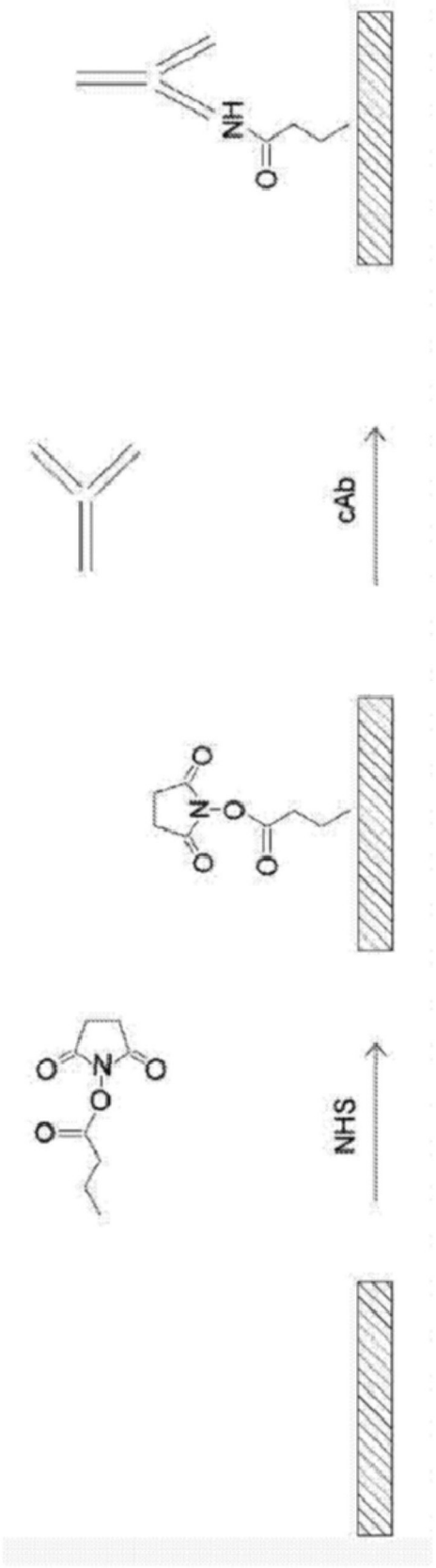


图94

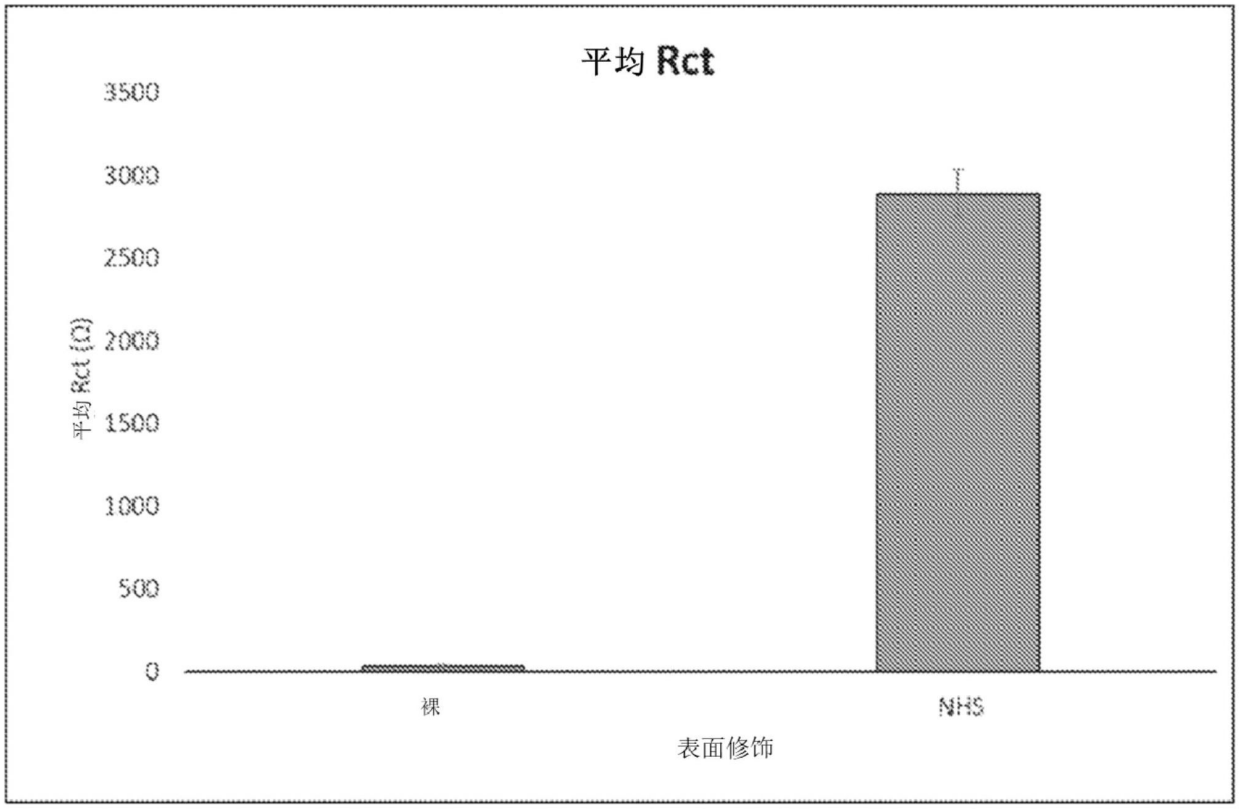


图95

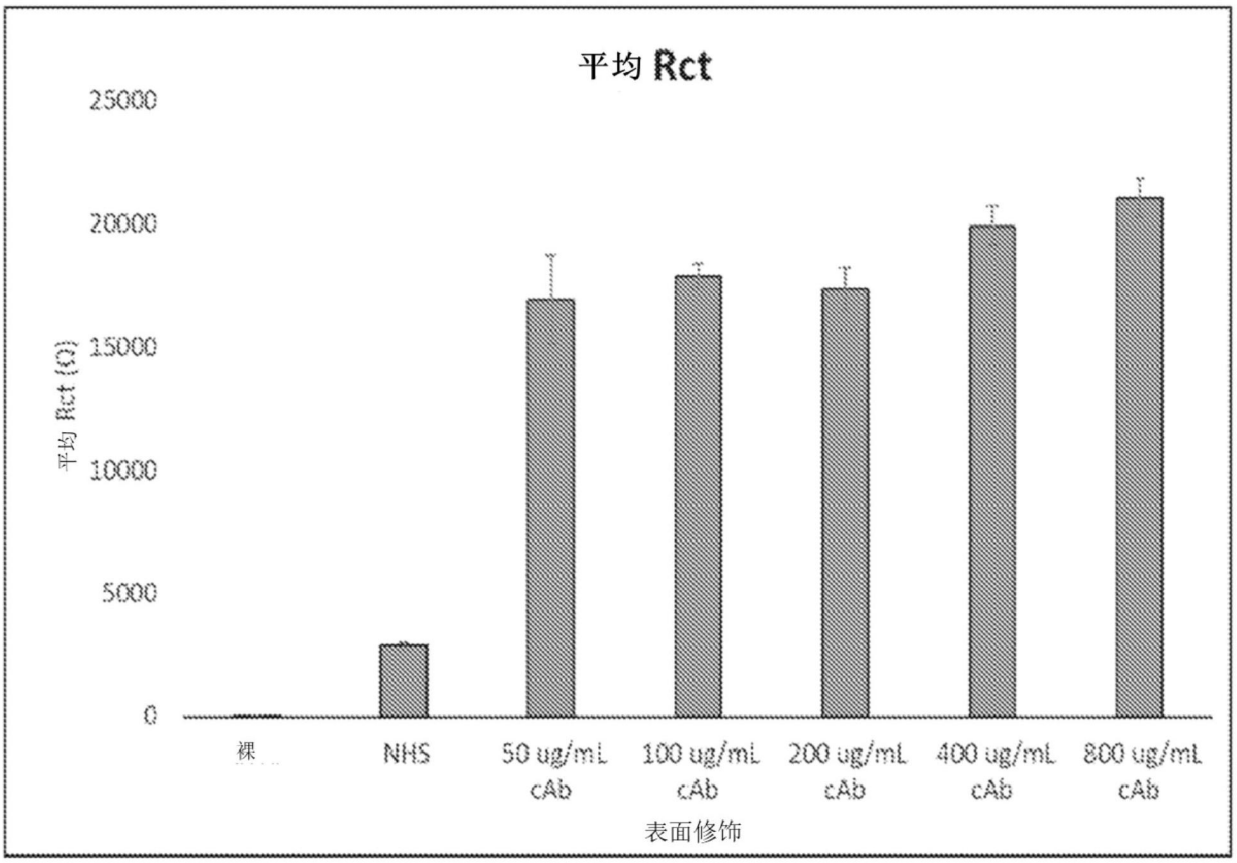
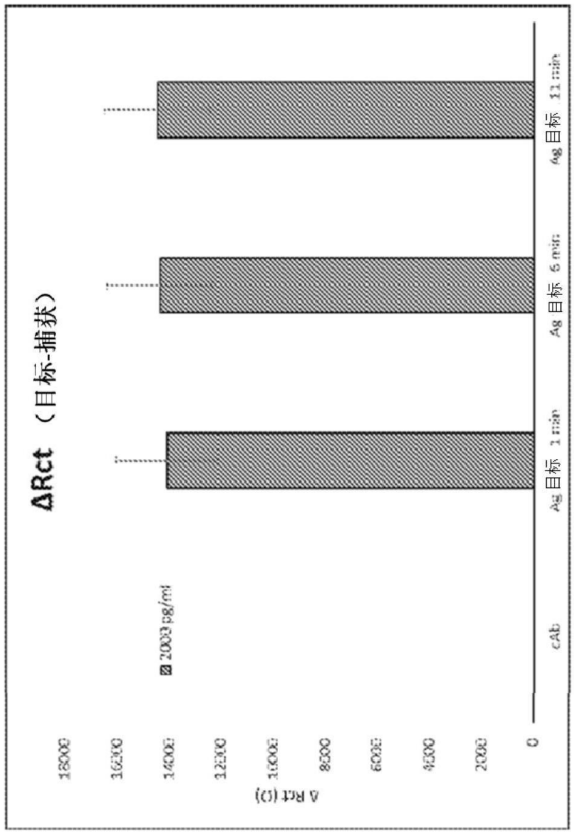

平均 Rct
25000
20000
15000
10000
5000
0
平均 Rct (Ω)
裸
NHS
50 ug/mL cAb
100 ug/mL cAb
200 ug/mL cAb
400 ug/mL cAb
800 ug/mL cAb
表面修饰

图96


ΔRct（目标-捕获）
Δ Rct (Ω)
18000
16000
14000
12000
10000
8000
6000
4000
2000
0
2000 pg/ml
cAb
Ag 目标 1 min
Ag 目标 6 min
Ag 目标 11 min

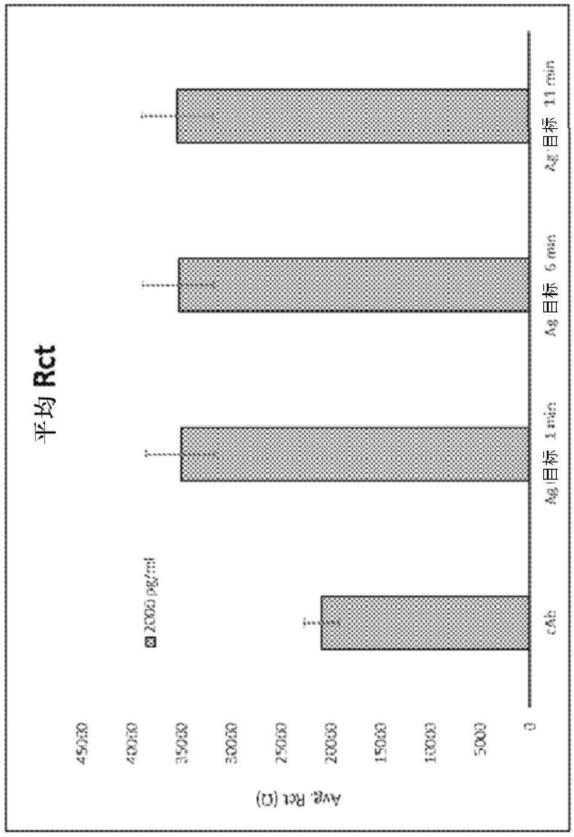

平均 Rct
Ave. Rct (Ω)
45000
40000
35000
30000
25000
20000
15000
10000
5000
0
2000 pg/ml
cAb
Ag 目标 1 min
Ag 目标 6 min
Ag 目标 11 min

图97